KTH Architecture and
the Built Environment

ARTIFICIAL GROUND FREEZING IN CLAYEY SOILS

LABORATORY AND FIELD STUDIES OF DEFORMATIONS DURING THAWING AT THE BOTHNIA LINE

TEDDY JOHANSSON

Doctoral Thesis

Division of Soil and Rock Mechanics
Department of Civil and Architectural Engineering
Royal Institute of Technology
Stockholm, Sweden 2009

TRITA-JOB PHD 1014
ISSN 1650-9501

www.kth.se

To my wife, Johanna and my children with all my love

The Häggvik tunnel in the spring of 2005 (Stockholm)

Don't be too optimistic; the light in the tunnel could be a train

(anonymous)

CONTENTS

ACKNOWLEDGEMENTS

The present research work has been carried out between the winter of 2003 and the spring of 2009 at the Royal Institute of Technology (KTH), division of Soil-and Rock Mechanics.

My warmest thanks go to my supervisor's Professor Staffan Hintze and Professor Håkan Stille, both at the Royal Institute of Technology, as well as to Professor Sven Knutsson at Luleå University of Technology (LTU) for their valuable assistance and viewpoints during the course of work of this thesis.

The author participated at the project Södra Länken 04 (SL04) in Stockholm during the stabilization of a future tunnel constructed with help of temporary soil freezing during the winter of 2000 to the spring of 2001. Large problems with deformations of the ground surface arose in conjunction with the thawing of the frozen construction. The research has been initiated by these phenomena and shaped with assistance of, among others, the research director at Skanska, Professor Kyösti Tuutti and the former director of research at Skanska Sweden, Professor Björn Täljsten. A warm thank you to Kyösti Tuutti and Björn Täljsten.

A reference committee consisting of people with diverse experience and knowledge in soil- and rock stabilization and freezing has followed the research. This group has worked as a discussion partner and has mainly assisted in competent reviewing of suggested test proposals.

The reference committee has consisted of:
Ph. D. Anne-Lise Berggren, Geofrost AS, Oslo
M. Sc. Lars Bjerin, the Swedish National Road Administration, Region Stockholm
Professor Lars-Olof Dahlström, NCC/Luleå University of Technology (LTU)
Ph. D. Anders Fredriksson, Golder Associates AB, Stockholm
Ph. D. Matti Kivelö, Kivelö Geoteknik AB, Karlskoga
Professor Sven Knutsson, Luleå University of Technology (LTU)
M. Sc. Gunnar Lejon, Botniabanan AB/the National Rail Administration (Banverket), Stockholm.
I wish to express my sincere appreciation to the help given by all the members of the reference committee.

Ph.D. Anders Fredriksson has during the course of the work also contributed with assistance in above all numerical calculations. Many thanks to Anders Fredriksson.

The instrumentation during the field studies has been accomplished with assistance of research engineer Per Delin and Elis Svensson at KTH, division of Soil-and Rock Mechanics. The co-ordination of the instrumentation and the registration of data has been carried out by M. Sc. Gunnar Lejon, at the Bothnia Line. The information from the instrumentation has been registered and compiled by personnel from the Bothnia Line, above all Eero Niemi. Warm thanks to all these contributors.

Many thanks to project manager Vesa Vaaranta, Lemminkäinen Construction, whose encouraging assistance and positive attitude have supported the work of this thesis. He has provided registered data for my use, thus allowing unique and important fieldwork to be performed.

Research engineer Per Delin has assisted with valuable knowledge and experience in the laboratory at Soil- and Rock Mechanics, KTH. Thank you Per.

Assistant professor Sven-Erik Rehnman has been most helpful during the course of my work. He has clarified discussions and contributed with valuable comments on paper- and report manuscripts. Thank you Sven-Erik.

Mrs. Lisa Embro-Klemesrud has helped and contributed with valuable viewpoints in regards to the linguistic adaptation of this thesis, and Mr. Jeffrey Stilwell has helped and contributed with valuable viewpoints in regards to the linguistic adaptation of articles, etcetera. Thank you Lisa and Jeff.

To compile data and solve specific problems, assistance is needed from a diverse group of people. Thank you to my colleagues at the division of Soil- and Rock Mechanics at KTH and Skanska.

I would also like to thank the financiers who have made this thesis possible, Skanska AB, The Research Consortium for highway, bridge and tunnel (Forskningskonsortiet Väg, Bro och Tunnel, VBT), KTH div of soil and rock mechanics and the Development Fund of the Swedish Construction Industry (Svenska Byggbranschens Utvecklingsfond, SBUF).

Finally, my special thanks are reserved to my beloved wife, Johanna and my children, for their boundless patience and continual encouragement during the innumerable weekends and late nights that I have spent in front of the computer, in the laboratory and at the test field. I would also like to thank my parents-in-law; Ylva and Rune who have been an invaluable help to our family during several years, when I, as well as Johanna have been finishing our academic careers.

Stockholm, the spring of 2009

Teddy Johansson

SUMMARY

In conjunction with the construction of the Södra Länken Project in Stockholm in the beginning of the 21st Century, an opportunity arose to employ a relatively unproven solution in regards to Swedish construction and design techniques. The design to be adopted for this project – artificial soil and rock freezing (AGF), intended to temporary stabilize and seal tunnels during construction. This method is quite common in Germany, UK, USA and France, and was actually adopted in Sweden as far back as 1884, when used on Lindmark's tunnel through the glacier esker, Brunkebergsåsen (Stockholm) and on the extension of the underground subway system at Tegelbacken (Stockholm) in 1952. The majority of the approximately 400 documented freezing projects have been performed in the last 70 years.

At the Södra Länken Project, temporary stabilisation and hydraulic sealing through freezing were performed at two different areas having poor rock coverage, both areas showed good results in conjunction with the tunnelling. However, during the thawing process, unexpectedly large deformations occurred which were related to the consolidation of the thawing clay.

This thesis considers the thawing process related to the settlement in fine-grained soils and describes the artificial freezing and thawing process, identifying differences and similarities with natural freezing. It also describes how different soil and rock parameters influence deformations and stresses during freezing and thawing in artificially frozen constructions. These descriptions are primarily based upon literature studies and case studies.

This thesis has primarily been limited to temporary stabilisation and hydraulic sealing of fine-grained soil through artificial freezing using brine as the cooling agent in connection with the building of tunnels.

The soil has been temporary stabilised and sealed through AGF on a section of approximately 90 metres of the contract of the Bothnia Line. At the frozen area, field studies are carried out; these results are used in the research of this thesis. The field studies started in connection with the shut off of the cooling machine, in the autumn of 2003. Soil samples are collected close to the frozen area. However, the samples assume to be undisturbed by the freeze process in the adjacent frozen construction. The soil samples' undisturbed and thawed properties are investigated in the KTH laboratory.

14 published methods to prognosticate the thaw settlement have been analysed. The analyses are primarily based on the use of the Bothnia soil properties. Moreover, the prognoses of the thaw settlement are also investigated in field studies and laboratory

studies. However, the results from the 14 analytic methods to prognosticate the thaw settlement are compared to the results from the field and laboratory studies. As a matter of fact, the dispersion of the results of the thaw settlement is very large. The results of the theoretically based methods show a prognosticated final thaw settlement of approximately 1.08 m, while the empirically based methods show a prognosticated thaw settlement varying between 1.93 m and 3.85 m. One explanation for this immense distribution is that the prognoses of the thaw-deformations are mainly related to permafrost and specific sites or soils. Nevertheless, the laboratory study of the Bothnia soil shows a relation between the thaw settlement magnitude (ε) and the ratio of the water content (w) and the plastic limit (w_p). The total resulted predicted thaw settlement, that is the settlement including the frost heave, was $\varepsilon = \Delta H/H = 7.0 \ln(w/w_p) + 7.8$, and in the same way, the predicted thaw settlement for undisturbed soil subjected to artificial freezing became $\varepsilon = \Delta H/H = 2.7\ w/w_p + 3.8$.

On completion of this thesis in the spring of 2009, the artificially frozen site at the Bothnia Line was still frozen. The thesis' laboratory and field studies are based on the Bothnia Line's temporary stabilizing and hydraulic sealing through AGF during the time period of the freezing between 2002 and 2003. During the course of the measuring, an unexpected load on the tunnel roof occurred, among other things, simultaneously as the ground surface unpredictably heaved approximately 0.1 m. This course of events is important to follow up, analyse and describe in further research. Furthermore, a theoretical analysis of the temperature influence of the thaw-related deformations is proposed, as well as an investigation of the influence of the low temperature durability is to be performed. The analysis should be based on the original water content and the original plastic limit, connected to the water content and the plastic limit after a freeze and thaw cycle.

Following general conclusion can be drawn from this thesis (all tests are based on one freeze-thaw cycle with a surcharge of the in situ pressure at the Bothnia frozen construction)

- the Bothnia soil water content decreased in mean approximately 14 % after a freeze-thaw cycle, which approximately corresponds to; $w_{th} = 0.8w - 1.5$
- the decrease of the water content has no correlation to the depth below ground surface, in contrast, there is a strong correlation between the undisturbed soil water content and the magnitude of the decrease in water content
- the soil attains a higher density after a freeze-thaw cycle under the in situ pressure at the same time as it becomes more permeable
- the soil liquid limit decreases after a freeze-thaw cycle, simultaneously as the relative share of clay and fine silt grains decreases while the relative share of more coarse grains increases
- the coarser and denser soil created after a freeze-thaw cycle obtains an increased preconsolidation pressure and an increased undrained shear strength
- registered temperatures in the frozen Bothnia construction are strongly influenced by heat from the surrounding atmosphere and sun radiation, due to heat conduction from the casing pipes, especially in the temperature range close to the phase change from ice to water
- the thawing of the frozen construction at the Bothnia Line has started adjacent to the casing pipes of the freeze pipes and the temperature control pipes. The thawed "windows" grant the deeper lying thawing soil water to migrate upwards to the ground surface.

SAMMANFATTNING

I samband med byggandet av Södra Länkenprojekten i Stockholm i början av 2000-talet, tillämpades för svenska förhållanden en relativt oprövad lösning för att temporärt stabilisera och täta tunnlar under tunneldrift, artificiell jord och bergfrysning (AGF). Tidigare har AGF tillämpats i Sverige bl a i samband med tunnelprojekt, exempelvis då Lindmark byggde tunneln genom Brunkebergsåsen i Stockholm 1884 och vid utbyggnaden av Stockholms tunnelbana 1952, vid Tegelbacken. Metoden är vanlig i bland annat Tyskland, Storbritannien, USA och Frankrike. De flesta av nära 400 dokumenterade frysprojekt har utförts efter 1940-talet.

På Södra Länkenprojekten stabiliserade och hydrauliskt tätade man temporärt två skilda tunnelavsnitt med dålig bergtäckning genom AGF, båda med lyckat resultat. Under tiningsförloppet uppstod däremot oväntat stora deformationer som relaterades till tiningssättning av lera.

Denna avhandling behandlar framför allt den tiningsrelaterade sättningen i finkornig jord och beskriver den artificiella frys- och tiningsprocessen med en identifiering av skillnader och likheter med naturlig frysning. Dessutom skildras hur olika jordparametrar påverkar deformationer och spänningar vid nedfrysning och upptining i artificiellt frysta konstruktioner. Beskrivningarna baseras i huvudsak på litteraturstudier och fallstudier.

Avhandlingen har i huvudsak begränsats till temporär stabilisering och hydraulisk tätning av finkornig jord med artificiell brinefrysning i samband med tunnelbyggnad.

På en av Botniabanans entreprenader har man i ett avsnitt på c:a 90 m stabiliserat och tätat jorden temporärt genom artificiell frysning. På det frysta området bedrivs fältförsök, som ansluter till forskningsområdet och beskrivs i denna avhandling. Fältförsöken inleddes i samband med att kylmaskinen stängdes av hösten 2003. Jordprover har tagits upp ur marken intill den frysta konstruktionen och betraktas som ostörda av frysprocessen. Provernas egenskaper har analyserats i KTH:s laboratorium dels som ostörda och dels som tinade.

14 publicerade analytiska metoder för att prognostisera tiningssättning har analyserats. Analyserna har framför allt baserats på Botniajordens egenskaper. Prognoserna för den tiningsinducerade deformationen har även studerats i samband med fältstudien och laboratorieförsöken. De 14 analytiska metoderna för att prognostisera tiningssättningen har jämförts med resultaten från laboratorieförsöken. Emellertid är spridningen på resulterande slutsättning mycket stor. Resultaten från de teoretiskt baserade metoderna visar att tiningssättningen blir c:a 1.08 m, medan resultaten från de empiriskt baserade metoderna

ger tiningssättning varierande mellan 1.93 m och 3.85 m. En anledning till den stora spridningen är att de empiriskt baserade prognoserna för tiningssättningarna är relaterade till framför allt permafrost och specifika jordar eller områden. Hur som helst, laboratoriestudien visar att det finns en korrelation mellan tiningskonsolideringens numerär (ε) och kvoten mellan vattenkvoten (w) och plasticitetstalet (w_p). Den resulterande totala prognostiserade tiningskonsolideringen, d v s sättningen inklusive tjälhävningen blev $\varepsilon = \Delta H/\mathrm{H} = 7.0 \ln(w/w_p) + 7.8$, och på samma sätt blev den prognostiserade tiningskonsolideringen för ostörd jord aktuell för artificiell frysning $\varepsilon = \Delta H/\mathrm{H} = 2.7\, w/w_p + 3.8$.

När detta arbete skrivs våren 2009 har det frysta området på Botniabanan ännu ej tinat. Avhandlingens laboratorie- och fältförsök baseras på Botniabanans temporära stabilisering och hydrauliska tätning genom frysning år 2002 till år 2003. Under mätningarna har man bl a konstaterat att det sker en oväntad lastuppbyggnad på tunneltaket, samtidigt som markytan oväntat hävt sig c:a 1 dm. Denna utveckling är viktig att följa upp, analysera och beskriva i fortsatta studier. Dessutom bör en undersökning av temperaturens inverkan på det nedfrysta jordmaterialets tiningsrelaterade deformation ingå i fortsatta studier. Analysen bör utgå från ursprunglig vattenkvot och plasticitetsgräns parade med vattenkvot och plasticitetsgräns, efter en frys- och tiningscykel.

Följande generella slutsatser kan dras (alla försök baseras på en frys- och tiningscykel under in situlast för den frysta Botniakonstruktionen)

- vattenkvoten i Botniajorden sjönk i genomsnitt med c:a 14 % efter en frys- och tiningscykel, vilket ungefär motsvarar; $w_{th} = 0.8w - 1.5$
- vattenkvotsminskningen har ingen korrelation till djupet under markytan, men det finns en stark korrelation mellan den ostörda jordens vattenkvot och minskningens storlek.
- jorden får en högre densitet efter tining under in situlasten, samtidigt som den blir mer permeabel
- flytgränsen blir lägre efter en frys- och tiningscykel samtidigt som den relativa andelen ler- och finsiltpartiklar minskar, medan andelen grövre partiklar ökar
- den grövre och kompaktare jorden som bildats efter tiningen får ett högre förkonsolideringstryck och en ökad skjuvhållfasthet
- registrerade temperaturer i den frysta Botnia konstruktionen påverkas starkt av foderrörens värmeledning av atmosfärstemperatur och solstrålning, då temperaturen nått vattnets fasomvandlingstillstånd från is till vatten
- tiningen av den frysta Botnia konstruktionen har startat kring foderrören för temperaturgivare och frysrör. De tinade "fönstren" bildar dräneringsvägar för det migrerande vattnet.

NOTATION

Key symbols used in the text are listed below. Others are defined as they first appear.

Greek Symbols

Symbol	Represents
α	soil parameter, thermal diffusivity, exponent for hydraulic conductivity
α_f	ground thermal diffusivity of frozen ground
α_u	ground thermal diffusivity of unfrozen ground
β	soil parameters, $d\rho_0/dT$, thermodynamic constant, coefficient of water expansion due to phase change [= 0.091]
γ, γ_t	total unit weight of soil
γ'	submerged (or effective) soil unit weight, submerged density
γ_d	dry unit weight
γ_{df}	dry unit weight of frozen soil
γ_{dth}	dry unit weight of thawed soil
γ_f	unit weight of frozen soil, frozen bulk density
γ_i	unit weight of ice
γ_m	material coefficient
γ_s	unit weight of solids
γ_{sat}	saturated unit weight
γ_w	wet unit weight, unit weight of water
δ	radial displacement
Δ	change (e.g. ΔT)
δ_f	radial displacement of frozen soil
δ_z	increment of pile length
ε_s^v	volumetric strain increment due to segregation heave
η_f, η_u	Poisson's ratio of the frozen and unfrozen soil, respectively
θ	absolute negative temperature, negative temperature
μ	viscosity, Poisson's ratio
ν	water migration rate to the heaving element
ξ	radius of the frozen cylinder, thickness of frozen soil layer
ρ	density
ρ'	submerged density

Symbol	Represents
ρ_d	dry density
ρ_{df}	dry density of frozen soil
ρ_f	frozen bulk density
ρ_i	density of ice
ρ_s	density of solid particles
ρ_{sat}	saturated density
ρ_t	bulk density
ρ_w	water density, density of water at 4 °C
ρ_0	density of water at 4 °C
σ	pressure, normal stress
Σ	sum
σ'	pressure, effective normal stress
σ_c	reference stress corresponding to a reference strain rate
σ_d	design compression strength
σ_{iw}	surface tension ice-water [≈ 0.0331 N m^{-1}]
σ_{no}	pressure, normal stress
$\sigma_{no}°$	pressure, normal stress without migrating water
σ_θ	reference strength at temperature θ
τ	shear strength
τ_d	dimensioning shear strength
τ_{fu}	undrained shear strength
τ_{futh}, $\tau_{fu,th}$	undrained shear strength of thawed soil
υ	coefficient of mass flow

Roman symbols

Symbol	Represents
A	area, area of ice-water interface, relative deformation, settlement in per cent
$\bar{A}$	thawing coefficient
a, b	soil parameters
$\bar{a}$	coefficient of relative compaction of frozen ground during thawing
A_0	thaw strain parameter
a_c	activity of clay, i.e. Skempton activity of clay
$a_{c,th}$	activity of clay for thawed soil, i.e. Skempton activity of clay
c	cohesion, heat capacity
C	distance from the cylinder axis at which the influence of the pressure (p) on the thawed soil can be neglected [$C >> \zeta$]
CL	clay content, i.e. the amount of particles less than 2 μm
c_u	undrained shear strength
C_u	uniformity coefficient
c_v, c_{vc}	coefficient of consolidation
c_{vf}	frozen soil, volumetric thermal capacity
c_{vu}	volumetric heat capacity, unfrozen soil
C_z	coefficient of curvature
d	radius, radius of pile
D	diffusion coefficient of moisture

Symbol	Represents
d_0	outer diameter of freeze pipe
D_{10}, D_{30}, D_{60}	ratio of the diameter of the particle size at 10 %, 30 % and 60 % respectively
e	void ratio
e_f, e_u	void ratio of frozen and unfrozen soil, respectively
E_f, E_u	coefficient of elasticity of the frozen and unfrozen soil
e_{f0}	initial void ratio of frozen
e_{th}	void ratio of thawed soil
F	percentage soil particles passing No. 200 sieve (0.075 mm) whole number
f_a	ad freeze stress
f_d	degree of mobilization
g	acceleration of gravity
G	specific gravity ($G = \rho / \rho_0$)
G_f	thermal gradient in the frozen soil
G_{ff}	thermal gradient in the frozen fringe
GI	group index (referring to AASHTO)
G_m	specific gravity of total soil mass ($G_m = \rho_t / \rho_0$)
grad T	gradient of temperature
grad T_f	gradient of temperature in the frozen element
G_s	specific gravity of solids ($G_s = \rho_s / \rho_0$)
G_w	specific gravity of water ($G_w = \rho_w / \rho_0$)
h	moisture ratio, height, thickness, total depth of entire soil layer tested
H	height, thickness
H_f	frozen soil layer thickness
H_{th}	thawed soil layer thickness
h_u	negative pressure
H_u	potential
H_w	total potential
I	hydraulic gradient, volumetric ice content
i, i_r	specific ice content, (”iceness”), iceness ratio
I_c	consistency index
$I_{c,th}$	thawed soil consistency index
I_l, I_L	liquidity index
$I_{l,th}$, $I_{L,th}$	thawed soil liquidity index
I_p	plasticity index
$I_{p,th}$	thawed soil plasticity index
k	thermal conductivity
K	experimental determined coefficient related to the soil and freezing conditions
$\bar{K}_f$	overall permeability
k, k_φ	hydraulic conductivity
k_0	hydraulic conductivity at -1 °C
k_1	thaw settlement factor
k_{air}	air thermal conductivity
k_f	frozen soil thermal conductivity
k_s	thermal conductivity of solids
k_u	soil characteristic parameter circumstantial among other things the spec surface, unfrozen soil thermal conductivity

Symbol	Represents
k_w	thermal conductivity of water, thaw settlement factor
l	height of specimen, thickness
L, l	volumetric latent heat of soil, volumetric latent heat of water
LL	liquid limit
l_s	length of the freezing isotherm in the element
l_u	thickness of unfrozen soil
m	soil parameter, soil constant, length of pile not embedded in permafrost
M	mass, compressibility modulus
M_g	mass of air
M_i	mass of ice
M_s	solids mass
M_t	total soil mass
M_{uw}	mass of unfrozen water
m_v	coefficient of volume compressibility
M_w	mass of water
n	porosity
OCR	overconsolidation ratio
p	pressure on the freezing cylinder surface, pressure of moisture
P, p	pressure, load, rate of energy removal
p_0	overburden pressure
p_e	applied pressure or effective overburden pressure
p_g	load on the beam
PP	plasticity index
p_u	excess pore pressure
p_w	total pressure potential (suction) at the freeze front
q	flow
Q	heat flux, water flux, amount of migrating water in the freeze process
q, q_0	stress applied to the surface
Q_p	load that can be developed by ad freeze on the pile surface
r	internal radius
R	thaw consolidation ratio
r_0	radius of the freezing pipe
r_c	radius of capillary
S	freeze pipe spacing
s, S	settlement
S_{max}	consolidation settlement
SP	segregation potential
SP*	redefined segregation potential
SP_0	the value of segregation potential obtained for zero applied pressure
S_r	degree of saturation
S_{rf}	degree of saturation of frozen soil
S_{ri}	degree of ice saturation of frozen soil
S_{ru}	degree of unfrozen water saturation
S_t	sensitivity, settlement at time t
t	time
T	temperature, estimated thickness of the frozen soil
T_0	initial temperature (before freezing, positive and constant)

Symbol	Represents
T_c	cold step temperature
T_f	the rate of cooling of the current frozen fringe, freezing temperature, temperature of the frozen zone of the soil
T_g	ground surface temperature [< T_{wf}]
T_i	freezing temperature of bulk water at the bottom of the fringe
T_{melt}	temperature of melting
T_n	the absolute value of temperature below 0 °C
T_s	segregation freezing temperature, surface temperature
T_u	temperature of the unfrozen zone of the soil
T_w	warm plate temperature
T_{wf}	freezing temperature, freezing temperature of pure water (i.e. 0 ºC)
u, u_b, u_w	pore water pressure
u_c	critical ground water velocity
u_i	pressure of ice
v	velocity, temperature difference
V	volume, volume of frozen sample
V_0	temperature gradient between the freeze pipe surface and the freezing point of water
V_{ff}	pore water velocity in the frozen fringe
V_g	volume of air
V_i	volume of ice [crystal]
v_o	water velocity, water intake flux
V_s	volume of solids, temperature gradient between the freeze pipe surface and the freezing point of water
V_{uw}, V_{wu}	volume unfrozen water
V_v	volume of voids
V_{vf}	volume of frozen voids
V_w	volume of water
w	soil water content
w_b	water content for frozen soil between ice layers
w_f	frozen soil water content
W_f	weight of frozen sample
w_i	ice content
w_j	water content after a virginal freeze-thaw cycle
w_l, w_L	liquid limit, water content due to ice inclusions
$w_{l,th}$, w_{lth}, $w_{L,th}$, w_{Lth}	thawed soil liquid limit
w_p	plastic limit
$w_{p,th}$, w_{pth}	thawed soil plastic limit
W_s	weight of solids
W_t	weight of sample
w_{th}	thawed soil water content
w_u	unfrozen water content
W_u	weight of thawed drained sample
w_v	water content due to pore ice
W_w	weight of water
x	depth below ground surface
X	coordinate, depth of frost penetration
$X(t)$	distance from the ground surface to the thaw plane at the time t

Symbol	Represents
Y	coordinate
χ	length of pile
Z	coordinate

Subscripts

Symbol	Represents
0	initial, water at 4 °C
air	air
d	dry
e	effective
f	frozen
ff	frozen fringe
g	gas, surface
i	ice
l	liquid
max	maximum
min	minimum
p	plasticity
r	relative, radial
s	solid phase, particle
sat	saturated
t	thawed, total
th	thawed
u	unfrozen
uw	unfrozen water
v	volume, vertical, voids
vf	frozen void …
w	water
z	vertical direction, depth
θ	absolute value of negative temperature

Acronyms, abbreviations and associations

Acronyms, abbreviations and associations	Represents
AASHTO	American Association of State Highway and Transportation Officials
AGF	Artificial ground freezing
ANOVA	Analyses of variance
Appl	Applied
ASCE	American Society of Civil Engineers
ASME	American Society of Mining Engineers. (American Society of Mechanical Engineers)
ATB väg 2004	General description for highway construction (published 2004 by Swedish National Road Administration)
Banverket	Swedish National Rail Administration
BGFS	British Ground Freezing Society

Acronyms, abbreviations and associations	Represents
Botniabanan AB	The company Botniabanan AB consist of the Swedish state, Kramfors, Örnsköldsvik, Nordmaling and Umeå rural districts. According to a principal agreement Botniabanan AB build the 190 km railway "Bothnia Line" between Ångermanälven and Umeå
Can	Canadian
CP	Code of Practice
CRREL	United States Army Cold Regions Research and Engineering Laboratory
EC	European Conference
FE(M)	Finite Element (Method)
Geot	Geotechnical
HB	Handbook
IAEG	International Association of Engineering Geologists
ICE	Institution of Civil Engineers
ICEC	International Cryogenic Engineering Conference
IC/IS	International Conference/Congress/Symposium
ICSMGE	International Conference on Soil Mechanics and Geotechnical Engineering
Inst	Institution/Institute
ISGF	International Symposium on Ground Freezing and Frost Action in Soils
ISSMFE	International Society for Soil Mechanics and Foundation Engineering
ISSMGE	International Society for Soil Mechanics and Geotechnical Engineering
J	Journal
JoB	Division of Soil and Rock mechanics at KTH (Avdelningen för Jord och Bergmekanik, in Swedish)
JOBFEM	Finite element program developed at KTH for geotechnical problems (Fredriksson, 1984) and is later on completed for various problems, e.g. temperature modelling
KTH	Royal Institute of Technology (Kungliga Tekniska Högskolan, in Swedish)
LN	Liquid Nitrogen
LNG/LPG	Liquefied Natural/Petroleum Gas
LTU	Luleå University of Technology (Luleå Tekniska Universitet, in Swedish)
Mem Vol	Memorial Volume
NATM	National Association of Testing Methods (USA)
NGI	Norwegian Geotechnical Institute
NSGF	National Symposium on Ground Freezing (recorded meetings of the BGFS)
Proc	Proceedings/transactions
RETC	Rapid Excavation and Tunneling Congress (USA)
Rpt	Report
SBUF	The Development Fund of the Swedish Construction Industry (Svenska Byggbranschens Utvecklingsfond, in Swedish)
SGF	Swedish Geotechnical Society (Svenska Geotekniska Föreningen, in Swedish)
SGI	Swedish Geotechnical Institute (Statens Geotekniska Institut, in Swedish)
SGU	Geological Survey of Sweden (Sveriges Geologiska Undersökning, in Swedish)
Soc	Society
SM & FE	Soil Mechanics and Foundation Engineering
Statens Vegvesen	Norwegian National Road Administration
Tech	Technical/Technology
Temp	Temperature/Temporary
TM	Technical memorandum
Transl	Translation

Acronyms, abbreviations and associations	Represents
(U)	Unpublished
USAAF	United States Army Air Forces
USACE	United States Army Corps of Engineers
Vägverket	Swedish National Road Administration

DESCRIPTION

Certain specialized terms used in current literature on frost and permafrost and in arctic and subarctic construction manuals, are also frequently used in this thesis. These terms and some other terms are clarified below.

Term	Description
Active layer (soil layer)	The annual frost zone in permafrost areas (USACE, 2006).
Annual frost zone	The top layer of the ground and the area subjected to annual freezing and thawing. In Arctic and Subarctic regions where the annual freezing penetrates to the permafrost table, the active layer (McFadden & Bennet, 1991).
Arctic region	The region in the north where the mean temperature for the warmest month is less than 10 °C and the mean annual temperature is below 0 °C (Freitag & McFadden, 1997).
Closed system	A condition when no source of free water is available during the freezing process other than that contained originally in the soil voids (Tsytovich, 1975).
Creep	Extremely slow continuing strain of soil material under stress.
Eutectic temperature	(From the Greek. eu't ktos 'easily fusible') the lowest temperature at which the equilibrium between the solid state and the fluid phase can exist. The eutectic temperature of H_2O-NaCl system is -21 °C (at about 23.3 % NaCl), i.e. the common salt will melt ice above this temperature. The eutectic temperature for H_2O-$CaCl_2$ system is -51 °C (Nationalencyklopedin [NE], 2005; Andersland & Ladanyi, 2004).
Excess ice	Ice in excess due to fractions that will be retained as water in the soil voids upon thawing. The establishing of excess ice in freezing soils normally constitutes from the excess water from the unfrozen soil (Andersland & Ladanyi, 2004).
Frost action	A universal term for freezing and thawing of soil moisture. It also covers the effect from the freeze and thaw process on these materials and on structures of which they are a part of (USAAF, 1987).
Frost heave	The raising of a soil layer because of ice formations in the underlying soil (Jumikis, 1966).

Term	Description
Frost susceptible soil	Soil that will encounter significant ice segregation when the essential moisture and freezing conditions are present (Beskow, 1935).
Ice segregation	The growth of ice in soil when in excess of the amount that would be produced by in place conversion of the original void moisture to ice. Ice segregation mostly appears as distinct lenses, layers and veins, often oriented normal to the freezing direction (Andersland & Ladanyi, 2004).
Liquid state of soil	Thawed soil with low or no effective stress.
Non frost susceptible soil	Cohesionless soil such as sand, gravel, etcetera, in which there is no significant ice segregation during normal freezing conditions (Beskow, 1935).
Open system	The condition where free water in excess of that contained originally in the soil voids is available to be encouraged to the surface of freezing to form segregated ice in frost-susceptible soil. This condition is due to the temperature gradient between the frozen part and the unfrozen part (Tsytovich, 1975).
Permafrost	Perennially frozen ground. It may be clarified more specifically as the thermal condition in the ground where temperatures below 0 °C persist over at least two successive winters and the intervening summer (USAAF, 1987).
Rheology	The study of the deformation and flow properties of materials.
Seasonal frost areas	The areas of the ground where there is significant freezing during the winter, but without development of permafrost (Freitag & McFadden, 1997).
Subarctic region	The regions adjacent to the "Arctic", where the mean temperature for the coldest month is below 0 °C, the mean temperature for the warmest month is above 10 °C, and where less than four months have a mean temperature above 10 °C. In general, subarctic land areas coincide with the circumpolar belt of dominant coniferous forest (Freitag & McFadden, 1997).
Thaw consolidation	The expression "thaw consolidation" embraces the study of the relative influence of the rate of thaw and the simultaneous process of water squeezing out of soil by self-weight of the soil or by applied load (Andersland & Ladanyi, 2004).
Thaw settlement	The term "thaw settlement" implies the volumetric changes due to water phase conversion and the subsequent consolidation of the soil as imposed stresses are transferred to the soil skeleton (Andersland & Ladanyi, 2004).

1 INTRODUCTION

1.1 BACKGROUND

Artificial freezing of soil and rock (AGF) in conjunction with tunnelling is developing in Sweden, among other countries (Johansson, 2005). The method is employed widely internationally and is mainly used for temporary stabilisation and sealing of soil and rock. Harris (1995) presents approximately 400 case studies written in a brief context. However, the cases are performed all over the world between the middle of the 19th century and the end of 20th century.

Artificial ground freezing as a method to temporarily stabilize and create hydraulic sealing in urban as well as in rural areas has been used in a number of Swedish construction projects, particularly during the last decade. The Bothnia Line (Stranneberget), and the South Link Road Construction in Stockholm (SL01 and SL04) and also Älvsjö storm water tunnel, are examples of recent tunnel projects accomplished through artificial freezing of soil and rock in Sweden. However, at the end of 2003, the contractor finished the ground freezing project for one contract area of the Bothnia railway line, namely, Stranneberget. At present, the contractor Skanska-Vinci stabilizes the faulty zone, Möllebackzonen of the Hallandsås project in southern Sweden (Stille, Sturk & Pilebro, 2007).

The earliest reported example of AGF in Sweden, is an AGF pedestrian subway in the middle of Stockholm (later referred to as Tunnelgatan). This was a successful pioneering effort, addressing a specific problem, which threatened the entire tunnel project in 1884. On the western flank of glacial clayey till, the overlying bedrock became progressively less stable. The use of AGF stabilized the ground and preserved the tunnel project, a decision made by the owner of the tunnel concession, Captain Lindmark (Cauer, 1885).

In many projects where it is desired to temporary stabilize and hydraulically seal soil and rock, chemical-or mineral-based grouting agents are used. Once the temporary construction has served its purpose, chemical-and mineral-based grouting substances are still remaining in the ground. During, for example, the stabilization and sealing of the 12 m long Hurum zone in the Oslo fjord, between 700 and 800 tons of cement grout were pumped into the zone without reaching adequate stabilization and sealing (Berggren, 1999, 2000; Eiksund, Berggren, & Svanø, 2001). Whereas, AGF was subsequently chosen as the method of stabilization and sealing, see chapter 2.

Temporary sealing and stabilization of soil and rock through freezing is, if used in the correct way, environmentally friendly and has many comparative advantages in relation to equivalent conventional methods. The temporary construction consists of frozen water, e.g. the ice creates a bonding agent between soil and rock particles that holds these together. When the temporary construction has served its purpose, the ground is thawed naturally or artificially and the natural groundwater can once again flow free.

In contrast to the Lindmark tunnel in the centre of Stockholm, the settlement in a number of Swedish artificial ground freezing projects dealing with fine grain soils has been reported undesirably and surprisingly large. In the majority of the reported cases, the surcharge has been inconsiderable or none existent. In the centre of Stockholm, a temporary stabilization and hydraulic sealing of a tunnel with AGF resulted, 2003, in a total thaw settlement of 0.70 m of the ground surface. Likewise, the settlement of an intersected 1.2 m in diameter shallow concrete sewer amounted to approximately 0.40 m. A pile footing, resting on point-bearing piles supports the sewer. Rescue operations of the sewer, like installations of soil piles, failed, see Figure 1.1. In the ground, "frozen windows" still remained and deluded the construction company (Bjerin, 2005).

Figure 1.1 Artificial ground freezing as an aid in tunnelling in the central of Stockholm, origin a thaw settlement of a 1.2 m in diameter shallow concrete sewer above the stabilized tunnel. Rescue operations of the settled sewer failed (on the left-hand side) and a brand new bypass sewer was built (on the right)

When freezing, particularly fine-grained soil, a zone, referred to as "the frozen fringe", is formed between the frozen and the unfrozen soils where both unfrozen water and ice crystals exist in chaos. In the frozen fringe, a hydraulic pressure gradient arises, with pore water suction close to the frozen soil. The pore water suction forms a source to a pore water flow against the frozen soil, where the water freezes and thus is able to form ice

lenses. However, enriching of the soil water is a self-defeating process and together with the released part of the original pore water, a reasonable amount of settlement can be expected.

When the frozen soil thaws, two opposite processes exist in the soil. There is consolidation, a reduction of porosity in connection with the pressure dispersion of the thawed water, and there is swelling of the clays. This condition is maintained at low pressures e.g. in soil near ground surface, and has the consequential effect that the soil void ratio increases. Thus, the effect is capable of resulting in a slight increase in the void ratio, particularly in soil close to the surface, and in a reduction in void ratio in the soil at deeper levels. If the soil after freezing and subsequent thawing has an increased void ratio, it means that the coefficient of consolidation of the thawed soil will be greater for the soil before freezing and vice versa (Tsytovich, 1975).

One problem with the freezing of soil and rock is that fine-grained clayey types of soils have showed a tendency to under certain circumstances, during the thawing process, create a pore water overpressure and to consolidate, despite a change in the external loading conditions. In certain cases, this condition can be a desired effect as the soil mass after a freeze- and thaw cycle acquires overconsolidated properties. Nevertheless, these side effects can create problems in urban areas with interruptions in the surroundings and undesired costs if, for example, a slide takes place in a slope or if the ground area is subjected to significant continuous settlements. Such an example is the stabilization and the hydraulic sealing with retaining structure at the area of Tegelbacken during the building of the underground railway from Central station to Slussen station in the centre of Stockholm, 1952 (Berglund, Österberg, Schütz & Heland, 1957). After the soil had thawed, large problems with consolidation settlements arose due to the freezing.

During the freezing, mineral particles and water are restructured, and in some cases, segregated ice with ice lenses is created. Fractures in the frozen soil can also arise at the frost front during the freezing process. These phenomena can lead to the thawing deformations. A number of different equations describe the size of the thawing deformations. The equations, however, are in general based upon site-specific soil properties and are usually adapted to permafrozen soils.

One finds extensive information concerning the permafrozen, cyclic, natural ground freeze- and thaw process in soil in shallow conditions in today's collected research concerning freezing of soil, see Knutsson (1982, 1983), Rydén (1985A, 1986), Kujala and Laurinen (1989), Kujala (1997) and Viklander (1997, 1998). Artificial freezing of deeper strata of soil and rock is, however, found under significantly different conditions. The differences are, above all, rapidity of the freezing, direction of the dispersion, states of stresses, soil-layer succession, that the deeper strata of soil have not been frozen cyclic and the fact that AGF normally affects soil that has never been frozen.

The field studies and the laboratory tests in this research study have been performed with soil from the freezing of the Bothnia Line in the vicinity of Stranneberget. The Bothnia Line is the railway link between Nyland, north of Kramfors, and Umeå. On one section of the railroad, the soil has been stabilized and hydraulically sealed through freezing, see Figure 1.2. The cooling down of the ground started in the spring of 2002 and was brought to a close in the autumn of 2003. The section that was frozen had poor rock coverage and measured nearly 100 metres. The existing instrumentation from this period has been completed and extensive examinations have been carried out at this site.

Figure 1.2 *Artificial ground freezing at one part of the Bothnia Line. In front of the mountain, Stranneberget, on the left-hand side, the brine supply systems for the installed freeze pipes in the ground. On the right-hand side, the cooling device, i.e. the storeroom of the cooling machinery*

This research project is important for the Swedish building construction industry in regards to both the extensive influence on the surroundings that frozen constructions initiate, particularly in urban areas, and to the new policy that EU advocates regarding constructions under ground. Likewise, the research project is also important for clients of great infrastructure projects e.g. frozen constructions such as the National Road Administration (Vägverket) and the National Rail Administration (Banverket). This project has been carried out in collaboration with the most influential clients of infrastructure such as the National Road Administration and the Botniabanan AB. In the same fashion, builders and contractors such as Skanska, NCC and Lemminkäinen have collaborated throughout the project and have contributed with valuable background material.

1.2 OBJECTIVES

The main objectives of this study are

- to describe and review the knowledge and current state of practice of artificial ground freezing
- to increase the understanding about the conceptual behaviour for prognosis of the vertical deformation concerning artificial ground freezing
- to compare and discuss results from laboratory and field studies concerning vertical deformation during thawing process for Bothnia soil.

1.3 SCOPE AND STRUCTURE

This thesis is written as a monograph and consists of eight chapters, which are briefly described in this section.

Chapter 1 is an introduction, which briefly describes the background of the work on thaw settlement, the objectives aimed in the framework of this research as well as the content of the present thesis.

Chapter 2 consists of a literature study containing a brief review of the; engineering of artificial ground freezing, field of application, refrigeration systems, soil energy transfer, soil water and soil ice, the differences and similarities between naturally frozen soil and artificially frozen soil, soil phase relations and case studies. However, chapter two also contains a thorough description of soil behaviour due to freezing and thawing.

Chapter 3 presents a case, the ground freezing project at the Bothnia Line, a railway to be built on the east coast in the middle of Sweden. The ground freezing projected is located near the mountain Stranneberget. The railway was constructed at a depth of approximately 20 m in sulphide rich clayey soil. Artificial ground freezing was estimated to be the most cost efficient method to be used due to environmental circumstances. The freezing started in the spring of 2002 and was terminated in the autumn of 2003.

Chapter 4 deals with freeze-thaw laboratory tests. Mainly undisturbed soil from the ground near the area to be frozen at the Bothnia Line is examined and described in the state of undisturbed as well as frozen and then thawed soil. Furthermore, the freeze-thaw tests with standard oedometers describe the soil behaviour. The differences between the undisturbed soil and the freeze-thawed soil properties, as well as the deformations due to the freeze-thaw tests, constitute a base for an estimation of the prognosticated deformation in the field at the Bothnia Line.

Chapter 5 deals with field tests at the artificial ground freezing project at Bothnia Line and depicts the thawing process and the expected thaw settlement. Furthermore, the installation of instruments and measurement readings as well as notable occurrences due to the case nature are described.

Chapter 6 depicts the analyses of foregoing chapters, i.e. the literature study, the field study as well as the laboratory study.

Chapter 7 consists of the general conclusions from the entire work.

Chapter 8 summarizes the recommendations for proposed future research associated with deformations during freezing and thawing due to artificial ground freezing.

1.4 EXTENT AND LIMITATIONS

This thesis relates to a part of the Bothnia Line. It deals with the behaviour of soil during thawing by means of temporary stabilization and hydraulic sealing of fine-grained soil through artificial freezing using brine as the cooling agent. However, the reason behind the problem consists of the final deformations due to the thawing process.

The extent of the literature review covers behaviours of artificial ground freezing and a brief description of naturally frozen ground is also included because a lot of research results from naturally frozen ground are taken and used in the artificially frozen ground design as well as in different calculations of artificial ground freezing. The description of naturally frozen ground is limited to give a brief understanding of the similarities and the differences between artificially frozen ground and naturally frozen ground.

The field study, i.e. the measurements at the Bothnia Line were limited to the beginning of the winter of 2004, approximately six months after the ground freezing was brought to close. Consequently, the frost heave at the frozen construction is not considered. The compilation of the measurements was accomplished in the summer of 2008 when the thawing of the ground had not yet been brought to an end. Furthermore, comparable analyses of different ground freezing projects, i.e. ground freezing projects from other regions, have not been made.

The laboratory study has been performed on clayey soils collected at the area close to the section subjected to ground freezing at the Bothnia Line. Results exist for laboratory tests from samples collected just above the tunnel axis at the end of the area to be frozen, gathered by the consultant company VBB-VIAK in 1999. However, no freeze-thaw tests were made, just routine tests on undisturbed samples. The soil samples subjected to freeze-thaw tests were collected beside the frozen area from three to ten metres below ground surface, during the period when the frozen construction was still frozen. The freeze-thaw tests were limited to one-dimensional tests in oedometers located in a climate chamber. Furthermore, the tests were performed under water supply and the oedometer equipment like the fixed ring container, the porous stone collar, the stamp, etcetera, were un-isolated. In addition, the tests were limited to one cooling temperature, near -10 °C.

2 LITERATURE STUDY

This chapter contains a literature review of important parameters used when describing soil behaviour related to thaw settlement as well as a brief presentation of the most common freeze technique. The chapter also gives further details about classifications with references to the behaviour of the soil in connection with settlement.

2.1 INTRODUCTION

When the free water in the soil freezes, it expands with approximately 9 %. Depending on the soil's water content, the soil will obtain a lower bulk density compared to the bulk density it had before the freezing. Due to the freezing, the soils initiate a frozen state where the horizontal and vertical directional expansion establishes a pressure and a frost heave (Beskow, 1935; Knutsson, 1982, 1983, 1984; Black & Hardenberg, 1991).

Later on, when the soil thaws, water will migrate and the soil will so consolidate. In conjunction with an artificially frozen construction for the stabilization of soil and rock during tunnelling, the construction changes from having been "supportive" to becoming a load on, above all, the tunnel roof. Not many extensive and comprehensive published articles exist discussing case studies and theoretical discourses regarding the load-construction of the tunnel roof when thawing. Uncertainties thus exist for how the frozen soil becomes a load on the permanent tunnel construction, that is to say if the frozen soil come off in larger portions and gradually adds to the load, or if the frozen soil slowly goes from a frozen state to a thawed with a proportional increase in the load (Johansson, 2005).

When frozen fine-grained soil thaws, the frozen unbounded water turns to liquid form and creates in conjunction with the process of the thawing a viscous mass consisting of soil and water. The initial elevation of the pore pressure will remain, depending on, among other things, the hydraulic conductivity and the capacity of the draining in the surrounding soil. During the phase of the elevation of the poor water there is in an opposite way a decrease in the effective stress and thus a lower bearing-capacity of the soil compared to if the soil had not been subjected to freezing (Knutsson, 1983; Rydén, 1985A).

It should be expected that the ground would heave during the freezing phase of the development of a stabilized and hydraulically sealed construction. During the following thawing phase, a settlement can be expected to reversely occur (Tsytovich, 1957, 1975).

There are several similarities between naturally frozen and artificially frozen soil. However, there are also many differences. By having knowledge of these differences, information from permafrost investigations and sciences can be used when designing artificially frozen constructions (Ladanyi & Sayles, 1978; Freitag & McFadden, 1997).

The freezing technique has obtained increased interest during the last years because of the raised requirements concerning the environment. Examples of areas of adaptation where the freezing technique of soil- and rock stabilization and sealing has been used or intended to be used are temporary creation of (Johansson, 2005)

- hydraulically sealed barrier and stable arch for tunnelling and rock cavern building
- stabilizing of soil- and rock slopes
- cofferdam to stabilize and seal shafts
- cofferdam to prevent the spreading of polluted groundwater
- stabilizing of contaminated ground to take care of the frozen contaminated soil and groundwater, i.e. "freeze dredging"
- sealing to prevent groundwater leakage between sheet piling and rock
- sealing of barrier in rock cavern in connection with the storing of cooled liquefied gas
- freezing of fine grained soil with subsequent thaw consolidation achieving an overconsolidated soil.

2.2 ARTIFICIAL FROZEN GROUND

In conjunction with the thawing process of the soil, water will escape from the thawed soil. This water originates from parts of the formed ice lenses and the water previously bound with the original soil particles, which upon freezing and restructuring lost parts of its capability to bond soil particles. When thawing occurs at a "slow" rate in relation to the permeability of the surrounding soil, the generated water will flow from the soil at about the same rate as it was produced, controlled by the surrounding soil's permeability. The water that is being squeezed out is induced by the self-weight of the soil as well as the applied load. If the rate of water generation exceeds the capacity of the discharge, excess pore water pressure exists. When this excess pore water is high and constant during a "long time", it will affect the soil's bearing capacity. Excess pore water reduces the soil bearing capacity considerably; the pore water pressure controls the effective stress in the soil and thereby the bearing capacity (Knutsson, 1983, 1998).

There are many similarities between naturally frozen and artificially frozen soil, unfrozen water and ice lenses exist, for example, in both cases. Ice lenses are developed in the same way in both cases, i.e. parallel to the freeze front. The frequency and thickness of the ice lenses decrease with depth, i.e. a decrease because of increased stress. When naturally frozen and artificially frozen fine-grained soil thaws, thaw consolidation occurs (Ladanyi & Sayles, 1978).

In civil engineering, i.e. geotechnical engineering, the expression "thaw settlement" refers to the volumetric changes due to water phase conversion and the subsequent consolidation of the soil as imposed stresses are transferred to the soil skeleton. However, the term "thaw consolidation" embraces the study of the relative influence of the rate of thawing and the simultaneous process of water being squeezed out of soil by self-weight of the soil or by applied load (Ladanyi & Sayles, 1978).

Researchers show a number of models that describe the effect of certain deformations related to the thawing of clayey soil. However, only a few models of thaw settlements predict such settlements related to AGF. On the other hand, in permafrost rural areas, these models are valuable engineering tools (Johansson, 2005).

This thesis deals particularly with such models predicting the thaw settlement in AGF-projects. Artificial ground freezing as a method to raise a stable, waterproof zone can be performed and used in different situations. In Sweden, artificial ground freezing has been carried out in several projects. The following approximately ten projects are examples:

- Excavation of the tunnel through Brunkebergsåsen (Tunnelgatan) in the centre of Stockholm, 1884, with aid of a frozen stabilized arch. With concession of owner, captain Knut S Lindmark (Cauer, 1885).
- Excavation of the subway close to Tegelbacken in the centre of Stockholm, 1954, with a frozen stabilized and waterproof zone near the transition of the point of sheet pile and bedrock (Berglund et al, 1957).
- Foundation of the house, "PK-huset", in the block Hästen (Hamngatan, Norrlandsgatan) in the centre of Stockholm, 1970, with a frozen stabilized and waterproof zone near the transition of the point of sheet pile and the bedrock (Lundahl & Sjökvist, 1972; Lundahl, 2008).
- Excavation of a sewage culvert to the wastewater treatment plant, Ryaverken in Gothenburg, with a frozen stabilized and waterproof arch, in the middle of 1970s (Bengtsson & Lundberg, 1977).
- Excavation of a storm water tunnel, "Älvsjö bräddavloppstunnel", 1999, with a frozen stabilized arch (Stille et al, 2000).
- Excavation of two ramp tunnels at the Södra Länken-project (SL04) in Sickla in the south of Stockholm, 2000, with a stabilized and waterproof arch (Stille & Johansson, 2001).
- Excavation of a tunnel at the Södra Länken-project (SL01) nearby Järnlunden in Stockholm, 2000, with a stabilized arch (Bjerin, 2005).
- Excavation of the railway tunnel, part of the Bothnia Line project (E5415) nearby the mountain, Stranneberget during 2003-2004, with a stabilized and waterproof arch (Vaaranta, 2004; Saarelainen, Korkitala-Tanttu & Viitala, 2004).
- Excavation of a part of a tunnel at the project Hallandsåstunneln through the zone Möllebackzonen started 2005, with a stabilized and waterproof circular torus (Stille et al, 2007).

Creating a frozen construction is relatively uncomplicated. A requirement is, however, that one, depending on the risk level of the project, recognizes the qualities of the soil and rock. The method is relatively insensitive to the contents of material and tolerates gap graded soil, provided that the moisture content exceeds approximately 10 % (Harris, 1995). On the other hand, Shuster (1980) presuppose a minimum saturation level of 10 %. In drainage areas, however, artificial infiltration or a water dam up may increase the water content and consequently increase the soil saturation. Whereas, heat injection is an enemy of a frozen construction via e.g. flowing ground water, i.e. an enforced convection (Shuster, 1980).

Stabilized and waterproofed soil constructions by means of ground freezing have numerous qualified advantages in comparison to other methods, see Figure 2.1. The

ground freezing method is preferable from the standpoints of being (Harris, 1995; Andersland & Ladanyi, 2004)

- productivity friendly
- safe for the working environment
- cost-effective
- friendly for the environment and the human being.

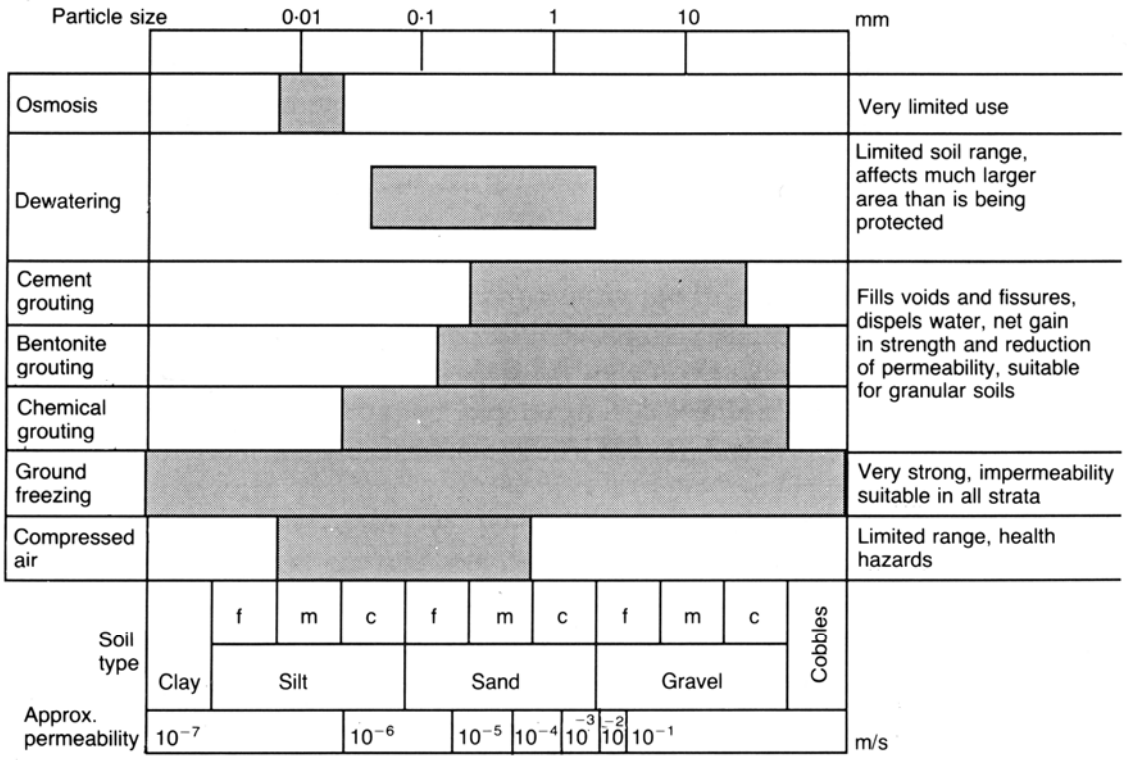

Figure 2.1 Soil stabilizing methods utility in different soils, after Harris (1995)

In contrast, in some situations, the ground freezing method has disadvantages for example that it is (Jumikis, 1966; Harris, 1995; Andersland & Ladanyi, 2004)

- energy intensive
- expensive, i.e. the initial high cost of mobilization for installation of cooling equipment and the freeze pipes etcetera
- expensive, since it is energy intensive to reduce the soil and pore water temperature, as well as the transforming of water to ice.

Disadvantages may also occur in some soil types; some examples are (Jumikis, 1966; Harris, 1995; Andersland & Ladanyi, 2004)

- thaw consolidation, this applies especially in fine grain soils
- excess pore pressure in conjunction with thawing, this applies especially in fine grain soils
- frost heave, this applies especially in fine grain soils, e.g. silty soils
- creep deformations, this applies in conjunction with loads
- drill hole precision, i.e. if the calculated maximised freeze pipe distance are exceeded
- heating of the frozen construction from ground water flow
- insufficient soil water content.

As the soil's strength increase when the temperature drops, the construction criteria to attain certain strength of frozen soil are normally based on the soil's expectancy to achieve a certain maximum temperature within a specific area. It is relatively easy to verify these construction criteria at the construction site as the development of the temperature in the soil is generally tracked with help of installed temperature sensors located at different depths and at different locations in plane (Jumikis, 1966; Harris, 1995; Andersland & Ladanyi, 2004). The temperature sensors are normally installed on, for example, a polyethylene hose that is then lowered down into a casing tube in the soil. Figure 2.2 shows the electric cables from the temperature sensors, installed at different depths in the steel casing tube.

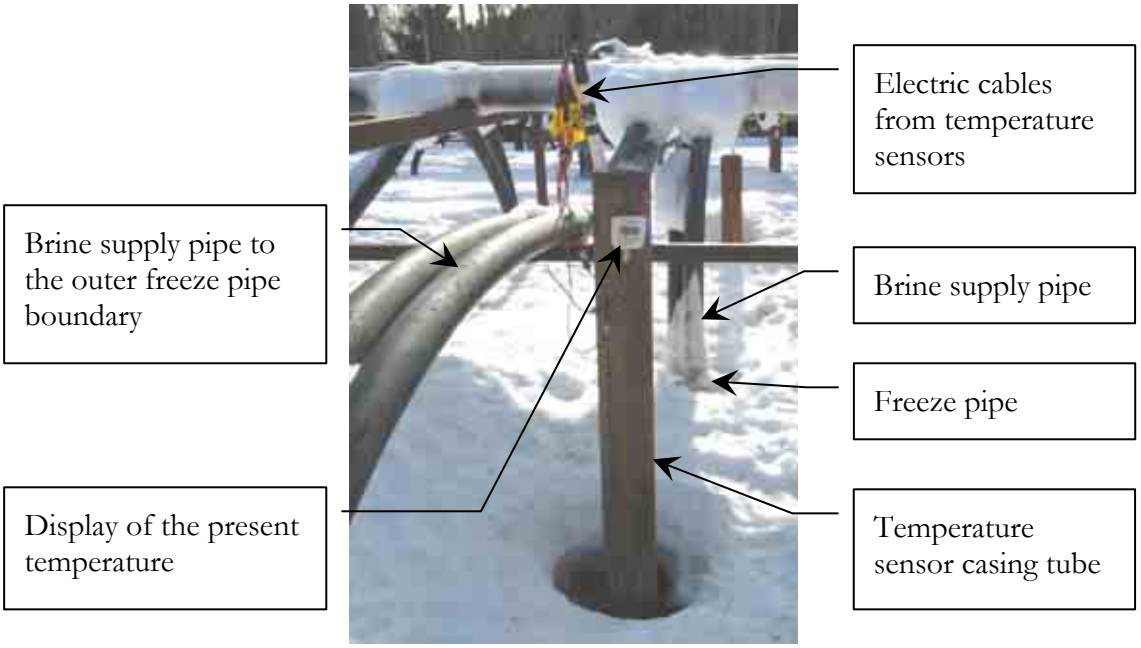

Figure 2.2 Temperature sensors installed at different depths in the ground are read manually or automatically via cables

2.2.1 In course of construction

In connection with "quite large constructions", one tries in general to dimension the frozen construction so that the stabilization capacity reach the construction criteria in about ninety days when brine freezing is used, and in about seven days when freezing with liquid nitrogen (Jumikis, 1966; Harris, 1995; Andersland & Ladanyi, 2004).

The artificially frozen construction in ground is created by installing freeze pipes (also called cooling-pipes) in the ground. To be able to freeze the ground to a certain temperature and so reach the desired strength and/or the desired waterproofing of the construction, one has to have knowledge of the material- and the geometric parameters so the time aspect and the necessary cooling effect can be judged. The agents of importance in regards to the freeze pipe design are (Jumikis, 1966; Shuster, 1980; Harris, 1995; Andersland & Ladanyi, 2004; Johansson, 2005)

- freeze pipe material
- freeze pipe effective cooling diameter, i.e. the cooling perimeter
- space of freeze pipes
- heat transfermedium temperature and velocity of flow.

Freeze pipes made out of steel are favourable as steel has better conductivity than, for example, most plastics on the market, i.e. "the plastic material" insulates the cold in the freeze pipe. A larger diameter is also favourable as the larger cold parameter cools the ground more efficiently. A shorter distance between the freeze-pipes is also preferable, as the frozen zone from respective freeze-pipe reaches other ones quicker when larger cooling effects per volume unite per definition is installed (Jessberger & Vyalov, 1978; Sanger & Sayles, 1978).

According to the freeze process of the ground, material- and geometric parameters for the thermal soil properties are (Jumikis, 1966; Sanger & Sayles, 1978; Shuster, 1980; Harris, 1995; Andersland & Ladanyi, 2004)

- volumetric water content
- thermal conductivity
- ground water flow
- freezing point (e.g. salinity of soil).

A low water content of the soil is favourable, partly because of that the amount of energy needed to the phase change of the water to ice is considerably lower and partly because the probability that the amount of unfrozen water bounded to the particles in the frozen soil is less (Shuster, 1980; Harris, 1995).

When the soil's particles have a high conductivity (thermal conductivity), the capacity to conduct heat is larger and less time is needed to, for example, cool down a volume of soil. High quartz content in the particles of the soil is especially favourable because the conductivity of quartz is three times larger than most other existing minerals in the soil particles (Sundberg, 1988).

Frozen constructions are sensitive to added heat in certain quantities. The flow of ground water through and close by a frozen construction can lead to unfrozen windows. The zone between two freeze pipes is especially sensitive at the time when the frozen soil is about to closure. If a gradient has risen on both sides of the pressure level of zero in the ground water (i.e. the ground water table) of the frozen construction, the groundwater can during certain circumstances, canalize to areas of the future frozen construction that are particularly rich in water and thus give rise to a flow of groundwater. Normally dimensioned frozen constructions usually manage to divert the added heat from a groundwater flow with a speed of about 2 m per 24 hours at freezing with brine and approximately 20 m per 24 hours during freezing with nitrogen (Sanger & Sayles, 1978).

Depending on how the frozen construction will work, if the structure is going to carry a load on a frozen arch in a tunnel with poor rock coverage (see Figure 2.3), or if it is going to act as a hydraulically sealed cofferdam construction in the ground, the freeze pipes will be placed accordingly (Figure 2.4). As cold brine circulates in the freeze pipes, a frozen zone is created successively around the freeze pipes. The frozen zones grow and with time it will close up around each freezing pipe and so form a homogenous frozen wall or roof (Jessberger & Vyalov, 1978; Sopko & Aluce, 2005), see Figure 2.4 and Figure 2.5. The spacing of the freeze pipes should not exceed about thirteen times their diameter unless analysis indicates that a larger relative spacing will be acceptable for particular application (Shuster, 1980). In the same fashion, Shuster (1980) depicts the criteria from the empirical data of projects with refrigeration pipes and presents the recommended freeze pipe diameter to be between 0.05 m and 0.15 m. Though, "theory indicates that the concepts and relationship should hold for larger diameter pipe, caution should be exercised in view of the lack of experience in this area. The relative spacing of the refrigeration pipe controls

the duration of the time necessary to complete satisfactory freezing more than any other controllable variable." (Shuster, 1980, p 866).

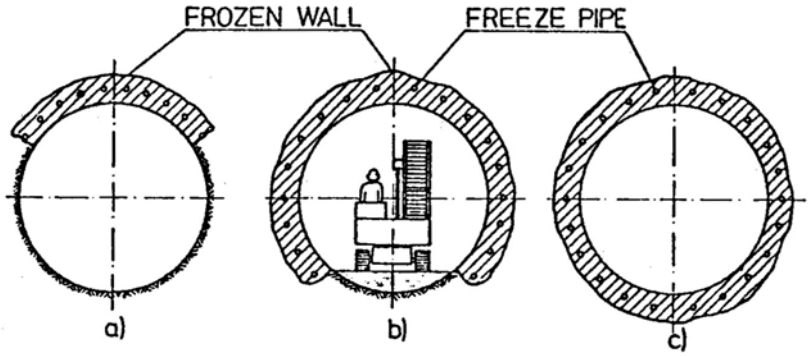

Figure 2.3 *Stabilizing of tunnels with AGF of different requirements, after Jessberger and Vyalov (1978)*

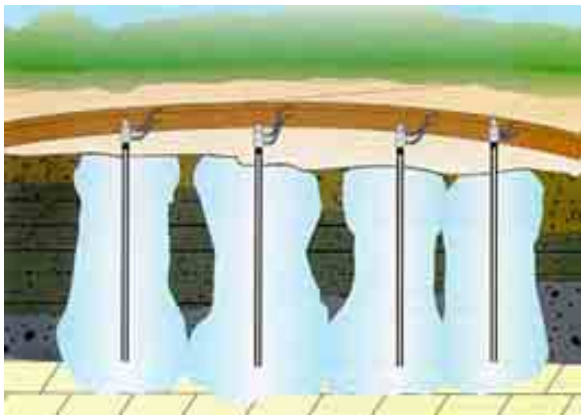

Figure 2.4 *Vertical cross-section, installed freeze pipes in the soil and rock. Depending on the thermal properties of the soil and rock, varied extension of the freezing in different materials takes place, modified after Sopko and Aluce (2005)*

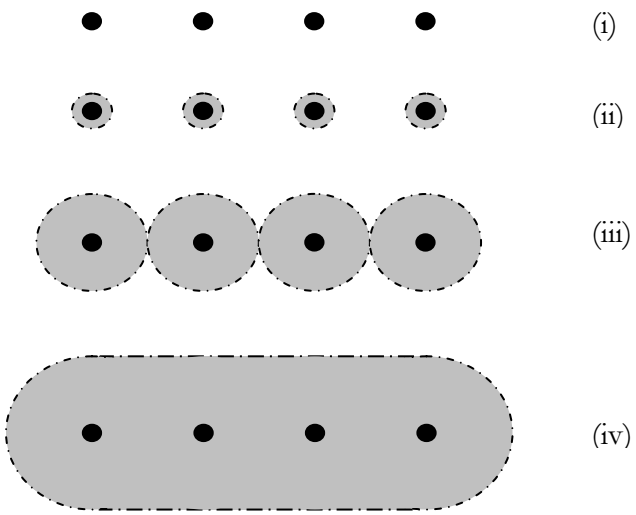

Figure 2.5 *Horizontal cross-section, installed freeze pipes in the soil and rock. Principal freezing extension step by step. From the top; i.) Installed freeze pipes, ii.) Freezing just started and a frozen zone is created increasingly, iii.) The frozen zones around the freeze pipes merge, iv.) The frozen zone have increased and created a frozen construction, i.e. a retaining wall and a cofferdam. Modified after Sopko and Aluce (2005)*

For frozen constructions that should only be hydraulically sealed, it is common that the frozen construction has grown according to (iii) in Figure 2.5, i.e. that the frozen zone keeps a temperature just under the freezing point of the ground water. However, in conjunction with that, frozen constructions should carry a load; the frozen zone is dimensioned so that a certain thickness of the zone holds the highest temperature as the frozen soils carrying capacity increases with a decreasing in temperature.

The frozen soil or the frozen rock will obtain a higher bearing capacity, i.e. more favourable properties than before freezing, whereas the frozen material takes on a viscous plastic behaviour. Thus, the magnitude and durability of the load therefore affect the deformation behaviour of the frozen mass. The colder the material is, the higher the bearing capacity becomes while the velocity of the deformations becomes lower. The behaviour depends on the "nature" of the ice and the amount of unfrozen water. On the other hand, an unfrozen mass that carries a load will creep and consolidate (Jessberger & Vyalov, 1978; Harris, 1995; Andersland & Ladanyi, 2004).

2.2.2 Cooling systems

Artificial soil- and rock freezing to stabilize and seal soil and rock can be accomplished with help of different types of cooling systems and in different ways. The cooling system can be adapted to the relevant situation depending on the local conditions. However, the cooling systems can be divided up into two main types (Knutsson, 1984C)

- indirect freezing
- direct freezing.

These systems are described below. Both systems require the heat in the ground to be removed, a process which is in both cases commonly performed by means of cooling pipes installed in the ground (Knutsson, 1984C). There are, however, exceptions, one of them being when storing ammoniac and petroleum based gases (propane etcetera), gases that are stored in liquid phase, either under high pressure or at temperatures below the vaporization point of the gas. The generic term for these gases is liquefied petroleum gases (LPG) (Aoki, Hibiya &Yoshida, 1990).

Indirect freezing

The indirect method uses either freeze pipes installed in the ground where the cold-carrier gets its energy supply via the mantle of the freeze pipe through heat conductivity, or an air-heater changer that blows chilled air towards a surface and in this way lowers the temperature of the ground, wall or roof (Cauer, 1885; Johansson, 2005).

Two closed and one open system is usually connected to a compressor unit as the central entity during indirect freezing. The two closed systems consist of the compressor-circuit and the cooling-circuit and the freeze pipes installed in the soil or/and rock. The open circuit system cools the compressor circuit's "warm" condenser, through a heat exchanger containing regular water, in smaller plants with air. The closed system with the cold transmitter, normally calcium chloride, gets its energy supply off the ground, as the cold transmitter (relatively seen) is colder than the ground. The energy is transmitted through the heat exchanger of the compressor circuit, the vaporizer. The larger motor effect, the larger cooling capacity, see Figure 2.6 (Jessberger & Vyalov, 1978; Harris, 1995).

The cooling machine is, casually speaking, called a "heat pump". The term "cooling machine" or "heat pump" varies depending on if one primarily takes care of the heat or the cold from the machine. The function is a circuit process and can be explained in the way that one uses the phase converted heat from the cold media hence the gas is converted to liquid form, see Figure 2.7. During the compression, the gas goes through a process, which

increases its energy content. The temperature and the pressure of the gas are raised. The compression is principally adiabatic. After the compression, the gas reaches the condenser. Parts of the hot gas condense in the condenser (with a pressure of 8-12 bars with ammonia) and thus give off phase converted heat to the cooling machine (Jumikis, 1966).

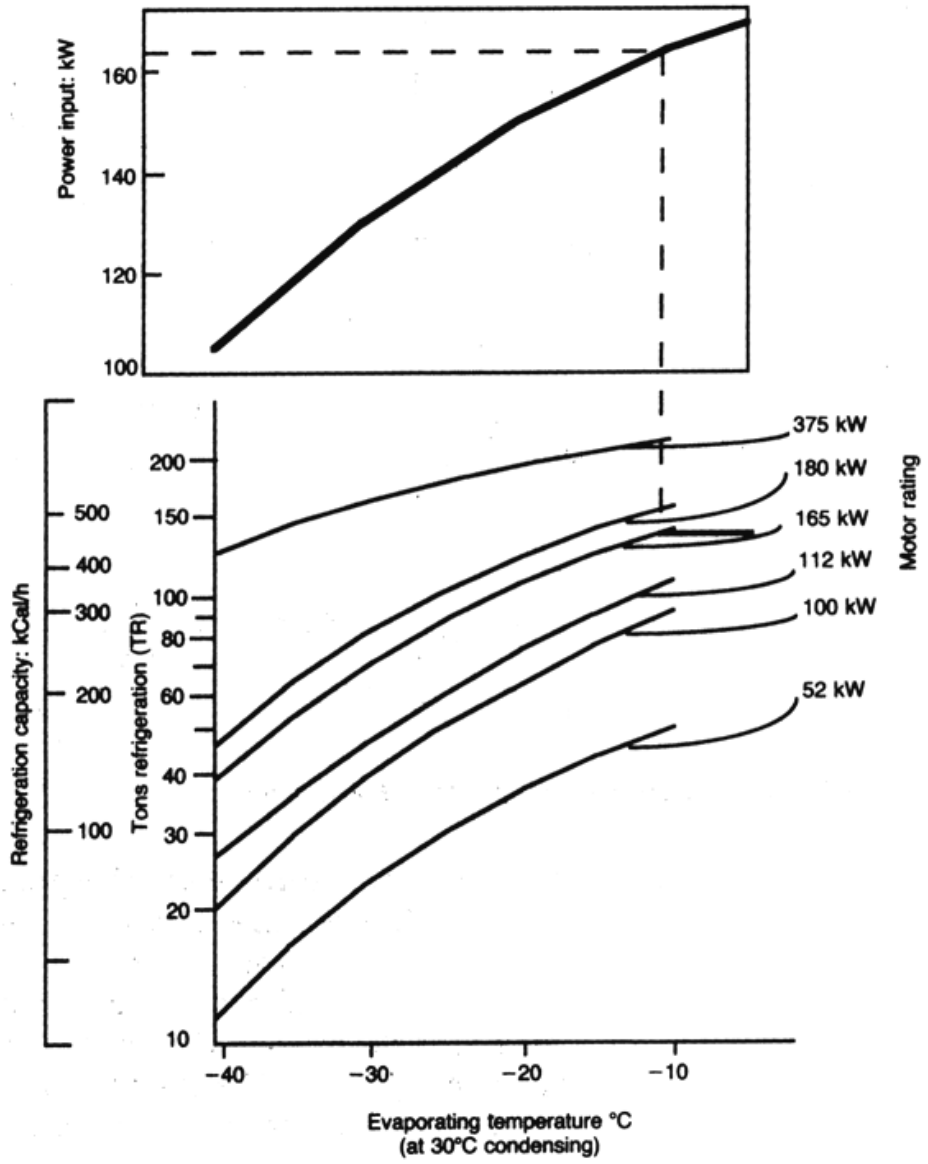

Figure 2.6 Magnitude determination of cooling machinery. The cooling machine capacity as a function of the evaporating temperature, at the condensing temperature 30 °C, after Harris (1995)

The cooling machine, whose primary aim is to produce cold, generally diverts the produced heat to the outdoor air via air coolers or cooling towers. A typical refrigerant in modern cooling machines is ammonia, which is an environmentally friendly product it regards to the nature but can be toxic for humans and mammals if existing at too high levels in the air (NE, 2005). Another refrigerant used, although less common in compressor cooling machines, is carbon dioxide. When the carbon dioxide is used in compressor cooling machines, this process typically takes place through direct vaporization in the cooling pipe, i.e. the refrigerant also acts as a cooling agent and vaporizes in the cooling pipe under high pressure instead of in a separate vaporizer that via heat exchange transmits heat from a brine system. However, circulation of carbon dioxide under high pressure in the cooling

pipe system therefore puts high demands on the tightness of the whole pipe system, including the freeze pipes (Johansson, 2005).

To obtain a frozen zone in the ground, usually an installation of a freeze pipes is required see Figure 2.7. The freeze pipe is normally supplied with an inflow stream of cold brine in the bottom of the pipes. Brine circulates with help of a circulation pump in the system with a varying temperature of -20 °C to -40 °C. The temperature varies depending on the cooling capacity of the cooling machine and on the amount of soil that has warmed up the heat transfermedium (Jumikis, 1966).

Brine consists of water and an additive that lowers the freezing point, typically calcium chloride ($CaCl_2$). Cold brine is heated by the mantle of the freeze pipe and is diverted to the top of the freeze pipe and then recycles back to the common return line. The diameter of the freeze pipe varies between 0.10 m and 0.25 m. The velocity of the brine ranges usually between 0.5 m and 0.7 m per second in the distributer pipe and the climbing rate in the freeze pipe is usually between 0.03 m and 0.05 m per second (Jumikis, 1966).

The freeze pipes can be connected in series into smaller groups of two to six freeze pipes and the groups can then be connected in parallel to the distribution pipe of the system. Another alternative is that each freeze pipe is connected in parallel to the distribution pipe, inflow- and return pipe (Jumikis, 1966).

The dimensioning of a frozen construction depends on, in addition to the thermal properties of the soil, also the cooling machines' capacity to deliver a flow of cold brine, the diameter of the freeze pipes, material and the freeze pipe spacing, see Figure 2.8.

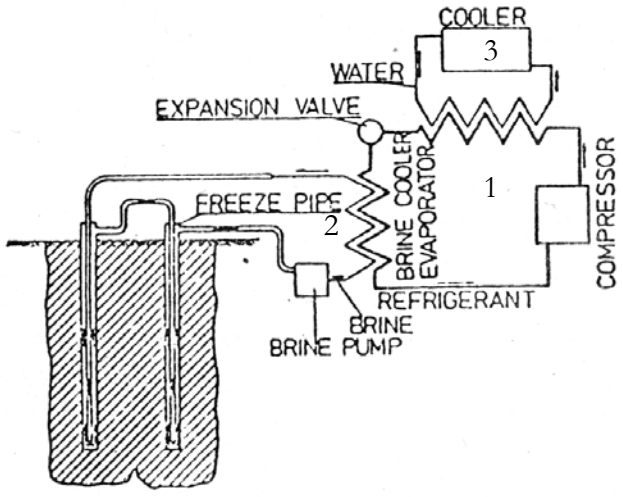

Figure 2.7 Indirect freezing through "brine freezing", schematic illustration: 1.) The compressor circuit, consisting of compressor, condenser and evaporator chamber. 2.) Brine cooling circuit consisting of evaporator chamber, brine pump unit and freeze pipes. 3.) Cooling circuit consisting of condenser chamber, cooler and cooling pump. The heat exchange takes place in the condenser and in the evaporator chamber. Modified after Jessberger (1980)

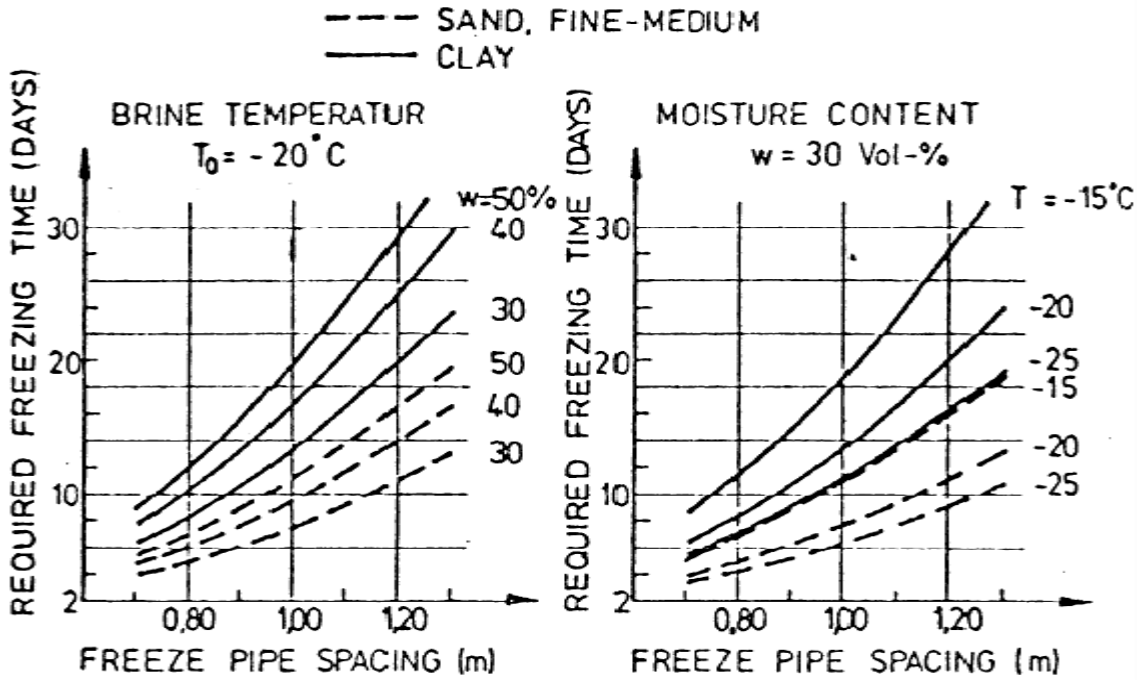

Figure 2.8 Artificial ground freezing with brine, required freezing time as a function of the freeze pipe spacing, after Jessberger and Vyalov (1978)

Direct freezing

The chilling of the ground with the direct method i.e. cooling by direct expansion, normally takes place with use of expanded liquid such as nitrogen (LN_2), solid carbon dioxide (CO_2), or liquid carbon dioxide (LCO_2) (Knutsson, 1984C).

The atmosphere consists of about 78 percentages by volume (or 75.5 percentage by weight) of nitrogen, typically in form of nitrogen gas (N_2). In the atmospheric pressure, nitrogen has a vaporization temperature of -196 °C. The production of nitrogen gas occurs most commonly through distillation of liquid air (NE, 2005). When using liquid nitrogen for soil- and rock freezing, the nitrogen is delivered in liquid form to the construction site in a heat insulated pressure tank. The nitrogen can, depending on the duration of the freezing, the location etcetera, be stored in a temporary working tank, or be distributed directly from the delivery tank of the truck, see Figure 2.10 (Veranneman & Rebhan, 1978; Stoss & Valk, 1979).

Nitrogen can normally by means of the pressure difference between the reservoir (5-15 bar) and the atmosphere directly to the cooling system via a distribution system, see Figure 2.9. When enriched with energy in the distribution system and in the cooling system, liquid nitrogen vaporizes simultaneously as it expands in volume approximately 600 times. The atmosphere consists of approximately 0.037 percentages by volume of carbon dioxide; the content increases with approximately 0.4 % annually because of human activity (NE, 2005). Solid carbon dioxide, (also so-called carbon dioxide snow or dry ice) has a boiling point, sublimation point, of -79 °C at atmospheric pressure, i.e. CO_2 phase changes directly into gas without creating liquid. The dry ice has a density of 1.56 ton m^{-3} (at 0 °C) and 1 kg creates 530 dm^3 of carbon dioxide in gas form (Handbook of Chemistry & Physics [HB of Chem & Phys], 2004; NE, 2005).

Liquid carbon dioxide is a "manufacture alternative" of solid carbon dioxide. Carbon dioxide is obtained, for example, as a bi-product when creating hydrogen for ammonia synthesis and through condensation of exhaust gases. When liquid carbon dioxide is used

as the cooling agent, this (process) usually occurs in connection with cooling via the compression plant where the carbon dioxide is used as a refrigerant and through direct vaporization as a cold transmitter, see above (Johansson, 2005; NE, 2005).

The media; liquid hydrogen is most common in direct ground freezing and however, uses essentially the same solution when it comes to the freeze pipe as the one being used when freezing with brine. The difference is above all that the material in pipe is adapted for the cold liquid (-196 °C), and also that the diameter of the pipe on freeze pipe is smaller, this because of that the cooling effect is significantly higher (Jessberger, 1980).

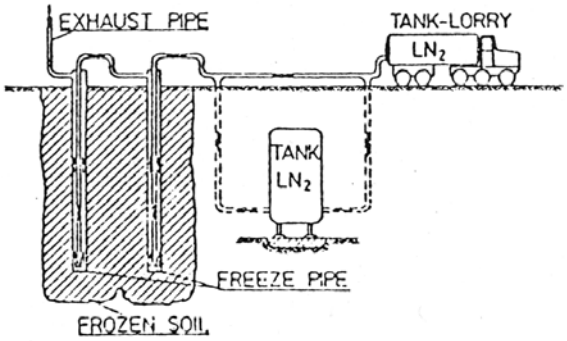

Figure 2.9 Direct freezing through "cooling by direct expansion", schematic illustration. Liquid nitrogen (LN_2) delivered in an insulated pressure tank (approximately 5-15 bar) to the area where the freezing will take place. The LN_2 is distributed in a tube system, evaporates in the freeze pipes and departs through the exhaust pipes into the atmosphere. After Jessberger (1980)

Figure 2.10 Cooling by direct expansion at the project Älvsjö storm water tunnel. The picture on the left-hand side shows the interim storage tank for liquid nitrogen. The picture on the right-hand side shows the freeze pipes organized at the tunnel arch. Photo Lasse Wilsson, Skanska

When freezing ground, the liquid nitrogen is released from the intermediate storage tank or directly from the tank lorry into the distribution system. A number of freeze pipes are typically connected in series to be able to use the temperature gradient in the nitrogen. The in series connected freeze pipes are in turn connected in parallel to the distribution system (Stille et al, 2000).

As soon as the liquid nitrogen is exposed to the relatively warm pipe surface, the liquid nitrogen vaporizes and is released into the atmosphere via an exhaust smokestack. At the vaporization of the LN_2, 199 kJ kg^{-1} (heat of vaporisation) "is taken" from the surroundings, and approximately 1 kJ kg^{-1} °C^{-1} heats the nitrogen (LN_2 thermal heat capacity) to the estimated exhaust temperature. Normally the nitrogen exhaust temperature determines the flow of the nitrogen in the system. However, several tests have shown that a temperature between -70 °C and -120 °C is economically favourable for the nitrogen exhaust gas (Veranneman & Rebhan, 1978).

The large temperature gradient allows a very quick freezing; it is generally dimensioned to achieve a hydraulically sealed barrier in approximately three days and a stable soil- and rock mass in about one week. The time span for freezing a soil- and rock volume depends on, among other things, the diameter of the cooling pipes and their spacing. Shuster (1972) has expressed the required time for the cooling as a function of the diameter of the cooling pipes and their spacing, see Figure 2.11.

The nitrogen consumption depends on many factors; a number of these are discussed later in this chapter. Veranneman and Rebhan (1978) specify the nitrogen consumption to approximately 800 kg LN_2 per cubic metre of soil. The size of consumption is based on 55 different artificial ground freezing projects with "normal" conditions, i.e. ground conditions with low water content and no groundwater flow. Nevertheless, a significant degree of uncertainty exist in regards to the consumption and empiricism shows a variation between 600 kg LN_2 m^{-3} of soil and 1 900 kg LN_2 m^{-3} of soil. However, the consumption to reach the frozen zone equals the consumption that is in turn needed to maintain the frozen zone during two to three weeks (Veranneman & Rebhan, 1978), see Figure 2.12.

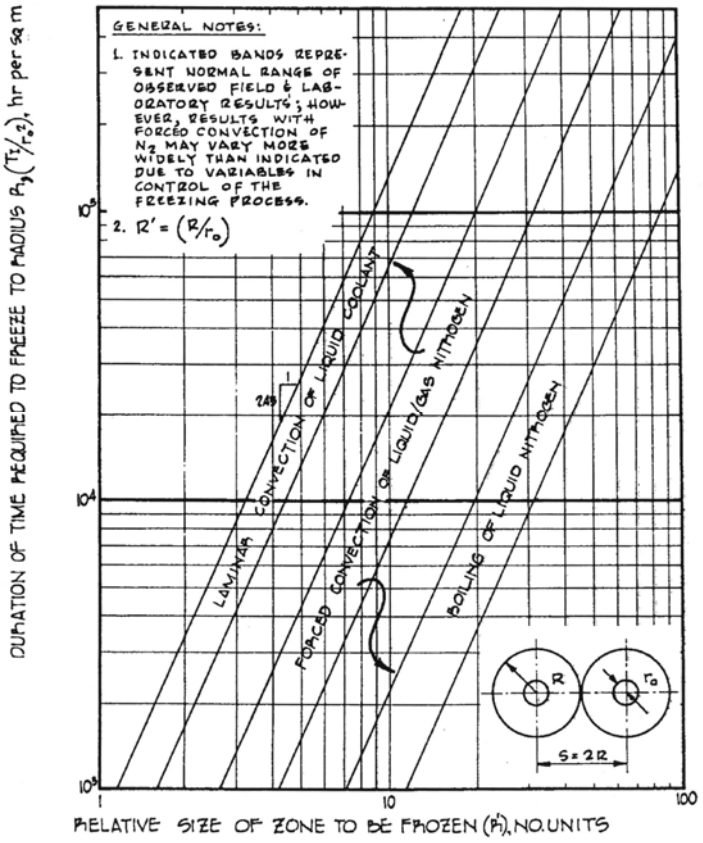

Figure 2.11 Cooling by direct expansion; schematic illustration of the required time to freeze v s the relative zone to be frozen, showing three different conditions of the nitrogen i.e. liquid, two phases and boiling, modified after Shuster (1972)

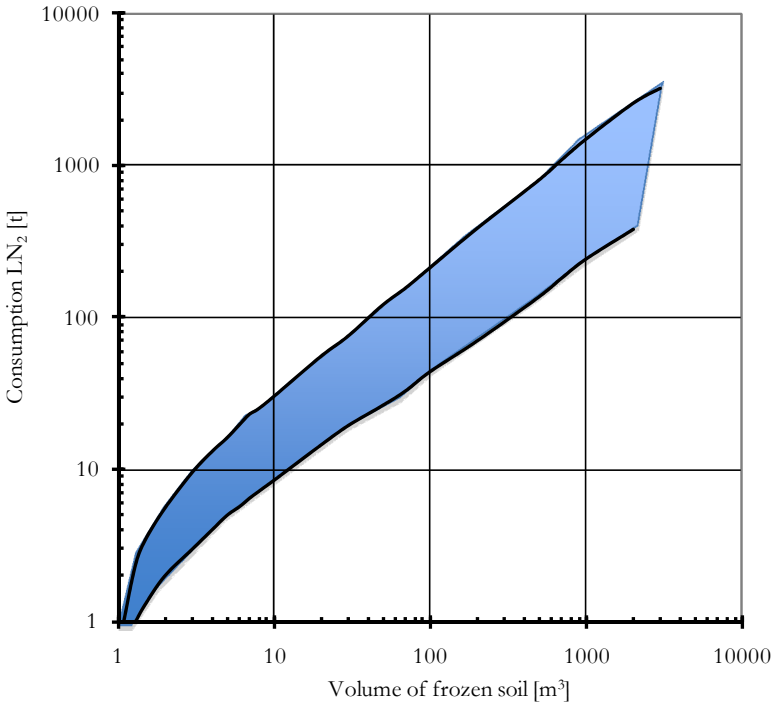

Figure 2.12 Cooling by direct expansion; the consumption of liquid nitrogen (in ton) as a function of the frozen soil volume (in cubic metre), modified after Veranneman and Rebhan (1978)

2.2.3 Artificial ground freezing as an aid in tunnelling

Freezing of soil and rock through the indirect or the direct method has advantages and disadvantages, see Table 2.1. Indirect freezing is typically used when having a fairly good amount of time to plan, project and freeze, as well as when a rather moderate flow of ground water exists in the future frozen zone. It is, however, advantageous to use the direct method when a hydraulically sealed and stable zone is desired. This method is yet more expensive, despite the initially lower cost of installation, compared to the indirect method, see Figure 2.13 (Stoss & Valk, 1978).

Siebe Gorman & Co practiced artificial freezing of soil and rock for the very first time in South Wales, England, 1862. The method was in the beginning used to stabilize shafts in the mining industry. Later, when it was possible to utilize horizontal drilling, the method was even employed in the (mining) drifts and in tunnels (Sanger & Sayles, 1978). Nevertheless, 1883, a mining engineer by name H Poetsch, patented the method in Germany; the ability to freeze constructions in the ground by the use of a cooling system and concentric freeze pipes and circulating brine (Jumikis, 1966). Furthermore, a large step was taken in 1962 when French engineers used liquid nitrogen in the freezing pipes to freeze soil and rock (Sanger & Sayles, 1978, from Ritter, 1962). Consequently, Harris (1995) has assembled approximately 400 documented freezing projects made during 1862-1990.

Table 2.2 shows a compilation of projects, according to Jones (1982) and others, which is mainly prepared during the last two decades. The table has a comparison of, among other things, deformations, i.e. amount of frost heave and thawing consolidation. The projects have been chosen with consideration of that they: are tunnel projects, have been accomplished during the last two decades, have published data and that there exist an element of artificial frozen soil.

Table 2.1 Comparison of freezing with nitrogen and brine, after Stoss and Valk (1978)

	Quality	LN_2	Brine
Site installations	Electric power	Not required	Required
	Water for cooling	Not required	Required
	Refrigeration plant	Not required	Required
	Storage tank	Required	Required
	Circulation pumps	Not required	Required
	Pipe system for distribution of coolant	Supply only	Supply and return
	Low temperature material for surface pipes, valves, etcetera	Required	Not required
	Low temperature material for freeze pipes	Not required	Not required
Execution of freezing	Physical condition of coolant	Liquid/vapour	Liquid
	Minimum temperature achievable (theoretic)	-196 °C	-34 °C, $MgCl_2$ -55 °C, $CaCl_2$
	Re-use of coolant	Impracticable	Standard
	Control of system	Difficult	Easy
	Shape of freeze wall	Often irregular	Regular
	Temperature profile in freeze wall	Great differences	Small differences
	Frost penetration	Fast	Slow
	Impact on freeze wall in case of damage to freeze pipe	None	Thawing effect
	Noise	None	Little

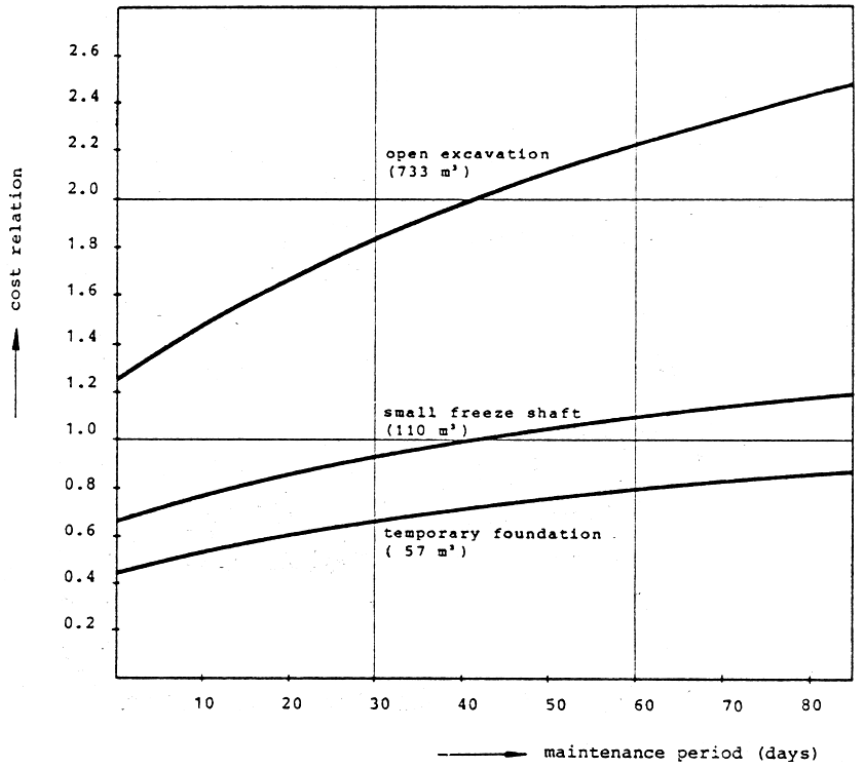

Figure 2.13 Cost relation due to the ratio LN_2 and Brine as a function of the durability and the project power requirement, after Stoss and Valk (1978)

Table 2.2 Details of recent tunnels constructed with the aid of artificial ground freezing, modified after Jones (1982) and others, see below the table

	Project	Type	Diameter or H × W	Duration		Position		Geology	Deformation		Comments
			[m]	σ [Days]	Σ [Days]	z_S [m]	z_w [m]		Heave [m]	Settlement [m]	
1	Charrat, sewer Switzerland	H	1.5	3		3.5	1.5-1	Varied, strata of silt, sand and gravel	0		LN_2, varied ground water level
2	Essen, underground railway Germany	AI	7×9	21		5.7-9.5	3-2.5	Ballast, silt	0	0.060	Tunnel 7×9 m
3	Kobe, existing cable tunnel Japan	CH	4.55	90	365	20		Varve sand and clay	0.04	0.08	Created a frozen zone around an existing tunnel
4	Oslofjord, road Norway	Ch	7×12	100	14/100	80	120	Glacial till; clay, sand, gravel			
5	Oslo, railway Norway	AH	Double single-track					Ballast, sandy gravel, limestone	0.025	0.04	
6	Stockholm, road (SL04)	AH	8×12	90	480	14	14	Clay, till	0.03	0.7	Deformations measured at a shallow sewer
7	Storebælt, railway Denmark	Ah	8.5 & 4.75	30		25-35	35-45	Clayey till			"Only minor settlement in about some millimetres"
8	Tokyo, watertight sealing Japan	Ch	3.14	45	>160	25	13	Clayey soil, clay, sand Silt, sand	0	0	Freeze pipes was inclined about 15° to the horizontal plane
9	Washington DC, sewer USA	CH	3.8	31	56	2.7	1.2	Clayey sand Sand and silt	0.125		Merging took place probably earlier

Note: **Type**; A = arch, C = complete cylinder, h = inclined (close to horizontal), H = horizontal, v = inclined (close to vertical), S = sheet. **Duration**; σ = time of refrigeration, **Σ** = total time of refrigeration. **Position**: z_S = covering, z_w = distance from the tunnel to the ground water table. **Deformation**: Maximum heave and settlement.

References: 1) Stoss and Valk (1979). 2) Valk (1980). 3) Konrad (2002). 4) Andreassen (1999); Berggren (1999); Berggren (2000); Eiksund, Berggren and Svanø (2001). 5) Josang (1980); Jones (1982). 6) Johansson (2000A, 2000B, 2005); Johansson and Hintze (2002). 7) Kofoed and Doran (1996); Murray and Eskesen (1997). 8) Takashi, Kiriyama and Kato (1979). 9) Jones and Brown (1979).

2.3 SOIL WATER AND SOIL ICE

Several interesting phenomena take place in connection with the freezing of water in the ground. The ice has mechanical properties that differ from those of water as well as a redistribution of water, i.e. a segregation of water coincides during the freezing process.

An effective stress generally exists in the soil skeleton. When ice-rich, fine-grained soils thaw under undrained conditions, the residual stress may be zero. However, various combinations of stress and thermal histories can result in the generation of significant residual stresses upon thawing (Nixon & Morgenstern, 1973).

At temperature levels close to below 0 ºC, i.e. below the freezing point, the soil water exists in three different phases; liquid, ice and vapour. The lower the temperature, however, the greater the volume that water assumes in a solid phase. Similarly, the lower the soil temperature, the greater the strength of the frozen soil, which obtains desirable properties that often are required for temporary constructions, i.e. low permeability and high strengths.

Overall, artificial freezing of soil and rock can be described as stored energy in the ground removed from the ground through a heat transfer medium, i.e. the energy existing in the ground is transferred into the atmosphere via circulating liquid quite colder than the ground. In the same fashion, a cooling device consisting of liquid nitrogen transfers energy from the ground to a comparatively colder liquid and convert the liquid to vapour. The energy enriched nitrogen gas mixes with the atmosphere and the transfer of energy from the ground to the atmosphere is completed. The frozen material in the soil and the rock are joined together with the frozen water, and the ice becomes a bond keeping the soil- and rock particles together.

An important component in regards to ground freezing is water and its properties. Water and ice possess distinct characters and their natures make an important foundation for the properties of the frozen and subsequently thawed soil. The definition of ice under these circumstances can be described as the solid water phase i.e. the ice phase. Different ice crystals are formed when liquid water and/or water in its vaporized form freezes.

The main difference between liquid and frozen water is the orientation of the molecules, which are formed according to a specific pattern in the solid phase, while the water molecules are unorganized and moving relatively each other in the liquid phase. Several ice structures can be formed depending on pressure and temperature. However, eleven ice structures are known, where ice Ih (hexagonal) is the only stable form existing in nature under "normal" atmosphere pressure. In nature, when water freezes into ice, the water molecules are connected into hexagonal circles, which in their turn are connected into greater patterns. When the ice crystal grows "unimpeded" in nature, such as the formation of a snowflake or an ice crystal formed by misty air, symmetrical patterns are always formed with a fundamental hexagonal structure. The reason for this phenomenon is that each new water molecule that connects to the crystal only has a few positions to choose between (Petrenko & Whitworth, 2002).

There is always a water film between the ice crystals in tempered ice, at lower temperatures the water amount decreases. At the point where three ice crystals meet, thin paths are created that can contain considerably more water. On the other hand, in clean ice the total amount of water is frozen at approximately -10 ºC. Because of this reason, the ice can be seen as "weakly penetrable" as long as the "water channels" are open. To re-organize the more irregular, accidental network in water to the well-organized tetrahedron network in

crystallized ice, latent heat is required. The energy, 334 kJ kg^{-1} released is thus called *latent heat* or *latent heat of fusion*. However, a comparable amount of heat is needed to melt the ice to water.

The specific heat capacity for water close to the melting point is 4.18 kJ kg^{-1} K^{-1} and for ice close to the melting point 2.04 kJ kg^{-1} K^{-1} (Knutsson, 1985A). Clean water can be supercooled to a temperature of -20 ºC; small water drops (1-10 μm) down to -40 ºC. Super cooling of the water is the formation of a metastable condition when water is cooled down under its normal freezing point, i.e. supercooled, see Figure 2.14. In ice Ih composition, each water molecule is tetrahedronly bound to four other water molecules with hydrogen compounds. The "open" structure leads to a significantly lower density than that of water. The density for nature ice varies between 890 and 950 kg m^{-3} while that of pure ice is 917 kg m^{-3}, the density also varies with the temperature, see Figure 2.15. Water has its maximal density at about 4 ºC; the distance between two adjacent oxygen atoms is then approximately 0.284 nm. The comparable distance in ice is 0.276 nm, this because each molecule on average is surrounded by a few more "neighbours" in water (4.5) than in ice (4) (Petrenko & Whitworth, 2002).

When water freezes to ice, its volume increases with approximately 9 %. This volume expansion leads to frost erosion in closed systems. On the other hand, the freezing point is lowered for ice with 0.0074 ºC bar^{-1} when under increased pressure (Petrenko & Whitworth, 2002). However, the highest pressure will develop when it is impossible for the water to expand during freezing. The pressure will reach a magnitude of 2 115 kgf cm^{-2} (approximately 200 MPa, author note) at a temperature of -22 ºC. On the other hand, the pressure will be much smaller at temperatures above -22 ºC (Tsytovich, 1975). To estimate the pressures that can arise when the water freeze with no possibility of volume expansion at temperature above -22 ºC, Tsytovich (1975) shows the empirical relation between the external pressure for temperatures above -22 ºC as a function of the thawing temperature of ice

$$\Delta p = 1 + 127\theta - 1.519\theta^2 \tag{2.1}$$

where Δp = pressure [kg f cm^{-2}] and θ = absolute negative temperature [º C]. See also the evaluation of the equation in Figure 2.16.

At normal conditions, i.e. normal atmospheric pressure and none saline water, ice melts at $\theta = 0$ ºC, as actually can be seen in Eq. (2.1) and in Figure 2.16. According to Eq. (2.1), at lower temperatures, a higher pressure is required, and also the ice will melt at the given negative temperature when the actual pressure is attained. As a result, according to Eq. (2.1) if the pressure is higher than estimated in Eq. (2.1), the water will not freeze at the specified negative temperature. On the contrary, the pressures illustrated in Eq. (2.1) will be the maximum pressures that ice can develop without melting under the effect of such external pressure at given negative temperatures. Tsytovich (1975) clarifies that these pressures can only be attained for water frozen in a closed system, in a rigid container. However, the pressure magnitudes developed in soils due to the frozen water will be lower than the pressures estimated in Eq. (2.1).

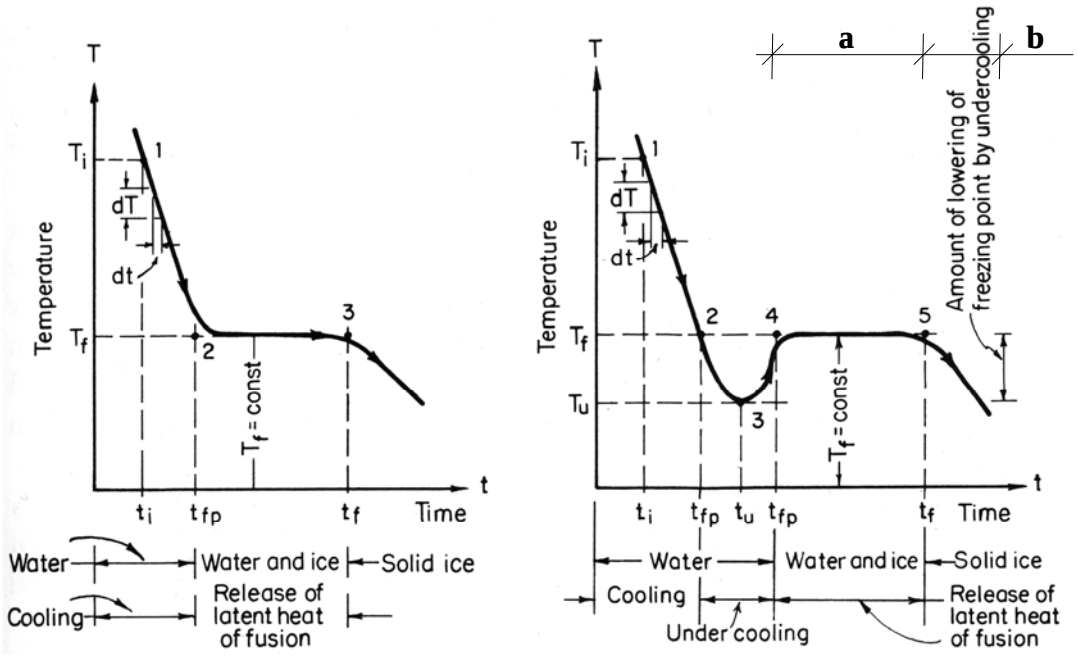

*Figure 2.14 Cooling-freezing curves; the picture on the left-hand side shows the cooling-freezing curve of pure water when not supercooled. The picture on the right-hand side shows the cooling-freezing curve of supercooled pure water. Free water freezes at **a**, at **b**, most of bound water is frozen and soils cools without latent heat effects, modified after Jumikis (1966)*

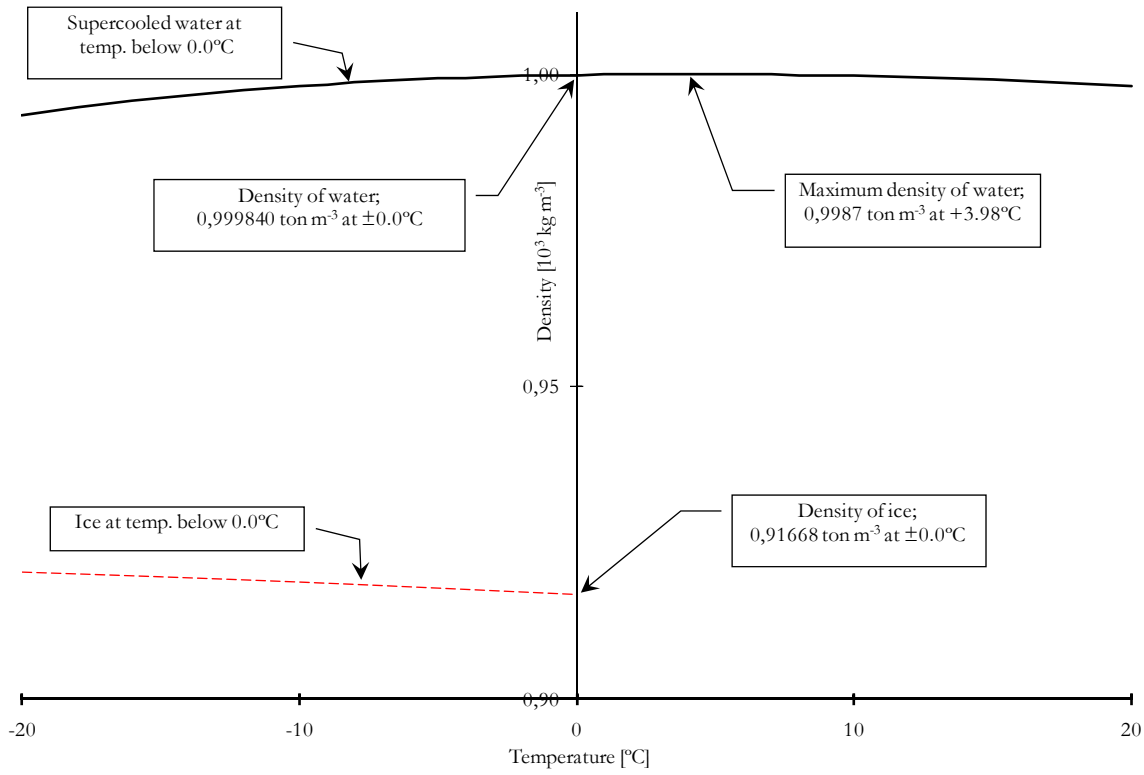

Figure 2.15 The variation of the density of water and ice vs. the temperature, after HB of Chem and Phys (2004) and Andersland and Ladanyi (2004)

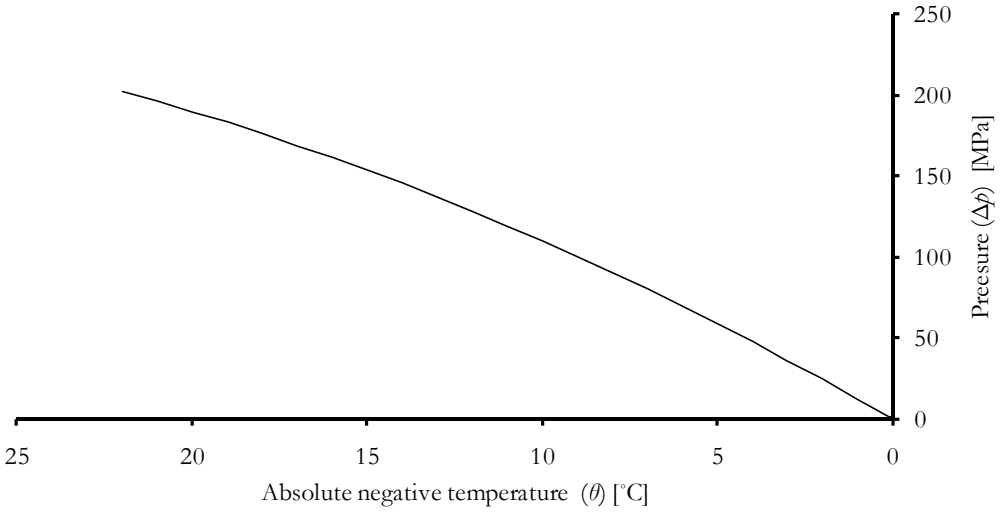

Figure 2.16 According to Eq. (2.1), empirical relation for the external pressure (kPa) as a function of thawing (melting) temperature of ice (absolute value of negative temperature in ºC), after Tsytovich (1975)

2.4 SOIL ENERGY TRANSFER

This section describes in brief the governing parameters affecting the properties of soil and rock in connection with stabilization and hydraulic sealing through freezing.

The energy or heat concept is synonymous with the motion of the atoms and the molecules; in solid material, the changes in the atoms' state of equilibrium, in gas and liquid the atoms' free motion. Larger energy contents contributes to more vigorous "heat motions".

Heat is energy transferred from one system to another because of a temperature gradient. The concept ("heat") is typically used in connection with a process where energy is added to a system, which thus goes from one state to another. This is, however, a static concept as separate molecules and atoms from a micro perspective continuously exchange energy.

When this micro perspective is seen from a wider view, no energy exchange is on average taking place. Systems with a thermal equilibrium have the same temperature everywhere. The energy exchange within a system or between different systems can take place with help of different parameters and in certain cases; there is an interaction between these parameters. The thermal parameters that particularly have an influence on soil- and rock freezing are (Jumikis, 1966)

- latent heat of fusion
- specific heat capacity
- convection
- heat conductivity.

In other cases, for example at extensions of district heating in ground, different thermal parameters have under certain conditions shown to be more important than those of importance during freezing of soil and rock. Placing of district heating in ground in areas with gravel and/or sandy moraine can have a drying effect on the moisture in the surrounding coverage because of relatively high temperatures of the district heating pipes in the ground (local conditions such as ground water levels, infiltration etcetera have an effect and can give rise to other circumstances) (Sundberg, 1988).

Water vapour diffusion and radiation are of importance in porous materials such as dry gravel and/or sandy moraine when under relatively high temperatures. Water vapour diffusion and radiation are in many cases also important as energy transporting parameters. The influences are, however, limited and can at high temperatures and with a dry material at the most add 10-20 % of the thermal conductivity (Knutsson, 1985A; Sundberg, 1988). Water vapour diffusion and radiation are significant as energy transporting parameters in many cases. These parameters have quite an insignificant effect in connection with soil freezing (Knutsson, 1985A).

Soil can be seen as a porous, three-phase composed medium when it is unfrozen, and a four-phase composition when frozen. The division of the soil element can be described as a solid-, a gas- and a liquid phase as well as a viscous "solid" phase when the soil is frozen. The soil type can be fairly well described depending on the knowledge of the different components' relative size. Diverse re-calculations of the different phases create important physical parameters for the calculations of soil freezing. Each one of the different components in the soil's three-phase structure has unique thermal properties (Knutsson, 1985A; Sundberg, 1988; Andersland & Ladanyi, 2004).

The soil's thermal qualities can be measured (in laboratories or in situ) or calculated. A calculation is only valid as a rough estimate and only for water saturated conditions, see Figure 2.17 (Sundberg, 1988).

In practice, the thermal heat transporting mechanisms in the ground can be divided into

- heat conductivity in soil particles, pore gas and pore water
- heat convection in pore gas
- heat radiation between particles
- water vapour diffusion
- specific heat capacity.

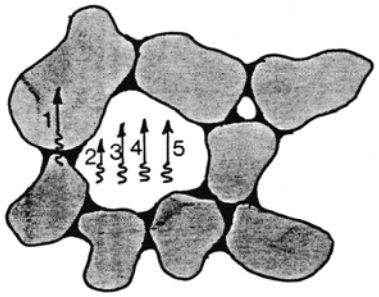

Figure 2.17 Soil heat transportation parameters, after Knutsson (1985A) are
1.) heat conductivity in particles and fluid
2.) heat conductivity in pore gas
3.) heat radiation between particles
4.) heat convection in pore gas

The different processes have different capacities in regards to transportation of thermal energy depending on the circumstances. The thermal conductivity is, at moderate temperatures and temperature differences, the dominating energy-transporting mechanism in regards to, for example, soil- and rock freezing. Natural convection and steam diffusion are more significant at high temperature gradients in permeable ground. Forced convection occurs, for example, in sand or gravel material in form of ground water flow (Sundberg, 1988).

2.5 NATURALLY FROZEN GROUND AND ARTIFICIALLY FROZEN GROUND, DIFFERENCES AND SIMILARITIES

Large areas in the northern hemisphere have naturally cold conditions; this concerns especially sporadic-, seasonally- or permafrozen ground. During the last centuries diverse activities like mining, oil exploitation etcetera have taken place in these areas. However, due to logistics, housing, construction etcetera, frozen grounds as well as thawing grounds have caused problems, among other things thaw settlement. To overcome these inconveniences, countries having these problems started researching naturally frozen ground. Therefore, knowledge of naturally frozen ground is relatively well described. This section describes the essential differences and the main similarities between naturally frozen ground and artificially frozen ground. A brief description of the main characteristics in permafrost landscapes and its genesis are given. In fact, there are several similarities between naturally frozen and artificially frozen soil. Nevertheless, there are also many differences. By having knowledge of these differences, information from permafrost investigations and sciences can be used when designing artificially frozen constructions (Ladanyi & Sayles, 1978; Freitag & McFadden, 1997).

Frozen ground is defined as soil and rock with a temperature below 0 °C. The definition is based solely on the temperature and is independent of the firmness of the ground, the water content and the ice content (McFadden & Bennet, 1991; Freitag & McFadden, 1997). However, Burdick, Rice and Phukan (1978, p 6) state, "Ground of any kind which stays colder than the freezing temperature of water throughout several years qualifies as permafrost. If the ground is dry sand, it is permafrost no less than if it was a conglomerate of soil particles cemented by ice.".

Cold areas are identified as having ground that has been frozen during several years or ground frost (*permafrost*) remaining in the ground at temperatures below 0 °C. The tundra is, above all, predominant in these areas, particularly in the arctic regions. Permafrozen areas can typically be divided into regions where permafrozen ground exists all over ("continuously permafrozen areas") or regions where permafrozen ground exists sporadically ("discontinuously permafrozen areas"), see Figure 2.18. However, it is assumed that the mean annual ground surface temperature have to be at least -3 °C for permafrozen ground to exist (Freitag & McFadden, 1997; Andersland & Ladanyi, 2004).

In the discontinuously permafrozen areas, the ground is frozen at a depth varying from less than 0.10 m, to depth of up to 100 m at the boundary zone to the continuously permafrozen areas. The ground frost in the continuously permafrozen areas, above all in the arctic regions, can, however, reach down to a depth of up to 1 km. In fact, the thickness, distribution and temperature of the ground frost are neither constant nor corresponding with the climate during the day in respective regions (Andersland & Ladanyi, 2004).

Seasonal frost areas, i.e. areas with recurring temperatures above 0 °C during an annual winter season, exist mainly in the subarctic climate areas, in areas where the taiga is widespread (Freitag & McFadden, 1997). However, the "cold areas" in the in the northern hemisphere border the 40th latitude. These are typically defined with an additional note that their southern border consist of a reoccurring ground frost depth of a minimum of 300 mm, once every ten years (Andersland & Ladanyi, 2004).

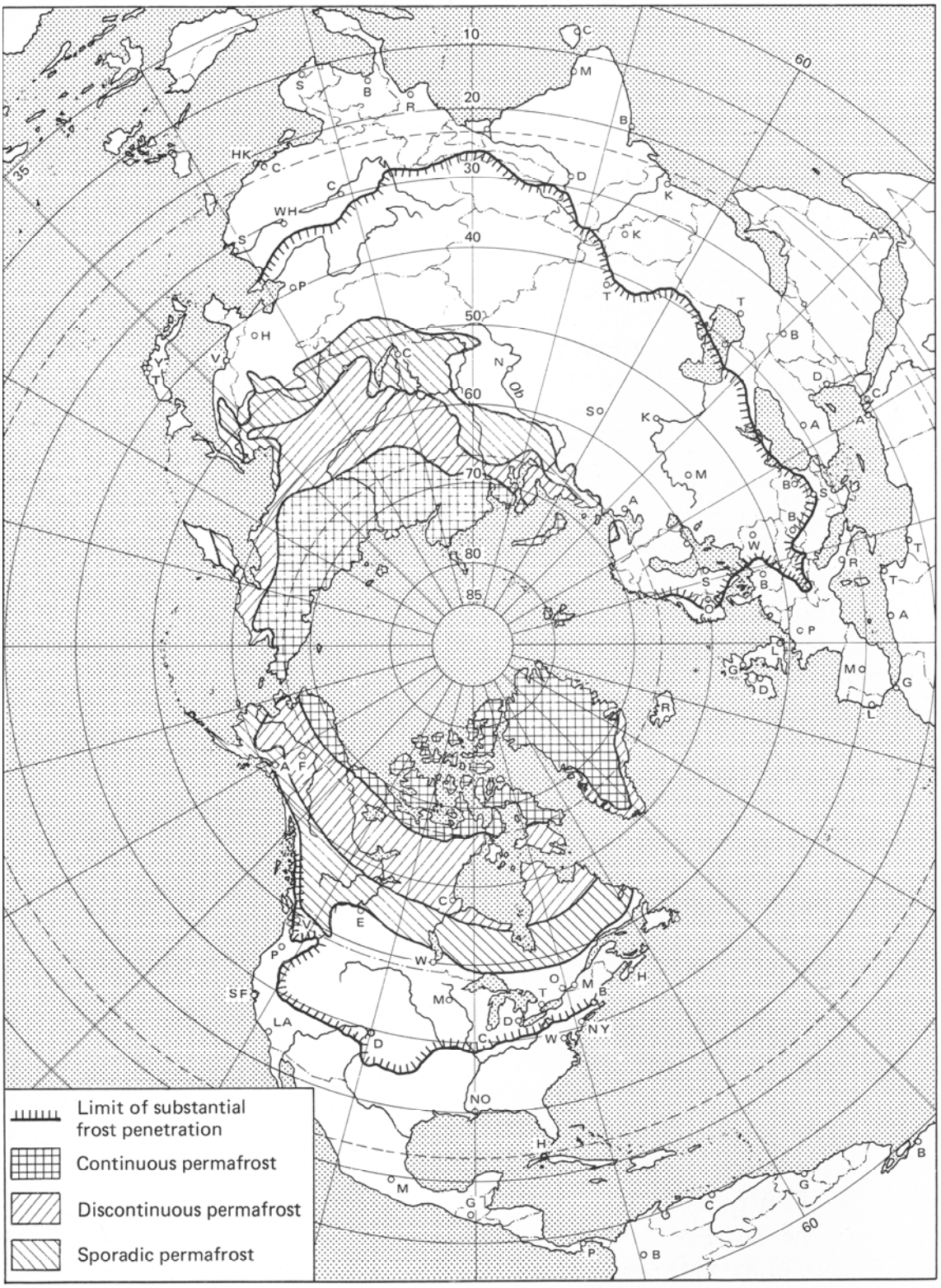

Figure 2.18 Areal distribution of permafrost in the northern hemisphere, after Burdick, Rice and Phukan (1978)

The continuous ground frost is in the cold areas superposed by an "active layer" consisting of seasonally frozen and thawed soil and rock. The ground frost of the active layer ranges from the northern part of the cold area down to the level of the continuous ground frost, while the surface cyclic frozen active layer only sporadically reaches the continuous ground frost further in the south. The active layer is so separated from the continuous ground frost by an unfrozen layer, see Figure 2.19. The thickness of the layer depends on many factors. In fact, besides the "hardness" of the winter, there is the influence of soil- and rock type, water content, snow depth, vegetation, drainability, as well as extension and orientation of ground slopes (McFadden & Bennet, 1991).

The characteristics of the terrain in the permafrozen areas are, above all, the qualities of the underlying ground. The most important qualities are (Freitag & McFadden, 1997; Andersland & Ladanyi, 2004)

- ice wedges
- pingos
- palsa
- ground ice
- thermokarst.

Ice wedges are created relatively close to the ground surface, near the surface of the continuous ground frost, see Figure 2.20. These wedges are wider at the top, vertical in their extension, and can grow 1-10 m deep and 1-3 m wide. The creation of the initial open crack is related to the falling winter temperatures – the surface layer shrink because of a temperature drop, but is held back by a more stable deeper layer. The cracks are subsequently filled with water during the summer period that freezes and expands the following winter. Cracks develop thus once again in the most water rich soil in connection with falling temperature (Freitag & McFadden, 1997). The thermal strain is normally larger in water rich soils as the ice has up to five times higher expansion coefficient that most soil particles. The rupture and crack formation occurs when tensile stress exceeds the frozen soil tensile strength (Andersland & Ladanyi, 2004).

Pingos are large, almost circular hills often occurring in an otherwise flat terrain. Pingos can be between 3 m and 70 m high and between 30 m and 650 m in diameter. The core consists of pure ice covered with soil or rock and vegetation. As a matter of fact, the solid ice core expands because of the seasonally continual addition of water from below, from example a seasonally thawed surface lake or artesian ground water (Freitag & McFadden, 1997).

Palsa is an elevated area in shape of a low hill or plateau. The size of a palsa varies between 1 m to 10 m height, up to 30 m wide and 150 m long. They are typically created in discontinuous, organic permafrost terrain. Palsa consist of a surface layer of a thick layer of peat that superimposes a core of permafrost. The permafrost core consists of ice lenses, each one, 2 cm to 3 cm thick. Ice lenses can cumulatively add up to half the height of the palsa. Despite the fact, the process of formation is discussed. One way of looking at the process is that ground ice has melted faster under the thin layers of peat and that these areas thus have sunk compared to areas with thicker layers of peat. Another way of looking at it is that the surface layer of peat encourages the formation of ice lenses due to its high thermal conductivity when wet, and low thermal conductivity when dry. Nevertheless, both ways of looking at the formation process tend to point in the direction that the freezing will become more effective than the thawing, particularly in comparison with mineral soil (Freitag & McFadden, 1997).

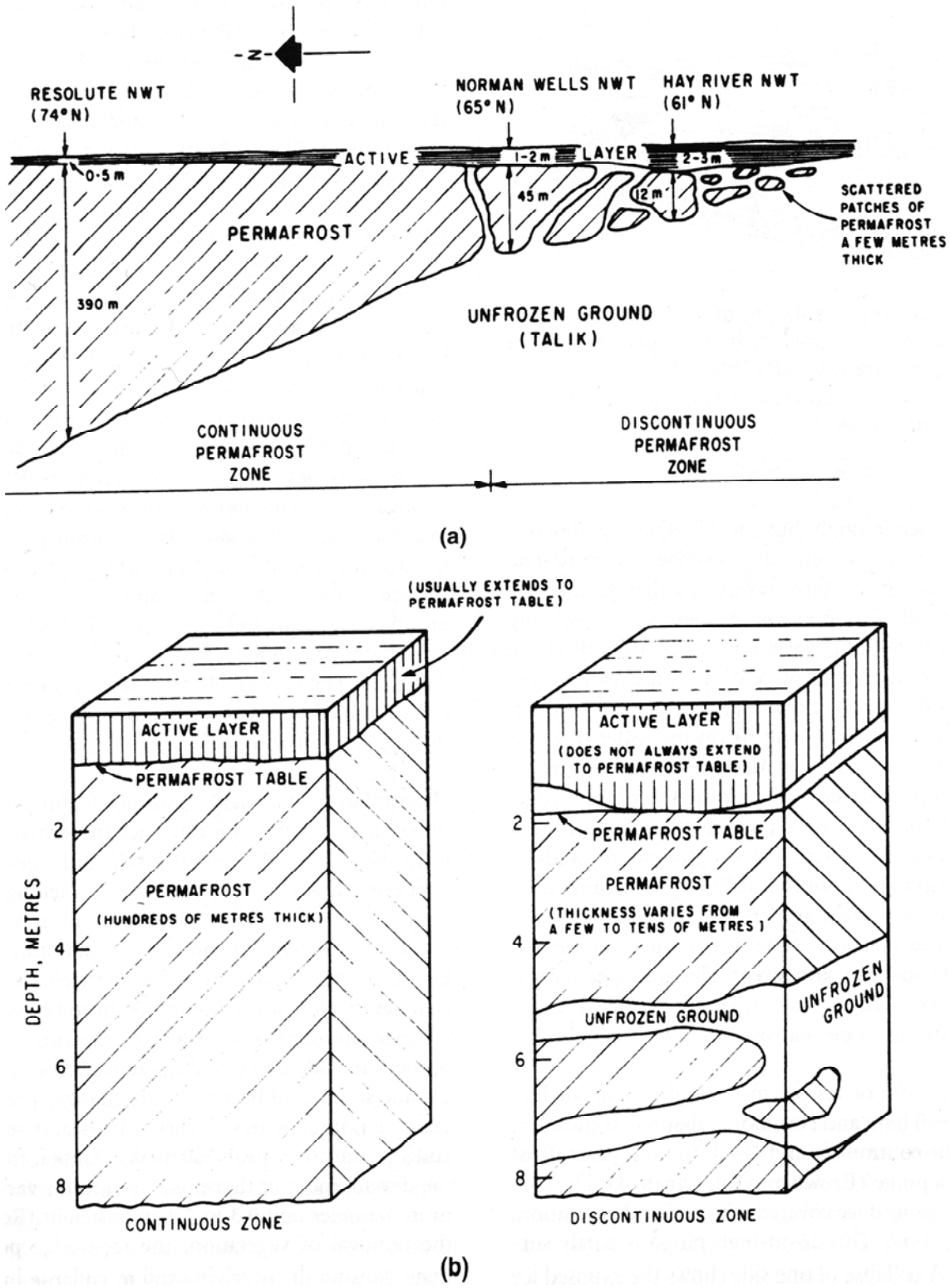

Figure 2.19 Different types of permafrost in cold regions. Drawing (a), the thickness of permafrozen soil layer and the active layer vs. the distance from the Arctic. Drawing (b), typical profile in the continuous zone as well as the discontinuous zone, after Brown, Johnston, Mackay, Morgenstern and Shilts (1981)

Ground ice is a general term for large masses of ice that exist below the ground surface. The origin for this ice can be glacier ice covered with soil, old ice wedges, pingos, large ice lenses, frozen surface dam or lake, etcetera (Freitag & McFadden, 1997; Andersland & Ladanyi, 2004).

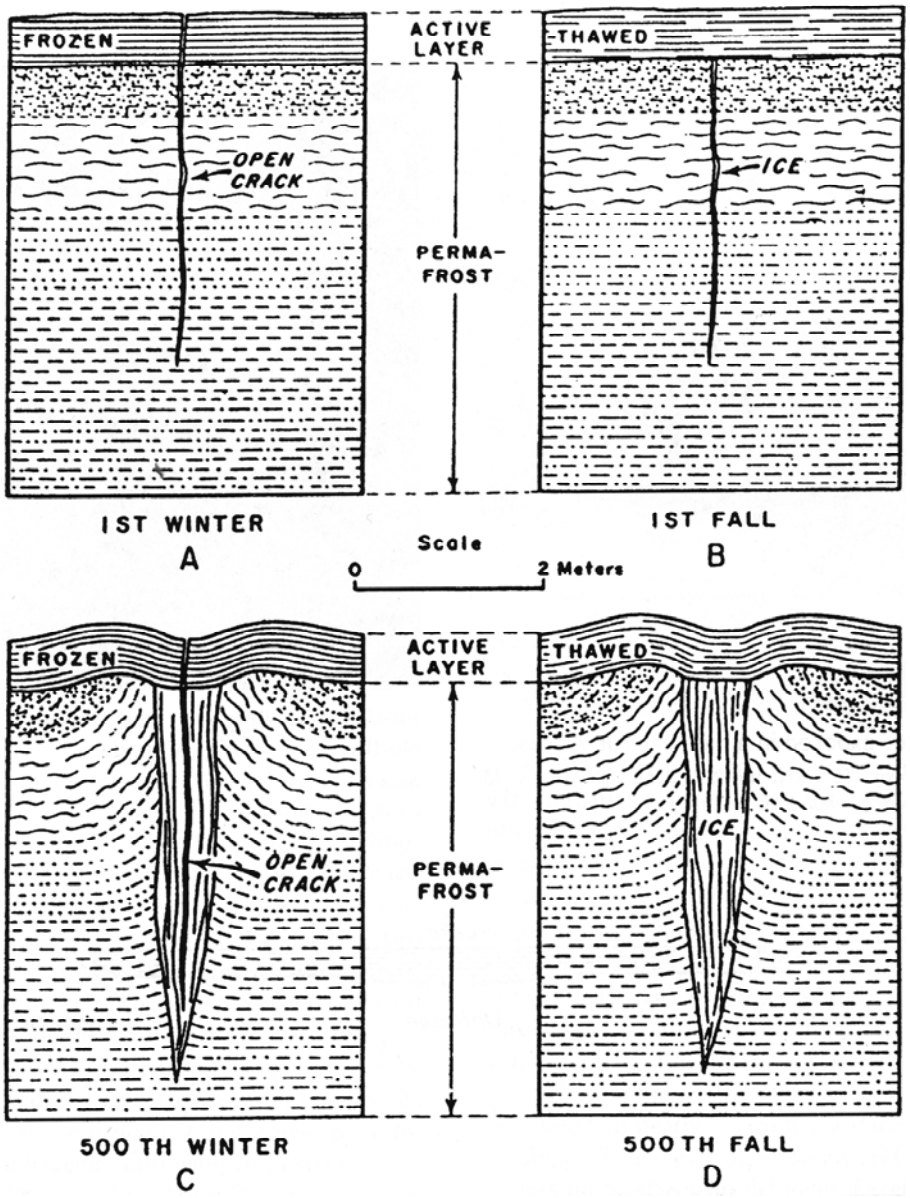

Figure 2.20 Schematic illustration of the ice wedge evolution according to the thermal contraction theory, after Lachenbruch (1963)

The permafrozen and the artificially frozen soil texture have a complex structure, including, mineral particles, gas inclusions, as well as interlayered ice crystals. However, Tsytovich (1975) has studied the textures in among other things ice layers from continuous ground frost and cyclic frozen soil in Igarka, Siberia. The texture for an ice crystal from continuous ground frost is shown in Figure 2.21. Tsytovich (1975, p 104) summarizes results from studies of the deformation mechanism of ice in glaciers and the texture of ice interlayers from permafrost:

i. The sizes of crystals in permafrost ice interlayers are larger than those in seasonally frozen soils by factors of 14 to 25, and have up to 500 times larger areas.
ii. The shapes of the ice crystals are irregular and often anomalous, with orientation of the principal optical axes parallel to the ice interlayer.
iii. At least three basic mechanisms of the deformation of ice should be notable: 1) Flow of ice in slow shear parallel to the base planes of the crystals without changing the structure of ice. 2) Destruction of the space lattice of the ice with molecular breakdown, recrystallization, intergranular shifting, and breakup into fragments with random structure. 3) Thawing of the ice under high shear stresses due to the heat of friction along planes of joints.

Tsytovich (1975, p 104)

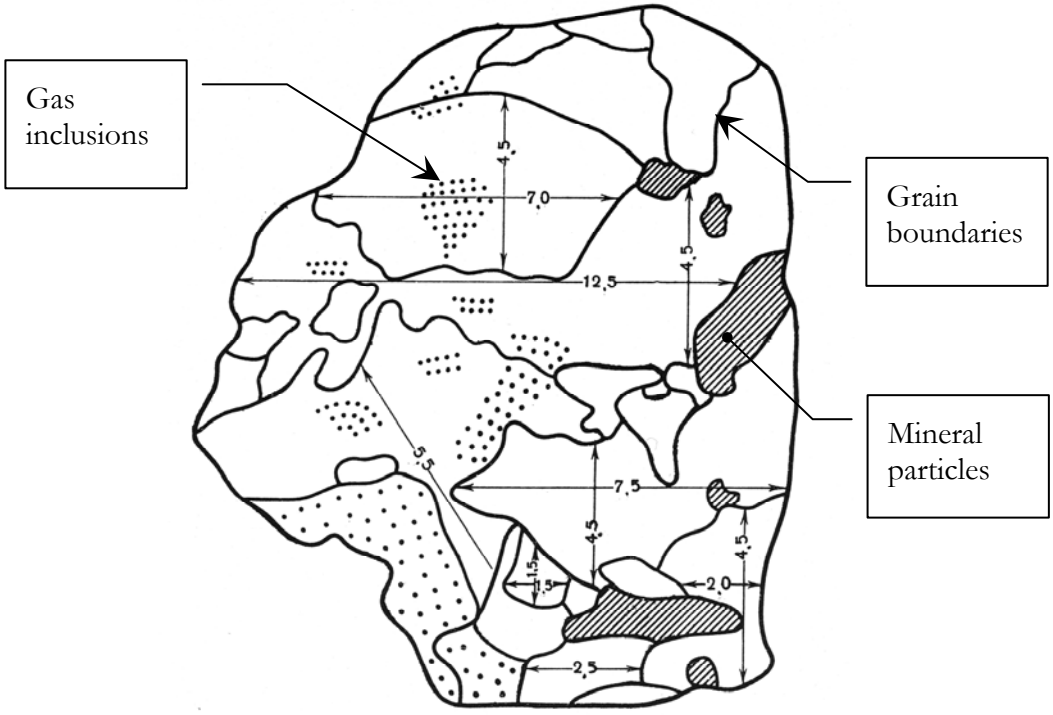

Figure 2.21 Schematic illustration of ice crystals from ice interlayer at a depth of two metres in permafrozen soil. Shaded areas are aggregates of mineral particles in the ice, circles represent gas inclusions and the solid lines correspond to grain boundaries. The crystal dimensions are specified in cm. Modified after Tsytovich (1975)

Thermokarst are regional formations associated with either discontinuous permafrost or previous permafrost conditions. The landscape is characterised by dams and sinkholes that lack normal shallow draining paths. However, these sinkholes in the ground layer develop when ice enclosures in deeper laying soil melt and top soil fall into and fill the cavities. In fact, the effect is largest in grounds consisting of silt material. As a result, once an opening has developed in the ground, it tends to fill up with water, which leads to subsequent melting (Freitag & McFadden, 1997).

The ground below the active layer has a constant temperature over -15 °C in areas with continuous ground frost. Besides the thermokarst areas and in the regions where ice wedges are created, the ice structure is dominated by horizontal ice lenses created through natural frost front that has moved further down. Conversely, artificially frozen soil is typically found in a different environment (McFadden & Bennet, 1991).

In contrast to the naturally frozen ground, the temperature in the artificially frozen ground is characterized by a large gradient with temperatures down towards -160 °C adjacent to the freeze pipes at cooling with liquid nitrogen and 0 °C at the freeze front (Harris, 1995; Andersland & Ladanyi, 2004).

A difference between naturally frozen and artificially frozen soil is that the naturally frozen soil may consist of both ice rich and ice poor soil. The ice lenses also tend to thin out with depth, while the artificially frozen soil in general consist of cohesion soil with low quantities of minerals, such as loose sand, silt, and loose clays below the ground water table. These soils tend to create segregated ice i.e. an oriented ice lens structure parallel to the freeze elements, thus giving rise to an anisotropic structure (Ladanyi & Sayles, 1978; Radd & Wolfe, 1978).

The installation of a freeze system can be optimized so that the creations of the ice lenses are advantageous for the frozen construction. This can occur because the orientation of the ice lenses generally coincide parallel with the direction of the freeze front (if they are built) and the ice crystals' orientation is of importance in regards to the mechanic properties. In artificially frozen soil, the temperature can be optimized so that the "right" strength in relation to the economy is achieved, while the temperature in naturally frozen material already is established and hard to influence (Vyalov et al, 1962, from Harris, 1995; Ladanyi & Sayles, 1978).

The soil in the continuous frozen areas is usually dimensioned for permanent constructions, i.e. long term loads up to 100 years. The situation is different for the artificially frozen constructions as the artificially frozen construction has been created under a shorter period, and is subsequently used under a relatively short period as a temporary construction that melts (McFadden & Bennet, 1991; Freitag & McFadden, 1997).

The main differences between artificially frozen soil and naturally frozen soil are summarized in Table 2.3.

Table 2.3 Identification of the main most important differences between naturally frozen ground as permafrozen and seasonally frozen together with artificially frozen ground, modified after Ladanyi and Sayles (1978) and Tsytovich (1975)

Aspect	Naturally frozen soil; seasonally frozen soil at shallow condition.	Naturally frozen soil; permafrozen soil.	Artificially frozen ground.
Type of ground	Normally ice rich, low mineral content, loose silt, sand, loose clayey soils.	Normally ice rich, low mineral content, loose silt, sand, loose clayey soils.	Any soil, poor of ice to ice rich.
Freezing process	1-dimensional freezing, discontinuous.	1-dimensionell freezing, permanent condition.	2-dimensionell freezing, continuous.
Stress condition	Low stress condition during comparatively brief period.	Low stress to high stress, permanent condition.	High stress during comparatively brief period.
Minimum temperature	Usually above -15 °C.	Hardly below -15 °C. Naturally controlled. Low variation in time.	Normally below -20 °C, or -160 °C using liquid nitrogen LN_2. Varied temperature.
Ice crystals[1]	1/25 to 1/14 size of corresponding ice crystals in permafrozen soil. The area is less than 1/500 of corresponding ice crystal in permafrozen area.	14 to 25 times larger than corresponding ice crystals in seasonally frozen soil. The area is up to 500 times larger than corresponding seasonally frozen soils. The shape of the ice crystals is irregular and often "strange", with the optic axes orientated parallel to the ice layer.	
Ice lenses	Usually horizontal. The thickness and the frequency decrease with increasing soil depth.	Usually horizontal. The thickness and the frequency decrease with increasing soil depth.	Usually parallel to the freeze tubes.
Establishing of mechanical design properties	In the frozen state; undisturbed specimens. Field and laboratory tests. In the thawed state; Relevant information can be received only/just when the soil is frozen Difficult to make prognosis because of unknown formed ice structures.	In the naturally frozen state, undisturbed specimens. Field and laboratory tests.	Relevant information cannot be achieved until the soil is frozen. Obscurely created ice structures may raise difficulties.

Note: 1) Tsytovich (1975)

2.6 SOIL PHASE RELATIONS

The soils geotechnical properties are significantly affected by the volume relations between its phases, i.e. between its particles, water and pore-gas. One additional phase exist in frozen soil – ice. The interaction between the phases can be explained in several different ways; the fundamental relations normally needed to describe the properties of a soil are illustrated in Figure 2.22.

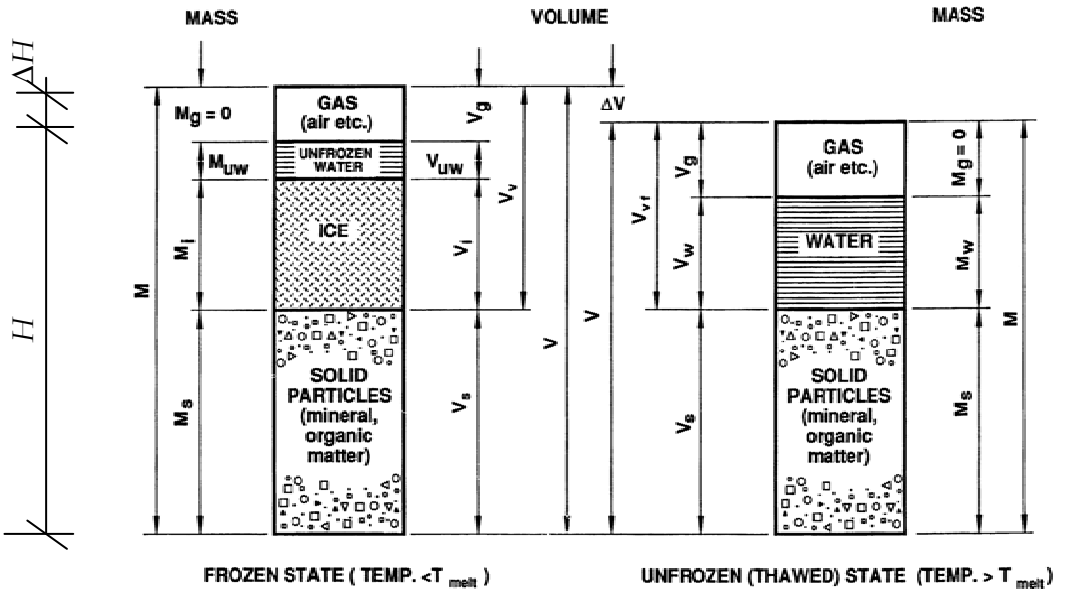

Figure 2.22 Schematic illustration of the relation "mass" and "volume" for frozen- and unfrozen soil. The variable, H characterizes a soil specimen's measured height or length and ΔH the measured change of height or length, modified after Andersland and Ladanyi (2004)

The soil types can be divided in- or classified in different systems depending on generics, composition, technical properties, structure, characteristic, chemical content, frost susceptibility, behaviour in regards to strength, etcetera. Nevertheless, several parallel classifications systems have historically been developed and modified. For instance, cohesion soil can be classified in many different ways. The methods of classification is founded on, for example (Beskow, 1951; Larsson, 1982; Karlsson & Hansbo, 2000)

i. the soils generic soil type classification
ii. the soils composition - components
iii. the soils physical properties, especially in relation to water
iv. the soils technical properties especially due to construction.

However, the systems can be combined and sub-classification system can be organized with consideration of, for example, particle size, petrographical – mineralogical (chemical) properties etcetera.

2.6.1 Water content

The water content is defined as the mass of water in relation to the mass of particles and is normally presented in (the unity) percentage, see Eq. (2.2). Soil above the water table normally contains both water and gas in the soil's pore volume, while soil under the water surface normally is water saturated. Although, the pores in organic soil under the water

table generally contain a certain amount of pore gas created from the biological process in the organic content. On the other hand, the water content for different water saturated soils is shown in Table 2.4. However, the degree of water saturation shows the percentage of the pore volume taken up by water, see Eq. (2.12).

Stress and deformations in frozen soil occur under the influence of temperature, phase change of water and soil particle redistribution. This process continues and accentuates during the course of the thawing. A settling often occurs during the relaxation, particularly in water rich fine soils i.e. rheology. The strong development of the rheological process in frozen soil is due to the singularity of its internal bonding structure where ice is an idealistic liquid body occupying the main role. Tsytovich (1975) lists three basic types of internal bonds, which must be distinguished in frozen soils:

i. Pure molecular bonds (van der Waals– London forces). These bonds are located at the contact points of the solid soil mineral particles. Their magnitude depends on the contact area, the mineral particles' spacing, compactness, and physiochemical nature. The bonds strengthen with increasing external pressure, while the mineral particles' stability on the contrary may be disturbed at some of the contacts.

ii. Ice-cement bonds, the most important bonds. These bonds are almost entirely responsible for the strength and deformation properties of the frozen soils. However, the bonds depend on "very many factors"; degrees of negative temperature, ice content (iceness), structure and coarseness of the ice inclusions and their positions with respect to direction of the forces in operation, unfrozen water content, gas inclusions, cavities in the ice, etcetera.

iii. Structural-textural bonds. These bonds depend on the conditions of formation, the shape and the subsequent existence of the frozen soils. Different structural elements of the frozen soils will be deformed differently depending on their composition and structure. However, structural anomalies, i.e. the presence of aggregates, open porosity, etcetera, will become an important factor. Consequently, the more inhomogeneous the frozen soil, the greater are the numbers of structural and constitutional shortcomings occurring in it, while its structural elements and the frozen soil as a whole will become weaker.

As discussed above, virgin artificial freezing of moist or water saturated soil is accompanied by significant textural and structural changes, therefore creating a new complex low-temperature structure. This structure arises due to the migration of pore water and dispersed mineral particles during the freeze process and the subsequent freezing of bonded pore water with its volume expansion. This volume expansion differentiates the soil through ice enclosures in form of ice lenses, compressed of mineral clusters, and separated layers of ice crystals. A range of different physiochemical processes such as coagulation of soil colloids (dispersed finely separated substances) and aggregation of soil particles and smaller clusters, occur in connection with the freezing of clay rich soil with high water content. This leads to a relatively high density of the soil aggregates, at the same time as the clay rich soil obtains a plastic consistency (Jumikis, 1966; Tsytovich, 1975).

Vertical fissures resembling splits due to drying are created because of the high under pressure at the freeze front of the frozen fringe. The increased permeability in the soil after a freeze-thaw cycle might be due the existence of a lower flow-resistance along the fractures. Experiments on, among other materials, CRREL clay and Hanover silt, have not shown fissuring, but on the contrary, an increased permeability (Chamberlain & Gow, 1978). Chamberlain and Gow suggest that certain differences in particle size and arrangement can explain these results. Nevertheless, Figure 2.23 depicts two idealized arrangements.

In the first case, Figure 2.23 illustrates a more coarse soil where sand and silt particles direct the degree of compaction while parallel parcels of clay particles having alternating directions move freely between the grains. The more coarse grains direct the deformability in this situation, while the clay particles direct the permeability. After a freeze-thaw cycle, the void ratio is basically the same as before the freezing. The clay particles have flocculated to a more compact structure compared to before the freezing, but a smaller volume of the pores is occupied by the clay particles with their bonded water and the permeability has thus increased, see Figure 2.23 (Chamberlain & Gow, 1978).

The second case in Figure 2.23 shows a soil where sand and silt particles lack contact with each other and "float" freely in a clay matrix amongst parallel parcels of clay particles having alternating direction. In the unfrozen mass, the clay mass directs both the compressibility and the permeability. A decrease in the void ratio occurs after a freeze-thaw cycle as the clay structure changes and creates a more compact structure compared to before the freezing. The permeability increases due to shrinkage fissures created during the freezing, see Figure 2.23 (Chamberlain & Gow, 1978).

The freezing and the following thawing cause considerable structural transformations of particularly clay rich soils, which leads to significant increases in the vertical permeability. The largest affect occurs in soils with high plasticity index and in soils with low surcharge. In soils made up of more coarse materials, where the compressibility is directed by incoming sand and silt particles, the increased permeability is caused by a reduction of the particle volume in the pore spaces during the freezing and the subsequent thawing (Chamberlain & Gow, 1978).

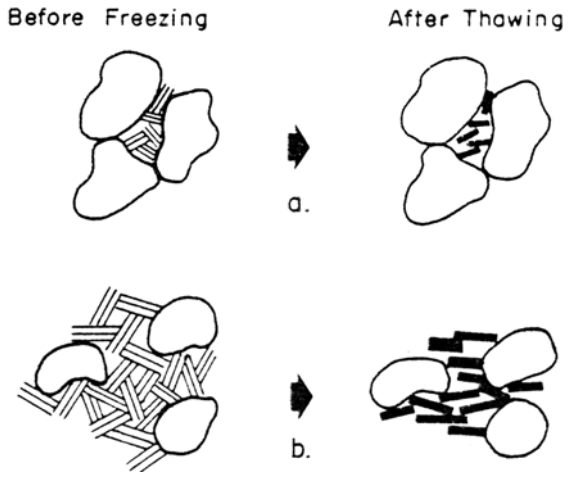

Figure 2.23 Illustration of idealized types of particle orientations for a.) Clayey silt and b.) Silty clay. Modified after Chamberlain and Gow (1978)

Pusch (1978) has performed freeze-thaw tests on two different clay types, one lacustrine and one marine, see Figure 2.30. The samples are taken at a depth of five metres and have a water content of 99-101 %, plasticity index 31-33 % and liquid limit of 69-82 % as well as a clay content of 67-77 %. However, the tests performed partly on undisturbed soil and partly on disturbed (remoulded) soil have shown that the particle aggregates in the clay have moved around without internal distortion in the temperature interval of 0 °C to -5 °C. Pusch (1978, 1979) indicates that a large amount of the bound water had not frozen in this interval. The clay structure is an influential agent during these circumstances, i.e. when the particle aggregates are small and completely porous but located close to each other, as for example in lacustrine clay, the amount of unfrozen enclosed water is large, and the mineral

surface is accessible to the pore water. On the contrary, salt water deposited clay will contain a slighter amount of unfrozen water because of it's large, compact particle aggregates separated by a large empty space, see Figure 2.24 (Pusch, 1978, 1979). The enclosed unfrozen water can be compared with the unfrozen water that arises between the "pure" ice crystals, see below and in Figure 2.25.

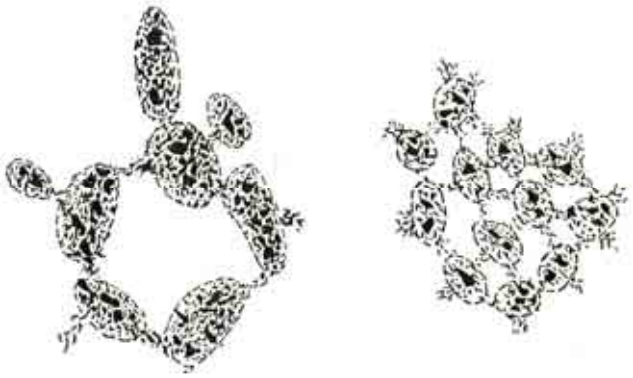

Figure 2.24 Undisturbed clay, schematic illustrated patterns. On the left-hand side, particle structure of marine clay and on the right-hand side lacustrine clay, modified after Pusch (1978)

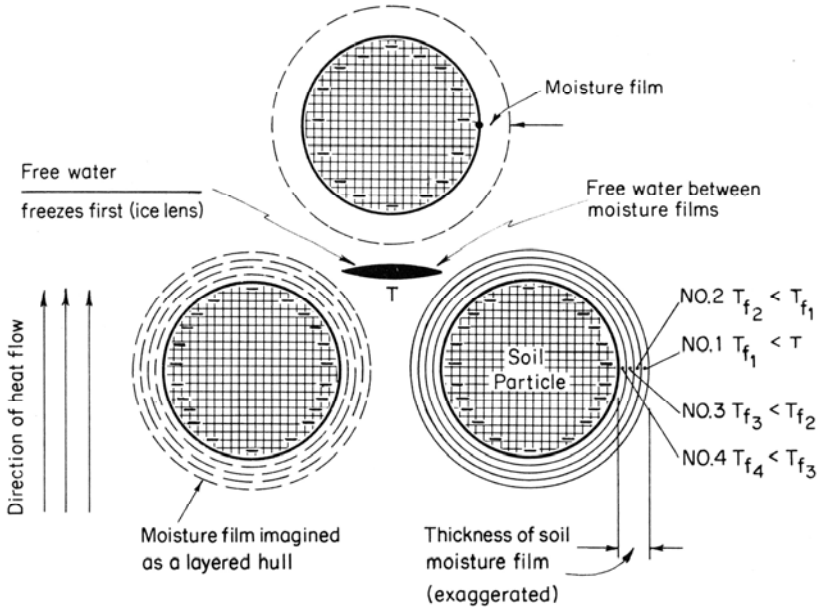

Figure 2.25 Symbolic illustration of freezing of soil moisture i.e. the free water and the moisture film around the soil particles, modified after Jumikis (1966)

Not all the water freezes at the same time when the freezing of pore water in the soil begins (Beskow, 1935; Pusch, 1962; Jumikis, 1966; Tsytovich, 1975; Knutsson, 1985A; Kujala, 1997). The progress of the freezing of the pore water depends on how strongly the water is bounded to the separate grains. In addition, the water is firmly bound to the grains in fine-grained soils, which is differently to more coarsely grained soils where, for example in medium sand almost all the water freezes to some degree below 0 °C. However, Jumikis (1966) has in laboratory tests shown that all the water is frozen at -78 °C in certain types of clay. In fact, the amount of unfrozen water depends greatly on the particle size and the clay particles specific area. The smaller the pores and the larger specific area of the clay structure, the lower the freezing point for the structure. The specific area can be related to

the soil's liquid limit. Figure 2.25 illustrates schematically how the unfrozen water bound to the soil particles freezes gradually in relation to the gradual fall in temperature; channels are thus created between the ice crystals that encourage passages of free water (Jumikis, 1966; Tsytovich, 1975; Knutsson, 1985A; Duquennoi, Fremond & Levy, 1989). The amount of unfrozen water as a function of temperature is shown in Figure 2.27 to Figure 2.30.

Figure 2.26 shows the adsorption-coat relation to the grain size for a coarsely grained soil (sand) and for a fine-grained soil (coarse clay). The respective tension spheres will lie as thin layers very close to the particle surface. When both soil types have equal loads, the load will be directly transferred to the contact surface in the more coarse soil, while the load in the fine-grained soil is transformed primarily in the pore water. "The adsorption water coats are in relation to the grain size very thin – if the soil type system is represented with the same particle size as the clay […] will the respective tension spheres lay as thin coats very close to the particle surface" (Beskow, 1935, p 43). For instance, if one presumes that both soils are subjected to the equal effective tension, the load in the more coarse soil will then be divided into fewer contact points than in the more fine-grained soil. The adsorption layers will in the more coarse soil become "significantly more squeezed out, between ice and soil particle will only a very thin adsorption layer, the most inner molecule layers to be located […]. The water flow to the ice crystals under-surface at the contact surfaces occurs through molecular migration – molecules from the adsorption-shale connect to the ice crystal, and are replaced via a fresh inflow of water […]. And the closer the water molecules are to the particle surface, the less mobility do they have, thus more firmly bound – the most interior molecule layers probably have a degree of stiffness comparable to the condition of solid bodies" (Beskow, 1935, p 44).

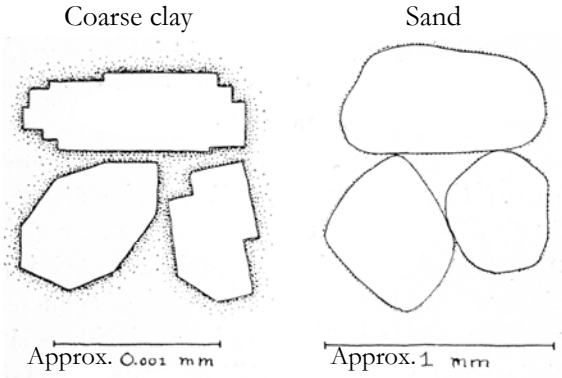

Figure 2.26 Schematic illustration of the relative importance of the adsorbed water films in fine-grained soil (coarse clay) and in coarse-grained soil (sand). The stippling depicts the magnitude of the force of adsorption, i.e. how much the water molecules are adhering to the particle surface. Both of the water-saturated soils are exposed to the same amount of moderate stress. Consequently, the surfaces of the sand grains have contact with each other, while the clay particles are separated by layers of adsorbed water. Modified after Beskow (1935)

The amount of unfrozen water depends on the surface force that determining the amount of water surrounding each respective particle. The closer one moves to the particles the larger becomes their force, which mainly consists of capillary- and adsorption forces. Consequently, the freeze temperature for the pore water close to the particles will so vary with the distance to the mineral particles, i.e. the freezing temperature will differ with the intensity of these forces. The mineral particles are thus surrounded by unfrozen water separating the ice from the mineral particles in the frozen soil (Beskow, 1935; Jumikis, 1966; Farouki, 2004).

Soil water content can be written

$$w\left[\%\right] = \frac{M_w}{M_s} 100 \tag{2.2}$$

where M_s = solids mass [kg], M_w = mass of water [kg] and w = water content [%].

The water content in the frozen soil forms by the sum of the unfrozen and the frozen water (Johnston, Ladanyi, Morgenstern & Penner, 1981; Andersland & Ladanyi, 2004)

$$w\left[\%\right] = w_u + w_i \tag{2.3}$$

and also (Johnston et al, 1981)

$$w\left[\%\right] = w_u + w_v + w_l \tag{2.4}$$

where w_i = total ice content [%], w_l = water content due to ice inclusions, such as ice lenses, ice crystals and coatings on soil particles [%], w_u = frozen soil, unfrozen water content at a given temperature [%] and w_v = water content due to pore ice [%].

The water content for frozen soil between the ice layers (w_b) then becomes (Johnston et al, 1981)

$$w_b\left[\%\right] = w_u + w_v \tag{2.5}$$

where w_b = water content for frozen soil between the ice layers, determined experimentally [%], w_u = frozen soil unfrozen water content at a given temperature [%] and w_v = water content due to pore ice [%].

All water contents are defined as the relationship between the water mass and the solid mass particles. Nevertheless, the values of the water content (w), the content of frozen soil between the soil layers (w_b) and the unfrozen water content in frozen soil (w_u) are normally determined experimentally. While the values of water content due to pore ice (w_v) and water content due to ice inclusions (w_l) normally are calculated due to Eq. (2.3) and Eq. (2.5) (Johnston et al, 1981). However, according to Fukada, Kim and Kim (1997) the unfrozen water content can be determined from the empirical equation

$$w_u\left[\%\right] = 21.18 e^{0.608\theta} \tag{2.6}$$

where w_u = frozen soil unfrozen water content at a given temperature [%] and θ = negative temperature [°*C*].

In the same fashion, Anderson and Tice (1971, from Sundberg, 1988) have shown that the theoretical connection for the course of the freezing is related to the soil's specific surface (which strongly increases with a decrease in grain size), see Figure 2.27. According to Anderson and Tice (1971, from Sundberg, 1988) the unfrozen water content can be calculated as stated by

$$w_u\left[\%\right] = \alpha T_n^{\beta} \tag{2.7}$$

where w_u = frozen soil unfrozen water content at a given temperature [%], T_n = (the absolute value of) temperature below 0 °*C* [°*C*] and β = characteristic soil parameter that depend on, among other things, the specific surface.

Frivik and Johansen (1980) have empirically shown that the freezing course in generally follows a straight line in a double logarithmic diagram with unfrozen water content and temperature below 0 °C as axis, as can be seen in Figure 2.28. While, Williams (1988)

empirically shows the unfrozen water content related to the dry density as a function of the freezing temperature, see Figure 2.29.

Similarly, Soviet scientists have also been described the amount of unfrozen water as a multiplication of the plastic limit and a soil characteristic parameter (Johnston et al, 1981)

$$w_u\left[\%\right] = k_u w_p \tag{2.8}$$

where w_u = frozen soil's unfrozen water content at a given temperature [%], w_p = plastic limit [%] and k_u = soil characteristic parameter circumstantial among others, the specific surface and the temperature [-].

The coefficient k_u that depend on above all the specific surface and temperature under 0 °C is empirically determined and shown in a double logarithmic diagram, see Figure 2.31.

The ratio between the mass of ice and the mass of water can be written (Johnston et al, 1981; Andersland & Ladanyi, 2004)

$$i_r\left[\%\right] = \frac{M_i}{M_w}100 \tag{2.9}$$

where i_r = relative ice content, i.e. "the iceness ratio" [%], M_i = mass of ice [kg] and M_w = total mass of water [kg].

On the other hand, for a soil constituting "layered or reticulate" structure, the relative ice content can be written (Johnston et al, 1981)

$$i_r\left[\%\right] = w_i - \frac{w_u}{w} = \left(w_v + w_l\right) - \frac{w_u}{w} \tag{2.10}$$

In the same fashion, Johnston et al (1981) depicts the relation for a frozen soil with a "massive structure"

$$i_r\left[\%\right] = \frac{w_v - w_u}{w} \tag{2.11}$$

where i_r = relative ice content, i.e. "the iceness ratio" [%], w = total water content [%], w_u = unfrozen water content [%] and w_v = water content due to pore ice [%].

The degree of saturation can be written (Lambe & Whitman, 1969)

$$S_r\left[\%\right] = \frac{V_w}{V_v}100 \tag{2.12}$$

where S_r = degree of saturation [%], V_v = volume of voids [m^3] and V_w = volume of water [m^3].

The total degree of saturation of frozen soil gives (dry soil, lack of ice; S_{ri} = 0 %, totally ice saturated soil; S_{ri} = 100 %. Ice density ρ_i = 916.8 kg m^{-3}) (Andersland & Ladanyi, 2004)

$$S_{rf}\left[\%\right] = S_{ri} + S_{ru} = \left(\frac{w_i \rho_w}{\rho_i} + w_u\right)\frac{G_s}{e} \tag{2.13}$$

where

$$S_{ri}\left[\%\right] = \frac{V_i}{V_v}100 \tag{2.14}$$

and

$$S_{ru}\left[\%\right]=\frac{V_{wu}}{V_v}100 \tag{2.15}$$

where G_s = specific gravity of solids = ρ_s/ρ_w [-], S_{rf} = total degree of saturation of frozen soil [%], S_{ri} = degree of ice saturation of frozen soil [%], S_{ru} = degree of unfrozen water saturation [%], V_i = volume of ice [m^3], V_v = volume of voids [m^3], V_{wu} = volume of unfrozen water [m^3], w_i = total ice content [%], w_u = unfrozen water content [%], ρ_i = density of ice [kg m^{-3}], ρ_s = density of solid particles [kg m^{-3}] and ρ_w = density of water at 4 ºC [kg m^{-3}].

Note that $\rho_w/\rho_i \approx 1.09$, and $2.6 < G_s \leq 2.8$ for mineral particles and $1.1 \leq G_s \leq 2.5$ for organic matter (Johnston et al, 1981).

Table 2.4 Soil water content, typical values of various saturated soils, after Pusch (1973)

Soil (saturated)	Water content (w) [%]	Remark
Peat	>500	Organic
Gyttja	150-300	
Clay, soft and medium	40-100	Non organic
Clay, stiff	10-30	
Silt	10-50	
Sand and gravel	10-35	
Till	5-10	

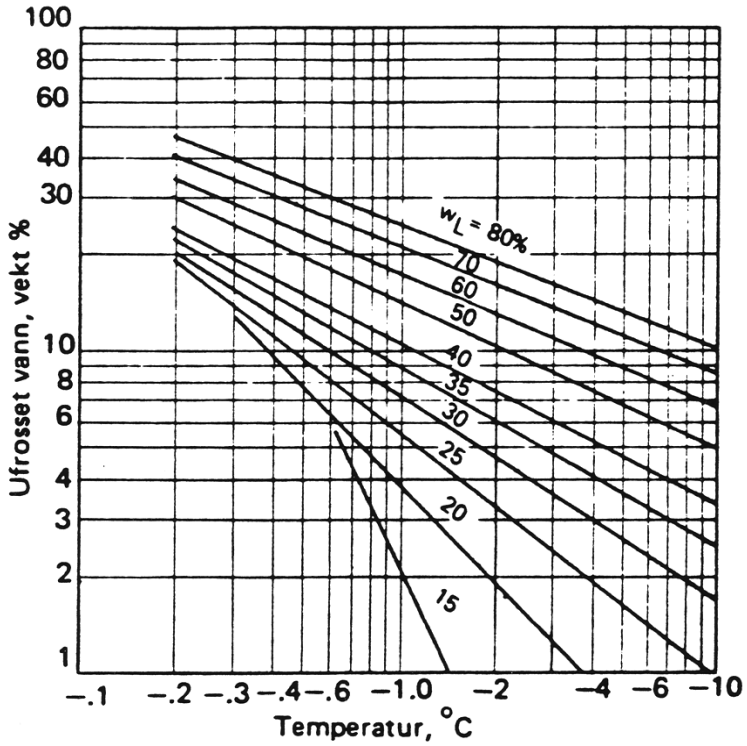

Figure 2.27 Amount of unfrozen water in various soils' liquid limit vs. the temperature below 0 °C, after Anderson and Tice (1971, from Knutsson, 1985A)

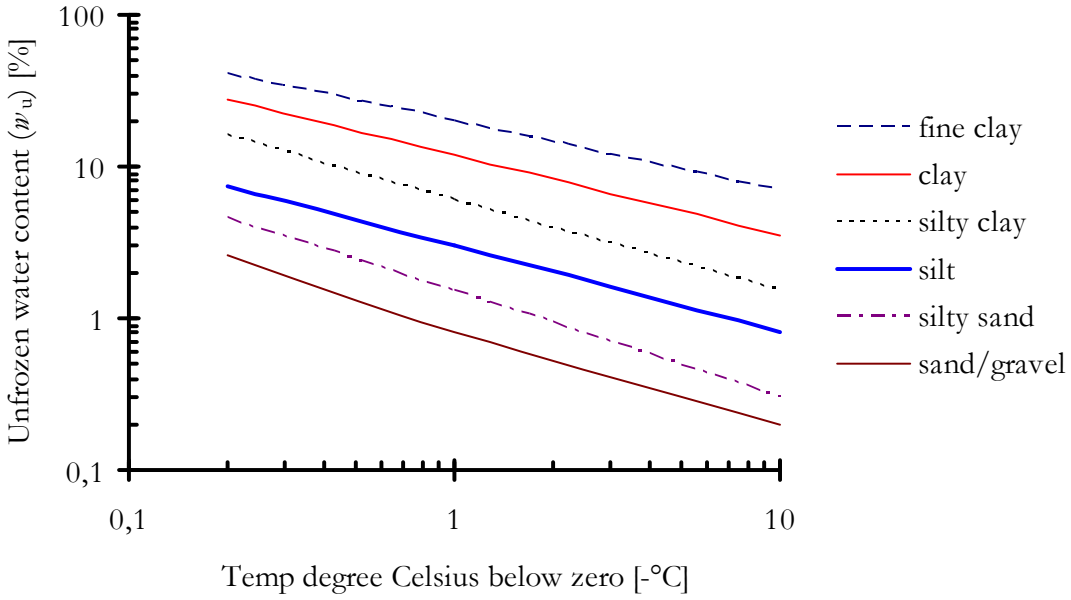

Figure 2.28 Unfrozen soil water content in various soils vs. the soil temperature below 0 °C, after Frivik and Johansen (1980), modified from Adolfsson, Franck, Rhen and Sällfors (1985)

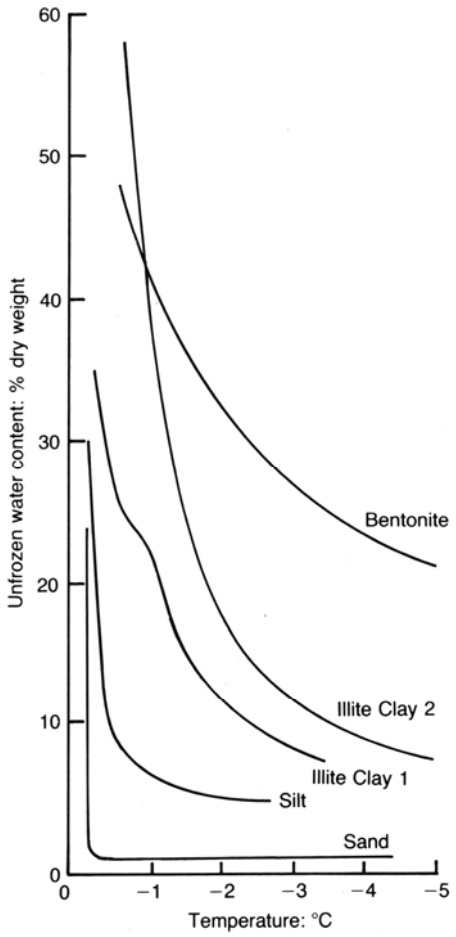

Figure 2.29 Unfrozen water content in various soils vs. the soil temperature below 0 °C, after Williams (1988, from Harris 1995)

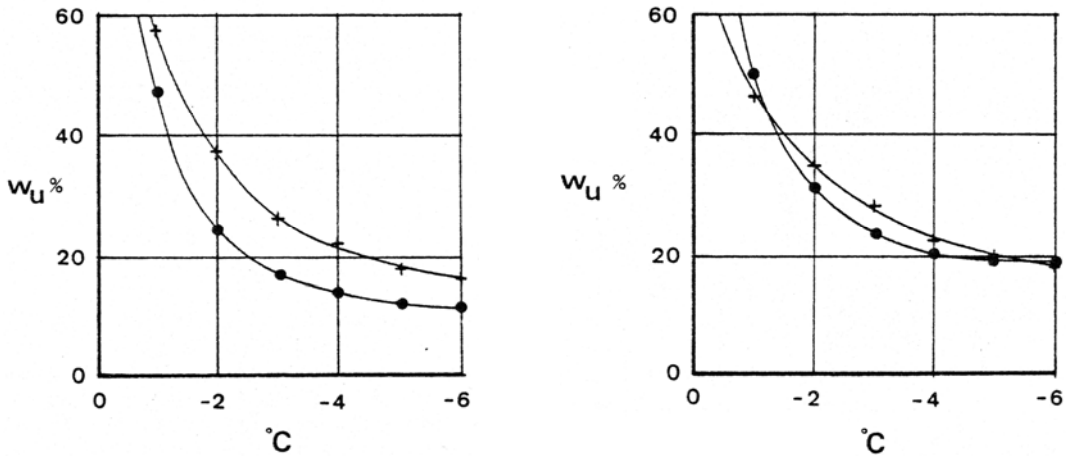

Figure 2.30 Unfrozen water content vs. the soil temperature. Two different clay types, one lacustrine (+Skå-Edeby) and one marine (• Lilla Edet). The figure on the left-hand side shows undisturbed clay. The figure on the right-hand side shows disturbed clay (remoulded). After Pusch (1978)

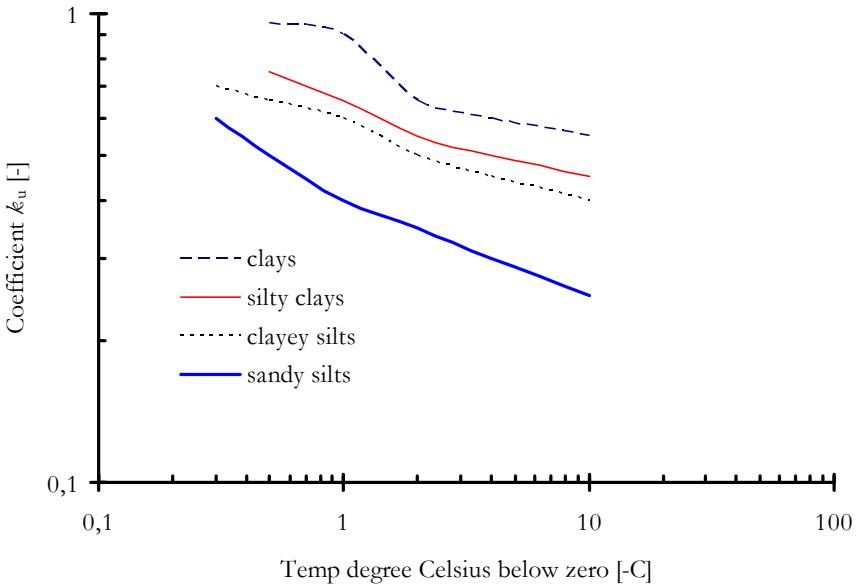

Figure 2.31 Coefficient k_u for unfrozen water content of various soils vs. the temperature below 0 °C, after USSR (1969, from Johnston, 1981)

2.7 FREEZING PROCESS

A number of physiochemical processes such as coagulation of soil colloids (dispersed finely divided substances), aggregation of clay particles and smaller clusters occur in connection with freezing of clayey soils with high water contents. This leads to that the density for the soil aggregates will become relatively high at the same time as the clayey soil gets a plastic consistency.

When freezing particularly fine-grained soils, a border zone is created during the freezing process between the frozen soil and the unfrozen soil where both free water and ice crystals exist in chaos. This zone is called frozen fringe. A hydraulic pressure gradient with

pore water under pressure next to the frozen soil arises in this edge zone. The effect of when water freezes at the ground frost front is the same as when the material dries out. However, in a frost susceptible material, the consequence is that pore water under pressure is created at the ground frost front, which tries to absorb water from the surrounding to normalize the pressure. Consequently, ice in the form of ice lenses or layers is created at the ground frost front. Depending on the properties of the soil material in relation to the endurance of the cold, the soil material can be more or less frost susceptible, i.e. the soil material's capacity to transport water to the freeze front gives the soil its ground frost heaving properties (Jumikis, 1966; Tsytovich, 1975).

The tensions and the prequalifications for the occurrence of deformations change during soil and rock freezing depend on, among other things, the temperature, ice/water's phase changes and particle rearrangement. These processes go on and accentuate during both the freezing phase and the thawing process. Different geophysical processes such as the creation of hydraulic pressure gradients because of temperature differences in the soil are generated in fine-grained soil with high levels of particularly silt fractions during the freezing. The pressure gradient that develops in the frost front gives origin to a pore water flow towards the relatively colder zone. Consequently, when this addition of pore water freezes, ice lenses with a quite high ice content are created in the soil which leads to that the soil mass expands and the frost will heave (Morgenstern, 1981).

The creation of ice lenses enriches the soil with water, and this together with in situ-water gives the frozen soil a lower bulk density and a higher water content compared to the original undisturbed soil (Harris, 1995).

Settlements arise during and after the thawing process in fine-grained soils with high contents of clay or silt. However, these settlements origin because of the draining of pore water during the simultaneous restructuring of the particles.

A determination of the soils' compression properties is often important for the establishing the foundation method, or to examine the influence of the environment due to changes of the ground water levels or loads. These properties can be decided with oedometer tests (CRS-tests or standard oedometer tests), compressometer tests or triaxial compression tests. The knowledge about the soils deformation properties under temperature influence is important at temporary stabilization and hydraulic sealing of soil and rock in urban areas, as large deformations can be initiated depending on which type of soil material has been frozen (Harris, 1995).

2.7.1 The soil frost action

Beskow (1935) has divided soil into six frost susceptible groups, with consideration of the soil's frost heaving and frost floating properties. The frost heaving and the frost floating properties are based on grain size, capillarity, and hygroscopicity. Presently, in Sweden classification according to, among others, Anläggnings AMA 98 (General material and work description for construction work 1998) and the National Road Administration (Vägverket) ATB VÄG 2004 (General technical description for highway construction, VÄG 2004), and SGF Laboratory direction, part 2; T21 (Swedish Geotechnical Organization for Laboratory directions), is used. Even if these classification systems are established for soils at shallow conditions, they can be used as guidance even for virgin freezing of deeper laying soils.

The National Road Administration has in *Allmän Teknisk beskrivning för Vägkonstruktion*, ATB VÄG 2004 (in Table A11.2), divided soil types for road technical use into four classes according to frost susceptibility. The classification is made with consideration of the soil

types' frost heaving properties during the frost process. The frost heaving behaviours are based mainly on the ratio of the fine grade soil.

SGF has in Karlsson and Hansbo (2000) divided the soil types into three frosts susceptible, with consideration on the soil's properties during frost heaving and thawing. This classification is based on the homogenous soil types' ratio of the fine grade soil, and gives approximate values of the judged frost susceptibility.

2.7.2 Deformations and stress conditions due to volume expansion during freezing

A "frost heave" occurs in shallow soils when "frost susceptible soils" expands. In deeper laying soil layers, depending on the circumstances is even the surrounding soil deformed of the frozen soils' expansion. This section describes the deformations that take place due to volume expansion in connection with freezing of the soil and the state of stress that occurs because of this deformation.

When water is transformed to ice, its volume increases with 9 %, see Figure 2.15. This volume expansion leads to "frost erosion" in closed systems. The freezing point for water is reduced with 0.0074 ºC bar^{-1} due to the increasing pressure in soil (NE, 2005). However, the volume increases in connection with that soil freezes, depending on the soil water content.

Freeze tests have shown that clay particles are accumulated in aggregates without inner interruptions during the freezing process. The tests have also shown that much of the water bounded to the particles do not freeze in the interval of 0 ºC to -5 ºC (Pusch, 1979). Different structures of the soil affect the freezing. The amount of unfrozen bound water increases radically when the pores of the particle accumulations are saturated of water, for example fresh water. The reason for this is that the minerals from the freshwater clay sediments expose a larger area against the pore water. On the contrary, salt-water clay sediments normally consisting of large particle aggregate and separated by larger distance from each other, contains a smaller amount of unfrozen water, compared to freshwater clay sediments (Pusch, 1979).

The freeze effect is the same as if the material has dried out when the water freezes at the freeze front. This can be compared to "freeze-drying" of provisions. The consequence is that the under pressure of the pore water created at the freeze front in frost susceptible soil, "absorbs" the water from adjacent areas in the frozen soil which in turn freezes on earlier frozen water. Ice lenses are then created in ground frost sensitive soils at the freeze front. Water saturated conditions are usually presumed in deeper laying soil in connection with soil-and rock stabilization and hydraulic sealing through freezing.

The clays consolidation process during thawing depends on many factors –physical and mechanical properties of water and ice are of important influential factors. The influence of structural changes in the permeability after a freeze- and thawing cycle, are best described through the stress development in the soil (Nixon & Morgenstern, 1973). The effective stress, i.e. the load taken up by the soil skeleton is proportional to the load minus the pore water pressure

$$\sigma' = \sigma - u \tag{2.16}$$

where u = pore pressure [kPa], σ = total stress, the soil specimen surcharge [kPa] and σ' = effective stress, the load on the soil skeleton [kPa].

Chamberlain and Gow (1978) show the theorized thaw consolidation process with help of Figure 2.32; undisturbed, unfrozen clay, consolidated at point *a* on the virgin compression

curve, i.e. the pore water pressure is zero and the effective stress according to Eq. (2.16) are the same size as the total stress. The sample is subsequently left to freeze with free access to water. During the freezing, the clay sample gets a net-increase of the void ratio to point *b*, because the water absorption from the reservoir and its (the water's) volume expansion. The strong under pressure created at the freeze front, explained above, causes an increase in the effective stress immediately in front of the freeze front. Segregated ice layers, i.e. separate bands of ice layers (and soil layers) are created and the soil bands obtain in this way overconsolidated properties at point *b'*. A development of the stress according to *b'-c* and finally to point *c* where the pore pressure is in equilibrium with existing load, take place under the thawing process. The clay sample has at point *c* gone through a net-decrease of the void ratio from point *a* to point *c*. Nevertheless, according to Chamberlain and Gow, the consolidation pressure under natural conditions can reach 3.8 MPa.

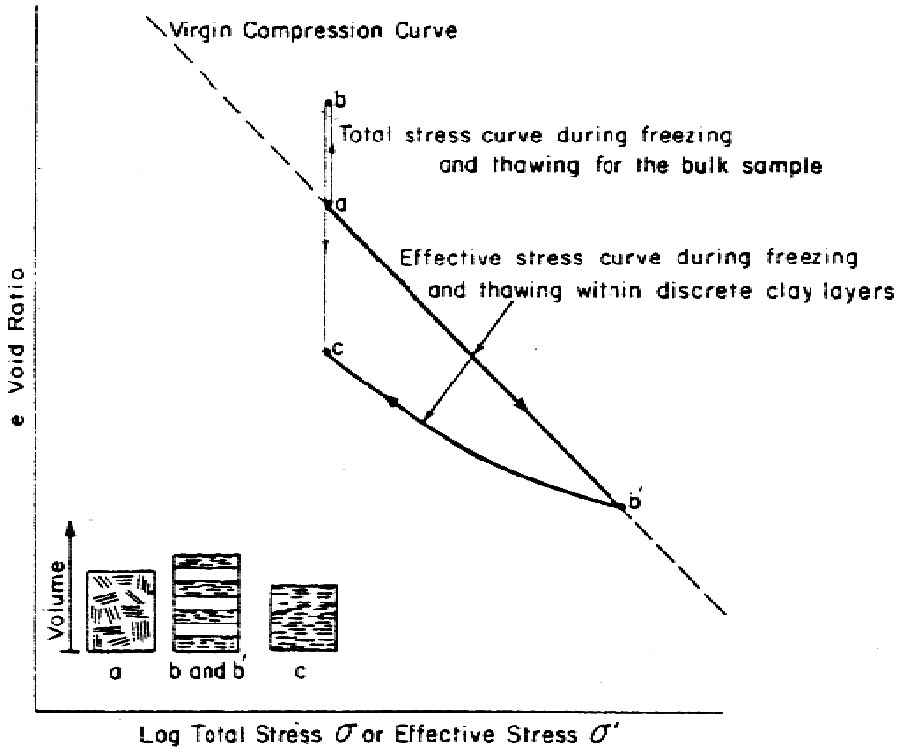

Figure 2.32 The void ratio as a function of the stress, under a freeze- and thaw cycle in clay. The undisturbed soil sample freezes with free access to water at ***a****. At* ***b****, the void ratio has increased because of water absorption and its volume expansion. Segregated layers with ice and clay are created, the clay gains overconsolidated properties at* ***b'****. The test is thawed during* ***b'-c*** *and gets at* ***c****, when the sample's pore pressure is equal with the load, a net-decrease in porosity (****a-c****), after Chamberlain and Gow (1978)*

As can be seen in Figure 2.33, Chamberlain and Gow (1978) show for the Morin clay that in both the void ratio vs. effective stress and the permeability vs. the void ratio planes, the curves for the unfrozen and the thawed states converge at the shrinkage limit void ratios. Chamberlain and Gow state that "this appears to indicate that the shrinkage limit void ratio is the value below which no changes in void ratio or permeability can be imparted by freezing and thawing" (pp 42-43). On the other hand, as can be seen in Figure 2.34, the shrinkage limit void ratio can not be observed for the CRREL clay. Chamberlain and Gow call attention to the fact that "some other factor may be limiting the effects of freezing and

thawing on these materials" (Chamberlain & Gow, 1978, p 43). However, Chamberlain and Gow report structural changes in consolidated clay slurries, which results in large increases in vertical permeability, the larger plasticity index, the larger vertical permeability.

Different properties of the soil create different conditions for the binding of water and grains, and also for the transportation of water to the freeze front from the unfrozen material, thus contributing to an increase in the water content of the frozen material. Considerable pressures can build up due to the heaving created when water is phase changed to ice; which has been accounted for above. In the freezing project of "Storebælt eastern railway tunnel in Denmark" 1994, the relation between hydraulic permeability and ground frost heaving was examined, see Figure 2.35 (Kofoed & Doran, 1996).

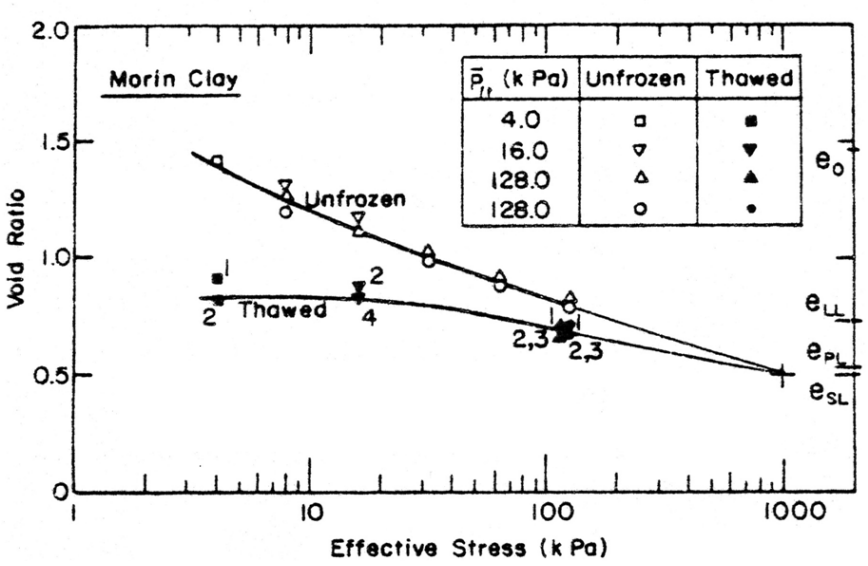

Figure 2.33 The effect of a freeze- and thaw cycle. The void ratio as a function of the effective stress for Morin clay, after Chamberlain and Gow (1978)

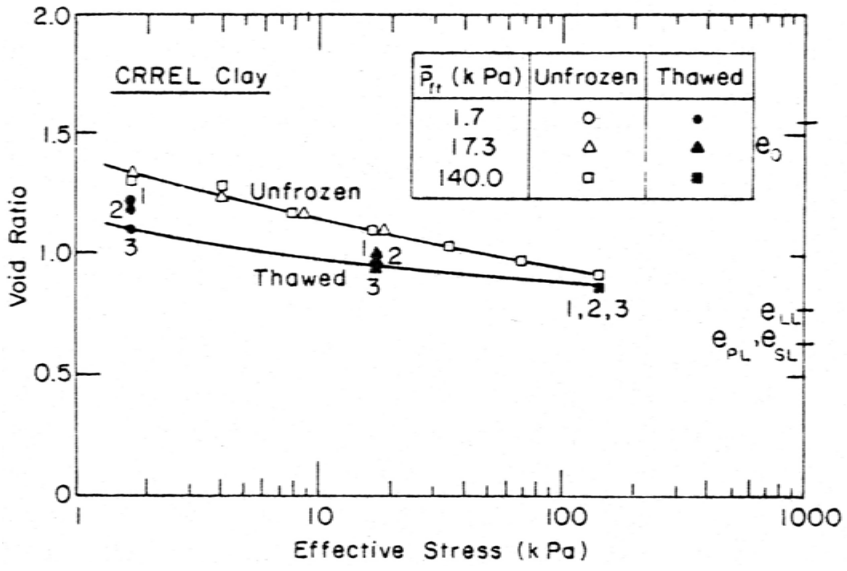

Figure 2.34 The effect of a freeze- and thaw cycle. The void ratio as a function of the effective stress for CRREL clay, after Chamberlain and Gow (1978)

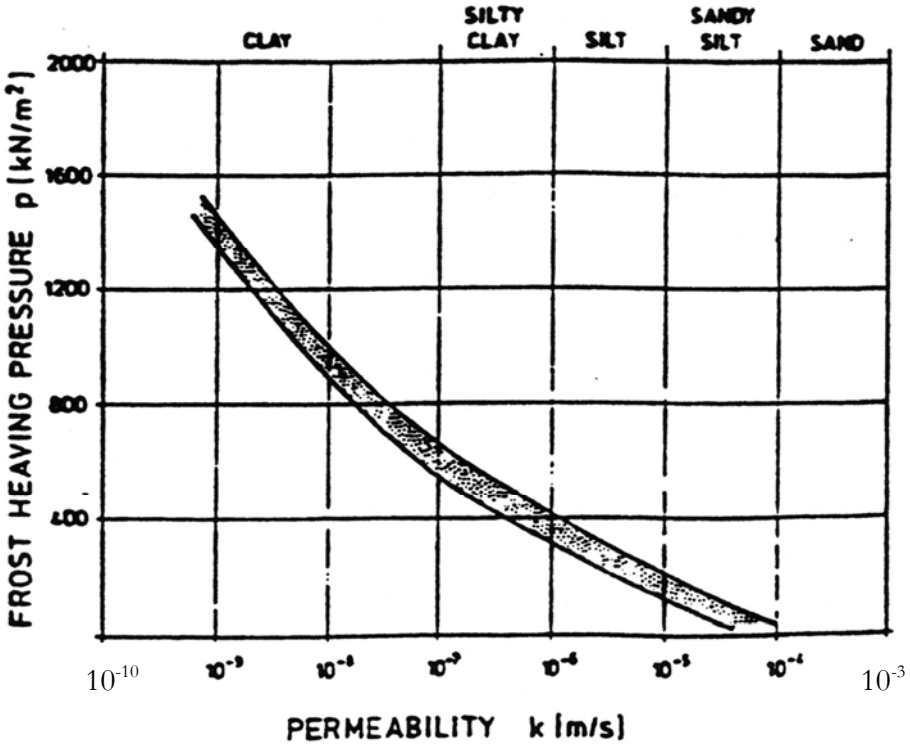

Figure 2.35 The ground frost heave pressure as a function of the soil's permeability, modified after Jessberger et al (1990, from Kofoed & Doran, 1996)

Beskow (1935) has described the challenges of ground frost for shallow condition, i.e. natural seasonally frozen ground. Hence, one example assumes that the creation of ground frost in sand, an "open pore system", does not generate heaving as the pore system allows water to flow downward (outward). Such a coarsely grained soil does not allow for the water molecules from the "warm" soil to "wedge" themselves in between the soil particles' surface and the ice surfaces of the freeze front. Consequently, no expansion occurs during such circumstances. This depends on the increase of the volume of water in connection with the phase change of the water from liquid to ice, which squeezes the equivalent quantity volume of water out of the pore system without an expansion of the pore system. Water-saturated sand will therefore decrease under the freezing to a corresponding grade of 1/10 of its original water volume (Beskow, 1935). However, in cases when sand creates a closed system, i.e. in a system where water cannot flow out of the system, an expansion will come about that equals 1/10 of the frozen water volume (Beskow, 1935).

Khakimov (1966) shows that the squeezed out water volume for deeper laying soil is equal throughout the whole sand layer's height during the growth of the frozen radius, during the course of the time. The water content of the saturated sand will hence decrease under the freezing process during the growth of the frozen radius (ξ) by dξ under the influence of the time dt according to (Khakimov, 1966)

$$\pi\left[\left(\xi+\mathrm{d}\xi\right)^2-\xi^2\right]n\alpha=2\pi k_\varphi I\xi\mathrm{d}t \tag{2.17}$$

where I = hydraulic gradient, k_φ = permeability of sand [m h^{-1}], n = porosity of sand, a = the coefficient of water expansion due to the phase change (water to ice, a = 0.091), ξ = frozen radius and dξ = the growth of the frozen radius during the time dt.

Neglecting the second-order infinitesimals in Eq. (2.17), obtaining (Khakimov, 1966)

$$\frac{\mathrm{d}\xi}{\mathrm{d}t} = \frac{k_\varphi I}{n\alpha} \tag{2.18}$$

notations see above.

Water saturated clayey soil has according to Khakimov (1966) low permeability. This results in that water that is "squeezed" out during the freezing barely gets absorbed by the unfrozen zone. A pore water pressure arises on the surface of the frozen cylinder partly because of the water expansion in connection with its phase change to ice, and partly because of the unfrozen clay's resistance. The pressure in the border zone between the frozen and the unfrozen water will create a displacement of the unfrozen soil; i.e. it will push unfrozen soil in a radial direction in relation to the frozen cylinder. In addition, Khakimov depicts the freeze process in sandy soil; "Assuming a freezing cylinder with the height of 1 m and a radius ξ lying at a considerable depth, the extent of the radial displacement can be determined by the following formula derived for a compound pipe" (Timoshenko, 1932, from Khakimov, 1966, p 57)

$$\delta = p(\xi - \delta)\left\{ E_\mathrm{u}^{-1}\left[\frac{C^2 + (\xi-\delta)^2}{C^2 - (\xi^2 - \delta)^2} + \eta_\mathrm{u}\right] + E_\mathrm{f}^{-1}\left[\frac{(\xi-\delta)^2 + r_0^2}{(\xi-\delta)^2 - r_0^2} - \eta_\mathrm{f}\right]\right\} \tag{2.19}$$

where C = the distance from the cylinder axis at which the influence of the pressure (p) on the thawed soil can be neglected [$C >> \xi$], E_f = compression modulus of the frozen soil, E_u = compression modulus of the thawed soil, p = pressure on the freezing cylinder surface, r_0 = radius of the freezing pipe, δ = radial displacement, ξ = radius of the freezing cylinder, η_f = Poisson's ratio for the frozen soil and η_u = Poisson's ratio for the unfrozen soil.

A simplification of Eq. (2.19); neglecting the term $(\xi-\delta)^2 C^{-2}$ as a very small fraction of unity, the load on the frozen cylinder's surface (p) and the radial displacement (δ) are "unknown". In the absence of a vertical displacement, Khakimov (1966) neglects the variation in volume of the soil skeleton with the temperature. However, Khakimov calculates the radial displacement of the frozen soil as

$$\delta_\mathrm{f} = \left[-1 + (1 + n\alpha i)^{1/2}\right]\xi \tag{2.20}$$

where δ_f = radial displacement of the frozen soil, i = "the iciness", n = porosity, a = coefficient for volume expansion of the water in connection with phase conversion to ice.

The compression module for frozen soil (E_f) is significantly larger that the compression module for thawed soil (E_u), therefore the displacement of the frozen can be estimated from the displacement of the thawed i.e. $\delta_\mathrm{f} \approx \delta_\mathrm{u}$ (Khakimov, 1966).

In a closed system the relation between ground frost heaving and initial content of pore water before freezing is described with the empirical equation (Changjiang & Chongyun, 1983)

$$\sigma_\mathrm{no} = ae^{-b/w} \tag{2.21}$$

where a and b = experimentally determined coefficients related to soil, temperature and area of the foundation plate, w = initial water content, σ_no = normal heave pressure acting upon the foundation bearing plate.

On the contrary, in an open system, the amount of pore water supplied during the freezing is more important. As a result, Changjiang and Chongyun (1983) report results from experiments showing; the greater the amount of water supplied, the larger the normal frost heave pressure will be. However, the empirical relationship can be expressed as (Changjiang & Chongyun, 1983)

$$\sigma_{no} = \sigma_{no}^{o} K Q \tag{2.22}$$

where K = experimental determined coefficient related to the soil and freezing conditions, Q = amount of migrating water in the freezing process, σ_{no} = normal heave pressure acting upon the foundation bearing plate, σ_{no}^{o} = normal frost heave pressure without migrating water.

Deformation due to creation of ice lenses, the capillary model

The ground frost heaving is, as mentioned above, a result of an increase in the soil's water content that occurs because of the migrating of water to the freeze front in connection with freezing. The increase in the soil's water content occur in ground frost susceptibility soil, generally in shape of segregated ice lenses or layers in the frozen soil. Whereas, the pressure difference between the ice and the water phase in the soil can be viewed as a fall in pressure in the pore water pressure, and it is this fall in pressure that is responsible for the migration of water to the freeze front (Williams, 1967).

The pore water pressure in the capillary model is related to the radius of the curvature of ice trying to penetrate through the pore neck, see Figure 2.36. However, the Kelvin equation gives the pressure difference between the ice and adjacent water (Williams, 1967; Harris, 1995)

$$u_i - u_w = \frac{\mathrm{d}\left(\sigma_{iw} A\right)}{\mathrm{d}V_i} \tag{2.23}$$

where A = area of ice-water interface (i.e. surface area of ice crystal (s)), u_i = pressure of ice (depending of vertical pressure such as the surcharge (γz) and the horizontal pressure similar to passive earth pressure), u_w = pressure of water, i.e. the pore water pressure ($\gamma_w(z-x)$), V_i = volume of ice crystal (s), σ_{iw} = surface tension ice-water, i.e. interfacial energy ice/water (≈ 0.0331 N m^{-1}, author note).

Simplifying Eq. (2.23), Williams (1967) presents the capillary model with the pores in the soil illustrated as cylindrical capillaries and the ice-water interface as hemispherical, when the interface is within a pore

$$u_i - u_w = \frac{2\sigma_{iw}}{r_c} \tag{2.24}$$

where r_c = radius of the curved interface. Note, the radius of the interface is less than the pore, since the presence of an adsorbed, unfrozen water layer on the pore walls, u_i = pressure of ice (depending of vertical pressure such as the surcharge (γz) and depending the horizontal pressure similar to passive earth pressure), u_w = pressure of water, i.e. the pore water pressure ($\gamma_w(z-x)$), σ_{iw} = surface tension ice-water, e.g. interfacial energy ice/water (≈ 0.0331 N m^{-1}, author note), see Table 2.5.

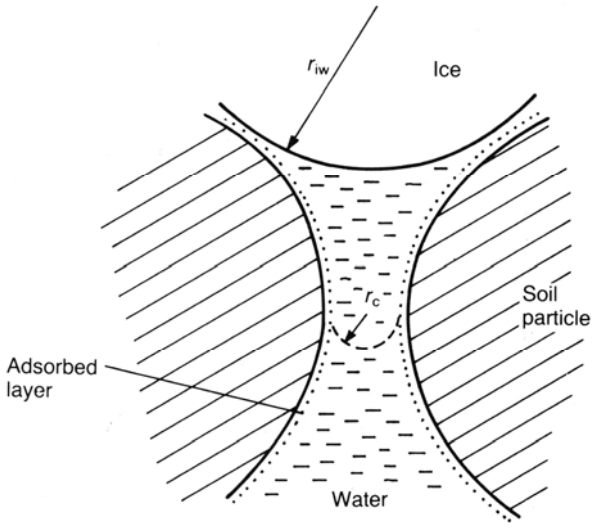

Figure 2.36 Schematic illustration of the pore neck in the capillary model, i.e. the theorized capillary pore, after Williams (1967, from Harris, 1995)

Table 2.5 Illustration of the pressure difference "$u_i - u_w$" that occur between the ice and the water phase for a few soils at the freeze front, modified after Williams (1967)

Soil type	$u_i - u_w = \frac{2\sigma_{iw}}{r_c}$ [kPa]
Coarse sands, or coarser material only	0
Medium and fine sands, or coarse silty sands	0-7.5
Medium silts, or mixed soils with small amounts <0,006 mm particle diameter	7.5-15
Largely fine silts, or silts with some clays	15-50
Silty clays	50-200
Clays	>200

Conversely, the capillary model can, yet, not be adopted on colloid soils where all water is absorbed (Harris, 1995).

Deformation due to ice lens build up, segregation potential model

Konrad and Morgenstern (1980, 1981, 1982, 1983) have developed another method, "segregation potential" (SP) that predicts one-dimensional frost heave to number velocity. The authors of the articles suppose that the over laying frozen soil does not partake in any mass transportation after that the ice lens is created, water is instead transported to the ice lens from the unfrozen zone through a thin zone of partly frozen soil, i.e. the frozen fringe.

When a soil sample freezes under different temperature steps on the "cold" side of the frozen fringe, but with the same temperature on the "warm" side, the water velocity towards the ice lens (v_0) will be proportional to the temperature gradient in the frozen fringe, see Figure 2.37 and Figure 2.38 (Konrad & Morgenstern, 1981)

$$v_o = \text{SP grad } T \tag{2.25}$$

where grad T = temperature gradient in the frozen fringe, SP = segregation potential, v_o = water intake flux (towards the frozen zone), and (Morgenstern, 1981)

$$\mathrm{SP} = \left| \frac{H_w - h_u}{T_s} \right| \bar{K}_f \tag{2.26}$$

$$\text{grad } T = \frac{T_w + |T_s|}{lt} = \frac{T_w}{l_u} \tag{2.27}$$

and where h_u = suction at the frozen-unfrozen interface, H_w = total potential, = overall permeability, l = thickness, l_u = thickness of the unfrozen soil, t = time, T_s = segregation freezing temperature andT_w = warm plate temperature, (notations see also Figure 2.38).

When the flow of water towards the ice lens can be calculated, can also the frost heave be calculated as the water freezes at the ground frost front on the ice lens. The heave of the soil will thus be proportional to the amount of water and the water's expansion in connection with its phase change during the freeze process. The SP will for a given soil have a connection between the heat flow and the mass flow (the water). This signifies that a slow freezing in practice gives a larger growth of ice lenses, see Figure 2.39**.** According to the same figure; if two identical samples are prepared with different boundary conditions, so that different temperature gradients are obtained between the frozen and the unfrozen soil, it will affect the thickness of the frozen fringe. That is, the freeze front advances the same distance (D*X*) in the same time (d*t*), but the result is a dissimilar temperature distribution, which is indicated by Figure 2.39. The size of the shaded area in the figure and the area of the frozen fringe at the time *t* can be interpreted as a measurement of the cooling of the frozen fringe (Morgenstern, 1981).

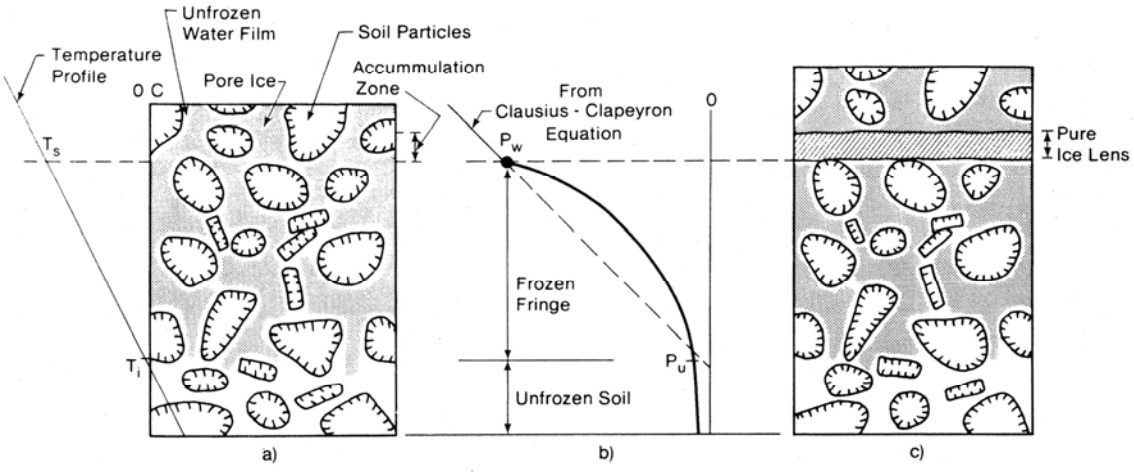

Figure 2.37 Illustration of the mechanisms for ice-lens creation a) shows the temperature gradient between the unfrozen soil and the ice lens, b) the pressure conditions and c) the heave as effect of ice lens creation, after Konrad and Morgenstern (1980)

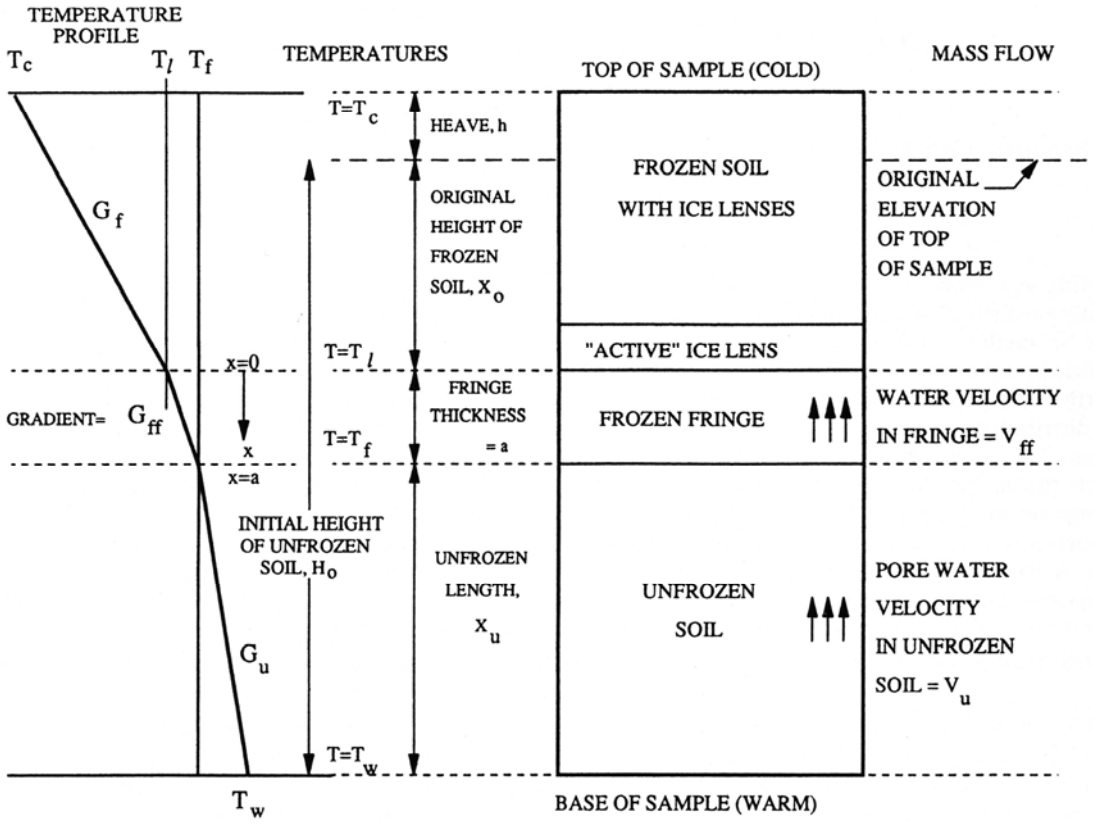

Figure 2.38 Idealized one-dimensional frost heave in a soil column, after Nixon (1992)

Konrad and Morgenstern (1981) show that the value of SP is given by a straight line of the function in Figure 2.40 and consists of the total pressure potential (under pressure) at the freeze front (p_w), the pressure potential between the frozen and unfrozen interface (p_u), the segregated freeze temperature (T_s) and the average hydraulic conductivity in the frozen fringe (Andersland & Ladanyi, 2004).

SP for a given soil decreases with increased overburden pressure. Konrad and Morgenstern (1981) show the influence of the load on the SP with the empirical equation (see also Table 2.6, Figure 2.41, Figure 2.42 and Figure 2.43) (Konrad & Morgenstern, 1981; Andersland & Ladanyi, 2004)

$$SP = SP_0 e^{-ap_e} \tag{2.28}$$

where a = empirical soil constant, p_e = applied pressure (or effective overburden pressure) and SP_0 = the value of SP obtained for zero applied pressure.

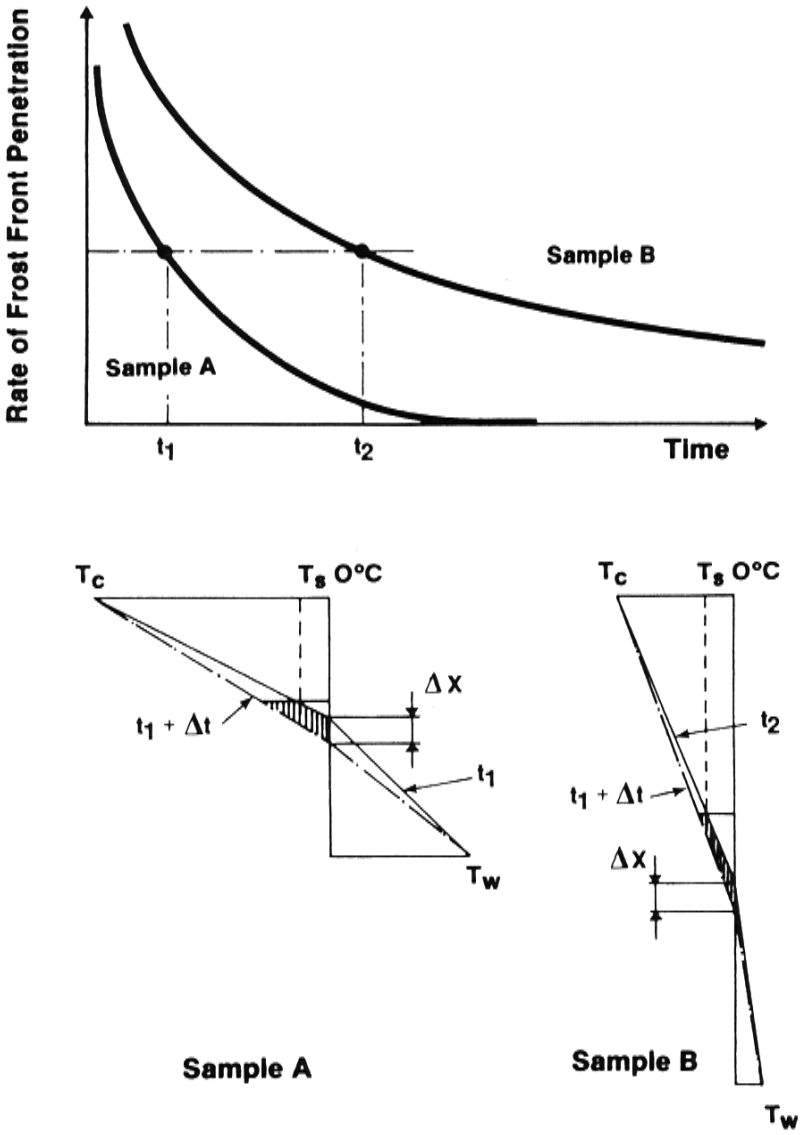

Figure 2.39 The influence of different freeze velocities on the frozen fringe. The sample A has a larger temperature gradient in the frozen fringe ($T_{cA} > T_{cB}$) at the same frost front advance (DX). The frozen temperature $T_{sA} = T_{sB}$. The shaded area together with the area of the frozen fringe represents the cooling of the frozen fringe, after Konrad and Morgenstern (1982)

When SP is calculated with consideration of stress and the soil constant, the heave rate can be calculated according to (Nixon, 1987)

$$\frac{\mathrm{d}h}{\mathrm{d}t} = \frac{1{,}09\mathrm{SP}^* \cdot G_\mathrm{f}}{1 + L \cdot \mathrm{SP}^* \cdot k_\mathrm{f}^{-1}} \tag{2.29}$$

where $\mathrm{d}h/\mathrm{d}t$ = the rate of the frost heave, G_f = temperature gradient in frozen soil, k_f = frozen soil thermal conductivity, L = volumetric latent heat of water and SP* = V_ff / G_ff ("redefined") segregation potential.

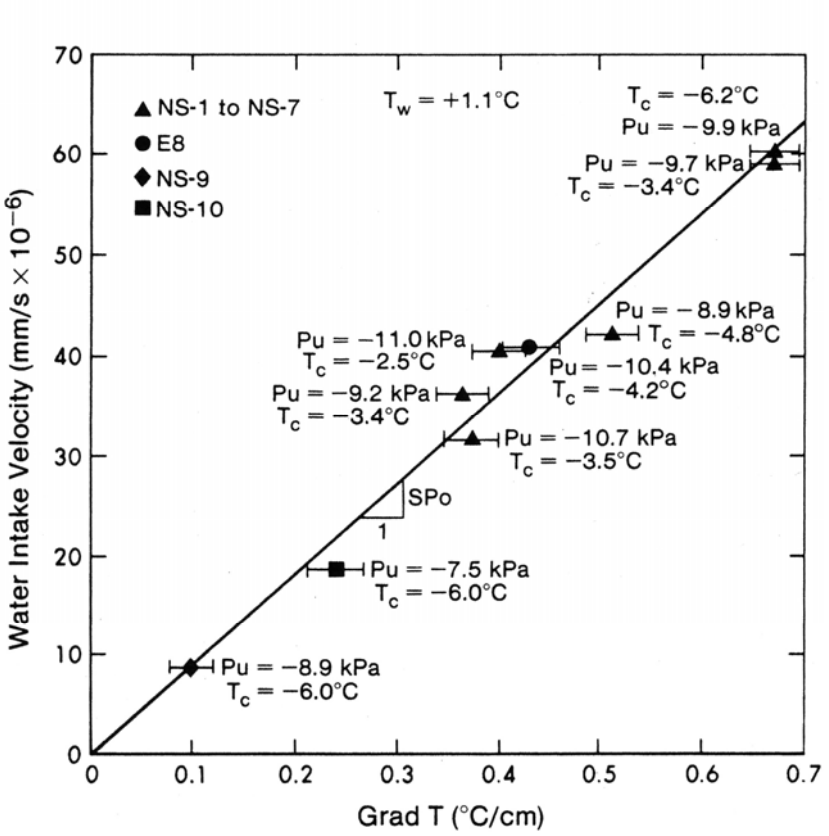

Figure 2.40 Active system during the creation of the ice lens, i.e. the relation between the velocity of the pore water towards the frost front and the temperature gradient in the frozen fringe, after Konrad and Morgenstern (1981)

The SP varies according to Nixon (1987) from 50 to $200 \cdot 10^{-5}$ mm^2 s^{-1} °C^{-1} for clay and clayey silt. The necessary hydraulic conductivity needed to predict the heave is given through the one-dimensional equation (Nixon, 1991)

$$\frac{V_{ff}}{G_{ff}} = SP^* = \left\{ \frac{L}{k_f} + \frac{\left[\frac{\alpha+1}{\alpha} \left(1{,}09\, p_0 - p_u \right) \right]^{\alpha}}{k_0 \beta^{1+\alpha}} \right\}^{-1} \tag{2.30}$$

where G_{ff} = temperature gradient in the frozen fringe, k_0 = hydraulic conductivity at -1 °C, k_f = thermal conductivity of frozen soil, L = volumetric latent heat of water, P_0 = overburden pressure [g cm^{-2}], p_u = excess pore pressure [g cm^{-2}], SP* = V_{ff}/G_{ff} ("redefined") segregation potential, V_{ff} = pore water velocity in the frozen fringe and β = thermodynamic constant equal to 12 400 cm water pressure per °C.

In addition, the subscript "ff" refers to the freezing fringe. Furthermore, "A plot of $(G_{ff}/V_{ff} - L/k_f)$ against $(1.09P_0 - P_u)$ on a log-log plot should have a slope of α and an intercept equal to $[(\alpha + 1)\, \alpha^{-1}]^{\alpha}\, (k_0\, \beta^{(1+\alpha)})^{-1}$." (Nixon, 1992, p 491). The ratio $L\, k_f^{-1}$ is close to being a constant for many soils and equal to a value of approximately 0.002 [mm^2 day^{-1} °C^{-1}]$^{-1}$ (Nixon, 1992).

The flow through the freezing fringe is assumed to be controlled by the Darcy's law. However, the hydraulic conductivity in the frozen soil in the "freezing fringe" is given through (Nixon, 1992)

$$k = k_0 \left(-T^{-\alpha}\right) \tag{2.31}$$

where k = hydraulic conductivity, k_0 = hydraulic conductivity at -1 °C, T = temperature [°C] and a = exponent for hydraulic conductivity (the slope of the relationship between k and ($-T$) on a log-log plot).

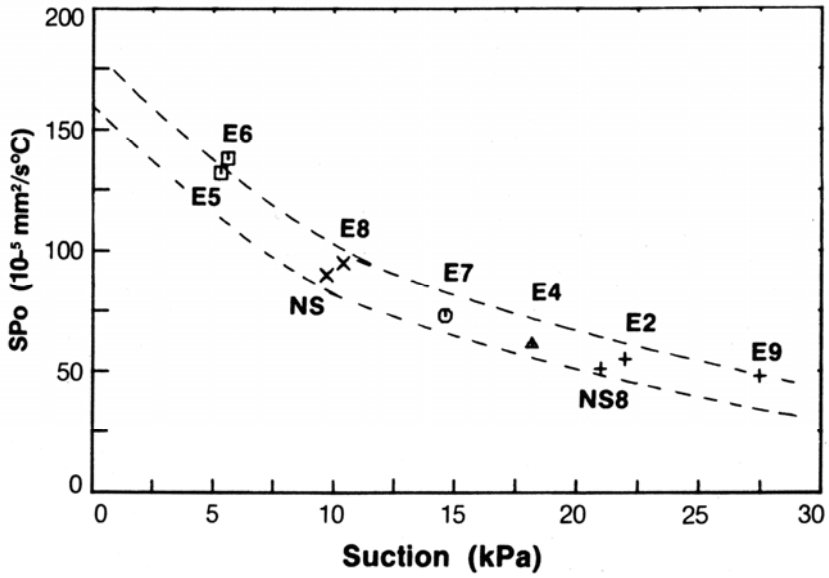

Figure 2.41 Segregation potential (SP) as a function of the under pressure (suction) in the frozen fringe for Devon silt, after Morgenstern (1981)

Konrad (1989B) has shown that the SP is dependent on both the surcharge and the salt content. Soil free of salts without a surcharge load that freezes gives according to tests SP = $200 \cdot 10^{-5}$ mm^2 day^{-1} °C^{-1}. In contrast to the soil free of salts, the same soil adopted with salts in pore water concentration of 8 g L^{-1} showed a considerable lower value of the SP; namely $50 \cdot 10^{-5}$ mm^2 day^{-1} °C^{-1}. This corresponds to a reduction of the SP of approximately 75 %.

Comparable tests on a soil free of salt and with a load amounted to 50 kPa gave a SP of $90 \cdot 10^{-5}$ mm^2 day^{-1} °C^{-1}. In the same fashion as in the test without a surcharge, the same soil adopted with salts in pore water concentration of 8 g L^{-1} and a surcharge load of 50 kPa also showed a considerable lower value of the SP amounted to approximately 78 % (Konrad, 1989B).

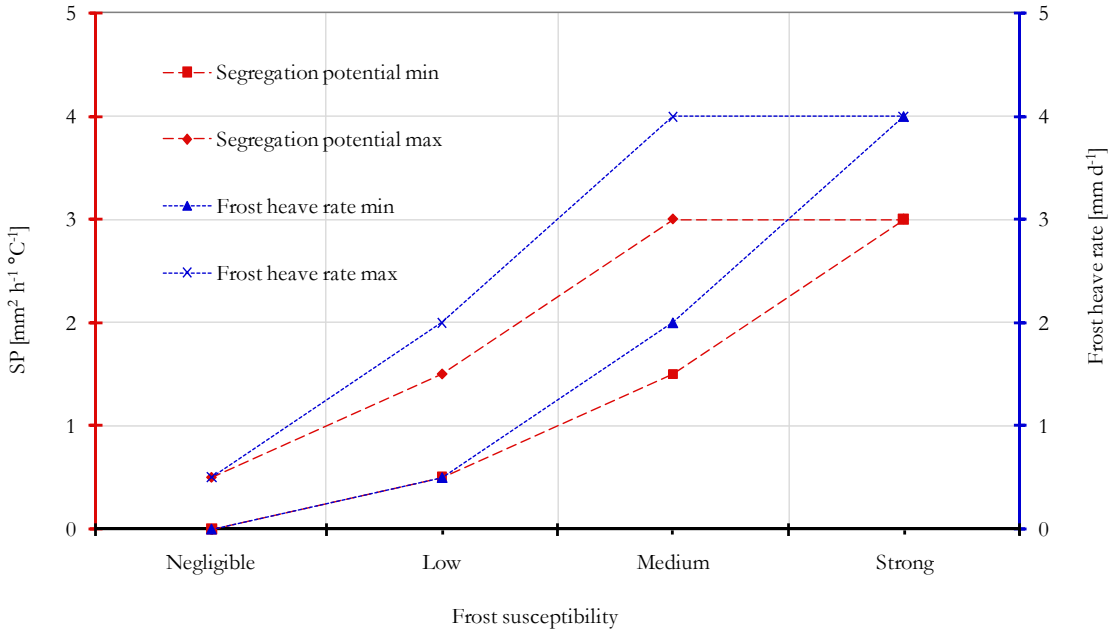

Figure 2.42 Segregation potential (SP) and the frost heave rate as a function of the frost susceptible from Table 2.6

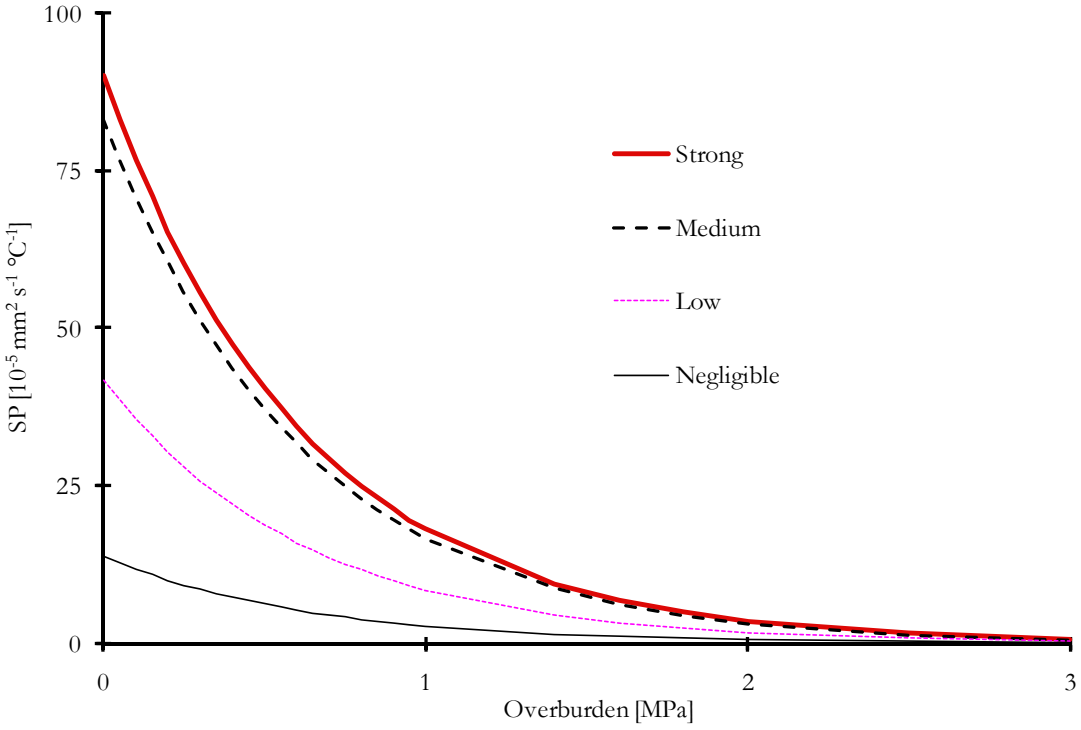

Figure 2.43 Segregation potential (SP), due to the frost susceptibility, the class and the overburden. The frost susceptibility classes denote "Strong", "Medium", "Low" and "Negligible". From Eq. (2.28) with SP values from Table 2.6 and α = -1.6 MPa^{-1}

Table 2.6 Frost susceptible soils, according to ISSMFE (1989), modified from Harris (1995)

Frost susceptibility class	Soil type (USCS)	Soil type (Equivalent)	Fines factor[1] (R_f)	Capillary rise[2] (H_C) [m]	Liquid limit (w_L)	Liquidity index[3] (I_L)	Plasticity index (I_p)	Segregation potential[4] (SP_c) [mm^2 h^{-1} °C^{-1}]	Segregation potential (SP_c) [×10^{-5} mm^2 s^{-1} °C^{-1}]	Frost heave rate[5] [mm days^{-1}]
Negligible	GW, GP, SW, SP	Gravel, sand	<2.5	<1		≤0	<1	<0.5	<14	<0.5
Low	CH	Clay high pl	2.5 – 5	1.0-1.5	>50	<0.25	≥7	0.5 - 1.5	14 – 42	0.5 - 2
Medium	CI	Clay	5 – 10	1.5-2.0	35-50	0.25 - 0.50	≥7	1.5 - 3.0	42 – 83	2 - 4
	OH[6], MH	Org clays, fine sand, silt			>50		≥7			
Strong	CL	Clay low pl			<35		≥7			
	ML	Silt	>10	>2	≤50	>0.50	<4	>3.0	>83	>4
	OL	Org silt low pl			35 - 50		≥7			

Note: Soils above the A-line with I_p between four and seven are borderline cases requiring the use of several methods.

1) Fines factor, $R_f = \frac{(\%\ \text{fines}) \times (\%\ \text{clay sizes in fine fraction})}{\text{liquid limit of fine fraction}}$, where fine fraction is below 74 μm. 2) Beskow (1951). 3) SNIP II - 15-74 (1975). 4) Konrad and Morgenstern (1981); Konrad (1987). 5) CRREL test; Chamberlain (1981). 6) Under A-line.

2.7.3 Freeze pipe carrying capacity

Locating of freeze pipes in casing pipes installed in ground gives an increased security against the spreading of brine in case of a breakage in the freeze pipe. Consequently, in the freezing contract next to Boston South station in Boston, Massachusetts, part of the project "Big Dig", there was a breakage in a large number of pipes, contributing to that brine flowed out. The freeze pipes had been installed without casing pipes in the ground with soil layers, each one with individual, very varying thermal properties. The consequence of the infiltration of freezing-point lowering liquid in the soil layers that were yet not frozen was that local unfrozen windows in the soil created a risk for instability and leakiness. Consequently, the installation of a freeze pipe in a casing pipe gives a larger protection against brine leakage affecting the surrounding ground. However, installation of freeze pipes directly in the ground without casing pipes results in a larger effective cooling surface, without an insulating ice layer between freeze pipes and casing pipes, as the thermal conductivity in, for example, clay normally is higher than for ice (Dijk & Bouwmeester, 2000A; Dijk & Bouwmeester, 2000B; Johansson & Hintze, 2002).

In fact, the risk for breakage in freezing pipes increases when the soil layers' thermal properties vary. Three adjacent layers with individual thermal properties can, if the middle layer freezes later then the surrounding, create stresses that can lead to fractures in the freezing pipe.

However, the largest load that can be carried by a freezing pipe is a load able to attach to the mantel of the freeze pipe, equal to the bonding strength (often termed "add freeze") Freitag and McFadden (1997). Nevertheless, Freitag and McFadden expresses the bearing capacity by add freeze for a pile in permafrost as

$$Q_p = \sum_{m}^{z} f_a (\pi d) \delta_z \tag{2.32}$$

where d = radius of the pile, f_a = add freeze stress that can be relied on over the life span of the structure, m = length of pile not embedded in permafrost, Q_p = load that can be developed by add freeze on the pile surface, z = length of the pile and δ_z = an increment of pile length.

In the same fashion, the strength that affects the pile in connection with ground frost heave is similarly dependant of the bond between the frozen soil and the pile (Freitag & McFadden, 1997).

2.8 THAW DEFORMATION

This section discusses the expected change of respective soil parameter and the expected thaw deformation. The thawing process has been divided into two different main sequences, namely, the condition immediate after the thawing has occurred and the condition after the thawed soil has settled. This thesis has mainly focused on the latter condition, i.e. when the thawed soil has consolidated under respective situ-stress. This is the present condition unless another condition is mentioned.

The migration of water from the clay particles occurs simultaneously as a change in the pH value of the water take place. As a matter of fact, the pH value is an indication of a solution's rate of "sour" or "basic", i.e. it explains the balance between hydrogen ions and

hydroxide ions, where a surplus of hydrogen ions gives a sour solution and vice versa. For instance, the pH value of a neutral solution equals seven at room temperature.

A change in the concentration of hydrogen ions in pore water indicates that a cation-process exists. "If the value of pH decreases the concentration of hydrogen cations of pore water increases. This is most likely a result of an exchange of loosely bound monovalent hydrogen to more strongly bound cations. This causes the decrease of the absolute value of zeta potential[1] and thus diminishes the repulse forces between clay particles." (Vähäaho, Lappalainen, Ryhänen, 1989, p 594). Furthermore, results from Vähäaho et al tests on three different soils show that the pH value decreases for each freeze-thaw cycle, see Figure 2.44.

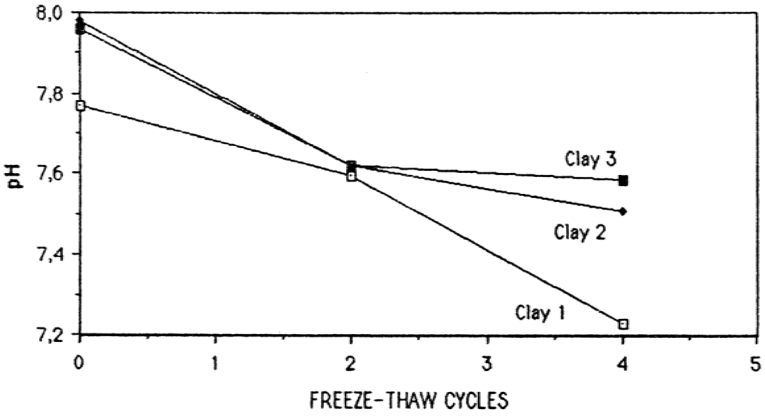

Figure 2.44 Cyclic freezing of three different clays. The value of pH of clay vs. the freeze-thaw cycles, after Vähäaho, Lappalainen and Ryhänen (1989)

Several researchers have studied the ranges of the thaw deformations of soil. A number of papers have been produced, and some of these calculations are presented below. In fact, the earliest reported thaw consolidation test was performed by Tsytovich and Sumgin (1937). Nevertheless, the calculations below normally depend on one soil parameter or in some cases more than one. However, some of these parameters are products of other parameters e.g. measurable, or converted to another soil parameter.

In addition, the thaw consolidation equations are divided into four groups, where the group characteristic is based on the most important soil parameter, namely

- thaw consolidation succeeded by excess pore pressure, one calculation presented
- thaw consolidation in permafrozen soil, due to void ratio change, two calculations presented
- thaw consolidation in permafrozen soil, due to unit weight change, three calculations presented
- thaw consolidation due to water content change, four calculations presented.

2.8.1 Thaw consolidation followed by excess pore pressure

Morgenstern and Nixon (1971) and Knutsson (1985B) show the one-dimensional consolidation of thawing soils in shallow conditions in terms of normalized pore pressure distributions.

[1] The zeta potential (or "streaming potential", or "electro-osmosis") constitutes the electric potential gradient between the ends of the capillary during fluid flow. The capillary fluid flow carry the electric charges in the electric dual conducting stratum in the capillary wall and cause an accumulation of electric charges in the end of the capillary.

As can be seen in Figure 2.45, the one-dimensional consolidation considers an increase in temperature at the ground surface, which continues to increase when moving deeper until reaching the soil's thawing state. However, this problem, the heat conduction problem, was originally used by Franz Neumann for the purpose of studying the formation of ice on still water. By the use of equations derived from thaw depths or frost-penetrating depths, several authors have presented solutions with similar approaches. Likewise, Stefan (1891) with Stefan's solution and Aldrich and Painter (1966) with modified Berggren equation developed equations similar to Neumann's solution, considering different parameters, depending on target application. However, Neumann gives two partial differential equations, originally for ice and water, as similar to the isotropic semi-infinite body of moist soil (Carslaw & Jaeger, 1959; Ingersoll, Zobel & Ingersoll, 1948; Jumikis, 1966). The two partial differential equations are, one for the frozen part

$$\frac{\partial T_{\mathrm{f}}}{\partial t} = \alpha_{\mathrm{f}} \frac{\partial^2 T_{\mathrm{f}}}{\partial x^2} \tag{2.33}$$

and the second for the unfrozen part of the soil

$$\frac{\partial T_{\mathrm{u}}}{\partial t} = \alpha_{\mathrm{u}} \frac{\partial^2 T_{\mathrm{u}}}{\partial x^2} \tag{2.34}$$

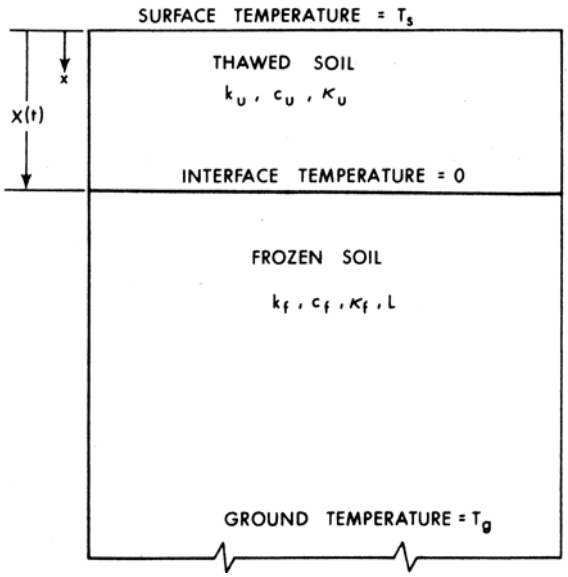

Figure 2.45 The Neumann problem, illustrated, after Nixon and McRoberts (1973)

Consequently, if we consider boundary conditions, perform mathematical approximations, carry out substituting equations, neglect volume change during phase change, neglect convection and heat flow, the analytic solution for the frozen zone becomes (Jumikis, 1966)

$$T_{\mathrm{f}} = T_{\mathrm{s}} + \left(T_{\mathrm{wf}} - T_{\mathrm{s}}\right) \cdot \frac{\operatorname{erf} \dfrac{x}{2\left(\alpha_{\mathrm{f}} t\right)^{1/2}}}{\operatorname{erf} \dfrac{m}{2\left(\alpha_{\mathrm{f}}\right)^{1/2}}} \tag{2.35}$$

and for the unfrozen zone (Jumikis, 1966)

$$T_u = T_0 - \left(T_0 - T_{wf}\right) \cdot \frac{1 - \operatorname{erf} \dfrac{x}{2\left(\alpha_u t\right)^{1/2}}}{1 - \operatorname{erf} \dfrac{m}{2\left(\alpha_u\right)^{1/2}}} \tag{2.36}$$

where

$$\operatorname{erf}(z) = [\text{denotes the error function}] = \operatorname{erf}(z) = \frac{2}{\sqrt{\pi}} \int_0^z e^{-s^2}\, ds \tag{2.37}$$

Similarly, the condition of the advancing thaw plane downwards for $x = X$ and $t > 0$, $T_f = T_u = T_{wf}$. This take place only when $x = 0$, $x = \infty$ and when $x = X$, i.e. the thickness of the thawed soil layer, is proportional to $t^{1/2}$. The thaw plane or the frozen front moving downwards can be written (Jumikis, 1966)

$$X(t) = mt^{1/2} \tag{2.38}$$

The soil constant m may be derived from Neumann's solution, for example (Jumikis, 1966; Lunardini, 1980)

$$L\rho_i w m \left(\pi\right)^{1/2} = \frac{k_f \left(\alpha_f\right)^{-1/2} \left(T_{wf} - T_g\right)}{e^{\frac{m^2}{4\alpha_f}} \operatorname{erf}\left\{m\left[2\left(\alpha_f\right)^{1/2}\right]^{-1}\right\}} - \frac{k_u \left(\alpha_u\right)^{-1/2} \left(T_0 - T_{wf}\right)}{e^{\frac{m^2}{4\alpha_u}} \left\{1\text{-}\operatorname{erf}\left[m\left[2\left(\alpha_u\right)^{1/2}\right]^{-1}\right]\right\}} \tag{2.39}$$

In the same fashion, Stefan (1891) derived a simple formula for the formation of ice, i.e. the relationship that must exist between the thickness, the time and the rate of freezing or melting of a sheet of ice on a lake of still water. In fact, Stefan (1891) simplified the conditions of that problem, by assuming, among other things, that the temperature of the water was everywhere constant and equal to zero. The fundamental equation (see Eq. (2.33)) then becomes (Ingersoll, Zobel & Ingersoll, 1948)

$$\frac{\partial T_f}{\partial t} = \alpha_f \frac{\partial^2 T_f}{\partial x^2} \tag{2.40}$$

The second equation, describing the unfrozen part of the soil is missing. It should be noted that T_f might be expressed in both time and place. The total differential can then be written (Ingersoll et al, 1948)

$$dT_f = \frac{\partial T_f}{\partial x} dx + \frac{\partial T_f}{\partial t} dt \tag{2.41}$$

Consequently, if we consider boundary conditions, perform mathematical approximations, carry out substituting equations, neglect volume change during phase change, neglect convection and heat flow, the analytic solution for the thawing plane becomes (Ingersoll et al, 1948; Knutsson, 1985B)

$$X\left(t\right) = \left(\frac{2T_s k_u t}{L\rho_u}\right)^{1/2} = \alpha t^{1/2} \tag{2.42}$$

where

$$\alpha = \left(\frac{2T_s k_u}{L'} \right) \tag{2.43}$$

Hence, in the same manner, rewriting Eq. (2.42), the thaw plane can be derived from the simpler Stefan's equation (Johnson, McRoberts & Nixon, 1984; Knutsson, 1985B)

$$X(t) = \left(\frac{2k_f \left(T_{wf} - T_g \right) t}{Lw\rho_d + 0.5c_{vf} \left(T_{wf} - T_g \right)} \right)^{1/2} \tag{2.44}$$

Likewise, Jumikis (1966), Morgenstern and Nixon (1971), Morgenstern (1981), Alexiades and Solomon (1993) found that properly fitting soil constants into this theory allowed the theory also to be applied to the frost penetration problem and the movement of the thaw plane in soils. As illustrated, in Figure 2.45, a gradual increase in temperature takes place simultaneously as the soil thaws and the thaw plane moves downward. The heat conduction problem for especially shallow conditions is proposed with Eq. (2.38) (Jumikis, 1966; Morgenstern & Nixon, 1971; Nixon, 1973; Morgenstern, 1981; Knutsson, 1985; Alexiades & Solomon, 1993).

According to Morgenstern and Nixon (1971), in the thawed region, with some assumptions e.g. that the theory of consolidation is valid, the soil is compressible, the soil particles is uncompressible, and the stress does not vary with time, the differential equation may be written

$$c_v \frac{\partial^2 u}{\partial x^2} = \frac{\partial u}{\partial t} \tag{2.45}$$

Morgenstern and Nixon (1971) expressed an analytical solution for the excess pore pressure with the boundary conditions expressed by Eq. (2.45) and

$$t = 0, X = 0 \tag{2.46}$$

$$q_0 + \gamma' X - u(X,t) = \frac{c_v \frac{\partial u}{\partial x}(X,t)}{\frac{dX}{dt}}, \qquad x = X(t), \qquad t > 0 \tag{2.47}$$

The complete solution of Eq. (2.45) with the differential constants derived from the boundary conditions is (Morgenstern & Nixon, 1971)

$$u(x,t) = \frac{q_0}{\operatorname{erf}(R) + e^{-R^2} R^{-1} (\pi)^{-1/2}} \operatorname{erf}\left[\frac{x}{2(c_{vc} t)^{1/2}} \right] + \frac{\gamma' x}{1 + (2R^2)^{-1}} \tag{2.48}$$

where

$$R = 0.5X(c_{vc} t)^{-1/2} = 0.5m(c_{vc})^{-1/2} \tag{2.49}$$

R is the term for the thaw consolidation ratio (Morgenstern & Nixon, 1971; Knutsson, 1985B).

According to Eq. (2.48), during the advancing of the thaw plane, the excess pore water pressure in the thawed zone can be evaluated. The knowledge of actual total soil pressure, the effective stress and the shear strength may be calculated in every soil level (Knutsson, 1985B). Similarly, Eq. (2.48) may be used to evaluate the settlement associated with the ice

water transformation, for the special case of no applied load (q = 0), which becomes (Morgenstern & Nixon, 1971)

$$S = 1 - \frac{1}{1 + 0.5R^{-2}} \tag{2.50}$$

Note that the pore pressure due to freeze thaw consolidation processes refers to the excess pore pressure. The hydrostatic pore pressure has no influence on the consolidation processes, for this reason, the excess pore pressure will be calculated.

2.8.2 Thaw consolidation in permafrozen soil, due to void ratio change

Silty and clayey soils are generally ice-rich, especially in layers or lenses of ice, and these ice formations are directed to increase the thaw settlements. Tsytovich (1975) suggested that the water intake during the freezing process agreed with the thaw settlement. However, Tsytovich proposed an equation (Eq. (2.51)) for permafrozen soil under uniform load with lateral expansion prevented, i.e. the one-dimensional problem. "The compression during thawing followed exactly the relation known from general soil mechanics for one-dimensional problem" (p 219)

$$s = \frac{h}{1 + e_{f0}} \left(\Delta e\right)_p \tag{2.51}$$

During the freeze-thaw process, several parameters alternate. For the consolidation process, one parameter in particular is urgent the changes in the void ratio.

Laboratory tests were performed where permafrozen soil was intended to thaw in an oedometer; Tsytovich (1975) anticipated a change in void ratio due to the applied load. As shown in Figure 2.46 during the thawing, the largest change in the porosity coefficient, i.e. the void ratio, occurs during the process of thawing.

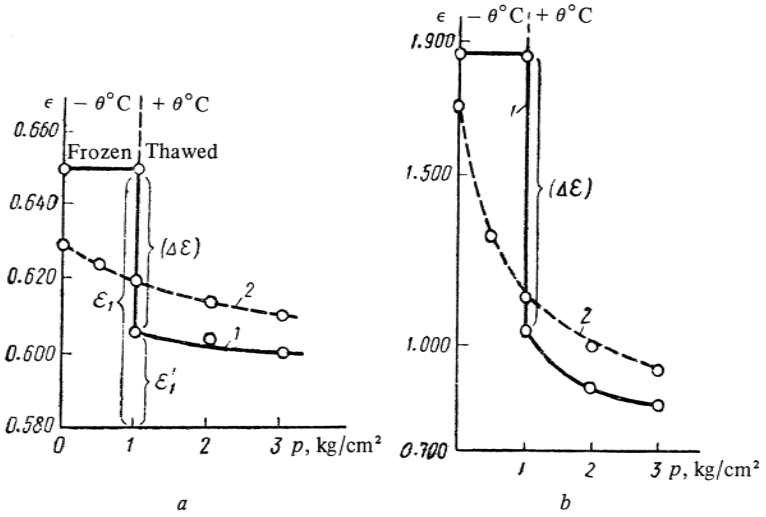

Figure 2.46 Laboratory experiments of an oedometer; Void ratio change in soil due to various loads. Figure a; sand and Figure b; clay. The curve (1) shows void ratio change after one freeze-thaw cycle and (2) shows the change of undisturbed soil, after Tsytovich (1975)

As can be seen in Figure 2.46, under laboratory conditions, the frozen soil void ratio decreases as the uniform load increases, but it is also obvious that the void ratios of the

frozen and then thawed soil decrease under a minor uniform load (under only the weight of the heating plunger; $p < 0.002$ kg cm^{-2}) (Tsytovich, 1975).

Eq. (2.51) can be rewritten, and give the relative settling of the soil layer under continuous load (Tsytovich, 1975)

$$\delta_{th} = \frac{s}{h} = \frac{\Delta e}{1 + e_{f0}} \tag{2.52}$$

where δ_{th} = the relative settling of the soil layer under continuous load with lateral expansion prevented.

Tsytovich (1975) has, as mentioned above, analysed the problems concerning thaw settlements due to permafrozen soil. The thaw settlements were expressed relative to the void ratio. The settlement was divided into two pieces, one referring to the thaw consolidation without overburden pressure, and one referring to settlements due to increment load. As can be seen in Figure 2.47, the void ratio change and the similar change in compaction load are strictly linear functions of the pressure within the range studied. The equation can be written in the form (Tsytovich, 1975)

$$\Delta e = A + p \tan \alpha \tag{2.53}$$

where A = change in the void ratios of thawing frozen soils with simultaneous compaction (does not depend on the external pressure), Δe = void ratio change, p = external load and tan a = inclination of the line.

Additionally, Tsytovich (1975) states the quantity tan a as the coefficient compaction of thawing soils, i.e. the denotation

$$\tan \alpha = a \tag{2.54}$$

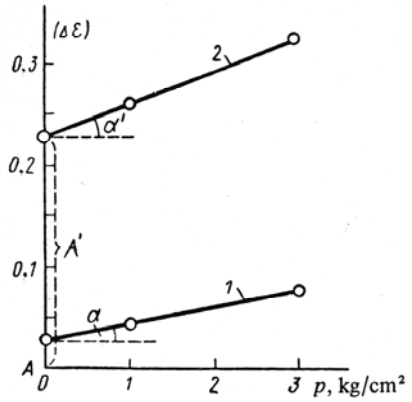

Figure 2.47 Void ratio change of frozen soil on thawing, due to external pressure (p). (Sand); (2) Clay, after Tsytovich (1975)

The frozen soil is assumed homogeneous, not involving ice lenses and other anomalies. After substitution of the term Δe in Eq. (2.52) and rearrangement of Eq. (2.53), the total settlement after a freeze-thaw cycle ($S = \delta_{th} h$) will then be rewritten as (Tsytovich, 1975)

$$S = h \frac{A}{1 + e_{f0}} + hp \frac{a}{1 + e_{f0}} = \bar{A}h + \bar{a}hp \tag{2.55}$$

where a = coefficient compaction of thawing soils, $\bar{a}$ = coefficient of relative (referred to the volume of the soil mineral particles) compaction of the frozen ground during thawing, A = change in the void ratios of thawing frozen soils with simultaneous compaction (does

not depend on the external pressure), $\overline{A}$ = thawing coefficient, e_{f0} = initial void ratio of the frozen soil, p = external pressure, h = total thaw depth of the entire soil layer tested and S = stabilized settling of the layer of thawed ground. Like Eq. (2.55), two separate terms are involved for prediction of the settling of foundations on thawing ground; the first term is assumed to represent thaw settling and does not depend on external load. The second term is the expression known from general soil mechanics for the stabilized settling of a soil layer under a continuous pressure. It depends on the magnitude of the compacting load and is known as the compaction settling for the duration of thawing. This equation shows the most important relationship for calculation of settling of thawing ground and is the basis for development of other methods (Tsytovich, 1975). However, Eq. (2.55) is limited for moderate loads up to 3-4 kg cm^{-2} (approximately 300-400 kPa, author note) (Tsytovich, 1975). In the same approach, Tsytovich describes the thaw settlement as

$$s_{th} = \overline{A}h + \overline{a}hp_e \tag{2.56}$$

where $\overline{A}h$ = thaw settling, $\overline{a}hp_e$ = compaction settling for moderate pressures in a soil layer with the thawing depth h and p_e = effective stress.

Andersland and Ladanyi (2004) predict thaw settlements in permafrozen soil. A permafrozen soil sample thaws in a one-dimensional consolidation device. A limitation consists of ice inclusions; in this test method, not more than 10 mm thin ice inclusions are permitted. "Thicker ice lenses require proportionally larger samples" (Andersland & Ladanyi, 2004). The thaw-strain parameter is defined and can be written (Nixon & Ladanyi, 1978; Andersland & Ladanyi, 2004)

$$A_0 = \frac{e_f - e_{th}}{1 + e_f} \tag{2.57}$$

where A_0 denotes the thaw strain parameter, e_f the frozen void ratio and e_{th} the thawed void ratio.

The conclusion that emerges from Eq. (2.57) is similar to Eq. (2.52), hence the void ratio gradient $\Delta e = e_f - e_{th}$.

Figure 2.48 shows the typical result of an oedometer thaw consolidation test of permafrozen soil; from point *a* to point *b*, a small decrease of the void ratio occurs due to the consolidation under the load of the effective stress. From point *b* to point *c*, a large change of the void ratio occurs, due to the ice-water phase change during the thawing process and the drainage of the excess pore water. The curve from point *c* to *d* illustrates the change of the void ratio under a surcharge load.

The relative settlement i.e. the vertical strain of the soil element thawed under a load of the effective stress for the soil field sample and an excessive overburden load is

$$\frac{\Delta H}{H} = \frac{e_f - e_{th}}{1 + e_f} + m_v \Delta\sigma = A_0 + m_v \Delta\sigma \tag{2.58}$$

where H denotes the thickness of the soil strata and m_v the coefficient of volume compressibility. As in the Tsytovich (1975) study (Eq. (2.52)), in Andersland and Ladanyi (2004) study (Eq. (2.58)) the thaw settlement under self-weight becomes a void ratio gradient between the frozen and thawed soil. However, Andersland and Ladanyi describes the settlement of the soil strata as

$$\Delta H = A_0 H_f + m_v \Delta\sigma H_{th} \tag{2.59}$$

where H_f and H_{th} will introduce a very small error that often is assumed to be negligible (Andersland & Ladanyi, 2004). The thaw settlement for layered soil strata, each with its own soil properties then becomes

$$\Delta H = \sum_{1}^{n} A_{0i} H_{fi} + \sum_{1}^{n} m_{vi} \Delta\sigma_i H_{thi} \tag{2.60}$$

where n denotes strata and i has values of 1 to n (Andersland & Ladanyi. 2004).

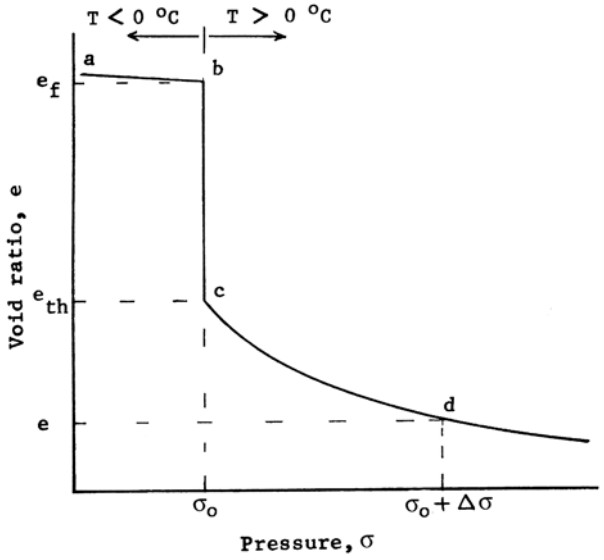

Figure 2.48 Representative void ratio versus pressure curve of frozen soil and the subsequent thawing. σ_0 denotes the effective overburden pressure for the field sample and $\Delta\sigma$ the surcharge load, after Andersland and Ladanyi (2004)

2.8.3 Thaw settlement in permafrozen soil, due to soil unit weight change

Crory (1973) described the thaw consolidation ratio as the relation between the dry unit weight of frozen soil and the dry unit weight of unfrozen soil, i.e. the thawed dry unit weight of soil. However, as can be seen in Figure 2.49, the frozen soil sample (a.) on thawing can expand (c.), experience no change of volume (d.) or consolidate (e.)

$$\frac{\Delta H}{H} = \frac{\gamma_{dth} - \gamma_{df}}{\gamma_{dth}} = 1 - \frac{\gamma_{df}}{\gamma_{dth}} \tag{2.61}$$

where H = soil sample's original height, ΔH = amount of expansion or axial strain, γ_{dth} = dry unit weight of thawed soil, γ_{df} = dry unit weight of frozen soil.

Again, the conclusion that emerges from Eq. (2.61) is similar to Eq. (2.52); hence, the void ratio can be obtained

$$e = \frac{V_v}{V_s} = \frac{\gamma_s}{\gamma_d} - 1 \tag{2.62}$$

Inserting the void ratio from Eq. (2.62) in Eq. (2.52) and rearranging, the equation Eq. (2.52) obtains the form of Eq. (2.61).

However, Crory (1973) found the total settlement in a stratum on thawing at a specific depth, computed by a summation of the strains of individual layers, as expressed by

$$S = \sum_{1}^{n} \left[\frac{\gamma_{dth} - \gamma_{df}}{\gamma_{dth}} \right] h_i \tag{2.63}$$

where S = total settlement, $(\gamma_{dth} - \gamma_{df})\gamma_{dth}^{-1}$ is the unit strain under the overburden and imposed structural pressure of the soil layer of thickness h_i and the individual layers of soil numbered from 1 to n.

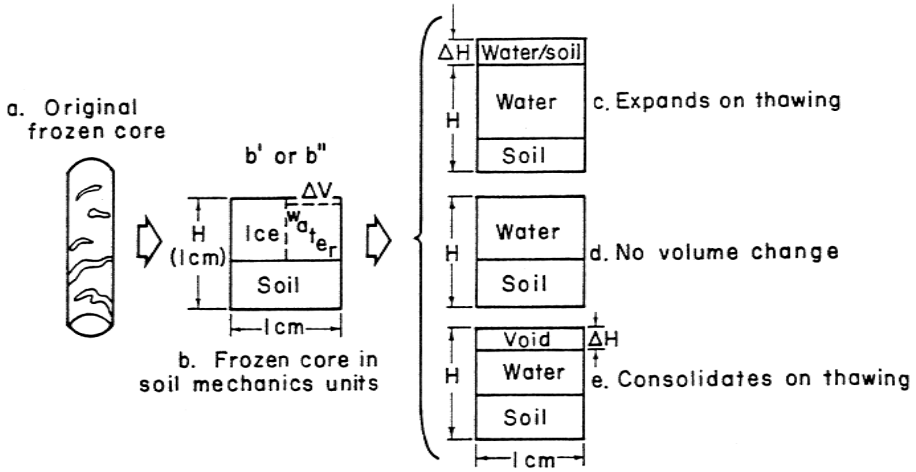

Figure 2.49 The basic volume relationships of frozen and thawed soil core, after Crory (1973)

Another method to determine the thaw settlement of permafrozen soil was proposed by Watson, Slusarchuk and Rowley (1973). As can be seen in Eq. (2.65), Watson et al (1973) consider the thaw settlement is affected by three parameters; a thaw settlement parameter and two compressibility terms, i.e. one due to the surcharge load and one due to the self-weight. Assuming the water table in thawed material is at the surface, the total settlement can be calculated by the following equation (Watson et al, 1973)

$$S = A_0 X + m_v \int_0^X \left(P + \gamma' X \right) \mathrm{d}X \tag{2.64}$$

or

$$S = A_0 X + m_v P X + \frac{m_v \gamma' X^2}{2} \tag{2.65}$$

where S = total settlement, A_0 = thaw-settlement parameter, X = depth of thaw front from the original surface, m_v = coefficient of volume compressibility due to vertical drainage, P = surcharge load and γ' = submerged unit weight of thawed soil.

On occasions where several layers of soil are present, the settlement of each stratum can be calculated separately and summed to the settlement of the total strata. For these situations, in Eq. (2.65), X becomes the depth of thaw (in any strata) and P corresponds to the effective load at the top of that stratum (Watson et al, 1973).

Watson et al (1973) showed two methods to determine the relative settlement parameter A_0; in Method 1, Crory (1973) equation (2.61) was used, i.e. the relation between frozen soil's dry density and thawed soil's dry density. In Method 2, the difference in volume between the frozen and thawed state was equated to the change in volume associated with melting the ice plus the volume of water expelled from the sample. The relationship can be expressed as (Watson et al, 1973)

$$A_{p2} = \frac{w_f \gamma_{df}}{90\gamma_w} + \frac{W_f - W_u}{\gamma_w V} \tag{2.66}$$

where A_{p2} = the relative settlement at some pressure, w_f = percentage frozen water content, γ_{df} = dry unit weight of frozen soil, γ_w = unit weight of water, W_f = weight of frozen sample, W_u = weight of thawed drained sample and V = volume of frozen sample.

Nixon and Ladanyi (1978) analysed Watson et al's (1973) results and supplemented them with their own data. Based on these data, they expressed the thaw settlement as

$$\frac{\Delta H}{H_f} = 0.90 - 0.868\left(\frac{\gamma_f}{\gamma_w} - 1.15\right)^{1/2} \pm 0.05, \quad 1.2 < \gamma_f / \gamma_w < 2.0 \tag{2.67}$$

Speer, Watson and Rowley (1973) analysed the relation between frozen bulk density and the corresponding thaw settlement for permafrozen silty and clayey soils in three sites close to the Mackenzie River and from a test site near Inuvik (N.E. in Canada). The test samples were collected from various depths down to approximately 13 m or "until the ice content was such that the thaw settlement would be negligible." (Speer et al, 1973, p 747). The samples were thawed under a load equivalent to the total overburden pressure at sample depth. The results of the thaw-settlement tests were compiled in a diagram in terms of thaw settlement versus frozen bulk density, as can be seen in Figure 2.50. Speer et al (1973) fitted a least-square curve to these data and obtained the equation

$$S = \frac{\Delta H}{H_f} = 73.60 - 101.8 \cdot \ln \gamma_f \pm 7.01\ \% \tag{2.68}$$

where S = settlement in percent and γ_f = frozen bulk density [g cm^{-3}]. "The residual standard variation was 7.01 %" (Speer et al, 1973, p 749). The limits of the equation defining the relationships are 1.09 g cm^{-3} and 2.05 g cm^{-3}. In soil samples with pure ice present a settlement of 100 % was envisaged. For densities between 2.05 and 2.16 g cm^{-3}, the thaw settlement was constant at 2 %. For values greater than 2.16 g cm^{-3}, the thaw settlement was assumed to be negligible (Speer et al, 1973).

Ladanyi (1994) analyzed Speer et al's (1973) and Johnston's (1981) results and expressed the relative settlement empirically as

$$\varepsilon_1 = 100\frac{\Delta H}{H_f} = 85\left[1 - \left(\frac{\rho_f}{\rho_w} - 1.10\right)^{1/2}\right] \pm 8 \tag{2.69}$$

Johnson et al (1984) expressed the one-dimensional total thaw settlement in terms of

$$S = A_0 X + m_v \int_0^X \left(P + \gamma' X\right) \mathrm{d}X \tag{2.70}$$

where S = the total settlement, A_0 = thaw settlement parameter, m_v = average coefficient of compressibility, P = surcharge load, X = depth to thaw front from original surface, γ' = submerged unit weight of thawed soil. It is assumed that the water table remains at the surface of the soil (Johnson et al, 1984). The determination of the parameter A_0 is presupposed from tests on a given sample. As can be seen in Figure 2.51, a best-fit linear relationship extrapolated to zero pressure defines the soil thaw settlement parameter A_0, and the line slope defines m_v.

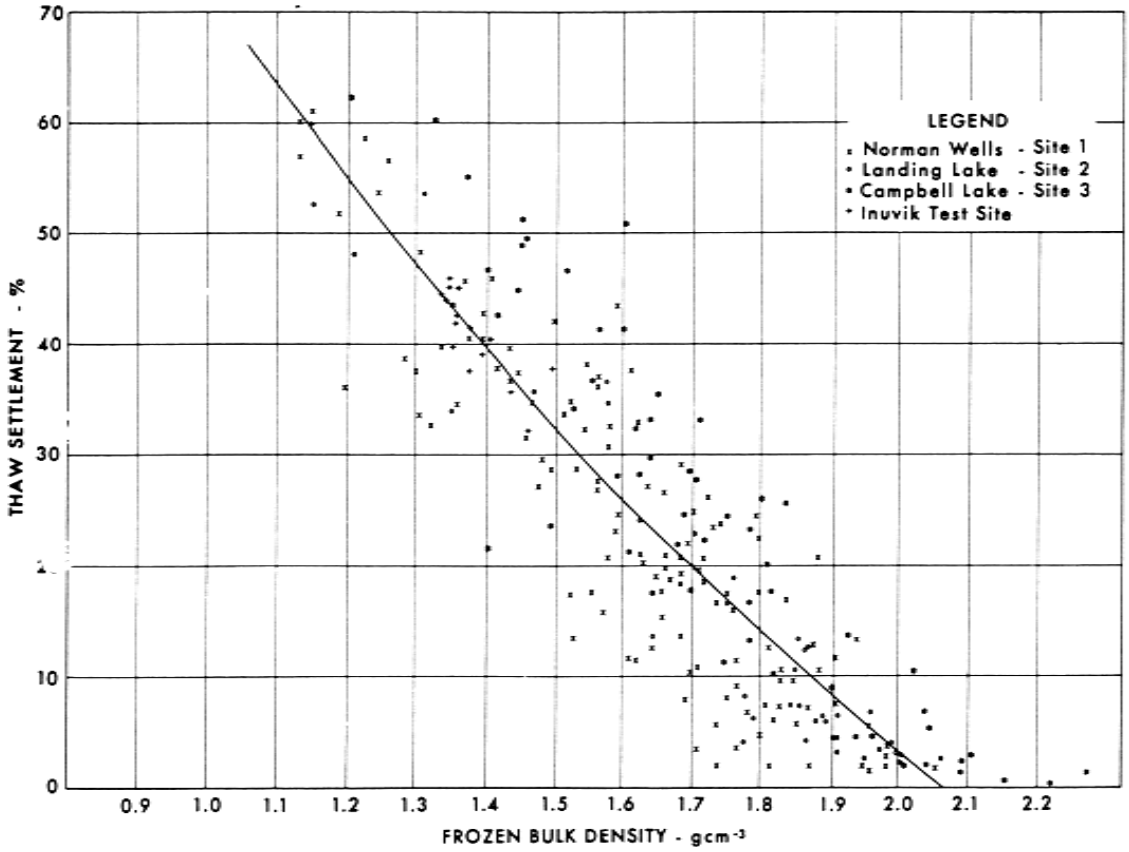

Figure 2.50 Thaw settlement versus frozen bulk density relationship, after Speer et al (1973)

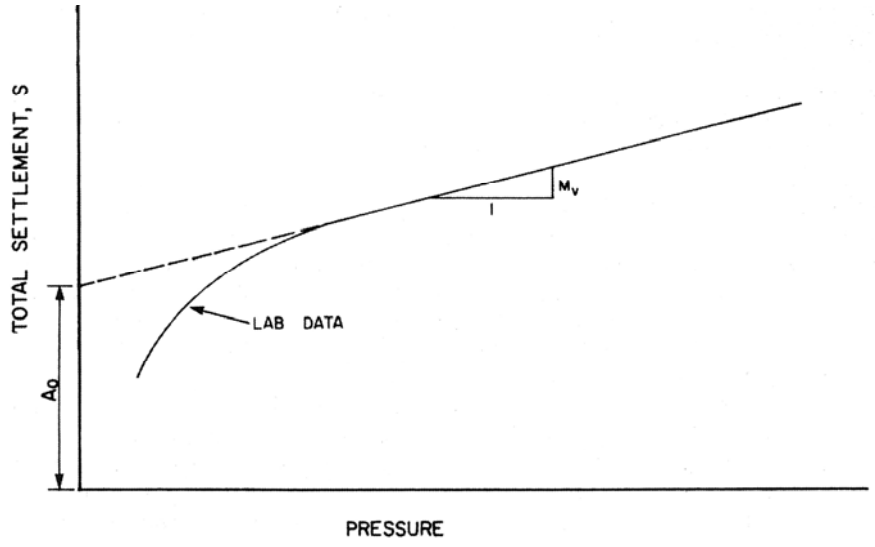

Figure 2.51 Total settlement vs. pressure, generalized form of thaw settlement test data, after Johnson et al (1984)

According to Figure 2.52, an analyse of Johnson et al (1984) plotted data from Mackenzie Valley soil samples in Figure 2.52, a rough best fit linear relationship of the line "thaw consolidate parameter A_0 vs. the frozen soil water content" is

$$A_0 = 40.43 \ln w - 128.02 \pm 8 \tag{2.71}$$

where A_0 = thaw settlement parameter, as can be seen in Figure 2.52 and w = original frozen soil water content. Eq. (2.71) is valid for soil water content interval ranging from 23 < w < 120 percent for Mackenzie Valley soil. Margin of error (±8 percent) is derived from Johnson et al (1984) best-fit curve on the same material.

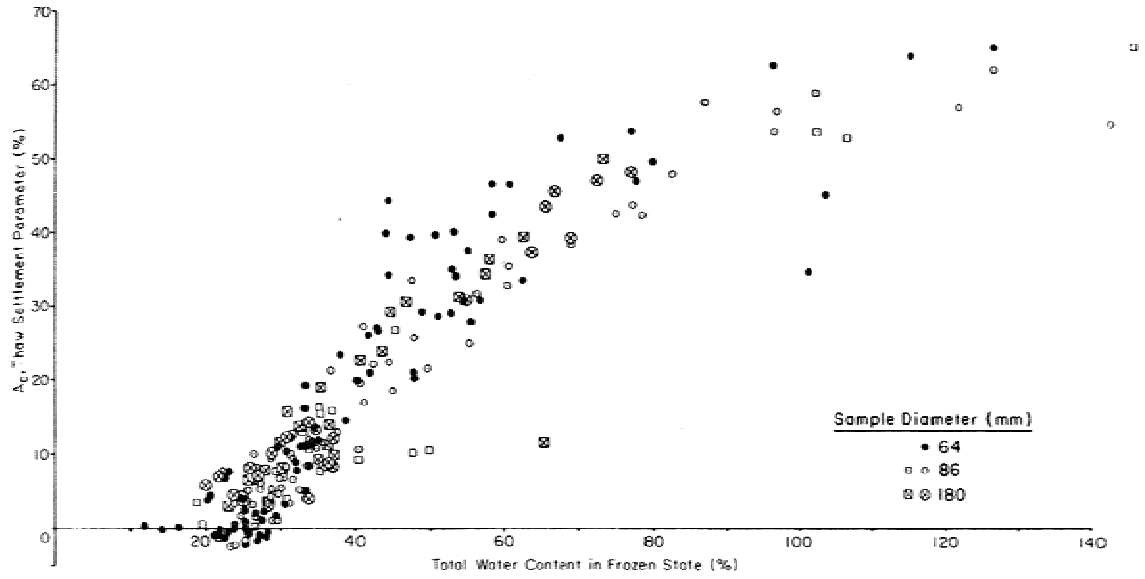

Figure 2.52 Thaw consolidation parameter A_0 vs. frozen soil water content of Mackenzie Valley soil, after Johnson et al (1984)

2.8.4 Thaw consolidation, due to water content change

According to Eq. (2.61), the deformation due to change in density, disregarding the unfrozen water is performed. However, Crory (1973) took into account the specific ice content (the "iceness ratio"); the influence of the 0.09 portion of the water contents i.e. the correction of the unfrozen water content. Hence, Eq. (2.61) takes the form (Crory, 1973)

$$\frac{\Delta H}{H} = \frac{w_f + 0.09 i_r w_f - w_{th}}{G_s^{-1} + w_f + 0.09 i_r w_f} \tag{2.72}$$

Using data from Johnson et al (1984) (see Figure 2.52); Ladanyi (1994) expressed the empirical equation

$$\varepsilon_1 = 100 \frac{\Delta H}{H} = 102.75 - \left[5,480.75 \left(w_f + 27.43 \right) \right] \pm 8\% \tag{2.73}$$

where w_f = total frozen soil water content.

Vähäaho (1988, 1991A) compared the thaw settlement properties of virginal frozen clay from China with virgin frozen clay from Helsinki. As can be seen in Figure 2.53, the resulting thaw settlement will then be equal to

$$A = k_1^{-1} w \tag{2.74}$$

where A = relative deformation i.e. the settlement in percent, $k_1 \approx 3$ and w = original water content in percent. The water content in the clay was measured before the freezing test and after virginal freezing and the subsequent thawing test. Likewise, Vähäaho (1988) found that the results agreed with a straight line in Figure 2.54 and belonged to the expression

$$w_j = k_w w \tag{2.75}$$

where w_j = water content after a virginal freeze-thaw cycle, in percent, $k_w \approx 2/3$ and w = original soil water content.

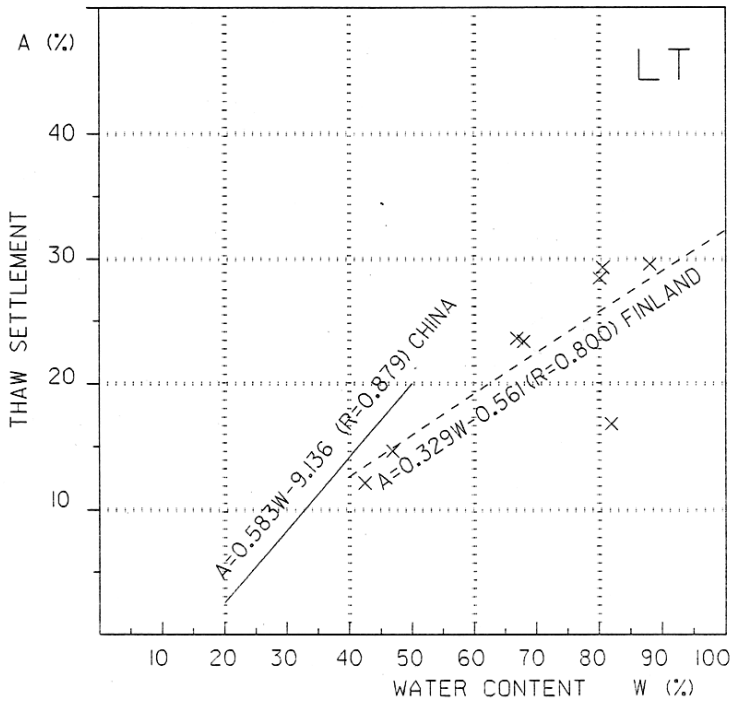

Figure 2.53 Diagram showing the relationship between the original water content and the thaw settlement of two different clayey soils; One clay from China (-) and the other from Finland (x), after Vähäaho (1991A)

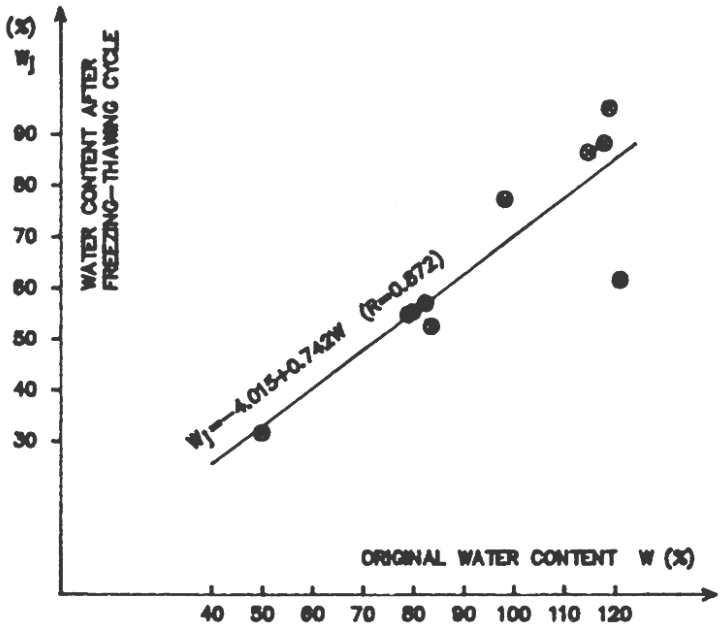

Figure 2.54 Soil water content after a freeze-thaw cycle vs. the original water content, after Vähäaho (1988)

As in Eq. (2.75) Vähäaho (1988) defines the thaw settlement in relation to the drop of water amount

$$A_{\mathrm{k}} = \left(1 - \frac{100 + 2.65 w k_{\mathrm{w}}}{100 + 2.65 w}\right) 100 \tag{2.76}$$

where A_{k} = thaw settlement in percent due to the drop of water content after one freeze-thaw cycle. Vähäaho (1988) recognized the decrease in soil water content to be about 4/5 of settlement, both in normal consolidation tests and in freeze-thaw tests. Thus, Eq. (2.76) can be rewritten as (Vähäaho, 1988)

$$A = \frac{5}{4}\left(1 - \frac{100 + \frac{2}{3} 2.65 w}{100 + 2.65 w}\right) 100 \tag{2.77}$$

Regarding analytical thaw consolidation equations, Table 2.7 shows the presented equations above, listed in alphabetical order according to authors.

Table 2.7 Combination of presented thaw deformation equations of soil, listed in alphabetical order according to authors

Author	Eq.	Eq. No.
Andersland and Ladanyi (2004)	$\frac{\Delta H}{H} = \frac{e_{\mathrm{f}} - e_{\mathrm{th}}}{1 + e_{\mathrm{f}}} + m_{\mathrm{v}} \Delta\sigma = A_0 + m_{\mathrm{v}} \Delta\sigma$	(2.58)
Crory (1973)	$\frac{\Delta H}{H} = \frac{\gamma_{\mathrm{dth}} - \gamma_{\mathrm{df}}}{\gamma_{\mathrm{dth}}} = 1 - \frac{\gamma_{\mathrm{df}}}{\gamma_{\mathrm{dth}}}$	(2.61)
Crory (1973)	$\frac{\Delta H}{H} = \frac{w_{\mathrm{f}} + 0.09 i_{\mathrm{r}} w_{\mathrm{f}} - w_{\mathrm{th}}}{\frac{1}{G_{\mathrm{s}}} + w_{\mathrm{f}} + 0.09 i_{\mathrm{r}} w_{\mathrm{f}}}$	(2.72)
Johnson et al (1984)	$S = A_0 X + m_{\mathrm{v}} \int_0^X \left(P + \gamma' X\right) \mathrm{d}X$	(2.70)
Johnson et al (1984)	$A_0 = 40.43 \ln w - 128.02 \pm 8$	(2.71)
Ladanyi (1994)	$\varepsilon_1 = 100 \frac{\Delta H}{H_{\mathrm{f}}} = 85\left[1 - \left(\frac{\rho_{\mathrm{f}}}{\rho_{\mathrm{w}}} - 1.10\right)^{1/2}\right] \pm 8$	(2.69)
Ladanyi (1994)	$\varepsilon_1 = 100 \frac{\Delta H}{H} = 102.75 - \left[5,480.75\left(w_{\mathrm{f}} + 27.43\right)\right] \pm 8\ \%$	(2.73)
Morgenstern and Nixon (1971)	$S = 1 - \frac{1}{1 + 0.5 R^{-2}}$	(2.50)

Author	Eq.	Eq. No.
Nixon and Ladanyi (1978)	$\frac{\Delta H}{H_f} = 0.90 - 0.868\left(\frac{\gamma_f}{\gamma_w} - 1.15\right)^{1/2} \pm 0.05,\ 1.2 < \gamma_f/\gamma_w < 2.0$	(2.67)
Speer et al (1973)	$S = \frac{\Delta H}{H_f} = 73.60 - 101.8 \cdot \ln \gamma_f \pm 7.01\ \%$	(2.68)
Tsytovich (1975)	$s = \frac{h}{1 + e_{f0}}\left(\Delta e\right)_p$	(2.51)
Vähäaho (1988)	$A = \frac{w}{k_1}$	(2.74)
Vähäaho (1988)	$A = \frac{5}{4}\left(1 - \frac{100 + \frac{2}{3}2.65w}{100 + 2.65w}\right)100$	(2.77)
Watson et al (1973)	$S = A_0 X + m_v P X + \frac{m_v \gamma' X^2}{2}$	(2.65)

2.9 CASE STUDIES

This section deals with three case studies, all three with different approaches to temporary frozen constructions, to get stability and/or a hydraulically waterproof zone. The three studies depicts

- Storebælt eastern railway tunnel, Denmark
- Hurum Weakness Zone in the Oslofjord tunnel, Norway
- tunnel in Kobe city, Japan.

A general limitation when considering a construction project case study, is typically that the project is well known and discussed if it has been "successful" but less known and discussed if it has been " unsuccessful". Few projects within this limited field have been described because of their possible miscalculated prognoses or faulty constructions, despite that, such projects should exist. This can partly be explained by that the persons involved in the construction process, such as the project's consultants and building contractors generally produce the articles from the projects. Few people besides the appointed parties involved in the construction have access to this information. Interruptions in the process often lead to disagreements concerning the construing of the agreement. Once the arguing parties agree on the "actual progress of events", this discussion leads to that the objective information is handled if it does not follow the agreement, i.e. the contract. This unfortunately leads to a self-censorship as it limits important information for increasing the knowledge for future projects.

The three projects are chosen because each one of them mainly treats an area of interest pertaining to this thesis. Storebælt eastern railway tunnel was built in Denmark during the 1990's for the purpose of together with the parallel built highway improve the connections between the islands Funen and Zealand. This thesis describes, above all, the method used to stabilize and hydraulically seal the geologically most requiring conditions in regards to the tunnel construction. However, the frozen constructions were planned to be accomplished on a relatively early stage of the construction process.

In connection with the building of the Oslo fjord tunnel, a highway connection south of Oslo in the late 1990's, a weak zone was surprisingly discovered, the Hurum Weakness Zone. This thesis describes, above all, the discussion around the stress conditions and the deformations during this construction process. Nevertheless, the frozen construction was not planned in the original building process, but was added after an unsuccessful attempt with cement grouting.

When the underground was going to be extended in the centre of Kobe, Japan, an older cable tunnel had to be "moved". The instruments used to predict possible deformations during the freezing-and thawing process are described in this thesis. However, the freezing around the existing tunnel in the end of the 1990's was planned at an early stage of the building process.

2.9.1 Ground freezing for tunnels and cross passages at Storebælt eastern railway tunnel, Denmark 1994

The Storebælt connection consists of the railroad- and the highway connection between the Danish islands Funen and Zealand via the small isle of Sprogø. The construction work on the connection started in 1988. The opening of the railway connection was in June 1997 and of the highway connection in June 1998. The connection is divided into mainly the West Bridge, the East Bridge and the East tunnel. The west bridge is a combination bridge for a railroad with two tracks and a main road with four lanes. The west bridge goes between Funen and Sprogø. However, between the isle of Sprogø and Zealand is the East Bridge with four lanes for the main road and closely parallel is the East tunnel for railroad traffic.

The East tunnel between the isle of Sprogø and Korsør on Zealand consists of two parallel single track tunnels and is located at its deepest point approximately 75 m under the surface of the sea and 50 m under the ocean bed.

Complicated geotechnical conditions resulted in that four cross passages between the two parallel tunnels, as well as the TBM junctions, were stabilized and hydraulically sealed through freezing.

Two freezing projects at the south tunnel are recapped in this thesis, the TBM junction and cross-passage, "Passage No. 8".

Introduction

The railroad connection under the Great Belt channel, or Storebælt consists of two bored parallel tunnel pipes, each one 7.4 km long with an outer diameter of 8.5 m. The tunnels that were driven through four TBM have 31 cross passages separated at a distance of 250 m. The centre distance between the tunnels is 25 m, while the cross passages are 17 m long with a diameter of 4.75 m (Kofoed & Doran, 1996; Murray & Eskesen, 1997).

Soil- and rock freezing was used on four cross passages and on the two TBM junctions. The freezing for cross passages were used in particular where there was a poor soil- and rock coverage and where the geotechnical conditions were complicated, the zones had

been observed in connection with the tunnelling of the main tunnels. The freezing of the cross passages created above all stable vaults over the zones that were to be excavated.

The tunnelling in the cross passages were shaped out of cast iron (Spheroidal Graphite Iron (SGI)). In the connection between the cross passage and the main tunnels, it consisted of cast in-situ concrete (Murray & Eskesen, 1997).

In connection with the tunnelling of the main tunnels with TBM machines, water transporting sand lenses could be observed at several cross passages. The sand lenses had hydraulic connection with the Belt Sea where freezing was used to stabilize a frozen arch of soil and to create a hydraulically sealed zone (Murray & Eskesen, 1997).

Geology

The predominant geology for the whole Eastern Tunnel can be divided into three main groups, see also Figure 2.55 (Murray & Eskesen, 1997)

i. Glacial moraine
ii. Upper Palaeocene marl
iii. Tertiary Lower Palaeocene Danian Limestone.

The glacial moraine consists of clayey moraine with layers of silt and sand moraines with inclusions of meltwater deposits. The moraine contains boulders of granite and gneiss up to three metres in sizes. The glacial deposits have become pre-consolidated of above laying glacier and are compact and dense (Murray & Eskesen, 1997).

The moraine can be divided into an upper and a lower layer, based on the lithological and geotechnical properties. The upper layer is homogenous clay moraine with a clay content about 20 % and an undrained vane shear strengths varying from less than 100 kPa up to 700 kPa (Murray & Eskesen, 1997). On the contrary, according to Kofoed and Doran (1996), the upper layer is homogenous clay moraine with clay content about 15 % and an undrained vane shears strengths typically greater than 200 kPa.

The subglacial till is less homogenous with elements of up to 20 % weight-percentage sand- and gravel deposits. The undrained vane shear strengths in the subglacial till vary from 200 kPa and to more than 700 kPa (Murray & Eskesen, 1997). Kofoed and Doran (1996) state that the subglacial till is dominated by clay with undrained vane shear strengths exceeding 500 kPa and with occurrences of sandy moraine with clay contents of less than 12 %. Furthermore, generous amounts of elements of melt water deposits consisting of clay- and silt fractions to highly permeable inclusions with sand and gravel deposits exist in the subglacial till. The permeability varies between 10^{-5} and 10^{-7} m s^{-1} (Kofoed & Doran, 1996).

The Upper Palaeocene marl is with help of classification according to British Standard (B.S. Classification), a weak to moderately weak rock with a compressive strength larger than 2 MPa. The marl is fissured and jointed with a permeability of between 10^{-4} and 10^{-6} m s^{-1}. Nevertheless, the lower Tertian Palaeocene Danish limestone is a weak, sandy and silty limestone, the tunnel, however, never reaches this depth (Kofoed & Doran, 1996; Murray & Eskesen, 1997).

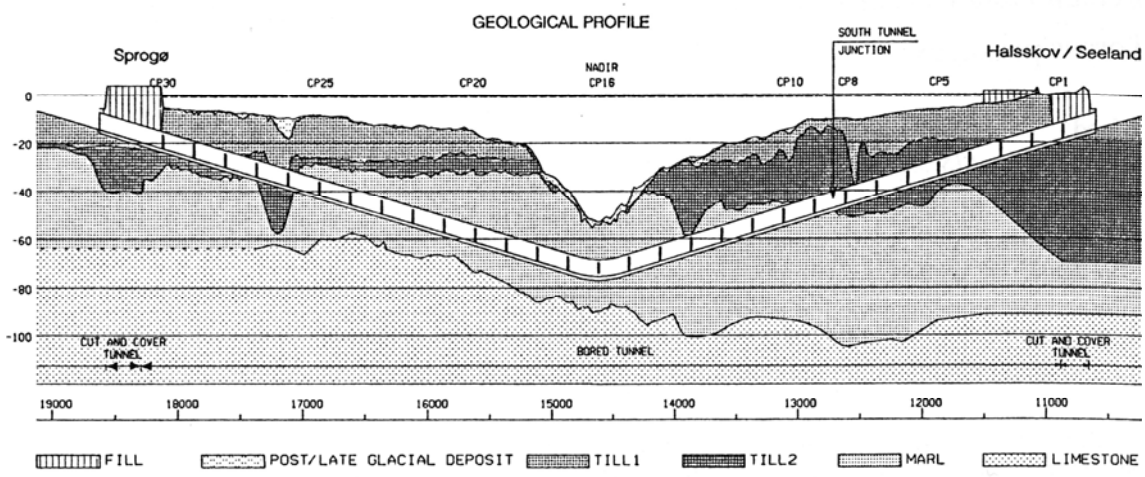

Figure 2.55 Geological longitudinal cross section, after Kofoed and Doran (1996)

Freeze technique and design

To reach temporary stability and the hydraulically sealed zone around the future tunnel, four steps in a process were performed (Kofoed & Doran, 1996)

i. pre-grouting of the zone that was to be frozen
ii. installation of freezing pipes and temperature control pipes
iii. installation of distribution system for brine between the freezing pipes and the cooling machine
iv. freezing and maintenance-cooling of the frozen soil mass during the service period.

Pre-grouting with cement bentonite grout was performed to lower the water circulation in the zone to be frozen (Kofoed & Doran, 1996).

Lost bit drilling technique with water as drilling fluid was used during the drilling for the installation of freezing pipes. The drill rods, dimension 60/75 mm, were used even as freezing pipes. The length of the freeze pipes were limited to about 10 m with consideration of the drill equipment's capacity, but in a few cases, freeze pipes with a length up to 20 m were installed. At the installation of freeze pipes in the TBM junction, these were installed from the shield of a "smaller drilling machine", see Figure 2.56 (Kofoed & Doran, 1996).

The freeze pipes were divided into groups of three to six pipes, connected in a series of 38/48 mm rubber hose. These systems were in turn connected parallel to two 100 mm distribution pipes. The freeze pipes were installed with a maximal spacing of 1.1 m around the future tunnel profile. The cooling medium consisted of a 25-30 weight percentage calcium chloride solution in water (Kofoed & Doran, 1996; Murray & Eskesen, 1997).

Four cooling machines were used during the tunnel project, each one suspended on the side of the main tunnel between two cross passages. The cooling capacity reached approximately 120 kW at an initial temperature of approximately -27 °C. The primary cooling agent, Freon R22 was used out of safety reasons (Kofoed & Doran, 1996; Murray & Eskesen, 1997).

One of the design criteria was; the temperature of -5 °C on a distance of 600 mm from the freeze pipe, the cooling time to reach this was calculated to thirty days.

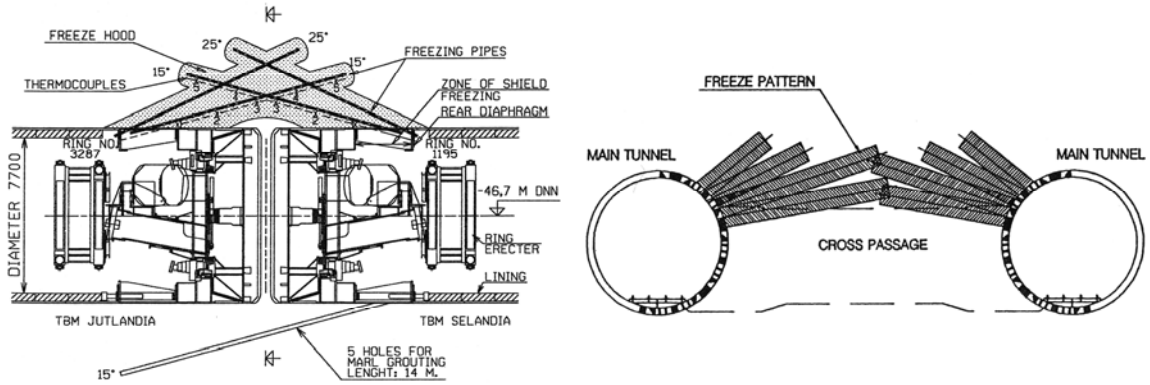

Figure 2.56 The two types of ground freezing were performed; TBM junction and cross passage. On the left-hand side, longitudinal cross section at the TBM junction. The picture on the right-hand side, cross-section at the cross passage, after Kofoed and Duran (1996)

At the Passage 8, one design criteria was that the temperature in the core of the frozen tunnel roof should be the at the most -10 °C and create a homogenously frozen arch with a thickness of 1.4 m along the whole cross passage.

In the TBM junction cavern of the southern tunnel, a design criterion was set to the target temperature -15 °C for a 2.5 m wide frozen core. This criterion was reached after approximately 30 days of freezing (Kofoed & Doran, 1996; Murray & Eskesen, 1997).

The frozen construction was used in two ways, primarily for creating an impermeable water barrier so that tunnelling could go on without risking that water would leak in, and secondly as a structural member providing a protective hood over the excavation (Kofoed & Doran, 1996; Murray & Eskesen, 1997).

Deformations and stresses

Different soil properties create different conditions for binding water to the grains and for transporting water to the freeze front from the unfrozen material that in this way increases the water content for the frozen material. Considerable pressures can be built up from heaving created when water phase change to ice, which has been discussed above. The relation between hydraulic permeability and frost heaving was examined in the freeze project, see Chap. 2.6.

In connection with the planning of the freezing for the cross passages, the designers were concerned that the pressure against the main tunnels caused frost heaving. The freeze pipes were, because of this concern, placed slanted in relation to the cross passage tunnels, i.e. installation of the freezing pipes parallel to the tunnel that was to be stabilized, was avoided thus only the pressure from the secondary heaving on the main tunnels was received. To further reduce possible frost heave, intermittent freezing was used. The results from the deformation measuring have shown that only "... deformations in the order of a few millimetres occurred during the freezing process ..." (Kofoed &Doran, 1996, p 395) and the deformations originating because of freezing were not considered to be present for the main tunnel lining (Kofoed &Doran, 1996). Furthermore, the SGI lining was designed for full overburden, i.e. the load of above laying water, soil and rock (Murray & Eskesen, 1997).

2.9.2 Ground freezing at Hurum weakness zone in the Oslofjord subsea tunnel, Norway 1999

To relieve the pressure on the heavy trafficked central parts of Oslo, a connection about 50 km south of Oslo was created to redirect the bypassing traffic over (under) the Oslofjord instead of having the traffic drive around the fjord and through Oslo. This saves about 25 km of road and approximately thirty minutes in time. The Oslo fjord connection thus creates a communication possibility between E18, which goes from Stavanger and follows the coast up towards Oslo, to E6, which goes from Oslo and continues down towards Malmo etcetera (Statens Vegvesen, 2005).

The Oslo fjord connection is totally 26.5 km long and consists of, inter alia, six tunnels and eight bridges. The project started in 1997 and is subdivided into five different section projects; these projects were completed at the same time. The traffic route opened for traffic during June of 2000 (Statens Vegvesen, 2005).

Introduction

The Oslo fjord connection consists of a two-lane highway, besides the tunnel section, which goes under water, and continues as a single-tunnel with three lanes. The single-lane road goes downwards in this section and the two-lane road upwards. To reduce the tunnel length, the tunnel however is inclined 7 % (Andreassen, 1999; Berggren, 1999; Berggren, 2000; Eiksund, Berggren & Svanø, 2001).

The tunnel under the Oslo fjord was included in the contract ”Parsell 4, Oslofjordtunnelen”, which goes between Verpen on Hurum in the west and Måna close by Dröbak in the east. The total length of the tunnel is 7.6 km whereof 7.2 km is located under the Oslo fjord.

Geology

The Oslofjord is formed along a number of faults and weakness zones; the vertical total displacement is estimated to 2 000 m. The preliminary examinations showed that especially three weakness zones crossed the tunnel’s projected length; see Figure 2.57 and Figure 2.58 (Eiksund et al, 2001).

Hurum weakness zone that was located closest to the Hurum country was considered to be the most critical one with the least rock coverage and the lowest seismic speed, 2,600 m s^{-1} (Eiksund et al, 2001). The examinations were accomplished with among other things core-drilling, one of the holes was accomplished with directional core drilling. The core material was noticed to contain crushed rock material and clay (Andreassen, 1999; Berggren, 2000; Eiksund et al, 2001).

The central parts of the Hurum zone consisted of the eroded long valley in the rock, filled with glacial deposits such as clay, sand, gravel and boulders measuring up to three metres. The base of the long valley is at the same level as the middle of the tunnel, i.e. three metres under the head of the tunnel and about 120 m under sea level. The tunnel’s lower part, under the Hurum zone consisted of fissured gneiss (Berggren, 2000).

The Hurum zone was identified early in the pre-investment study and additional examinations were therefore performed, such as seismic, core-drilling, and soil- rock penetration test to establish the extent and the content (Andreassen, 1999; Backer & Blindheim, 1999).

The core material in the zone was established to consist of crushed rock with elements of clay. When core-drilling, however, it was not discovered that the Hurum zone had a high water pressure, i.e. a static hydraulic pressure of 12 bar and that it contained loosely layered soil (Berggren, 2000; Eiksund et al, 2001).

The 12 m wide zone with glacial deposits was discovered at preliminary probing in connection with the tunnelling (Andreassen, 1999). Further tests showed that the upper half of the tunnel area merged with loosely stored glacial moraine on the bottom of the Oslofjord. The zone, consisting of sand gravel and blocks, had high permeability. In the lower part of the tunnel area, under the Hurum weakness zone, it consisted on the other hand of hard but fissured rock (Eiksund et al, 2001).

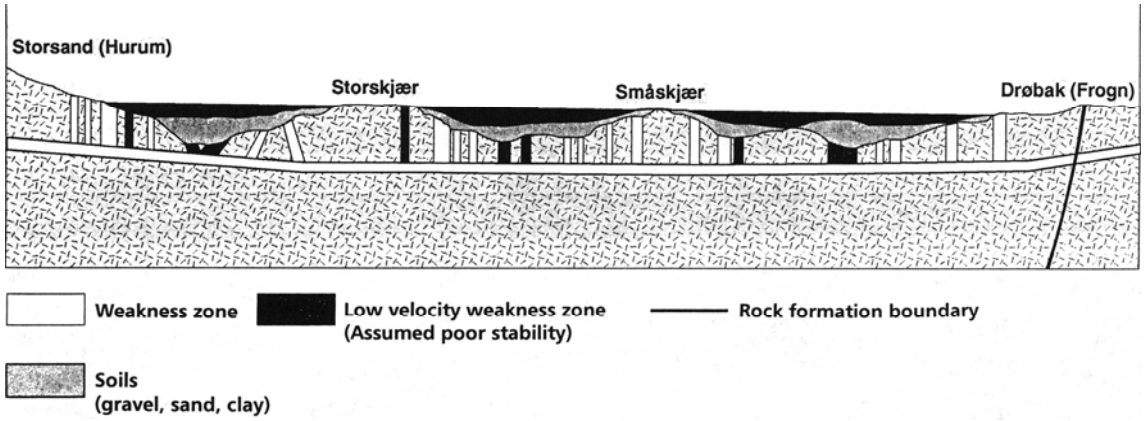

Figure 2.57 Oslofjord subsea tunnel, longitudinal cross section, after Backer and Blindheim (1999)

Freeze technique and design

The driving of the tunnel was accomplished primarily through conventional drilling and blast of the tunnel area on four fronts, one from the west, one from the east and two from a working tunnel with portalling on the western lakeside (Storsand). The advance was on average 30 m to 40 m per week at each respective front (Eiksund et al, 2001).

Probing with three 30-m holes with 15 m overlap was performed during the driving process. In connection with driving from the working tunnel's western front towards Hurum, the zone was penetrated during probing and water was flushed in the tunnel. It was concluded that the Hurum zone was in hydraulic contact with the water in the Oslo fjord, 40 m under the ocean bed and 120 m under the water surface, i.e. 12 bar hydrostatic water pressure (Andreassen, 1999; Berggren, 2000). "The weakness zone is the bottom of a channel probably cut by a glacial melting river." (Eiksund et al, 2001, p 1731).

To gain more knowledge about the zone, the driving process stopped 17 m from the zone and further tests were made. Having acquired new knowledge about the zone's hydraulic and geological properties, it was decided in January 1998 that a 47-m^2 bypass tunnel was going to be built 15 m to 20 m under the Hurum zone. The bypass tunnel, totally 350 m long, connected 150 m west of the Hurum zone in April 1998. After having even driven the tunnel from the west towards the zone, 46 m un-driven tunnel was saved whereof it was acknowledged that about 12 m of it was part of the Hurum zone (Andreassen, 1999).

The tunnel was driven from the Hurum side towards the Hurum zone. One unsuccessful attempt to stabilize and seal the zone with 700 tons of cement grouting was made and the zone was frozen as an alternative method. One of the main reasons why freezing was chosen as the stabilizing and sealing method, was that the method was considered safe since it was hard to obtain representative tests from the zone because of the relatively high water pressure. The uncertainties in regards to the material in the zone contributed to that many stabilizing and sealing methods gave too significant uncertainties, while the freezing was considered a way to stabilize and seal the material that the tests' results were varying between (Backer & Blindheim, 1999).

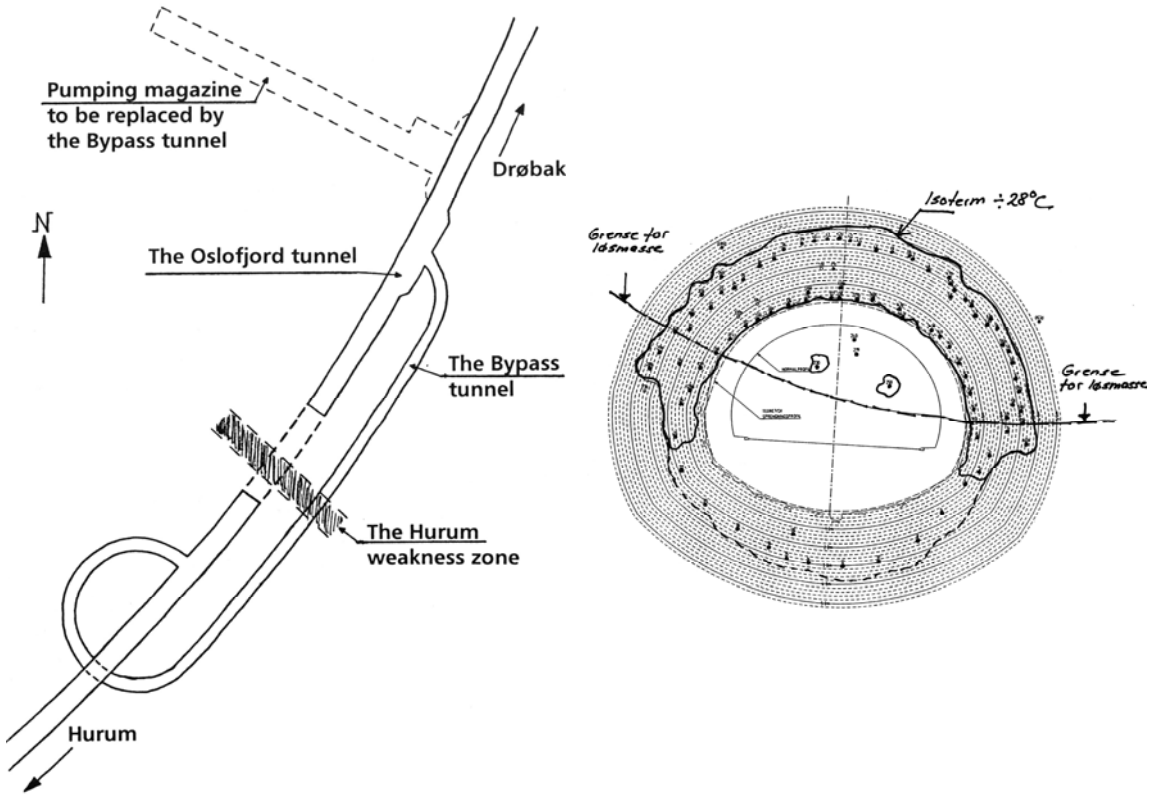

Figure 2.58 Hurum weakness zone; on the left-hand side, schematic plan showing the bypass tunnel crossing the weakness zone at a lower level, modified after Backer and Blindheim (1999). On the right-hand side, cross-section of the Hurum weakness zone, showing the -28 °C isotherm, one design criteria. Modified after Andreassen (1999)

Freezing as a stabilizing and hydraulically sealing method was decided upon in April 1998. The freezing started in April 1999, the tunnelling of the frozen zone started in August 1999 and the break-through occurred in November 1999 (Berggren, 2000).

Deformations and stresses

Berggren (1999) describes the design of the frozen mass using an arching effect of shell type structure around the tunnel, because of the frozen mass' high compression strength and low tension strength. However, the starting point is a pressure ring with throughout yielding around the tunnel, where the surface tension according to classical plasticity theory is replaced by the designed pressure (σ_d) for the frozen material, see Figure 2.59. The tangential stress along the internal radius (r) is critical. Nevertheless, the surcharge (p) on the frozen zone, the pressure ring, is then aloud to be maximum (Berggren, 1999; Eiksund et al, 2001)

$$p_g \leq \sigma_d \ln\left(\frac{r+T}{r}\right) \tag{2.78}$$

where p_g = load on the beam, r = internal radius, T = estimated thickness of the frozen soil and σ_d = design compression strength.

Rearranging Eq. (2.78) gives the requisite thickness of the frozen zone for a circular tunnel (Berggren, 1999; Eiksund et al, 2001)

$$T = r\left(e^{p_g/\sigma_d} - 1\right) \tag{2.79}$$

With consideration of the significant depth in the ground, Eq. (2.79) gives an unrealistically large frozen zone (20 m) (Eiksund et al, 2001). "Other solutions thus had to be considered" (Berggren, 1999, p 20.3). According to Eiksund et al (2001), a complete tunnelling cycle of 2 m to 3 m long rounds could be performed by installing a concrete lining before advancing to the next section.

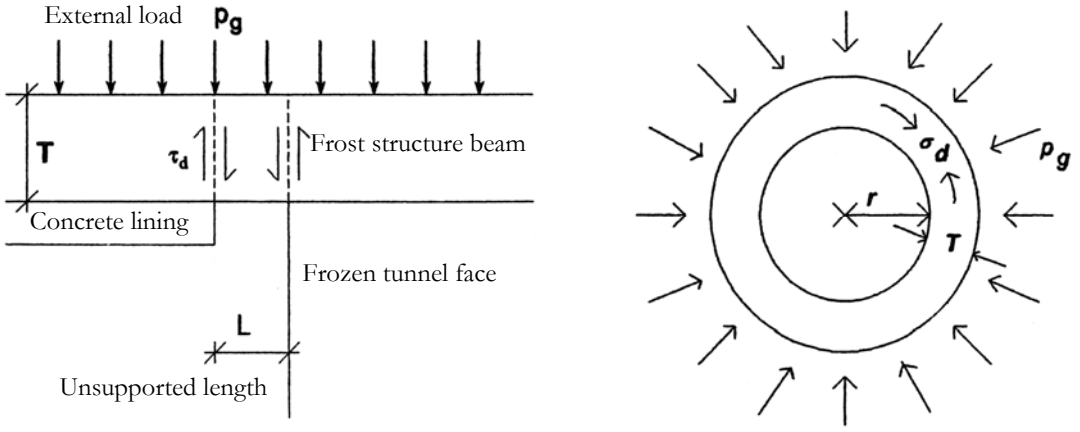

Figure 2.59 Design of the frozen ground as an aid in tunnelling at Hurum. On the left-hand side, illustration of the necessary thickness of the frozen structure, bearing between the frozen tunnel face and the concrete lining. On the right-hand side, Stress relations at a circular shaped opening according to plasticity theory, modified after Berggren (1999)

To minimize the frozen construction, a plain beam model was used as an estimation model. The beam is supported by on the one hand concrete lining, on the other hand the frozen tunnel face, see Figure 2.59 (Eiksund et al, 2001; Berggren, 2000). However, the length of the unsupported frozen construction, i.e. the "open length" is given through the state of equilibrium discourse (Berggren, 2000)

$$Lp_g = 2\sum T\tau_d \tag{2.80}$$

where L = unsupported length of the frozen beam, P_g = load on the beam, T = dimensioning thickness of the beam and τ_d = dimensioning shear strength of the beam.

The loads are made up by the approximately 80 m of permeable soil above the tunnel, as well as the hydrostatic water pressure (12 bar). In the model of estimation, the hydrostatic water pressure was assigned to 1 200 kPa and the above load of soil to 200 kPa, i.e. a total load (p_g) of 1 400 kPa. However, the load factor was assigned to be 1.0 (Berggren, 2000).

The strength properties, its temperature-, and time dependence are decided through laboratory tests on the actual material. The creep model for frozen soil material that was developed by Berggren (1983) was used to design the frozen zone. In the creep model, the creep strength is defined as maximal surcharge allocated over the material over a given time without that the material's deformation rate becomes constant. The reference strength (σ_θ) is dependant of the temperature, the mobilization degree (f_d) is dependant of the duration and was decided together with the material coefficient (γ_m) through Berggren's (1983) creep model the dimensioned creep strength (σ_d), see also Figure 2.60

$$\sigma_{\mathrm{d}} = \frac{f_{\mathrm{d}}\sigma_{\theta}}{\gamma_{\mathrm{m}}} \tag{2.81}$$

where f_{d} = degree of mobilization at the design load duration, γ_{m} = material coefficient, dependent of risk and project. The value is chosen in accordance with the Norwegian recommendations, normally between 1.2 and 2.0 (Berggren, 2000), σ_{d} = design compressive strength and σ_{θ} = reference strength at temperature θ (the unconfined compression strength) and at constant rate of strain of 1 % per minute.

Core drilling was performed in the unstabilized zone to perform freeze tests in laboratory environment. Only "two small pieces" from the cores of the core drilling was judge undisturbed, the rest was "disturbed" because of flushing of fine material in connection with the core-drilling. The material from the core-drilling was mixed, packed and saturated with seawater, before they were frozen and laboratory tests were performed (Berggren, 2000).

The temperature dependant strength (unconfined compression tests) was decided through tests at -10 °C, -20 °C and -28 °C. The strength at -10 °C was low in relation to earlier tests (Berggren, 2000). Figure 2.60 shows that the frozen soil strength "develops" faster at temperatures lower than the eutectic temperature for sodium chloride, -21.3 °C (Andreassen, 1999; Berggren, 2000). However, Berggren's interpretation of this phenomenon is that the presence of the salt rich pore water affects both the cohesion material and the friction material.

Unconfined compression tests have been accomplished to analyze the degree of mobilization for a material from the weakness zone in a temperature of -28 °C, see Figure 2.60. Because of that, the material in the tests showed a relatively low strength at "high" temperatures, it was decided that the design temperature should be -28 °C. The reference strength (σ_0) at this temperature was 8 000 kPa (Berggren, 2000).

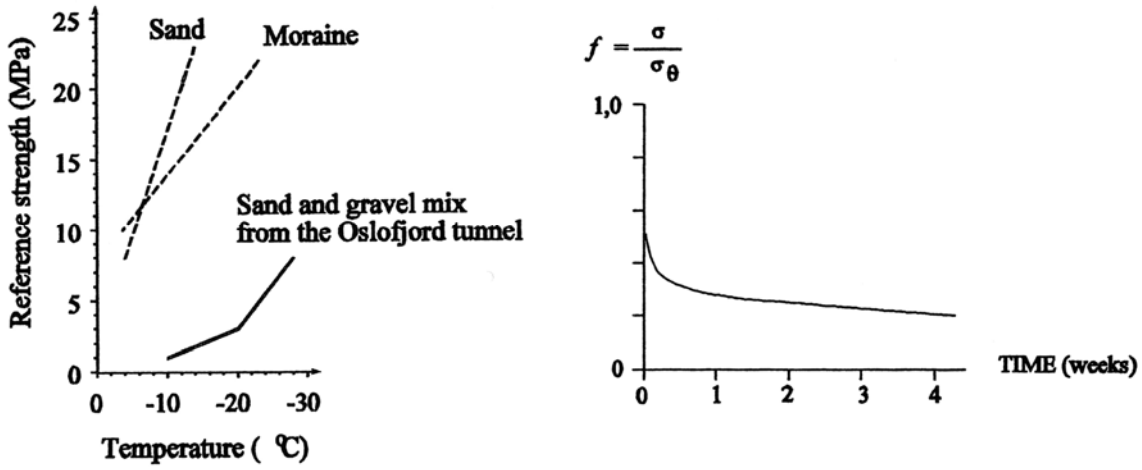

Figure 2.60 On the left-hand side; design values of reference strength, results from laboratory studies. At the right-hand side, design values for the degree of mobilization as a function of the time, after Berggren (2000)

The time schedule for each round of drilling, blasting, mucking out and lining was one week. The dimensioned stand-up-time was two weeks; this gave a degree of mobilization (f_{d}) of 0.25, see Figure 2.60 (Berggren, 2000).

Because of the serious consequences that a possible break in the frozen construction could lead to, the material coefficient (γ_m) to 1.6 was established. The level was based upon among other things (Berggren, 2000)

- the material in the frozen construction was judged to be stronger than the material tested in the laboratories
- the three-dimensioned carrying effect is favouring in relation to the one-dimensional beam model
- the possibility to close the tunnel face if a breakage would occur was good.

The dimensioned compressive strength according to Eq. (2.81) with variables placed according to above was 1 250 kPa. The shear strength (τ_d) was assigned to half of the dimensioned strength, which is 650 kPa, as no other tests were made on this parameter (Berggren, 2000).

The length of each round could be calculated from Eq. (2.80) using the above variables. A 3 m thick frozen zone with a temperature not exceeding -28 °C gives, for example, an allowed opening length of 2.7 m, and a complete driving cycle became 2.2 m with consideration of overlapping; see Figure 2.61 (Berggren, 2000).

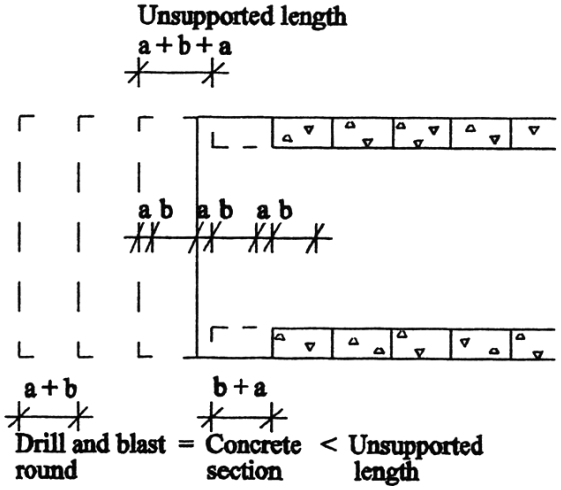

Figure 2.61 Illustration of the different lengths in a drill and blast round between the tunnel support and the tunnel face, after Berggren (2000)

There were three requirements that had to be accomplished before the driving of the tunnel through the frozen construction could start (Andreassen, 1999; Berggren, 2000)

i. the frozen zone around the future tunnel had to be sealed
ii. the soil in the weakness zone in the tunnel face had to be frozen
iii. the temperature between the two rows of freeze pipes had to be at least -28 °C.

A concrete wall, designed to handle hydrostatic water pressure of 13.5 bar had been built between the tunnel face and the rest of the tunnel. According to the safety routines, the tunnel should be evacuated under the water level. There was also a vehicle accessible to lock the door in the concrete wall in case of a leakage in connection with the blasting. Nevertheless, to prevent that rocks and blocks would fall down from the broken up frozen surface, a 0.20 m layer of shotcrete was applied on the vault and in the front. The shotcrete had been equipped with an accelerator, and compressive strength of 1 MPa was received after 15 minutes and 5 MPa after three hours. However, no problems arose in connection with the application of shotcrete against the cold surface. Furthermore, the permanent

lining was dimensioned for ”full hydrostatic water pressure” and consisted of 1.2 m concrete in the bottom and 1.0 m in vault (Berggren, 2000).

2.9.3 Ground freezing around an existing tunnel in Kobe, Japan 1996

The authorities in Kobe City, Japan, made a decision to extend the subway system consisting of two tunnel pipes with an outer diameter of 5.4 m. Because of the design limitations, the lower of the two tunnel pipes came to cross an existing cable tunnel, straight underneath the Motomachi Avenue. The cable tunnel belongs to Nippon Telegraph and Telephone Corporation (NTT) (Kamata et al, 2000).

NTT's cable tunnel has a diameter of 4.55 m and is located approximately 20 m under street level. To solve the problem with the meeting of the two tunnels it was decided that a new 40.7 m long NTT tunnel was to be built directly underneath the existing tunnel. The existing stretch of tunnel that was blocking the subway was removed, see Figure 2.62 (Kamata et al, 2000; Konrad, 2002).

Introduction

The freezing method was chosen to create a strong, frozen mass around the existing NTT tunnel so that one part of the existing NTT tunnel could be torn down. The new tunnel and later even the subway pipe were going to be built at the same time. Nevertheless, as the project was located in the heart of Kobe City, it was important to reduce the freeze- and thaw induced deformations with consideration of the existing buildings, particularly a 6.0 m wide wastewater culvert located 4.0 m under street level and in the close vicinity of the centre line of the future subway (Konrad, 2002).

Geology

The soil conditions at the Kobe tunnel consisted of sequences of none frost susceptible materials such as sand- and gravel strata layered with frost susceptible, fine-grained materials such as sandy clay. The groundwater's zero pressure level was about 3.5 m under street level and its salinity was judged negligible. The rate of the ground water was lower than 1 mm per day, see Figure 2.62 (Kamata et al, 2000; Konrad, 2002).

NTT tunnel is located at a depth of 20 m, under an existing wastewater tunnel (Kamata et al, 2000).

Freeze technique and design

The cooling machines were located at ground surface, 210 m from the frozen section. Three cooling machines, each one with a cooling effect of 150 kW at -25 °C ($CaCl_2$), stabilized and hydraulically sealed the temporary construction during 390 days.

The freeze system in the ground consisted of 328 freeze pipes, divided into 104 sub-vertical pipes installed from the ground surface and 106-curved freeze pipes (referred to as tulip pipes) installed in curved form, from the existing NTT tunnel through directional drilling. Furthermore, from the inside of the tunnel, 224 “short” freeze pipes were installed radial. In the central parts of the tunnel, a cross section of four 0.10 m vertical freezing pipes with a centre distance of 1.0 m and a circular “tulip pipe” dimensioning 0.25 m and with a spacing of 0.7 m (Konrad, 2002).

The freezing started on August 3rd, 1997 and went on during one year in the vertical freeze pipes. The freezing through the tulip pipes began in September the same year and the driving of the tunnel started three months after that the cooling had begun, i.e. during November 1997. When the cooling was finished and there was no longer a need for the temporary construction, the thawing process was accelerated through circulation of “hot water” at +55 °C in the tulip pipes (Konrad, 2002).

The freeze project was dimensioned so that the temporary stabilized construction had reached a max temperature of -10 °C with a thickness of at least 1 m after 90 days.

Up to four layers consisting of sandy clay are affected by the freezing, see Figure 2.62. As it could be expected that these layers most likely are frost susceptible, it is possible that they would affect the surrounding construction (Konrad, 2002).

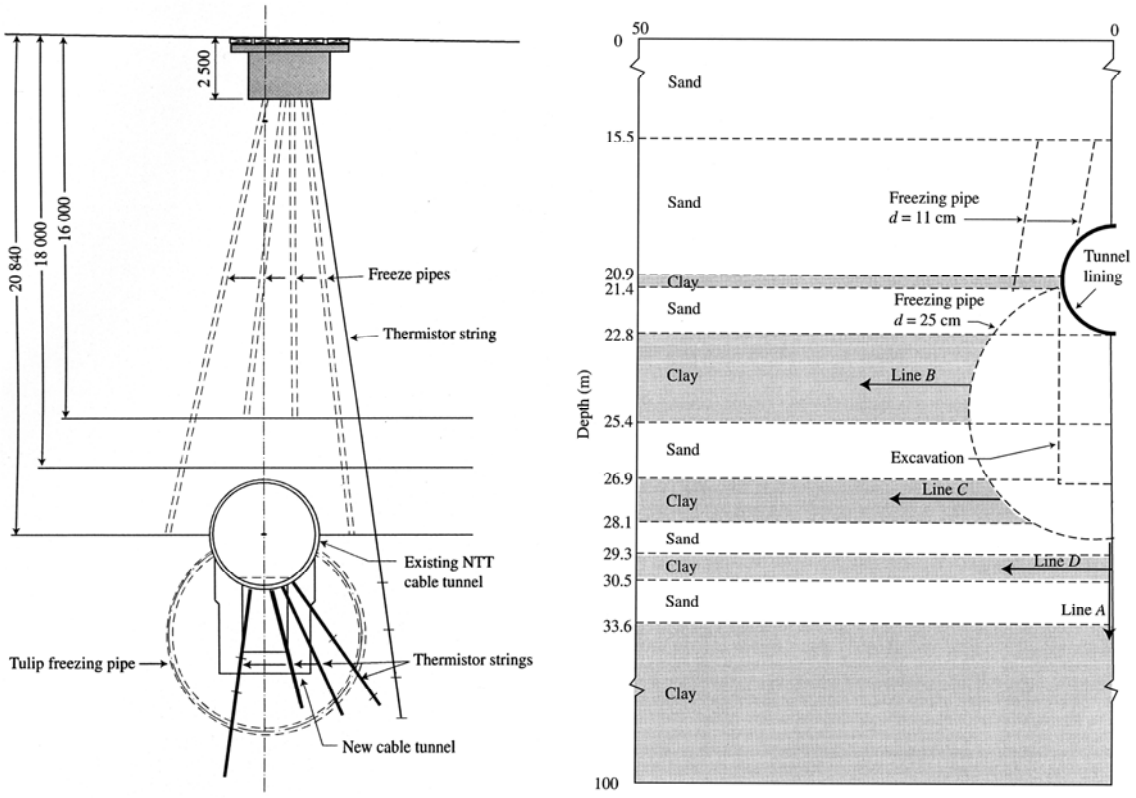

Figure 2.62 On the left-hand side; Cross section; freezing around existing tunnel. At the 'tunnel crossing' between the existing cable tunnel (NTT) and the subway's lower tunnel pipe was connected to the NTT tunnel via the building of a new short tunnel (the rectangular) under the subway, after Konrad (2002). On the right-hand side; cross section showing the geology for the frozen tunnel, after Konrad (2002)

Deformations and stresses

The segregation potential (SP) is in, among others, Konrad and Morgenstern (1981) and Konrad (1987) defined as the relation of the rate of the frost heave to the temperature gradient in the frozen fringe. The SP model has earlier been used successfully in different projects, particularly in one-dimensional (1D) simulation of heaving.

Many field problems can, according to Konrad (2002), be solved with two-dimensional thermal simulation when predicting, above all, the water content increase due to ice lens creation during the freeze process. One-dimensional simulation of frost heave is, however, advantageous as the stress in the frost front is of the same number as the surcharge. When adapting two-dimensional frost simulation, the interaction between the loads and the SP must be taken in to consideration, as well as one has to ensure oneself of the compatibility between the load and the deformation (Konrad, 2002).

Numerical frost problem models using rigid net are not correct in situations when the frost heaving is relatively large and therefore induces stress, which in turn affects the rate of the

water to the freeze front. Models that apply deformable nets based on modulation of volumetric deformations are truer (Konrad, 2002).

A change in volume occurs in frost susceptible soil principally through ice lens formations created by migrating water, which in turn has frozen on the segregated freeze front. The volumetric strain increment due to segregational heave is calculated with help of SP-function (Konrad, 2002)

$$\mathrm{d}\varepsilon_{\mathrm{s}}^{v} = \frac{\Delta V_{\mathrm{s}}}{V} = \frac{\rho_{\mathrm{w}}}{\rho_{\mathrm{i}}} l_{\mathrm{s}} v \frac{\Delta t}{A}, \quad \text{with } v = \mathrm{SP}\left(\sigma_{\mathrm{n}}\right) \mathrm{grad}\, T_{\mathrm{f}} \tag{2.82}$$

where A = element area, grad T_{f} = temperature gradient in the frozen element, l_{s} = length of the freezing isotherm in the element, SP = segregation potential, Δt = time step, V = element volume, ΔV_{s} = element volumetric expansion due to the segregational heave, = volumetric strain increment due to segregational heave, v = water migration rate to the heaving element, ϱ_{i} = density of ice, ϱ_{w} = density of water and σ_{n} = stress normal to the frost front.

To predict the freeze- and thaw inducing deformations around the freezing pipe, the following method was used (Konrad, 2002):

i. Establishing of SP for sandy clay and relation between SP and applied normal stress, by freezing undisturbed tests gradually with different overburden loads.
ii. Establishing of boundary conditions for temperature via use of 2D thermal simulation in a longitudinal section parallel to the tunnel axis. Three simulations were accomplished for (*a*) vertical freeze pipes in water saturated sand; (*b*) "the tulip freezing pipes" in sand and (*iii*) "tulip freezing pipes" in sandy clay. The thermal simulations give a good approximation of the temperature field around the freezing pipes as a function of time.
iii. Establishing of the water content increase during the freezing process in a cross section, perpendicular to the tunnel axis with a SP-2Dmodel. The boundary conditions from (ii) are used in the model. The deformations are calculated with help of an anisotropic strain tensor where the majority of the expansion strain is normal to the frost line in each element.
iv. The establishing of thaw consolidation using the anisotropic volume change tensor, where the main axis for the strain is horizontal and vertical. As all surplus pore water is accumulated in each element during the course of freezing, it will instantly disappear as soon as the melting process occurs in the element. Once again, it is emphasized that the main direction for the deformation during the thawing is different from the main direction of the heaving.

The soil samples were taken at a level of 23.5 m below the ground surface and were frozen from top to bottom at a temperature of -10 °C. Figure 2.63 shows a freeze- and thaw test of the samples №1 to №5 which confirms a structural change in the soil after a freeze-and thaw cycle, this is illustrated by the deformation of 1 % (Konrad, 2002).

From results of laboratory tests with frozen soil samples assembled in Table 2.8, as well as knowledge about SP_0 (= $110 \cdot 10^{-5}$) and the soil consonant α, these also from laboratory experiments, SP can be calculated according to (2.83). The results from these calculations are accounted for in Figure 2.63 and in Table 2.8, with SP as a function of the normal stress (Konrad, 2002)

$$\mathrm{SP} = 110 \cdot 10^{-5} \mathrm{e}^{a\sigma_{\mathrm{n}}} \ [\mathrm{mm^2\ s^{-1}\ ^oC^{-1}}] \tag{2.83}$$

where a = soil consonant from laboratory experiments; -1.6 MPa^{-1} and σ_n = stress normal to the frost front [MPa].

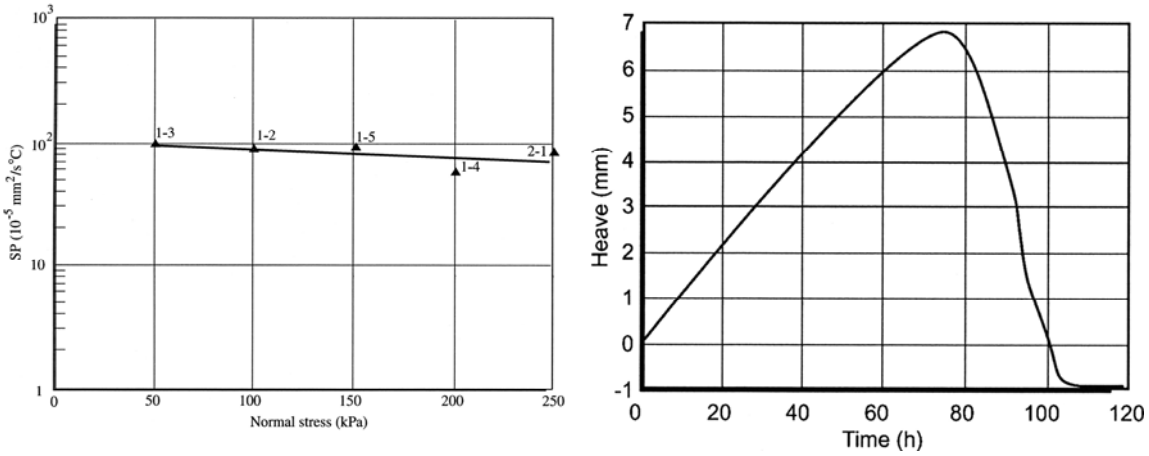

Figure 2.63 On the left-hand side; frost heave laboratory tests of the segregation potential for Kobe clay, after Konrad (2002). On the right-hand side; a result from a freeze-, thaw test, sample № 1 to № 5, after Konrad (2002)

Table 2.8 Summary of results from frost heaving tests, after Konrad (2002)

Test №	Water content (w) [%]	Normal stress (σ_n) [kPa]	Heave rate ($dh\ dt^{-1}$) [mm h^{-1}]	Temperature gradient (grad T) [°C mm^{-1}]	Segregation potential [10^{-5} mm^2 s^{-1} °C $^{-1}$]
1 - 1	43	250			
1 - 2	46	100	0.13	0.0385	94
1 - 3	43	50	0.15	0.04	104
1 - 4	43	200	0.085	0.04	60
1 - 5	44	150	0.096	0.0275	97
2 - 1	36	250	0.095	0.0314	84

SP-2D (cross section) was used in connection with the analyzing of freeze-, thaw simulation, the surcharge-deformation relation used to calculate the volumetric expansion induced stress field during frost heave was based upon the values shown in Table 2.9. The values originate from Johnston (1981) (Konrad, 2002).

Table 2.9 Soil parameters for Kobe clay, after Konrad (2002)

	Deformation modulus (E) [MPa]	Poisson ratio (υ)	Yield stress (σ_y) [MPa]
Clay, unfrozen	11.2	0.3	
Sand, unfrozen	25	0.3	
Clay, frozen	$13.75(-T)^{1.18}$	0.3	$0.531(-T)^{0.404}$
Sand, frozen	$27.5(-T)^{1.18}$	0.3	$1.06(-T)^{0.404}$

Note: Deformation modulus after thawing (E_f); 0.25E. T = temperature.
Tunnel lining: $E_u = E_f = 2 \cdot 10^4$ MPa; $\nu = 0.3$

Figure 2.64 shows the deformation of the ground surface above the temporary freeze-stabilized tunnel after three months freezing, i.e. at the point when the frozen construction has reached its design criteria and the excavation can begin. The image also illustrated the deformations in the ground surface after one year of freezing as well as after another year of thawing. When the cooling has reached the design criteria after three months, a heave in the ground of about 0.03 m above the tunnel has then occurred. The construction receives

intermittent maintenance cooling during the passive phase to minimize heaving. The heaving of the ground surfaces measures after one year of freezing, whereof nine months is passive freezing, 0.048 m right over the tunnel axis. The vertical movements in the ground surface decrease on the other hand with the distance from the tunnel axis. The maximal vertical movements decrease on an average of 0.001 25 m per metre at the distance between 10 m and 30 m from the tunnel centre axis. The total observed and prognosticated settlements of the ground surface above the tunnel axis are shown in Figure 2.64.

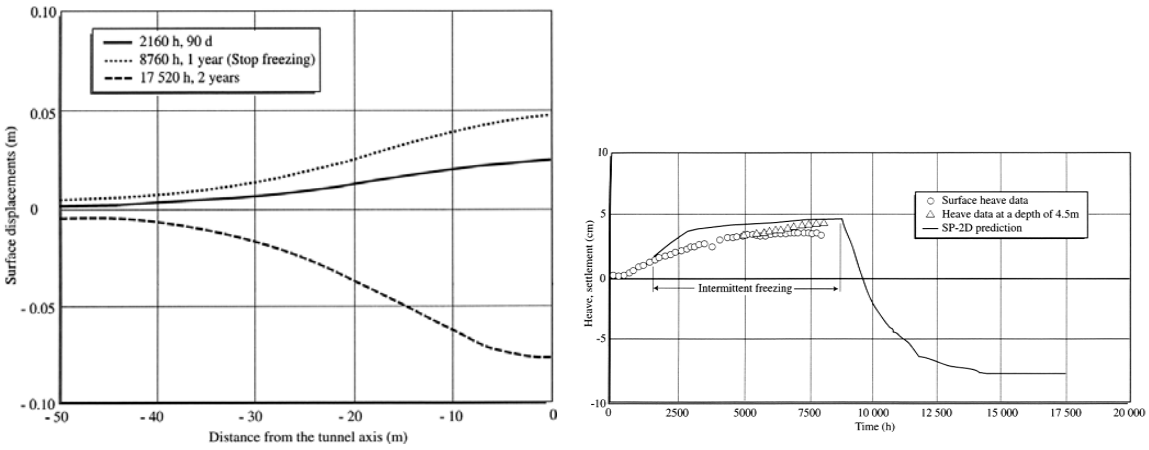

Figure 2.64 On the left-hand side; prognosis of the deformation of the ground surface through SP-2D after the freezing phase (90 days), when the cooling is finished (1 year) as well as 1 year after terminated cooling, Konrad (2002). On the right-hand side; estimated deformation and observed deformation during the freezing process (frost heave) for ground surface and at a depth of 4.5 m above the tunnel axis, after Konrad (2002)

Table 2.9 shows the original water content average reaching 45 %; this was taken as a representative value for all clay layers in freeze- and thaw calculations. The assumed water content for the compact water saturated sand was 18 %, while the water content in the medium compact sand was set to be 15 %. The water content increased significantly in the frost susceptible clay layers close by the advancing frost front. After one year of freezing, the water content increased to approximately 60 % in the clay layers along the lines C and D, see Figure 2.62. The freezing of the migrating water did not contribute to any significant vertical deformation; however, a horizontal expansion primarily occurred (Konrad, 2002).

During the thawing process, all surplus water in each soil element will eventually migrate from the soil element, i.e. if a thaw consolidation occurs. The extent of the deformation is calculated with consideration of that all surplus pore water accumulated in each soil element during the freezing would escape out of the soil element when thawed. This simulation did not, however, take into account the structural changes in the soil. The size of the structural change is, as mentioned above, 1 %. The settlements occur as soon as the thawing is completed for each element. Nevertheless, this simplification does not affect the settings' total number; it solely influences the time dependence of the settings, which in turn corresponds with SP-2D (Konrad, 2002).

In fact, the rate of the thawing deformation is in reality dependant on the surrounding soil's hydraulic conductivity. Thus, the rate of the thaw consolidation will become lower than the rate of the thawing, unless the surrounding soil is draining (Konrad, 2002). However, the thaw consolidations are two to three times larger than the frost heave in

larger projects with horizontal tunnels. In this project the thaw consolidation were 2.7 times larger than the frost heave (Konrad, 2002).

The expected thaw settlement, approximately 0.13 m for the shallow wastewater tunnel, was too large of deformation for the tunnel construction to handle considering possible breakage in the construction and subsequent leakage. Because of this reason, injection of grout in the clay layers during the thawing process was suggested to reduce deformations due to thawing. On the contrary, the estimated settlement due to thawing for wastewater was less than 0.010 m (Konrad, 2002).

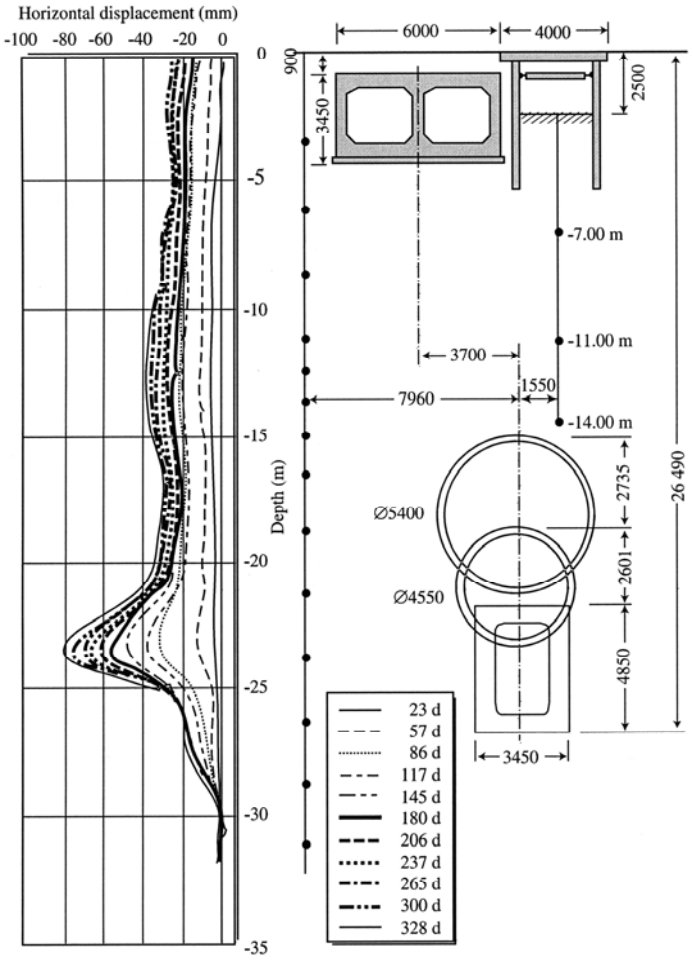

Figure 2.65 Cross section perpendicular to the tunnel axis, horizontal deformation as a function of the depth. Negative deformation, - movement from the freeze area, after Konrad (2002)

Horizontal deformations were observed through inclinometers, installed approximately eight metres from the NTT tunnel's centre line. The measured results are shown in Figure 2.65. Figure 2.65 also illustrates that the deformation after one year of freezing was 20-30 mm in a zone reaching from the ground surface down to a depth of 20 m. The largest horizontal deformation is measured at 24 m depths in height with the new NTT tunnel, middle of the clay layer Line B, see Figure 2.62, one year after the beginning of the freezing.

2.10 CONCLUSION

The literature study covers; 1.) Artificially frozen ground. 2.) Transference of soil energy. 3.) Soil water and soil ice. 4.) Naturally frozen ground and artificially frozen ground, differences and similarities. 5.) Freeze process. 6.) Soil phase relations. 7.) Thaw deformation equations of soil. 8.) Case studies.

The literature study's chapter about artificial freezing of soil and rock in connection with tunnelling shows that:

- Ground freezing used to stabilize and seal soil and rock can primarily come about either through freezing with liquid nitrogen or with compressor cooling machines. The direct method, however, i.e. ground freezing with liquid nitrogen is fast, but proportionally expensive.
- To create a hydraulically sealed construction with liquid nitrogen normally takes about three days once the cooling equipment is installed. Creating a comparable sealed construction with the "indirect method", i.e. with a compressor-cooling machine, generally takes a few weeks once the cooling system is installed.
- There is always a water film between the ice crystals in tempered ice and at lower temperatures the water amount decreases. As a result, thin water paths are created that can contain considerably more water and as long as the water channels are open, the ice can be seen as "weakly penetrable".
- Generally, the degree of unfrozen water depends on; grain size, mineral and temperature.
- The division of the soil element can be described as a solid phase, a gas phase and a liquid phase as well as a viscous "solid" phase when the soil is frozen.
- There are several similarities between naturally and artificially frozen ground. However, there are also many differences. The main differences are; the lowest temperature condition, temperature gradients, stress conditions and durability.
- The frost heaving and the frost floating properties are based on grain size, capillarity and hygroscopicity.
- Several researchers have studied the ranges of thaw deformations of soil without excess load and a number of papers have been produced. As a result, two main groups of thaw settlement predictions can be perceived, theoretical equations and equations taking into account site specific conditions. Moreover, the majority of the presented solutions originate from naturally frozen soil, e.g. permafrozen soil.
- The main parameters that are sensitive to prediction of thaw settlement of soil without excess load according to the theoretical equations are ; void ratio change, e.g. amount of frozen water content, iceness ratio and thawed soil water content.
- Soil water content is the most sensitive parameter when predicting thaw deformation without excess load, due to a specific site. Furthermore, this parameter is completed with various soil dependent constants and variables.
- The case studies show that in general, artificial ground freezing projects are easy to verify during construction. When the temporary construction is fulfilled, the permanent construction takes over the load.

3 GROUND FREEZING AT THE BOTHNIA LINE

This chapter contains descriptions of the ground freezing project at the Bothnia Line and explains the underlying reasons for why the artificial ground freezing method was used. It includes an introduction to the subsequent chapters concerning the laboratory and the field studies, as well as it gives the basic soil parameters presented in the tender document. However, chapter 4, Laboratory study, presents the laboratory studies performed on undisturbed soil and freeze-thawed soil from the area closed to the frozen construction at the Bothnia Line. Similarly, Chapter 5, Field study and prognoses at the Bothnia Line, depicts the field study performed at the Bothnia Line as well as a prognosis of the temperature development in the frozen construction.

3.1 INTRODUCTION

During the construction of the AGF at Stranneberget at the Bothnia Line, the author had the opportunity to do research at the AGF site. Therefore, valuable measurements are conducted for settlements, load build-up on the tunnel roof, temperatures and pore pressures. This thesis deals particularly with in situ soil monitoring during the thawing period of virgin artificially frozen ground. The study of the Bothnia Line ground freezing project has been performed in order to identify and calculate the effect of the thaw settlement. These results are analyzed and presented in the chapter of the field study. Soil samples from different depths have similarly been collected from areas close to the frozen zone. These samples were analysed in the laboratory and the results are presented in the chapter discussing the laboratory studies. Consequently, this process agrees with the hypothesis to collect soil samples from an area that is to be stabilized through artificial ground freezing and to examine these samples in a laboratory and so from the results prognosticate the future final settlement.

For the construction of the tunnel near Stranneberget (at the Bothnia Line in the middle of Sweden, see Figure 3.1 and Figure 3.2), a 100 m tunnel was built with artificial ground freezing techniques (AGF). Extraordinary in situ measurements of temperature, stress on the tunnel roof and deformations of the ground surface were performed during the thawing period in order to estimate the effects of the ground freezing techniques. Due to an increase in water content, resulting from ice lens formation and water volume increase

when the water turned to ice, a decrease in water content during the subsequent thawing was expected as a result of thaw settlement.

The single-track railway line named the Bothnia Line is located in the middle of Sweden between Örnsköldsvik and Umeå on the east coast. The railway line penetrates the mountain, Stranneberget, in a tunnel seven km northeast of Örnsköldsvik. In the northern part of the mountain Stranneberget, the tunnel is redirected from the rock and at shallow grounds, it passes through clayey soil. However, the tunnel passes mostly through good conditions of reinforced rock with shotcrete and wide space bolting. In contrast to the rock tunnel, the tunnel through the clayey soil was built with artificial ground freezing techniques combined with shotcrete. In the same fashion, the instant lining of the good rock became the final assembled tunnel, while, the instant lining of the tunnel in the clayey soil had to be finished with a cast concrete lining. Nevertheless, in order to temporarily increase the stability and the underground water caulking in the clayey soil, artificial ground freezing was to be performed on a 95 m stretch of the tunnel (Botniabanan, 2001A).

The artificial freezing was included in a contract totalling 1 580 m of embankment and tunnel (chainages 12+780-14+360). The purchasing form for the contract was a negotiated purchase with the remuneration type of a fixed price not linked to the cost-of-living index. In addition, the type of the contract was; "... build contract with responsibility for design of tunnel portal, concrete tunnels with associated earth/rock geodesign in the form of freezing, road bridge for route E4, plus construction of the tunnel mouth for servicing the tunnel ..." (Botniabanan, 2001A). This contract was worth around SEK 161 million (Botniabanan, 2001B).

Figure 3.1 Location of the Ground freezing at the Bothnia Line, modified after CIA (2008)

There was a proposition in the tender documents to freeze two areas, area 13+522 to 13+615 (west) and also area 13+740 to 13+850 (east). The two areas resemble each other but the rock surface level in the east area is located closer to the ground surface. However, the contractor decided to install jet pillars for the eastern area and artificial freezing for the western area, see Figure 3.3 (Botniabanan, 2001A).

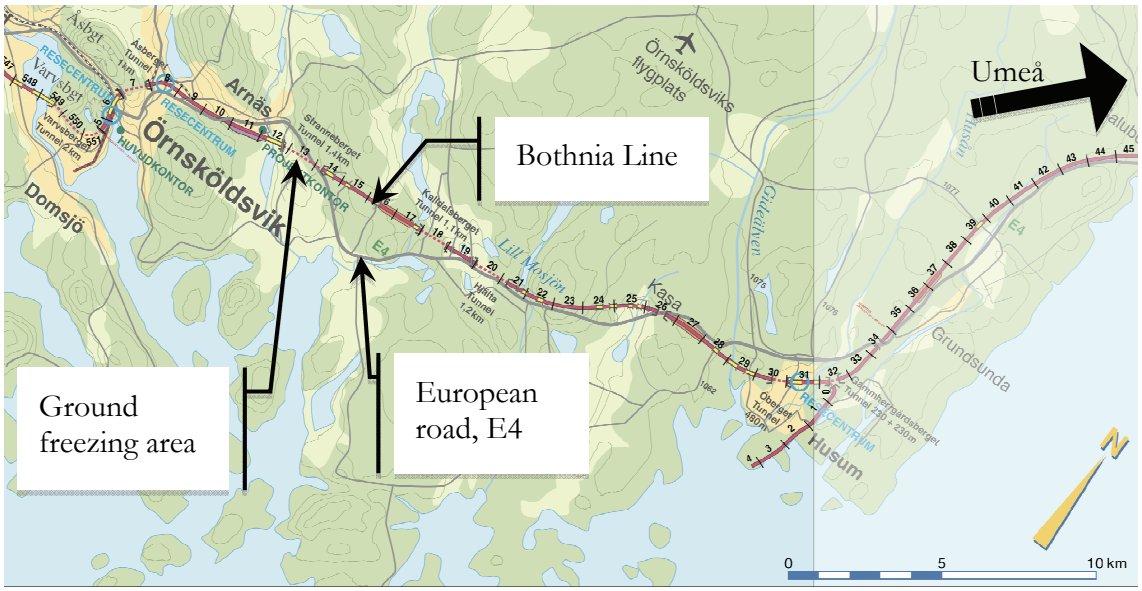

Figure 3.2 *Location of the ground freezing area, a section of the Bothnia Line, modified after Botniabanan (2008)*

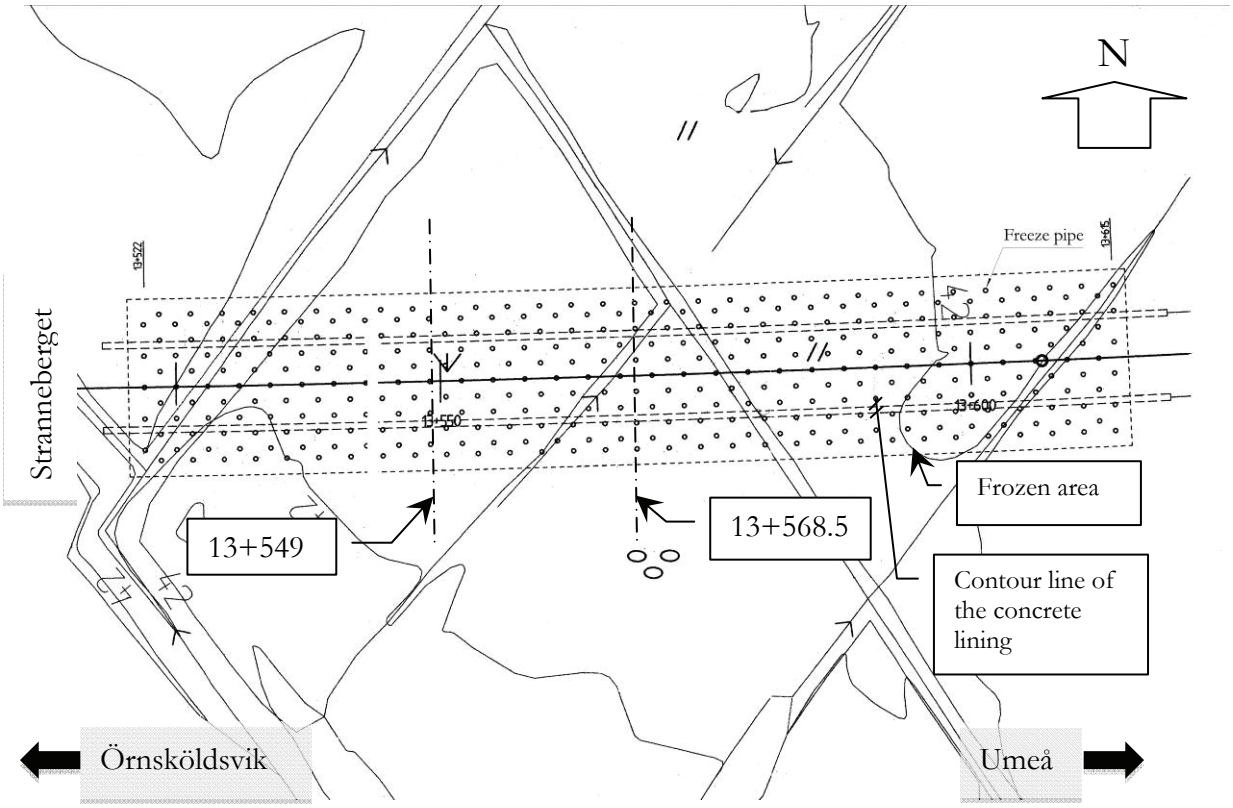

Figure 3.3 *Bothnia Line, principal plan for chainages 13+522 to 13+615. The horizontal projection shows the proposed geometry of the freeze pipe installation, and the monitoring sections in chainages 13+549 and 13+568.5, modified after Botniabanan (2001A)*

3.2 GEOLOGY

The actual soil consisted of approximately 2 m of loose peat and gyttja overlaying postglacial sulphide rich silty clay, see Table 3.1. The thickness of the clay reached up to 11 m and covered an approximately 7 m thick glacial till and the Precambrian bedrock, as can be seen in Figure 3.4 (Botniabanan, 2001A).

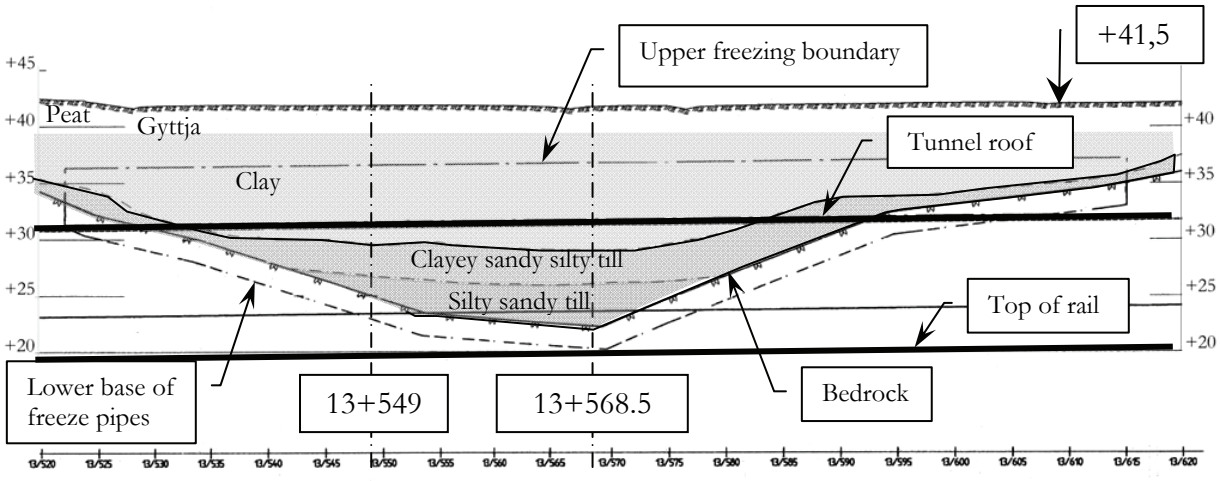

Figure 3.4 *Longitudinal profile of the ground freezing area at the Bothnia Line, illustrating the soil stratum and the vertical tunnel position between chainages 13+522 and 13+615. In the same fashion, the figure shows the monitoring sections in chainages 13+549 and 13+568.5. Modified after Botniabanan (2001A)*

Table 3.1 *The Bothnia Line; the clay's properties at depths of 4 m to 10 m, testing site in chainage 13+573 in the tunnel centre, drill hole TN467, after Botniabanan (2001A)*

Level [m]	Bulk density [t m^{-3}]	Water content [%]	Undrained shear strength [kPa]	Sensitivity [-]	Liquid limit [%]	Coefficient of consolidation [10^{-8} m^2 s^{-1}]
4.0	1.48	92	7.3	29	70	2.5
6.0	1.54	77	13.0	19	68	
8.0	1.51	80	13.0	15	72	80
10.0	1.69	61	11.0	69	44	15

3.3 FREEZE TECHNIQUE AND DESIGN

The reinforcement through ground freezing was stretched over a soil pit from rock to rock. In the clayey areas, artificial ground freezing was performed by means of brine glaciations. This method was estimated to be the most cost-effective method (Vaaranta, 2004). One major reason for choosing ground freezing was the unfavourable contents of sulphide in the soil, which required special soil treatment. Hence, the artificial ground freezing method appeared to be the most advantageous method when looking at the economical aspects as well as the most environmentally friendly method (Saarelainen et al, 2004; Vaaranta, 2004).

The freezing equipment was designed for soil freezing temperatures at approximately -35 °C with a 90-day freezing period. The estimated effective output of the freezing equipment was 650 kW with a capacity of 350 $m^3 h^{-1}$ of the brine pump unit. The ground was frozen by way of approximately 350 freeze pipes organized according to Figure 3.3 and installed at various depths, see Figure 3.5 and Table 3.2 (Botniabanan, 2001A; Vaaranta, 2004). The design criterion was an achieved frozen zone, a frozen arch of 3 m out of the tunnel contour with an average temperature of -15 °C. However, when the average temperature of the frozen arch reached -15 °C, even the tunnel soil intended for subsequent excavating was frozen and had stabilized together as a hydraulic seal, thus securing a hydraulic bottom heave and a stable tunnel face. In the same fashion, the frozen tunnel soil made normal rock tunnelling procedures possible, i.e. usage of the same drill and blast system, and equipment. In contrast to the tunnelling in the solid rock, the frozen soil tunnelling was performed with slightly reduced rounds, maximum 2.5 m and with a higher density of charge (Vaaranta, 2004).

Table 3.2 The design criteria of the frozen construction in chainages 13+522 – 13+615, proposed in the Bothnia Line tender document (Botniabanan, 2001A)

Parameter	**Criterion**
Brine	Running temperature -35 °C
Design temperature	”Temperature mean value” -15 °C in a 3 m thick arch
Casing pipes (steel)	Dimension 219.1· 4.0, tolerance in plan 0.1 m, max deviation of inclination 1 %. 341 pcs. totally installed length; 4 620 m
Freeze pipes	193.7 mm (steel pipe), internal pipe 64 mm (polythene tube)
Freezing time	90 days
Required power	Min 650 kW (calculated on the outgoing brine feeder)
Pump wells	6 pcs. (3 pcs. at each side of the frozen construction)
Observation wells	8 pcs. (4 pcs. at each side of the frozen construction)
Temperature sensor casing tubes	10 pcs. (3 pcs. temperature sensors in each casing tube)
Freeze pipe geometry	Distances between the outer freeze pipes; 94.5 m along the tunnel, 15 m across the tunnel at the central part and 12 m across the tunnel at the ends of the tunnel. Spacing in the longitudinal direction, 3 m in each freeze pipe row. Every other row of freeze pipes at half spacing displacement. Distance between individual freeze pipes, about 2 m in a diagonal network. Spacing across the tunnel, 4 m in the centre of the tunnel and 3.5 m at the edges. Every other freeze pipe row at half spacing displacement. Figure 3.5 and Figure 3.3 show the freeze pipe geometry.

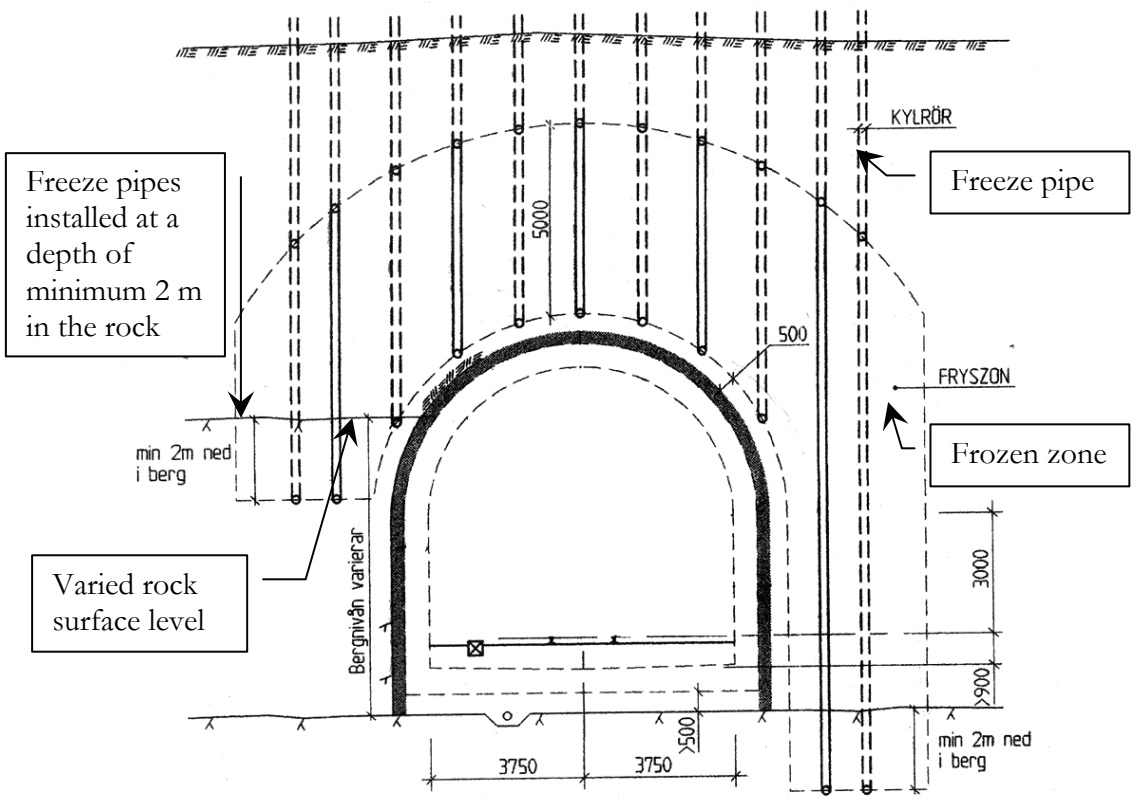

Figure 3.5 Tunnel section with a circular arc, showing various installation depths of freeze pipes, after Botniabanan (2001A)

From December 2001 until April 2002, the tunnel contractor installed the freeze pipes in the ground and established the artificial ground freezing unit. In the middle of April 2002, the contractor started the freezing. However, after approximately five months, in the middle of September, the freezing criteria were fulfilled and the tunnelling started. The tunnelling carried on with a pilot in the frozen soil without stopping until it had completed the full section. The temporary support consisted of the frozen ground maintained by keep-alive temperature, as well as a shotcrete layer of 0.25 m. The tunnelling with temporary support was completed in November 2002, and the cast of the in situ concrete lining started in January 2003. However, in May 2003, the in situ cast concrete lining was finished, and the contractor shut off the cooling device in September 2003. During this time, the soil was frozen by maintained keep-alive temperature for nearly 17 months from the starting of the cooling device until the shut off (Vaaranta, 2004; Saarelainen et al, 2004).

4 LABORATORY STUDY OF BOTHNIA SOIL

This chapter contains laboratory tests accounts of the behaviour and the properties of undisturbed soil and thawed soil i.e. the differences in the soil's behaviours and properties before and after the artificial ground freezing takes place. The chapter is mainly divided into four parts i.e.; *A.*) Soil phases' basic relations, showing traditional geotechnical engineering routine tests for Bothnia undisturbed and thawed soil. *B.*) Soil behaviour, CRS-tests and oedometer tests, showing, above all, Bothnia undisturbed soil deformation properties. *C.*) Grain size distribution tests, showing especially Bothnia soil grain size distribution for undisturbed and thawed soil. *D.*) Soil freeze-thaw laboratory tests, showing, above all, the Bothnia soil deformation on freezing and thawing.

4.1 INTRODUCTION

When soil freezes, mineral particles and water are restructured and in some cases segregated ice with ice lenses are also created. This chapter considers an experimental study carried out by the author in one-dimensional deformation tests for Bothnia soil in a standard oedometer. Based upon the literature study, a number of soil parameters are selected. The essential undisturbed and thawed soil properties and soil behaviour are examined for Bothnia soil. The key results from the laboratory tests are compared with the literature study and to a certain degree, with the results from the field study. These results are discussed in chapter 6.

4.2 MATERIAL

The soil materials originate solely from the area close to the frozen construction, nearby Stranneberget at the Bothnia Line (Örnsköldsvik).

4.2.1 Sampling

Figure 4.1 shows a plan of the geometric design of the installed freeze pipes and the locations where the soil samples have been collected. From Figure 3.4 rock levels, soil profiles as well as the extent of the soil-and rock freezing are shown from a vertical section through the freeze area.

The soil material has been collected from soil considered undisturbed, i.e. not affected by temperature changes in the frozen zone, but representative for the soil in the frozen construction. The soil samples have been collected with standard piston sampler. The sample series of February 24th, 1999 has been collected by VBB-VIAK in connection with preliminary examinations (published in the tender documents) before the freeze construction was established.

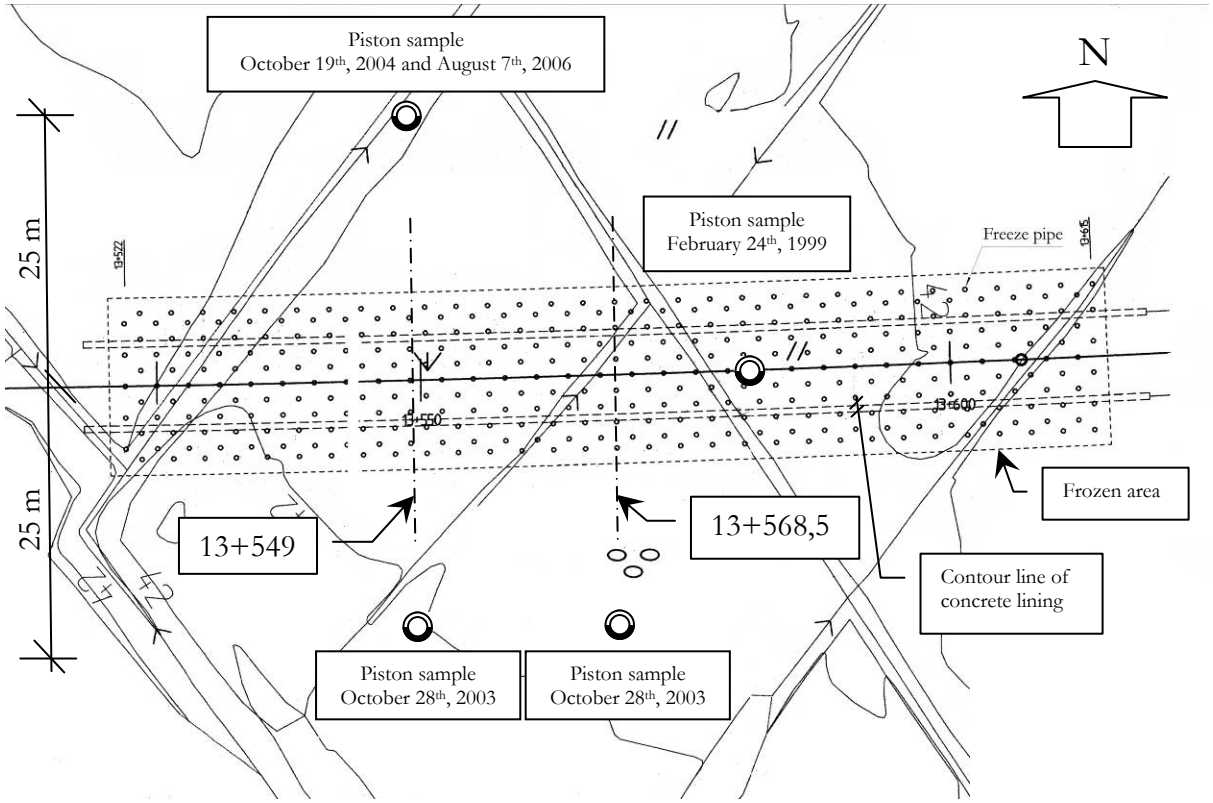

Figure 4.1 The frozen area at the Bothnia Line close to Stranneberget. Principal plan drawing of chainage KM 13+520 to 13+610. The plan shows the suggested freeze pipe geometry for a dimensioned freeze zone of 5 m around the tunnel periphery, as well as points for soil specimens pick up and the two test cross sections, modified after Botniabanan (2001A)

4.2.2 The occasions for the collecting of soil specimens

The soil specimens have being gathered at four times, namely:

i. February 24th, **1999**, VBB-VIAK collected and analysed the soil specimens
ii. October 28th, **2003**, KTH collected and analysed the soil specimens
iii. October 19th, **2004**, KTH collected and analysed the soil specimens
iv. August 7th, **2006**, KTH collected and analysed the soil specimens.

4.3 BASIC CHARACTERISTIC OF SOIL

The characteristics of the material were determined from geotechnical engineering routine laboratory tests, carried out on the Bothnia clayey soils.

4.3.1 Sample preparation

The sample preparation, i.e. the sample performance and interpretation of the laboratory examinations have been done according to the Laboratory Committee of the Swedish Geotechnical Society (Laboratoriekommittén inom Svenska Geotekniska Föreningen, SGF), part 10, in cases where no other source is mentioned. However, the sample preparations as well as the sample performance have been carried out at the Royal Institute of Technology (KTH). Nevertheless, the Swedish consultant company VBB-VIAK performed the soil specimens collected on February 24th, 1999, prior to the establishing of the frozen construction.

4.3.2 Performance

The characteristics of the material were determined from the undisturbed Bothnia soil. For the soil collected 2006 even the characteristics of the thawed soil were determined. The determined soil parameters are

- density
- water content
- limit of consistencies
- void ratio
- undrained shear strength and sensitivity
- organic content.

Performed geotechnical engineering routine laboratory tests for each depth as well as the time of certain occasions are shown in Table 4.1.

Table 4.1 Performed geotechnical engineering routine laboratory tests on Bothnia soil, distribution at the time of collection, state of disturbances and depth below ground surface. See also the locations of sampling in site layout in Figure 4.1

Depth [m]	February 24th, **1999** TN467 Chainage 13+580 In the centre Undisturbed	October 28th, **2003** Chainage 13+549 and 13+568.5 25 m south Undisturbed	October 19th, **2004** Chainage 13+549 and 13+568.5 25 m north Undisturbed	August 7th, **2006** Chainage 13+549 and 13+568.5 25 m north Undisturbed	August 7th, **2006** Chainage 13+549 and 13+568.5 25 m north Frozen-thawed[1]
3		ρ, w, w_l, w_p, τ_{fu}	ρ, w, w_l, w_p, τ_{fu}	ρ, w, w_l, w_p, τ_{fu}	ρ_{th}, w_{th}, w_{lth}, $w_{p,th}$, τ_{futh}
4	ρ, w, w_l, w_p, τ_{fu}	ρ, w, w_l, w_p, τ_{fu}	ρ, w, w_l, w_p, τ_{fu}	ρ, w, w_l, w_p, τ_{fu}	ρ_{th}, w_{th}, w_{lth}, $w_{p,th}$, τ_{futh}
5		ρ, w, w_l, w_p, τ_{fu}	ρ, w, w_l, w_p, τ_{fu}	ρ, w, w_l, w_p, τ_{fu}	ρ_{th}, w_{th}, w_{lth}, $w_{p,th}$, τ_{futh}
6	ρ, w, w_l, w_p, τ_{fu}	ρ, w, w_l, w_p, τ_{fu}	ρ, w, w_l, w_p, τ_{fu}	ρ, w, w_l, w_p, τ_{fu}	ρ_{th}, w_{th}, w_{lth}, $w_{p,th}$, τ_{futh}
7		ρ, w, w_l, w_p, τ_{fu}	ρ, w, w_l, w_p, τ_{fu}	ρ, w, w_l, w_p, τ_{fu}	ρ_{th}, w_{th}, w_{lth}, $w_{p,th}$, τ_{futh}
8	ρ, w, w_l, w_p, τ_{fu}	ρ, w, w_l, w_p, τ_{fu}	ρ, w, w_l, w_p, τ_{fu}	ρ, w, w_l, w_p, τ_{fu}	ρ_{th}, w_{th}, w_{lth}, $w_{p,th}$, τ_{futh}
9			ρ, w, w_l, w_p, τ_{fu}	ρ, w, w_l, w_p, τ_{fu}	ρ_{th}, w_{th}, w_{lth}, $w_{p,th}$, τ_{futh}
10	ρ, w, w_l, w_p, τ_{fu}		ρ, w, w_l, w_p, τ_{fu}	ρ, w, w_l, w_p, τ_{fu}	ρ_{th}, w_{th}, w_{lth}, $w_{p,th}$, τ_{futh}

Note: ρ denotes; soil bulk density, w denotes; soil water content, w_l denotes liquid limit, w_p denotes plastic limit, τ_{fu} denotes undrained shear strength. The addition of index; th denotes thawed soil. The terms south and north derive from the location according to the tunnel centre axis. The term "In the centre" denotes the location above the tunnel centre axis.

1. Frozen-thawed denotes soil sample pre-consolidated, frozen and thawed in an oedometer under in situ effective stress, i.e. the thawed soil properties.

4.4 DEFORMATION CHARACTERISTIC

Several CRS-tests (Constant Rate of Strain tests) and standard oedometer tests have been performed to examine soil properties related to, above all, compression, permeability, etcetera. However, CRS-tests have been performed on undisturbed Bothnia soil collected

i. February 24th, **1999**, VBB-VIAK collected the samples, made the tests and the appropriate analyses
ii. October 28th, **2003**, KTH collected the samples, made the tests and the appropriate analyses
iii. October 19th, **2004**, KTH collected the samples, made the tests and the appropriate analyses
iv. August 7th, **2006**, KTH collected the samples, made the tests and the appropriate analyses.

Standard oedometer tests were performed on undisturbed Bothnia soil collected and analysed

i. October 28th, **2003**, the soil specimens were collected and analyzed at KTH, for the depths 6 m and 8 m.

CRS-tests were performed on thawed soil collected and analyzed

i. August 7th, **2006**, the soil specimens were collected and analyzed at KTH**.**

Standard oedometer test were performed on thawed Bothnia soil collected and analysed

i. October 28th, **2003**, the soil specimens were collected and analyzed at KTH, for the depths 5 m and 8 m
ii. October 19th, **2004**, the soil specimen was collected and analyzed at KTH, for the level 7 m.

4.4.1 Sample preparation

CRS-tests have been evaluated according to SS027126 based on, inter alia, Laboratory Committee of the Swedish Geotechnical Society (Laboratoriekommittén inom Svenska Geotekniska Föreningen, SGF), part 10.

Since the hydraulic conductivity (k) is temperature dependent, the coefficient of consolidation (c_v) is consequently also temperature dependent due to that the viscosity of water alters depending on the water temperature. Measured values of the coefficient of consolidation and hydraulic conductivity from the CRS-tests are therefore reduced by the correction factor 0.7; therefore, the induced respective value subsequently corresponds with the in situ temperature, i.e. approximately 7 ºC (Sällfors & Andréasson, 1985).

4.4.2 Performance

CRS-tests on undisturbed soil samples from depths of 4 m, 8 m and 10 m below ground surface level were performed by VBB-VIAK on February 24th, 1999. The tests originated from the testing position TN467 next to chainage 13+580; straight in the tunnel's centre line, approximately 30 m east of the other tests performed by KTH. In fact, the sampling occurred before the establishing of the frozen construction, see Figure 4.1. CRS-tests on undisturbed soil samples collected on October 28th, 2003 were performed by KTH, JoB. However, the samples originate from respective metre-level, from 3 m to 10 m below the ground surface. The tests originate from chainages 13+549 and 13+ 568.5, approximately 25 m south the tunnel centre axis. CRS-tests on undisturbed soil samples collected on

October 19th, 2004 were performed by KTH, JoB. However, the samples originate from respective metre-level, from 3 m to 10 m below the ground surface. The tests originate from chainages 13+549 and 13+ 568.5, approximately 25 m north the tunnel axis.

CRS-tests on soil samples collected 1999, 2003 and 2004 were performed at room air temperature, approximately 20°C, in KTH, JoB laboratory. The experiments were performed during one to two days with a deformation rate of 0.0035 mm min^{-1}. However, pore pressure, surcharge and deformation were continually registered during the experiment. Two CRS-tests were performed at each entire metre-level from 3 m to 10 m below the ground surface, see Table 4.2

Prior to the CRS-tests, geotechnical engineering routine tests were performed; the determined undisturbed soil parameters were for the most part

- water content and density, see Table 4.1
- undrained shear strength with falling cone see Table 4.1
- liquid limit and plastic limit, see Table 4.1
- grain size distribution, see part 4.7.3

CRS-tests on samples collected on August 7th, 2006 were performed at room temperature of approximately 20°C at KTH, Soil and Rock Laboratory. In contrast to the CRS-tests mentioned above, the 2006 tests have been carried out during one to two days with a strain rate of 0.002 mm min^{-1}. However, during the tests, pore pressure, stress and strain were recorded. Two CRS-tests were performed at each entire metre-level from 3 m to 10 m below the ground surface, see Table 4.2.

Table 4.2 Performed CRS-tests on Bothnia soil, distributed according to date of collection and depth below ground surface, see also the locations of sampling in site layout in Figure 4.1

Depth [m]	February 24th, **1999** TN467 Chainage 13+580 In the centre	October 28th, **2003** Chainage 13+549 and 13+568,5 25 m south	October 19th, **2004** Chainage 13+549 and 13+568,5 25 m north	August 7th, **2006** Chainage 13+549 and 13+568,5 25 m north
3		CRS-u	CRS-u	CRS-u, CRS-f
4	CRS-u	CRS-u	CRS-u	CRS-u, CRS-f
5		CRS-u	CRS-u	CRS-u, CRS-f
6		CRS-u	CRS-u	CRS-u, CRS-f
7		CRS-u	CRS-u	CRS-u, CRS-f
8	CRS-u	CRS-u	CRS-u	CRS-u, CRS-f
9		CRS-u	CRS-u	CRS-u, CRS-f
10	CRS-u	CRS-u	CRS-u	CRS-u, CRS-f

Note: CRS-u denotes; CRS-test on undisturbed soil sample, CRS-f denotes; CRS-test on thawed soil sample, i.e. a sample consolidated, frozen and thawed under its in situ pressure together with the subsequent CRS-test. The terms south and north derive from the location according to the tunnel centre axis. The term "In the centre" denotes the location above the tunnel centre axis.

Freeze-thaw tests have been performed on four standard oedometers simultaneously in climate chambers. The oedometers were numbered from №1 to №4, see chapter 4.6.1. However, after having performed the freeze-thaw tests, routine parameters of soil were determined from two of the oedometers, namely, oedometer №1 and №2. The determined routine soil parameters were

- water content
- density
- liquid limit and plastic limit.

After performed freeze-thaw tests, the deformation characteristics were determined via CRS-tests for two of the oedometers, namely, oedometer №3 and №4. Each test was removed from the oedometer ring of the standard oedometer and installed in the oedometer ring of the CRS-equipment. The CRS-tests were performed at a room temperature of about 20 ºC at KTH, JoB laboratory. The duration of the tests were one to two days with a deformation rate of 0.002 mm min^{-1}. Time, pore pressure, load and deformation were continuously registered during the tests. Two tests were performed at each entire metre-level, i.e. one test from each oedometer №3 and №4, from depths of 3 m to 10 m.

4.5 GRAIN SIZE DISTRIBUTION

The laboratory tests were performed in two different series, namely No. 7321 and No. 7420. Eva Sjöström at the Institute for Surface Chemistry (Ytkemiska institutet (YKI)) performed the tests. The testing pertains to soil from the Bothnia Line collected with piston sampler on August 7th, 2006.

4.5.1 Sample preparation

The materials from the tests were collected from undisturbed material from piston, undisturbed material dried in oven (105 °C) and from freeze-thawed material in oedometers. The oedometer tests were performed through pre-consolidation of the soil sample at approximately 7 °C, freezing at approximately -10 °C, as well as thawing at a temperature of 7 °C. In addition, all tests originated from the area next to the Bothnia Line's freeze stabilized construction and is considered undisturbed.

For series number 7321, the grain size distribution was decided from eight different samples. These samples consisted of soil from levels of: 3 m, 5 m, 7 m and 9 m.

For series 7420, the grain size distribution was determined from four different samples, from the same depths as from series number 7321. The materials from the samples were collected from undisturbed material from piston (not dried).

The test sample was placed in a 250 ml glass container. Approximately 100 ml of distilled water was added; the sample was cut into smaller pieces with a scalpel and hence added. Moreover, the samples were subsequently stirred during two hours with 0.05 m magnetic stirrer of 250 rpm. A few drops of the sample were taken out during the stirring and transferred into a measuring cell. The diluted sample was left while stirred in the instrument for two minutes before the reading was done. The testing was repeated three times with the same sample in the cell and two sample selections were made for each test.

4.5.2 Performance

The grain sizes distributions of the samples have been determined with light diffraction according to Mie theory. The testing's were performed with Malvern Mastersizer 2000, see Figure 4.2. The apparatus measures the particle size and the particle distribution for emulation, suspension and dry powders with help of light diffraction technique. The test interval for the apparatus is particle size between 0.02 μm to 2 000 μm. The source of light is a He-Ne-laser generating light with a temperature stable wavelength of 0.633 μm. A number of detectors collect the light diffraction from different angles. The dispersion

pattern is via knowledge about density and refraction index for the sample and the medium transferred into numbers that are re-calculated to a volume based particle size distribution for the sample.

Figure 4.2 Determination of grain size distribution has been made by laser diffraction with Malvern Mastersizer 2000, photo ATA Scientific Pty Ltd

4.6 SOIL FREEZE-THAW LABORATORY TESTS

This chapter contains a description of the simulation of the freeze-and thaw cycle of freezing and thawing in laboratory environment intended to as accurately as possible imitate the maximal heaving-, and thawing levels that can occur in the area of the artificially frozen construction at the Bothnia Line.

The thaw deformation is affected by the temperature of the cool down, i.e. the lower the temperature of the cool down the larger the thaw deformation. This occurs because clay particles of smaller (relative) size, consisting of a larger share of bounded water, contribute to the aggregation process in which larger clay particles have already taken part. The content of fine grain particles in clay together with the water content, water saturation ratio, and hydraulic conductivity, are of great importance by influencing the thaw deformations, since the capacity to bind water hydroscopic etcetera increases with smaller grain size, and the capacity to transport water to the frozen zone decreases with a reduced hydraulic conductivity. While, these behaviours are significant for the soil's capacity to transport water and for the soil's deformation behaviours during thawing. The likeliness of fine-grained soil to create segregated ice is greater during slow freezing than during rapid freezing.

To be able to analyse the soil's properties, with consideration of above all the thaw deformation, tests with standard oedometer have been performed in a climate chamber (see Figure 4.3 to Figure 4.5), i.e.

i. the test was pre-consolidated to the effective stress equivalent to the in situ stress at the test site during approximately one day at a temperature of +7 ºC
ii. freezing during approximately one day at a temperature of -10 ºC
iii. thawing during approximately one day at a temperature of +7 ºC.

As can be seen from Figure 4.3 and Figure 4.4 the pilot study is performed with soil samples collected at the depths of 5 m and 8 m below the ground surface. The test shows the performance of two different soil samples from different ground levels with altered soil water content. The soil sample from the depth of 5 m had original soil water content (w) of 106 % while the soil sample from the depth of 8 m had original water content of 48 %.

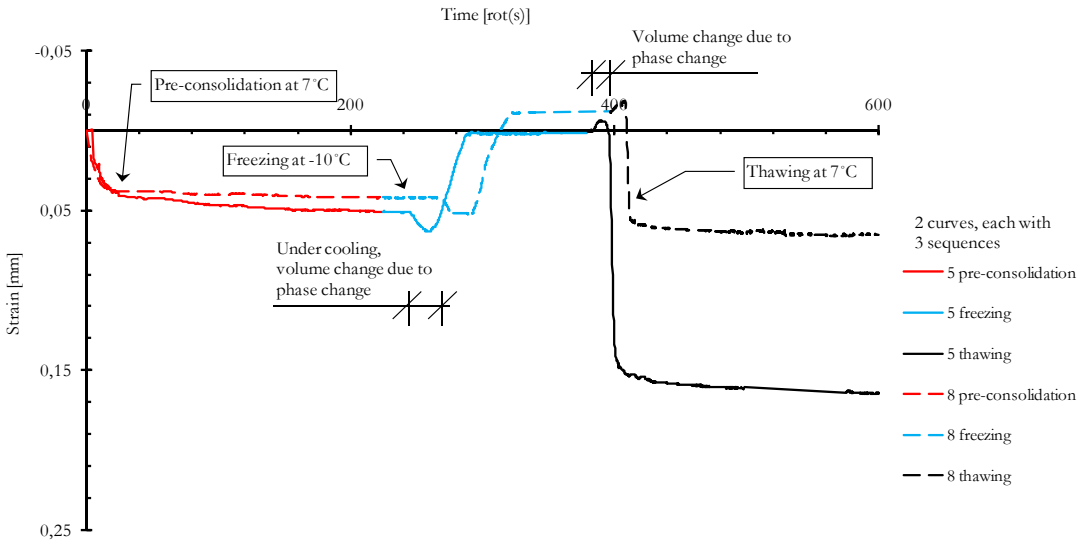

Figure 4.3 *Illustration of a typical deformation derived from one-dimensional freeze-thaw soil oedometer test. The two-sided drainage pilot test performed with sulphide rich clay from the Bothnia Line shows pre-consolidation within the duration of half a day, freezing at -10 °C during one day and the subsequent thawing during a second day. The test shows the deformation from the depths of 5 m and 8 m below the ground surface, i.e. two curves, each with the three sequences; pre-consolidation, freezing and thawing. Each soil samples have a surcharge load of in-situ effective soil stress. Concerning figure denotations, see also Figure 2.14, page 25*

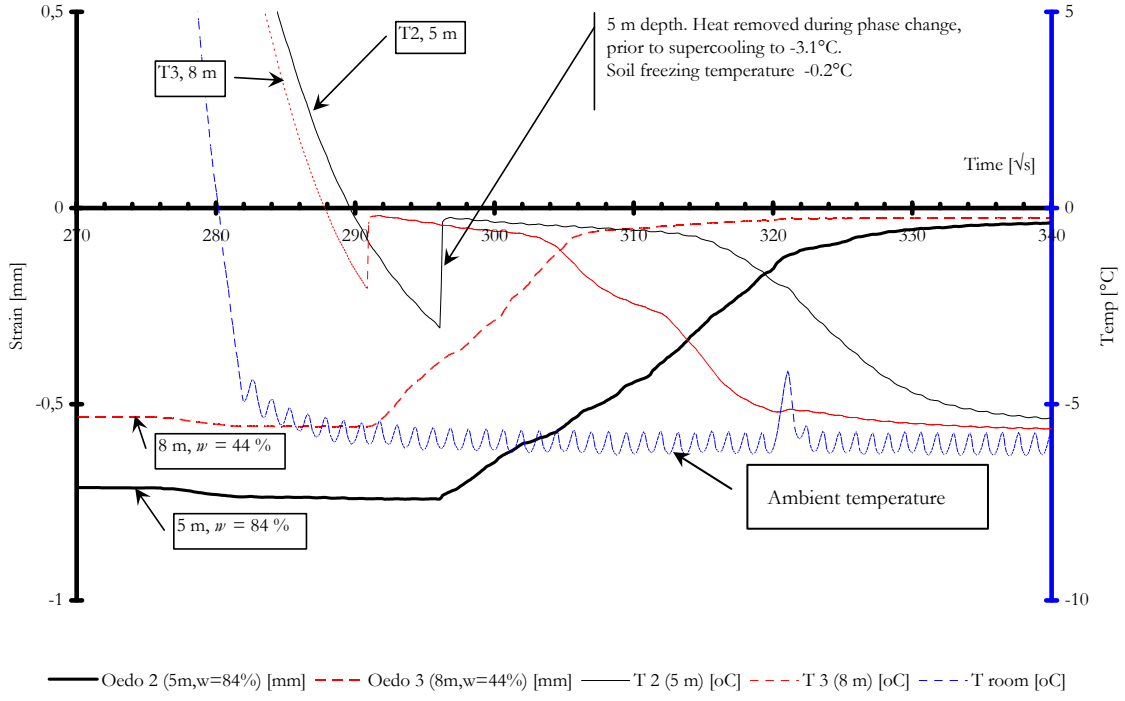

Figure 4.4 *Performed freeze-thaw tests of two Bothnia soil specimens collected from 5 m and 8 m depths below the ground surface. The test shows the registered air temperature and the soil specimen's temperature, as well as the soil specimen's deformation as function of the time in root-seconds. The soil specimens were applied with a surcharge load of the in-situ effective stress level. The pilot study shows the volume expansion during the freezing, compared to the air temperature, as well as the soil temperature. The two tests were performed simultaneous*

Figure 4.4 shows the temperature decrease in the surrounding atmosphere and the subsequent temperature decrease in the soil samples. The slope of the cooling curve illustrates the rate of the gradually falling temperature. Thus, the moister the sample, the longer it takes until the freezing occur. As can be seen in Figure 4.4, the time for the freezing of the soil water is characterized by the nearly horizontal temperature curve anticipated by the super cooling. The horizontal curve represents two water phases i.e. water and ice and the release of latent heat of fusion. As a result, the volume expansion starts immediately as the water phase change effectuates.

Figure 4.5 The oedometer equipment, enumeration from the centre; oedometer ring (white), below; top porous stone collar (red), in the top; stamp (steel), ultimately, the bottom porous stone collar, i.e. the fixed ring container (red)

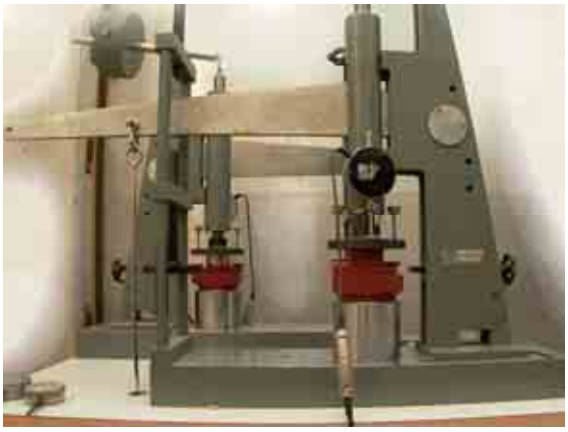

Figure 4.6 Experiment set up in two different oedometers, type SGI X completed with digital registration of the soil deformation. In the red fixed ring container, the installed soil specimens

Figure 4.7 Soil specimen from the Bothnia Line fitted in the oedometer ring, before the test

Figure 4.8 Soil specimen from the Bothnia Line dismounted from the oedometer ring subsequent to test. Re-measuring with the purpose of checking the total deformation

4.6.1 Performance

The freeze-thaw tests were performed with four oedometers simultaneously in a climate chamber. The oedometers of type SGI X, equipped with digital registration of the deformation, were enumerated from №. 1 to №. 4. During the tests, time and deformations were registered. Before the freeze-thaw tests, several basic soil parameters were defined likewise for one or two soil samples of each soil level, e.g.

- water content and density
- undrained shear strength (in fall-cone apparatus)
- liquid limit (in fall-cone apparatus) and plastic limit
- soil deformation behaviour (CRS-test at 20 ºC)
- soil grain size distribution (in laser diffraction app., for the depths 3, 5, 7 and 9 m).

The freeze-thaw tests were performed in the following sequence: firstly, the Bothnia soil sample was placed in an oedometer ring, Figure 4.7; secondly, the sample was installed in a standard oedometer, positioned in a climate chamber with an ambient temperature of seven degree Celsius, see Figure 4.6. The tests were conducted with a static load consisting of the sample in situ effective stress. During the tests, the vertical deformation was registered as a function of time. The tests were performed in steps

- pre-consolidation during approximately one day at an ambient temperature of 7 ºC
- cooling down for one day at an ambient temperature of -10 ºC
- thawing during one day at an ambient temperature of 7 ºC.

The performed freeze-thawed tests' basic soil parameters were subsequently defined, as well as the soil deformation behaviour was subsequently defined according to A and B below.

A: Immediately after the freeze-thaw tests were performed, the following basic parameters were defined from the two oedometers, namely oedometer №1 and oedometer №2

- water content and soil bulk density
- undrained shear strength (in fall-cone apparatus)
- liquid limit (in fall-cone apparatus) and plastic limit
- soil deformation behaviour (CRS-test performed at 20 ºC)
- soil particle distribution (in laser diffraction app., for depths of 3, 5, 7 and 9 m).

B: Directly after the freeze-thaw tests, the following parameter were defined from the two oedometers, namely oedometer №3 and oedometer №4

- soil deformation behaviour (CRS-test performed at 20 ºC).

The performances of the freeze-thaw tests from the soil collected on October 28th, 2003, were completed as a pilot study. However, the tests were conducted according to the general description above. In contrast, just two oedometers were in use at each test and also some of the basic soil parameters and the soil deformation behaviour were not defined. Two freeze-thaw test series of soil collected on October 28th, 2003 were performed, namely

- test series I from two different depths of 5 m and 8 m
- test series II from the depth of 5 m.

The performances of the freeze-thaw tests from the soil collected on October 19th, 2004, were completed according to the general description above. Only two tests from soil at each depth were on the contrary performed this time, and also only, the basic parameters, soil density and water content were defined before the freeze-thaw test and after the test.

Two freeze-thaw tests series of the soil collected on October 19th, 2004 were performed, namely

- test series I from depths of 3, 4, 5, 6, 7, 8, 9 and 10 m
- test series II from depths of 3, 4, 5, 6, 7, 8, 9 and 10 m.

The performances of the freeze-thaw tests from the soil collected on 7th August, 2006, were completed according to the general description, above.

4.7 RESULTS

This part presents the results from the laboratory tests, demonstrated in the previous sections. The results for each test consists of

- soil phase basic relations
  (density, water content, limit of consistencies, void ratio, undrained shear strength and organic content)
- soil behaviour from CRS-tests and standard oedometer tests
  (preconsolidation pressure, effective stress, overconsolidation ratio, coefficient of consolidation, permeability, compressibility modulus)
- grain size distribution
- soil freeze-thaw laboratory tests
  (freeze-thaw one-dimensional deformation tests).

4.7.1 Soil phase basic relations

The fundamental properties of the soil have been examined at KTH (Royal Institute of Technology), div. JoB (div Soil and Rock mechanics). The sample series of February 24th, 1999, is collected and analysed by VBB-VIAK. The results in this chapter are mainly presented with help of diagrams, while the numerical values are generally presented in table format in appendix.

Previous studies of the soil in the region where the Bothnia Line is located have shown that the soil is iron sulphide rich (Larsson, Westerberg, Albing, Knutsson & Carlsson, 2007; Botniabanan, 2001A; Schwab, 1976). Ocular inspection as well as odour test of the Bothnia soil samples collected by KTH show that the results from these examinations correlate with previous studies.

The undisturbed soil bulk density has been calculated from soil samples collected on October 28th, 2003; October 19th, 2004; and August 7th, 2006. VBB-VIAK calculated the soil's undisturbed bulk density from samples collected on February 24th, 1999. The results are presented in Figure 4.9. The number of samples calculated per sampling occasion and the number of samples creating the mean value are presented in Appendix, laboratory tests, Table A.1.

Figure 4.9 shows the mean value of three calculations of the thawed bulk density from samples collected on October 19th, 2004 and August 7th, 2006. These results are compared with the mean value of six calculations of undisturbed soil from the total number of sampling occasions, which is compared with the mean value of undisturbed and thawed soil from respective samples collected on October 19th, 2004 and August 7th, 2006.

The estimated bulk density for the undisturbed soil is based on the thawed soil's bulk density and the deformation development that occurred during the sampling.

The dry density for undisturbed soil has been calculated for samples collected on October 28th, 2003, October 19th, 2004 and August 7th, 2006. VBB-VIAK has calculated the undisturbed soil's dry density for February 24th, 1999. The results are presented in Appendix.

The soil samples from all depths from 3 m to 10 m have been assumed water saturated. Due to the hydrostatic water zero pressure level within the frozen zone and the area close

to the frozen construction lies at the same level as the ground surface at the moment the zero pressure level lies at its lowest position i.e. artesian ground water.

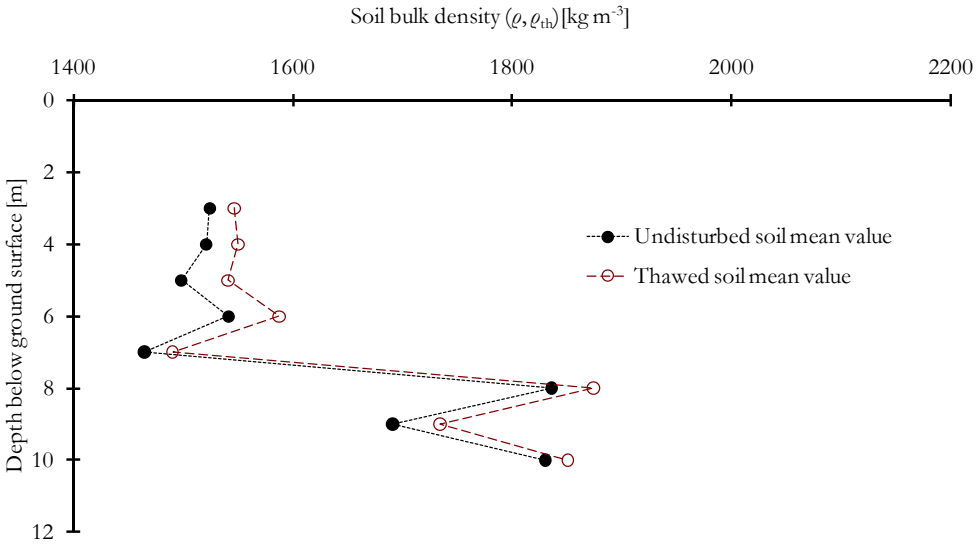

Figure 4.9 Soil bulk density; mean value for undisturbed soil and for thawed soil. The values are based on deformation tests. Samples collected on October 19th, 2004 and August 7th, 2006

The water content of undisturbed soil has been calculated for samples collected on October 10th, 2003, October 19th, 2004 and August 7th, 2006. VBB-VIAK calculated the undisturbed soil's water content of February 24th, 1999. The results of the mean value of the water content for each sampling occasion are accounted for in Figure 4.10, Figure 4.11, and as numerical values presented in tables in Appendix. However, in Figure 4.11, the mean value of five calculations of the thawed soil's water content from October 19th, 2004 and August 7th, 2006 are compared with the mean value of eight calculations of undisturbed soil from all sampling occasions and the mean value from respective samplings of undisturbed and unfrozen soil from October 19th, 2004 and August 7th, 2006.

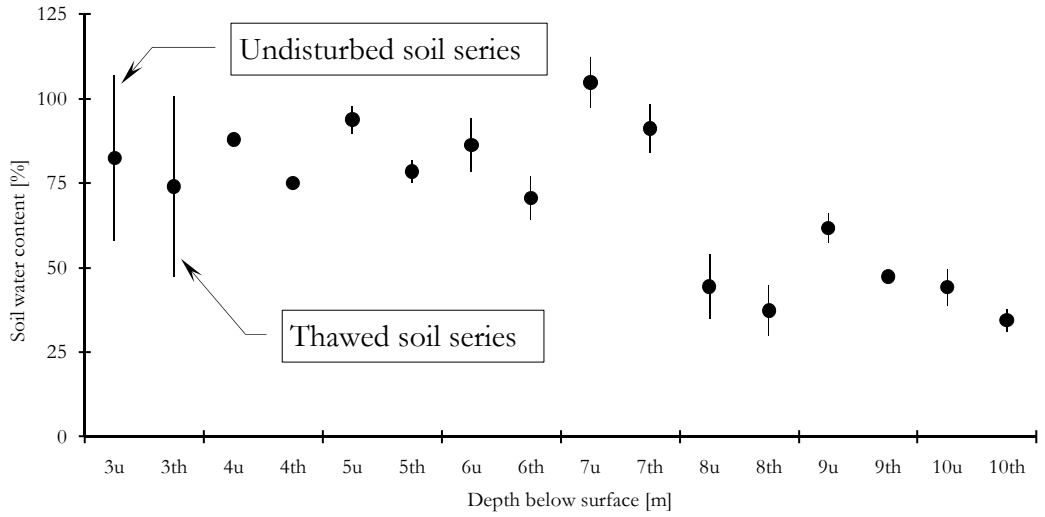

Figure 4.10 Soil water content; two series, undisturbed soil (u) and thawed soil (th). The individual 90 % confidence intervals for the means of the soil water content as a function of the depth below the ground surface, all values included. The dots denotes the mean values and the line's ends points the lowest and highest value at 90 % confidence level. The values are based on deformation tests for samples collected on October 19th, 2004 and August 7th, 2006

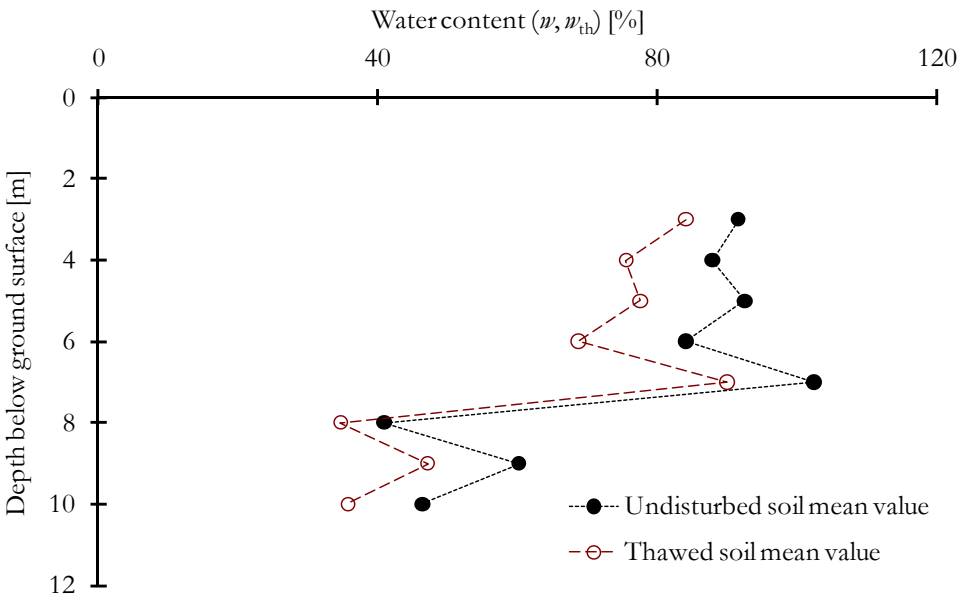

Figure 4.11 Soil water content; mean value for undisturbed soil and for thawed soil. The values are based on deformation tests. Samples collected on October 19th, 2004 and August 7th, 2006

Liquid limit (w_L) has been determined by fall-cone apparatus. However, the liquid limit has been determined for undisturbed soil collected on October 28th, 2003, October 19th, 2004 and August 7th, 2006. VBB-VIAK determined the undisturbed soil's liquid limit of samples collected on February 24th, 1999. The liquid limit for the thawed soil was determined from samples collected on August 7th, 2006. The mean value for all calculations is presented in Figure 4.12. All measured values of liquid limit are also shown as numerical values and diagrams in Appendix.

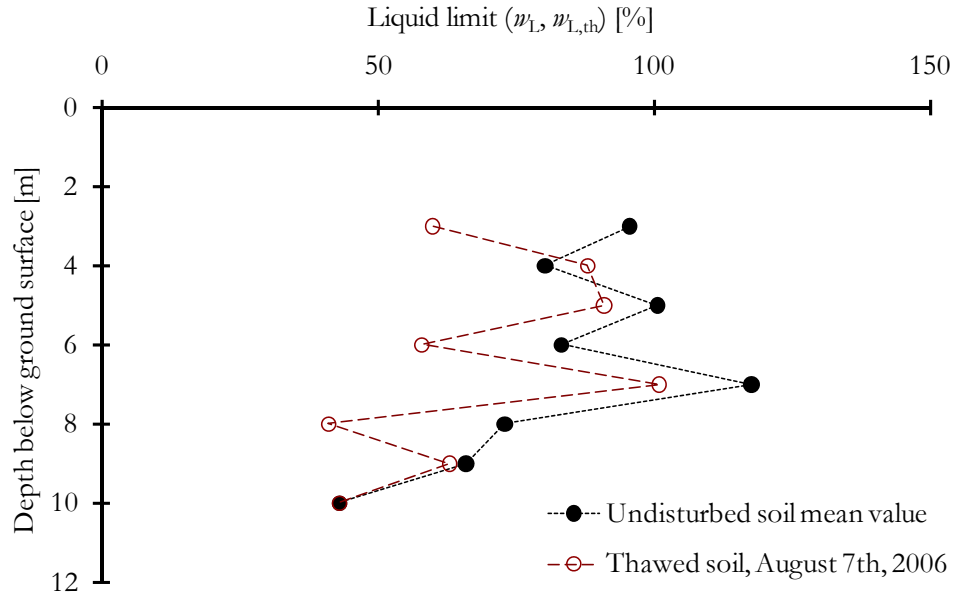

Figure 4.12 Liquid limit; mean value for undisturbed soil, samples collected 1999, 2003, 2004 and 2006 and for thawed soil, samples collected 2006

Plastic limit (w_p) has been determined for undisturbed soil from samples collected on October 28th, 2003, October 19th, 2004, and August 7th, 2006. However, the calculated mean value for all calculations, totally three is presented in Figure 4.13. The plastic limit for

thawed soil has been determined from soil collected on August 7th, 2006. The results of the calculated plastic limit are presented in Figure 4.13. All measured values of the plastic limit for undisturbed soil as well as for thawed soil are also accounted for in Appendix.

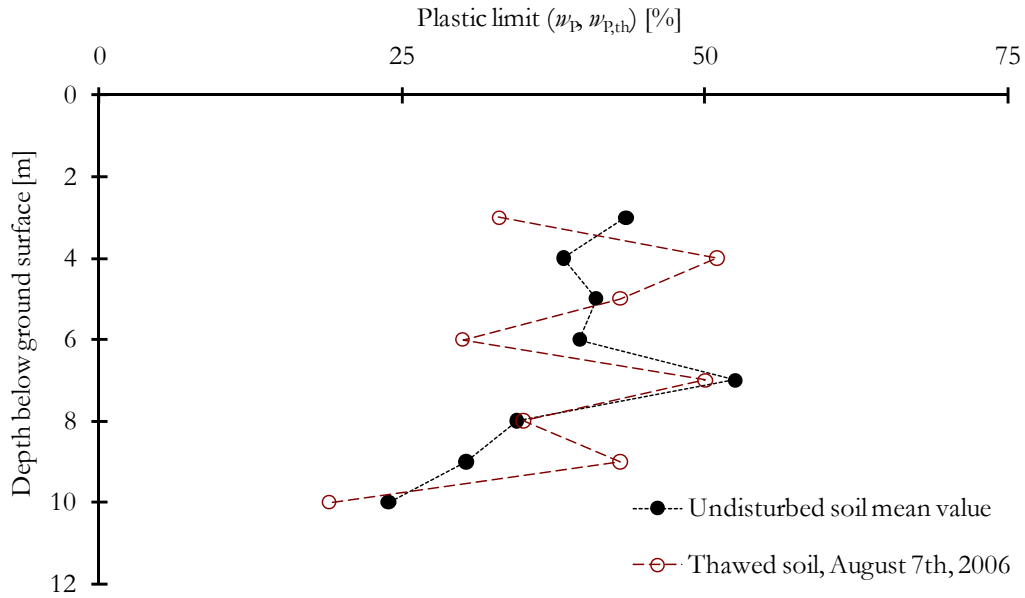

Figure 4.13 Plastic limit; mean value for undisturbed soil, samples collected 2003, 2004, and 2006 and the plastic limit for thawed soil collected 2006

Plasticity index ($I_p = w_L - w_p$) for undisturbed soil has been determined from samples collected on October 28th, 2003, October 19th, 2004 and August 7th, 2006. However, plasticity index for thawed soil was determined from soil collected on August 7th, 2006. The results of calculated plasticity index are presented in Figure 4.14, whereas plasticity index values are based on values presented in Figure 4.12 and Figure 4.13. Furthermore, all measured values of the plasticity index for undisturbed soil as well as for thawed soil are also accounted for in Appendix.

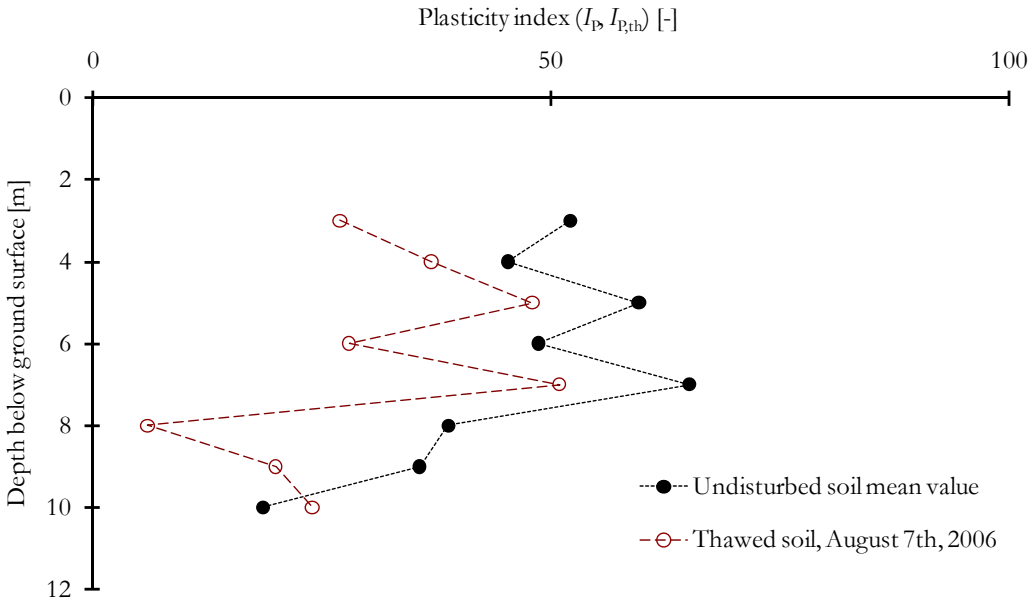

Figure 4.14 Plasticity index; mean value for undisturbed soil, samples collected 2003, 2004 and 2006 and for thawed soil collected 2006

Void ratio (e, e_{th}) has been determined for undisturbed soil collected on February 24th, 1999, October 28th, 2003, October 19th, 2004 and August 7th, 2006. The void ratio for thawed soil has been determined from samples collected on October 19th, 2004 and August 7th, 2006, see Figure 4.16. All measured values of void ratio for undisturbed soil (four occasions) and for thawed soil (two occasions) are shown in tables in Appendix.

The calculated values for plasticity index and for the liquid limit for respective depth below ground surface are presented in Casagrande's plasticity chart, see Figure 4.15. The Swedish "A-line" in the diagram is presented according to Larsson (1982). Plasticity index (I_c) as a function of the liquid limit (w_L) has been determined for undisturbed soil from samples collected on October 28th, 2003, October 19th, 2004 and August 7th, 2006, as well as for thawed soil from samples collected on August 7th, 2006. The results from respective plasticity index for undisturbed soil and thawed soil originates from results presented in Figure 4.14, page 114, and also from results in Appendix. Nevertheless, the values of undisturbed soil as well as thawed soil liquid limit originate from Figure 4.12, page 113, and from Appendix.

The soil's undrained shear strength (τ_{fu}) has been determined by fall-cone apparatus. The undrained shear strength has been determined for undisturbed soil collected on February 24th, 1999; October 28th, 2003; October 19th, 2004; and August 7th, 2006. The undrained shear strength ($\tau_{fu,th}$) for thawed soil has been determined for samples collected on August 7th, 2006. The soil's undrained shear strength for undisturbed soil and for thawed soil is presented in Figure 4.17 All calculated values of the undisturbed soil undrained shear strength (four totally) and for thawed soil (one occasion) are shown in table in Appendix.

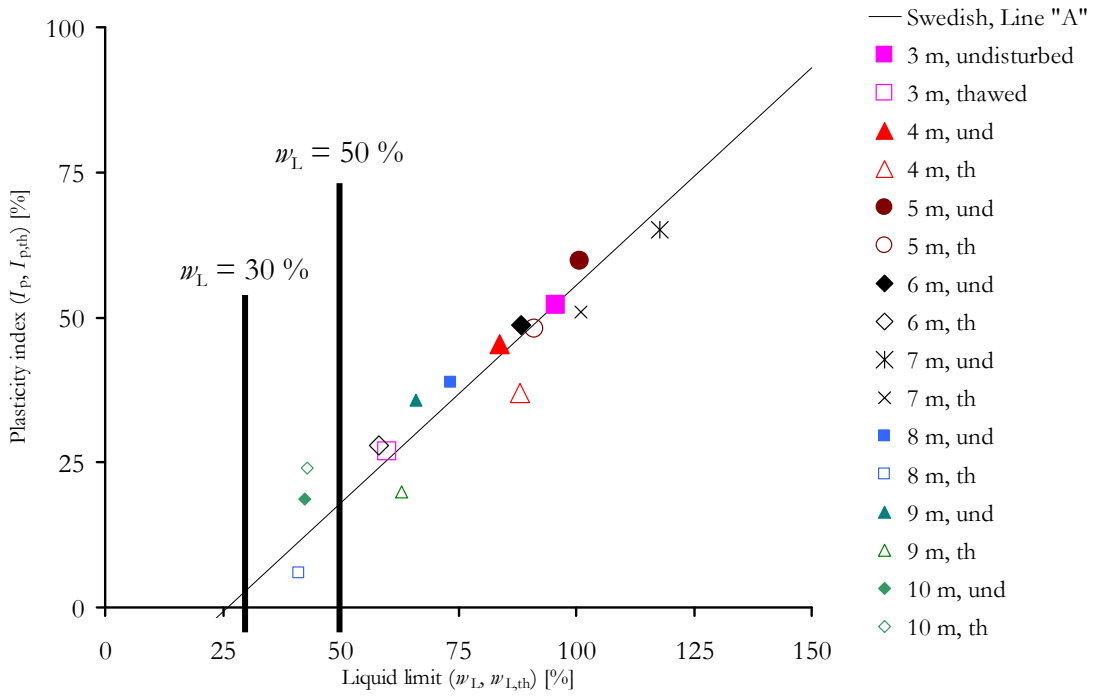

Figure 4.15 Casagrande's plasticity chart with the border lines at liquid limits 30 % and 50 % as well as the Swedish "A-line". The mean value for undisturbed samples collected on October 28th, 2003, October 19th, 2004 and August 7th, 2006 ("undisturbed" and "und"), as well as for thawed samples collected on August 7th, 2006 ("thawed" and "th")

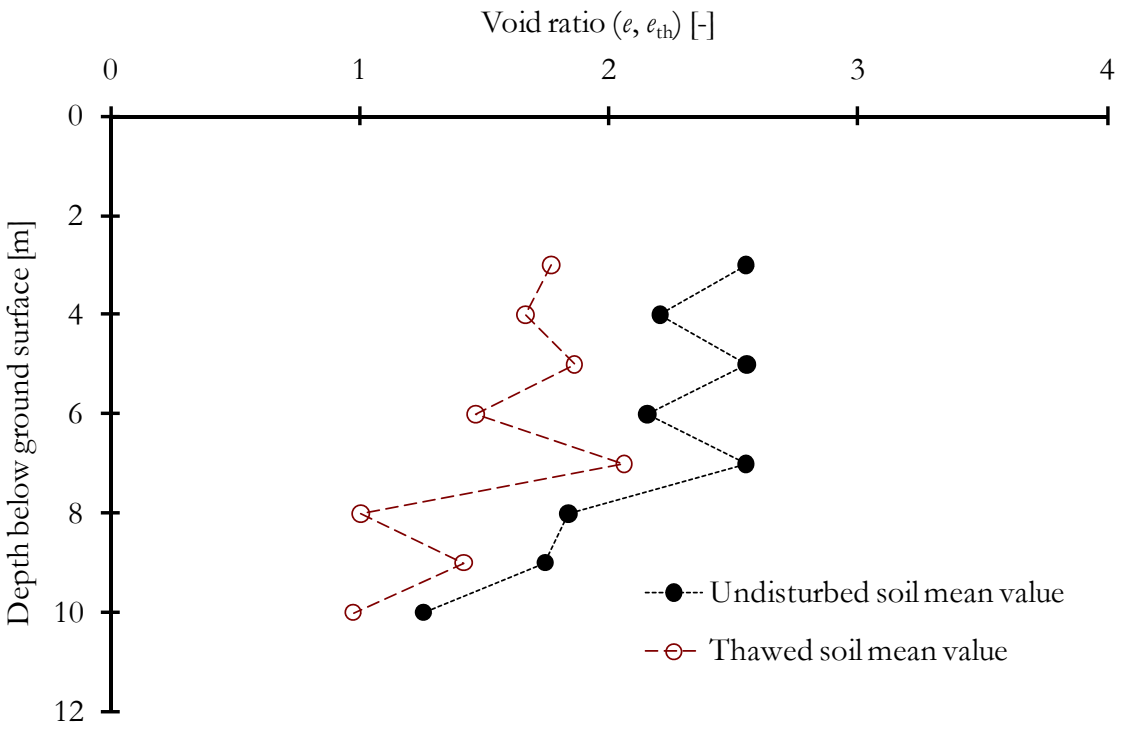

Figure 4.16 Void ratio for undisturbed soil for samples collected on February 24th, 1999; October 28th, 2003; October 19th, 2004; August 7th, 2006 as well as thawed soil for samples collected on October 19th, 2004 and August 7th, 2006

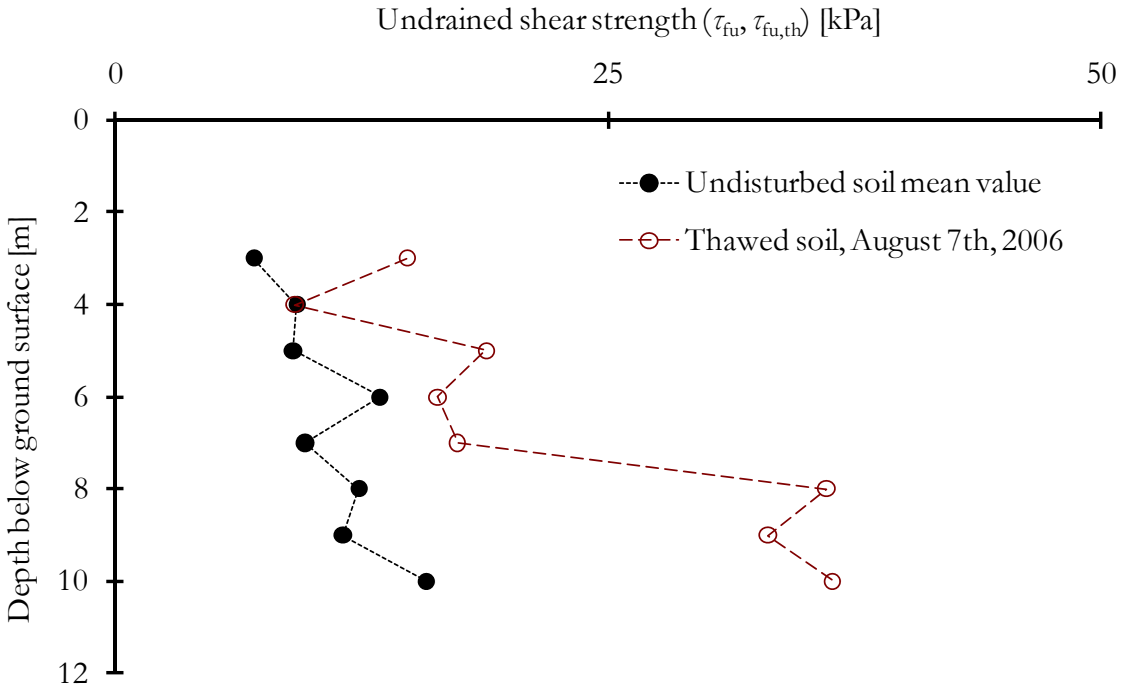

Figure 4.17 Undrained shear strength for undisturbed soil for samples collected on February 24th, 1999; October 28th, 2003; October 19th, 2004; August 7th, 2006 as well as for thawed soil from samples collected on August 7th, 2006

4.7.2 Soil behaviour, CRS-tests and oedometer tests

The preconsolidation pressure has been evaluated in CRS-tests. Soil samples collected on August 7th, 2006 were performed in CRS-tests according to SS027126. However, soil samples collected on 1999, 2003 and 2004 were performed at a different deformation rate (0.0035 mm min^{-1}). These results are presented in Appendix. The results of the evaluation for soil collected on August 7th, 2006 are presented in Figure 4.18.

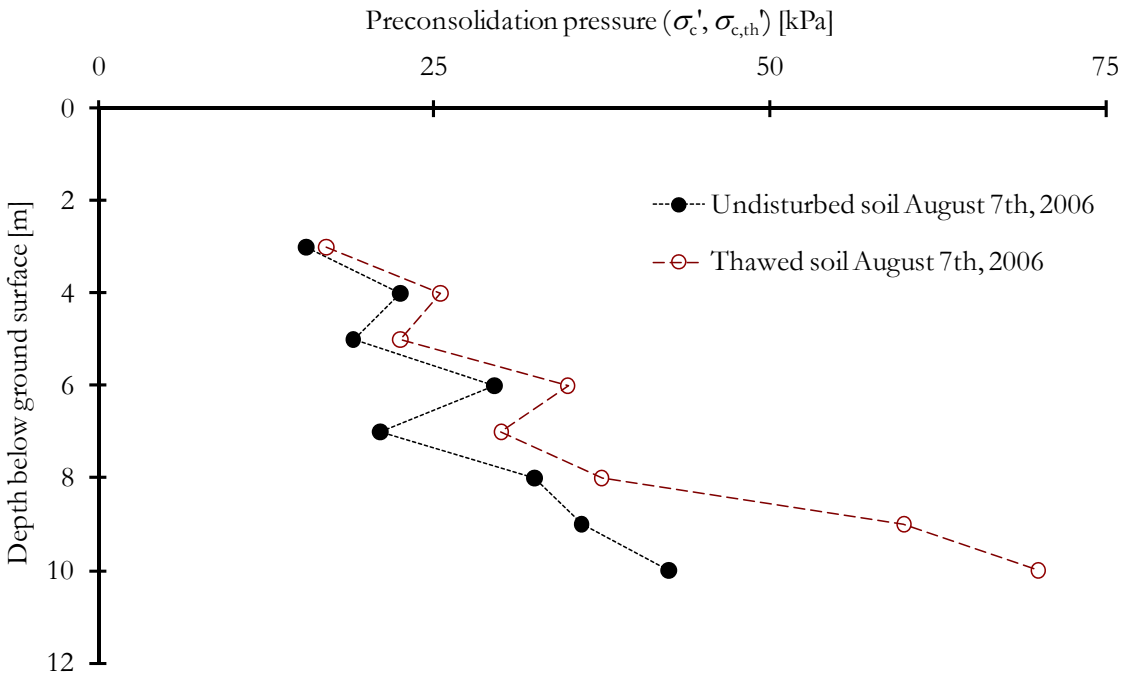

Figure 4.18 The preconsolidation pressure for undisturbed soil and freeze-thawed samples collected on August 7th, 2006

Knowledge about the vertical in situ-pressure as well as the actual preconsolidation pressure at respective depths below ground surface is required when calculating the overconsolidation ratio. Table A.40 in the Appendix shows the calculated effective stress of respective depths below ground surface, which is based on existing bulk density and hydrostatic pore water pressure. Moreover, Figure A.1, page VII, shows the overconsolidation ratio.

4.7.3 Grain size distribution

Measuring of grain size distribution has been performed on samples collected on August 7th, 2006. The measuring was accomplished with laser diffraction. The results from the measuring are given in volume distribution and as mean value of two sample series. The volume distribution is, however, the same as weight distribution if the density does not change between different size fractions.

Grain size distribution has been measured for

i. undisturbed sample
ii. undisturbed, dried sample
iii. consolidated, frozen and thawed sample in oedometer.

Grain size distribution has been presented in the fractions, clay, silt and sand, see Table 4.3.

Table 4.3 Grain size distribution for undisturbed soil (undist), undisturbed, dried soil (und, dr), as well as consolidated, frozen and thawed in oedometer (th), determined through laser diffraction. The mean value of two mean values creating a series

	Clay			**Silt**			**Sand**		
	Fine	Medium	Coarse	Fine	Medium	Coarse	Fine	Medium	Coarse
Grain size distribution	$d <$ 0.2 μm [%]	0.2 μm $< d <$ 0.6 μm [%]	0.6 μm $< d <$ 2 μm [%]	2 μm $< d <$ 6 μm [%]	6 μm $< d <$ 20 μm [%]	20 μm $< d <$ 60 μm [%]	60 μm $< d <$ 200 μm [%]	200 μm $< d <$ 600 μm [%]	$d >$ 600 μm [%]
3 m undist[1]	-	2.8	16.9	54.2	23.7	2.1	0.3	-	-
3 m und, dr[2]	-	2.9	19.8	34.1	24.8	11.0	7.1	0.4	-
3 m th[3]	-	2.3	16.8	44.9	31.9	3.4	0.7	-	-
5 m undist[1]	-	0.8	4.2	14.0	43.6	23.8	9.7	3.3	0.5
5 m und,dr[2]	-	0.9	4.6	16.2	36.5	28.1	11.5	2.2	0.0
5 m th[3]	-	0.7	3.3	9.5	37.7	31.3	12.4	4.0	1.0
7 m undist[1]	-	0.7	3.5	10.8	41.0	32.5	10.5	0.9	-
7 m und, dr[2]	-	1.1	4.9	13.0	31.8	32.2	16.1	1.0	-
7 m th[3]	-	0.7	3.3	8.9	37.8	36.0	11.1	2.1	0.0
9 m undist[1]	-	4.0	21.1	39.9	29.3	5.1	0.5	0.2	-
9 m und, dr[2]	-	2.6	19.5	38.5	27.8	9.0	2.3	0.1	-
9 m th[3]	-	2.6	15.5	36.6	39.5	5.2	0.5	-	-

Note: 1 denotes undisturbed soil sample, 2 denotes undisturbed dried soil sample, 3 denotes consolidated, frozen and thawed soil under a load of the in situ effective pressure.

Table 4.4 shows the alterations i.e., the calculated differences between the original undisturbed content and the thawed content for respective fraction. Table 4.5 shows the relative alterations i.e., the calculated relative differences between the original undisturbed content and the thawed content for each fraction.

Table 4.4 Grain size distribution as a percentage of the difference between undisturbed and thawed soil. Positive value denotes a fraction increase [percentage unit]

	Clay			**Silt**			**Sand**		
Level [m]	Fine $d <$ 0.2 μm [%]	Medium 0.2 μm $< d <$ 0.6 μm [%]	Coarse 0.6 μm $< d <$ 2 μm [%]	Fine 2 μm $< d <$ 6 μm [%]	Medium 6 μm $< d <$ 20 μm [%]	Coarse 20 μm $< d <$ 60 μm [%]	Fine 60 μm $< d <$ 200 μm [%]	Medium 200 μm $< d <$ 600 μm [%]	Coarse $d >$ 600 μm [%]
3 m		-0.4	-0.1	-9.3	8.2	1.3	0.4	0.0	0.0
5 m		-0.2	-0.8	-4.5	-5.9	7.5	2.7	0.7	0.5
7 m		-0.0	-0.2	-1.9	-3.2	3.5	0.6	1.1	0.0
9 m		-1.4	-5.5	-3.3	10.2	0.1	0.0	-0.2	0.0

Table 4.5 *Grain size distribution, the relative change between the undisturbed and the thawed soil. Positive value denotes a relative fraction increase [calculated as percentage]*

	Clay			**Silt**			**Sand**		
Level [m]	Fine $d <$ 0.2 μm [%]	Medium 0.2 μm $< d <$ 0.6 μm [%]	Coarse 0.6 μm $< d <$ 2 μm [%]	Fine 2 μm $< d <$ 6 μm [%]	Medium 6 μm $< d <$ 20 μm [%]	Coarse 20 μm $< d <$ 60 μm [%]	Fine 60 μm $< d <$ 200 μm [%]	Medium 200 μm $< d <$ 600 μm [%]	Coarse $d >$ 600 μm [%]
3 m		-15	-1	-17	34	61	127		
5 m		-20	-20	-32	-13	31	27	22	90
7 m		-2	-5	-18	-8	11	6	119	
9 m		-35	-26	-8	35	3	3	-100	

Figure 4.19 and Table 4.6 show the activity of the Bothnia clay for the depths of 3 m, 5 m, 7 m and 9 m below the ground surface. Figure 4.20 shows the influence of gradation on plasticity index for the depths of 3 m, 5 m, 7 m and 9 m below the ground surface. Table 4.6 shows several basic geotechnical engineering parameters where

$$C_u = \frac{D_{60}}{D_{10}} \tag{4.1}$$

$$C_z = \frac{D_{30}^2}{D_{10} D_{60}} \tag{4.2}$$

$$\mathrm{GI} = (F - 35)\left[0.2 + 0.005(\mathrm{LL} - 40)\right] + 0.01(F - 15)(\mathrm{PI} - 10) \tag{4.3}$$

$$a_c = \frac{I_p}{\mathrm{CL}} \tag{4.4}$$

where C_u denotes the *uniformity coefficient* for indication of the grain gradation and expresses the ratio of the diameter of the particle size at 60 % (D_{60}) and the ratio of the diameter of the particle size at 10 % (D_{10}).

C_z denotes the coefficient of curvature (or concavity) and sometimes used as a measurement of the shape of the grain-size distribution curves (Craig, 1974), where D_{10} denotes the ratio of the diameter of the particle size at 10 %, the denotations of D_{30} and D_{60} as stated above.

Group index (GI) is included in the American Association of state highway and transportation officials (AASHTO) classification of soils and soil-aggregate mixtures. The classification system divides the soil into mainly seven groups (National Soil Survey Handbook [NSSH], 2007), where F denotes percentage passing No. 200 sieve (0.075 mm), whole number, LL denotes liquid limit and PI denotes plasticity index. Finally, a_c denotes the activity of clay and constitutes the ratio between the plasticity index (I_p) and the clay content (CL) i.e. the amount (in percentage) of particles less than 2 μm.

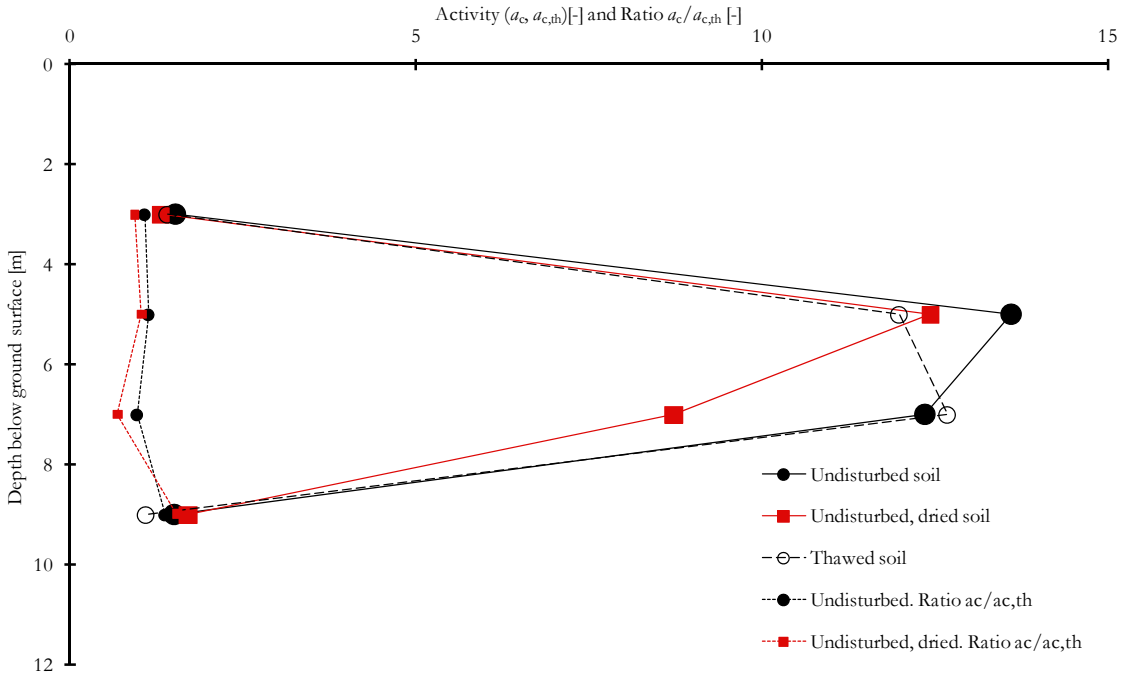

Figure 4.19 The activity and activity ratio of undisturbed soil. The activity as well as the relation between the activity before and after the freezing for the depths of 3 m, 5 m, 7 m, and 9 m below ground surface. Sample series of August 7th, 2006

The results of the grain size distribution presented as passing volume percentage for respective particle size is shown in charts, for the depth of 3 m below the ground surface in Figure 4.21, for 5 m in Figure 4.23, for 7 m in Figure 4.24 and finally for 9 m in Figure 4.25.

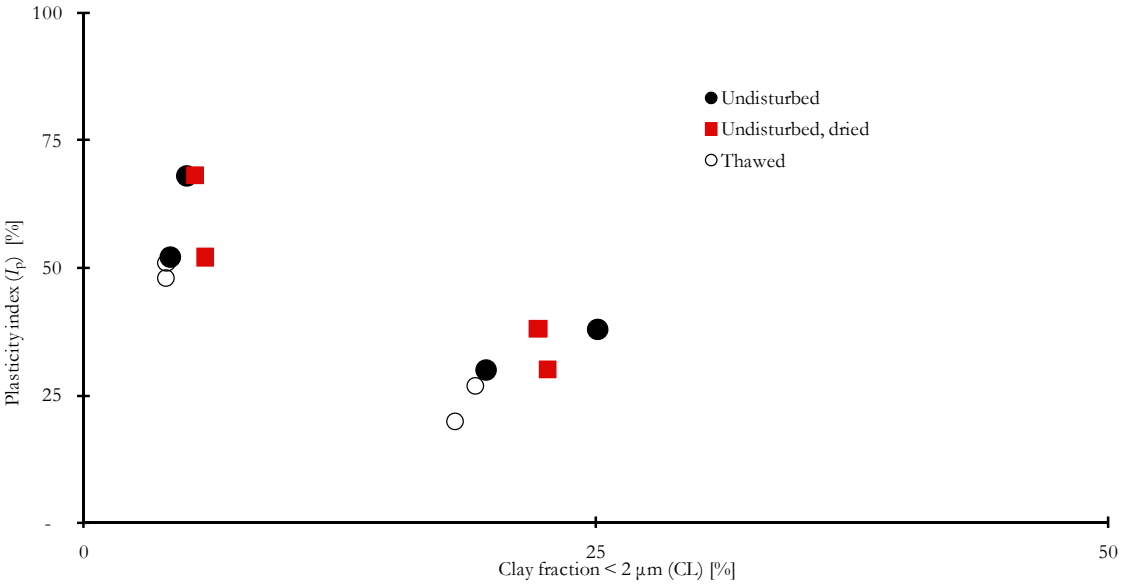

Figure 4.20 Relation between plasticity index and clay content for depths of 3 m, 5 m, 7 m and 9 m below ground surface. Sample series of August 7th, 2006

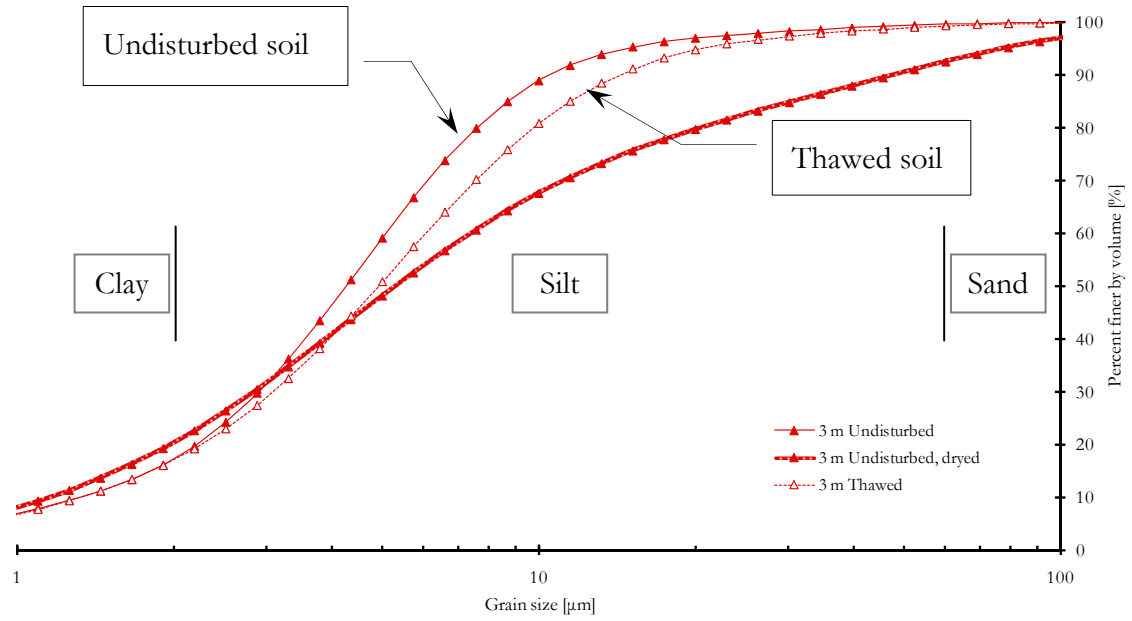

Figure 4.21 Grain size distributions for undisturbed soil, for undisturbed dried soil, and for thawed soil, mean value of two sample series respectively. Sample series collected 3 m below ground surface on August 7th, 2006

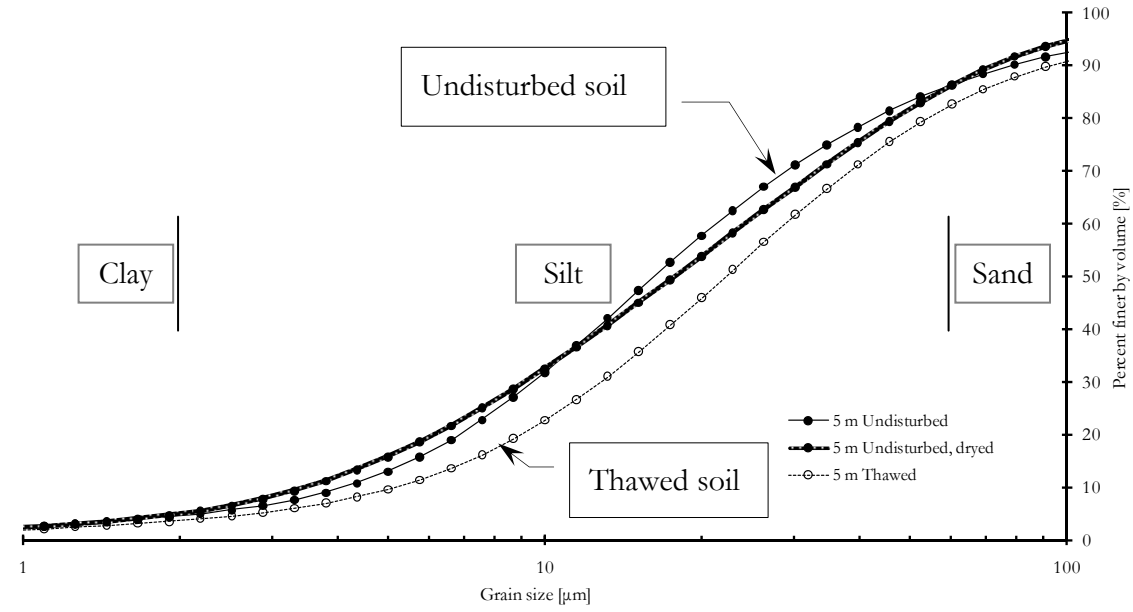

Figure 4.22 Grain size distributions for undisturbed soil, for undisturbed dried soil, and for thawed soil, mean value of two sample series respectively. Sample series collected 5 m below ground surface on August 7th, 2006

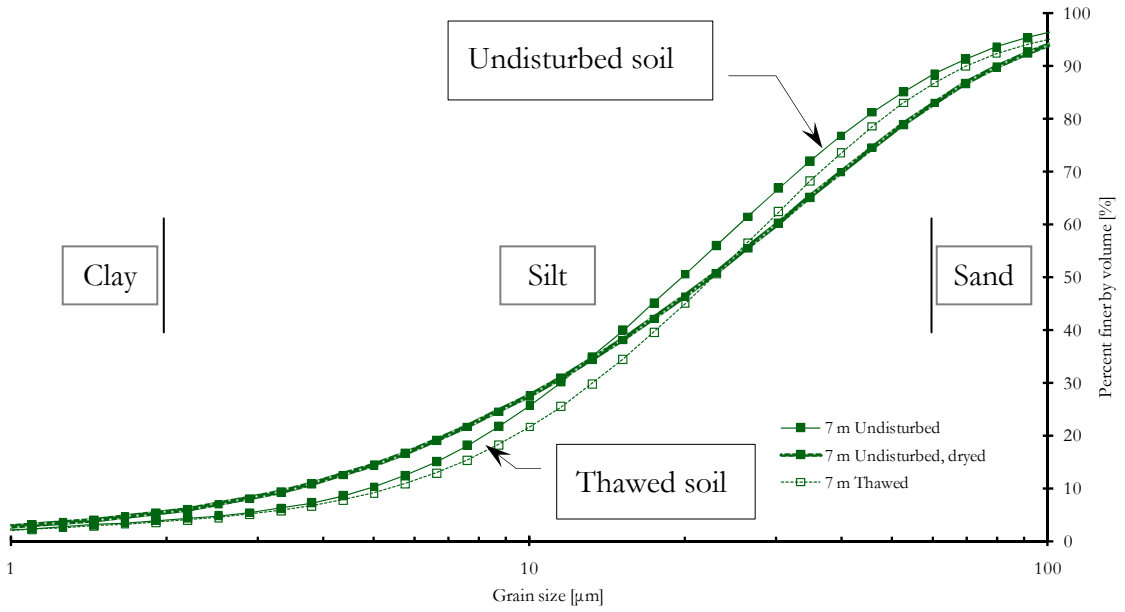

Figure 4.23 Grain size distributions for undisturbed soil, for undisturbed dried soil, and for thawed soil, mean value of two sample series respectively. Sample series collected 7 m below ground surface on August 7th, 2006

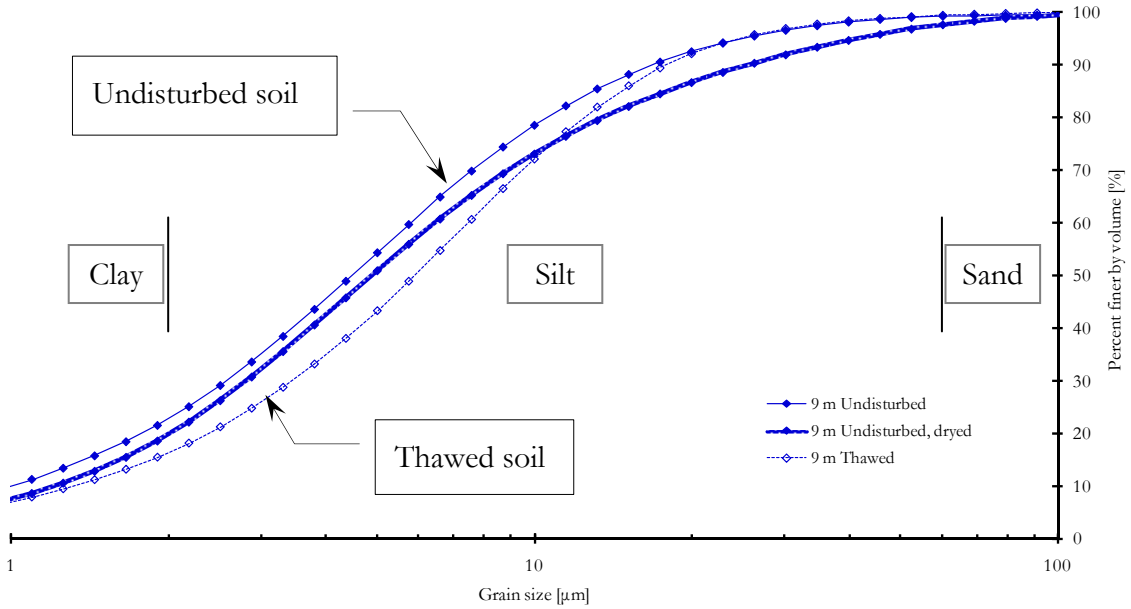

Figure 4.24 Grain size distributions for undisturbed soil, for undisturbed dried soil, and for thawed soil, mean value of two sample series respectively. Sample series collected 9 m below ground surface on August 7th, 2006

Table 4.6 to Table 4.8 present a summary of grain size distribution, taking into account the relative presence as well as the numerical values of undisturbed material, undisturbed, dried material and thawed material from freeze-thaw tests in standard oedometer for respective depth.

Table 4.6 Measured and calculated coefficients for undisturbed and dried (u,dr) as well as pre-consolidated, frozen and thawed soil (th), for the depths of 3 m, 5 m, 7 m, and 9 m below ground surface. Sample series on August 7th, 2006

	D_{10}	D_{30}	D_{60}	F	CL	w_L	I_p	C_u	C_z	GI	a_c	Ratio $a_c/a_{c,th}$
	[mm]	[mm]	[mm]	[%]	[%]	[%]						
3 m u	1.3	2.9	5.1	99	20	53	37	3.8	1.25	40	1.5	1.1
3 m u,dr	1.2	2.8	7.4	94	23	53	37	6.4	0.94	37	1.3	0.9
3 m th	1.3	3.1	6.1	99	19	60	12	4.6	1.19	21	1.4	
5 m u	4.1	9.5	21.3	89	5	110	49	5.2	1.03	59	13.6	1.1
5 m u,dr	3.5	9.2	24.3	90	5	110	49	7.0	0.99	60	12.4	1.0
5 m th	5.2	12.8	28.9	86	4	91	48	5.6	1.09	50	12.0	
7 m u	4.9	11.4	25.4	92	4	117	36	5.2	1.05	53	12.4	1.0
7 m u,dr	3.5	11.1	30.0	88	6	117	36	8.5	1.16	50	8.7	0.7
7 m th	5.4	13.3	28.6	91	4	101	51	5.3	1.15	59	12.7	
9 m u	1.0	2.6	5.8	99	25	70	31	5.8	1.14	40	1.5	1.4
9 m u,dr	1.2	2.8	6.5	98	22	70	31	5.4	1.02	39	1.7	1.6
9 m th	1.3	3.5	7.5	99	18	63	20	5.7	1.21	29	1.1	

Note: F = percentage passing No. 200 sieve (0.075 mm), whole number, CL = clay content, LL = liquid limit, PI = plasticity index. GI = (F-35)[0.2+0,005(LL-40)]+0.01(F-15)(PI-10)

Table 4.7 Classification according to Karlsson and Hansbo (1989) of undisturbed and thawed soil for the freeze area at the Bothnia Line according to; liquid limit (w_L), plasticity index (I_p), liquidity index (I_L), consistency index (I_c), shear strength (τ_{fu}), sensitivity (S_t), and ignition loss (Ign-loss). Sample series on August 7th, 2006, sample series for ignition loss from October 28th, 2003

Level [m]	w_L i	$w_{L,th}$ i	I_p i	$I_{p,th}$ i	I_L ii	$I_{L,th}$ ii	I_c ii	$I_{c,th}$ ii	τ_{fu} iii	$\tau_{fu,th}$ iii	S_t iv	$S_{t,th}$ iv	Ign-loss v
3	HP	HP	HP	HP	HF	P	HF	P	ML	L	M	M	
4	MH	MH	HP	HP	P	P	P	P	L	ML	L	L	
5	MH	MH	MH	HP	P	P	P	P	ML	L	L	M	LO
6	MH	HP	HP	HP	P	FH	P	HF	L	L	M	L	LO
7	MH	MH	MH	MH	P	P	P	P	ML	L	M	M	
8	HP	MP	HP	LP	P	FH	P	HF	L	HF	M	M	MS
9	HP	HP	HP	MP	P	P	P	P	ML	HF	M	M	
10	MP	MP	MP	MP	P	P	P	P	L	HF	M	M	

Note: i: IP = None plastic, LP = Low plasticity, MP = Medium plasticity, HP = High plasticity, MH = Very high plasticity
ii: FH = Stiff – medium stiff, P = Plastic, HF = Medium liquid – liquid
iii: ML = Very soft, L = Soft, HF = Medium stiff, F = Stiff, MF = Very stiff
iv: L = Low-sensitive, M = Medium-sensitive, H = High-sensitive
v: LO = Low-organic soils, MO = Medium-organic soils, OS = High –organic soils, MS = Mineral soils

Table 4.8 Classification according to Karlsson and Hansbo (1989) of undisturbed and thawed soil of the freeze area at the Bothnia Line according to; uniformity coefficient (C_u) , coefficient of curvature (C_z) , hydraulic conductivity (k) , overconsolidation ratio (OCR) , frost activity (Frost) as well as Skempton activity of clay (a_c) (Skempton, 1953). Sample series on August 7th, 2006

Level [m]	C_u i	$C_{u,th}$ i	C_z ii	$C_{z,th}$ ii	k iii	k_{th} iii	OCR iv	OCR_{th} iv	Frost v[1], vi[2]	$Frost_{th}$ v[1], vi[2]	a_c vii	$a_{c,th}$ vii
3	E	E	W	W	Cl	Cl	U	U	III[1],4[2]	III[1],4[2]	A	A
4					Cl	Cl	U	N	III[1],4[2]	III[1],4[2]		
5	Me	Me	W	W	Cl	Cl	U	U	III[1],4[2]	III[1],4[2]	A	A
6					Cl	Cl	U	N	III[1],4[2]	III[1],4[2]		
7	Me	Me	W	W	Cl	Cl	U	U	III[1],4[2]	III[1],4[2]	A	A
8					fi-si	fi-si	U	U	III[1],4[2]	III[1],4[2]		
9	Me	Me	W	W	Cl	Cl	U	N	III[1],4[2]	III[1],4[2]	A	N
10					Cl	Cl	U	N	III[1],4[2]	III[1],4[2]		

Note: i: E = Even-graded, Me = Medium-graded, Ma = Multi-graded.
ii: W = Well graded, P = Poorly graded.
iii: fi-si = Medium silt – Fine silt, Cl = Clay.
iv: U = Underconsolidated, N = Normally consolidated or lightly overconsolidated, O = Overconsolidated.
v: Group I = Frost-insusceptible soils (also called "frost-free"), Group II = Moderately frost-susceptible soils, Group III = Strongly frost-susceptible soils.
vi: Frost-susceptible class 1 = None frost heaving soils, 2 = Slightly frost heaving soils, 3 = Moderate frost heaving soils, 4 = Strongly frost heaving soils.
vii: L = Inactive clay, N = Normal clay, A = Active clay.
1: Classification according to Karlsson and Hansbo (2000).
2: Classification according to ATB Väg 2004 (Vägverket, 2004).

4.7.4 Soil freeze-thaw laboratory tests

The pre-consolidation, i.e. the primary consolidation (at +7 °C) is ignored in all freeze-thaw tests according to Figure 4.3, page 108. Testing of samples collected on October 19th, 2004. The tests consist of two series with one freeze-thaw test per depth, i.e. 3 m to 10 m below ground surface. The results from 3 m to 6 m in Series I are shown in Figure 4.25. The results from Series II, 3 m to 6 m, the results from 7 m to 10 m in Series I, and also the results from 7 m to 10 m in Series II are presented in Appendix.

Mean value for interpreted maximal heaving, and the thaw settlement (heaving included) in relation to the depths below ground surface are presented in Figure 4.26 for samples collected on October 19th, 2004 and in Figure 4.27 for samples collected on August 7th, 2006. Furthermore, heaving of the frozen soil has been presented with the mean value and two-sided 90 % - interval of confidence for each depth below ground surface in Figure 4.28 for samples collected on October 19th, 2004 and in Figure 4.32 for samples collected on August 7th, 2006. In addition, thaw settlement for the frozen soil (heaving not included) has been presented with the mean value and two-sided 90 % - interval of confidence for each depth below ground surface in Figure 4.29 for samples collected on October 19th, 2004 and in Figure 4.33 for samples collected on August 7th, 2006. Finally, the thaw settlement for frozen soil (heaving included) has been presented with the mean value and two-sided 90 % - interval of confidence for each depth below ground surface in Figure

4.30 for samples collected on October 19th, 2004 and in Figure 4.34 for samples collected on August 7th, 2006.

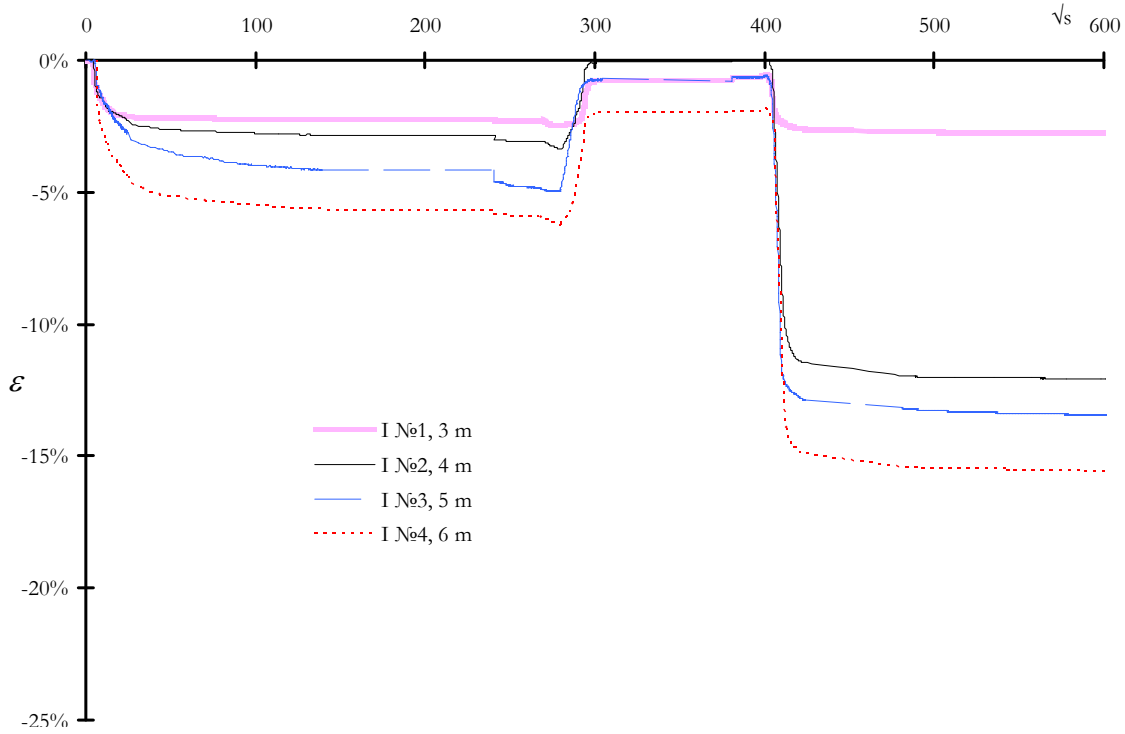

Figure 4.25 Soil strain due to freezing and thawing. Freeze-thaw tests in oedometer for the depths of 3 m to 6 m below ground surface. Series I, on soil from samples collected on October 19th, 2004. Abscissa in the unit; square root of seconds

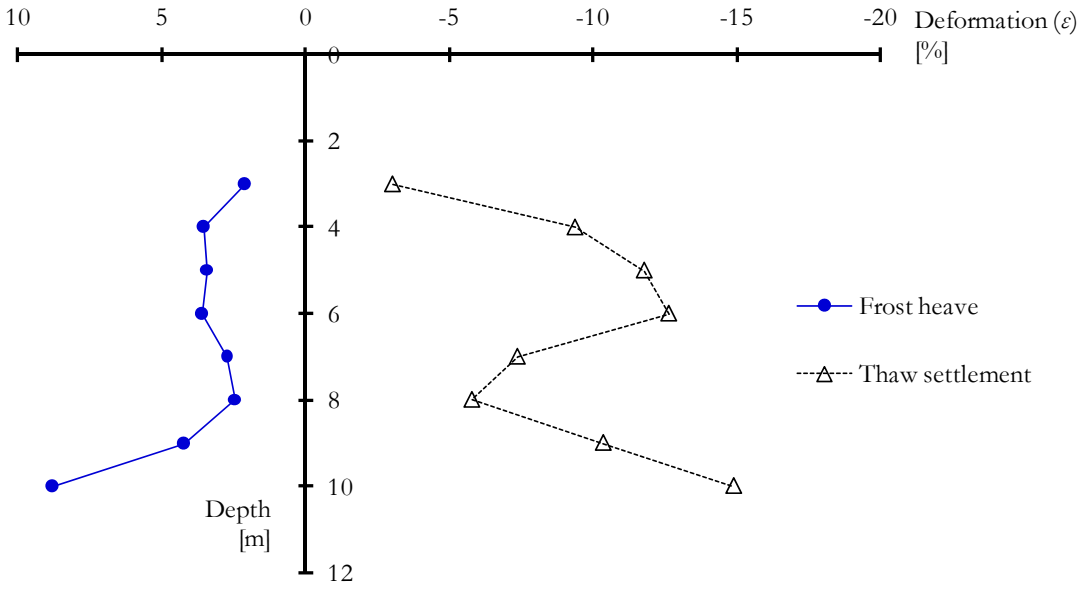

Figure 4.26 Soil strain due to freezing and thawing. Frost heave series and net thaw-settlement series. Thaw settlement with the frost heave not included. Results from freeze-thaw tests in oedometer, mean value for respective depth below ground surface. Samples collected on October 19th, 2004

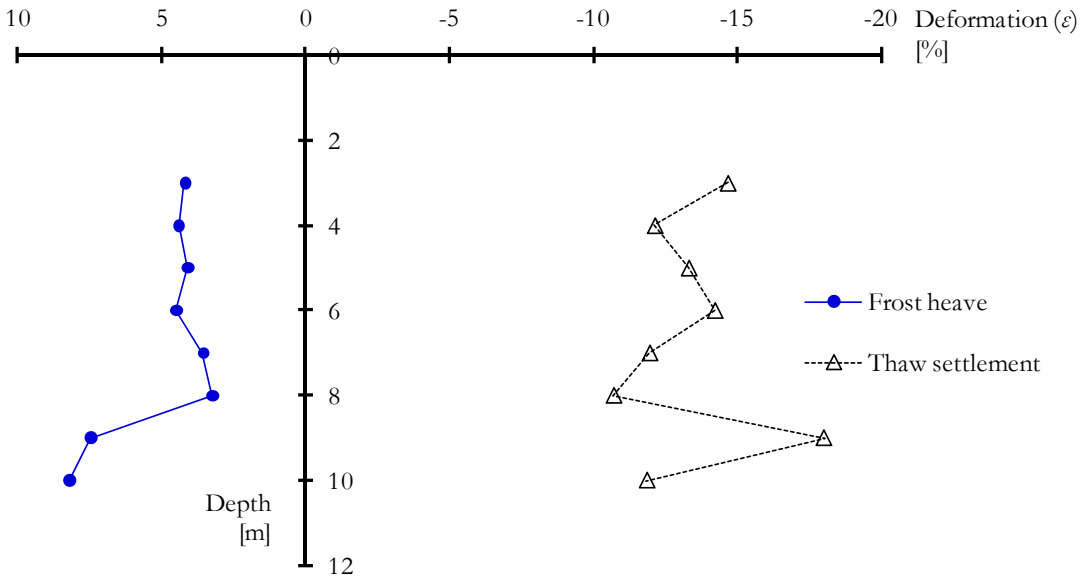

Figure 4.27 Soil strain due to freezing and thawing. Frost heave series and net thaw-settlement series. Thaw settlement series with the frost heave not included. Results from freeze-thaw tests in oedometer, mean value for respective depth below ground surface. Samples collected on August 7th, 2006

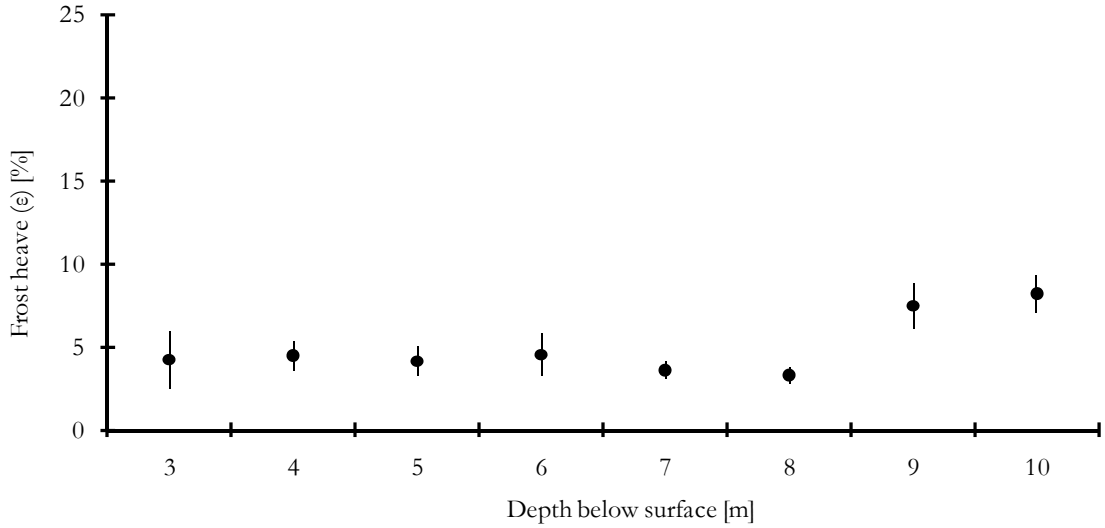

Figure 4.28 Frost heave and the 90 % interval of confidence. Results from freeze-thaw tests in oedometer, mean value for respective depth below ground surface. Samples collected on August 7th, 2006

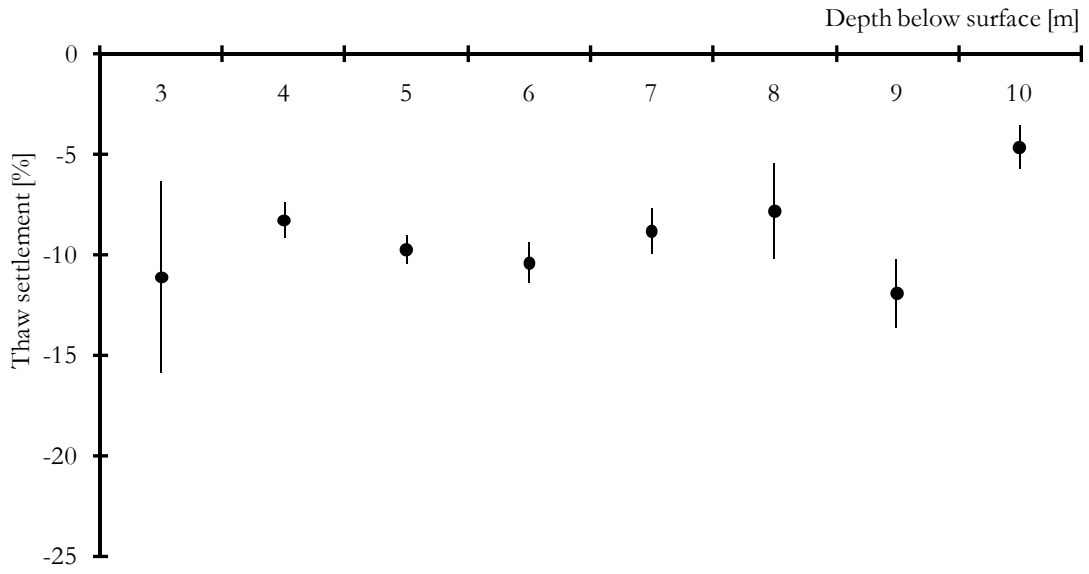

Figure 4.29 Net thaw settlement and the 90 % interval of confidence. Results from freeze-thaw tests in oedometer, mean value for respective depth below ground surface. Samples collected on August 7th, 2006

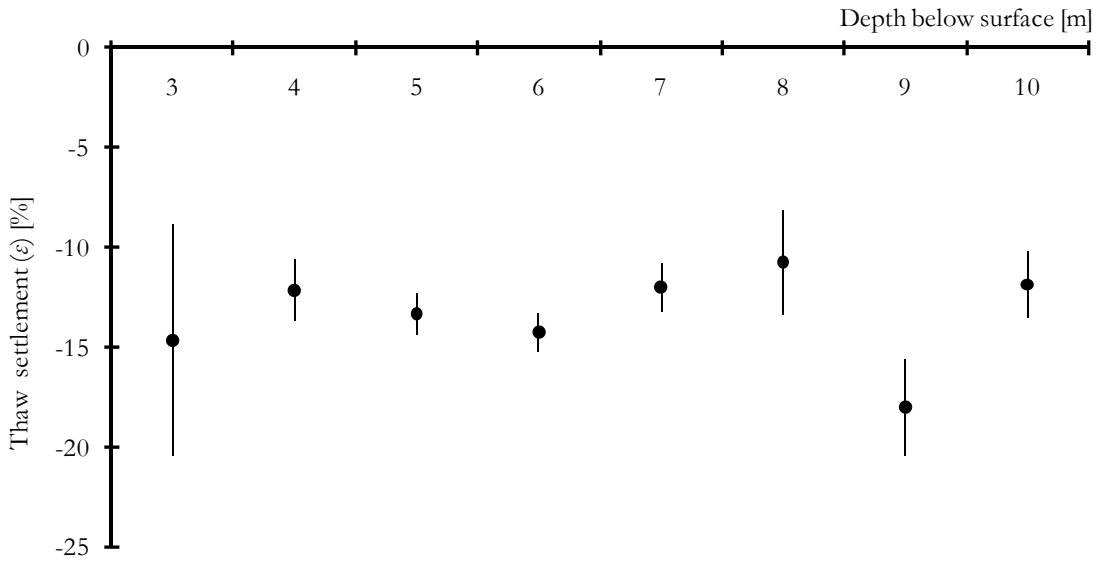

Figure 4.30 Thaw settlement and the 90 % interval of confidence. Results from freeze-thaw tests in oedometer, mean value for respective depth below ground surface. The resulted thaw settlement includes the frost heave. Samples collected on August 7th, 2006

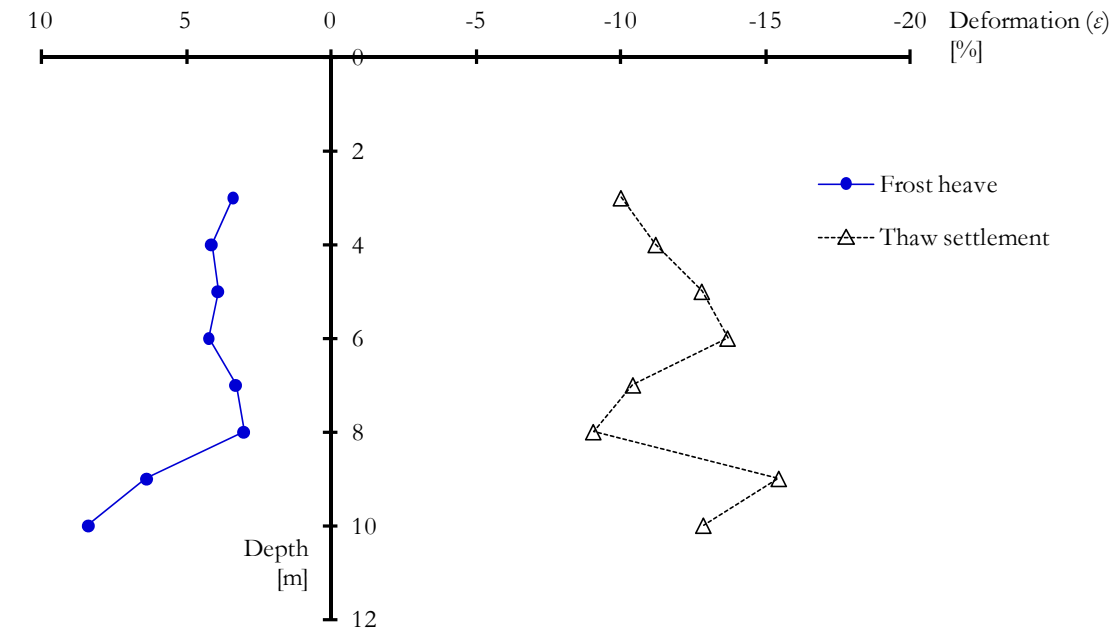

Figure 4.31 Soil strain due to freezing and thawing. Frost heave series and thaw-settlement series. Thaw settlement with the frost heave included. Results from freeze-thaw tests in oedometer, mean value for respective depth below ground surface. Samples collected on October 19th, 2004 and on August 7th, 2006

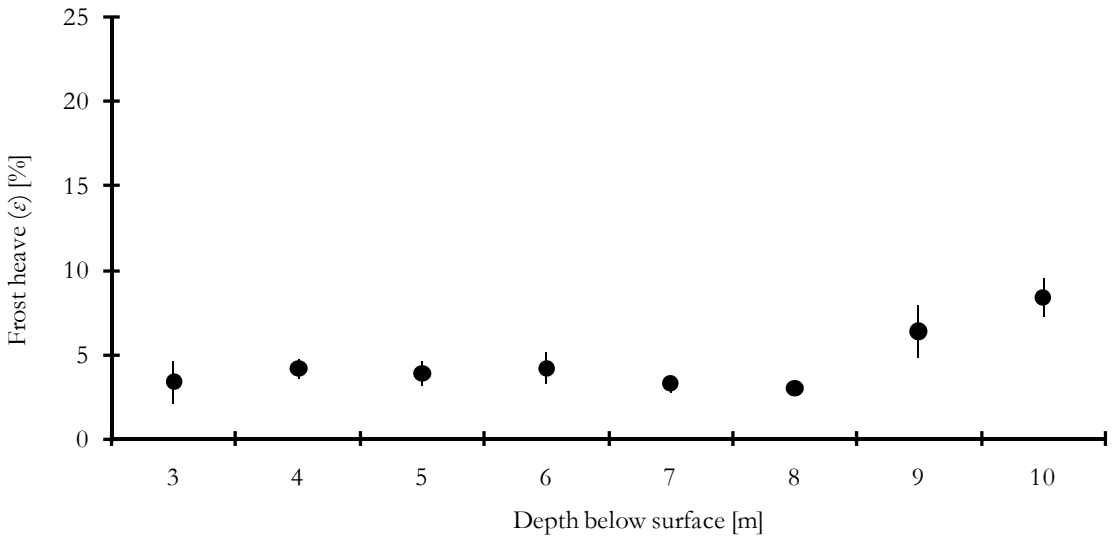

Figure 4.32 Frost heave and the 90 % interval of confidence. Results from freeze-thaw tests in oedometer, mean value for respective depth below ground surface. Samples collected on October 19th, 2004 and on August 7th, 2006

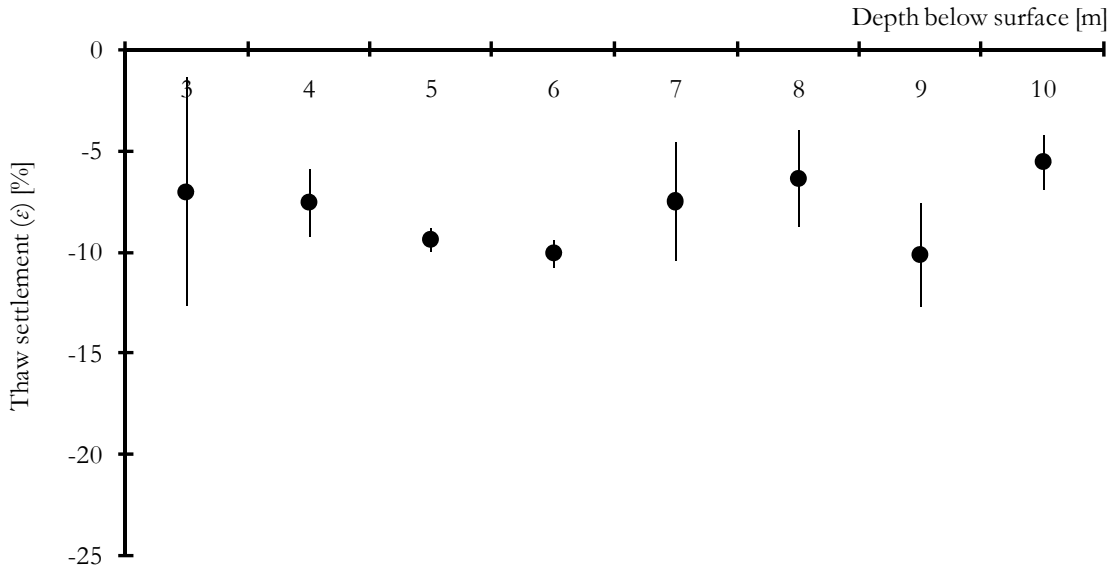

Figure 4.33 Freeze-thaw test in oedometer, mean value for respective depths below ground surface. The figure shows the thaw settlement with the pre-consolidation and the frost heave not included and 90 % interval of confidence. Samples collected on October 19th, 2004 and on August 7th, 2006

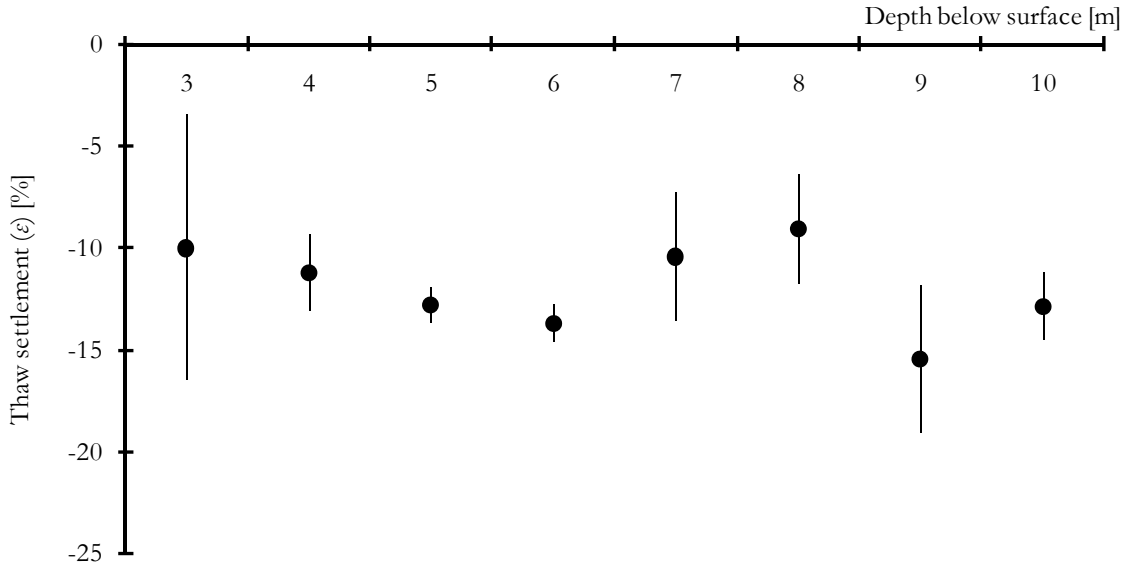

Figure 4.34 Freeze-thaw test in oedometer, mean value for respective depths below ground surface. The figure shows the thaw settlement with the pre-consolidation not included and 90 % interval of confidence. Samples collected on October 19th, 2004 and on August 7th, 2006

The results from samples collected on August 7th, 2006 freeze-thawing has been performed at one occasion for each depth below ground surface, four samples simultaneously, i.e. the experiments have been performed one time per standard oedometer for each depth. The results showing the difference between the oedometers are presented in Figure 4.35. The figure shows the mean value of all depths for each oedometer, as well as two-sided 90 %-interval of confidence for respective oedometer.

Analyses of variance (ANOVA) tests the hypothesis that each sample comes from the same underlying probability distribution against the alternative hypothesis that the underlying probability distribution is not the same for all samples. A hypothesis testing with the zero-hypothesis, *"Each standard oedometer goes a sample from the same underlying probability distribution as the other standard oedometers"* gives a table value for $F_{\alpha = 0.05} = 2.96$ with 3 and 27 degrees of freedom (i.e. hypothesis test at 95 %-level of significance). The zero-hypothesis rejected at signification level α if and only if F (= MST/MSE) $\geq F_{0.05}$. Due to that the laboratory experiments' F-value (= 1.31) is below $F_{0.05}$ (= 2.96), the hypothesis can not be rejected, meaning that if no difference exists between the oedometers and the laboratory experiments, they can be compared at a 95 % signification level (Johnson, 2000). However, Figure 4.35 shows the mean value for all tests of each oedometer as well as the two-sided 90 % interval of confidence.

The tests consist of four series with one freeze-thaw test per depth, i.e. from 3 m to 10 m below ground surface. The results from 3 m depth are presented in Figure 4.36 and the results from 4 m to 10 m depth in the Appendix.

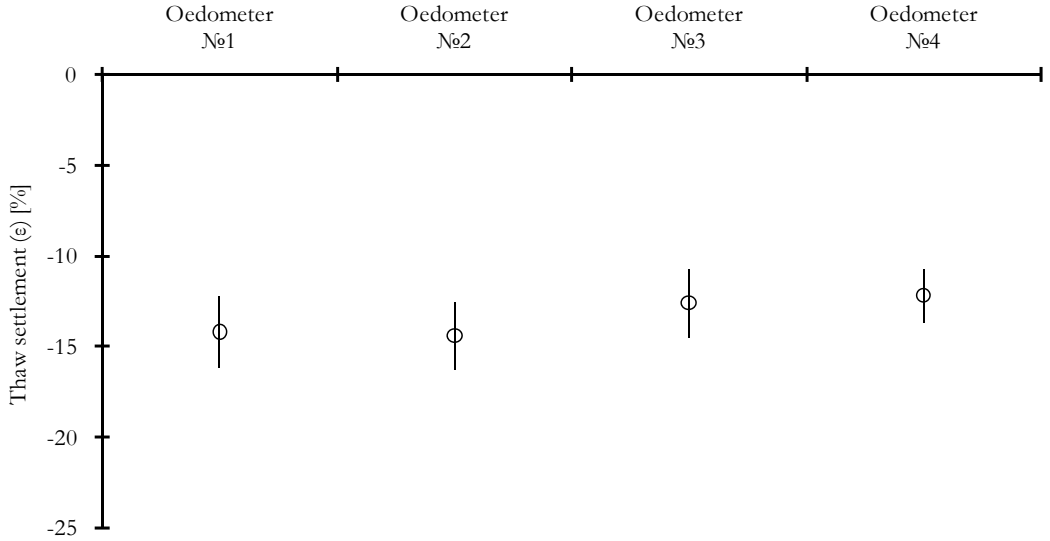

Figure 4.35 Sample series of August 7th, 2006. Comparison of the results from four oedometers relating to thaw settlement, involving eight experiments, i.e. one experiment per depth (besides oedometer №2 which has seven tests). The figure shows the mean values of all readings on respective standard oedometer and respective two-sided 90 % - interval of confidence

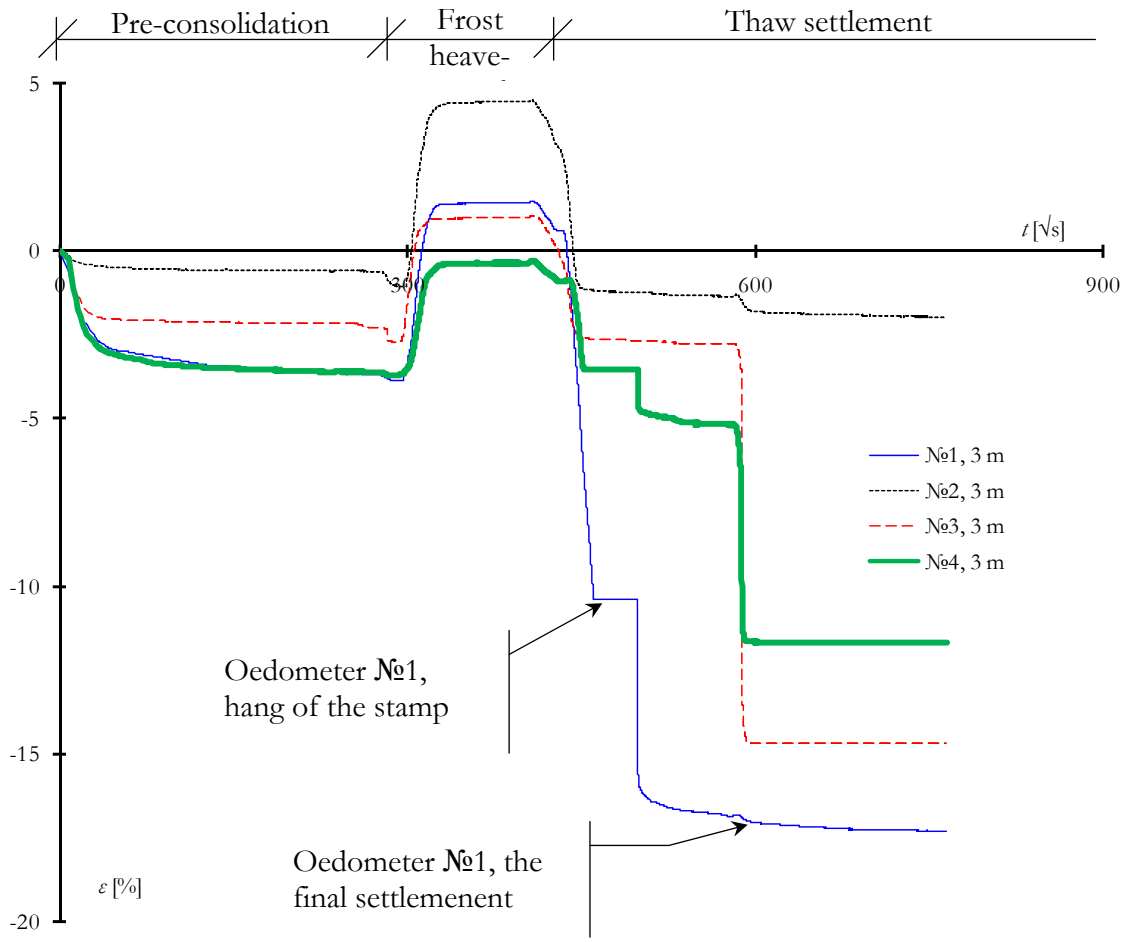

Figure 4.36 Typical freeze-thaw test. Deformation as a function of time (square root second). Freeze-thawing in oedometer № 1 to №4, for the depth of 3 m below ground surface. Abscissa in units of square root of seconds. Sample series of August 7th, 2006. Depend upon the light surcharge at the depth of 3 m (in situ effective stress); hang of the oedometer stamp during the settlement can accrue

4.8 CONCLUSION

The laboratory study mainly covers; 1.) Soil phase basic relations, showing traditional geotechnical engineering routine tests for Bothnia undisturbed and thawed soil. 2.) Soil behaviour, CRS-tests and oedometer tests, showing above all Bothnia undisturbed soil deformation properties. 3.) Grain size distribution tests, showing particularly Bothnia soil grain size distribution for undisturbed and thawed soil. 4.) Soil freeze-thaw laboratory tests, showing above all the Bothnia soil deformation on freezing and thawing.

However, the laboratory study's chapter about soil properties and freezing and thawing soil behaviours shows on one hand the undisturbed soil properties;

- The soil consists of sulphide rich, silty clay.
- The soil from 3 m to 7 m depths consists of organic mineral soil, from 8 m to 10 m depth of mineral soil.
- The soil is according to SGF (i.e. Karlsson and Hansbo (1989)) classification considered "strongly frost-susceptible" and according to ATB Väg 2004 classification as "very frost heaving".

On the other hand after the laboratory freeze-thaw tests;

- Thaw settlement occurs at all depths.
- The thaw settlement magnitude is a function of the ratio between the liquidity limit and the plasticity limit for the undisturbed soil.
- The thaw settlement is a function of the ratio between the water content and the plasticity limit for the undisturbed soil.
- The porosity decreases on average 6 % after the freeze-thawing.
- The void ratio decreases on average approximately 14 % after the freeze-thawing.
- The water content decreases on average 11 %-units after the freeze-thawing.
- The amount of particles less than 6 μm (fine silt) decreases and the amount of particles in, above all, fractions larger than 6 μm (medium silt) increase after the freeze-thawing.
- The preconsolidation pressure increases after a freeze-thaw cycle.

5 FIELD STUDY AND PROGNOSES AT THE BOTHNIA LINE

This chapter contains descriptions of the field studies at the Bothnia Line as well as explanations of the necessity of each measurement. The chapter also presents the test results and a brief discussion around the soil behaviour, the measurements and the test reading.

5.1 INTRODUCTION

The primary aim of the field study is to observe the thaw settlement without any surcharge load at the ground freezing project at the Bothnia Line. The theories of the thaw settlement and the laboratory studies of the thaw settlement will be compared with the thaw settlement in the field study. However, as can be seen in the chapter of the literature study, the extent of the thaw settlement depends on several parameters and has to be monitored and measured.

This thesis deals particularly with in situ soil monitoring during the period of thawing of virgin artificial ground freezing. The study of the Bothnia Line ground freezing project has been done in order to identify and calculate the effect of the thaw settlement.

Extraordinary in situ measurements of temperature, stress on the tunnel roof and deformations of the ground surface were performed during the thawing period, in order to estimate the effects of the ground freezing techniques. However, the monitoring systems at the Bothnia Line consist of

i. monitoring systems for the temperature development in the frozen zone during the thawing
ii. monitoring system for the load build-up on the tunnel roof during the thawing
iii. monitoring system for the pore pressure build-up during the thawing
iv. monitoring system for the vertical deformation first for the freezing ground and secondly for the thawing ground, i.e. possible frost heave and the thaw settlement.

5.2 SITE CONDITIONS AND MATERIALS

The frozen construction site is located below an arable and pasture land, close to the mountain Stranneberget. During the thawing, artesian ground water collects in ponds at various locations between the freeze pipes, due to settlement of the ground surface, see Figure 5.1.

Figure 5.1 The frozen construction site at the Bothnia Line in July, 2007, approximately five years after the cooling machine was turned off. Chainage 13+615 in the foreground and chainage 13+520.5 in the background near the mountain, Stranneberget. The visible parts of the freeze pipes have been cut off at the present ground surface level and will be covered by a soil layer and joined with the adjacent ground surface

5.2.1 Soil condition

The actual soil consisted of approximately 2 m loose peat and gyttja overlaying postglacial sulphide rich silty clay. The foregoing chapter 'Ground freezing at the Bothnia Line' as well as the chapter 'Laboratory study' depicts the soil parameters at each soil stratum, presented in the tender documents and also from laboratory studies at KTH.

5.2.2 Artificial ground freezing

During the period from December 2001 until April 2002, the tunnel contractor installed the freeze pipes in the ground and established the artificial ground freezing unit. In the middle of April 2002, the contractor started the freezing. However, after approximately four months, in the middle of September, the freezing criteria were fulfilled and the

tunnelling started. The tunnelling with temporary support was fulfilled in November 2002, and the cast of the in situ concrete lining started in January 2003. However, in May 2003, the in situ cast concrete lining was finished, and the contractor shut off the cooling device in September 2003. During this time the soil was frozen by maintained keep-alive temperature for nearly 17 months from the starting of the cooling device until the shut off.

5.2.3 Field test instrumentation

Before the ground freezing started, the contractor installed temperature sensors in casing tubes, i.e. Platinum Resistance Thermometers, Pt100. The sensors were concentrated in five sections, originally to control the frozen state of the ground support. However, the temperature sensors are still reading individually at the ground surface.

During the summer of 2003, chainages 13+549 and 13+568.5 ground level gauges were installed at 2.5 m depth in two control sections. The ground level gauges were being distributed at 2 m, 5 m, 10 m, 15 m and 20 m symmetrically at both sides of the tunnel axis as well as perpendicular to the tunnel axis. The ground level gauge located at 10 m south of the tunnel centre axis at both control sections were installed at a depth of 7 m. The vertical ground motion is measured by means of geodetic levelling of the top of a 3 m invar rod, i.e. a half metre above the ground surface. In the same fashion, the installed ground level gauges at 10 m south of the tunnel centre axis were completed with piezometers at the same depth as the ground level gauges at 7 m.

5.3 TEMPERATURE DISTRIBUTION

This part deals with on one hand the temperature prognoses during the thawing of the frozen construction at the Bothnia Line, on the other hand, the field temperature observations at the Bothnia Line at the time of the shut off the cooling device. A good agreement between prognoses and measured values of the temperature in grounds generally mean that the soil's technical properties are described well, above all when considering of the soil material's water content.

5.3.1 Prognosis

Based on the information from above; time schedule, ground profile, soil condition, ground freezing equipment and freeze pipe organisation, a prognosis of the soil temperature development during the freezing was performed by the tunnel contractor. This prognosis of the soil temperature development during the freezing, as well as the temperature based strength of the ground freezing project at the Bothnia Line are mainly described by Saarelainen et al (2004). Likewise, the prognosis of the temperature development during the thawing has been carried out using the (geo-mechanical and) geo-temperature computer program JOBFEM. The soil temperature prognoses during the thawing in JOBFEM are based on the measured data of the soil. The measured soil temperature distribution in the soil at the moment the freezing device has been shut off is shown in Figure 5.14. Likewise, the calculated temperature distribution in the soil at the same time is presented in Figure 5.2. It is of great importance to notice that the original ground temperature was near 7 °C.

The ground temperature is of essential importance for the frozen soil's strength during the construction stage as well as it is important for the following thawing process of the frozen soil and the subsequent thaw settlement. The soil's temperature guides the settlement rate, among other things, during the consolidation process, as the pore water's viscosity is

strongly affected by the temperature. The temperature profile in the soil is thus important when it comes to being able to see the development of the thaw settlement.

The contractor has registered the temperature development of ground via temperature sensors installed in the winter of 2002. Readings have been performed by the contractor and mainly by personals from Botniabanan AB after that the ground freezing contract was finished. However, through regular soil sounding the upper frost front have established by KTH, div of soil and rock mechanics.

The soil and rock thermal properties are judged in the tender documents, Botniabanan (2001A). The estimated thermal properties of the soil are based on the current densities, the water content and the contents of minerals. The estimated thermal properties of the soil are shown in Table 5.1.

Table 5.1 Soil thermal properties at Bothnia Line (Botniabanan, 2001A)

Material	Heat conduction T < 0 °C [W m^{-1}]	Heat conduction T > 0 °C [W m^{-1}]	Heat capacity T < 0 °C [MJ m^{-3} $°C^{-1}$]	Heat capacity T > 0 °C [MJ m^{-3} $°C^{-1}$]	Latent heat of fusion [MJ m^{-3}]
Clay	2.33	0.92	2.19	3.59	166.4
Clayey sandy silty till	2.43	1.04	2.18	3.47	152.3
Silty sandy till	2.72	1.92	2.17	2.7	63.3
Bedrock	2.72	2.72	1.80	1.80	0.3

Before the installation of the cool-down device took place, the contractor performed a thermal prognosis for the chilling stage and the maintenance temperature stage. Fredriksson (2005) carried out a thermal prognosis for the thawing stage i.e. at the time of the shut off of the cooling equipment. Likewise, the thermal prognoses based on the numerical method analysis have been carried out for the thawing duration of 12, 24 and 36 months as well as the thermal condition at the moment of the shut off of the cooling device, illustrated in Figure 5.2, Figure 5.3 Figure 5.4 and Figure 5.5.

The thaw phase simulation in a numerical method analysis that has been carried out in the numerical computer program JOBFEM (Finite element method in soil and rock mechanics) is based on measured temperatures from the temperature sensors installed in the soil at the time for shut off of the cooling device. Likewise, during the thawing the outdoor temperature and the temperature in the tunnel were set to the annual mean outdoor temperature for the district.

Figure 2.4 shows that the temperature around the tunnel holds a temperature of about -23 °C where the thickness is approximately 3.8 m when the cooling machine is terminated. The temperature adjustment of the ground continues during the thawing process and at the same time as the temperature increases relatively quickly in the colder areas, the zero-degree isotherm is moving out in the earlier unfrozen areas. The temperature of the core has already after three months increased to -10 °C on an area measuring 1 m wide and an altitude of approximately 2 m.

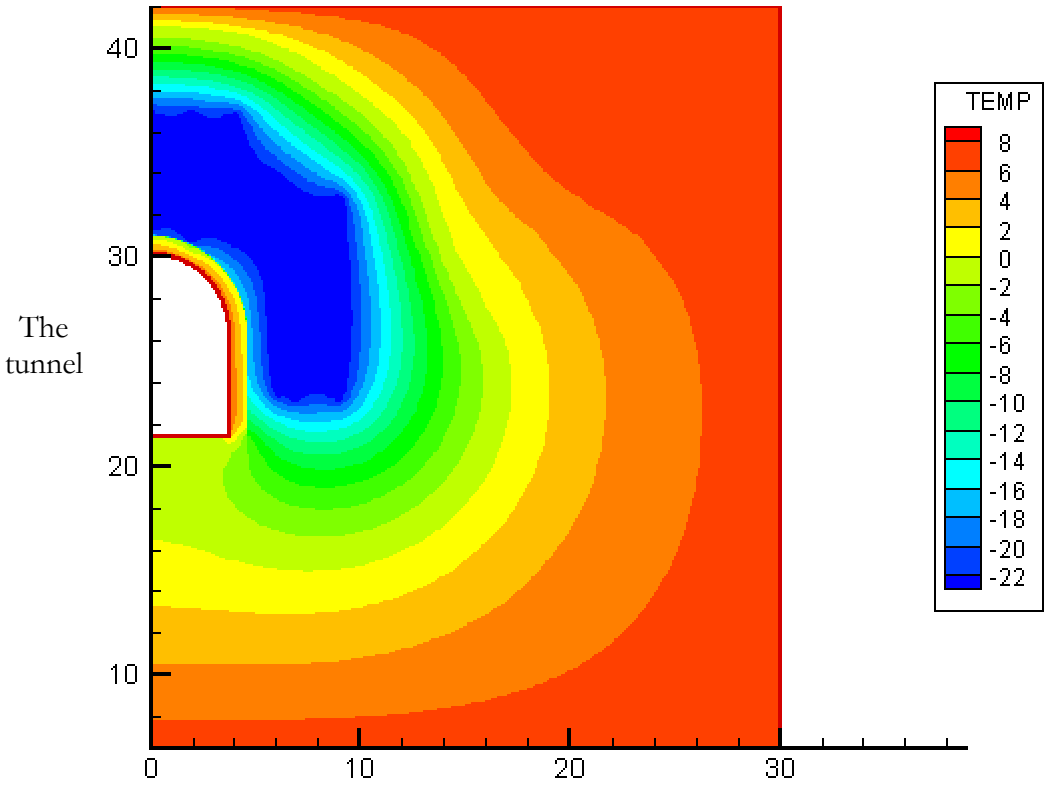

Figure 5.2 *Soil temperature distributions around the tunnel at the time of the shut off of the cooling device, i.e. September 2003. The temperature distributions are based on measured temperatures from the temperature sensors, after Fredriksson (2005)*

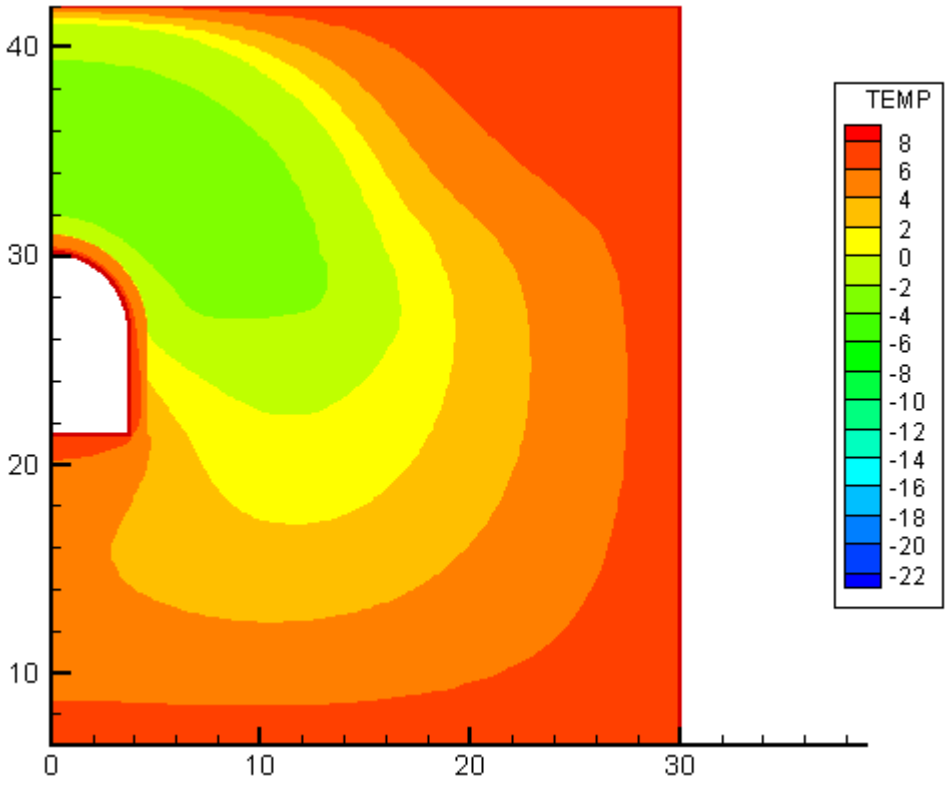

Figure 5.3 *Soil temperature distribution around the tunnel, 12 months after the cooling device was shut off, i.e. the prognosis for September 2004, based on the measured temperatures at the time of September 2003. After Fredriksson (2005)*

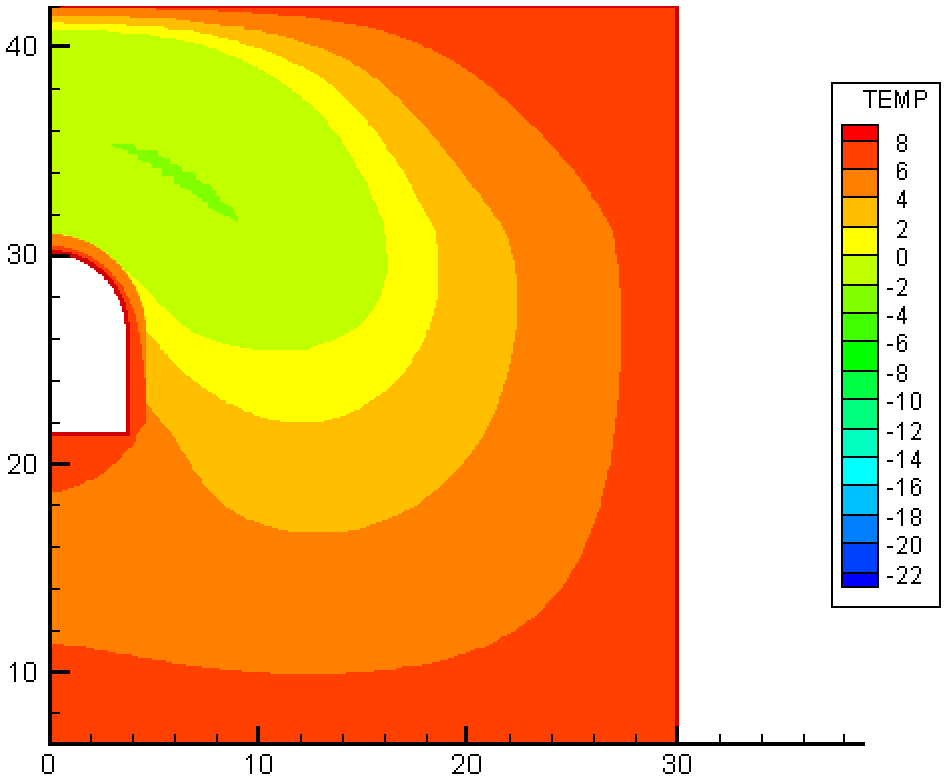

Figure 5.4 *Soil temperature distribution around the tunnel, 24 months after the cooling device was shut off, i.e. the prognosis for September 2005, based on the measured temperatures at the time of September 2003. After Fredriksson (2005)*

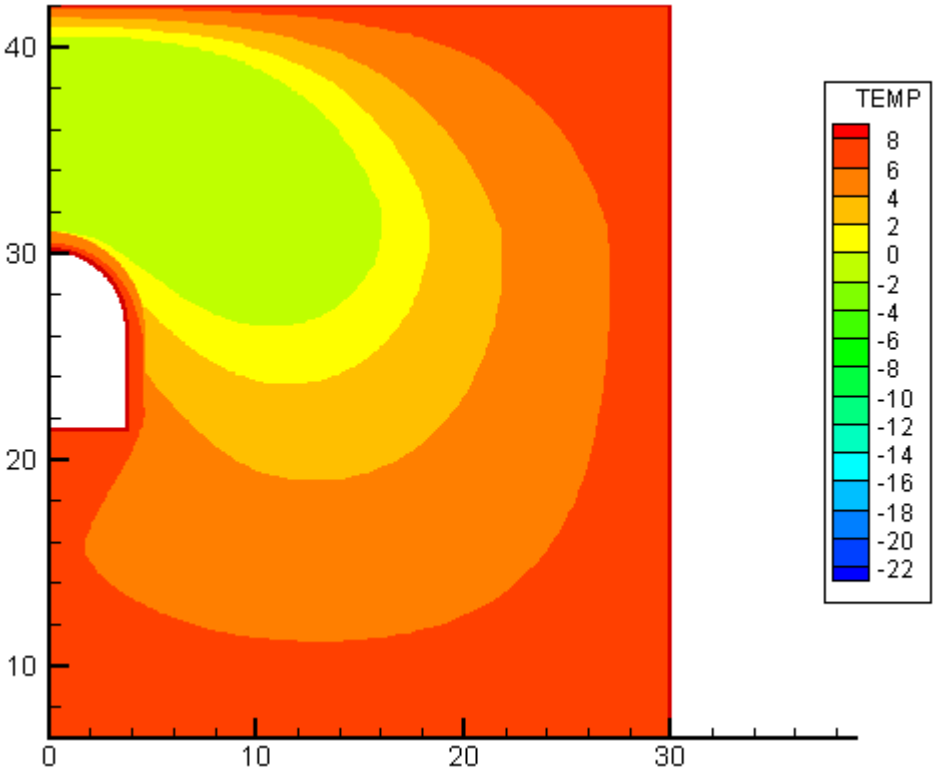

Figure 5.5 *Soil temperature distribution around the tunnel, 36 months after the cooling device was shut off, i.e. the prognosis for September 2006, based on the measured temperatures at the time of September 2003. After Fredriksson (2005)*

5.3.2 Performance

The temperature development during the freezing and the thawing process has been registered in temperature sensor casing tubes installed by the contractor in connection with the installation of freeze pipes in the ground. The temperature sensor casing tubes are installed in five sections (the freezing area is limited by chainage 13+520.5 and 13+615), (see Appendix). The temperature sensor distribution in each temperature sensor casing tube varies from two temperature sensors to seven temperature sensors. However, the temperature sensor distribution in each section, i.e. each chainage is

- 13+525, three temperature tubes with a total of six temperature sensors
- 13+549, five temperature tubes with a total of 22 temperature sensors
- 13+568.5, four temperature tubes with a total of 28 temperature sensors
- 13+579, three temperature pipes with a total of 28 temperature sensors
- 13+601, four temperature pipes with a total of eight temperature sensors.

The installed temperature sensors were of type Pt100, i.e. platinum resistance thermometers, see Figure 5.5. The principle of operation is to measure the resistance of a platinum element. The Pt100 has a resistance of 100 ohms at 0 °C and 138.4 ohms at 100 °C (Pentronic, 2005). Figure 5.5 shows the manual reading of the instantaneous temperature.

Figure 5.6 On the left-hand side temperature sensor, type Pt100. On the right-hand side; manual reading of the soil temperatures at different depths

5.4 LOAD BUILD-UP ON THE TUNNEL ROOF DURING THE THAWING

This part deals with partly the prognoses of the load build-up on the tunnel roof during the thawing of the frozen construction at the Bothnia Line, and partly the observed tunnel roof loads at the Bothnia Line after that the cooling device was terminated.

The expected load build-up on the tunnel roof consists of the overlaying thawing soil, together with the pore water pressure. The frozen soil will relatively promptly during the thawing process turn into a viscous soil. This is, nevertheless, fairly hard to prognosticate in detail as the soil is not a continuum but has shifting properties concerning its water and mineral content etcetera. It is presently unclear how the soil's bearing capacity becomes a load on, for example, the tunnel roof when the thawing process continues through the original frozen material. In the beginning i.e. when the frozen mass consists of a massive frozen vault over the tunnel, the frozen vault will have a bearing capacity ("stand-up-time") depending on, among other things, the soil particles' size distribution, mineral content, water content, temperature, etcetera. Once the frozen construction thaws, this will occur, above all, partly from the excavated, permanently stabilized tunnel and partly from the ground surface (in this case). With consideration of first and foremost the geometrical conditions, the soil closest to the tunnel will thaw radial from the tunnel's periphery. Depending on the soil's rheology, properties when the soil goes from a frozen to a thawed condition, the soil will, during a certain course of time and partly with help of cohesion gradually or continually go from having had a bearing capacity to instead become a load on the tunnel roof. The registration of the load build-up on the tunnel roof will show the rheological significance for the course of the load build- up.

The load build-up on the tunnel has been registered by load-cells on the tunnel's roof installed by the contractor and KTH div. JoB, spring 2003. The readings have been accomplished mainly by personnel from the Bothnia Line and to a certain degree personnel from KTH div. JoB.

5.4.1 Prognosis

The prognosis for the load build-up on the tunnel roof consists of the boundary conditions, namely

- the soil is still frozen next to the tunnel
- the soil has partly thawed and created an open aquifer with hydraulic contact with the outer layer of ground water aquifers
- all soil is thawed.

When the soil is still frozen and has not started to "creep", the load on the lining is then 0 kPa. Due to, above all, convection in the relatively warmer tunnel and further the tunnel linings conductivity, a rather thin thawed zone is created around the tunnel where the ground water can get contact with surrounding aquifer and flowing can occur. The thawed zone's thickness above the tunnel roof was about 1 m according to Figure 5.2, three years after the cooling machine was terminated, see Figure 5.5. The load on the tunnel roof of solely soil then becomes approximately 10 kPa, during the first three years after the shut of the cooling machine. According to the Bothnia Line (Botniabanan, 2001A), there is a hydrostatic zero-pressure level for ground water located at the ground level and in some areas also for artesian ground water located about 1 m above the ground level, the load on the tunnel roof made up of solely water thus becomes approximately 125 kPa. The total load on the tunnel roof becomes about 135 kPa. When all the soil has thawed and consolidated, the load on the tunnel roof will then become approximately 120 kPa for soil and approximately 125 kPa for water that is a total load of about 245 kPa.

5.4.2 Performance

The load build-up that is expected to happen when the frozen soil has thawed has been registered via installed soil pressure cells on the tunnel roof; see Figure 5.7 and Figure 5.8.

The soil pressure cells (max load 5 bar) are placed in the control sections 13+549 and 13+568.5, i.e. totally two pressure cells are installed. The installations were done in May and June 2003.

Pressure cell

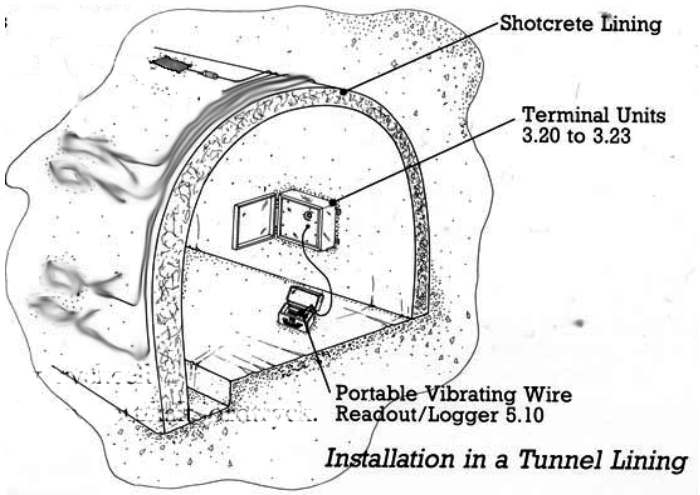

Figure 5.7 Principle section showing installation of soil pressure cell with cabling, modified after Soil instruments ltd (2003)

The pressure cells were installed "embedded" in a layer of tunnel draining mat/rug of about 0.05 m thick ice/soil layer on the temporary shotcrete shell. The pressure cells are of type "vibrating wire pressure cells" and are read manually via cables in the tunnel.

Figure 5.8 Installations in the tunnel at the Bothnia Line, figure of the left-hand side, soil pressure cell to be installed. Figure of the right-hand side, soil pressure cell installed above the insulation behind 0.25 m shotcrete

The first reading of the pressure cells, after the "zero reading" at the time of the installation, was done December 3rd, 2003. Readings of the pressure cells have been done mainly by personnel from the Bothnia Line and to a certain degree also by personnel from KTH, div. JoB. The readings have been made about once a month.

The surcharge on the pressure cells is registered as a total pressure (σ), i.e. the sum of the surcharge of soil and the load of hydrostatic pore water pressure ($\sigma = \sigma' + u$), see Figure 5.24 to Figure 5.26.

5.5 PORE PRESSURE BUILD-UP DURING THE THAWING

This part deals with prognoses of the soil pore pressure build up during the thawing of the frozen construction at the Bothnia Line, and the critical ground water velocity concerning to nearly frozen construction and the observed soil pore pressures during the thawing.

Flowing water in connection with frozen constructions is unfavourable as the running water adds heat to the frozen construction (Shuster, 1980). Flows up to 2 m day^{-1} can generally be accepted for brine freezing without that special measures need to be taken (Jumikis, 1978; Harris, 1995). When freezing with nitrogen, flows up to 20 m day^{-1} are accepted (Harris, 1995). However, it is recorded that flow-rates of up to 50 m day^{-1} have been successfully frozen using nitrogen, although with a significant increase in consumption (Shuster, 1972).

The flowing would be able to arise across the frozen construction as there is a pore water gradient where the ground water in the area south of the frozen construction has a zero-pressure level that lies on a higher geodetic level than the ground water in the area north of the frozen construction. The frozen soil will relatively momentary become a thawed viscous soil during the thawing process. This makes possible a situation with freely flowing water. Nevertheless, this is fairly difficult to prognosticate in detail, as the soil is not a continuum but have shifting properties because of, for example, its mineral content etcetera. The flowing water can affect the course of thawing by convective heat transportation and thus the rate of settlement. It is therefore important to measure the pore water pressure levels as the pore pressure gradient can indicate possible flowing.

This part consists of a prognosis for critical groundwater velocity through the frozen area, particularly after that the cooling machine has been shut off, as well as registered pore water pressure.

5.5.1 Prognoses

Sanger and Sayles (1978) have proposed a closed form solution for determining the critical ground water velocity in connection with artificial ground freezing constructions, performed as brine glaciations

$$u_c = \frac{V_s}{V_0} \frac{k_f}{4S \ln\left(\frac{S}{2d_0}\right)} \tag{5.1}$$

where u_c = critical ground water velocity [m days^{-1}], V_s = temperature gradient between the freeze pipe surface and the freezing point of water [K], V_o = temperature gradient between the surrounding soil and the freezing point of water [K], k_f = frozen soil and rock thermal conductivity [W m^{-1} K^{-1}], S = freeze pipe spacing [m] and d_o = outer diameter of freeze pipe [m].

A rough estimation of the critical ground water velocity, with Sanger and Sayles's (1978) Eq. (5.1) using the following initial values, has been done. However, Sanger and Sayles (1978) reservations have been considered (see Johansson, 2005)

V_s = 24 [K] the period July 3rd, 2002 - August 14th, 2002, see Figure 5.12 and Figure B.6, page XLI
V_o = 9 [K] estimated
k_f = according to Table 5.1
S = 3 [m] (Botniabanan, 2001A)
d_o = 219.1 · 10^{-3} [m] (Botniabanan, 2001A).

Table 5.2 shows the results of the estimated critical ground water velocity for the different soil materials.

The critical velocity is considered to have its largest influence on the frozen construction right when it is about to close up, that is when the water is phase change to ice (Sanger & Sayles, 1978). The soil volume that should be stabilized and sealed through freezing encompasses about 11 900 m^3 and does not make up a continuum.

The areas in the ground that is to be frozen but that holds a larger part water, and the area that contains fine grain material with a larger share bounded water which freezes first at temperatures lower than approximately -3 °C to -5 °C, close up later than other areas. In fact, a possible effect when the frozen construction closes itself is that groundwater flows arise in the areas that per definition close up later and give origin to unfrozen "channels". The flowing water requires much larger cooling effect, which can be accomplished by, for example, supplementation of denser freeze pipe installations or by local freezing with liquid nitrogen (Sanger & Sayles, 1978).

During the period July 3rd, 2002 to August 14th, 2002, a large number of temperature sensors, Figure 5.12 and Figure B.6, in the design zone (see design criteria, Table 3.2) have temperatures of around 0 °C, i.e. when latent heat bonds in water/the ice medium. This is confirmed by theories (Johansson, 2005). The illustrations also show that the measured temperature gradient between entering and exiting brine has increased significantly to approximately 11 °C to once again drop approximately three to four degrees Celsius around August 20th 2002. This can be explained partly by that the chilling of the cooling machine's condenser has been under-dimensioned with consideration of the high outside temperature and partly with consideration of that too many freezing pipes have been connected for the cooling machine's delivered effect.

Ground water flowing through the area that to be frozen can be estimated with help of Darcy's law

$$v = ki = \frac{q}{A} = k\frac{h}{l} \tag{5.2}$$

where; A = area of flow, normal to the flow direction [m^2], h = the height of the flow length [m], i = hydraulic gradient, k = permeability [m $dygn^{-1}$], l = flow length [m], q = flow [m^{-3} $dygn^{-1}$] and finally v = calculated ground water velocity, mean value [m $days^{-1}$].

An estimation of the critical velocity with Darcy's law, Eq. (5.2) including following initial values gives

h = the height of the flow length 5 m, see Figure 5.10
k = permeability, see Table 5.2
l = length of flowing 30 m.

The critical ground water velocity for the different materials does not become dimensioned, see Table 5.2. No groundwater flowing will occur in the clay layer or the clayey moraine due to the soil's low permeability.

Table 5.2 Bothnia Line; estimated ground water velocity according to Eq. (5.2) and the estimated critical ground water velocity according to Eq. (5.1)

Material	Level below the ground surface [m]	Critical ground water velocity [m day^{-1}]	Estimated ground water velocity [m day^{-1}]
Clay	4 - 10	0.27	0.000 01 - 0.000 06
Clayey, sandy, silty till	13 - 15	0.28	0.000 14
Silty, sandy till	15 - 19	0.31	0.001 4
Bedrock	19 -	0.31	-

5.5.2 Performance

The pore water pressure in the clay together with possible shifting in the load is of large significances for the consolidation process. Regular measuring of the pore pressure and the ground water level was done in ground water observation pipes in and around the freeze area from April 2002.

The pore water pressure development close to the frozen construction has been recorded by standard vibrating wire piezometer installed in the spring of 2003, by KTH, division of soil and rock mechanics, see Figure 5.9. The piezometer tip comprises a porous element integral with a diaphragm type vibrating wire pressure transducer, installed in the drill hole at a depth of approximately 7 m. A screened cable connects the transducer direct to the readout unit. However, the vibrating wire pressure transducer consists of a vibrating steel wire, fasten at one end to the sensor element body. The wire vibration at its resonant frequency is relative to the tension in the wire.

The readings have been done principally by personnel from the Bothnia Line and to a certain degree by personnel from KTH, Div. JoB, see Figure 5.9.

According to examinations accounted for in tender documents (Botniabanan, 2001A), there is a hydraulic gradient between the area south of the tunnel and the area north of the tunnel as well as periodically artesian ground water in the whole area above the future tunnel.

Flowing water makes up an important parameter for time consumption, need of effect, placing of freezing pipes etcetera in connection with freezing of temporary constructions to achieve desired stability and hydraulic sealing. The Bothnia Line (Botniabanan, 2001A) has in tender documents proposed that a well system should drain away the possible water flow in and in the surrounding of the frozen zone.

Three well points (for ground water pumping) were installed on the southern side of the freeze area, and three infiltration wells on the northern side. The aim with the placing of the well systems was that if the hydraulic gradient became unfavourable, i.e. it would be disadvantageous to the freezing process if the frozen construction in a hydraulic state would act as a dam construction. If a hydraulic gradient would arise above the freeze area, it would be a possibility of pumping ground water from the wells on the side of the upward flow to the side of the downward flow and in this way decrease the hydraulic gradient.

The zero pressure level of the ground water has been registered in existing ground water observation pipes and wells. During the tunnelling, it has been established that a certain

decrease in the groundwater's zero pressure level has occurred, this depending on where the observation points were located.

Figure 5.9 *On the left-hand side; piezometer mounted on the conduit at the ground level gauge. On the right-hand side; manual reading the vibrating wire piezometer at ground surface*

.

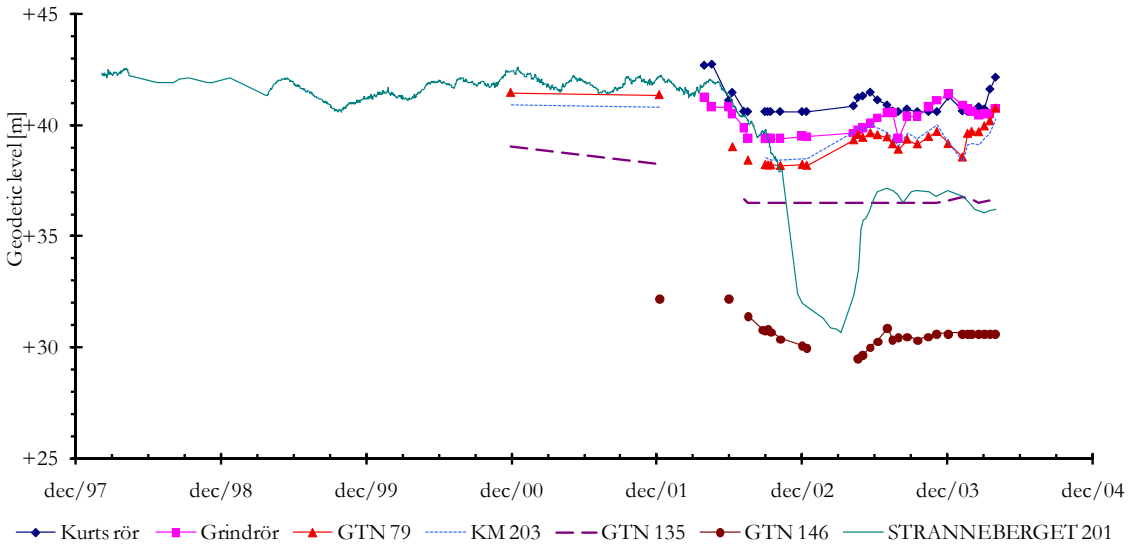

Figure 5.10 *The ground water fluctuation next to the freeze area on the Bothnia Line. The registration of the ground water levels has been accomplished regularly from 2002-2004 (Hammarbäck, 2005)*

Two combined measuring instruments, each consisting of a piezometer and a ground level gauge were fixed together before they were installed in the ground at chainages 13+549 and

13+568.5. The "vibrating wire piezometers" and the ground level gauges were installed on October 28th, 2003 at chainages 13+549 and 13+568.5. The installations were performed 10.2 m and 10.4 m south of the tunnel centre at a depth of 7 m. These points were located 1.5 m into the frozen zone at the time of the installation.

5.6 VERTICAL DEFORMATIONS; FROST HEAVE AND THAW SETTLEMENT

This part deals with the prognoses of the vertical soil deformations during the thawing of the frozen construction at the Bothnia Line, and the observed vertical deformations at the Bothnia Line after the time of cooling device was shut off.

As mentioned in previous chapter, during the freezing, a vertical heave might come about from the water expansion due to the phase change and/or when segregated ice originates in the boundary layer between the frozen soil and the unfrozen soil. On the contrary, when the frozen construction thaws, a vertical settlement is expected thus, the frozen construction mainly consists of fine-grained soil, like, silt and clay. After thawing, the Bothnia soil will first become a viscous mass, and depending on the course of draining, the clayey soil will consolidate and is expected to be overconsolidated. The course's boundary conditions, i.e. the maximum heaving and the size of the settlements are stimulated in laboratories and are thoroughly accounted for separately.

The registration of the deformation in connection with the thawing for a temporary artificially frozen construction of soil and rock is unusual. The connection between the field registered deformation and the laboratory environment registered deformation is central to this work. When the connection between these circumstances can be pointed out, the deformations can then also be pre-decided which is important at construction sites in urban areas.

The development of the vertical deformation above the frozen construction has been registered by ground level gauges installed at a depth comparable to 2.5 m. The gauges were installed by KTH, Div. JoB, in the spring of 2003, see Figure 5.11. Readings via geodetic height determination have been made principally by personals from the Bothnia Line.

When creating a frozen construction, a relatively slow ground frost heave can be expected during the freeze phase and when the frozen construction thaws, i.e. during the thawing process a rather fast thaw settlement can be expected.

This section includes a prognosis for the settlement of the ground surface above the frozen area after that the cooling machine was shut off, as well as registered vertical deformation.

5.6.1 Prognoses

Gauges with a registration level under the seasonal ground frost level have been installed on the freeze area of the Bothnia Line.

The frost heave can be described as a function of partly the enclosed water's expansion and partly the water enrichment and its expansion. An enriching of the water occurs in, above all, surface laying silty soils. On the freeze stabilized sections of the Bothnia Line, the main part consists of the frozen crosscut of sulphide rich clay (approximately 3 m to 10 m deep), as well as gyttja and peat (from ground surface to a depth of approximately 3 m), see Table 3.1 and Figure 3.4.

A strictly simplified prognosis of the total frost heave has been made during the freeze phase when "almost" all the water in the soil had frozen. With guidance of the literature chapter, the thesis Johansson (2005), the soils properties (Table 3.1 and Figure 3.4) as well as oedometer tests, the prognosticated expansion and the accumulated heaving are presented in the previous chapter. However, the laboratory tests discussed in following chapter form the basis for respective analytical solutions that have resulted in a prognosticated settlement.

In fact, the deformation of the frozen area can be expected to occur when the area freezes and to certain degree when it thaws. During the period between the freezing and the thawing, i.e. when the temperature in the frozen zone increases from low temperatures to temperatures around freezing, 0 °C, it is then expected that the frozen zone undergoes a thermal volume expansion during which the zone goes from a relatively cold temperature to a warmer. The expansion equals on an average approximately $5 \cdot 10^{-5}$ K^{-1} (Nordling & Österman, 2004; Ingelstam, Rönngren & Sjöberg, 1999) depending on the degree of water saturation, frozen and unfrozen water share, mineral content, etcetera. This means a heaving due to thermal expansion equal to approximately ten mm for the frozen zone, when the temperature increases from about -20 °C to 0 °C in the approximately 10 m thick frozen zone.

5.6.2 Performance

The soil's deformation is registered with ground level gauges installed in control sections, 13+549 and 13+568.5. Ten ground level gauges at an approximate depth of 2.5 m under ground level have been installed at respective control section. This depth is located under the expected ground frost depth, which has been estimated to be at the most about 1 m (peat).

The ground level gauges are symmetrically divided on approximately 2 m, 5 m, 10 m, 15 m and 20 m from the tunnel centre axis on the northern respective the southern side of the tunnel centre. The two sections where the ground level gauges are installed in are shown in Figure 3.3.

The gauges were installed on October 26th, 2003. A hole for each gauge was drilled with aid of a casing tube in the unfrozen ground, above the frozen ground. The hole was subsequently filled with sand to a thickness of about 0.2 m. The foot of the gauge was put on the sand and surrounded with another 0.2 m of sand. The space above the sand, around the gauge's protection pipe, was re-filled with existing drill cuttings see Figure 5.11. Invar rods ending approximately 0.5 m above ground surface were mounted from the gauge foot at a depth of 2.5 m.

To prevent add freeze forces, etcetera on the invar rods during the course of the post freeze, the rods were equipped with casing pipes of PEN20. Nevertheless, the casing pipes were removed after the refill around the protection casing.

In connection with the installation of piezometers approximately 10 m south the tunnel centre, the installation was completed with ground level gauges placed at the same level as the pore pressure sensors were installed, which is 7 m under the ground surface. The ground level gauges' labels and positions are referred to in the Appendix.

The ground level gauges' height level was read via conventional levelling against one of the National Rail Administration fixed points for the Bothnia Line. The gauge's reading point consists of one end of the connection invar rod located about 0.5 m above ground surface level.

Figure 5.11 Installation of ground level gauges. Illustration to the left; ground level gauges with protection casing (four). Illustration to the right; sealing of the mounted ground level gauges with sand

A number of ground level gauges were damaged in connection with the restoration work at the freeze area during the autumn of 2004. The installation was completed in October 19th, 2004 with ground level gauges for chainage13+549 in points; 20 m, 15 m and 2 m north of the tunnel centre axis, as well as 20 m south of the tunnel centre. In sections 13+568.5, the installation was supplemented with new gauges in points 20 m, 15 m, 10 m and 5 m north of the tunnel axis centre as well as 20 m south of the tunnel centre axis.

5.7 RESULTS

This part deals with the observed and registered results from the soil temperature measurements, the loads on the tunnel roof, the soil pore pressure and finally the vertical soil deformations.

5.7.1 Temperature distribution

The temperature development in the ground is interesting as the time for the settlement process' start depends on the temperature. As explained above and below, the soil profile consists mainly of clay, but has strata of clayey, sandy silty till that turns into silty sandy till underneath. According to Table 5.1, the heat capacity of frozen clay is approximately 2.2 MJ m^{-3} °C^{-1}. It takes about 45 MJ m^{-3} to receive a temperature increase from -20 °C to 0 °C. On the other hand, according to Figure 5.2 it takes about 165 MJ m^{-3} to phase change ice to water, i.e. it takes approximately four times more energy for the phase conversion than for the temperature increase from -20 °C to 0 °C.

The thawing occurs, according to JOBFEM calculations (see above), during a relatively quick levelling of the temperature in the ground, at the same time as the frozen zone continues to expand another metre until 24 months after the shut off of the cooling machine when the frozen zone "stands still" until complete thawing is attained, see Figure 5.17 till Figure 5.19.

The prognosis shows, Figure 5.17, 12 months after the shut off of the cooling machine, that the temperature is still -3 °C in a core comparable to -2 °C isotherm, at the time when the cooling machine is shut off. The temperature development stops during a relatively long period of time, as the phase change requires such a large amount of energy when the temperature in the ground gets closer to zero degrees Celsius.

The observed temperature development at each the stratum of the ground freezing area presents in Figure 5.14. The diagram shows the mean value of all observed temperatures from thermocouples at assorted span as well as the average temperature value of all installed thermocouples. The distributions of the thermocouples at the ground freezing area are summarized in Appendix.

In the control section, chainage 13+549, see Figure 5.12, the temperature development is shown in three temperature control pipes located at 3 m, 6 m, 5 m and 9 m south of the tunnel centre and in a temperature control pipe located about 6 m north of the tunnel centre. The ground level is at the geodetic level approximately +42.0. The temperature sensors in the pipes are distributed from four metres down to 14 m and 16 m under the ground surface in respective pipes.

In control sections 13+568.5, see Figure B.6, the temperature development is shown in three temperature control pipes located straight above the tunnel centre, 4 m and 8 m north of the tunnel centre as well as a temperature control pipe 8 m south of the tunnel centre. The ground level is at a geodetic level of approximately +42.0. The temperature sensors in the pipes are distributed from 4 m down to 21 m and 22 m under the ground surface in respective pipe.

The theoretic contour of the tunnel is in the ceiling approximately +30.1 and +30.3 (in chainage 13+549 and 13+568.5 respectively), i.e. about 12 m under the ground surface.

The temperatures of the freeze area's outer edge zone are in the west registered in the chainage 13+525 and in the east registered by the chainage 13+601, see figures in Appendix.

At the temperature readings July 7th, 2006, it was established that all sensors registered temperatures above 0 °C, except the sensors; 3.3.1 located at the geodetic height +38.0, straight above the tunnel's centre axis in chainage13+568.5 and the sensor 3.3.2, located in the same temperature control pipe at the geodetic level +36.0 see Figure 5.12 to Figure B.8.

The results from the soil sounding August 7th, 2006, shows that the frozen zone's upper border exists at a geodetic level varying between +36 and +39 in both of the soil sounding length chainages 13+549 and 13+568.5, see Figure 5.15, Figure 5.17 and Figure 5.19.

The temperature development in the frozen area is presented quantitatively by being divided into three different temperature intervals: The number of measuring values above 0 °C (expected thawed zone), the number of measuring values that at respective time is 0 °C (expected frozen soil, intermediate temperature), as well as the number of measuring values below 0 °C (expected frozen soil), see Figure 5.13. However, there are a total of 58 (still) working sensors.

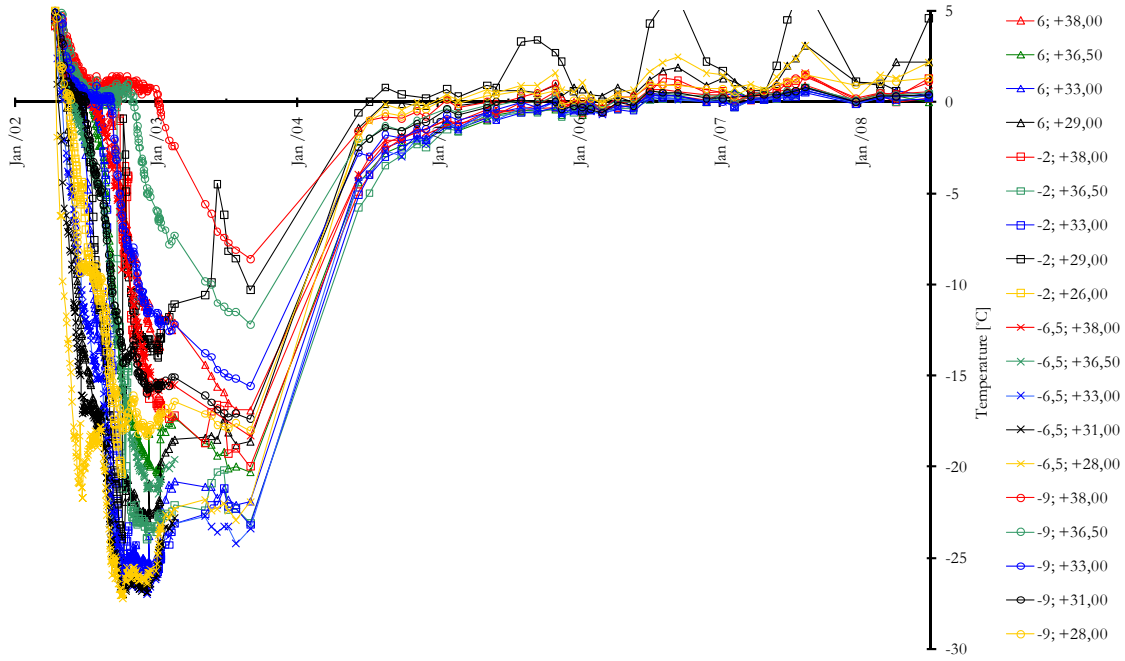

Figure 5.12 The temperature development for chainage 13+549 at the Bothnia Line, from April 16th, 2002 to June 26th, 2008. The registration of the temperature originates from 3 temperature control pipes located; 2, 6, 5 and 9 m south of the tunnel centre as well as a temperature control pipe located 6 m north of the tunnel centre axis. The temperature sensor in each temperature control pipe is placed at geodetic level from +38,00 down to about +26,00. The temperature control pipes are noted positive north of the tunnel and refer to the distance to the tunnel centre

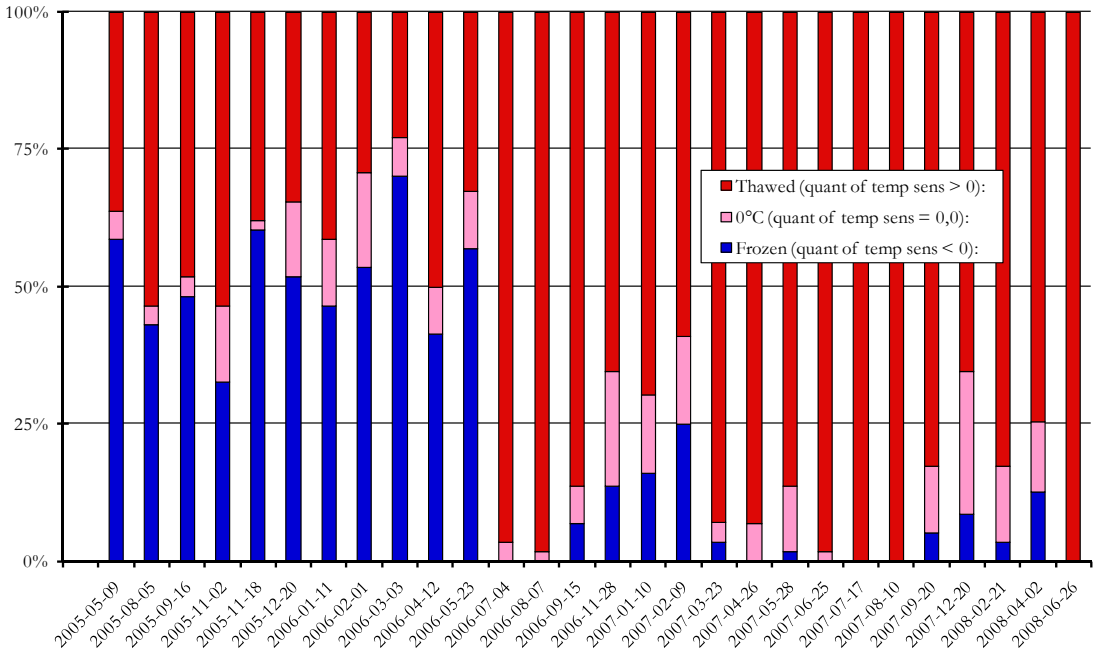

Figure 5.13 Quantitative estimate of the soil temperature distribution during the period September 5th, 2005 to June 26th, 2008. There are a total of 58 temperature sensors registering the temperature. The illustration shows the temperature development for the frozen construction as a percentage of the distribution of the amount of temperature sensors registering temperatures above 0 °C (expected thawed soil), 0 °C (intermediate temperature) as well as 0 °C (expected frozen soil)

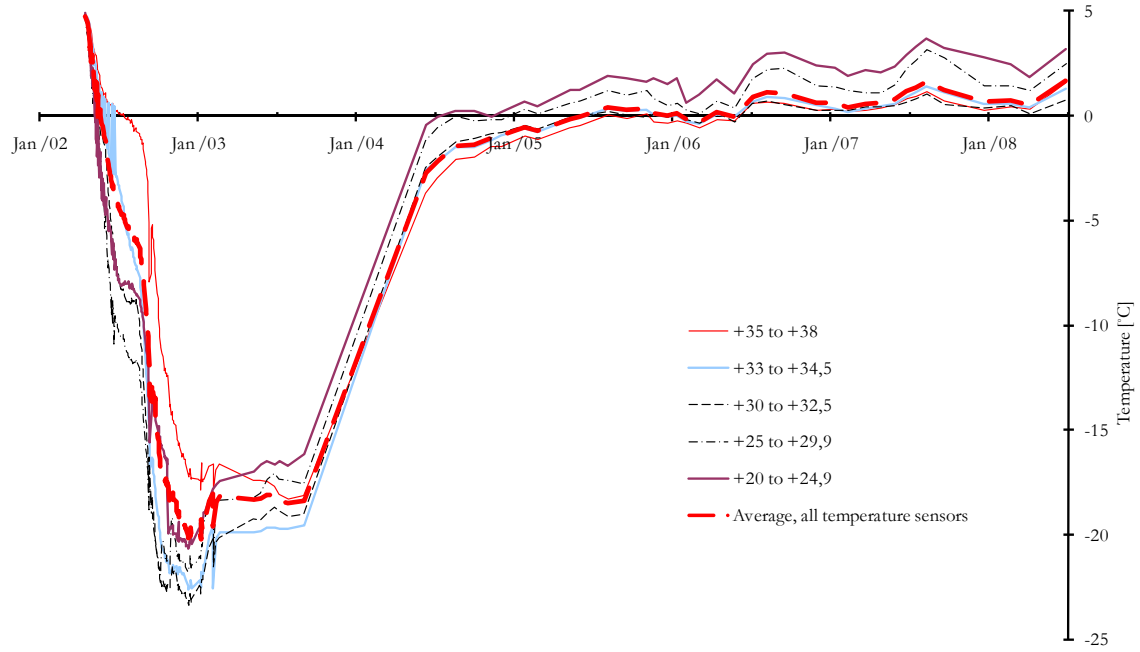

Figure 5.14 Observed temperatures at the ground freezing area at the Bothnia Line. Thermocouples assorted span of geodesic levels showing temperatures [°C] vs. days. The geodesic level of ground surface, +41.5 and of the tunnel roof approximately +30

To verify the frozen zone calculated in the JOBFEM program, i.e. the actual frost front, regular manual sounding have been performed in each control section i.e. chainage 13+549 and chainage 13+568.5. Likewise, the manual sounding was carried out in October 2003, June 2004, October 2004, June 2005, November 2005, and August 2006 and also in July 2007. Manual sounding was performed by sounding in points; above the tunnel centre located about 2 m and 5 m from the tunnel centre as well as more frequently where the horizontally frozen upper surface turned in to steep incline.

The ground surface is approximately horizontal and located in sections at a geodetic level of about +41.7; see Figure 5.15 and Figure 5.17. The sounding results in chainage 13+549 and chainage 13+568.5 show that the frozen zones horizontal upper surface during the period October 28th, 2003 to June 10th, 2004 (approximately seven months) thawed about 0.8 m, i.e. the freeze front has retarded from the geodetic level of approximately +41.2 to about +40.4.

The frozen zone's location shows an unchanged position during the period June 10th, 2004 to October 19th, 2004 (approximately four months); see Figure 5.15 and Figure 5.17.

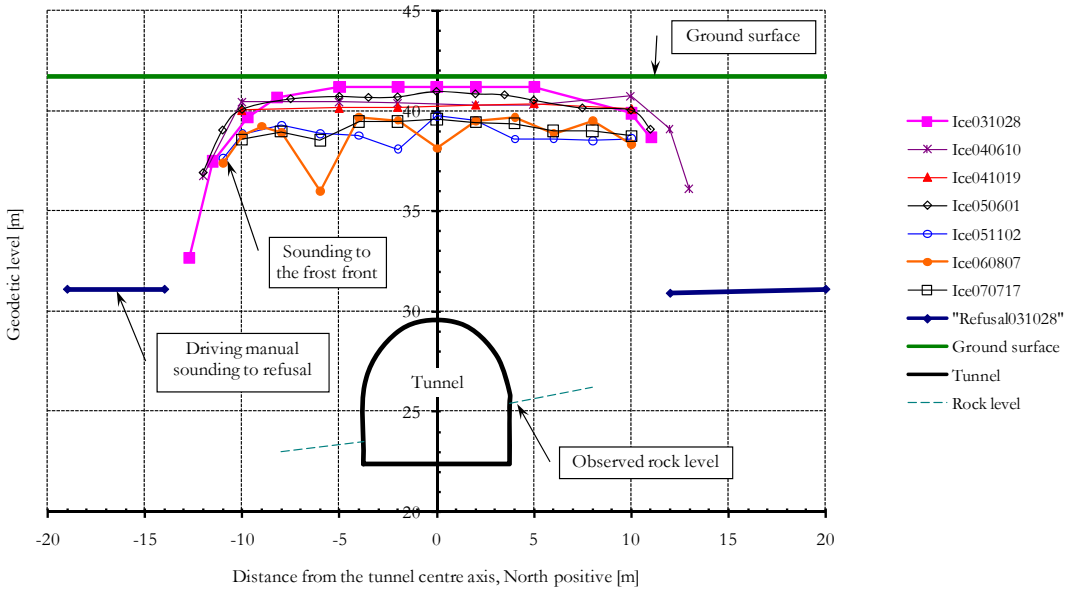

Figure 5.15 Cross section at the Bothnia Line, chainage 13+549; the frozen zone's development after the shut off of the cooling machine. The manual sounding results October 2003, June 2004, October 2004, June 2005, November 2005 as well as August 2006, i.e. 1, 9, 13, 21, 25 and 35 months after the shut off of the cooling machine

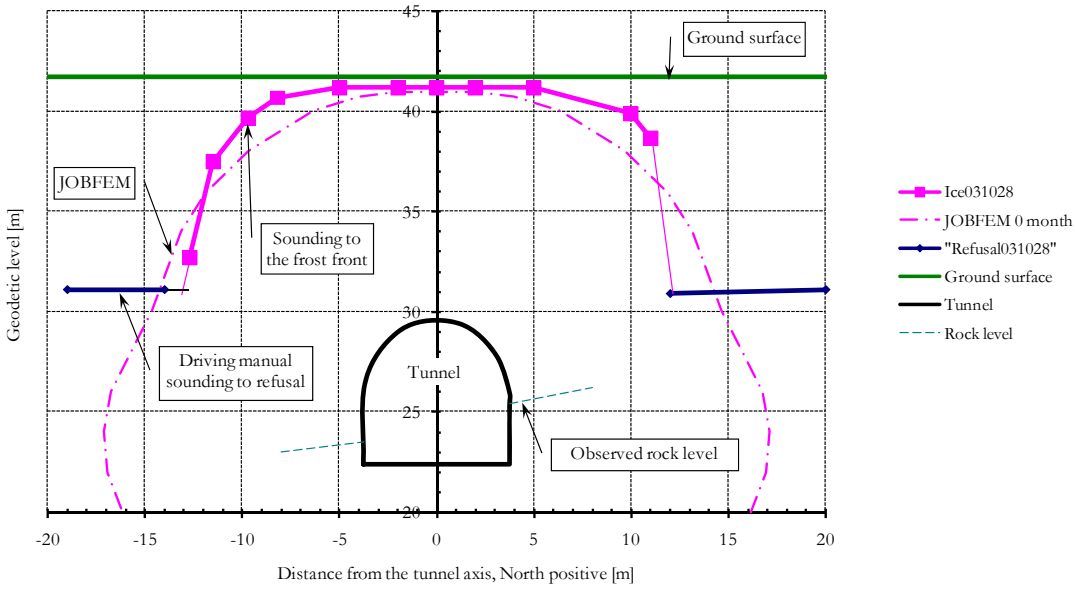

Figure 5.16 Cross section at the Bothnia Line, chainage 13+549; the frozen zone's development after the shut off of the cooling machine. The results of the manual sounding from sounding October 28th, 2003, that is one month after the shut off of the cooling machine, have been compared with numerical calculation for the time when the cooling machine was shut off

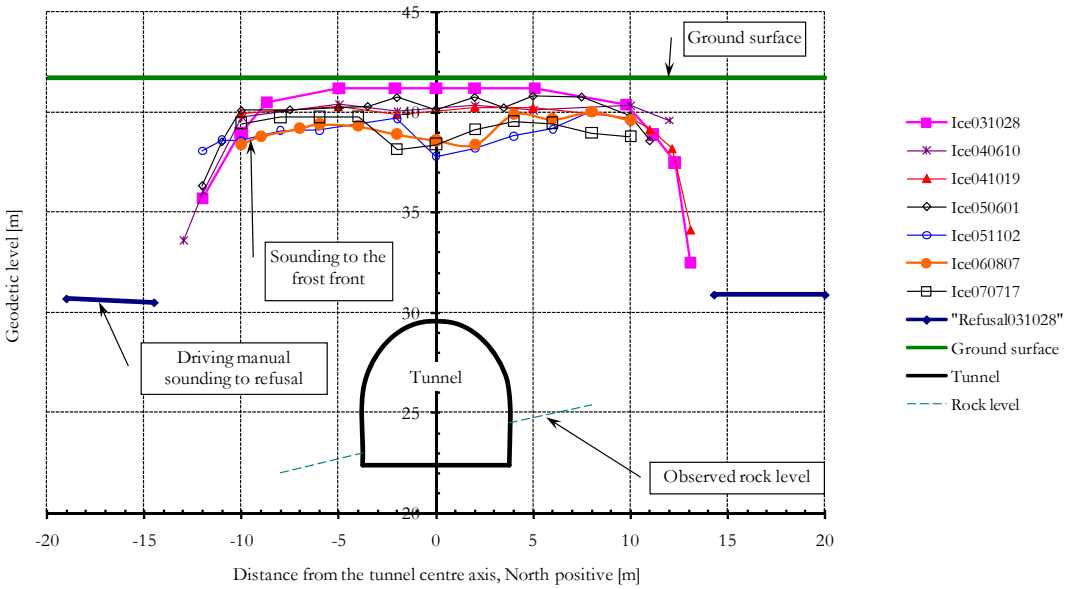

Figure 5.17 Cross section at the Bothnia Line, chainage 13+568.5; the frozen zone's development after the shut off of the cooling machine. The sounding results from the sounding October 28th, 2003, June 10 th, 2004 and October 19th, 2004, i.e. 1, 9, 13, 21, 25, and 35 months after the shut off of the cooling machine

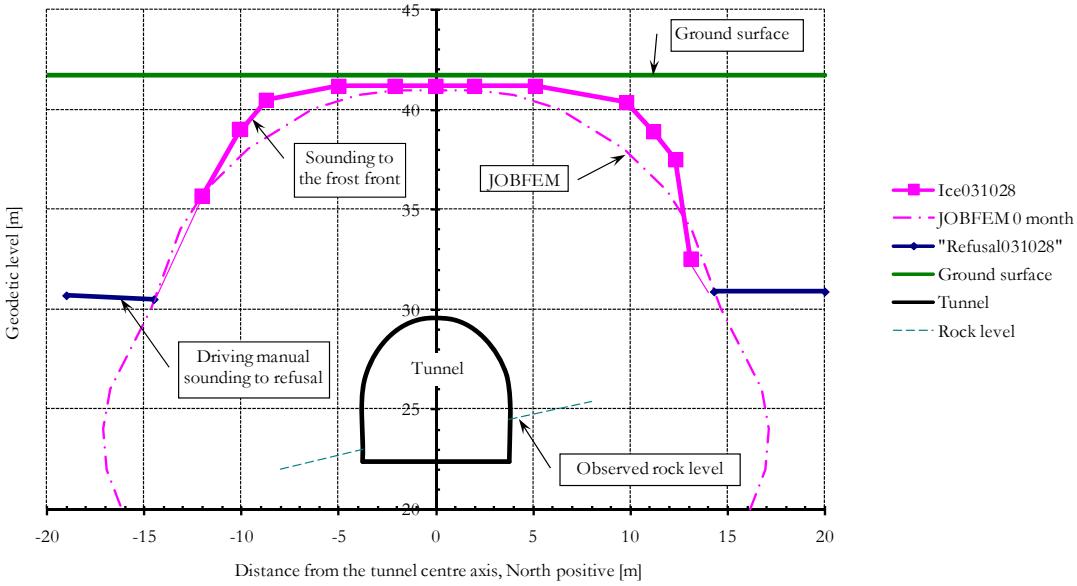

Figure 5.18 Cross section at the Bothnia Line, chainage 13+568.5; the frozen zone's development after the shut off of the cooling machine. The manual sounding results from sounding October 28th, 2003, i.e. one month after the shut off of the cooling machine, have been compared with numerical calculation for the time when the cooling machine was shut off

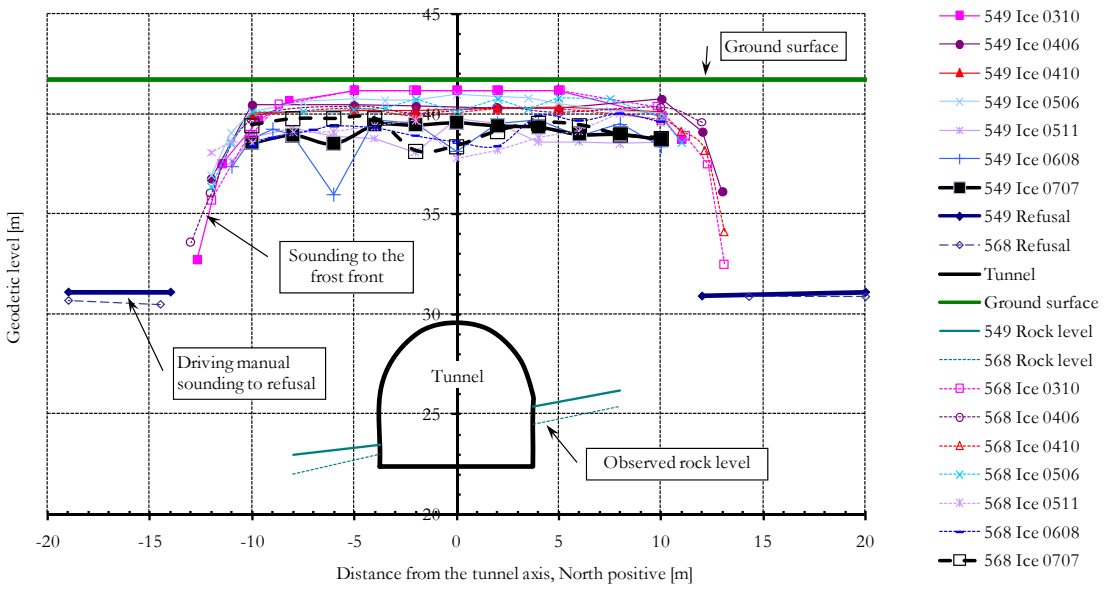

Figure 5.19 Cross section at Bothnia Line, chainage 13+549 and 13+568.5; the development of the frozen zone after the cooling machine shut off. Results from manual soundings; Oct 2003, June 2004, Oct 2004, June 2005, Nov 2005, Aug 2006, i.e. 1, 9, 13, 21, 25, 35 and also 46 month after the cooling device shut off

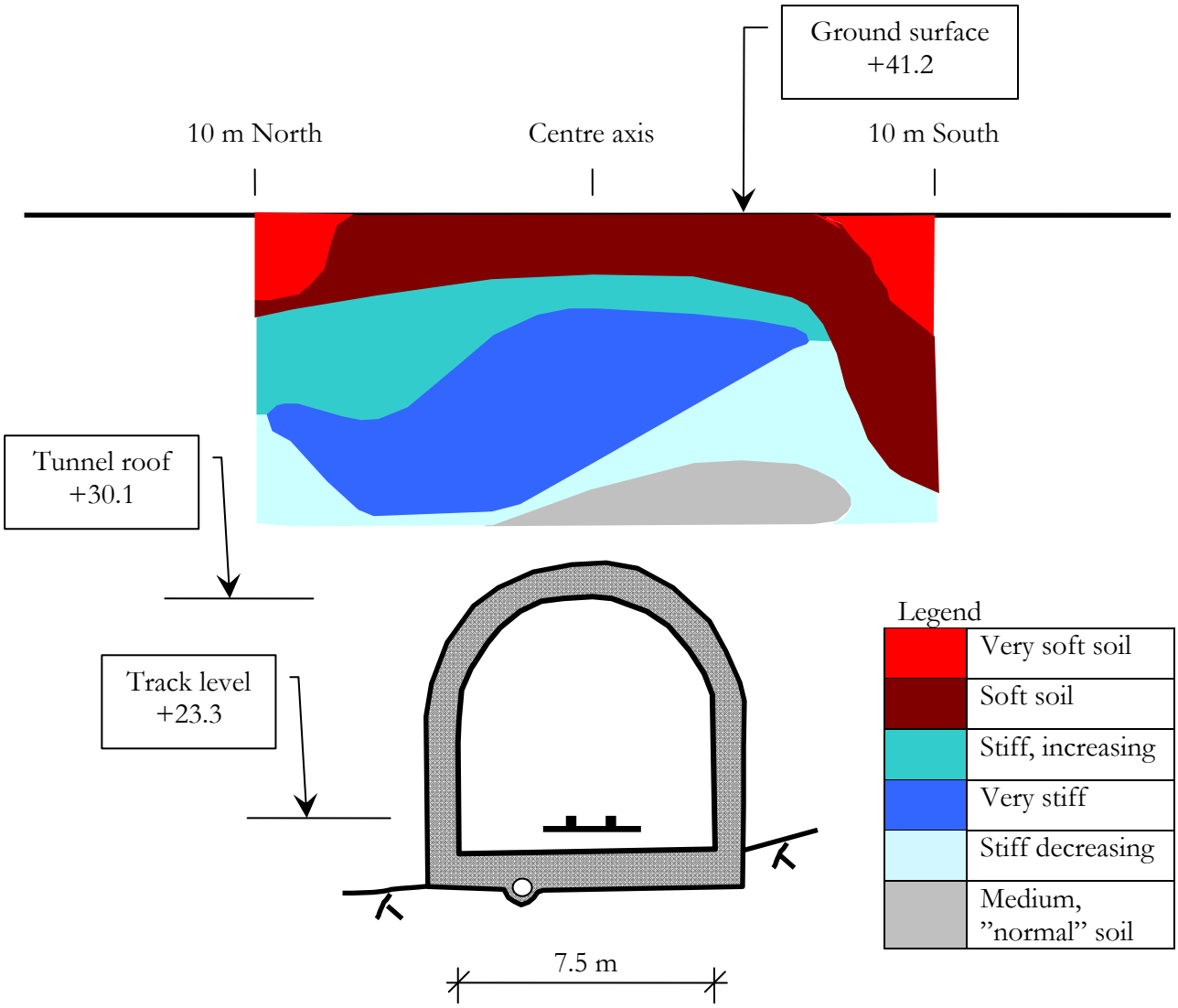

Figure 5.20 Diagram, showing interpretation from soil-rock penetration test at chainage 13+549. The test was performed in September 2007, three years after the cooling device was shut off. Any "stiff" areas are interpreted as frozen soil, otherwise thawed

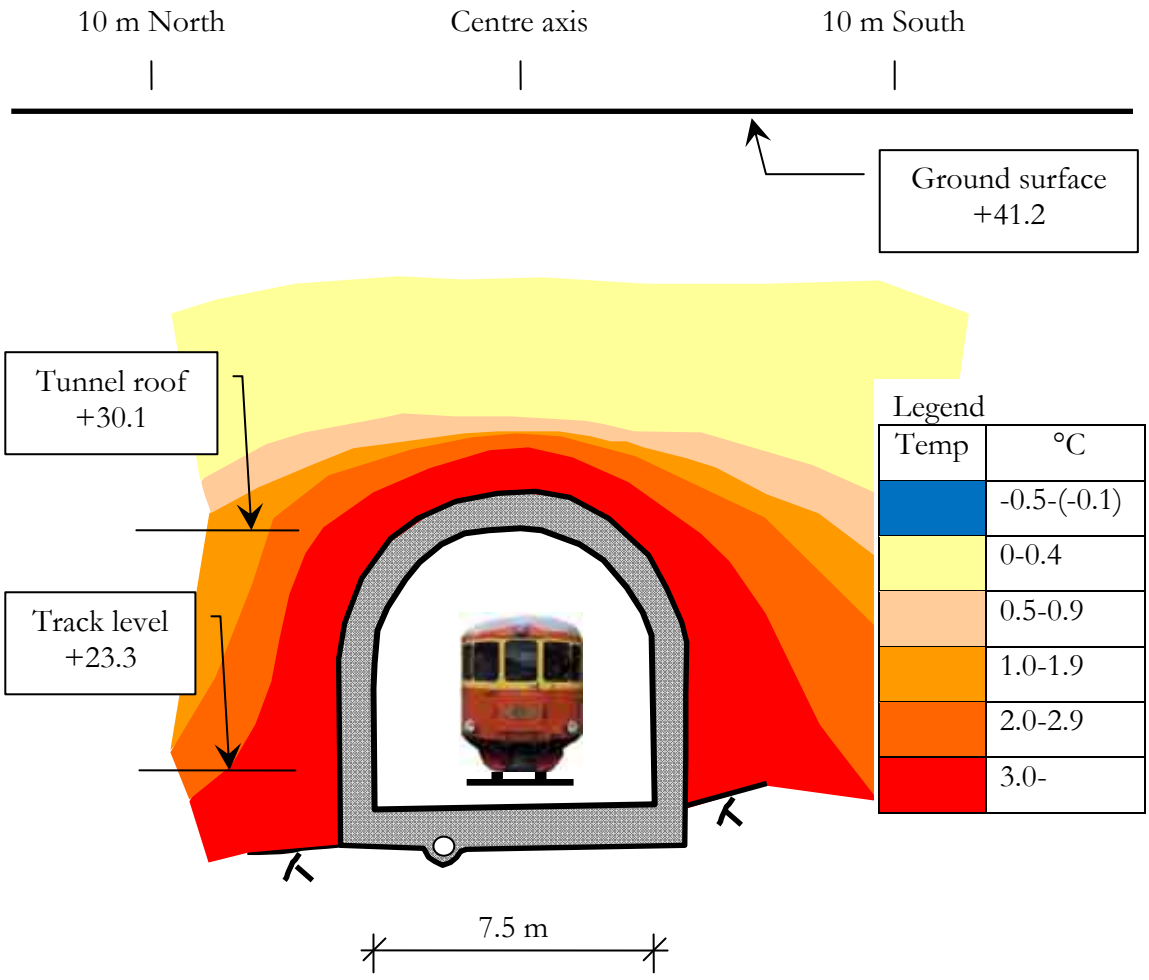

Figure 5.21 Measured temperatures in the temperature control tubes at the chainage 13+549. September 2007

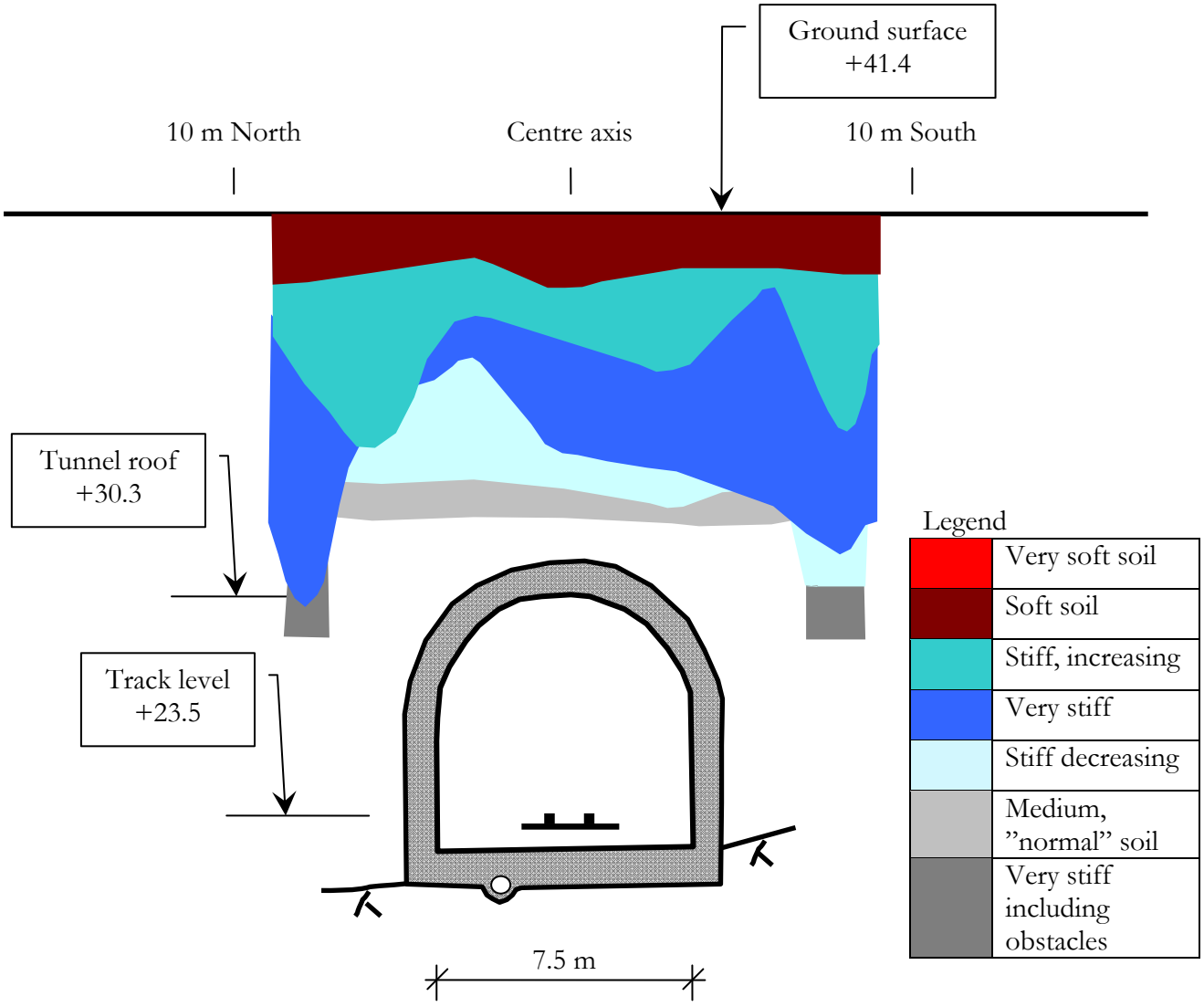

Figure 5.22 Diagram, showing interpretations from soil-rock penetration test at chainage 13+570. The test was performed in March 2008, three and a half years after the cooling device was shut off. Any "stiff" areas are interpreted as frozen soil, otherwise thawed, except the area "Very stiff including obstacles", this area is interpreted as a nearly thawed till

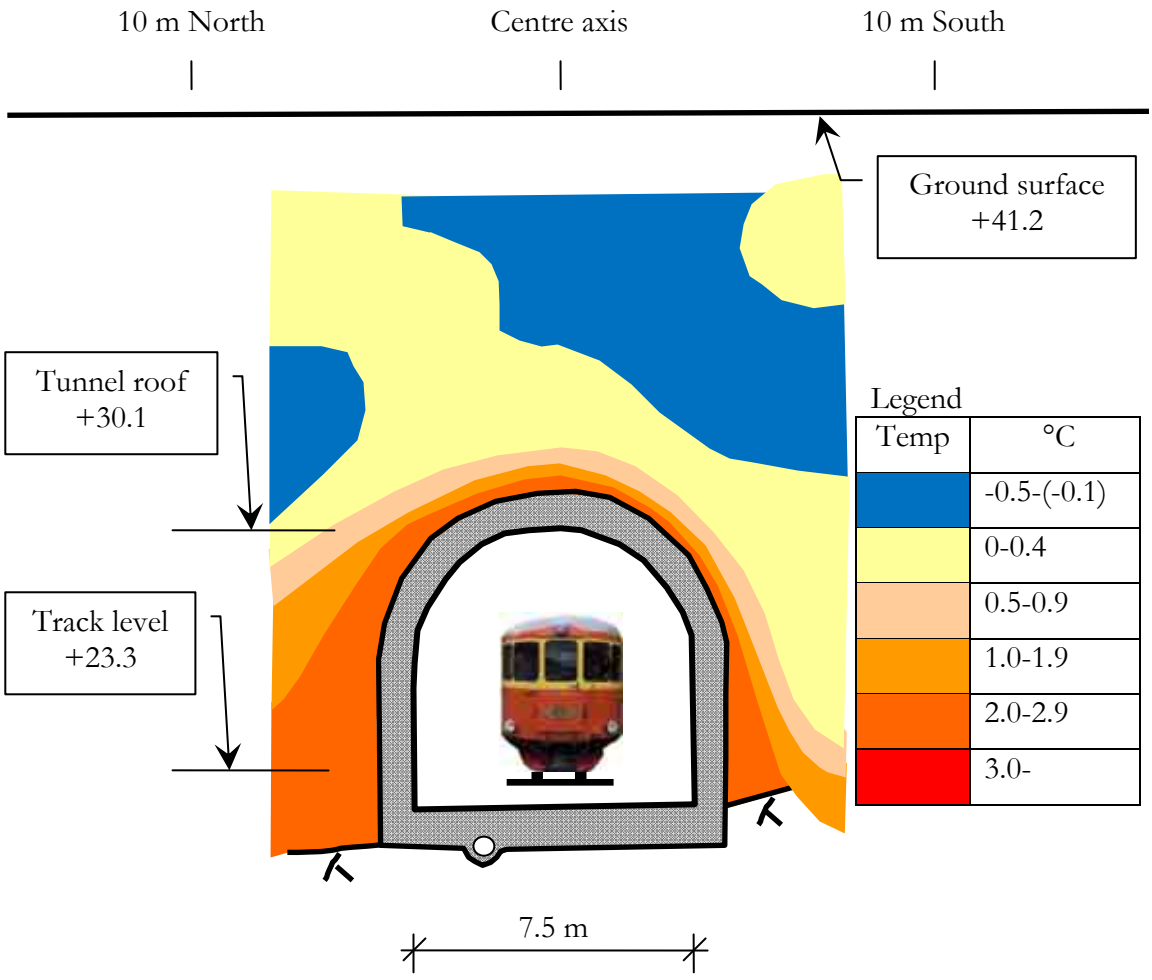

Figure 5.23 Measured temperatures in the temperature control pipes at the chainage 13+568.5. March 2008

5.7.2 Load build-up on the tunnel roof during the thawing

The registration of the development of surcharge on the tunnel roof started with manual readings December 3rd, 2003. The load on the pressure cell at chainage 13+549 suddenly after installation decreased to the lowest value February 20th, 2004, hence the pressure cell scale is set to 0 kPa at this reading.

After this reading the pressure increased quite fast until a peak of approximately 205 kPa was noted, January 24th, 2005. However, the load on the pressure cell after this reading fell to a pressure of approximately 150 kPa August 5th 2005, see Figure 5.24 and Figure 5.26.

Unlike the pressure cell at 13+549, the pressure cell at 13+568.5 has a quite smooth development from the first reading in December 2003 of approximately 60 kPa, until June 2008 of approximately 150 kPa, see Figure 5.25 and Figure 5.26.

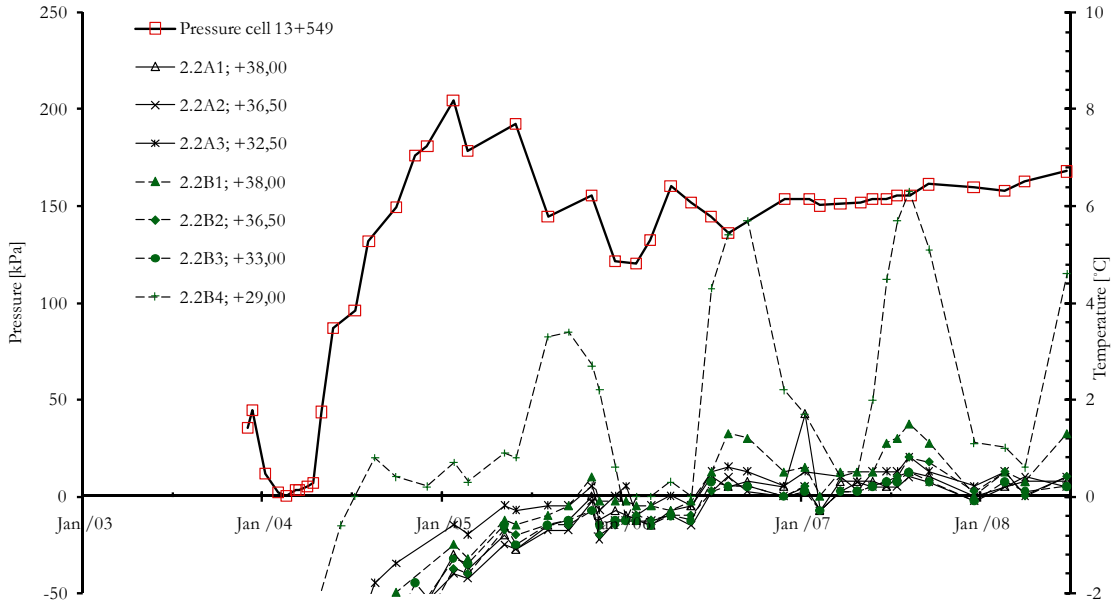

Figure 5.24 The Bothnia Line: Development of surcharge on the tunnel roof's lining for control chainage 13+549 is presented with close-by temperature sensors. The pressure cell is located at approximately +30.0. The temperature control pipe 2.2A and B are located about 2 m south of the tunnel centre in chainage 13+549

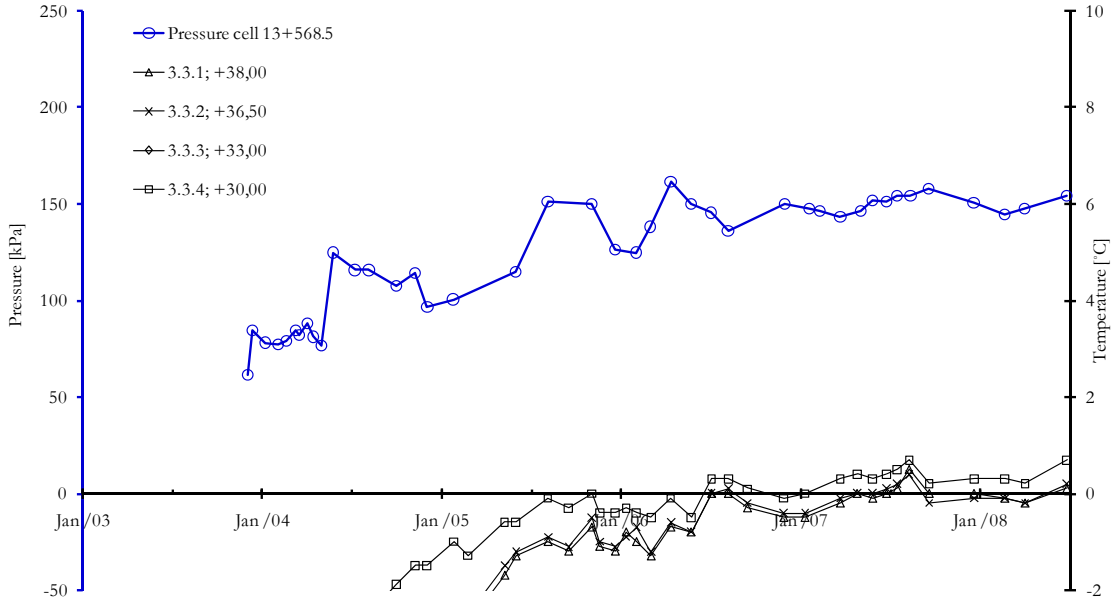

Figure 5.25 The Bothnia Line: Development of the surcharge on the tunnel roof's lining for control chainage 13+568.5 is presented with close-by located temperature sensors. The pressure cell is located at approximately +30.0. The temperature control pipe 3.3 is located in the middle of the tunnel centre in chainage 13+568.5

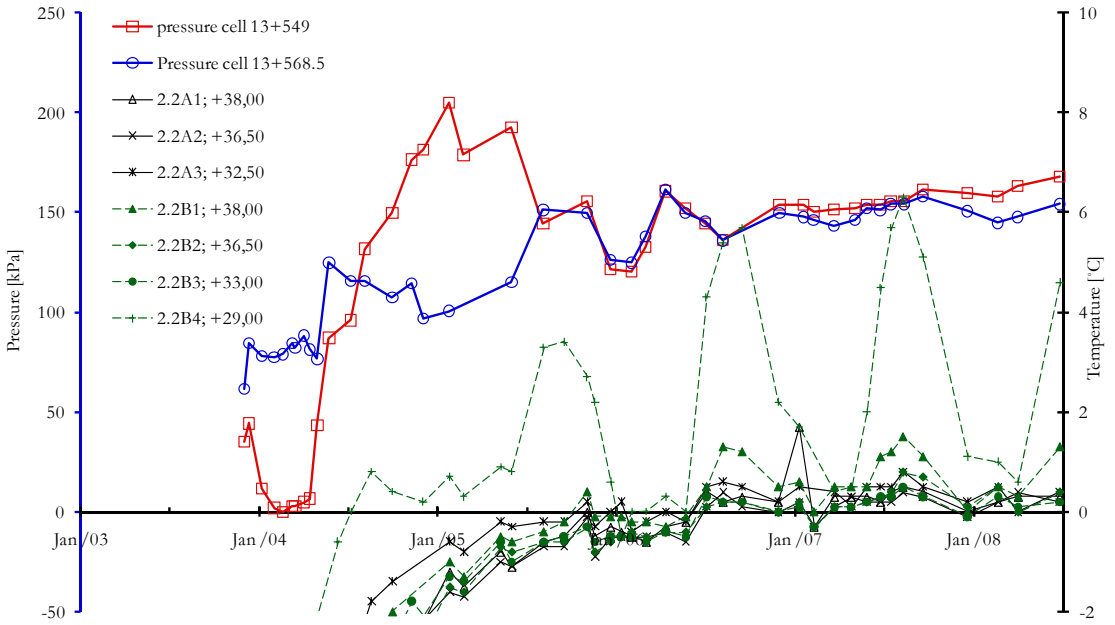

Figure 5.26 Pressure cells on the top of the tunnel lining at approximately +30 showing the pressure at chainage 13+549 and 13+568.5. Temperature sensors located in chainage 13+549, approx 2.3 m south of the tunnel centre line. The pressure cells are located approx +30.0. The temperature control pipe 2.2A and B are located approx 2 m south of the tunnel centre in chainage 13+549

5.7.3 Pore pressure build-up during the thawing

As can be seen in Figure 5.27, no real soil pore pressures have been registered in the piezometers, in neither chainage 13+549 nor 13+568.5. However, the soil temperature has increased to approximately +0,5 °C in this area in June 2008.

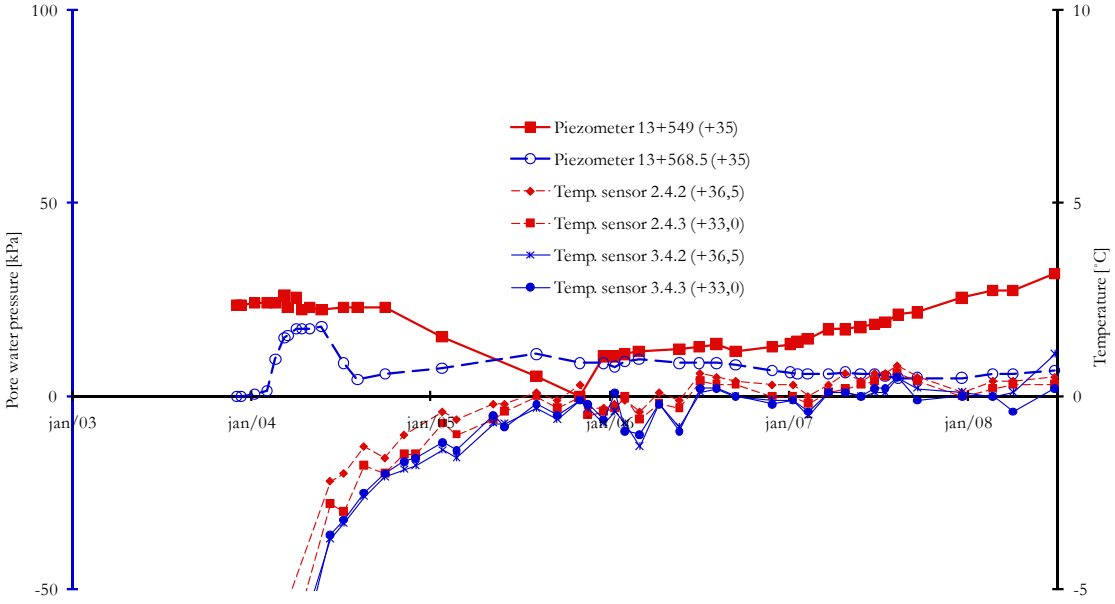

Figure 5.27 Pore water pressure measured in two of the installed control sections 13+549 and 13+568.5. The piezometers are installed 7 m under the ground surface at +35, approx 10 m south of the tunnel centre. The temperature is shown for temperature control pipe 2.4 (TG11, see catalogue of co-ordinates in the Appendix) close to the piezometer in chainage 13+549 and for temperature pipe 3.4 (TG10) close-by the piezometer in chainage 13+568.5

5.7.4 Vertical deformation

In chainage 13+549, the ground level gauges are located 2 m, 5 m and 10 m from the tunnel's centre axis in the frozen zone up until the manual sounding June 1st, 2005. From the time of the manual sounding November 2nd, 2005, all ground level gauges are located in unfrozen soil, see Figure 5.15. The ground level gauge 2 m south of the tunnel axis in chainage 13+549 was installed October 19th, 2004.

Figure 5.28, below shows that the central ground area in chainage 13+549 above the tunnel has a constant change in volume (i.e. a heave) during the period counted from the first registration on February 10th, 2004, to August 2005, for the sensors 10 m to 5 m north as well as 10 m, 5 m and 2 m south of the tunnel's centre axis. The deformation is comparable to a heaving of about 0.003 m per month during this period of time. The ground level gauge 2 m north of the tunnel's centre axis that was installed on October 19th, 2004 has a similar development after the installation as the comparable gauge south of the tunnel's centre axis. Figure 5.15 shows that the gauges are located in the frozen zone during this period of time.

Temperature measuring shows that the ground area since the measuring on July 4th, 2006, according to all sensors have thawed, see Figure 5.12 to Figure B.6. According to ground sounding, however, Figure 5.19 and JOBFEM calculations, Figure 5.5, the ground area was still frozen (August 7th, 2006), in principle the same geometry as the frozen zone had at the time when the cooling machine was turned off.

The temperature of the ground varied between -5 °C and -15 °C, at the time of the first measuring occasion, see Figure 5.12 and Figure B.6. At the measuring in January 2005, the temperature had increased a comparable 5 °C to 12 °C; see Figure 5.12 and Figure B.6.

The frozen area is limited to approximately 13 m north and south of the tunnel's centre axis. The soil where the gauges 20 m and 15 m north and 20 m south of the tunnel's centre axis have thus never experienced a freezing.

In sections 13+568.5, ground level gauges are located 2 m, 5 m and 10 m from the tunnel's centre axis in the frozen zone up until the sounding June 1st, 2006. From the time of the sounding on November 2nd, 2005, are all gauges but the one 10 m north of the tunnel axis, located in unfrozen ground, see Figure 5.17.

Figure 5.29 below, shows that the central ground area in chainage 13+568.5 above the tunnel has a constant volume change, heaving during the period counted from the first registration February 10th, 2004 to August 2005, for the sensors 2 m north as well as 5 m and 2 m south of the tunnel's centre axis. The deformation is comparable to a heaving of approximately 0.003 m per month during this period of time. The ground level gauge 5 m north of the tunnel's centre axis that was installed October 19th, 2004, has a similar development after the installation as the comparable gauge south of the tunnel's centre axis. Figure 5.17 shows that the gauges are located in the frozen zone during this period of time.

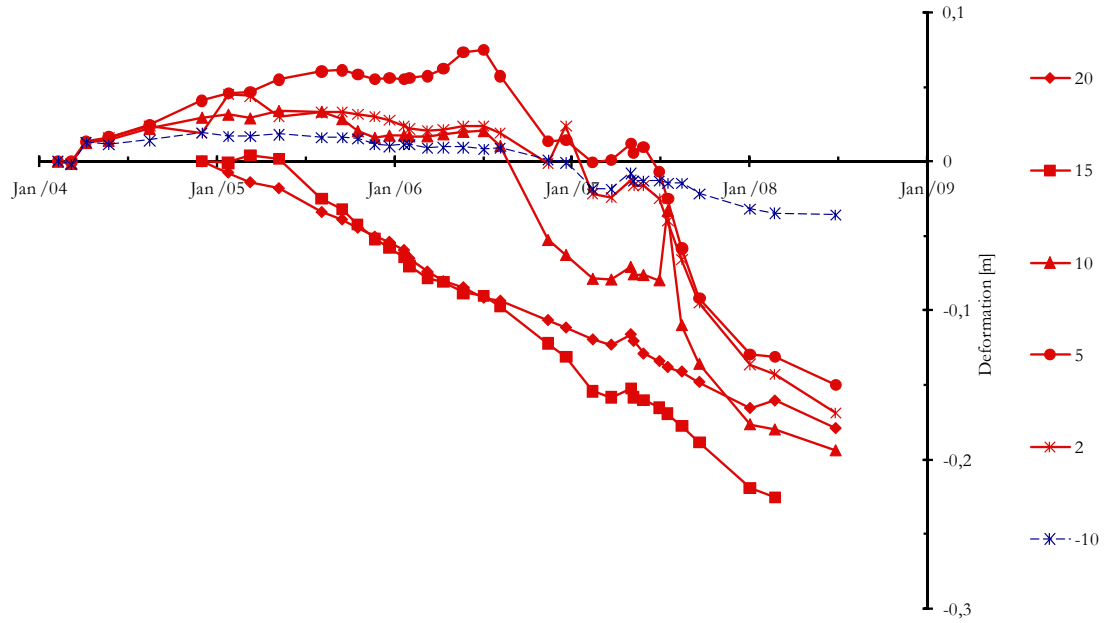

Figure 5.28 *Chainage 13+549. Soil deformation registered with ground level gauges. The ground level gauges are located about 2.5 m below the ground surface. Gauge "-10pt" is located 7 m under ground surface. The values are mean values of one gauge located north of the tunnel centre axis and one located south of the tunnel centre axis, at the same distance from the centre axis*

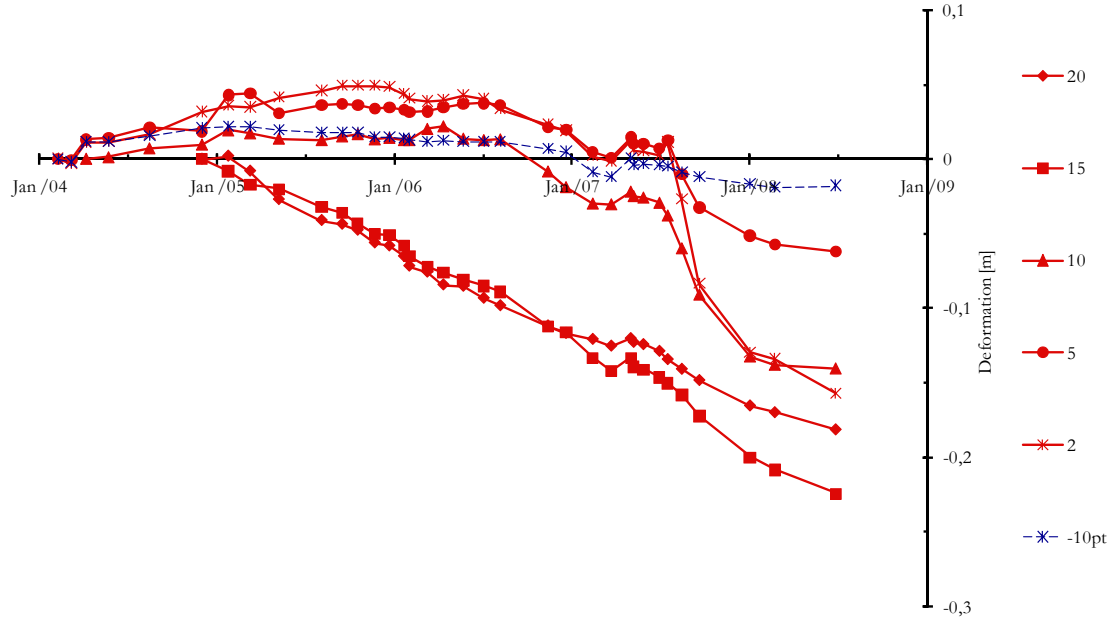

Figure 5.29 *Chainage 13+568.5. Soil deformation registered with ground level gauges. The ground level gauges are located about 2.5 m under ground surface. Gauge"-10pt"is located 7 m under the ground surface. The values are mean values of one gauge located north of the tunnel centre axis and one located south of the tunnel centre axis, at the same distance from the centre axis*

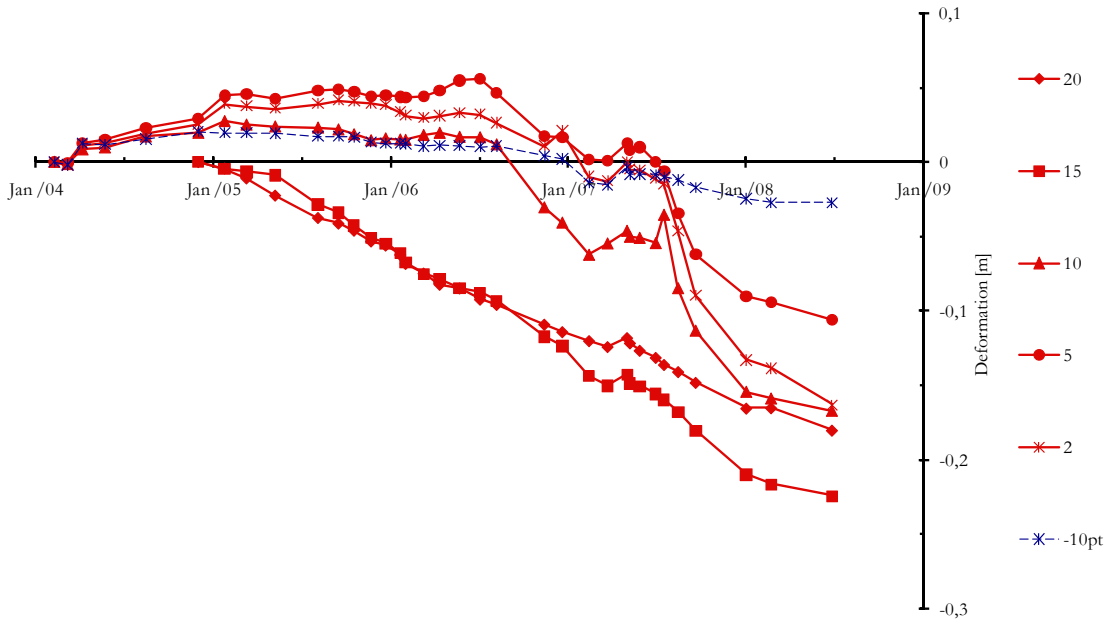

Figure 5.30 *Chainage 13+549 and 13+568.5. Soil deformation registered with ground level gauges. The ground level gauges are located about 2.5 m under ground surface. Gauge "-10pt" is located 7 m under the ground surface. The values are mean values of the gauges located north of the tunnel centre axis and the gauges located south of the tunnel centre axis, at the same distance from the centre axis in chainage 13+549 and 13+568.5*

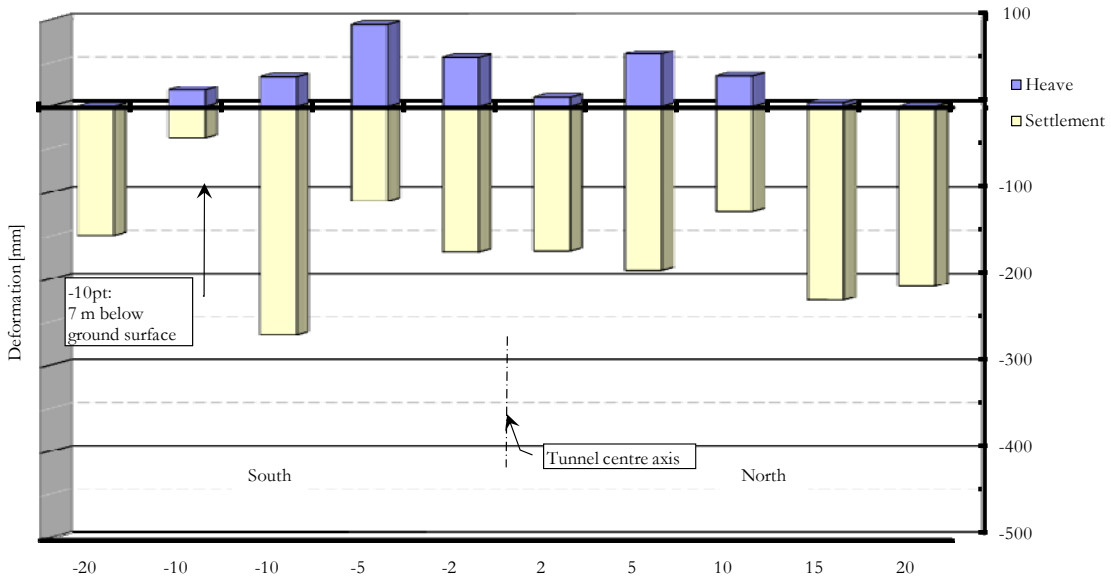

Figure 5.31 *Chainage 13+549. Deformations of the ground above the frozen tunnel, maximal heaving and setting up until June 2008. The deformations are measured via ground level gauges in the section at distances 20 m, 15 m, 10 m, 5 m and 2 m north and south of the tunnel centre. The ground gauges are located about 2.5 m under the ground surface. Gauge "-10pt" is located 7 m under ground surface. The distances are positive north of the tunnel*

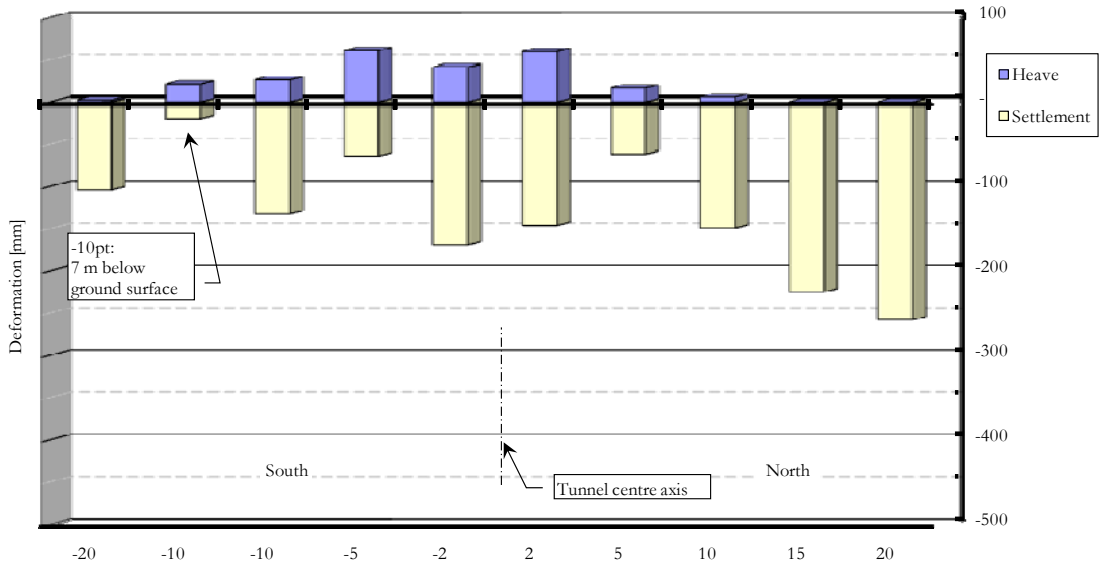

Figure 5.32 Chainage 13+568.5. Deformations of the ground above the frozen tunnel, maximal heaving and setting up until June 2008. The deformations are measured via ground level gauges in the section at distances 20 m, 15 m, 10 m, 5 m and 2 m north and south of the tunnel centre. The ground gauges are located about 2.5 m under the ground surface. Gauge "-10pt" is located 7 m under ground surface. The distances are positive north of the tunnel

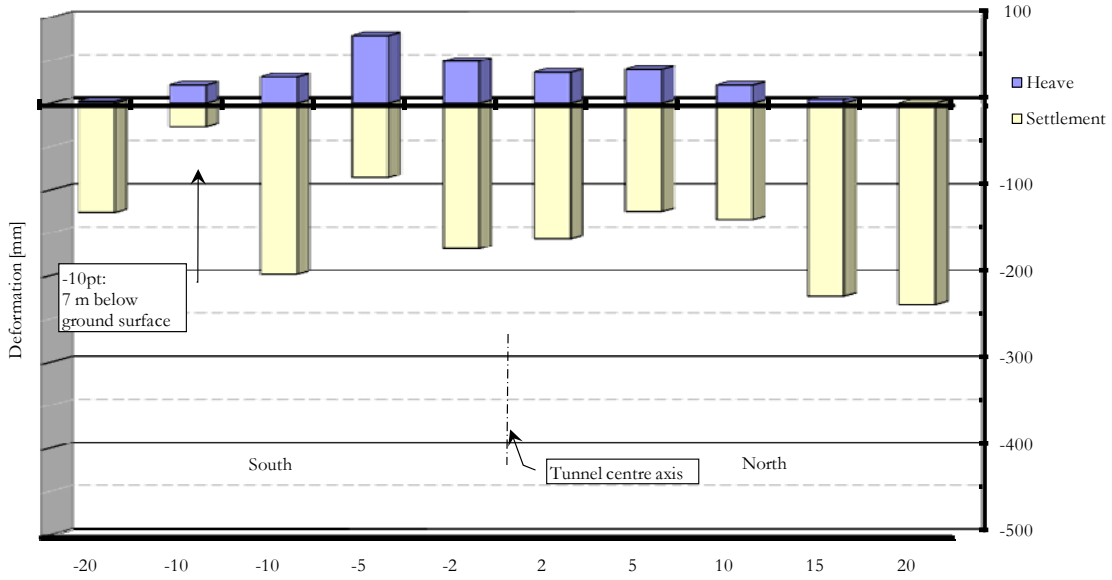

Figure 5.33 Chainage 13+549 and 13+568.5. Mean value of the deformations of the ground above the frozen tunnel, maximal heaving and setting up until June 2008. The deformations are measured via ground level gauges in the section at distances 20 m, 15 m, 10 m, 5 m and 2 m north and south of the tunnel centre. The ground gauges are located about 2.5 m under the ground surface. Gauge "-10pt" is located 7 m under ground surface. The distances are positive north of the tunnel

5.8 CONCLUSION

The field study mainly covers; 1.) Temperature distribution in the thawing soil. 2.) Load build-up on the tunnel roof during thawing. 3.) Pore pressure build-up during the thawing. 4.) Vertical deformation.

Conclusions from the field study at the Bothnia Line are:

- Overall, the artificial ground freezing method appears to be the most advantageous method when considering the economical aspects as well as it is also the most environmentally friendly method.
- The freeze pipe diameter exceeded Shuster's (1980) recommended maximum diameter of approximately 50 %. The freeze pipe spacing was approximately nine times the freeze pipe diameter, i.e. fulfilled Shuster's (1980) recommendations.
- An estimated ground water flow was prevented by the pump wells and infiltration wells system. Hence, no unfrozen windows were reported.
- The temporary method during the tunnel excavation in soft soil, i.e. the artificial ground freezing together with the shotcrete, was successful and permitted the underground project to proceed according to the time schedule.
- On the whole, during the thawing, the temperature prognosis follows the temperature progress in the ground.
- The load build-up on the tunnel roof seems to be a slow growing surcharge throughout the thawing (until the normal conditions take place, i.e. the normal temperature and the normal effective stress).
- The installed piezometers have not delivered any values from the 7 m depth, probably due to the ground still is frozen at the piezometer locations.
- The frozen ground close to the freezing point heaved surprisingly after six months of thawing, probably due to excess pore pressure in the thawed soil close to the tunnel. In the same fashion, the excess pore pressure is probably due to ground water supply from the nearly 100 m higher Stranneberget.
- The thawing started close to the tunnel and probably in the bedrock. While the thawing underneath the ground surface had not yet begun.
- The settlement due to the thawing started in the soil close to the frozen construction in soil that had never previously been frozen. This settlement can be due to that the thawed soil close to the tunnel had decreased in volume.

6 ANALYSES AND DISCUSSIONS

This chapter contains analyses of theories, field and laboratory studies as well as a discussion around these studies.

6.1 INTRODUCTION

The examined soil material discussed in this thesis has been collected solely in the area adjacent to the frozen construction next to the mountain Stranneberget along the Bothnia Line (Örnsköldsvik) where the field studies have also been performed.

6.2 ALTERATIONS OF SOIL PARAMETERS DUE TO THAWING OF VIRGIN BOTHNIA SOIL

The literature study lists vital parameters important to the thaw settlement and the changes it goes through due to thawing. The following parameters are studied in laboratory; water content, density, limit of consistencies, preconsolidation pressure, void ratio, undrained shear strength and sensitivity. The results from the undisturbed Bothnia soil are compared with the results from the thawed Bothnia soil at each level below ground surface, respectively. Furthermore, a matched pairs *t* test establishes if a change occurs in the soil parameter (Johnson, 2000). Table 6.1 shows the results; whether there is a change in the soil parameter, or not at 0.05 level of significance. The matched pairs *t* test assures that the samples are dependent, i.e. that the samples originate from the same location, are collected and tested under same conditions, etcetera. The collection of signed differences between the undisturbed and the thawed samples is treated as a random sample of size n from a population having the mean μ_D. The matched pairs *t* test interprets $\mu_D = 0$ as an indication that the means of the two responses are the same and $\mu_D > 0$ as an indication that the mean response of the first is higher than that of the second, and vice versa (Johnson, 2000).

6.2.1 Water content

As can be seen in Figure 4.11 the water content decreases due to the freezing and the subsequent thawing process. This finding is proved by a matched pairs *t* test at 0.05 level of significance ($t = 10.00 > t_{\alpha=0.05} = 1.89$) (Johnson, 2000), see Table 6.1. Moreover, the evidence is very strong since a computer calculation gives a *P* value $1.07 \cdot 10^{-5}$. Consequently, construction of a 90 % confidence interval for the mean of a paired difference of the water content change shows that we are 90 % confident that between 9.4 % and 13.7 % a reduced amount of soil water content takes place after the thawing, independently of the depth below ground surface. This behaviour is a fundamental driving

force for the genesis of the thaw settlement under self-weight for deeper lying soils. The behaviour concerning the decrease of the water content that emerges from this study is in accordance with that in Vähäaho (1988, 1991A).

Figure 4.10 shows the individual 90 % confidence intervals for the means of the soil water content as a function of depth below ground surface. Considering the graph, no correlation exists between the decrease in soil water content and the depth below ground surface. The figure also shows the general rule of thumb, the deeper in the ground the lower soil water content. Hence, this study shows that a large amount of soil water content in the upper strata does not in general result in a larger soil water decrease due to thawing. Despite the fact, the study shows that there is a strong relationship between the original soil water content and the decrease of soil water content due to the thawing. A best-fit curve with a correlation coefficient of 0.9 for the strata from 3 m to 8 m shows the correlation between the decreased water content (w-w_{th}) and the original water content (w) to be approximately $0.15w + 1.51$. In contrast, the results show no correlation between the degrees of the original water content and the magnitude of settlement (see Appendix, laboratory tests, Figure A.2, page X), this conclusion differs from that in Vähäaho (1988, 1991A).

6.2.2 Soil bulk density

As can be seen in Figure 4.9 and Table 6.1 the soil bulk density becomes denser for thawed soil, compared to undisturbed soil. This phenomenon is a result of the pore water migration and the subsequent thaw settlement. The behaviour concerning soil density change that emerges from this part of the study is related to that in Crory (1973), Johnson et al (1984), Johnston (1981), Ladanyi (1973), Speer et al (1973) and Watson et al (1973), despite the fact that the magnitude differs.

6.2.3 Void ratio

A decreased water content and an increased density as a result of thawing lead to a decreased void ratio. Hence, the void ratio is the relation of volume of voids and the volume of solids and is demonstrated in Table 6.1 and Figure 4.16. This behaviour concerning the void ratio change that emerges from this part of the study is similar to that in Tsytovich (1975) and Andersland and Ladanyi (2004), while the magnitude, however, differs.

This study shows that thawed soil from the Bothnia Line becomes denser and hence obtains a decreased void ratio. Generally, in geotechnical aspects, these behaviours also obtain a less permeable soil, i.e. a soil with less hydraulic conductivity. In contrast, the Bothnia Line thawed soil becomes more permeable; this statement is proved by Table 6.1 and the results in Table A.25 and Table A.26. In the same fashion, Chamberlain and Gow (1978) argues that thawed clayey soil causes a large increase in vertical permeability. Whereas Chamberlain and Gow reported that the increase was greatest for the soil with the largest plasticity index and that the increase in general was smaller for soil at the highest applied stress levels. In contrast to Chamberlain and Gow's study, this study has no such correlation (see Appendix, laboratory tests, Figure A.3, page XIV (and Figure A.2, page X)).

6.2.4 Preconsolidation pressure and overconsolidation ratio

The preconsolidation pressure and the overconsolidation ratio increase for thawed soil, compared to undisturbed soil, see Table 6.1, Figure 4.18 and Figure A.1 (Appendix, laboratory tests, page VII). The resulted preconsolidation pressure and overconsolidation

ratio occur at all investigated depths. This behaviour is a result of the migrated pore water and the subsequent thaw settlement.

Table 6.1 Matched pairs t test for soil parameters. The use of 0.05 level of significance to test whether alterations of soil parameter due to thawing take place. The undisturbed Bothnia soil parameters for each depth are compared to the thawed Bothnia soil parameter at corresponding depth. ($t_{\alpha=0.05}$ and P value from Johnson (2000))

Soil parameter	t	$t_{\alpha=0.05}$ (From table)	Estimation	P value (Calculated, single sided)	Decision: There is a difference
Bulk density	-9.26	1.89	$t = \|-9.3\| > t_{\alpha=0.05}$	$1.77 \cdot 10^{-5}$	**Yes**
Liquid limit	2.57	1.89	$t = \|2.6\| > t_{\alpha=0.05}$	0.018	**Yes**
Overconsolidation ratio	-7.13	1.89	$t = \|-7.1\| > t_{\alpha=0.05}$	$9.4 \cdot 10^{-5}$	**Yes**
Permeability	-3.00	1.89	$t = \|-3.0\| > t_{\alpha=0.05}$	0.010	**Yes**
Plastic limit	0.02	1.89	$t = \|0.02\| < t_{\alpha=0.05}$	0.494	**No**
Plasticity index	3.79	1.89	$t = \|3.8\| > t_{\alpha=0.05}$	0.003	**Yes**
Preconsolidation pressure	-2.77	1.89	$t = \|-2.8\| > t_{\alpha=0.05}$	0.014	**Yes**
Sensitivity	0.98	1,89	$t = \|1.0\| < t_{\alpha=0.05}$	0,180	**No**
Undrained shear strength	-3.67	1.89	$t = \|-3.7\| > t_{\alpha=0.05}$	0.004	**Yes**
Void ratio	8.01	1.89	$t = \|8.0\| > t_{\alpha=0.05}$	$4.51 \cdot 10^{-5}$	**Yes**
Water content (mean value 2004 and 2006)	10.00	1.89	$t = \|10.0\| > t_{\alpha=0.05}$	$1.07 \cdot 10^{-5}$	**Yes**
Water content (2006)	10.38	1.89	$t = \|10.4\| > t_{\alpha=0.05}$	$8.38 \cdot 10^{-6}$	**Yes**
Water content (2004)	6.98	1.89	$t = \|7.0\| > t_{\alpha=0.05}$	$1.07 \cdot 10^{-4}$	**Yes**

6.2.5 Limit of consistencies

Liquid limit decreases due to thawing, see Table 6.1 and Figure 4.12. In fact, this tendency shows a change in the soil structure. As a result, the undisturbed soil has a greater tendency to attract water to the soil particle surfaces. We should then expect that the water content at which the undisturbed and thawed soils begin to behave as a liquid would be greater for undisturbed soil than for thawed soil (Lambe & Whitman, 1969). These circumstances are confirmed by the investigation of the grain size distribution. As can be seen in Table 4.4 and Table 4.5 the amount of clay and fine silt particles decreases after a freeze-thawing cycle, hence there is an increase of the coarser particles. The results illustrate a coarser soil structure for thawed soil, i.e. the fine grain particles create aggregates. This conclusion is similar to that in Chamberlain and Gow (1978).

This phenomenon, the creation of conglomerates from clay particles, forms new aggregates with particle size equalling medium silt and coarse silt. However, the obtained thawed soil with a new coarse soil structure attains a more permeable soil, probably due to the larger distance between the soil particles (i.e. between soil aggregates), not because of cracks

similar to that in Chamberlain and Gow (1978). (Chamberlain and Gow obtained an average crack thickness of 0.07 – 0.15 mm). The Bothnia soil samples from the freeze-thaw tests did not obtain any visible cracks. On the other hand, freeze-thaw tests of Bothnia soil samples without any surcharge or with a light weight surcharge due to the in situ pressure, showed visible polygonal shrinkage cracks.

This study shows no change of plastic limit in a matched pairs *t* test for undisturbed soil and thawed soil, see Table 6.1 and Figure 4.13. Whereas, the plasticity index presented in Table 6.1 and Figure 4.14 shows a decrease for thawed soil.

6.2.6 Undrained shear strength and sensitivity

As can be seen in Table 6.1 and Figure 4.17 undrained shear strength increases for thawed soil at all depths. However, no change occurs for sensitivity for thawed soils, see Table 6.1, Table A.33 and Table A.36.

6.3 TEMPERATURE DEVELOPMENT AT THE BOTHNIA LINE'S FROZEN CONSTRUCTION

The temperature development measured in the temperature sensors and the frozen zone's geodetic level measured via sounding in the soil from the ground level, follow in principle prognosticated temperature development in the finite element program, JOBFEM. One anomaly in the temperature development can, nevertheless, be established parallel with-, and in the middle of the freeze area, where the thawing has caused an unfrozen "ditch" in the frozen soil.

An important note in regards to the field conditions is the fact that the freeze pipes and the temperature measuring pipes are still installed in the ground when this is being written. A comparison of measured temperatures and the actual frozen zone shows the measured temperatures to be above the freezing point, despite the magnitude of the frozen zone (see chapter 4 and 5). Manual sounding has showed that the soil has thawed next to the freeze pipes and the temperature measuring pipes. The freeze pipes as well as the temperature pipes contain water that froze during the course of the freezing. This ice/water has thawed through temperature conduction and via forced convection conducted (down) the heat and so contributed to the thawing of the surrounding soil. The frozen soil will thus be similar to a "Swiss Cheese" full of thawed holes. The temperature measuring does therefore not show the correct temperature of the soil. Hence, the thawing process takes place faster than the JOBFEM-analyses due to the freeze pipes' heat conduction.

6.4 GROUND HEAVING AT THE BOTHNIA LINE'S FROZEN CONSTRUCTION

During the freezing phase when creating a stabilized and hydraulically sealed construction at Stranneberget at the Bothnia Line, it can be expected that heaving will occur in the ground as well as thaw settlement can occur in a comparable way during the subsequent thawing phase. The vertical deformation has mainly been measured at a frost-free level at a depth of about 2.5 m under the ground surface, as well as via two ground level gauges installed approximately 7.5 m under the ground surface in the still frozen mass (July 2008).

The frozen construction went through a surprising heaving during its initial stage when the temperature had balanced out to a level of about -1 °C in the frozen construction. The largest heaving occurred in chainage 13+549 (in the measuring section closest to the Stranneberget) in the gauge 5 m south of the tunnel centre. The heaving was largest in May

2006 and was registered to be 0.095 m above the level when the reading of the gauges started (February 2004).

During the period from July 2004 until January 2005, the registered load on the pressure cell in section 13+549 increased from about 96 kPa to 205 kPa and then decreased to about 135 kPa in August 2006, see Figure 5.24. Because of that the load on the pressure cell consists of partly thawed soil (10 kPa, see prognosis) and partly a hydrostatic water pressure (205 – 10 kPa), the hydrostatic water pressure will act against the surrounding frozen soil-rock with an uplift force (and against the tunnel's lining). The uplift force, i.e. the hydrostatic water pressure, can originate due to that the permeability in the frozen zone and its edge zone are high enough. The weight of the frozen soil above the tunnel roof is about (11 m × 1.60 kN m^{-3} =) 175 kPa. During the period July 2004 to August 2006, the hydrostatic water pressure is larger than the weight of the frozen soil, thus exerting a static load on the frozen vault.

It is important to note that the measuring of the ground surface's heaving started in February 2004, six months after the shut off of the cooling machine. As can be seen by the measuring, the heaving is in large linear and can so have started earlier and in such a case actually have contributed to a larger heaving than the one presently registered.

The load on the soil (hydrostatic water pressure on the frozen zone's underside) can be divided into three periods of time, see Figure 5.26:

i. July – September 2004 (three months) load of hydrostatic water pressure on average (135 – 100 kPa) 35 kPa, mean temperature in the soil in average number during the period about -3 °C.
ii. October 2004 – May 2005 (eight months), load of hydrostatic water pressure on average (180 – 100) 100 kPa, mean temperature in the soil in average number during the period about -2 °C.
iii. June 2005 – August 2006 (fifteen months) load of hydrostatic water pressure on average (150 – 100 kPa) 50 kPa, mean temperature in the soil in average number during the period about -1 °C.

The expansion of the frozen area can to a certain degree be explained by the thermal expansion of about 0.005 m occurring as the temperature increases from about -10 °C to about -1 °C. One explanation for the heaving can be that the ground water creats infiltration water from the relatively higher Stranneberget produces a hydrostatic ground water pressure between the sealed tunnel pipe and the relatively sealed frozen construction. The hydrostatic ground water pressure creates in such a way an "upward directed" load on the frozen construction, with consideration of the relatively high temperature (approximately -1 °C) the frozen soil mass had a low bearing capacity (that is the frozen soil mass had a relatively high likeliness to creep). When the frozen construction subsequently begun to thaw in the edge zone, the hydrostatic pressure had been equalized in relation to the zone outside the earlier frozen construction and the thaw settling had been initiated, largest in number in the edge zone of the frozen construction.

The mass is, according to JOBFEM- calculations and observations of the temperature in the frozen zone, frozen together with the rock base on both sides of the tunnel lining. An approximately 1 m thawed zone of soil and rock surrounds the tunnel lining. One argument that possibly stresses this is that the load appears to be dependent on the season.

Thus, the frozen construction that has been carrying its own weight during the excavation and been deformed downward vertically is, during the above described conditions, relived from its load. As the upward directed pressure between the tunnel lining and the frozen

construction is larger than its own weight, this result is a time dependant up-ward directed deformation, a heaving.

6.5 NATURALLY FROZEN GROUND AND ARTIFICIALLY FROZEN GROUND AND THE SUBSEQUENT THAWING

The majority of the presented thaw settlement equations in the literature study are intended for permafrozen soil. In other words, the soil specimens from the permafrozen soil have undergone the soil water phase change and developed the frost heave in situ (if frost heave occur), and also probably during years, decades or centuries developed segregated ice lenses in situ. The literature chapter concerning the permafrozen soils shows different developed ground qualities, for example, ice wedges, pingos, palsa, etcetera. Commonly for these ground qualities, which forms the shape of the terrain, is the involved water. In fact, due to the involved soil (mineral particles, gas inclusions, and interlayered ice crystals), temperature development, the water supply and the underlying bedrock, various shapes will develop in the terrain. This ongoing process shows that the permafrozen soil is not a "dead material"; hence, the water migration forms the continuously changing terrain in the landscapes.

One of the conspicuous parameters of the thaw settlement is the amount of ice inclusions in the frozen soils. The literature chapter shows that the naturally frozen soils, the permafrozen soils, have a relatively high temperature and therefore a higher amount of unfrozen water. These phenomena contribute to the water migration and consequently the build up of ice lenses.

In addition, a vital part of the thaw settlement is the ice lens orientation. Normally, a horizontal ice lens orientation results in an increased thaw settlement compared to that of a pure vertical ice lens orientation. However, ice lenses normally form parallel to the freeze front, i.e. in naturally frozen soils practically horizontal.

In contrast to naturally frozen ground, artificial ground freezing quickly creates a frozen construction, (generally) made out of virgin soils. However, a construction made via artificial ground freezing only lasts for a short period of time and thaws after having served its purpose. Moreover, artificial ground freezing normally presupposes installed freeze pipes in the ground and the freeze pipe orientation will vary with the project's characteristics. The freeze pipe pattern induces the cooling effect in the ground. However, in the soil various phenomena will occur simultaneously during freezing and thawing, due to where in the pattern the soil particles are located, i.e. during the freezing, soil close to the freeze pipe exist in a low temperature condition with a relatively large temperature gradient, compared to soil halfway between the freeze pipes.

Figure 6.1 shows a schematic artificial ground freezing consisting of three freeze pipes installed vertically in the soil. The figure illustrates five stages in the soil freezing process, depicted by the five equilateral triangles. In the first stage (i), the freeze process has just started and in the final stage (v), the frost front has merged and all the soil is frozen. However, during the freezing, water phase change takes place as well as water migration from the unfrozen soil towards the frost front. Simultaneously, various phenomena occur in each stage, inter alia, soil's expansion; in the first stage during the initial freeze phase lateral expansion occur, in the second and third stage, the intermediate phase, both lateral and vertical expansion take place, and finally in the fourth and fifth stage, i.e. the final freezing phase only vertical expansion occur. Nevertheless, during the initial freeze phase, the frost front conditions allow the soil to expand in the most favourable direction i.e. perpendicular to the frost front. In the intermediate freezing phase, the frost fronts have

approached each other and the gaps between the frost fronts decrease. This situation increases the horizontal resistance due to the former compression of the intervening soil and encourages the vertical expansion. Finally, in the final freeze phase, the freezing columns have merged and lateral expansion is prevented, as a result, only vertical expansion is allowed.

Whereas, naturally frozen soils generally have horizontal frost fronts (at least parallel to the ground surface) and in general a moderate temperature, artificially frozen ground has a complex frost front situation and almost always a relatively low temperature.

The laboratory tests in this thesis are performed with undisturbed soil. The soil specimens originate from the area close to the frozen construction at the Bothnia Line. However, according to the explanation above and Figure 6.1, various stress conditions are expected during freezing and thawing depending on where the specimen is located. In other words, if the soil specimen is located close to the freeze pipe, the specimen obtains a stress strain relation dissimilar to a specimen located halfway between the freeze pipes.

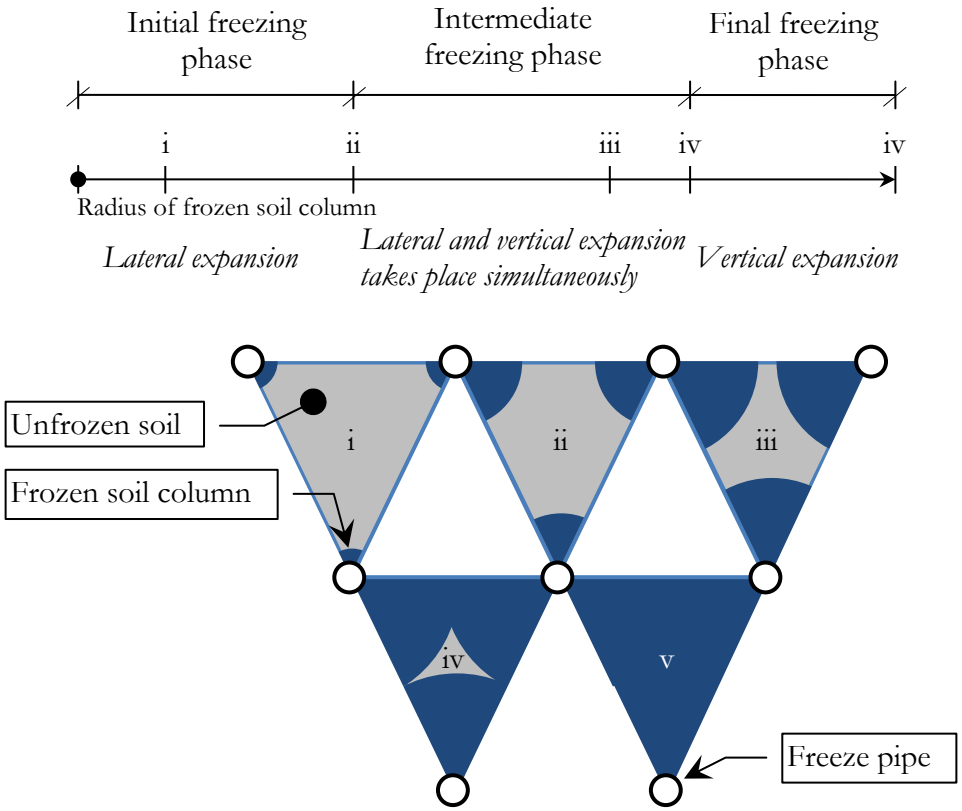

Figure 6.1 *The artificial ground freezing process divided into five schematic stages (i-v) and three schematic phases at vertical freeze pipe orientation. In the upper figure, the stages and phases at the corresponding radius of the frozen soil column. In the lower figure, an illustration of the freezing process at each of the five phases respectively. In the initial freezing phase only lateral expansion occurs, in the intermediate freezing phase, lateral and vertical expansion take place simultaneously and in the final phase, only vertical expansion takes place*

6.6 THAW SETTLEMENT

When the frozen fine-grained soil thaws, the bound water turns to liquid form and creates during the thawing stage a viscous mass consisting of soil and water. The initial increase of the pore water pressure remains depending on, among other things, the permeability and the surrounding soil's draining capacity. During the stage when the pore pressure increase, a decrease in the effective stress occurs in a comparable way and therefore also a lower bearing capacity of the soil than the one existing if the soil would have not been affected by freezing. It is thus important to be able to follow the pore pressure development in the soil so that one, together with the temperature in the surrounding soil and thaw settlement, measured with settlement gauges, is able to follow the different controlling parameters' effect on the thaw consolidation.

Continuous measuring of the ground's temperature is important for the following thawing process of the frozen soil and the subsequent thaw settlement. The soil's temperature, among other things, controls the consolidation ratio during the consolidation process, as the pore water's viscosity is strongly dependent of the temperature. The temperature profile in the soil is thus important for the following of the development of the thaw consolidation.

The course of thawing so begins at an early stage around the steel pipes and the risk for considerable adhesive forces on the freeze pipes are therefore minimal compared to if the thawing would have been initiated by the surrounding. Hence, relatively short draining paths arise in the thawing soil and the soil will consolidate relatively momentary.

The detailed laboratory analysis of the Bothnia soil shows an empirical relationship between the thaw settlement and determining soil parameters. Although, in the soil strata at 9 m and 10 m below ground surface an anomaly exists. These strata are bounded by the lower stratum of clayey, sandy, silty till and influenced by silty interlayers. The silty layers in the specimens disturb the freeze-thaw tests in the oedometers, since the silty material has extraordinary frost susceptibly properties. Consequently, the relatively small specimen cannot be representative for a larger amount of ground and therefore creates a scale error. The depths of 9 m and 10 m are thus flagged as outliers and as a result these observations are dropped. Despite the fact, a best-fit curve with a correlation coefficient of 0.8 for the strata from 3 m to 8 m shows the correlation between the thaw settlement and the ratio of the water content and plastic limit (see Figure 6.3)

$$\varepsilon = \frac{\Delta H}{H} = 2.7\frac{w}{w_{\mathrm{p}}} + 3.8 \tag{6.1}$$

where ε = strain, w = undisturbed soil water content and w_{p} = undisturbed soil plastic limit.

In the same manner the total thaw settlement obtained with consideration of the frost heave in the oedometer tests (see Figure 6.4)

$$\varepsilon = \frac{\Delta H}{H} = 7.0\ln\left(\frac{w}{w_{\mathrm{p}}}\right) + 7.8 \tag{6.2}$$

where ε = strain, w = undisturbed soil water content and w_{p} = undisturbed soil plastic limit.

The comparisons of the freeze thaw deformations in the oedometer and the results of Eq. (6.1) and Eq. (6.2) is located in Appendix.

The detailed laboratory analysis also shows the empirical relationship between the frost heave and the ratio of water content and plastic limit, see Figure 6.2. However, the predicted frost heave is given by

$$\varepsilon = \frac{\Delta H}{H} = 1.8 \ln\left(\frac{w}{w_p}\right) + 2.7 \tag{6.3}$$

where ε = strain, w = undisturbed soil water content and w_p = undisturbed soil plastic limit.

The thaw settlement is predicted according to the soil characterization from the Bothnia Line and the thaw settlement equations above. In Figure 6.5 the predicted vertical settlement for each stratum from every thaw settling equation above are showed. As can be seen in Figure 6.6, regarding the Bothnia Line soil behaviour, the total accumulated thaw settlement for each stratum from every thaw settling equation above is calculated. As can be seen in Figure 6.5 and Figure 6.6, a variation in the predicted settlement arises, both in the total predicted ground surface settlement and in each predicted soil stratum.

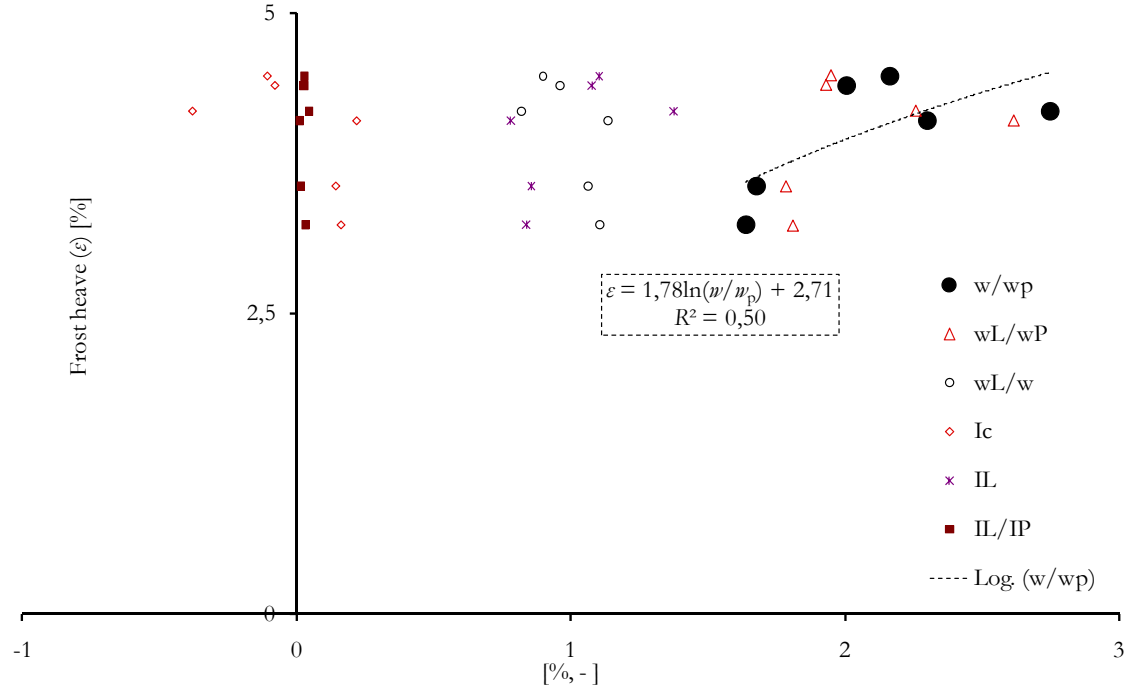

Figure 6.2 Frost heaving as a function of soil parameters. Soil sample series of August 7th, 2006, consisting of depths from 3 m to 8 m below ground surface

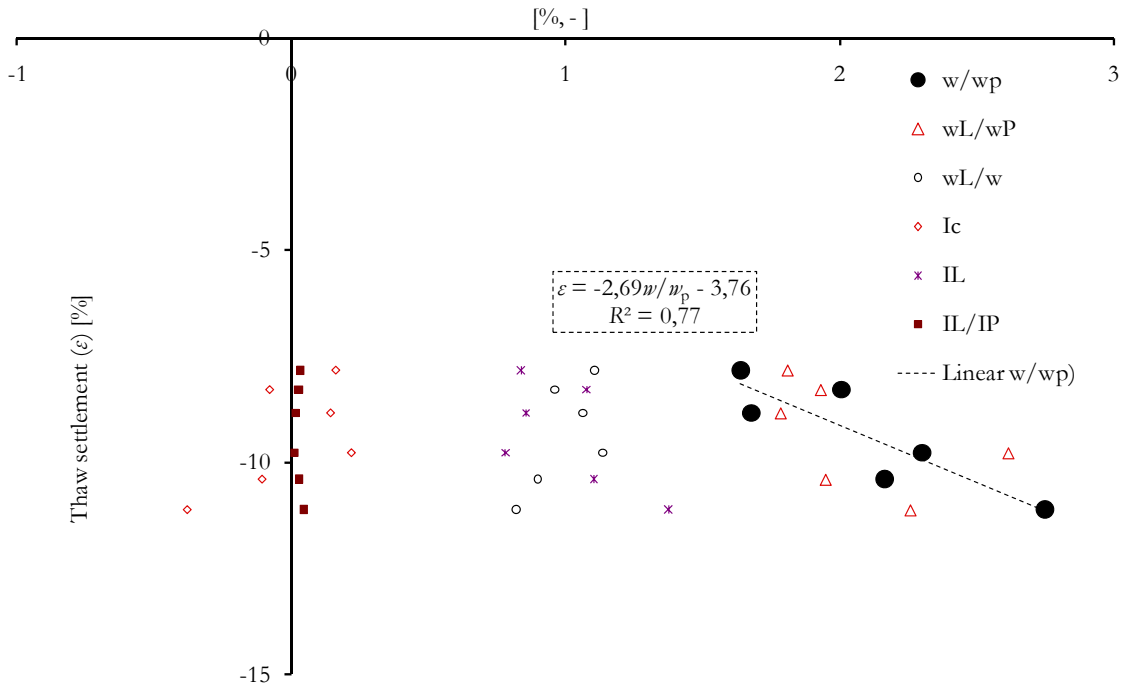

Figure 6.3 *Thaw strain as a function of soil parameters i.e. the settlement magnitude determined from the level of consolidated, undisturbed soil. Soil sample series of August 7th, 2006, consisting of depths from 3 m to 8 m below ground surface*

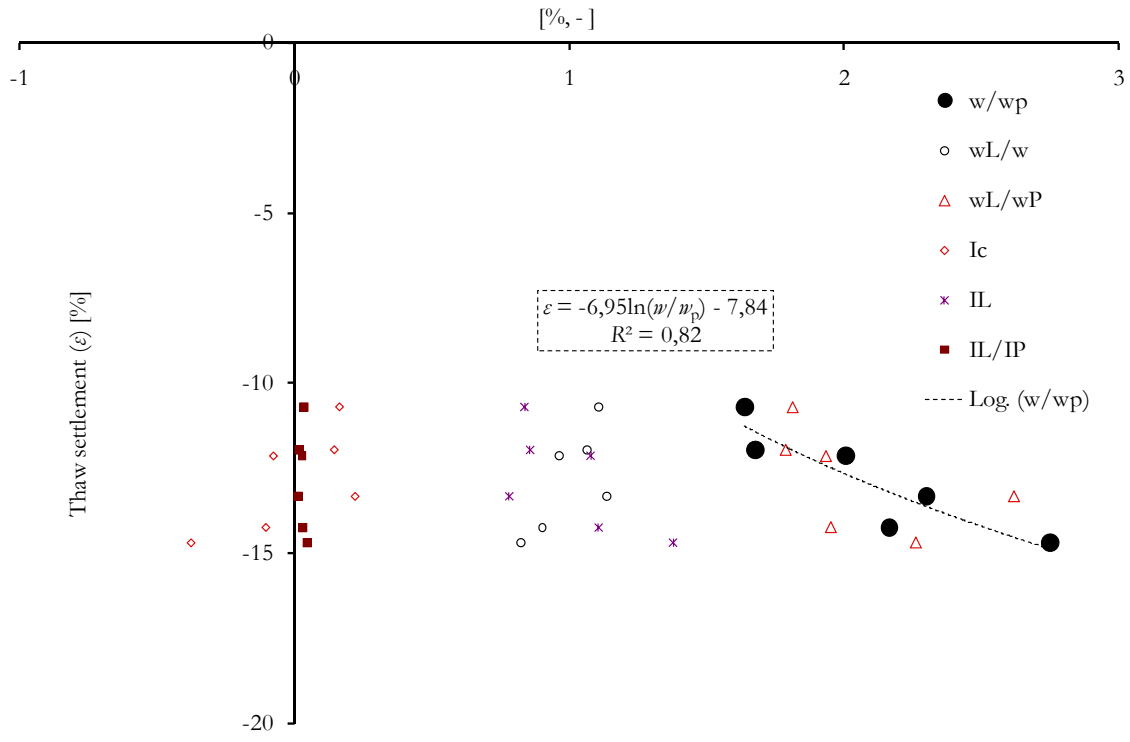

Figure 6.4 *Total thaw settlement as a function of soil parameters i.e. the settlement magnitude determined from the level of frost heave (heave + settlement). Soil sample series of August 7th, 2006, consisting of depths from 3 m to 8 m below ground surface*

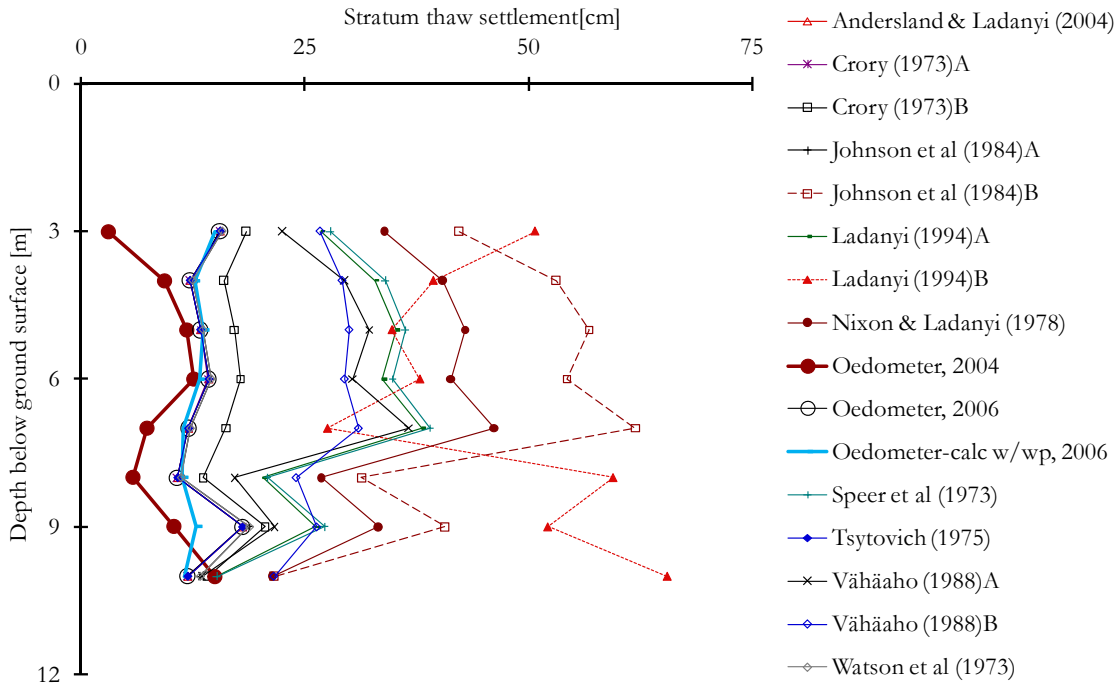

Figure 6.5 *Deformation, the total thaw settlement of every soil strata. The resulted thaw settlement originates from the Bothnia Line soil behaviour, calculated with the equations above. The presented settlement named "Oedometer, 2006" originates from oedometer tests on representative depth of the Bothnia Line soil*

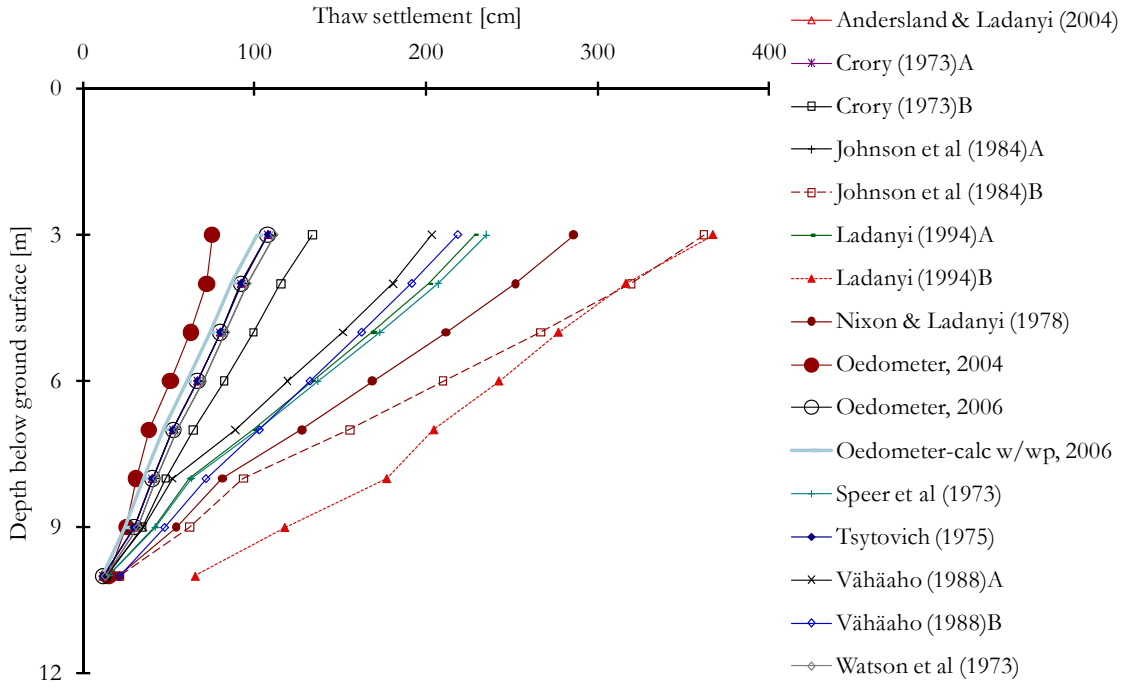

Figure 6.6 *The total accumulated thaw settlement. The resulted thaw settlement originates from the Bothnia Line soil behaviour, calculated with equation above. The presented settlement named "Oedometer, 2006" originates from oedometer tests on representative depth of the Bothnia Line soil*

Analyses of each equation to calculate the thaw settlings according to articles above show that the theoretical equations primary based on water content change, i.e. a bulk density

change provides nearly the same result for the thaw settlement. The equations above, based on the water content change are

- Andersland and Ladanyi (2004), Eq. (2.58)
- Crory $(1973)_A$, Eq. (2.61)
- Crory $(1973)_B$, Eq. (2.72)
- Johnson et al $(1984)_A$, Eq. (2.70)
- Tsytovich (1975), Eq. (2.52)
- Watson et al (1973), Eq. (2.65).

These thaw settlement equations consider no more than the water content change during the thaw process, from the original frozen soil until the soil is completely thawed; therefore, the results of these equations in Figure 6.5 and Figure 6.6 are nearly identical. Crory $(1973)_B$, Eq. (2.72), on the other hand, took into consideration the specific ice content. In fact, the iceness ratio i.e. $(w_f - w_u) / w_f$ consider the clay content and the sub-zero temperature, the lower the temperature, the higher the iceness ratio.

In contrast to these theoretical equations, a handful of empirical equations consider the local soil properties when predicting the thaw settlement, as can be seen in Figure 6.5 and Figure 6.6. Equations depicting the thaw settlement based on empirical data

- Johnson et al $(1984)_B$, Eq. (2.71)
- Ladanyi $(1994)_A$, Eq. (2.69)
- Ladanyi $(1994)_B$, Eq. (2.73)
- Nixon and Ladanyi (1978), Eq. (2.67)
- Speer et al (1973), Eq. (2.68)
- Vähäaho $(1988)_A$, Eq. (2.74)
- Vähäaho $(1988)_B$, Eq. (2.77).

Johnson et al's $(1984)_B$, Eq. (2.71) shows the thaw settlement, based on frozen bulk density in fine-grained lacustrine soils with a wide range of ice contents, at different points along the Mackenzie Valley, based on Speer et al's (1973) data. However, the thaw strain data for soils along the trans-Alaska pipeline route have been correlated with frozen bulk density. Johnson et al $(1984)_B$ analysed the data in Figure 2.52 and made a best-fit linear relationship of the line thaw consolidate parameter A_0 vs. the total water content. As can be seen in Figure 6.6, the settlement in the example at Bothnia Line will exceed at least 3 m, nearly 30 % of the total soil depth.

In the same fashion, Ladanyi $(1994)_A$ used Speer et al's (1973) data and made a best-fit linear relationship of the line thaw consolidate parameter A_0 vs. the frozen bulk density, Eq. (2.69). As can be seen in Figure 6.6, the settlement in the example at Bothnia Line will exceed at least 2 m, nearly 20 % of the total soil depth.

Again, Ladanyi $(1994)_B$ used Speer et al's (1973) thaw settlement data and presented a best-fit linear relationship of the line thaw consolidate parameter A_0 vs. the total water content, Eq. (2.73). As can be seen in Figure 6.6, the thaw settlement in the actual example at Bothnia Line will exceed at least 4 m, nearly 40 % of the total soil depth.

Like Johnson et al $(1984)_B$, Ladanyi $(1994)_A$ and Ladanyi $(1994)_B$, also Speer et al (1973) analysed the relation between frozen bulk density and the corresponding thaw settlement from different points along the Mackenzie Valley, see Eq. (2.68). As can be seen in Figure 6.6, the thaw settlement in the example of the Bothnia Line will exceed at least 2 m, nearly 20 % of the total soil depth, by using this equation.

Johnson et al $(1984)_B$, Ladanyi $(1994)_A$, Ladanyi $(1994)_B$, Nixon and Ladanyi (1978) and also Speer et al (1973) used data from different points along the Mackenzie Valley and presented altered best-fit linear relationships of the line thaw consolidate parameter A_0 vs. the frozen bulk density or vs. total water content. These Canadian results are based on measurements connected with thawing of permafrost. In contrast, Vähäaho $(1988)_A$ and $(1988)_B$ used results from investigations on clay in the Helsinki area, in Finland and on "native thin clay from China" (Vähäaho et al, $1988)_A$ and $(1988)_B$. Likewise, the use of Vähäaho's $(1988)_A$ and $(1988)_B$ calculation methods of the thaw settlement in the example at Bothnia Line shows a thaw settlement exceeding at least 2 m, nearly 20 % of the total soil depth. However, in the Bothnia Line example the results from the Vähäaho $(1988)_A$ and $(1988)_B$, Ladanyi $(1994)_A$ and Speer et al (1973) thaw-settlement calculations are in the same range.

The results from the oedometer tests show a total thaw settlement of the ground surface of approximately 1.08 m. Likewise, the results from theoretical methods to calculate the thaw settlements agree with the laboratory oedometer tests, whereas the results from the theoretical methods are based on the laboratory tests.

The results from the theoretical studies estimate the thaw settlement of the ground surface to be approximately 1.08 m, while the results from the empirical studies predicting thaw settlements methods fluctuate between 1.93 m and 3.85 m.

One explanation for the range of the empirical thaw settlement estimations could be that they originate from unique test areas; however, the majority of thaw settlement equations originate from the same area. The conclusion that emerges from this study is that thaw settlement ratio in permafrozen clayey soils differ from the thaw settlement ratio in virgin artificially frozen ground.

6.6.1 Comparison of measurements at site and FEM analyses of the thaw settlement

The course of events of the thaw settlement has been simulated in JOBFEM. The simulation has been performed via coupled analysis, i.e. the course of the settlement has been connected to the course of the thawing. The simulation of the course of the thawing has been accounted for in the field study chapter and is based on, among other things, the measured temperatures in the soil at the time of the shut off of the cooling plant. The thaw settlement is related to the temperature change as the thaw settlement occurs momentarily when the temperature in respective element exceeds 0 °C. The decrease in volume is assumed to have happened instantly, i.e. the pore water migrates momentarily. This assumption is based on, among other things, the results from the laboratory tests where the thaw deformation occurred very fast in all tests. The thaw settlement is assumed to be the mean value of the volumetric thaw deformation, 13.37 %, which derives from the laboratory tests for all depths. The volume decrease occurs as an initial strain in the same way as one analyzes the effect of volume change due to changes in temperature. The results from the coupled FEM analyses shows the prognosticated thaw settlement after 12 months in Figure 6.7, after 36 months in Figure 6.8, after 60 months in Figure 6.9, and finally at the time for final soil settlement in Figure 6.10 after 228 months (19 years).

Figure 6.11 shows a comparison of the measured deformations of the Bothnia Line and the deformations in JOBFEM. The accounted for measurements for the deformations are based on the average number of the deformations in the gauges on respective distances, 2 m, 5 m, 10 m, 15 m and 20 m from the centre of the tunnel in both control sections, 13+549 and 13+568.5. The values for the deformations in JOBFEM are calculated for the opposite points of the plane and for the representative depths of gauges, i.e. 2 m, 5 m,

10 m, 15 m and 20 m from the tunnel centre as well as at a depth of 2.5 m. Even gauge 10pt, 10 m from the tunnel centre at the depth of 7.5 m is accounted for in the figure.

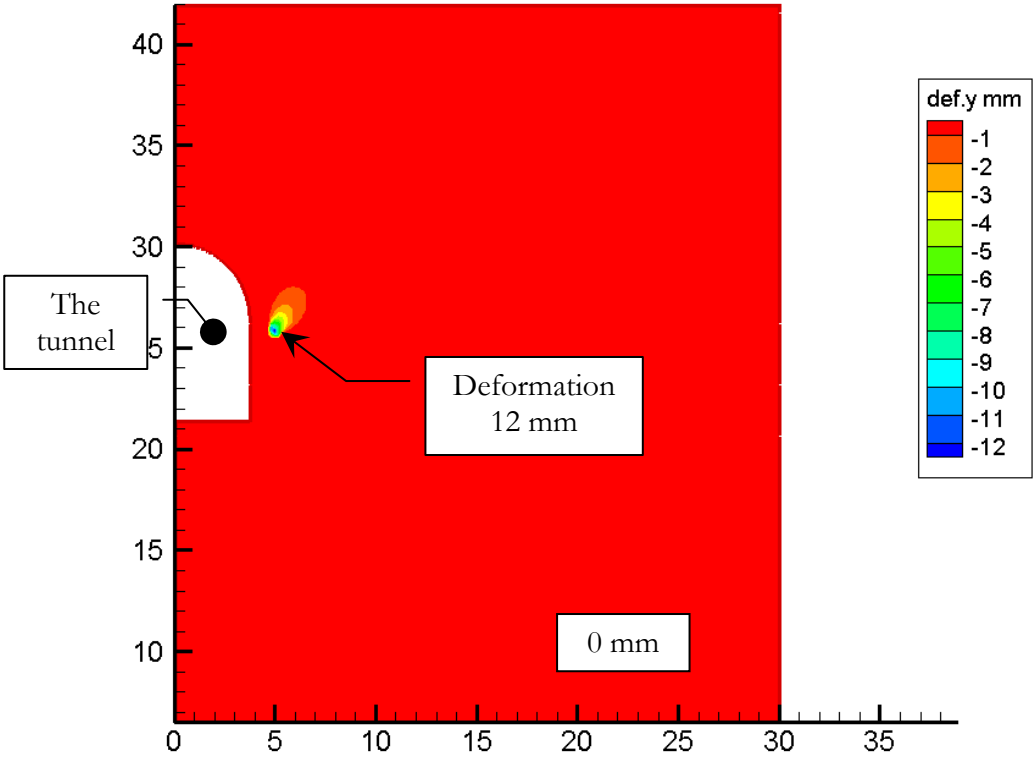

Figure 6.7 *Soil settling distribution around the tunnel 12 months after that the cooling device was shut off, i.e. the prognosis for September 2004, based on the measured temperatures at the time of September 2003 and the volumetric strains in oedometer tests. Calculated in JOBFEM*

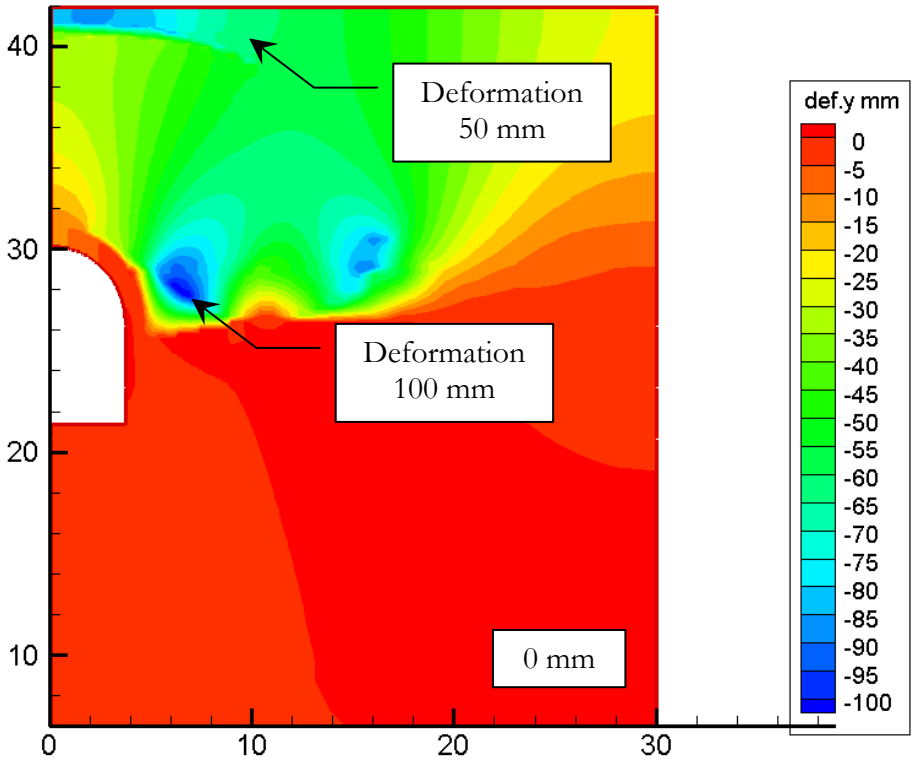

Figure 6.8 *Soil settling distribution around the tunnel 36 months after that the cooling device was shut off, i.e. the prognosis for September 2006, based on the measured temperatures at the time of September 2003 and the volumetric strains in oedometer tests. Calculated in JOBFEM*

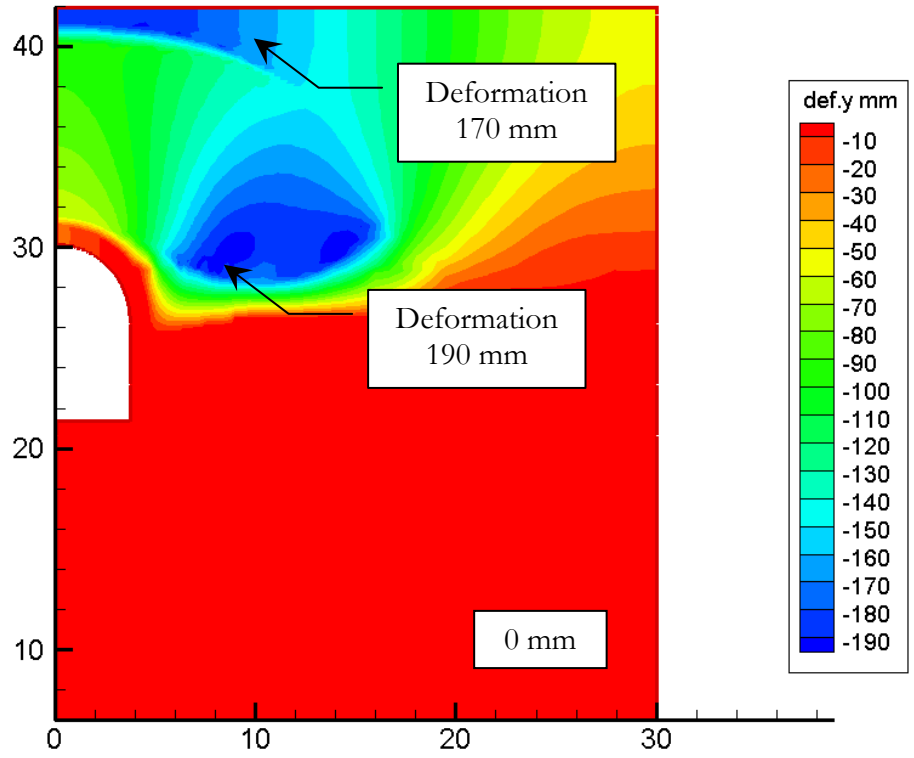

Figure 6.9 *Soil settling distribution around the tunnel 60 months after that the cooling device was shut off, i.e. the prognosis for September 2008, based on the measured temperatures at the time of September 2003 and the volumetric strains in oedometer tests. Calculated in JOBFEM*

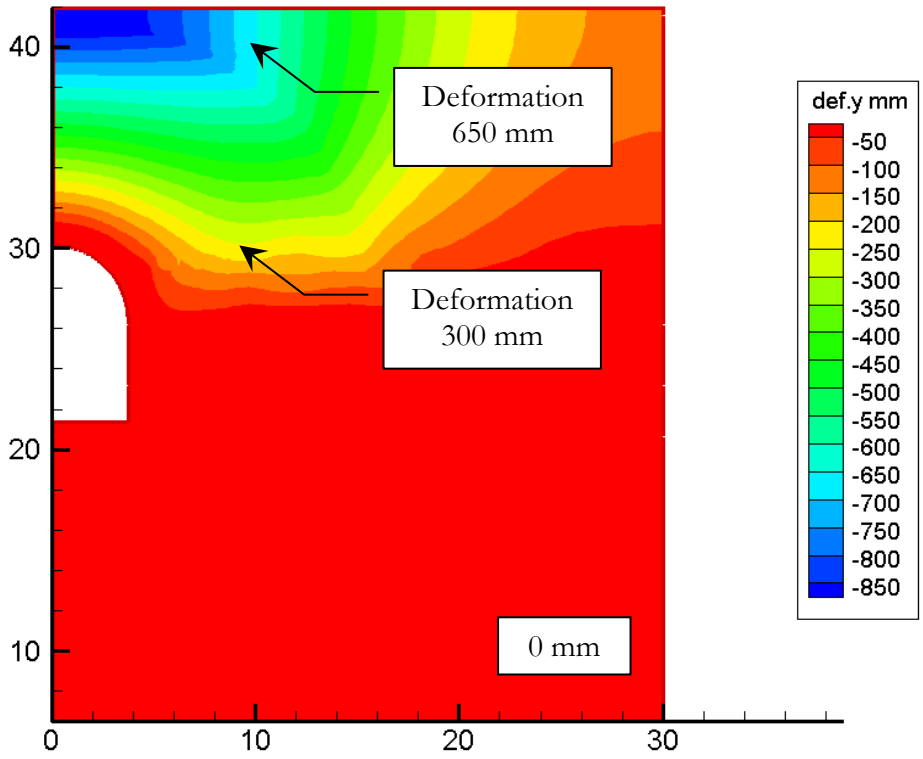

Figure 6.10 *Soil settling distribution around the tunnel 228 months after that the cooling device was shut off, i.e. the prognosis for the final soil settlement on September 2022, based on the measured temperatures at the time of September 2003 and the volumetric strains in oedometer tests. Calculated in JOBFEM*

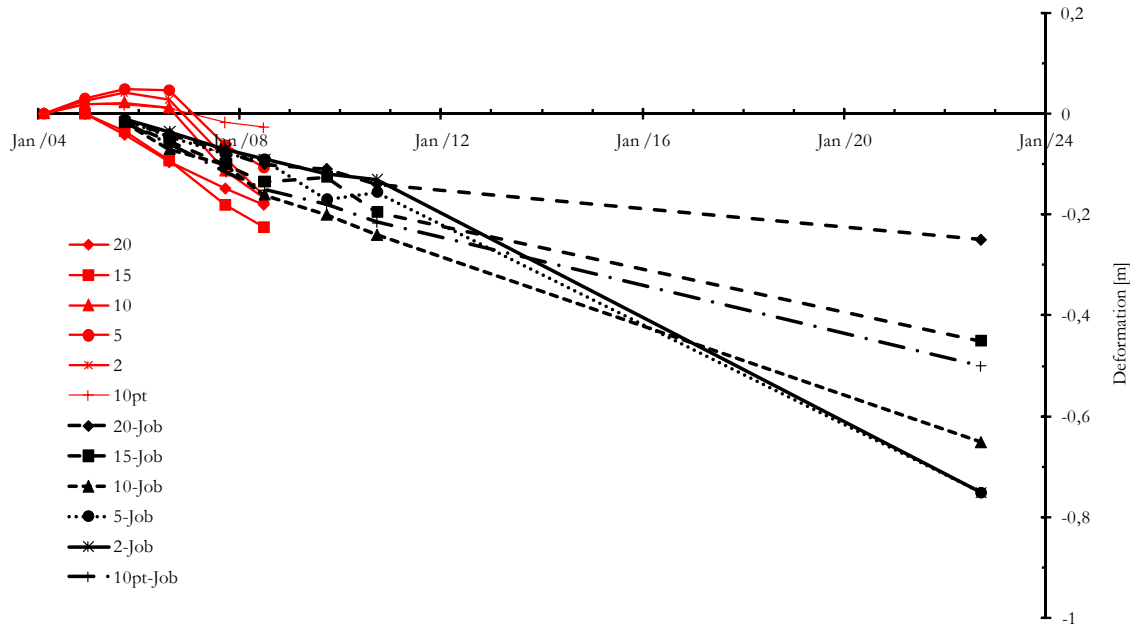

Figure 6.11 Soil settling distribution around the tunnel. Comparison of the measured settling (continuous lines) at the Bothnia Line and the calculated settlement (dotted lines) in JOBFEM. The line numbers refers to the distance between the tunnel centre and the measuring point, i.e. the ground level gauge

6.7 TUNNEL ROOF LOAD

In connection with the thawing of an artificially frozen construction to stabilize soil and rock during tunnel construction, the construction goes from having been ”supportive” to being a load on, above all, the tunnel roof. Case studies and theoretical discourses of size and time concerning the load build-up on the tunnel roof have not yet been published. Uncertainties therefore exists regarding how the frozen soil becomes a load on the tunnel line, i.e. if the frozen soil ”let go” in larger portions and gradually contributes to an added load, or if the frozen soil slowly goes from frozen condition to thawed condition with a proportionally add-on to the load. The regular measuring of the load on the tunnel roof is thus important when it comes to being able to draw conclusions for how the process of the load build-up acts on the permanent construction during the course of the thawing.

The settlings started in the soil outside the frozen construction, i.e. in soil that had not been frozen. The settlings originated most likely from the volume decrease that the thawed soil next to the tunnel lining gave rise to. The temperature measuring together with JOBFEM calculations confirm partly that the soil next to the tunnel lining has thawed and partly that the soil outside the frozen construction, where the settlings are the largest, has not been frozen. The pressure cells on the tunnel lining’s roof register the successive increase in the load that coincides with that the soil is still frozen according to the temperature sensors and manual soil soundings, but thawed in a segment connected to the tunnel.

6.8 CASE STUDIES

The three case studies concerning Storebælt eastern railway tunnel, Hurum Weakness Zone and the tunnel in Kobe city show a variety of challenges. The AGF was in an early stage fitted into the schedule for the Storebælt tunnel and the Kobe tunnel. However, in the case

of the Hurum weakness zone, AGF was agreed upon in a late decision due to the hidden problem.

The freeze pipes in the Storebælt tunnel were installed with an inclination to the prospective tunnel to minimize deformations and stresses due to frost heave. When the designed temporary frost construction was achieved, maintenance freezing was performed with intermittent freezing. These actions, as reported, prevented deformations and unfavourable stresses. Surprisingly, no problems due to marine environment have been reported. The site location expects strength reductions and therefore unfavourable creep of the frozen construction, due to salinity. On the other hand, the temporary frozen construction was reported to allow reliable tunnelling.

In the Hurum weakness zone, grouting was used in the first attempts to stabilize and seal the zone. As this method proved unsuccessful it was opted for to freeze with brine. One reason for this choice of freezing was the difficulty to achieve representative samples of the material. Core samples were collected and they were mixed and packed. The attempted freezing of the samples showed that the strength grew faster during the eutectic temperature, thus requiring a relatively low design temperature. With consideration of saline content, stress situation, risk for flowing ground and load-bearing capacity, the lengths of the rounds were maximized to 2.2 m. The choice of freeze method was made at a late stage contributed to that it took relatively long time before the zone could be passed. The marine environment with a relatively high saline content in the water added however uncertainties in regards to the strength.

During the freezing of the existing Kobe tunnel, the frost heave was estimated to be 0.05 m above the axis of the tunnel after one year of freezing. The observed frost heave became about 0.04 m. The calculations for the frost heave were performed with help of segregation potential (SP). As the tunnel roof was located approximately 18 meters under the ground surface, the heave became about 0.2 %. With consideration of that the freezing was performed with vertical, inclined, radial and horizontal freeze pipes in a ground made up of different layers of sand and clay where the spreading of the freeze pipes also varied vertically and horizontally, the concluded calculated heave must be pure luck. During the freezing the expansion will, due to the phase change of the water and the creation of ice lenses occur during very complex conditions. Depending on how the cooling effect is distributed to the freeze pipes, expansion will occur both vertically and horizontally, see Figure 6.1. This distribution is very difficult to predict during circumstances such as those reported from the Kobe tunnel. During the thawing of the frozen construction, the thawed area was chemically injected intermittently to avoid damage caused by the thaw settlement. This thaw settlement was estimated to 0.13 m on the above located wastewater pipe. Knowing the results, an alternative stabilization method to freezing might have been preferable in this case as the freeze method had to be supplemented with a second stabilization method throughout the whole course of the thawing.

6.9 CONCLUSION

Conclusions from the analysis and discussions, concerning the AGF at Bothnia Line are:

- A change in soil parameters occurs due to thawing of the Bothnia soil, namely; bulk density, liquid limit, overconsolidation ratio, permeability, preconsolidation pressure, undrained shear strength, void ratio and water content.
- No change in following soil parameters occurs due to thawing of Bothnia soil, namely, plastic limit and sensitivity.

- The driving force for the amount of migrated pore water due to thawing has no correlation to the depth below ground surface and no or very little correlation to the original water content.
- A part of naturally frozen soil and another part of artificial frozen soil with similar contents of particles, have different behaviour for thawed soils. This is generally due to altered water content in the state of ice inclusions.
- The occurred ground heaving at the Bothnia Line, six months after the cooling machine was shut off is probably, due to a pore water increase inside the frozen construction and hence, outside the tunnel lining.
- The results from the theoretical studies estimate the thaw settlement of the ground surface at the Bothnia Line to be approximately 1.08 m, while the results from the empirical studies predicting thaw settlements methods fluctuate between 1.93 m and 3.85 m.
- The laboratory study shows an empirical relationship between the thaw settlement and the ratio of water content and plastic limit.
- Analyses in JOBFEM shows a final settlement of approximately 0.65 m above the tunnel (entire width) that gradually decreases to approximately 0.25 m at a distance of 20 m from the tunnel centre axis.
- The prognosticated temperature followed the measured temperature during the period of measurements (approximately six years).
- The load on the tunnel roof was constantly increasing, due to the continuously thawing soil loading up on the tunnel roof.

7 GENERAL CONCLUSIONS

This thesis concerns artificial ground freezing and covers; 1.) A brief description of the effects of various Bothnia soil parameters and their effects on the thaw deformation. 2.) Analyses, reviews and validations of the state of the art and theories of prognoses for vertical deformation, i.e. the thaw settlements in fine-grained soil during the thawing process for Bothnia soil conditions. 3.) A proposed empirical method for estimating the thaw settlement using observed soil properties at the frozen construction at The Bothnia Line. The following main conclusions can be drawn from this thesis:

The thaw settlement process in clayey soils, due to artificial freezing and the subsequent thawing, is a process which depends on several soil parameters, namely; void ratio, water content, particle size distribution, mineral content and whether the present soil has been frozen or not. Laboratory tests of Bothnia soil depict alterations of various soil parameters. During the freeze-thaw process in the Bothnia soil, several parallel processes take place. However, the soil water content decreases in mean approximately 14 % (with exception of the depths nine and ten metres below ground surface). The decreases of soil water content have no correlation to the depth below ground surface. On the other hand there is a strong relationship between the original water content and the decrease of the water content. A best-fit curve with a correlation coefficient of 0.9 for the strata from 3 m to 8 m shows the correlation between the decreased water content (w-w_{th}) and the original water content (w) to be approximately $0.15w + 1.51$. In addition, the degree of decreased water content has a vague correlation to the magnitude of settlement. In the same fashion, the tests show no correlation between the degree of original water content and the magnitude of settlement.

The laboratory freeze-thaw tests show that the soil becomes denser, the preconsolidation pressure and the overconsolidation ratio increase for thawed soil compared to undisturbed soil, as a result of the freeze-thaw induced pore water migration and the settlement under self-weight. Hence, soils with a decreased soil water content and an increased density due to thawing lead to a decreased void ratio. Generally, in none temperature influenced geotechnique, these results lead to a less permeable soil, whereas, the CRS-tests of the thawed soil show a more permeable soil. Furthermore, the liquid limit decrease due to thawing and the amount of clay and fine silt particles decreases after thawing, hence the amount of coarser particles increases. These results show that a process where finer particles create a coarser soil due to thawing do exists. In addition, the thawed soil is more permeable, probably due to the higher amount of coarser particles, rather than vertical cracks due to the freeze process reported by Chamberlain and Gow (1978). Consequently,

the coarser and denser soil with a higher preconsolidation pressure created due to freeze-thaw process increases the undrained shear strength.

Whereas naturally frozen soils generally have horizontal frost fronts (at least parallel to the ground surface) and in general a moderate temperature permitting unfrozen water to migrate and continuously form different landscapes. The artificially frozen ground on the other hand, has a complex frost front situation and almost always a relatively low temperature, hence an in comparison low unfrozen water content. The magnitude of frost heave depends on the amount of water content phase change and the ability to create ice lenses. On the other hand, the magnitude of the thaw settlement generally depends on the ability to migrate bound water, and secondly the ability to create ice lenses. Generally, ice lenses build up normal to the frost front, regardless of if it is naturally frozen soil or AGF. In fact, slow freezing with low temperature gradients is generally favourable for ice lens creation. Therefore, naturally frozen soil has a relatively high content of ice lenses; consequently, the thaw settlement is normally in larger than e.g. AGF soil. As a matter of fact, the frost heave and the thaw settlement in an AGF project depends on the soil properties and the orientation of the freeze pipes. Moreover, a behaviour of a soil sample taken in the ground before the frozen construction takes place should perform in various ways if the sample is localised close to a freeze pipe or localised halfway between the freeze pipes. In other words, during freezing, soil close to the freeze pipe exists in a low temperature condition with a relatively large temperature gradient, compared to soil halfway between the freeze pipes.

Laboratory tests of the Bothnia soil show a correlation between thaw settlement vs. the ratio of water content and plastic limit. Hence, the results from laboratory routine tests of soil samples collected from the area close to the frozen construction at the Bothnia Line, prognosticate the future final thaw settlement. A proposed 1-dimensional empirical method to estimate the final thaw settlement at Bothnia soil condition is (Eq. (6.2)) $\varepsilon = \Delta H/H = 7.0 \ln(w/w_p) + 7.8$, where w is the original water content of the undisturbed soil and where w_p is the original plastic limit of the undisturbed soil. In the same fashion, a proposed 1-dimensional empirical method to estimate the frost heave at the Bothnia Line is (Eq. (6.3)) $\varepsilon = \Delta H/H = 1.8 \ln(w/w_p) + 2.7$. Nevertheless, using the 1-dimensional thaw strain mean values from the freeze-thaw tests in a 2-dimensional JOBFEM analysis, shows a result of a final settlement of approximately 0.65 m above the Bothnia tunnel. The thaw settlement gradually decreases to approximately 0.25 m, at a distance of 20 m from the tunnel centre axis.

Historically, authors have been presenting a variety of mathematical equations describing the thaw consolidation process. Nevertheless, soil parameters influence the thaw settlement ratio in the equations in different ways. This study calculates the thaw settlement ratio with presented equations. Calculations with Bothnia soil properties resulted in an estimated thaw settlement ratio varying from 1.1 m to approximately 3.9 m using the presented equations. In most cases existing mathematical, analytic equations describe the thaw settlement processes concerning the local conditions the equations primarily have been created for. Therefore, using the reported equations, a great scattering of results is attained.

According to the field temperature measurements and the JOBFEM analyses of the Bothnia Line frozen construction, the temperature measurements seems to present appropriate temperatures in the ground until temperatures close to ice/water phase change. This study shows that the temperature sensor casing tubes and the freeze pipe casing pipes of steel have a considerable influence on the thawing effect of the ground, especially at temperatures close the phase change of ice/water. Hence, at the moment the phase change took place, the manual sounding at the Bothnia Line frozen construction shows a distinct

difference between the frozen ground and the thawed soil close to the temperature sensor casing tubes and the freeze pipe casing pipes. As a result the ground consisted of frozen soil and vertical thawed soil pits round the steel casing pipes, i.e. metaphorically speaking, the ground can be compared to a "Swiss cheese".

The field study at the Bothnia Line's frozen construction shows that the ground surface performs a settlement. On the contrary, the first year of measuring, which begun approximately half year after the cooling machine was terminated, the ground surface surprisingly heaved approximately 1 dm. This phenomenon is probably due to artesian ground water. However, as the frozen construction thawed and permitted the ground water to communicate with the surrounding area, the ground surface commenced to settle. Measurements show a settlement closed to the prediction in JOBFEM, while, the measured settlement in the field seems to develop faster, at least until this day. On the other hand, the occurrence of the surprising heave raises difficulties to prognosticate the thaw settlement, based on the field study. As a result, this experience shows the necessity to begin the measurements at an early stage.

Pressure cells at the Bothnia Line tunnel roof were frequently read because of the issue concerning if the soil above the tunnel roof would crash on the roof in large chunks due to thawing. The conclusion of the reading of the pressure cells is that the soil create the load build-up on the tunnel roof successively and coincides with the soil's successive thawing, i.e. the soil does not crush on the roof in large chunks due to thawing.

Case studies show that AGF is an assured method to stabilize and create watertight constructions with comparative benefits to other methods. The strength of AGF constructions is unsophisticated to verify. On the other hand, the AGF method is relatively expensive to establish, and in fine grain soils AGF might create frost heave and thaw settlements. Nevertheless, an essential experience regarding AGF shows that the measurements should start preferably before the establishing of the ground freezing equipment.

8 SUGGESTIONS FOR FURTHER RESEARCH

Vähäaho et al (1989) shows that the pore water pH value decreases for each freeze-thaw cycle. The migration of the pore water from the clay particles occurs simultaneously as a change in the pH value of the pore water takes place. This change of the pH value may be a marker for the magnitude of thaw settlement. On the other hand, Vähäaho et al also shows that the change in the pH value after freeze-thaw cycles varies in three different clays. This is an indication that the clay mineral may also be a marker for the magnitude of thaw settlement.

Konrad and Morgenstern (1980, 1981, 1982, 1983) show that the deformations due to ice lens build up during freezing could be estimated by using the segregation potential method (SP). However, SP calculations depend on inter alia the temperature gradient in the frozen fringe, i.e. the freeze rate. This freeze rate may be a marker for the magnitude of the thaw settlement.

Sulphide rich clayey soils are sensitive to the influence of oxygen. Generally, the unaffected sulphide rich soils are black. However, due to oxidation the soil becomes gray-green and aging of the soil during the storage may affect the reliability of the thaw consolidation tests.

Pusch (1978), Anderson and Tice (1971), Frivik and Johansen (1980) show the relation between unfrozen water content and soil temperature. Hence the lower soil temperature the lower unfrozen water content. The unfrozen water content depends on inter alia the grain size distribution and the clay mineral content. Nevertheless, the influence of the freeze temperature may affect the thaw settlement ratio.

The use of tube filling in the temperature sensor casing tubes affects the measured temperature in field conditions, e.g. a fill of water in the casing tubes becomes liquid when unfrozen, as a result, the liquid creates a self induced convection and hence, the temperature sensors in the casing tube will be affected.

During the freezing, several processes take place in the field, e.g. ground frost heave. The resulted information is important for the estimation of the final thaw settlement.

As can be seen in the chapter "Field study and prognoses at the Bothnia Line", the casing tube material (steel) affects the thawing rate. Due to the casing tube material and the casing tube pattern in the ground the thaw rate will be influenced. This influence should be considered in the thaw estimations.

The work presented in this thesis suggests several topics for further research. Such work may cover partly laboratory and field studies. The Laboratory studies suggest that this complementary research concern

- the pH alteration during thawing
- the influence of various types of clay on the thaw consolidation
- the influence of the freeze rate on the thaw consolidation
- the age of especially sulphide rich clay specimens
- the influence of the freeze temperature on the thaw consolidation.

The field studies suggests that this complementary research concerns

- the influence of various case tube fillings on the measured temperature vs. the actual temperature
- early installation and reading of instrumentation in field, preferably before the freezing takes place
- the influence of the casing tube material on the thaw rate.

Follow up the development of thaw settlement of virginal freezing of clayey soils via studies of future artificial ground freezing projects concerning the suggested thaw settlement equation.

REFERENCES

Adolfsson, K., Franck, P.-Å., Rhen, I. & Sällfors, G. (1985). *Frysning av lera i jordvärmelager* (Rap 19). Göteborg: Chalmers univ of tech.

Aldrich, H.P. Jr & Painter, H.M. (1966). *Depth of frost penetration in non-uniform soil.* (Spec rep 104). Hanover NH: CRREL.

Aldrich, H.P. (1956). Frost penetration below highway and airfield pavements. *Highw res Board Bull 135*. Pp 124-149.

Alexiades, V. & Solomon, A.D. (1993). *Mathematical modelling of melting and freezing process.* Washington: Hemisphere publ corp.

Alkire, B. (1977). Generalized thaw settlement of soil. *15th Symp on Eng Geol and Soils Eng, USA, Pocatello, Idaho.* Pp 133-147.

Alkire, B. (1978). Some factors that affect thaw strain. *Transp Res Rec; 675*. Pp 6-10.

Andersland, O. & Ladanyi, B. (2004). *Frozen Ground Engineering.* New Jersey: Wiley.

Anderson, D. & Tice, A. (1971). Low temperature phases of interfacial water in clay-water systems. *Soil Sci Soc of Am J, vol 35(1).* Pp 47-54.

Andreassen, F. (1999). Oslofjordstunnelen, Erfaringer fra frysing og driving gjennom frysesonen. *Referat fra foredrag fra Fjellspreng d, Bergmek d, Geotekn d, Oslo.* Pp 18.1-18.15.

Aoki, K., Hibiya, K. & Yoshida, T. (1990). Storage of refrigerated liquefied gases in rock caverns: Characteristics of rock under very low temperatures. *Tunneling and Undergr Space Techn, vol 5, №4.* Pp 319-325.

Assur, A. (1963). Discussion on creep of frozen soils. *1st Int conf on permafrost, USA, West Lafayette, Indiana.* Pp 339-340.

Axelsson, K., Jouper, B. & Rydén, C.-G. (1988). Experimentell bestämning av portrycksutvecklingen i tinande jord. *Nordiska geoteknikermötet 1988*. Ss 9-13.

Backer, L. & Blindheim, O. (1999). The Oslofjord subsea road tunnel. Crossing of a weakness zone under high water pressure by freezing. In T. Alten et al (Eds.), *Challenges for the 21st century* (pp. 309-316). Rotterdam: Balkema.

Bengtsson, H. & Lundberg, B. (1977). *Grundförstärkning med frysning vid tunneldrivning* (Tech rep). Stockholm: Svenska Riksbyggen-BPA Byggprod AB.

Bergaya, F., Theng, B.K.G. & Lagaly, G. (2008). *Handbook of clay science*. Oxford: Elsevier.

Berggren, A.-L. (1983). *Engineering creep models for frozen soil behaviour.* Dr thesis, Univ of Trondheim, Norwegian Inst of Tech, Geotech Div.

Berggren, A.-L. (1997). *Grunnfrysing* (Tech rep). Oslo: Geofrost Eng AS.

Berggren, A.-L. (1999). Frostkonstruksjonen i Oslofjordstunnelen. *Referat fra foredrag fra Fjellsprengningsdagen, Bergmekanikdagen, Geoteknikdagen, Oslo.* Pp 20.1-20.17.

Berggren, A.-L. (2000). The Oslofjord subsea tunnel, a case record. *9th Int symp on ground freezing, Belgium, Louvain-la-Neuve.* Pp 267-272.

Berglund, H., Österberg, S., Schütz, F. & Heland, H. von (1957). *Teknisk beskrivning av Stockholms tunnelbana* (Tech rep). Stockholm: Norstedt & Söner.

Beskow, G. (1935). *Tjälbildningen och Tjällyftningen: Med särskild hänsyn till vägar och järnvägar. Soil freezing and frost heaving* (Meddelande №48, SGU Ser. C, №375). Stockholm: Statens Väginstitut.

Beskow, G. (1951). *Amerikansk och Svensk Jordklassifikation: Speciellt för vägar och flygfält. American and Swedish Soil Classification: Especially for highways and airfields* (Handling №111). Göteborg: Chalmers Tekn Högskola.

Bjerin, L. (2005). *Oral discussions on the ground freezing at the Södra Länken project, SL01.*

Black, P.B. & Hardenberg, M.J. (1991). *Historical perspectives in frost heave research, the early works of S. Taber and G. Beskow* (Spec rep № 91-23). USACE, CRREL.

Botniabanan. (2001A). *Örnsköldsvik – Husum, del 2, Contract area 5415, "Tunnel- och terrasseringsarbeten Km 12+780 – 14+360"* (Tender documents for the Bothnia Line ["Botniabanan"], in Swedish). Örnsköldsvik/Stockholm: Botniabanan AB.

Botniabanan. (2001B). *Lemminkäinen bygger tunnel genom Stranneberget.* Access in November, 2001, from Botniabanan AB, www.botniabanan.se.

Botniabanan. (2008). *Botniabanan. Delprojekt Arnäsvall (km 536+200 – 32+500).* Access in January, 2008, from Botniabanan AB, www.botniabanan.se.

Broms, B. & Yao, Y. (1964). Shear strength of soil after freezing and thawing. *ASCE, Soil Mech and Found Div. J. vol* (90), No. SM4. Pp 1-25.

Brown, E., Johnston, G., Mackay, N., Morgenstern, N. & Shilts, W. (1981). Permafrost distribution and terrain characteristics. In G. Johnston (Ed.), *Permafrost Engineering Design and Construction* (pp. 31-72). New York: Wiley.

Burdick, J.L., Rice, E.F. & Phukan, A. (1978). Cold regions: Descriptive and Geotechnical aspects. In O. Andersland & D. Anderson (Eds.), *Geotechnical engineering for cold regions* (pp. 1-29). New York: McGraw-Hill inc.

Carslaw, H.S. & Jaeger, J.C. (1959). *Conduction of heat in solids,* (2nd ed.). Oxford: Clarendon press.

Cauer, W. (1885). Gefrierverfahren beim Bau eines Tunnels in Stockholm. *Zentralblatt der Bauverwaltung,* №51. Pp 537-538.

Chamberlain, E. & Gow, A. (1978). Effect of freezing and thawing on the permeability and structure of soils. *1st Int symp on ground freezing, Germany, Bochum.* Pp 31-44.

Chamberlain, E. & Gow, A. (1979). Effect of freezing and thawing on the permeability and structure of soils. *Eng Geol.* Pp 73-92.

Chamberlain, E. (1981). *Frost susceptibility of soil: Review of index tests* (Spec rep 81-2). Hanover NH: CRREL.

Chamberlain, E. (1989). Physical changes in clays due to frost action and their effect on engineering structures. *1st Int Symp on Frost in Geot Eng, Finland, Saariselkä.* Pp 863-893.

Changjiang, T. & Chongyun, Y. (1983). Research on the frost-heaving force of soils. 4th *Int conf on permafrost, Alaska, Fairbanks.* Pp 1273-1277.

CIA. (2008). *Map of Europe.* Access in November, 2008, from Central Intelligence Agency, www.cia.gov.

Craig, R.F. (1974). *Soil mechanics.* London: Van Nostr Reinh comp.

Crory, F. (1973). Settlement associated with the thawing of permafrost. *2nd Int Conf on Permafrost, USSR, Yakutsk.* Washington DC: US Nat acad of scie. Pp 599-607.

Crory, F. (1984). Consolidation of permafrost upon thawing. In N. Yong & F. Townsend (Eds.), *Sed/cons models. Predictions and validation* (pp 399-410). San Francisco, CA: ASCE.

Crory, F., Isaacs, R., Penner, E., Sanger, F. & Shook, J. (1984). Design for frost heave conditions. In Berg L. & Wright E. (Eds.), *Frost action and its control* (pp 22-44). Hanover NH: *ASCE.*

Czurda, K.A. (1983). Freezing effects on soils: comprehensive summary of the ISGF 82. *5th Int Symp on Ground Freezing, UK, Nottingham.* Pp 93-107.

Davis, E.H. & Poulos, H.G. (1968). The use of elastic theory for settlement prediction under three-dimensional conditions. *Géotechnique, vol* 18. Pp 67-91.

Dijk, P. van & Bouwmeester, W. van den Bos (2000A). *Freezing in Boston* (Published report). Noordwijkerhout, Netherland: Soft Ground Technology.

Dijk, P. van & Bouwmeester, W. van den Bos (2000B). Large scale application of artificial ground freezing. *Conf on soft gr tech, Netherlands, Noordwijkerhout.* Pp 315-330.

Duquennoi, C., Fremond, M. & Levy, M. (1989). Modelling of thermal soil behaviour. *1st Int Symp on Frost in Geot Eng, Finland, Saariselkä.* Pp 895-915.

Dysli, M. (1993). Where does the water goes during ice lence thaw? *2nd Int Symp on Frost in Geot Eng, Alaska, Anchorage.* Pp 45-50.

Eiksund, G., Berggren, A.-L. & Svanø, G. (2001). Stabilisation of a glacifluvial zone in the Oslofjord subsea tunnel with ground freezing. *15th Int Conf on Soil Mech and Geotech Eng, Turkey, Istanbul.* Pp 1731-1736.

Farouki, O.T. (2004). Ground thermal properties. In C. Esch (Ed.), *Thermal analysis Constr, and monoring meth for gr freezing* (pp 259-276). Virginia: ASCE.

Fredriksson, A. (1984). *Analys av geotekniska problem med finita elementmetoden – tillämpad på lera under odränerade förhållanden (Finite element analysis of geotechnical problems – applied to undrained conditions in clay).* Dr thesis (in Swedish), KTH, Div of Soil and Rock Mech.

Fredriksson, A. (2005). *Thermal prognoses in JOBFEM for the thawing process of the frozen area at the Bothnia Line, contr 5415*. Oral discussions at Golder Associates AB, Stockholm.

Freitag, D. & McFadden, T. (1997). *Introduction to cold regions engineering*. N Y: ASCE.

Frivik, P.-E. & Johansen, Ø. (1980). *Thermal properties of soils and rock. Ground freezing, preprints*. Trondheim: NTH, Inst for Kjöleteknikk.

Fukada, M., Kim H.-S. & Kim, Y.-C. (1997). Preliminary results of frost heave experiments using standard test sample provided by TC8. *8th Int Conf on Ground Freezing and frost action in soils, Sweden, Luleå*. Pp 25-41.

Graham, J. & Au, V.C.S. (1985). Effects of freeze-thaw and softening on natural clay at low stresses. *Can Geot J, vol* (22). Pp 69-78.

Hammarbäck, S. (2005). *Ground water measurements: Ground water data from Stranneberget at the Bothnia Line*. Stockholm/Örnsköldsvik: Botniabanan AB.

Handbook of chemistry and physics (85th ed.). (2004). Boca Raton, FL: CRC-Press/Taylor and Francis.

Harris, J. (1995). *Ground freezing in practice*. London: Telford.

Hashin, Z. & Shtrikman, S. (1962). A variational approach to the theory of the effective magnetic permeability of multiphase materials. *J appl phys vol* (33). P 3125.

Heller-Kallai, L. (2008). Thermally modified clay minerals. In F. Bergaya, B.K.G. Theng & G. Lagaly (Eds.), *Handbook of clay science* (pp 289-308). Oxford, UK: Elsevier.

Ingelstam, E., Rönngren, R. & Sjöberg, S. (1999). *TEFYMA, Handbok för grundläggande teknisk fysik, fysik och matematik*. Helsingborg: Sjöbergs Bokf.

Ingersoll, L.R., Zobel, O. & Ingersoll, A.C. (1948). *Heat conduction with engineering and geological applications*. New York: McGraw-Hill Book comp inc.

ISSMFE. (1989). *Work report 1985-1989 of the Techn Com on Frost. TC8. IS VTT94, Frost in Engineering*. H Rathmeyer (Ed.), Finland, Espoo.

Jessberger, H. & Vyalov, S. (1978). General report. *1st Int symp on ground freezing, Germany, Bochum vol* (2). Pp 15-20.

Jessberger, H. (1978). General report. *1st Int symp on ground freezing, Germany, Bochum*.

Jessberger, H. (1980). Theory and application of ground freezing in civil engineering: Review. *Cold regions science and technology,* 3. Pp 3-27.

Jessberger, H. (1987). Artificial freezing of the ground for construction purposes. In F.G. Bell (Ed.)*, Ground engineer's reference book* (ch 31). London: Butterworths & co Ltd.

Jessberger, H. & partner Gmbh, Bochum. (1990). *Ground freezing conception of cross passages at Great Belt Tunnel, Denmark* (Internal report).

Johansson, T. (2000A). *Jordfrysning i samband med tunneldrivning*. Master's thesis, (in Swedish), KTH, Div of Soil and Rock Mech.

Johansson, T. (2000B). *Frysteknik i samband med undermarksbyggande* (Internal research report) Stockholm: Skanska.

Johansson, T. & Hintze, S. (2002). *Frysteknik: Utveckling av produktionsteknik för att stabilisera och täta jord vid undermarksbyggande: Grundläggande samband, användningsområden och erfarenheter* (SBUF-Utvecklingsprojekt 1071). Stockholm: SBUF-Skanska.

Johansson, T., Hintze, S., Stille, B. & Matérn, M. (2002). *Utveckling av strategiskt viktiga områden inom jord- och bergfrysning* (Internal research report). Stockholm: Skanska.

Johansson, T. & Hintze, S. (2003). Frysteknik -för att täta jord och berg. *Bygg & Teknik, № 1* (in Swedish). Pp 59-64.

Johansson, T. & Stille, B. (2003). *SGF metoddatablad: Frysteknik* [Brochure]. Stockholm: SGF, jordförstärkningskommittén.

Johansson, T. (2004). *The use of ground freezing at the MBZ in the Hallandsås project: Comments about volume increase and thaw-consolidation, due to the freezing process* (Internal research report). Stockholm: Skanska.

Johansson, T. (2005). *Frysning av jord och berg vid tunnelbyggande. Studier av deformationer och spänningar, etapp 1*. Licentiate thesis (in Swedish), KTH, Div of Soil and Rock Mech.

Johansson, T. (in press). Thaw consolidation ratio in clayed soils due to artificial fereezing and subsequent thawing – analytic equations comparisons. *To be submitted.*

Johnson, T., McRoberts, E. & Nixon, J. (1984). Design implications of subsoil thawing. In R.L. Berg & E.A. Wright (Eds.), *Frost action and its control* (pp 45-103). N Y: ASCE.

Johnson, R.A. (2000). *Miller & Freund's: Probability and statistics for engineers* (6th ed.). Upper Saddle River, NJ: Prentice Hall Int, inc, Int ed.

Johnston, G.H. (1981). *Permafrost Engineering Design and Construction.* Toronto: Wiley.

Johnston, G.H., Ladanyi, B., Morgenstern, N.R. & Penner, E. (1981). Engineering characteristics of frozen and thawing soils. In G.H. Johnston (Ed.). *Permafrost Eng Design and Constr* (pp 73-148). Toronto: Wiley.

Jones, J. & Brown, R. (1978). Design of tunnel support systems using ground freezing. *1st Int Symp on Ground Freezing, Germany, Bochum.* Pp 235-246.

Jones, J. & Brown, R. (1979). Design of tunnel support systems using ground freezing. *Eng Geol, vol* (13). Pp 375-395.

Jones, R. (1982). Ground movements associated with artificial freezing. *3rd Int Symp on Ground Freezing, USA, Hanover, NH.* Pp 295-304.

Josang, T. (1980). Ground freezing techniques used for tunneling in Oslo City Centre. *2nd Int Symp on Ground Freezing, Norway, Trondheim.* Preprints. Pp 969-979.

Jumikis, A. (1966). *Thermal Soil Mechanics.* New Brunswick, NJ: Rutgers univ press.

Jumikis, A. (1978). Cryogenic texture and strength aspects of artificially frozen soils. *1st Int Symp on Ground Freezing, Germany, Bochum.* Pp 75-85.

Kamata, T., Morioka, T., Suzue, T., Hirano, T., Hashimoto, T., Konda, T. et al. (2000). Application of freezing method to shift down an existing tunnel. *9th Int Symp on Ground Freezing, Belgium, Louvain-la-Neuve.* Pp 345-350.

Karlsson, R. & Hansbo, S. (Eds.). (1989). *Soil Classification and Identification* (Perf and Interpr of Lab Investig, Part 2). Stockholm: SGF lab com.

Karlsson, R. & Hansbo, S. (Eds.). (2000). *Jordarternas Indelning och Benämning* (Geot Labanv, Del 2). Stockholm: SGF Labkom.

Kay, B.D. & Perfect, E. (1988). State of the art: Heat and mass transfer in freezing soils. *5th Int Symp on Ground Freezing, UK, Nottingham*. Pp 3-21.

Kersten, M. (1948). Apparatus for measuring thermal conductivity of soil. *2nd Int Conf on Soil Mech and Found Eng, Netherlands, Rotterdam*, *vol* (3). Pp 162-165.

Kersten, M. (1949). *Thermal properties of soils* (Bull no 28). USA, Minneapolis: Univ of Minnesota. Inst of Technology.

Khakimov, R. (1966). *Artificial freezing of soils: Theory and practice*. (A. Barouch, Trans.). Jerusalem: Monson. (Orig work publ 1957).

Klein, J. (1979). The application of finite elements to creep problems in ground freezing. *3rd Int Conf on Num Methods in Geomech, vol* (1). Pp 493-502.

Knutsson, S. (1982). Field study of instrumented gullies and manholes in frost-susceptible soils. *3rd Int Symp on Ground Freezing, USA, Hanover, NH*. Pp 367-374.

Knutsson, S. (1983). *En teoretisk modell för beräkning av porvattentryck och sättningar i tinande jord* (Teknisk Rapport 1983:35). Luleå: LTU.

Knutsson, S. (1984A). Inverkan av cyklisk frysning på lerors konsistensgränser. *Nordiska Geoteknikermötet, Sweden, Linköping, vol* (1), Pp 337-344.

Knutsson, S. (1984B). Tjäle och frost. In S. Avén (Ed.). *Handboken bygg: Geoteknik* (pp. 526-537). Stockholm: Liber.

Knutsson, S. (1984C). *Jordförstärkning, frysning*. In S. Avén (Ed.). *Handboken bygg: Geoteknik* (pp. 438-443). Stockholm: Liber.

Knutsson, S. (1985A). *Jordmaterials värmetekniska egenskaper* (Rapport 85:09). Luleå: LTU.

Knutsson, S. (1985B). *Hållfasthet/bärighet i tinande tjäle* (Rapport 1985:32). Luleå: LTU.

Knutsson, S. (1985C). *Thermal properties of bentonite based barriers*. Licentiate thesis, LTU, Dep of Civ and Mining Eng.

Knutsson, S. (1998). *Soil behaviour at freezing and thawing*. Dr thesis, LTU, Dep of Civ and Mining Eng.

Knutsson, S. & Johansson, T. (2005). Konsekvenser av frysning och tining på finkornig jords egenskaper. *Bygg & Teknik, № 1* (in Swedish). Pp 48-52.

Knutsson, S. & Rydén, C.-G. (1984). Porvattenövertryck i tinande jord - en teoretisk modell. *Nordiska Geoteknikermötet, Sweden, Linköping, vol* (1). Pp 345-352.

Kofoed, N. & Doran, S.R. (1996). Storebælt Eastern Railway Tunnel, Denmark – Ground freezing for tunnels and cross passages. *Int symp on geot aspects of undergr constr in soft ground*, *UK, London*. Pp 391-398.

Konrad, J.-M. & Morgenstern, N. (1980). A mechanistic theory of ice lens formation in fine-grained soils. *Can Geot J, vol* (17). Pp 473-486.

Konrad, J.-M. & Morgenstern, N. (1981). The Segregation Potential of a Freezing Soil. *Can Geot J, vol* (18). Pp 482-491.

Konrad, J.-M. & Morgenstern, N. (1982). Prediction of frost heave in the laboratory during transient freezing. *Can Geot J, vol* (19). Pp 250-259.

Konrad, J.-M. & Morgenstern, N. (1983). Frost heave prediction of chilled pipelines buried in unfrozen soils. *Can Geot J, vol* (21). Pp 100-115.

Konrad, J.-M. (1987). Procedure for Determining the Segregation Potential of Freezing Soils. *Geot Testing J, vol* (Jun, 10-2). Pp 51-58.

Konrad, J.-M. (1989A). Effect of freeze-thaw cycles on the freezing characteristics of a clayey silt at various overconsolidation ratios. *Can Geot J, vol* (26). Pp 217-226.

Konrad, J.-M. (1989B). Segregation potential-pressure-salinity relationships near thermal steady state for clayey silt. *Can Geot J, vol* (27). Pp 203-215.

Konrad, J.-M. (1999). Frost susceptibility related to soil index properties. *Can Geot J, vol* (36). Pp 403-417.

Konrad, J.-M. (2002). Prediction of freezing-induced movements for an underground construction project in Japan. *Can Geot J, vol* (39). Pp 1231-1242.

Kujala, K. & Laurinen, K. (1989). Freeze-thaw effects on thaw settlement and pore pressure. *1st Int Symp on Frost in Geot Eng, Finland, Saariselkä*. Pp 523-533.

Kujala, K. (1997). Estimation of frost heave and thaw weakening by statistical analyses and physical models. *8th Int Conf on Ground Freezing and frost action in soils, Sweden, Luleå*. Pp 31-41.

Lachenbruch, A. (1963). Contraction theory of ice-wedge polygons: A qualitative discussion. *1st Int Conf on Permafrost, USA, West Lafayette, Indiana*. Pp 63-71.

Ladanyi, B. & Sayles, F. (1978). Mechanical properties. *1st Int Symp on Ground Freezing, Germany, Bochum, vol* (2). Pp 5-13.

Ladanyi, B. (1994). *Design and maintenance of transportation infrastructures in Northern regions*. Manual for the ministry of transp of Québec. (From Andersland & Ladanyi, 2004).

Lambe, T. & Whitman, R. (1969). *Soil Mechanics*. New York: Wiley.

Larsson, R. (1982). *Jords egenskaper* (Information 1). Linköping: SGI.

Larsson, R., Westerberg, B., Albing, D., Knutsson, S. & Carlsson, E. (2007). *Sulfidjord, geoteknisk klassificering och odränerad skjuvhållfasthet* (Report 69). Linköping: SGI.

Lunardini, V. (1980). *The Neumann solution applied to soil systems* (CRREL Report; 80-22). Hanover, NH: Springfield, Va.

Lundahl, B. & Sjökvist, K. (1972). Djup grundläggning med komplikationer. *Väg och Vattenbyggaren nr* 5. Pp 256-262.

Lundahl, B. (2008). *Excavations in the block Hästen in the centre of Stockholm in the beginning of 1970:s.* Oral discussions.

Mackay, J.R. (1985). Pingo ice of the western Arctic coast, Canada. *Can J Earth Sci,* 22(10). Pp 1452-64.

McFadden, T. & Bennet, L. (1991). *Construction in cold regions.* New York: Wiley.

Morgenstern, N. & Nixon, J. (1971). One-dimensional consolidation of thawing soils. *Can Geot J, vol* (8). Pp 558-565.

Morgenstern, N. & Smith, L. (1973). Thaw-consolidation tests on remoulded clays. *Can Geot J, vol* (10). Pp 25-40.

Morgenstern, N. (1981). Geotechnical engineering and frontier resource development. *Géotechnique, vol* (31), No. 3. Pp 305-365.

Murray, M.J. & Eskesen, S.D. (1997). Design and construction of cross passages at the Storebælt Eastern Railway Tunnel. *Int Conf on Tunneling, Inst of Mining and Metallurgy and the British Tunnelling soc, UK, London*. Pp 463-479.

Mäkelä, H. (1979). The laboratory tests on frozen soil of the Cluuvi cleft. *Nordiska geoteknikermötet, Finland, Esbo*. Pp 709-717.

NE. (2005). Swedish National Encyclopedia.

Niemi, E. & Bylund, P. (2005). *Planritning over Frysområdet på Botniabanans entreprenad 5415*. Örnsköldsvik: Botniabanan AB.

Nixon, J. & Ladanyi, B. (1978). Thaw consolidation. In O. Andersland & D. Anderson (Eds.), *Geotechnical engineering for cold regions,* (pp. 164-215). New York: McGraw-Hill inc.

Nixon, J. & McRoberts, E. (1973). A study of some factors affecting the thawing of frozen soils. *Can Geot J, vol* (10). Pp 439-452.

Nixon, J. & Morgenstern, N. (1973). Residual stress in thawing soils. *Can Geot J, vol* (10). Pp 571-580.

Nixon, J. (1973). Thaw-consolidation of some layered systems. *Can Geot J, vol* (10). Pp 617-631.

Nixon, J. (1987). Ground freezing and frost heave. *Int Symp on Cold Regions Heat Transfer.* Pp 1-10.

Nixon, J. (1991). Discrete ice lens theory for frost heave in soils. *Can Geot J, vol* (28). Pp 843-859.

Nixon, J. (1992). Discrete ice lens theory for frost heave beneath pipelines. *Can Geot J, vol* (29). Pp 487-497.

Nordling, C. & Österman, J. (2004). *Physics Handbook for science and engineering.* Lund: Studentlitteratur.

Novikov, F. (1978). Pressure of thawing soils on concrete lining of vertical mine shaft. *1st Int Symp on Ground Freezing, Germany, Bochum*. Pp 175-182.

NSSH. (2007). *National Soil Survey Handbook*. Washington, DC: U.S. Department of Agriculture, Natural Resources Conservation Service.

Penner, E. (1956). *Soil moisture movement during ice segregation* (Bull no 135). Highway Res Board. Washigton, DC: Nat Acad of Scie-Nat Res Council.

Pentronic. (2005). *Resistanstermometrar, Pt100*. Product specification. Access in March, 2005, from Pentronic, www.pentronic.se.

Petrenko, V. & Whitworth, R. (2002). *Physics of ice*. New York: Oxford university press.

Pilebro, H. & Johansson, T. (2008). *Jernbanetorget, Nitrogenfrysning Brunn S3* (Internal report). Stockholm: Skanska.

Pusch, R. (1962). *Clay Particles their shape and arrangement in relation to some important physical properties of clays* (Handlingar Nr 40). Norrköping: Statens Råd för Byggnadsforskning.

Pusch, R. (Ed.). (1973). *Densitet, vattenhalt och portal* (Försl till Geot Lab Anv, Del 7). Stockholm: SGF Labkom.

Pusch, R. (1978). Unfrozen water as a function of clay microstructure. *1st Int Symp on Ground Freezing, Germany, Bochum*. Pp 103-107.

Pusch, R. (1979). Unfrozen water as a function of clay microstructure. *Eng geology, 13*. Pp 157-162.

Radd, F. & Wolfe, L. (1978). Ice lens structures, compression strengths and creep behaviour of some synthetic frozen silty soils. *1st Int Symp on Ground Freezing, Germany, Bochum*. Pp 115-130.

Redlund, M. (1976). Grundförstärkning genom frysning räddar gamla stan? *Byggnadsindustrin, №27*.

Ritter, C. (1962). Recent developments in liquefaction and transportation of natural gas. *Chem Eng Progress vol* (58) № 11. Pp 61-69.

Rowley, R., Watson, G. & Auld, R. (1973). Performance of a 48-in. Warm-oil pipeline supported on permafrost. *Can Geot J, vol* (10). Pp 282-303.

Rydén, C.-G. (1985A). Pore pressure in thawing soil. *4th Int symp on ground freezing, Japan, Sapporo*. Pp 223-226.

Rydén, C.-G. (1985B). *The CBT-Oedometer, an apparatus for one-dimensional thawing tests of frozen soil samples* (Tech rep 1985:043T). Luleå: LTU.

Rydén, C.-G. (1986). *Pore pressure in thawing soil, theory and laboratory determination*. Licentiate thesis, LTU, Dep of Civ and Mining Eng.

Saarelainen, S. & Gustavsson, H. (2001). Thaw weakening of subgrades in Finland. *15th Int Conf on Soil Mech and Geot Eng, Turkey, Istanbul, vol* (3). Pp 2183-2186.

Saarelainen, S. (1997). Field and laboratory methods for determining deformation properties in thawing soils. *8th Int Conf on Ground Freezing and frost action in soils, Sweden, Luleå*. Pp 53-62.

Saarelainen, S., Korkitala-Tanttu, L. & Viitala, J. (2004). Railway tunnelling in frozen ground on Bothniabana. *5th Int conf on case hist in geot eng, USA, New York, paper 6.06*. Pp 1-5.

Saka, F., Tanaka, M., Hara, H. & Takimoto, K. (1994). Application of freezing method to launch a large diameter shield tunnel. *7th Int Symp on Ground Freezing, France, Nancy*. Pp 281-288.

Sanger, F. & Sayles, F. (1978). Thermal and rheological computations for artificially frozen ground construction. *1st Int Symp on Ground Freezing, Germany, Bochum*. Pp 95-113.

Schwab, E.F. (1976). *Bearing capacity, strength and deformation behaviour of soft organic sulphide soils*. Dr thesis, KTH, Dep of Soil and Rock Mech.

Sellmann, P.V. & Brocket, B.E. (1992). *Digging fozen ground with a ripper bucket* (Spec Rep 92-15). Hanover NH: CRREL.

Sheng, D. (1994). *Thermodynamics of freezing soils, theory and application*. Dr thesis, LTU, Dep of Civ and Mining Eng.

Shuster, J. (1972). Controlled freezing for temporary ground support. *1st Conf on N Am Rapid Exc and Tunnelling, USA, Chicago, Illinois, vol* (2). Pp 863-895.

Shuster, J. (1980). Engineering quality assurance for construction ground freezing. *2nd Int symp on ground freezing, Norway, Trondheim*. Pp 863-879.

Skempton, A.W. (1953). The Colloidal "activity" of clays. *3rd Int Conf on Soil Mech and Found Eng, Switzerland, Zürich, vol* (1). Pp 60-64.

Skempton, A.W. & Bjerrum, L. (1957). A contribution to the settlement analysis of foundations on clay. *Géotechnique, vol* (7). Pp 168-178.

Slusarchuk, W., Watson, G. & Speer, T. (1973). Instrumentation around a warm oil pipeline buried in permafrost. *Can Geot J, vol* (10). Pp 227 – 245.

SNiP II-15-74. (1975). *Bases and foundations of buildings and structures. Moscow*. (From Harris, 1995).

Soil Instrument Limited. (2003). *Remediation: Product specification*. Access in March, 2003, from www.groundfreezing.com.

Sopko, J. & Aluce, G. (2005). *Artificial ground freezing for environmental remediation*. Access in January, 2005, from www.groundfreezing.com.

Speer, T., Watson, G. & Rowley, R. (1973). Effects of ground-ice variability and resulting thaw settlements on buried warm-oil pipelines. *2nd Int Conf on Permafrost, Siberia, Yakutsk*. Pp 746-752.

Statens Vegvesen. (2005). *Public information*. Access in January, 2005, from www.vegvesen.no.

Stefan, J. (1891). *Ann Phys. u. Chem*. (Wiedemann) N.F. vol 42. Pp 269-286.

Stepanov, Y. & Kholin, N. (1979). Determination of stress field during thawing of frozen ground. *Soil mech and found eng, vol* (6), no 2. Pp 94-98.

Stille, B. & Johansson, T. (2001). Frysning som jordförstärkningsmetod. *Nat Symp on Grundläggningsdagen 2001, Sweden, Stockholm*. Pp 217-231.

Stille, B., Brantmark, J. & Wilson, L. (2000). Dimensionering av frysta tunnlar-två projekt i Stockholm. *Nat Symp on Grundläggningsdagen 2000, Sweden, Stockholm*.

Stille, B., Sturk, R. & Pilebro, H. (2007). Drivning av pilottunnel genom Möllebackzonen. *Väg & Vattenbyggaren nr 1*. Pp 50-54.

Stoss, K. & Valk, J. (1978). Chances and limitations of ground freezing with liquid nitrogen. *1st Int Symp on Ground Freezing, Germany, Bochum*. Pp 303-311.

Stoss, K. & Valk, J. (1979). Uses and limitation of ground freezing with liquid nitrogen. *Eng geology, 13*. Pp 485-494.

Sundberg, J. (1988). *Thermal properties of soils and rocks* (Report no 35). Linköping: SGI.

Sällfors, G. & Andréasson, L. (Eds.). (1985). *Kompressionsegenskaper* (Geot Lab Anv, Del 10). Stockholm: SGF lab com.

Takashi, T., Kiriyama, S. & Kato, T. (1979). Jointing of two tunnel shields using artificial underground freezing. *Eng Geol, 13*. Pp 519-529.

Terzaghi, K. (1966). *Theoretical Soil Mechanics* (14th ed.). New York: Wiley.

Tidfors, M. (1987). *Temperaturens påverkan på lerors deformationsegenskaper, -en laboratoriestudie*. Licentiate thesis, Chalmers Univ of tech.

Tsytovich, N. (1957). The fundamentals of frozen ground mechanics (New investigations). *Int conf on soil mech and found eng, vol 1*. Pp 116-119.

Tsytovich, N. (1975). *The Mechanics of frozen ground*. Washington, DC: Scripta book co.

Tsytovich, N.A. & Sumgin, M.I. (1937). *Principles of mechanics of frozen ground* (USSR Acad sci press. Trans 19). Hanover N H: CRREL.

USAAF. (1987). *Arctic and subarctic construction general provisions* (Technical manual TM 5-852-1/AFR 88-19, vol 1). USA: Joint Dep of Army and the Air force.

USACE. (2006). *Ice engineering*. Washington: USACE.

Vaaranta, V. (2004). *Tunnelling in frozen ground at the Bothnia Line, 2002-2003*. Oral discussions.

Valk, J. (1980). The successful application of an unusual ground freezing method to secure tunnel excavation. *2nd Int symp on ground freezing, Norway, Trondheim*. Pp 79-83.

Veranneman, G. & Rebhan, D. (1978). Ground consolidation with liquid nitrogen (LN_2). *1st Int Symp on Ground Freezing, Germany, Bochum*. Pp 289-302.

Viklander, P. & Knutsson, S. (1994). Deformation and compaction of frozen soils. *7th Int Symp on Ground Freezing, France, Nancy*. Pp 109-115.

Viklander, P. (1995). *Frysnings- och tiningscyklers inverkan på jords permeabilitet* (Tech rep 1995:12T). Luleå: LTU.

Viklander, P. (1997). *Compaction and thaw deformation of frozen soil: Permeability and structural effects due to freezing and thawing*. Dr thesis, LTU, Dep of Civ and Min Eng.

Viklander, P. (1998). Permeability and volume changes in till due to cyclic freeze/thaw. *Can Geot J, vol* (35). Pp 471-477.

Vyalov, S., Gmoshinskii V.G., Gorodetskii, S.E., Grigorieva, V.G. & Zaretskii, Iu. K. (1962). *The strength and creep of frozen soils and calculations for ice-retaining structures* (CRREL trans 76). Hanover, N H: CRREL.

Vägverket. (2004). *Allmän teknisk beskrivning, VÄG 2004* (Vägv A11.2, Publ 2004:111). Borlänge: Vägverket.

Vähäaho, I. (1988). Soil freezing and thaw consolidation results for a major project in Helsinki. *5th Int Symp on ground freezing, UK, Nottingham*. Pp 219-223.

Vähäaho, I. (1991A). Effects of thaw consolidation on clay, *10th European conf on soil mech and found eng, Italy, Florence, vol* (2). Pp 625-628.

Vähäaho, I. (1991B). *The effects of thaw consolidation on geotechnical properties of clay* (Report 51). Helsinki: Geot dept, City of Helsinki.

Vähäaho, I., Lappalainen, V. & Ryhänen, H. (1989). Thaw consolidation of frozen clays of post-glacial origin in Helsinki. *1st Int Symp on Frost in Geot Eng, Finland, Saariselkä*. Pp 583-600.

Wallis, S. (2000). Tunnel Jacking in Boston. *World Tunnelling, Sept, 2000*.

Watson, G., Slusarchuk, W. & Rowley, R. (1973). Determination of some frozen and thawed properties of permafrost soils. *Can Geot J, vol* (10). Pp 592-606.

Williams, P.J. (1967). *Properties and behaviour of freezing soils* (Publ №72). Oslo: NGI.

Williams, P.J. (1988). Thermodynamic and mechanical conditions within frozen soils and their effects. *5th Int Conf on Permafrost, Norway, Trondheim, vol* (1). Pp 493-498.

Wind, H. (1978). The soil freezing method for large tunnel constructions. *1st Int Symp on Ground Freezing, Germany, Bochum*. Pp 119-121.

Yong, R., Cheung, C. & Sheeran, D. (1978). Prediction of salt influence on unfrozen water content in frozen soils. *1st Int Symp on Ground Freezing, Germany, Bochum*. Pp 87-101.

A APPENDIX, LABORATORY TESTS

This supplementary chapter shows results from the laboratory tests. The results are performed in standard geotechnical tests and in standard oedometer. The test samples originate from the Bothnia Line.

Table A.1 shows the number of samples per selection of samples creating a mean value for respective sampling level.

Table A.1 The number of samples per selection of samples creating a mean value for respective sampling level (3 m to 10 m below the ground surface)

Sampling		1999-02-24*	2003-10-28	2004-10-19	2006-08-07	**Total**
Bulk density	ρ	1	1	3	3	**8**
	ρ_{th}			1	2	**3**
Dry density	ρ_d	1	1	2	4	**8**
	$\rho_{d,th}$			2	4	**6**
Water content	w	1	1	3	3	**8**
	w_{th}			3	2	**5**
Limit of consistencies	w_L, w_p, I_p, I_L, I_c	1	1	1	1	**4**
	$w_{L,th}$, $w_{p,th}$, $I_{p,th}$, $I_{L,th}$, $I_{c,th}$				1	**1**

*Solely level, 4 m, 6 m, 8 m and 10 m below ground surface

Table A.2 shows the undisturbed soil bulk density based on the weight and the geometry of the soil samples in the tare.

Table A.2 Undisturbed soil bulk density (ρ), all measured at KTH's laboratory, except values from February 24th, 1999 which was measured by VBB-VIAK [kg m^{-3}]

Level [m]	1999-02-24	2003-10-28	2004-10-19 "Routine"	2004-10-19 SeriesI	2004-10-19 SeriesII	2006-08-07 "Routine"	2006-08-07 ρ_1	2006-08-07 ρ_2	2006-08-07 ρ_k	**Mean**	**Std-dev**
3		1349	1486	1492	1481	1610		1610		1505	98
4	1480	1516	1546	1493	1523	1524	1521	1528		1516	21
5		1480	1521	1515	1503	1428	1402		1454	1472	46

Level [m]	1999-02-24	2003-10-28	2004-10-19 "Routine"	2004-10-19 SeriesI	2004-10-19 SeriesII	2006-08-07 "Routine"	2006-08-07 ρ_1	2006-08-07 ρ_2	2006-08-07 ρ_k	**Mean**	**Std-dev**
6	1540	1480	1557	1602	1559	1569	1558	1570	1581	1557	34
7		1526	1487	1491	1509	1465	1468	1418	1508	1484	34
8	1510	1480	1747	1857	1761	1717	1709	1723	1720	1692	120
9			1662	1627	1643	1636	1644	1618	1645	1639	14
10	1690		1748	1706	1678	1880	1837	1880	1672	1761	90
Mean:	1555	1472	1594	1598	1582	1604	1591	1621	1597	1579	44
Std-dev:	93	64	109	131	101	145	150	147	102		

Table A.3 shows the undisturbed soil bulk density of the samples collected on October 19th, 2004. Table A.4 shows the undisturbed soil bulk density of samples collected on August 7th, 2006. The values of the undisturbed soil bulk density are based on the pre-consolidated samples due to freeze thaw tests in oedometer, i.e. the assumption of the density of the solid particles (ρ_s = 2 650 kg m^{-3}), solid mass and the volume of soils due to the pre-consolidation oedometer strain.

Table A.3 Undisturbed soil bulk density (ρ). All values are based on the freeze-thaw tests at KTH laboratory, test series I and II, collected on October 19th, 2004 [kg m^{-3}]

Level [m]	Series I	Series II	**Mean**	**Std-dev**
3	1446	1366	1406	56
4	1483	1519	1501	25
5	1493	1493	1493	0
6	1568	1537	1552	22
7	1456	1493	1474	26
8	2019	1856	1938	115
9	1695	1677	1686	13
10	1772	1706	1739	46
Mean:	1616	1581	1599	25
Std-dev:	201	155		

Table A.4 Undisturbed soil bulk density (ρ). All values are based on the freeze-thaw tests at KTH laboratory, soil specimens collected on August 7th, 2006 [kg m^{-3}]

Level [m]	Oedometer №1	Oedometer №2	Oedometer №3	Oedometer №4	**Mean**	**Std-dev**
3	1632	1618	1579	1606	1609	22
4	1537	1529	1538	1543	1537	6
5	1489	1507	1507	1521	1506	13
6	1494	1655	1614	1612	1594	69
7	1459	1472	1474	1467	1468	7
8	1715	1762	1774	1760	1753	26
9	1690	1615	1643	1660	1652	31
10	1940	1824	1861	1861	1871	49
Mean:	1620	1623	1624	1629	1624	4
Std-dev:	161	123	134	130		

Table A.5 shows the thawed soil bulk density. The values are based on samples, which were pre-consolidated, frozen and thawed in oedometer. Before and after drying in a heating oven, the samples were weighed and the volumes were measured.

Table A.5 Thawed soil bulk density (ρ_{th}), are all measured in KTH laboratory [kg m^{-3}]

Level [m]	2004-10-19 SeriesI	2004-10-19 SeriesII	2006-08-07 "Routine"	2006-08-07 ρ_{th2}	2006-08-07 ρ_{th3}	**Mean**	**Std-dev**
3	1506	1563	1690	1649	1618	1630	53
4	1548	1579	1550	1574	1540	1561	19
5	1590	1591	1520	1551	1526	1547	32
6	1611	1622	1540	1612	1682	1614	58
7	1495	1578	1470	1485	1499	1508	48
8	1932	1862	1770	1783	1810	1806	41
9	1788	1726	1730	1720	1631	1702	47
10	1797	1784	1900	1874	1796	1838	57
Mean:	1658	1663	1646	1656	1638	1651	11
Std-dev:	160	114	160	139	128	135	20

Figure A.9 and Figure A.10 show the estimated thawed soil bulk density. The values of the undisturbed soil bulk density are based on the freeze thaw tests in oedometer, i.e. the assumption of the density of the solid particles (ρ_s = 2 650 kg m^{-3}), water saturated soil (S_r = 100 %), pre-consolidated solid mass and the volume of soils based on the oedometer strain.

Table A.6 Thawed soil bulk density (ρ_{th}).Test series I and II, collected on October 19th, 2004 [kg m^{-3}]

Level [m]	Series I	Series II	**Mean**	**Std-dev**
3	1449	1377	1413	51
4	1542	1546	1544	3
5	1553	1554	1554	1
6	1626	1608	1617	13
7	1458	1557	1507	70
8	2039	1910	1975	91
9	1734	1748	1741	10
10	1835	1781	1808	38
Mean:	1654	1635	1645	14
Std-dev:	204	168		51

Table A.7 Thawed soil bulk density (ρ_{th}). Test series collected on August 7th, 2006. The value of the thawed soil bulk density for oedometers №3 and №4 are based on the soil bulk density mean value from oedometers №1 and №2, and also the oedometer strain [kg m^{-3}]

Level [m]	Oedometer №1	Oedometer №2	Oedometer №3	Oedometer №4	**Mean**	**Std-dev**
3	1690	1618	1633	1633	1644	32
4	1550	1540	1557	1557	1551	8
5	1520	1526	1539	1539	1531	9
6	1540	1682	1647	1647	1629	62

Level [m]	Oedometer №1	Oedometer №2	Oedometer №3	Oedometer №4	**Mean**	**Std-dev**
7	1470	1499	1492	1492	1488	13
8	1770	1810	1797	1797	1793	17
9	1730	1631	1676	1676	1678	40
10	1900	1796	1835	1835	1841	43
Mean:	1646	1638	1647	1647	1644	4
Std-dev:	149	118	121	121		

Table A.8 shows the undisturbed soil dry density, before and after drying in a heating oven the samples were weighed and the volume was measured.

Table A.8 Undisturbed soil dry density (ρ_d), all values are measured at KTH laboratory, except values from February 24th, 1999, which were measured by VBB-VIAK [kg m^{-3}]

Level [m]	1999-02-24	2003-10-28	2004-10-19	2006-08-07	**Mean**	**Std-dev**
3		581	762	996	780	208
4	771	838	854	853	829	39
5		718	796	743	753	40
6	870	744	890	902	851	73
7		795	763	725	761	35
8	839	744	1205	1119	977	220
9			1007	981	994	18
10	1050		1222	1361	1211	156
Mean:	882	737	937	960	879	100
Std-dev:	119	87	188	209	151	57

Table A.9 shows the undisturbed soil dry density. The values are based on samples which were subjected to freeze-thaw tests in oedometer, i.e. the assumption of the density of the solid particles (ρ_s = 2 650 kg m^{-3}), water saturated soil (S_r = 100 %), primary consolidated solid mass and the volume of soils based on the oedometer strain.

Table A.9 Undisturbed soil dry density (ρ_d). All values are measured at KTH laboratory in connection with the freeze-thaw tests. The test series are collected on October 19th, 2004 and August 7th, 2006. The value of the thawed soil bulk density for oedometers №3 and №4 are based on the soil bulk density mean value from oedometers №1 and №2, and also the oedometer strain [kg m^{-3}]

Level [m]	2004-10-19 SeriesI	2004-10-19 SeriesII	2006-08-07 Oedo№1	2006-08-07 Oedo№2	2006-08-07 Oedo№3	2006-08-07 Oedo№4	**Mean**	**Std-dev**
3	720	595	959	992	895	936	849	157
4	795	845	809	787	822	828	814	22
5	813	810	754	759	777	788	783	25
6	912	882	770	994	926	932	903	75
7	732	811	691	722	729	717	734	41
8	1637	1388	1113	1185	1208	1192	1287	194
9	1116	1107	1015	884	964	973	1010	89
10	1239	1163	1388	1201	1285	1282	1260	78
Mean:	995	950	937	941	951	956	955	21
Std-dev:	323	223	251	199	214	210	237	

Table A.10 shows the undisturbed soil dry density. The values are based on samples which were subjected to freeze-thaw tests in oedometer, i.e. the assumption of the density of the solid particles (ρ_s = 2 650 kg m^{-3}), water saturated soil (S_r = 100 %), primary consolidated solid mass and the volume of soils based on the oedometer strain.

Table A.10 Thawed soil dry density ($\rho_{d,th}$). All values are measured at KTH laboratory in connection with the freeze-thaw tests. Test series are collected at 2004-10-19 and at August 7th, 2006. The value of the thawed soil bulk density for oedometers №3 and №4 are based on the soil bulk density mean value from oedometers №1 and №2, and also the oedometer strain [kg m^{-3}]

Level [m]	2004-10-19 SerieI	2004-10-19 SerieII	2006-08-07 Odo№1	2006-08-07 Odo№2	2006-08-07 Odo№3	2006-08-07 Odo№4	**Mean**	**Std-dev**
3	721	605	1108	992	1017	1017	910	199
4	871	877	883	867	895	895	881	12
5	888	890	835	845	865	865	865	22
6	1005	976	867	1096	1039	1039	1004	78
7	735	894	755	802	790	790	794	55
8	1668	1462	1237	1301	1279	1279	1371	165
9	1178	1201	1172	1014	1085	1085	1123	73
10	1341	1254	1445	1278	1340	1340	1333	66
Mean:	1051	1020	1038	1024	1039	1039	1035	11
Std-dev:	323	229	257	205	210	210	239	

The in situ vertical stress conditions are based on the actual water table at the level of the ground surface. Table A.11 shows the estimated undisturbed, in situ, soil, vertical effective stress (σ_v'). Table A.12 shows the estimated thawed, in situ, soil, vertical, effective stress ($\sigma_{v,th}$'). The results from 2006 in Table A.12 are based on the mean value of two tests, everything else from one test sample at each depth. The results are based on the CRS-tests with the exception of the results from 1999, which are based on the VBB-VIAK results.

Table A.11 Undisturbed soil, vertical effective stress, σ'_v. The values are based on the actual water table at the ground surface level [kPa]

Level [m]	1999-02-24	2003-10-28	2004-10-19	2006-08-07	**Mean**	**Std-dev**
3		18	20	23	21	2
4	25	24	25	31	26	3
5		28	31	38	32	5
6	35	33	36	47	38	6
7		39	41	54	45	8
8	46	43	48	64	50	9
9			55	70	63	11
10	59		63	78	67	10
Mean:	41	31	40	51	41	31
Std-dev:	15	9	15	19	15	9

Table A.12 Thawed soil, vertical effective stress, $\sigma'_{v,th}$, The values are based on the actual water table at ground surface level [kPa]

Level [m]	2004-10-19	2006-08-07	2006-08-07	**Mean**	**Std-dev**
3	15	17	22	18	4
4	21	24	27	24	3
5	28	29	33	30	2
6	35	36	38	36	1
7	41	41	43	42	1
8	49	49	50	50	1
9	57	56	58	57	1
10	66	64	67	65	1
Mean:	39	40	42	40	2
Std-dev:	18	16	15	16	

Preconsolidation pressures are interpreted from CRS-laboratory tests, see Table A.13, and Table A.14. Figure A.1 shows the estimated overconsolidation ratio (OCR).

Table A.13 Undisturbed soil preconsolidation pressure, σ'_c [kPa]

Level [m]	1999-02-24	2003-10-28	2004-10-19	2004-10-19	2006-08-07	2006-08-07	**Mean**	**Std-dev**
3		6	12	8	13	18	11.4	4.7
4	23	13	23	20	23	22	20.7	3.9
5		20	22	25	23	15	21.0	3.8
6		25	30	35	27	32	29.8	4.0
7		40	20	22	20	22	24.8	8.6
8	40	45	50	40	25	40	40.0	8.4
9		42	45	48	38	34	41.4	5.5
10	38	-	55	40	45	40	36.3	18.8
Mean:	33.7	23.9	35.0	32.9	26.8	27.9	29.6	2.8
Std-	9.3	17.2	14.7	10.7	10.2	9.9	12.3	2.9

Table A.14 Thawed soil preconsolidation pressure, σ'_c, interpreted from CRS-tests [kPa]

Level [m]	2006-08-07	2006-08-07	**Mean**	**Std-dev**
3	16	18	17	1.4
4	23	28	26	3.5
5	20	25	23	3.5
6	45	25	35	14.1
7	30	30	30	-
8	30	45	38	10.6
9	60	60	60	-
10	70	70	70	-
Mean:	36.8	37.6	37.2	0.6
Std-dev:	19.7	18.7	19.2	

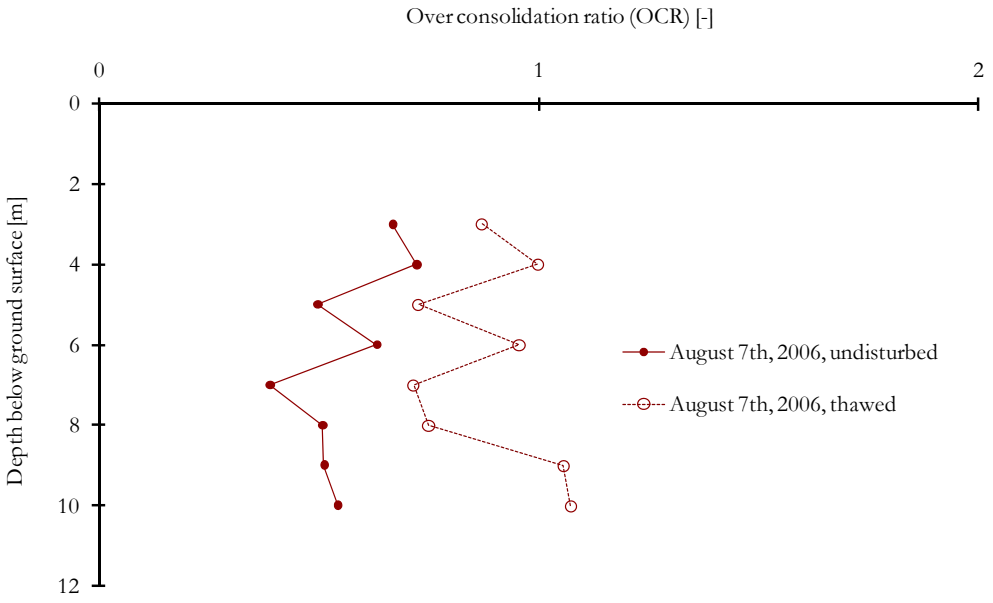

Figure A.1 Overconsolidation ratio, the values are based on Table A.11 to Table A.14

Table A.15 and Table A.16 show the undisturbed soil water content (w) obtained by weighing the undisturbed soil, drying in heating oven and weighing again.

Table A.15 Undisturbed soil water content (w), all values measured at KTH laboratory, except values from February 24th, 1999, which were analysed by VBB-VIAK [%]

Level [m]	1999-02-24	2003-10-28	2004-10-19 "Routine"	2004-10-19 SeriesI	2004-10-19 SeriesII	2006-08-07 w_1	2006-08-07 "Routine"	2006-08-07 w_2	**Mean**	**Std-dev**
3		132	95	89	92	73	57	55	85	26
4	92	81	81	88	81	89	72	75	82	7
5		106	91	83	86	83	96	97	92	8
6	77	99	75	66	74	74	74	75	77	10
7		92	95	89	85	97	109	100	95	8
8	80	99	45	35	44	53	53	55	58	21
9			65	62	59	64	69	67	64	4
10	61		43	50	54	39	39	36	46	9
Mean:	78	102	74	70	72	71	71	70	76	11
Std-dev:	13	17	21	20	17	19	23	22	19	

Table A.16 Undisturbed soil water content (w), mean values for each collected test occasion. Samples collected on February 24th, 1999, were analysed by VBB-VIAK and are based on only one sample per level [%]

Level [m]	1999-02-24	2003-10-28	2004-10-19	2006-08-07	**Mean**	**Std-dev**
3		132	95	62	96	35
4	92	81	81	79	83	6
5		106	91	92	96	8
6	77	99	75	74	81	12
7		92	95	102	96	5
8	80	99	45	53	69	25
9			65	67	66	1

Level [m]	1999-02-24	2003-10-28	2004-10-19	2006-08-07	**Mean**	**Std-dev**
10	61		43	38	47	12
Mean:	78	102	74	71	79	14
Std-dev:	13	17	21	21	18	

Table A.17 and Table A.18 show the thawed soil water content (w_{th})obtained by weighing the thawed soil sample, drying in heating oven and weighing again.

Table A.17 Thawed soil water content (w_{th}), i.e. the soil water content after pre-consolidation, freezing and thawing under the in situ effective stress in an oedometer [%]

Level [m]	2004-10-19	2004-10-19	2004-10-19	2006-08-07	2006-08-07	**Mean**	**Std-dev**
3	86	85	73	58	63	73	13
4	77	76	70	71	78	74	4
5	83	68	68	75	81	75	7
6	68	64	62	64	54	62	5
7	91	88	70	91	87	85	9
8		29	35	42	39	36	6
9	62	41	48	49	61	52	9
10	47	40	42	34	41	41	5
Mean:	73	61	58	60	63	63	6
Std-dev:	15	22	15	19	18	18	

Table A.18 Thawed soil water content (w_{th}), mean values at each test occasion [%]

Level [m]	2004-10-19	2006-08-07	**Mean**	**Std-dev**
3	81	61	71	15
4	74	74	74	0
5	73	78	75	4
6	65	59	62	4
7	83	89	86	4
8	21	40	31	14
9	50	55	53	3
10	43	37	40	4
Mean:	61	62	61	0
Std-dev:	22	18	19	

Figure A.19 and Table A.21 show the undisturbed soil water content. The values are based on samples, which were subjected to freeze-thaw tests in oedometer, i.e. the assumption of the density of the solid particles (ρ_s = 2 650 kg m^{-3}), water saturated soil (S_r = 100 %), primary consolidated solids mass and the volume of soils based on the oedometer strain.

Figure A.20 and Table A.22 show the thawed soil water content. The values are based on samples, which were pre-consolidated, frozen and thawed in oedometer, i.e. the assumption of the density of the solid particles (ρ_s = 2 650 kg m^{-3}), water saturated soil (S_r = 100 %), the mass of solids and the volume of soils based on the oedometer strain after the thawing.

Figure A.2 shows the undisturbed soil water content, relative change of water content after freezing and relative thaw deformation in oedometer for samples collected on October 2004 and August 2006.

Table A.23 and Table A.24 show the void ratio for undisturbed soil and thawed soil respectively.

Table A.19 Undisturbed soil water content (w) for samples collected on October 19th, 2004. Calculated values are based on the oedometer deformations [%]

Level [m]	Oedo №1	Oedo №2	**Mean**	**Std-dev**
3	104	134	119	21
4	91	84	87	5
5	89	87	88	1
6	77	77	77	0
7	102	88	95	10
8	25	36	30	8
9	55	56	55	0
10	49	56	52	5
Mean:	74	77	76	2
Std-dev:	28	29		

Table A.20 Thawed soil water content (w_{th}) for samples collected on October 19th, 2004. Calculated values are based on the oedometer deformations [%]

Level [m]	Oedo №1	Oedo №2	**Mean**	**Std-dev**
3	101	127	114	19
4	77	76	77	1
5	75	75	75	0
6	62	65	63	2
7	98	74	86	17
8	22	31	26	6
9	47	45	46	1
10	37	42	39	4
Mean:	65	67	66	1
Std-dev:	28	30		

Table A.21 Undisturbed soil water content (w) for samples collected on August 7th, 2006. Calculated values are based on the oedometer deformations. Oedometers №3 and №4's initial values come from the freeze thaw mean value of oedometers №1 and №2 [%]

Level [m]	Oedo №1	Oedo №2	Oedo №3	Oedo №4	**Mean**	**Std-dev**
3	70	58	67	63	64	5
4	90	86	89	88	88	2
5	98	93	99	98	97	3
6	94	78	96	95	91	8
7	111	108	109	111	110	2
8	54	52	50	51	52	2
9	67	68	62	63	65	3
10	40	44	39	39	40	2

Level [m]	Oedo №1	Oedo №2	Oedo №3	Oedo №4	**Mean**	**Std-dev**
Mean:	78	73	76	76	76	2
Std-dev:	24	22	25	26		

Table A.22 Thawed soil water content (w_{th}), calculated values after pre-consolidation, freezing and thawing in oedometer for soil collected on August 7th, 2006. Oedometers №3 and №4's initial values come from the freeze thaw mean value of oedometers №1 and №2 [%]

Level [m]	Oedo №1	Oedo №2	Oedo №3	Oedo №4	**Mean**	**Std-dev**
3	53	58	53	53	54	3
4	75	71	75	75	74	2
5	82	75	82	82	80	3
6	78	64	78	78	74	7
7	95	91	95	95	94	2
8	43	42	43	43	43	1
9	48	49	48	48	48	1
10	31	34	31	31	32	1
Mean:	63	60	63	63	62	1
Std-dev:	22	19	22	22		

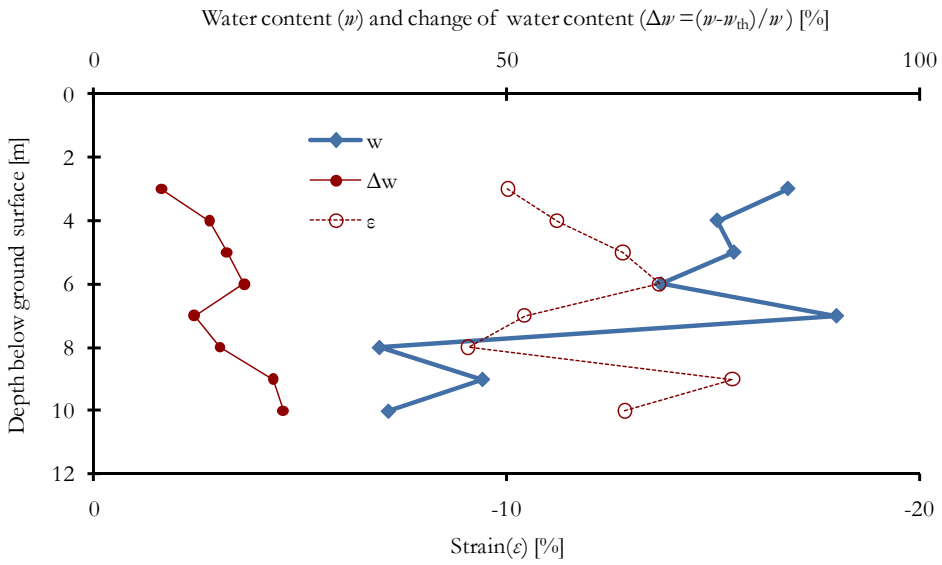

Figure A.2 Undisturbed soil water content (w), relative change of water content after freezing (Δw) and relative thaw deformation (ε) in oedometer for samples collected on August 2006

Table A.23 Undisturbed soil void ratio (e), all samples analyzed at KTH, except samples collected on February 24th, 1999, which were analysed by VBB-VIAK [-]

Level [m]	1999-02-24	2003-10-28	2004-10-19	2006-08-07	**Mean**	**Std-dev**
3		3.5	2.5	1.6	2.6	0.9
4	2.4	2.1	2.1	2.1	2.2	0.2
5		2.8	2.4	2.4	2.6	0.2
6	2.0	2.6	2.0	2.0	2.2	0.3
7		2.4	2.5	2.7	2.6	0.1
8	2.1	2.6	1.2	1.4	1.8	0.7
9			1.7	1.8	1.7	0.0
10	1.6		1.1	1.0	1.3	0.3
Mean:	2.1	2.7	2.0	1.9	2.1	0.4
Std-dev:	0.3	0.5	0.6	0.5	0.5	

Table A.24 Thawed soil void ratio (e_{th}), i.e. soil specimen pre-consolidated, frozen and thawed in oedometer under load of in-situ effective stress [%]

Level [m]	2004-10-19	2006-08-07	**Mean**	**Std-dev**
3	2.4	1.1	1.8	1.0
4	1.9	1.4	1.7	0.3
5	2.0	1.7	1.9	0.2
6	1.7	1.2	1.5	0.3
7	2.3	1.8	2.1	0.3
8	1.1	0.9	1.0	0.2
9	1.5	1.4	1.4	0.1
10	1.0	0.9	1.0	0.0
Mean:	1.7	1.3	1.5	0.3
Std-dev:	0.5	0.3	0.4	

Table A.25 shows the undisturbed soil hydraulic conductivity and Table A.26 shows the thawed soil hydraulic conductivity, the values are based on CRS-tests.

Table A.25 Undisturbed soil hydraulic conductivity (permeability, k) [m s^{-1}]. All samples are analyzed at KTH, except samples collected on February 24th, 1999, which were analysed by VBB-VIAK [%]

Level [m]	1999-02-24	2003-10-28	2004-10-19	2004-10-19	2006-08-07	2006-08-07	**Mean**	**Std-dev**
3		3.0E-09	1.4E-08	8.8E-08	4.2E-09	2.7E-09	2.2E-08	3.7E-08
4	2.2E-09	2.5E-09	1.7E-09	2.1E-09	2.1E-09	1.9E-09	2.1E-09	2.9E-10
5		3.7E-09	1.4E-09	8.9E-10	2.8E-09	3.1E-09	2.4E-09	1.2E-09
6		3.6E-09	1.4E-10	9.5E-10	1.4E-09	1.2E-09	1.5E-09	1.3E-09
7		3.2E-09	1.1E-08	4.6E-09	1.7E-09	7.8E-10	4.2E-09	4.0E-09
8	7.3E-10	5.6E-09	2.4E-08	4.7E-08	1.6E-08	1.4E-08	1.8E-08	1.6E-08
9		5.0E-09	2.2E-09	2.7E-09	3.7E-09	2.1E-09	3.1E-09	1.2E-09
10	5.2E-10		2.8E-09	1.2E-09	3.0E-09	4.7E-09	2.4E-09	1.6E-09
Mean:	1.2E-09	3.8E-09	7.1E-09	1.8E-08	4.3E-09	3.8E-09	6.4E-09	6.2E-09
Std-dev:	9.3E-10	1.1E-09	8.4E-09	3.2E-08	4.6E-09	4.3E-09	8.6E-09	

Table A.26 Thawed soil hydraulic conductivity (permeability, k) [m s^{-1}]

Level [m]	2006-08-07	2006-08-07	Mean	Std-dev
3	6.2E-09	3.4E-09	4.8E-09	2.0E-09
4	6.2E-09	4.7E-09	5.4E-09	1.1E-09
5	4.7E-09	3.7E-09	4.2E-09	6.6E-10
6	6.5E-09	3.7E-09	5.1E-09	1.9E-09
7	6.9E-09	3.5E-09	5.2E-09	2.4E-09
8	1.8E-08	9.9E-09	1.4E-08	6.0E-09
9	5.0E-09	1.1E-08	7.9E-09	4.2E-09
10	4.7E-09	2.3E-09	3.5E-09	1.7E-09
Mean:	7.3E-09	5.3E-09	6.3E-09	1.5E-09
Std-dev:	4.6E-09	3.2E-09	3.9E-09	

Table A.27 to Table A.32 show limit of consistencies.

Table A.27 Undisturbed soil liquid limit (in fall-cone apparatus) ($w_{L,cone}$), all samples are analyzed at KTH, except samples collected on February 24th, 1999, which were analysed by VBB-VIAK [%]

Level [m]	1999-02-24	2003-10-28	2004-10-19	2006-08-07	**Mean**	**Std-dev**
3		137	97	53	96	42
4	70	76	90	85	80	9
5		91	101	110	101	10
6	68	99	84	82	83	13
7		113	123	117	118	5
8	72	116	47	57	73	30
9			62	70	66	6
10	44		46	39	43	4
Mean:	64	105	81	77	82	17
Std-dev:	13	21	27	27	22	

Table A.28 Thawed soil liquid limit (in fall-cone apparatus) ($w_{L,th,cone}$), i.e. soil consolidated, frozen and thawed in oedometer under load of in-situ effective stress [%]

Level [m]	1999-02-24	2003-10-28	2004-10-19	2006-08-07	**Mean**	**Std-dev**
3				60		
4				88		
5				91		
6				58		
7				101		
8				41		
9				63		
10				43		
Mean:				68.1		
Std-dev:				22.5		

Table A.29 Undisturbed soil plastic limit (w_P) [%]

Level [m]	1999-02-24	2003-10-28	2004-10-19	2006-08-07	**Mean**	**Std-dev**
3		62	45	23	43	19
4		35	36	44	38	5
5		39	42	42	41	2
6		41	36	42	40	3
7		42	50	65	52	12
8		45	27	31	34	9
9			29	32	30	2
10			24	24	24	0
Mean:		44.0	36.1	38.0	39	4
Std-dev:		9.4	9.2	13.7	11	

Table A.30 Thawed soil plastic limit ($w_{P,th}$) [%]

Level [m]	1999-02-24	2003-10-28	2004-10-19	2006-08-07	**Mean**	**Std-dev**
3				33		
4				51		
5				43		
6				30		
7				50		
8				35		
9				43		
10				19		
Mean:				38.0		
Std-dev:				10.8		

Table A.31 Undisturbed soil plasticity index ($I_p = w_L - w_P$) [%]

Level [m]	1999-02-24	2003-10-28	2004-10-19	2006-08-07	**Mean**	**Std-dev**
3		75	52	30	52	23
4		41	54	41	45	7
5		52	59	68	60	8
6		58	48	40	49	9
7		71	73	52	65	12
8		71	20	26	39	28
9			33	38	36	4
10			22	15	19	5
Mean:		61.33	45.13	38.68	48	12
Std-dev:		13.31	18.58	16.19	16	

Table A.32 Thawed soil plasticity index ($I_{p,th} = w_{L,th} - w_{P,th}$) [%]

Level [m]	1999-02-24	2003-10-28	2004-10-19	2006-08-07	**Mean**	**Std-dev**
3				27		
4				37		
5				48		
6				28		
7				51		
8				6		
9				20		
10				24		
Mean:				30.13		
Std-dev:				14.83		

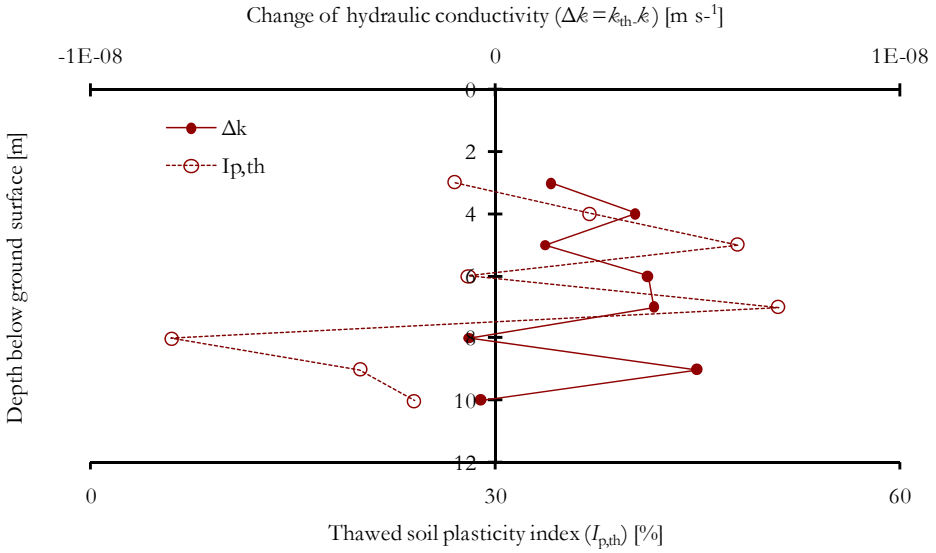

Figure A.3 Change of hydraulic conductivity ($\Delta k = k_{th} - k$) and thawed soil plasticity index ($I_{p,th}$) vs. Depth below ground surface. Samples collected on August 2006

Table A.33 to Table A.38 show results related to fall-cone apparatus i.e. the undrained shear strength or the soil sensitivity.

Table A.33 Undisturbed soil undrained shear strength (in fall-cone apparatus) (τ_{fu}) [kPa]

Level [m]	1999-02-24	2003-10-28	2004-10-19	2006-08-07	**Mean**	**Std-dev**
3		3.0	8.3	10.0	7	3.6
4	7.3	6.2	8.5	15.0	9	3.9
5		7.1	8.5	11.4	9	2.2
6	13.0	7.9	11.8	21.1	13	5.6
7		9.5	8.0	11.4	10	1.7
8	13.0	7.4	14.6	14.5	12	3.4
9			12.9	10.2	12	1.9
10	11.0		15.8	20.5	16	4.7
Mean:	11	7	11	14		
Std-dev:	2.7	2.2	3.2	4.4		

Table A.34 Remoulded "undisturbed" soil shear strength (in fall-cone apparatus) (τ_{fu}) [kPa]

Level [m]	1999-02-24	2003-10-28	2004-10-19	2006-08-07	**Mean**	**Std-dev**
3		0.5	1.2	1.1	0.9	0.4
4	0.3	0.9	1.1	2.0	1.1	0.7
5		2.6	1.2	1.9	1.9	0.7
6	0.7	1.3	1.5	2.1	1.4	0.6
7		1.2	1.9	1.2	1.4	0.4
8	0.8	1.2	1.4	1.5	1.2	0.3
9			0.3	0.7	0.5	0.3
10	0.2		0.3	1.3	0.6	0.6
Mean:	0.5	1.3	1.1	1.5	1.1	0.4
Std-dev:	0.3	0.7	0.6	0.5	0.5	

Table A.35 Undisturbed soil sensitivity (S_t)

Level [m]	1999-02-24	2003-10-28	2004-10-19	2006-08-07	**Mean**	**Std-dev**
3		5.6	6.6	9.4	7.2	2.0
4	29.0	6.7	7.9	7.4	12.7	10.9
5		2.8	6.9	6.1	5.3	2.2
6	19.0	6.1	8.0	9.9	10.7	5.7
7		8.2	4.3	9.2	7.2	2.6
8	15.0	6.1	10.1	9.6	10.2	3.7
9			50.7	14.3	32.5	25.7
10	69.0		54.3	16.2	46.5	27.2
Mean:	33.0	5.9	18.6	10.2	16.9	11.9
Std-dev:	24.7	1.8	21.0	3.4	14.8	

Table A.36 Thawed soil undrained shear strength (in fall-cone apparatus) ($\tau_{fu,th}$) [kPa]

Level [m]	1999-02-24	2003-10-28	2004-10-19	2006-08-07	**Mean**	**Std-dev**
3				14.8		
4				9.1		
5				18.8		
6				16.3		
7				17.4		
8				36.1		
9				33.1		
10				36.4		
Mean:				22.8		
Std-dev:				10.7		

Table A.37 Remoulded thawed soil undrained shear strength (in fall-cone apparatus) ($\tau_{fu,th}$) [kPa]

Level [m]	1999-02-24	2003-10-28	2004-10-19	2006-08-07	**Mean**	**Std-dev**
3				0.9		
4				2.0		
5				1.9		
6				2.1		
7				2.0		
8				1.9		
9				2.8		
10				2.3		
Mean:				2.0		
Std-dev:				0.5		

Table A.38 Thawed soil sensitivity ($S_{t,th}$)

Level [m]	1999-02-24	2003-10-28	2004-10-19	2006-08-07	**Mean**	**Std-dev**
3				15.6		
4				4.7		
5				9.8		
6				7.8		
7				8.8		
8				18.6		
9				11.9		
10				15.8		
Mean:				11.6		
Std-dev:				4.7		

The organic content have been estimated by measuring the ignition loss at three different levels below the ground surface, namely 5 m, 6 m and 8 m, The results derive from samples collected on 28th, October 2003, see Table A.39 and Figure A.4.

Table A.39 Undisturbed soil ignition loss from samples collected on 28th, October 2003

Level [m]	1999-02-24	2003-10-28	2004-10-19	2006-08-07	**Mean**	**Std-dev**
3						
4						
5		4.6				
6		3.4				
7						
8		1.3				
9						
10						
Mean:		3.1				
Std-dev:		1.7				

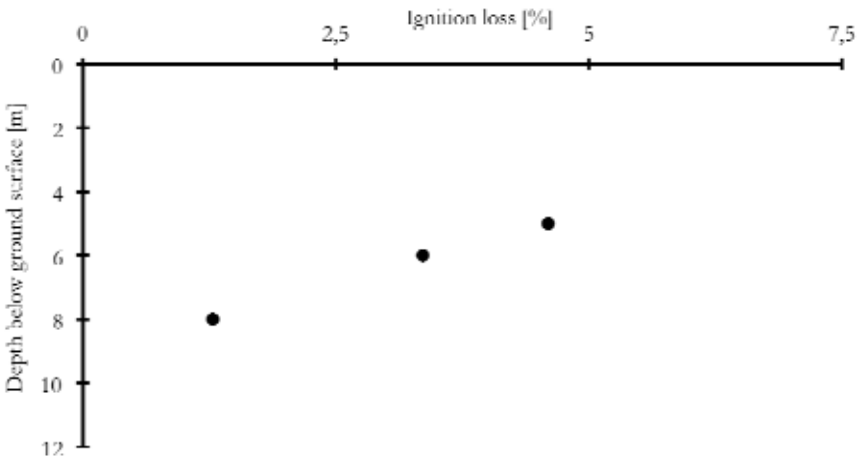

Figure A.4 The ignition loss for undisturbed soil at samples collected on October 28th, 2003. Samples originate from 5 m, 6 m and 8 m depth below ground surface

Grain size distribution was investigated of soil collected on August 7th, 2006. The samples originating from level 3 m, 5 m, 7 m and 9 m below the ground surface. The tests have been performed in the laser equipment, Malvern Mastersizer 2000. However, the results originate from two equivalent tests, i.e. the mean value. Figure A.5 shows a plot of each sample from respective level illustrating the relative volume.

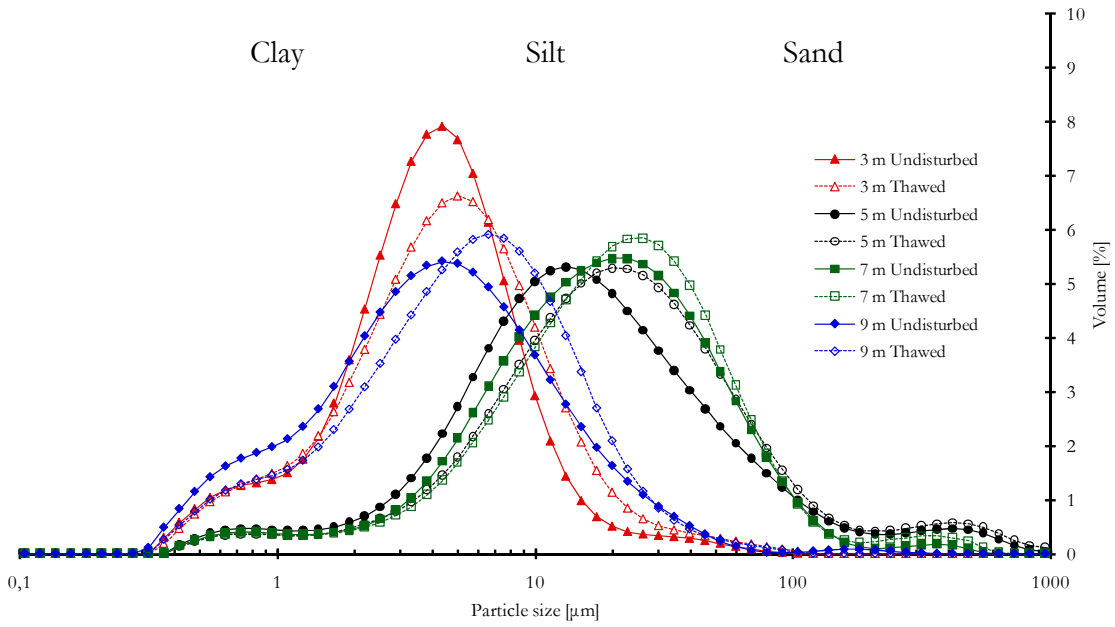

Figure A.5 Undisturbed soil and thawed soil grain size distribution, showing the mean value from two tests series. The soil originates from August 7th, 2006

In the same fashion, Figure A.6 to Figure A.9 show the three different soil grain size distributions at each level, namely; undisturbed soil, undisturbed, dried soil and thawed soil (i.e. pre-consolidated, frozen and thawed soil sample under the in-situ effective stress). However, the plots show the contained relative volume of the grain size.

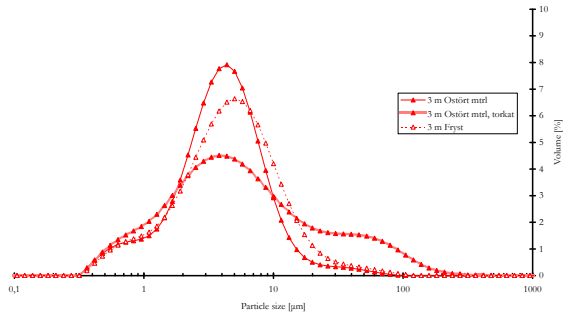

Figure A.6 *Grain size distribution for undisturbed soil, undisturbed, dried soil and thawed soil at a depth of 3 m below ground surface*

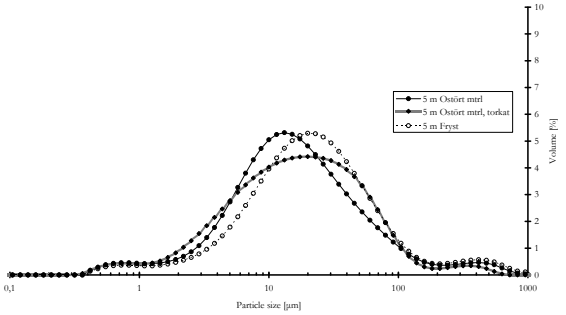

Figure A.7 *Grain size distribution for undisturbed soil, undisturbed, dried soil and thawed soil at a depth of 5 m below ground surface*

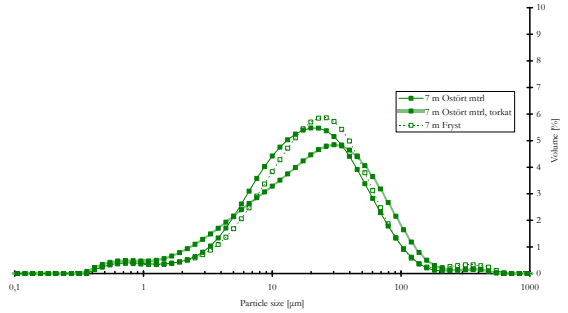

Figure A.8 *Grain size distribution for undisturbed soil, undisturbed, dried soil and thawed soil at a depth of 7 m below ground surface*

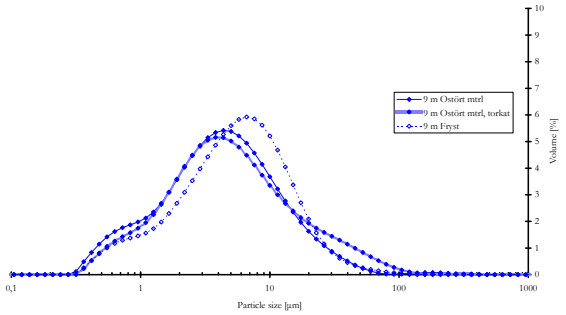

Figure A.9 *Grain size distribution for undisturbed soil, undisturbed, dried soil and thawed soil at a depth of 9 m below ground surface*

The freeze-thaw tests were performed in a climate chamber with standard oedometers. However, the oedometer one-dimensional pressure at each level below the ground surface corresponded to the actual in-situ effective stress. Table A.40 shows the actual in-situ stress.

Table A.40 Oedometer stress at each level for the freeze thaw tests, i.e. the static stress in the oedometer freeze thaw tests during the pre-consolidation, freezing and thawing

Level [m]	Vertical. stress [kPa]	Effective stress [kPa]
1	17.5	7.5
2	35.0	15.0
3	49.9	19.9
4	65.3	25.3
5	80.5	30.5
6	96.1	36.1
7	111.0	41.0
8	128.4	48.4
9	145.1	55.1
10	162.5	62.5

Oedometer freeze-thaw tests of Bothnia soil, collected on October 28th, 2004

Figure A.10 and Figure A.13 show the results from the freeze-thaw laboratory tests. The deformations for the depths between 3 m to 10 m have been registered in two test series per level. Each test series consists of simultaneous performed freeze-thawing in four standard oedometers. These results are presented in Table A.42 to Table A.45. However, the results for each registered deformation for the mean value of both tests series are presented for each level in Table A.41.

Table A.41 Compilation of oedometer freeze-thaw tests for Bothnia soil, 3 m to 10 m below the ground surface. Mean values for measured deformations in two different tests series, namely Series I and Series II (i.e. totally 1+ 1 = 2 oedometer tests at each ground level). Soil collected on October 19th, 2004

Level	Pre-consolidation	Heave	Thaw-Settlement	Calc net Heave (H)	Calc net Settlement (S)	Calc total Settlement (H + S)
m	[mm]	[mm]	[mm]	[%]	[%]	[%]
3	-0.55	-0.14	-0.74	2.1	-1.0	-3.0
4	-0.69	0.00	-1.88	3.5	-6.2	-9.4
5	-0.96	-0.31	-2.63	3.4	-8.7	-11.8
6	-1.00	-0.32	-2.80	3.6	-9.5	-12.6
7	-1.03	-0.51	-1.94	2.7	-4.9	-7.4
8	-0.76	-0.28	-1.43	2.5	-3.5	-5.8
9	-2.00	-1.24	-3.20	4.2	-6.6	-10.4
10	-1.75	-0.15	-3.10	8.8	-7.4	-14.9

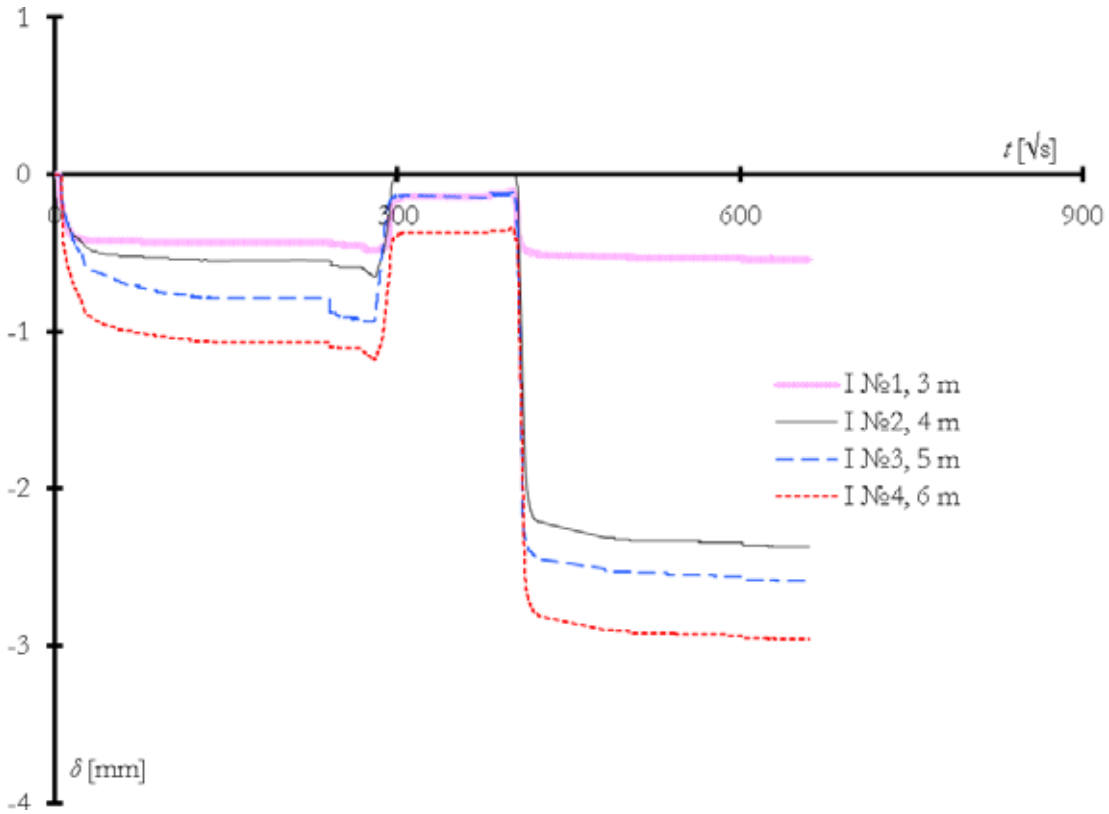

Figure A.10 Oedometer freeze-thaw laboratory tests from the depths of 3 m to 6 m below the ground surface for Bothnia Line soil. The figure shows the results of four simultaneous performed freeze-thaw oedometer tests for oedometer №1 to №4 in Series I for soil collected on October 19th, 2004

Table A.42 Freeze-thaw tests from the depths of 3 m to 6 m below the ground surface. Measured deformations for series I in the four oedometers, namely oedometer №1 to №4. Bothnia soil collected on October 19th, 2004

[mm]	3 m	4 m	5 m	6 m	**Mean**	**Std-dev**
Pre-consolidation	-0.48	-0.65	-0.94	-1.18	-0.81	0.31
Heave	-0.10	0.01	-0.11	-0.34	-0.14	0.15
Thaw settlement	-0.53	-2.33	-2.55	-2.93	-2.09	1.07
Net [%]						
Pre-consolidation	-2.400	-3.250	-4.700	-5.900	-4.063	1.550
Heave	1.900	3.300	4.150	4.200	3.388	1.074
Thaw settlement	-2.150	-11.700	-12.200	-12.950	-9.750	5.093

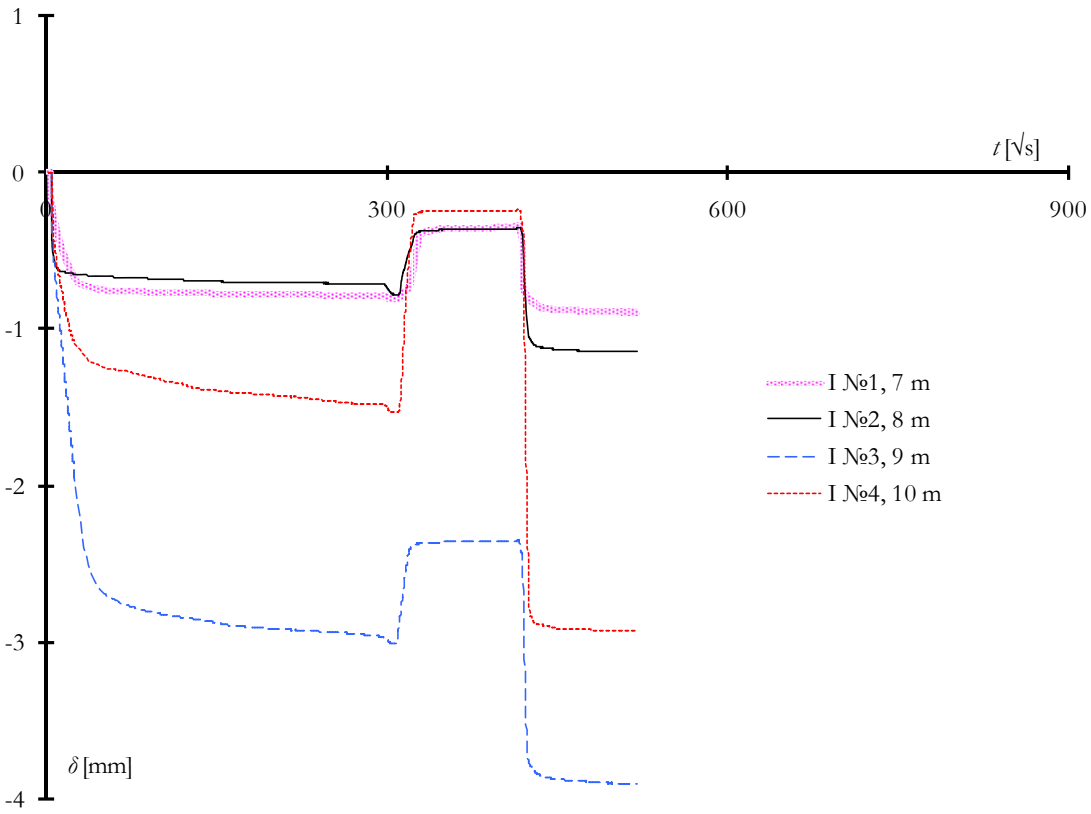

Figure A.11 Oedometer freeze-thaw laboratory tests from the depths of 7 m to 10 m below the ground surface for Bothnia Line soil. The figure shows the results of four simultaneous performed freeze-thaw oedometer tests for oedometer №1 to №4 in Series I for soil collected on October 19th, 2004

Table A.43 Freeze-thaw tests from the depths of 7 m to 10 m below the ground surface. Measured deformations for series I in the four oedometers, namely oedometer №1 to №4. Bothnia soil collected on October 19th, 2004

[mm]	7 m	8 m	9 m	10 m	**Mean**	**Std-dev**
Pre-consolidation	-0.81	-0.78	-3.00	-1.53	-1.53	1.04
Heave	-0.34	-0.35	-2.34	-0.23	-0.82	1.02
Thaw settlement	-0.89	-1.14	-3.90	-2.93	-2.22	1.44
Net [%]						
Pre-consolidation	-4.1	-3.9	-15.0	-7.7	-7.6	5.20
Heave	2.3	2.2	3.3	6.6	3.6	2.01
Thaw settlement	-2.8	-3.9	-7.8	-13.6	-7.0	4.84

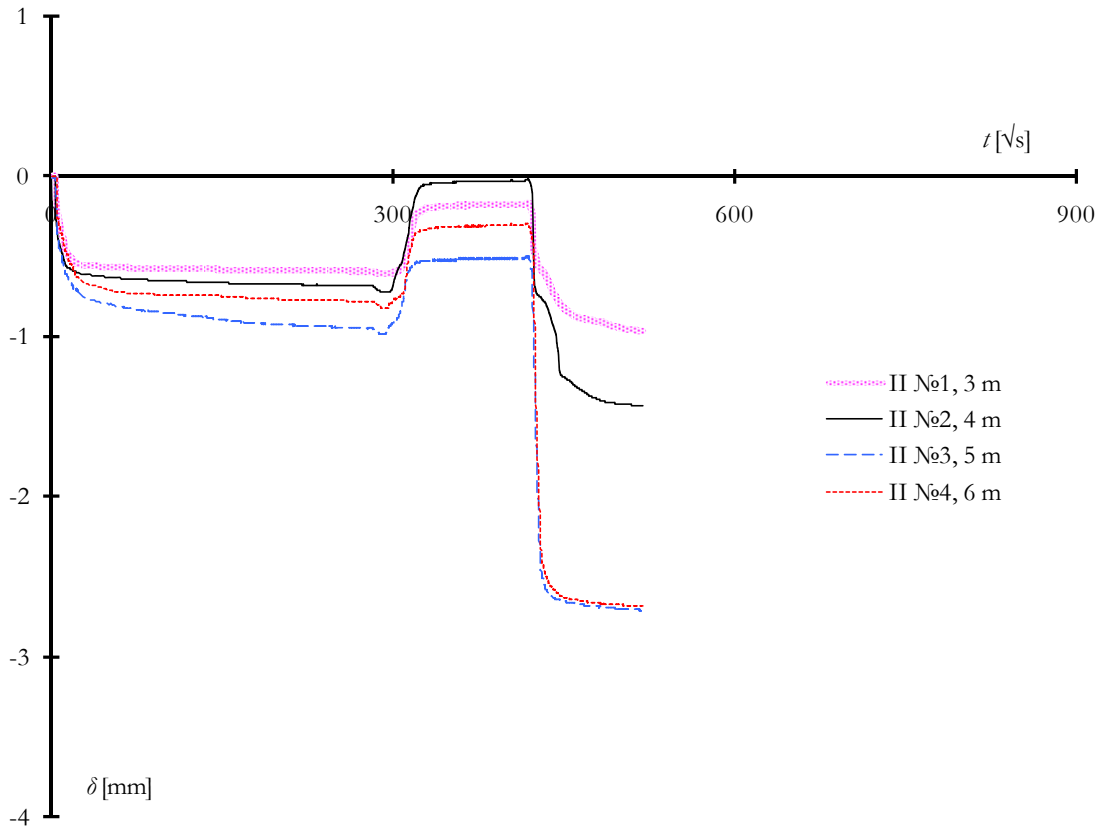

Figure A.12 Oedometer freeze-thaw laboratory tests from the depths of 3 m to 6 m below the ground surface for Bothnia Line soil. The figure shows the results of four simultaneous performed freeze-thaw oedometer tests for oedometer №1 to №4 in Series II for soil collected on October 19th, 2004

Table A.44 Freeze-thaw tests from the depths of 3 m to 6 m below the ground surface. Measured deformations for series II in the four oedometers, namely oedometer №1 to №4. Bothnia soil collected on October 19th, 2004

[mm]	3 m	4 m	5 m	6 m	**Mean**	**Std-dev**
Pre-consolidation	-0.61	-0.72	-0.98	-0.82	-0.78	0.16
Heave	-0.17	-0.01	-0.50	-0.29	-0.24	0.21
Thaw settlement	-0.95	-1.42	-2.70	-2.67	-1.94	0.89
Net [%]						
Pre-consolidation	-3.1	-3.6	-4.9	-4.1	-3.9	0.79
Heave	2.2	3.6	2.4	2.7	2.7	0.60
Thaw settlement	-3.9	-7.1	-11.0	-11.9	-8.5	3.70

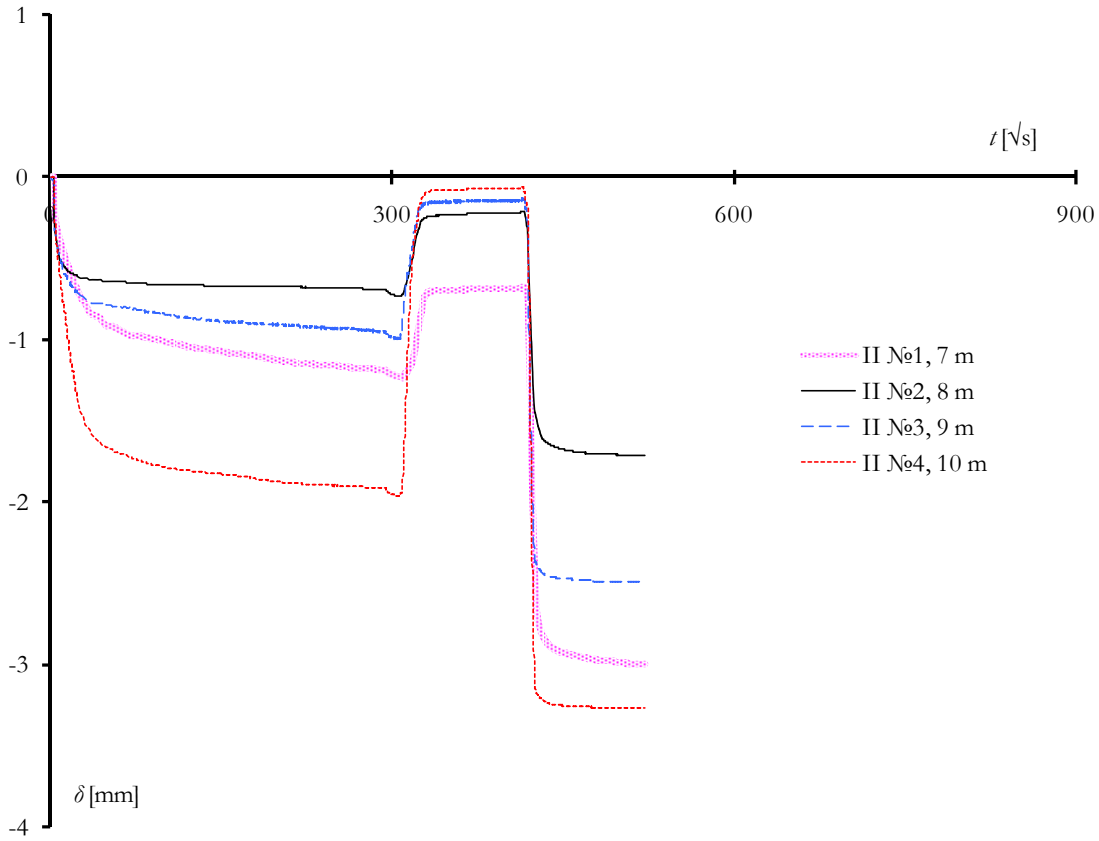

Figure A.13 Oedometer freeze-thaw laboratory tests from the depths of 7 m to 10 m below the ground surface for Bothnia Line soil. The figure shows the results of four simultaneous performed freeze-thaw oedometer tests for oedometer №1 to №4 in Series II for soil collected on October 19th, 2004

Table A.45 Freeze-thaw tests from the depths of 7 m to 10 m below the ground surface. Measured deformations for series II in the four oedometers, namely oedometer №1 to №4. Bothnia soil collected on October 19th, 2004

[mm]	7 m	8 m	9 m	10 m	**Mean**	**Std-dev**
Pre-consolidation	-1.24	-0.73	-1.00	-1.96	-1.23	0.53
Heave	-0.68	-0.21	-0.13	-0.06	-0.27	0.28
Thaw settlement	-2.99	-1.71	-2.49	-3.27	-2.62	0.68
Net [%]						
Pre-consolidation	-6.2	-3.7	-5.0	-9.8	-6.2	2.64
Heave	2.8	2.6	4.4	9.5	4.8	3.22
Thaw settlement	-11.6	-7.5	-11.8	-16.1	-11.7	3.49

Oedometer freeze-thaw tests of Bothnia soil, collected on August 7th, 2006

Figure A.14 to Figure A.21 and Table A.47 to Table A.54 show the results from the freeze-thaw laboratory tests of Bothnia soils collected on August 7th, 2006. The deformations for the depths between 3 m to 10 m have been registered in one test series per level. Each test series consists of simultaneous performed freeze-thawing in four standard oedometers. However, the results for each registered deformation for the mean value of the four tests in each tests series are presented for each level in Table A.46.

Table A.46 Freeze-thaw tests from the depths of 3 m to 10 m below the ground surface. Mean values of measured deformations in the four oedometers at each series, namely oedometer №1 to №4. Bothnia soil collected on August 7th, 2006

Level	Pre-consolidation	Heave	Thaw Settlement	Heave (H)	Settlement (S)	Thaw Settlement (H + S)
[m]	[mm]	[mm]	[mm]	[%]	[%]	[%]
3	-0.67	0.14	-2.82	4.2	-11.1	-14.7
4	-0.78	0.07	-2.37	4.4	-8.3	-12.1
5	-0.96	-0.18	-2.82	4.1	-9.8	-13.3
6	-1.66	-0.84	-3.57	4.5	-10.4	-14.2
7	-1.03	-0.36	-2.71	3.6	-8.8	-12.0
8	-1.03	-0.42	-2.52	6.9	-7.8	-10.7
9	-1.13	0.27	-3.38	7.4	-11.9	-18.0
10	-0.81	0.77	-1.70	8.2	-4.6	-11.9

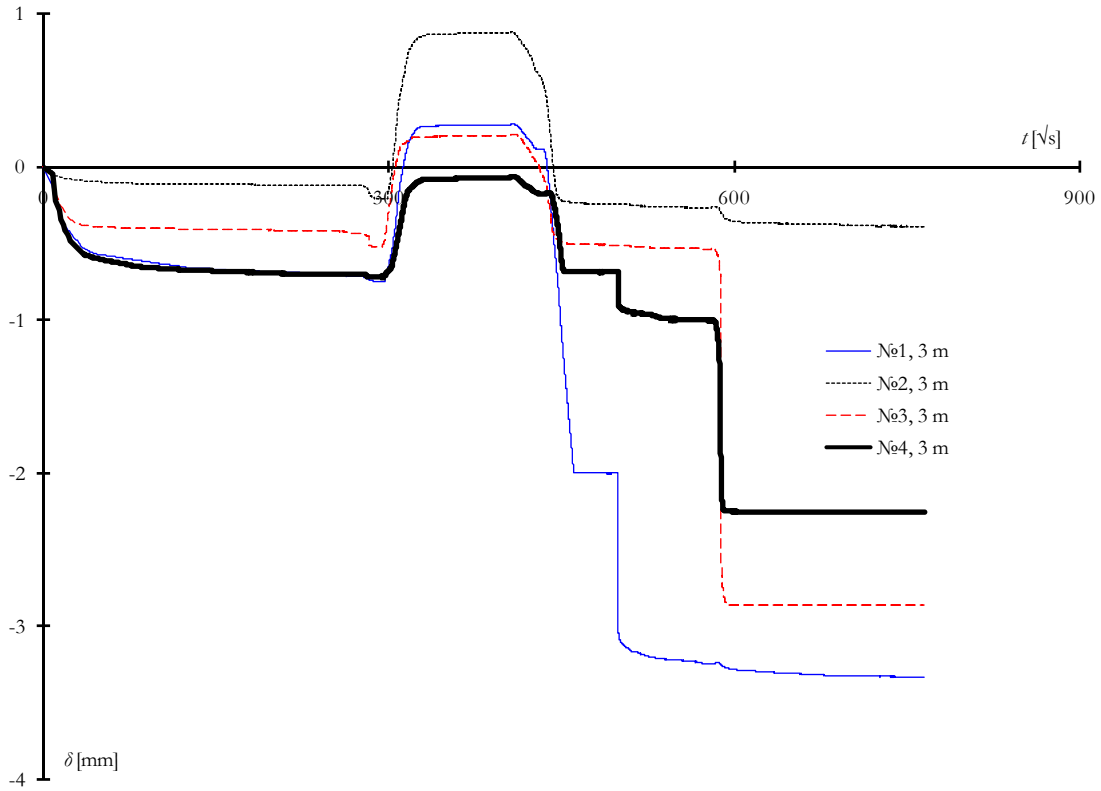

Figure A.14 Oedometer freeze-thaw laboratory tests at a depth of 3 m below the ground surface for Bothnia Line soil. The figure shows the results of four simultaneous performed freeze-thaw oedometer tests for oedometer №1 to №4. The results from oedometer №2 are cancelled due to disturbances in the deformation pattern

Table A.47 Freeze-thaw tests at a depth of 3 m below the ground surface. Measured deformations in the four oedometers, namely oedometer №1 to №4. Bothnia soil collected on August 7th, 2006. The results from oedometer №2 are cancelled due to disturbances in the deformation pattern

[mm]	№1	№2	№3	№4	**Mean**	**Std-dev**
Pre-consolidation	-0.75	~~-0.21~~	-0.53	-0.72	-0.67	0.12
Heave	0.28	~~0.89~~	0.21	-0.06	0.14	0.18
Thaw settlement	-3.33	~~-0.39~~	-2.86	-2.26	-2.82	0.54
Net [%]	[%]					
Pre-consolidation	-3.7	~~-1.1~~	-2.6	-3.6	-3.3	0.60
Heave	5.4	~~5.5~~	3.8	3.4	4.2	1.02
Thaw settlement	-18.8	~~-6.4~~	-15.7	-11.4	-15.3	3.71

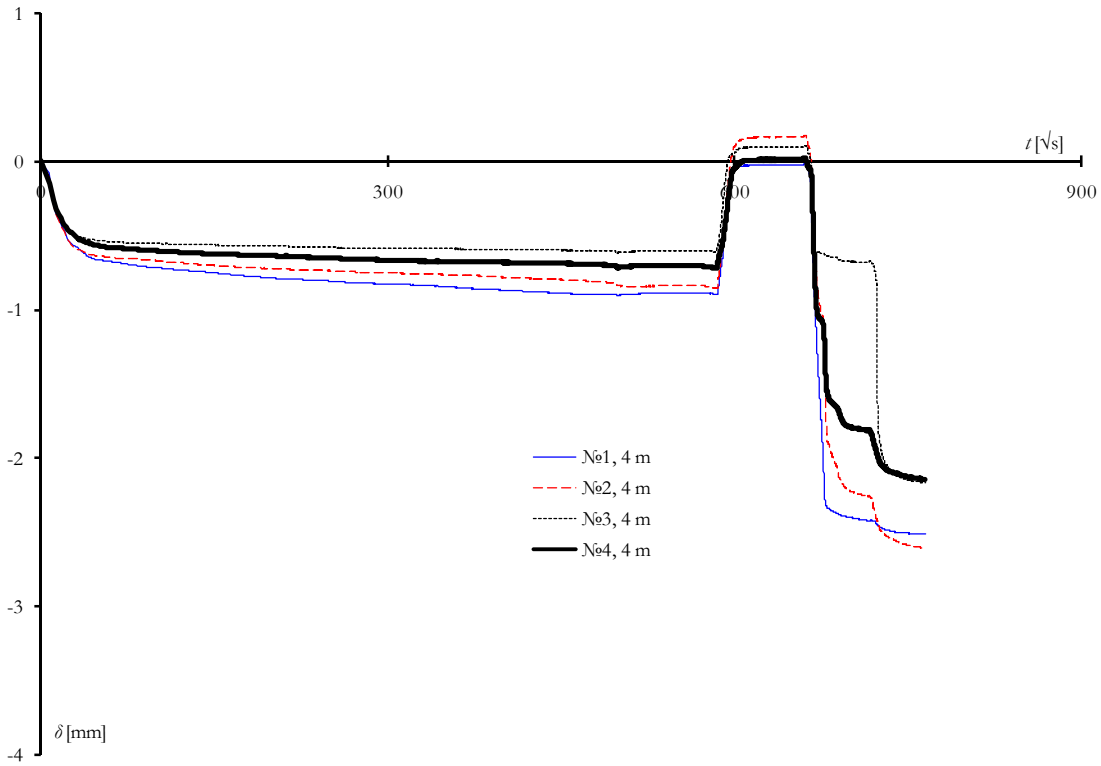

Figure A.15 Oedometer freeze-thaw laboratory test at a depth of 4 m below the ground surface for Bothnia Line soil. The figure shows the results of four simultaneous performed freeze-thaw oedometer tests for oedometer №1 to №4

Table A.48 Freeze-thaw tests at a depth of 4 m below the ground surface. Measured deformations in the four oedometers, namely oedometer №1 to №4. Bothnia soil collected on August 7th, 2006

[mm]	№1	№2	№3	№4	**Mean**	**Std-dev**
Pre-consolidation	-0.90	-0.86	-0.61	-0.73	-0.78	0.13
Heave	-0.02	0.17	0.11	0.02	0.07	0.09
Thaw settlement	-2.52	-2.62	-2.18	-2.15	-2.37	0.24
Net [%]	[%]					
Pre-consolidation	-4.5	-4.3	-3.1	-3.6	-3.9	0.66
Heave	4.6	5.4	3.7	3.9	4.4	0.76
Thaw settlement	-13.1	-14.6	-11.8	-11.3	-12.7	1.47

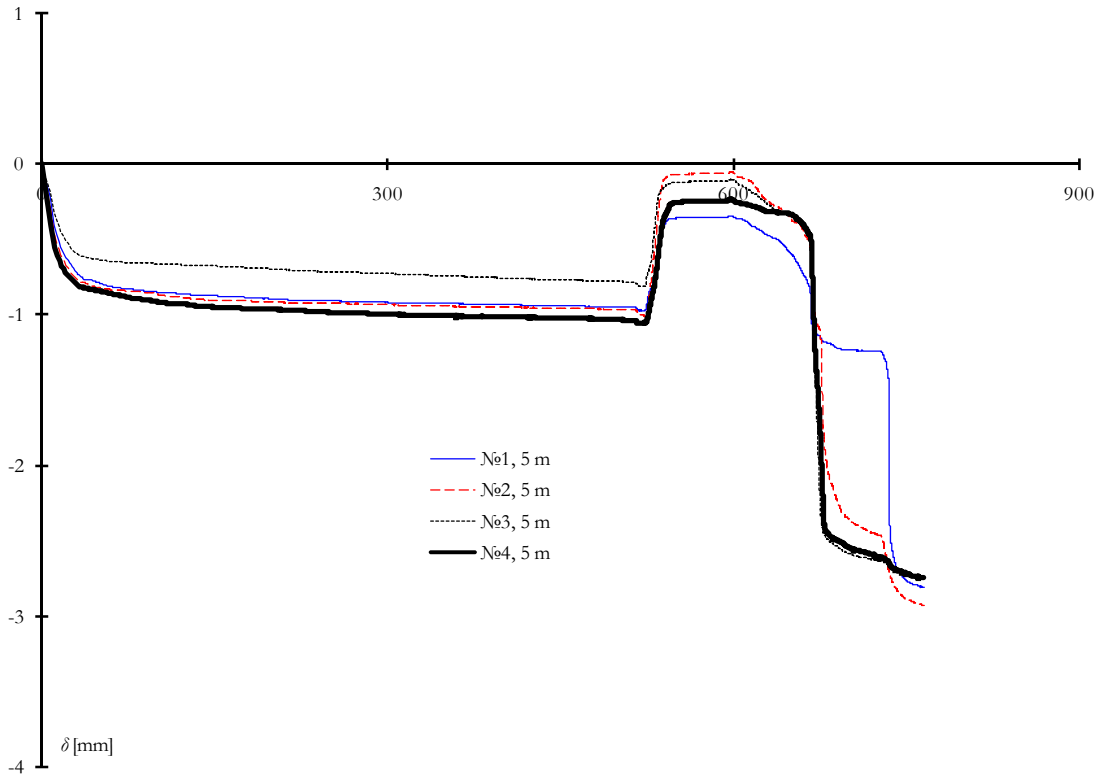

Figure A.16 Oedometer freeze-thaw laboratory test at a depth of 5 m below the ground surface for Bothnia Line soil. The figure shows the results of four simultaneous performed freeze-thaw oedometer tests for oedometer №1 to №4

Table A.49 Freeze-thaw test at a depth of 5 m below the ground surface. Measured deformations in the four oedometers, namely oedometer №1 to №4. Bothnia soil collected on August 7th, 2006

[mm]	№1	№2	№3	№4	**Mean**	**Std-dev**
Consolidation	-0.98	-1.01	-0.81	-1.06	-0.96	0.11
Heave	-0.34	-0.05	-0.10	-0.24	-0.18	0.13
Thaw consolidation	-2.83	-2.95	-2.76	-2.75	-2.82	0.09
Net [%]	[%]					
Consolidation	-4.9	-5.0	-4.1	-5.3	-4.8	0.54
Heave	3.3	5.0	3.7	4.4	4.1	0.75
Thaw consolidation	-13.1	-15.3	-13.9	-13.3	-13.9	0.98

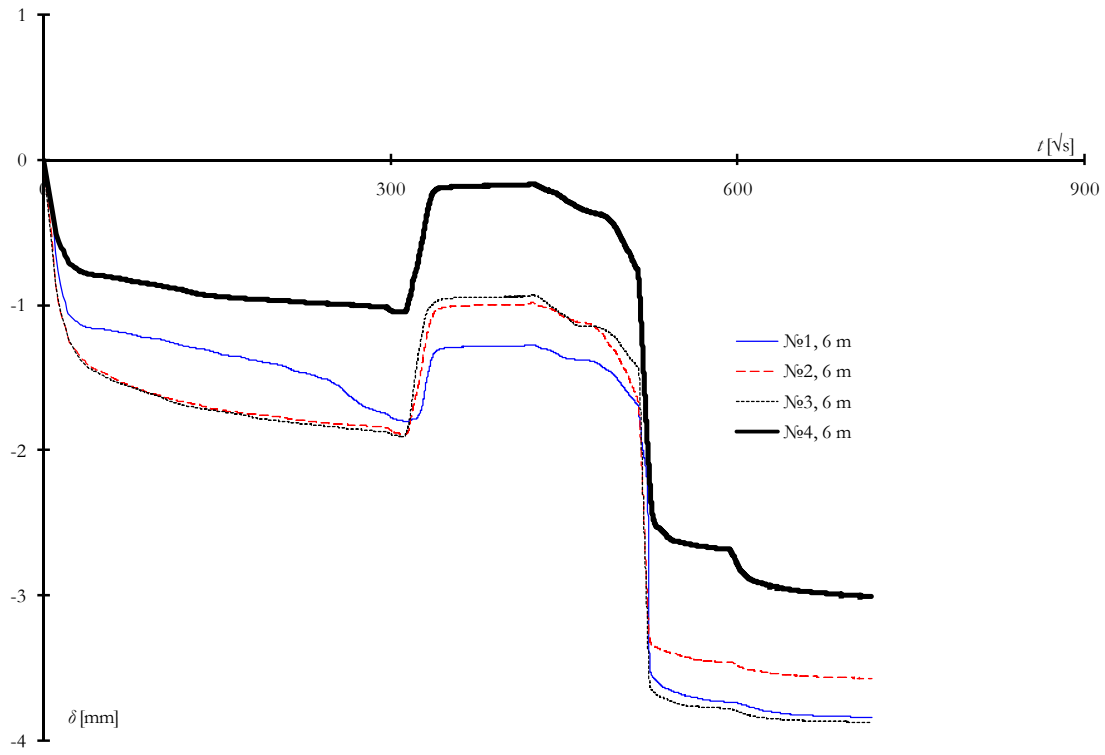

Figure A.17 Oedometer freeze-thaw laboratory test a depth of 6 m below the ground surface for Bothnia Line soil. The figure shows the results of four simultaneous performed freeze-thaw oedometer tests for oedometer №1 to №4

Table A.50 Freeze-thaw tests at a depth of 6 m below the ground surface. Measured deformations in the four oedometers, namely oedometer №1 to №4. Bothnia soil collected on August 7th, 2006

[mm]	№1	№2	№3	№4	**Mean**	**Std-dev**
Consolidation	-1.80	-1.89	-1.91	-1.05	-1.66	0.41
Heave	-1.27	-0.99	-0.94	-0.16	-0.84	0.48
Thaw consolidation	-3.84	-3.57	-3.87	-2.99	-3.57	0.41
Net [%]	[%]					
Consolidation	-9.0	-9.4	-9.5	-5.2	-8.3	2.06
Heave	2.9	5.0	5.4	4.7	4.5	1.09
Thaw consolidation	-14.1	-14.2	-16.2	-15.0	-14.9	0.98

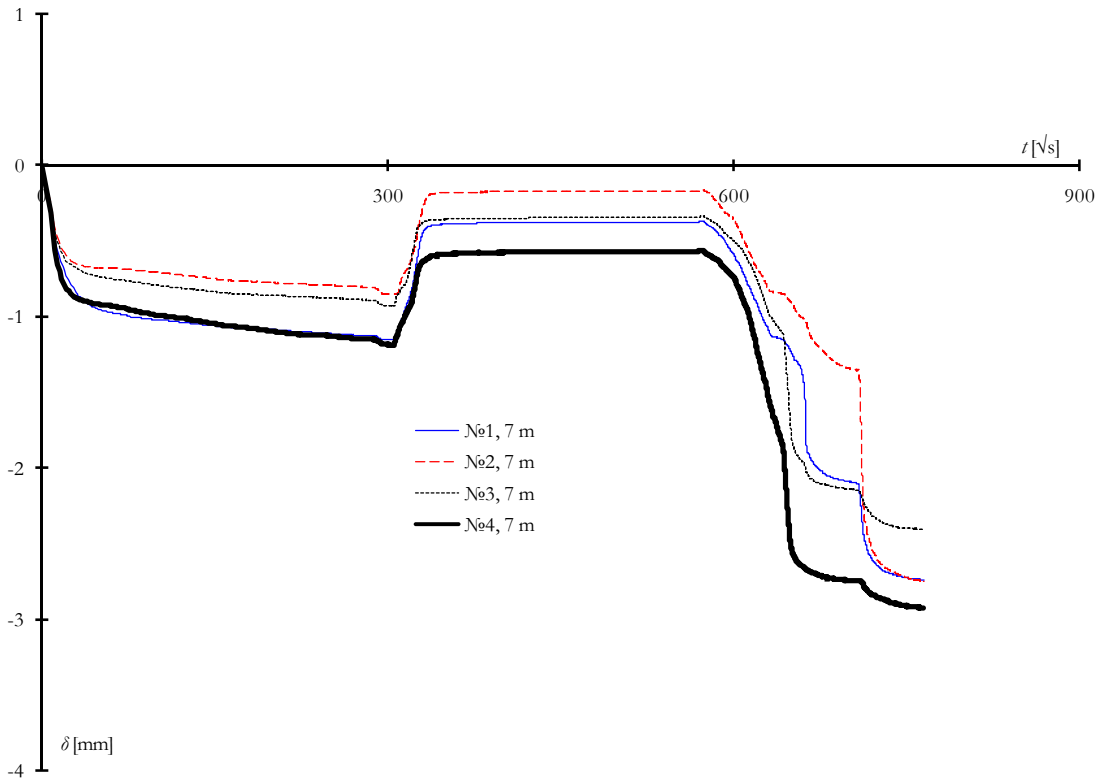

Figure A.18 Oedometer freeze-thaw laboratory tests at a depth of 7 m below the ground surface for Bothnia Line soil. The figure shows the results of four simultaneous performed freeze-thaw oedometer tests for oedometer №1 to №4

Table A.51 Freeze-thaw tests at a depth of 7 m below the ground surface. Measured deformations in the four oedometers, namely oedometer №1 to №4. Bothnia soil collected on August 7th, 2006

[mm]	№1	№2	№3	№4	**Mean**	**Std-dev**
Consolidation	-1.15	-0.85	-0.93	-1.19	-1.03	0.16
Heave	-0.37	-0.16	-0.34	-0.56	-0.36	0.16
Thaw consolidation	-2.74	-2.75	-2.41	-2.93	-2.71	0.22
Net [%]	[%]					
Consolidation	-5.8	-4.3	-4.7	-5.9	-5.2	0.81
Heave	4.2	3.6	3.1	3.4	3.6	0.44
Thaw consolidation	-12.6	-13.5	-10.9	-12.6	-12.4	1.10

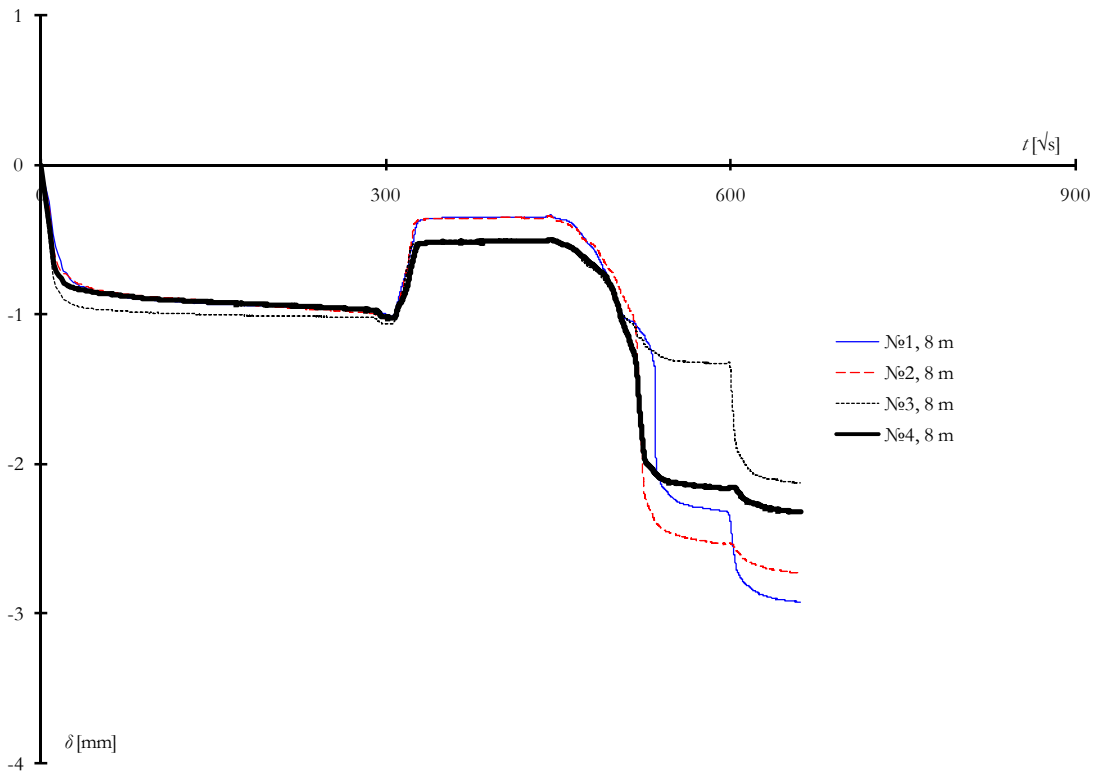

Figure A.19 Oedometer freeze-thaw laboratory tests at a depth of 8 m below the ground surface for Bothnia Line soil. The figure shows the results of four simultaneous performed freeze-thaw oedometer tests for oedometer №1 to №4

Table A.52 Freeze-thaw tests at a depth of 8 m below the ground surface. Measured deformations in the four oedometers, namely oedometer №1 to №4. Bothnia soil collected on August 7th, 2006

[mm]	№1	№2	№3	№4	**Mean**	**Std-dev**
Consolidation	-1.01	-1.03	-1.07	-1.02	-1.03	0.02
Heave	-0.34	-0.34	-0.49	-0.50	-0.42	0.09
Thaw consolidation	-2.91	-2.72	-2.12	-2.32	-2.52	0.36
Net [%]	[%]					
Consolidation	-5.0	-5.2	-5.3	-5.1	-5.2	0.12
Heave	3.5	3.6	3.0	2.8	3.2	0.41
Thaw consolidation	-13.5	-12.5	-8.6	-9.6	-11.1	2.36

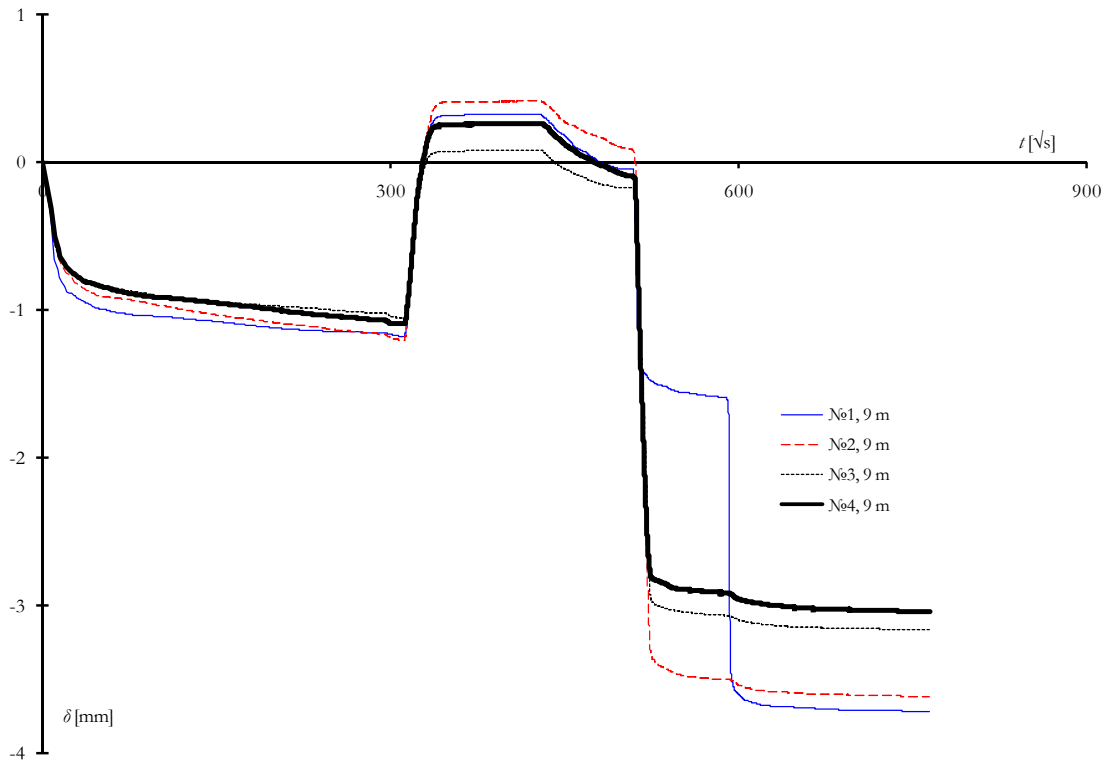

Figure A.20 Oedometer freeze-thaw laboratory tests at a depth of 9 m below the ground surface for Bothnia Line soil. The figure shows the results of four simultaneous performed freeze-thaw oedometer tests for oedometer №1 to №4

Table A.53 Freeze-thaw tests at a depth of 9 m below the ground surface. Measured deformations in the four oedometers, namely oedometer №1 to №4. Bothnia soil collected on August 7th, 2006

[mm]	№1	№2	№3	№4	**Mean**	**Std-dev**
Consolidation	-1.18	-1.21	-1.06	-1.09	-1.13	0.07
Heave	0.32	0.41	0.08	0.26	0.27	0.14
Thaw consolidation	-3.71	-3.62	-3.16	-3.04	-3.38	0.33
Net [%]	[%]					
Consolidation	-5.9	-6.1	-5.3	-5.5	-5.7	0.36
Heave	8.0	8.6	6.0	7.2	7.4	1.14
Thaw consolidation	-21.5	-21.5	-17.1	-17.5	-19.4	2.41

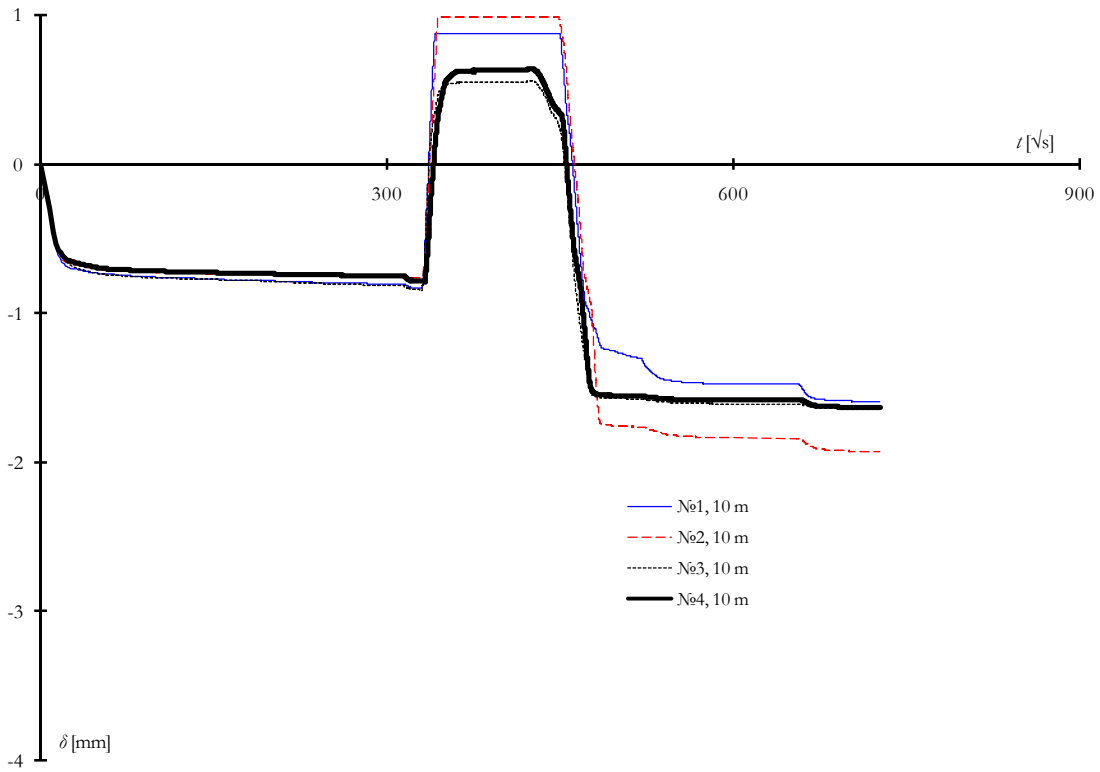

Figure A.21 Oedometer freeze-thaw laboratory tests at a depth of 10 m below the ground surface for Bothnia Line soil. The figure shows the results of four simultaneous performed freeze-thaw oedometer tests for oedometer №1 to №4

Table A.54 Freeze-thaw tests at a depth of 10 m below the ground surface. Measured deformations in the four oedometers, namely oedometer №1 to №4. Bothnia soil collected on August 7th, 2006

[mm]	№1	№2	№3	№4	**Mean**	**Std-dev**
Consolidation	-0.83	-0.77	-0.84	-0.79	-0.81	0.04
Heave	0.88	0.99	0.56	0.64	0.77	0.20
Thaw consolidation	-1.60	-1.93	-1.64	-1.63	-1.70	0.15
Net [%]	[%]					
Consolidation	-4.2	-3.8	-4.2	-3.9	-4.0	0.19
Heave	8.9	9.1	7.3	7.4	8.2	0.95
Thaw consolidation	-12.9	-15.1	-11.5	-11.8	-12.8	1.66

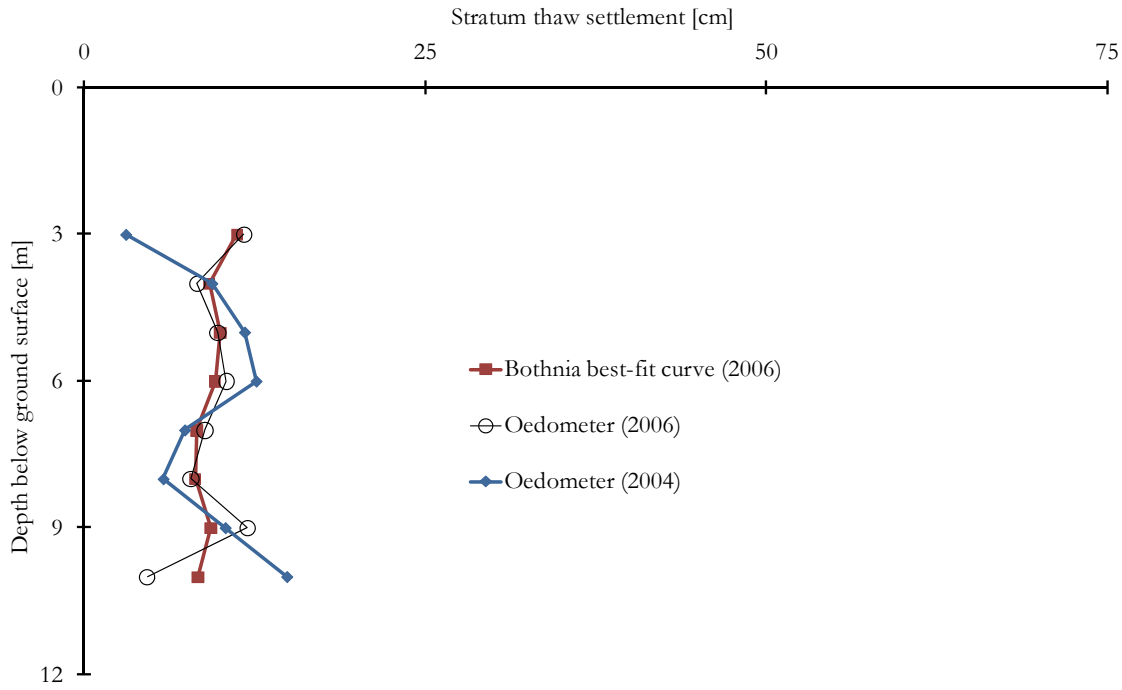

Figure A.22 Oedometer freeze-thaw tests, the figure shows the mean value of the resulted stratum thaw settlement from specimens collected on October 19th, 2004 and August 7th, 2006. The figure also shows the resulted best-fit curve of the stratum thaw settlement from specimens collected on August 7th, 2006

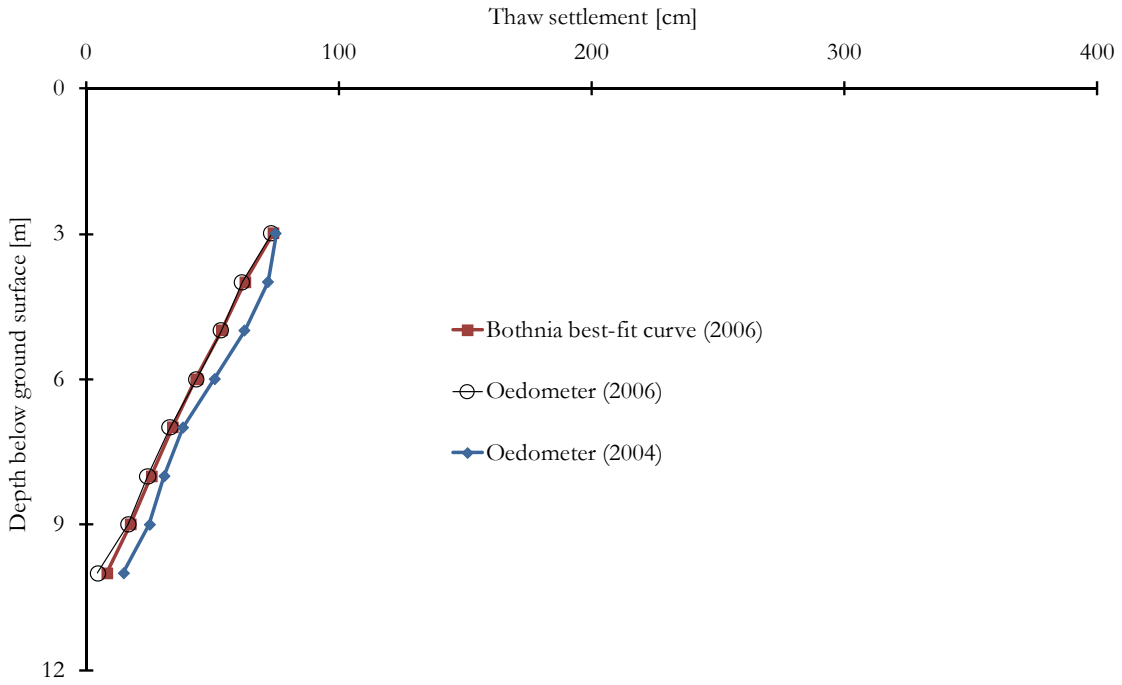

Figure A.23 Oedometer freeze-thaw tests, the figure shows the mean value of the resulted thaw settlement from specimens collected on October 19th, 2004 and August 7th, 2006. The figure also shows the resulted best-fit curve of the thaw settlement from specimens collected on August 7th, 2006

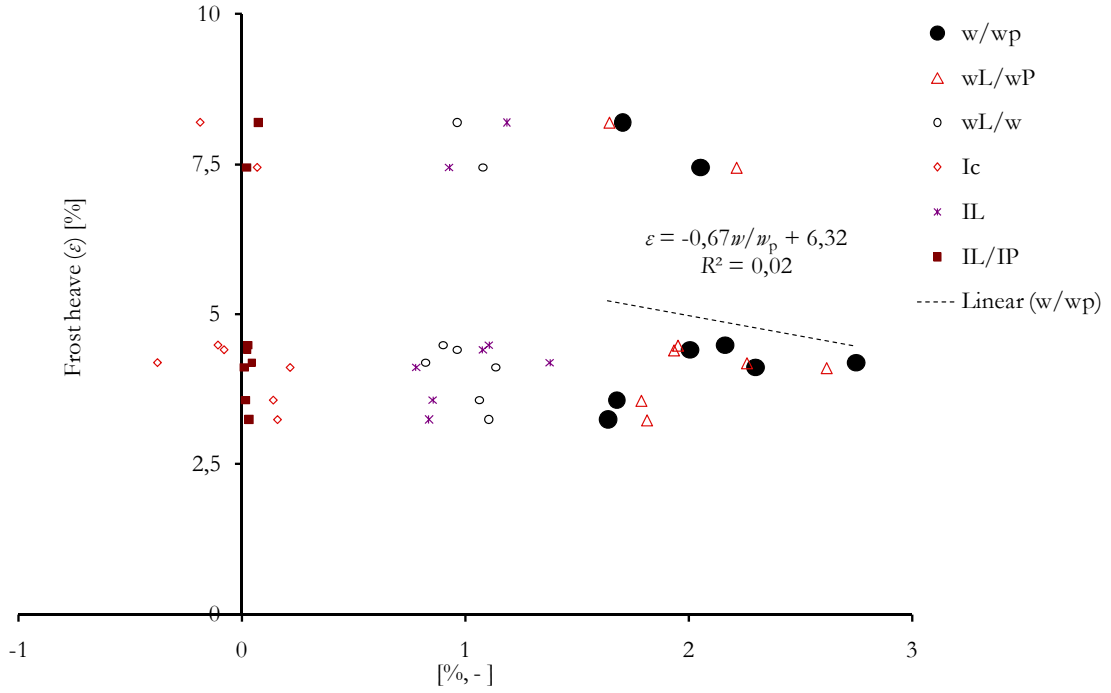

Figure A.24 Frost heave as a function of soil parameters. Soil sample series of August 7th, 2006, consisting of samples from 3 m to 10 m depths

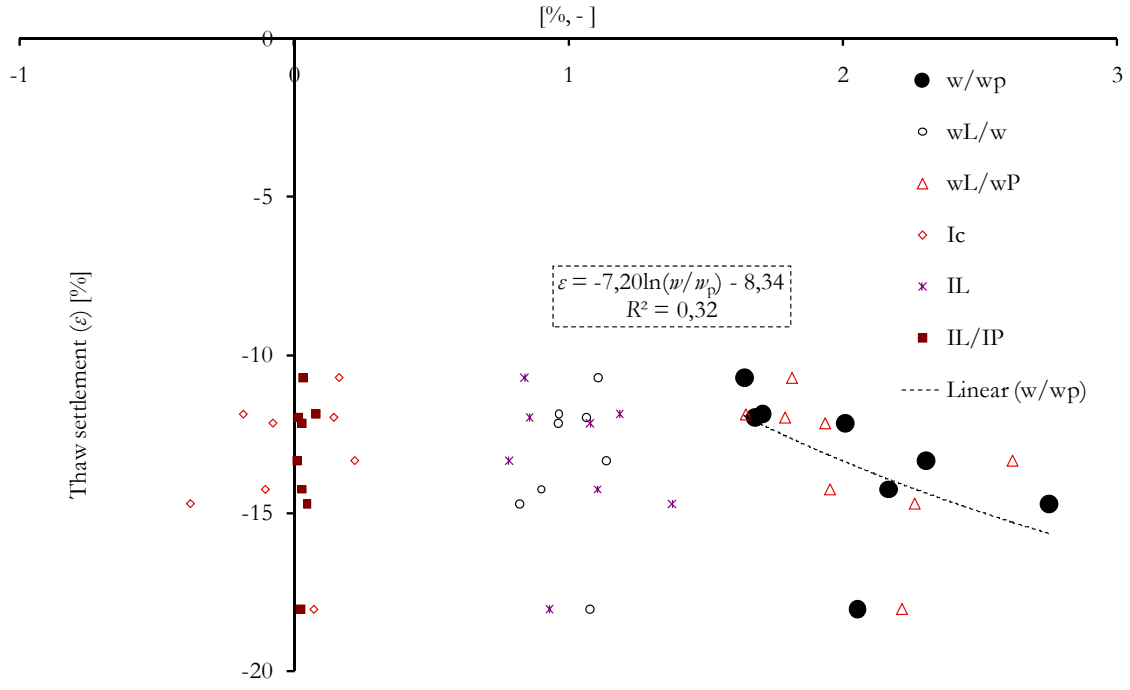

Figure A.25 Thaw settlement as a function of soil parameters. Soil sample series of August 7th, 2006, consisting of depths from 3 m to 10 m below ground surface

B APPENDIX, FIELD STUDY

This supplementary chapter shows results from the field tests at the Bothnia Line.

Ground alteration measurements

The deformations of the ground at the Bothnia Line have being measured with ground level gauges in chainage 13+549 and 13+ 568.5. Figure B.1 and Figure B.2 show the soil deformations at a depth of approximately 2.5 m.

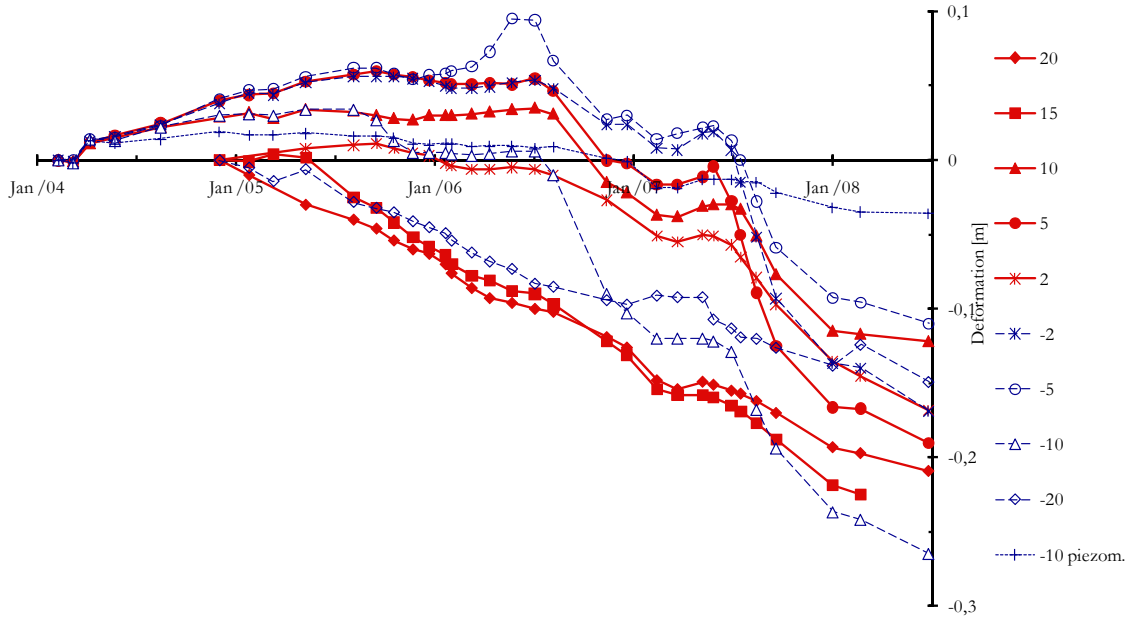

Figure B.1 Chainage 13+549. Soil deformation registered with ground level gauges. The ground level gauges are located about 2.5 m below the ground surface. Gauge "-10pt" is located 7 m below the ground surface. The gauges are noted positive north of the tunnel and refer to the distance to the tunnel centre axis

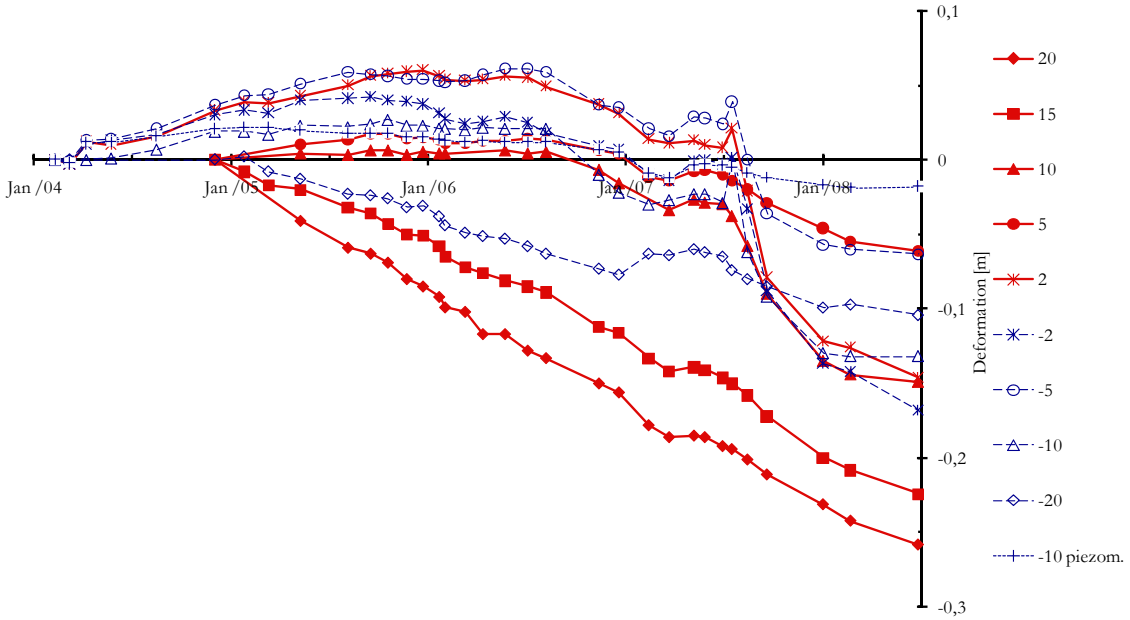

Figure B.2 *Chainage 13+568.5. Soil deformation registered with ground level gauges. The ground level gauges are located about 2.5 m below the ground surface. Gauge"-10pt" is located 7 m below the ground surface. The gauges are noted positive north of the tunnel and refer to the distance to the tunnel centre axis*

Temperature measurements

The frozen construction at the Bothnia Line is limited to chainages 13+520.5 and 13+615; hence, the length of the frozen construction is 94.5 m. Table B.1 to Table B.6 show the distribution of the temperature sensor casing tubes, as well as the distribution of the temperature sensors (Botniabanan, 2006). Hence, Figure B.3 to Figure B.8 show the registered temperature in the temperature sensors.

Table B.1 *Chainage of the temperature sensor casing tubes. The table shows the longitudinal vertical cross section at the tunnel centre. Schematic illustration of the temperature sensors casing tubes distribution*

km	**13+525**	**13+549**	**13+568.5**	**13+579**	**13+601**
	3 casing tubes	5 casing tubes	4 casing tubes	3 casing tubes	4 casing tubes

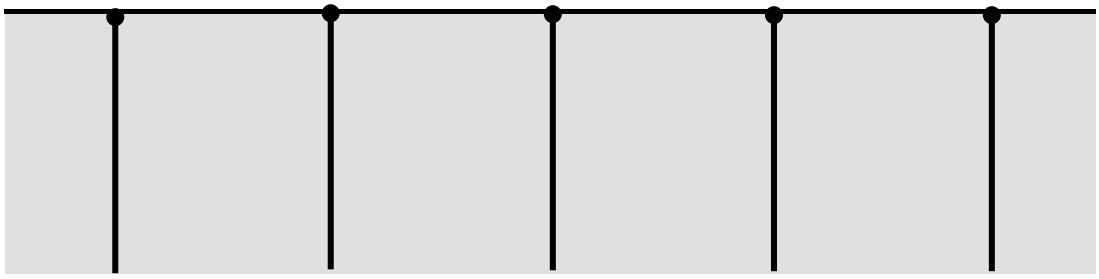

Table B.2 *Chainage 13+525. Temperature sensor casing tubes No. 1.1, 1.2 and 1.3. Three temperature sensor casing tubes containing six temperature sensors, distributed across the tunnel as well as at depth. The tunnel roof geodetic level (inside) is approximately located at +29.84*

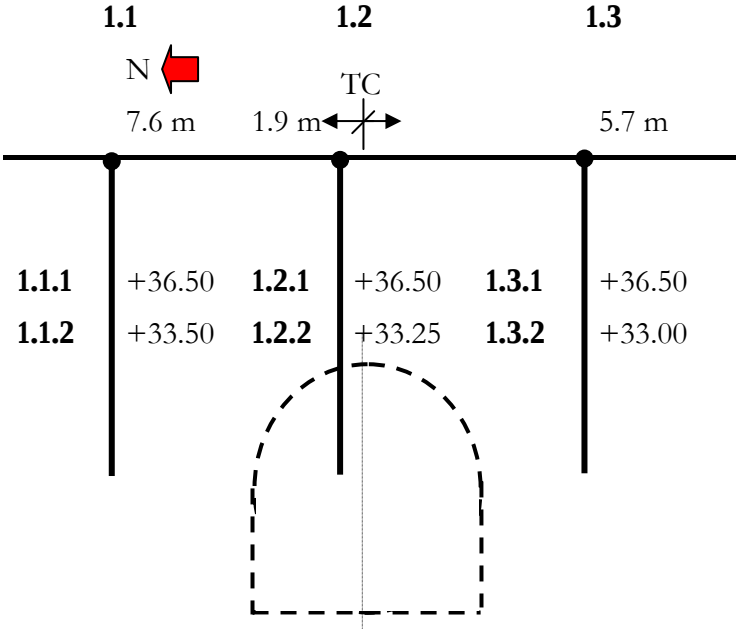

Table B.3 *Chainage 13+549. Temperature sensor casing tubes No. 2.1, 2.2A, 2.2B, 2.3 and 2.4. Five temperature sensor casing tubes containing a total of twenty-two temperature sensors, distributed across the tunnel as well as at depth. The tunnel roof geodetic level (inside) is approximately located at +30.08*

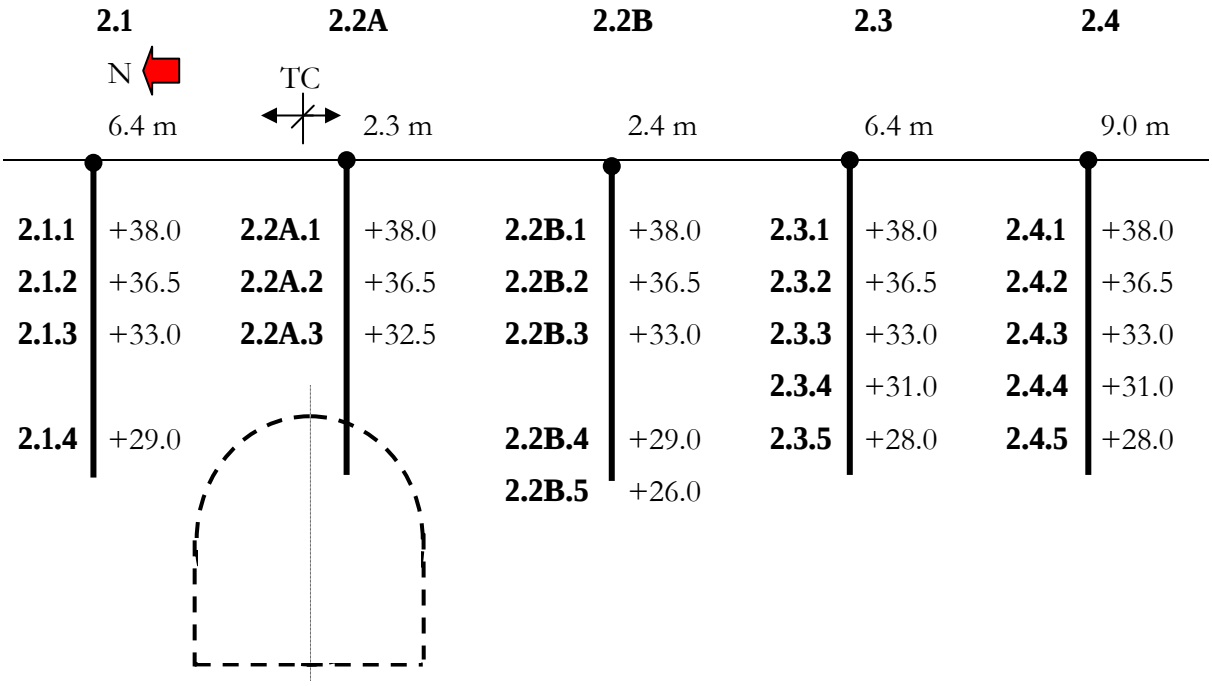

Table B.4 *Chainage 13+568.5. Temperature sensor casing tubes No. 3.1, 3.2, 3.3 and 3.4. Four temperature sensor casing tubes containing a total of twenty-eight temperature sensors, distributed across the tunnel as well as at depth. The tunnel roof geodetic level (inside) is approximately located at +30.28*

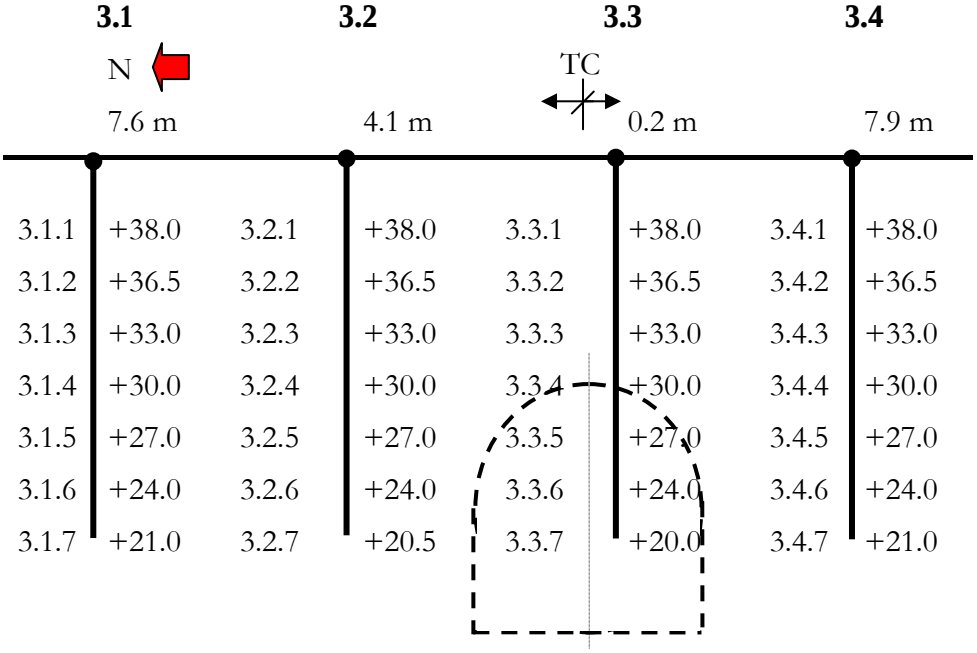

Table B.5 *Chainage 13+579. Temperature sensor casing tubes No. 4.1, 4.2 and 4.3. Three temperature sensor casing tubes containing a total of fourteen temperature sensors, distributed across the tunnel as well as at depth. The tunnel roof geodetic level (inside) is approximately located at +30.38*

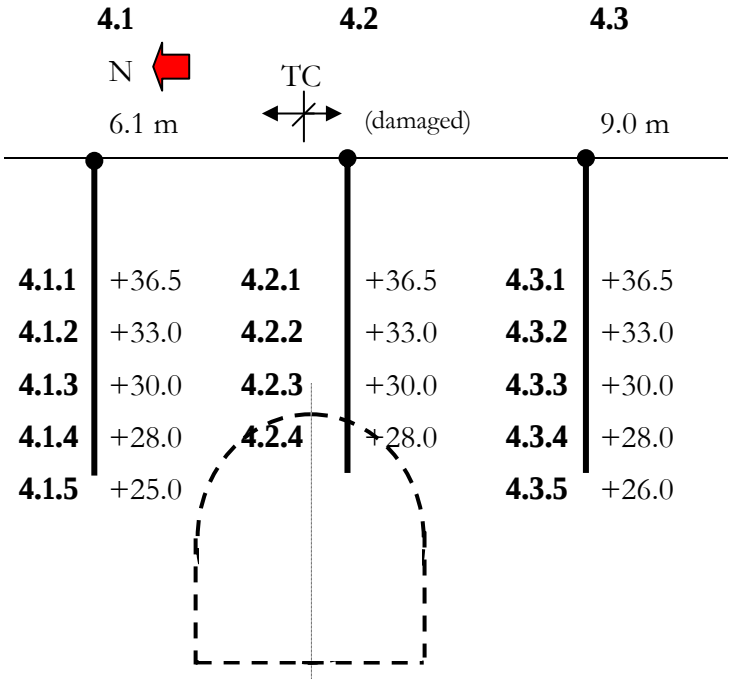

Table B.6 *Chainage 13+601. Temperature sensor casing tubes No. 5.1, 5.2, 5.3 and 5.4. Four temperature sensor casing tubes containing a total of eight temperature sensors, distributed across the tunnel as well as at depth. The tunnel roof geodetic level (inside) is approximately located at +30.60*

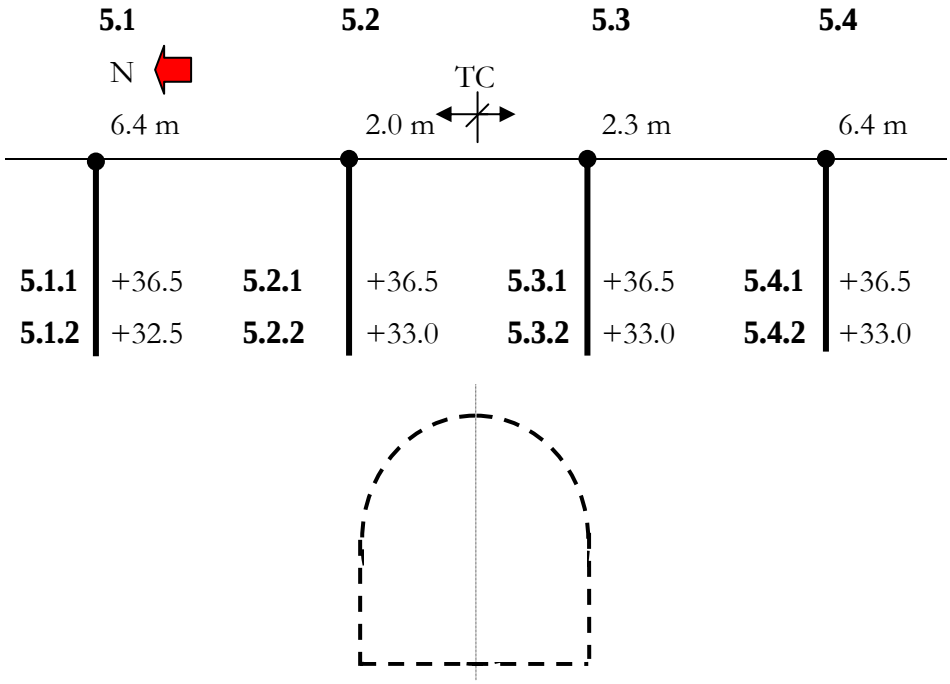

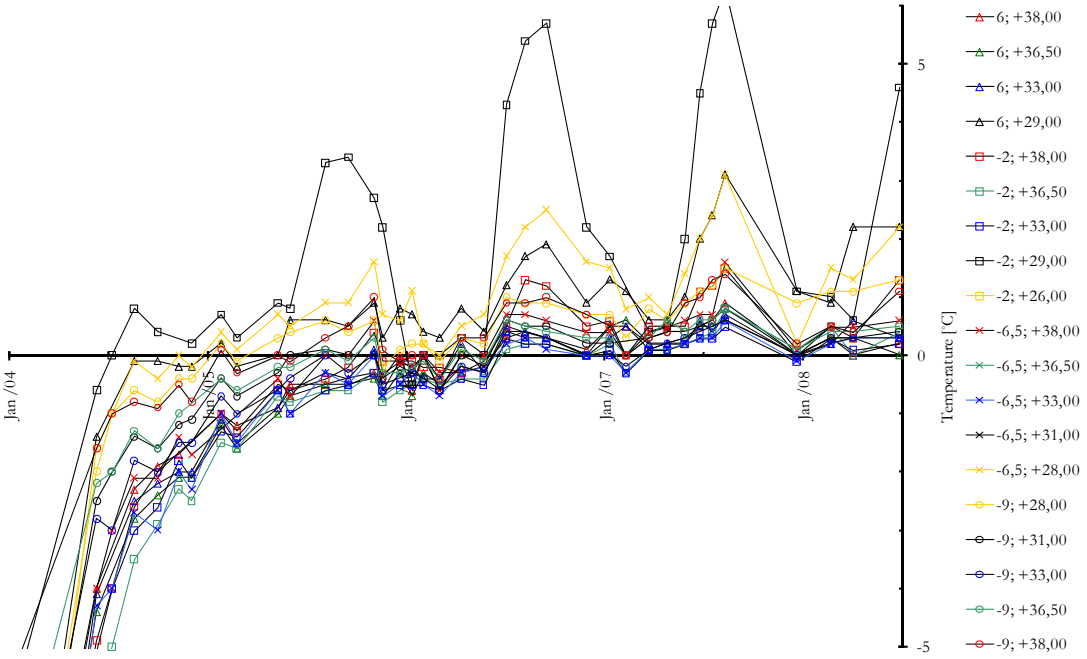

Figure B.3 *The temperature development for chainage 13+549 at the Bothnia Line from July 1st, 2004 to June 26th, 2008, according to Figure 5.12. The temperature sensor casing tubes are noted positive north of the tunnel and refer to the distance to the tunnel centre axis*

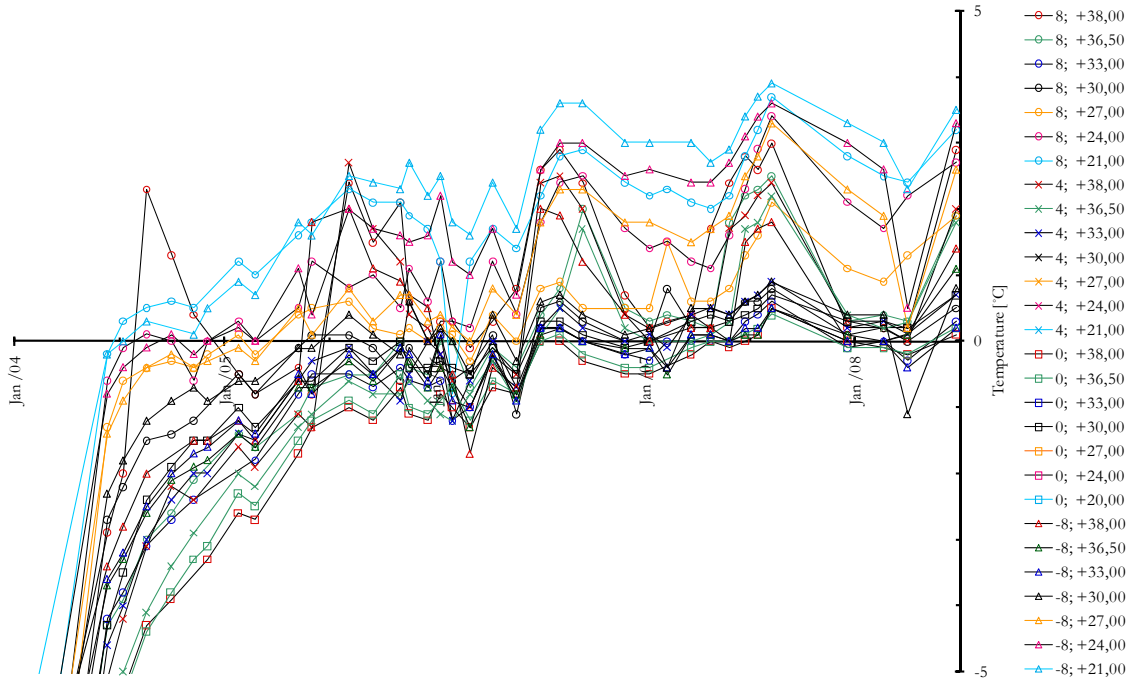

Figure B.4 *The temperature development for chainage13+568.5 at the Bothnia Line, from July 1st, 2004 to June 26th, 2008, according to Figure B.6. The temperature sensor casing tubes are noted positive north of the tunnel and refer to the distance to the tunnel centre axis*

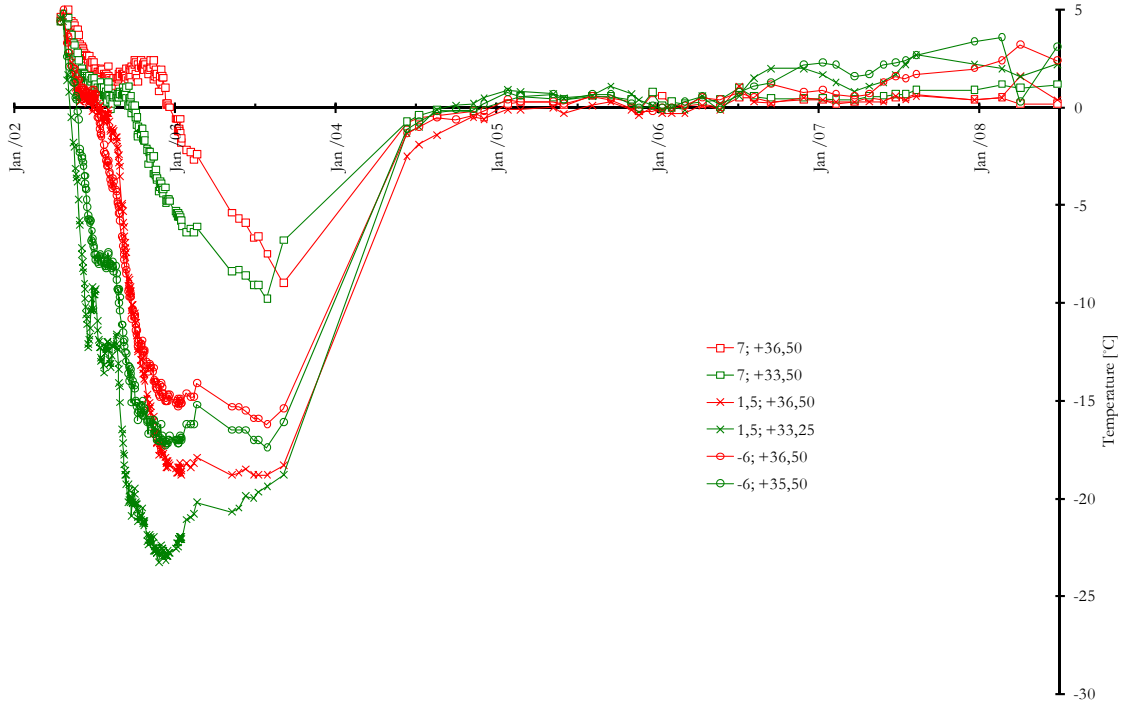

Figure B.5 *The temperature development for chainage 13+525 at the Bothnia Line, from April 16th, 2002 to June 26th, 2008. The temperature registrations originate from the temperature casing tubes located; 7 m and 1.5 m north, and 6 m south of the tunnel centre axis. The temperature sensor in each temperature sensor casing tube is located at the levels +36.50 and +33.50. The temperature sensor casing tubes are noted positive north of the tunnel and refer to the distance to the tunnel centre axis*

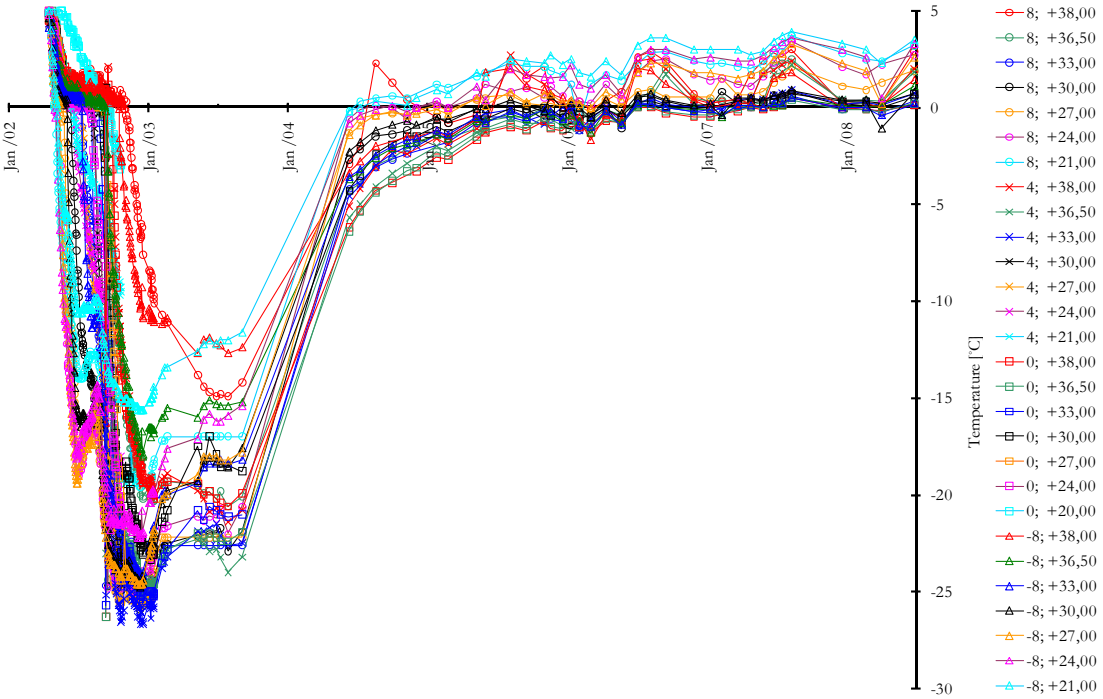

Figure B.6 *The temperature development for chainage13+568.5 (N tunnel centre), from April 16th, 2002 to June 26th, 2008. The temperature registration derive from three temperature control pipes located; 0.4 m and 8 m north of the tunnel centre as well as one temperature control pipe located about 8 m south of the tunnel centre axis. Temperature sensor in each temperature control pipe is placed at a geodetic level of +38.00 down to +20.00. The temperature pipes are noted positive north of the tunnel and refer to the distance to the tunnel centre axis*

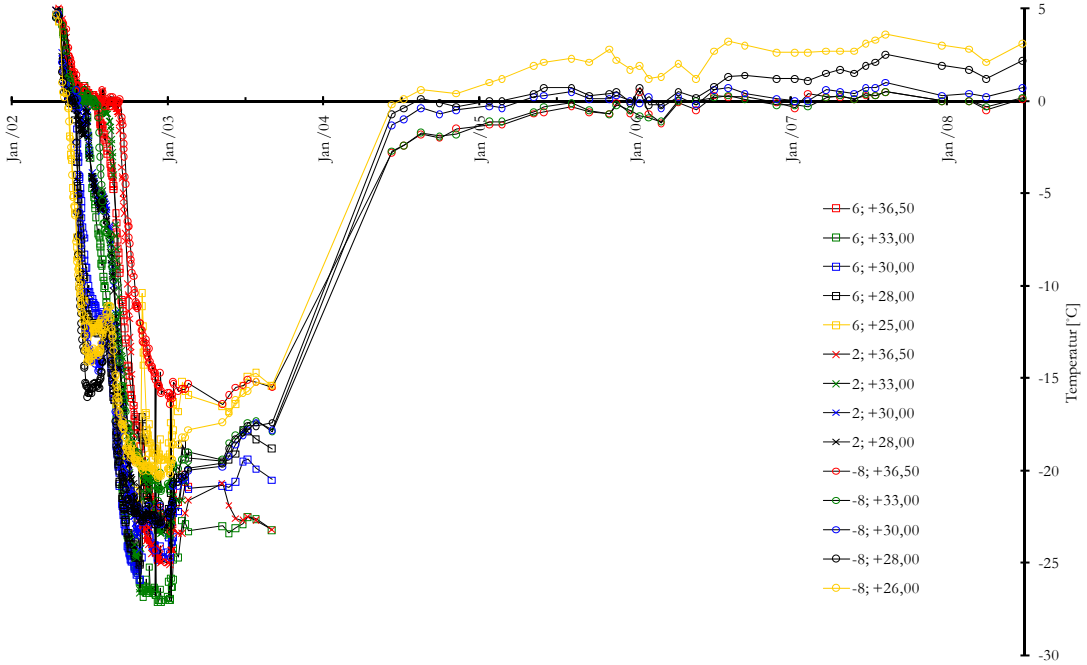

Figure B.7 *The temperature development for chainage13+579 at the Bothnia Line, from April 16th, 2002 to June 26th, 2008. The temperature registrations originate from three temperature sensor casing tubes located; 6 m and 2 m north, and 8 m south of the tunnel centre axis. The temperature sensor in each temperature sensor casing tube is located at a geodetic level between +36.50 and +25.00 to +28.00*

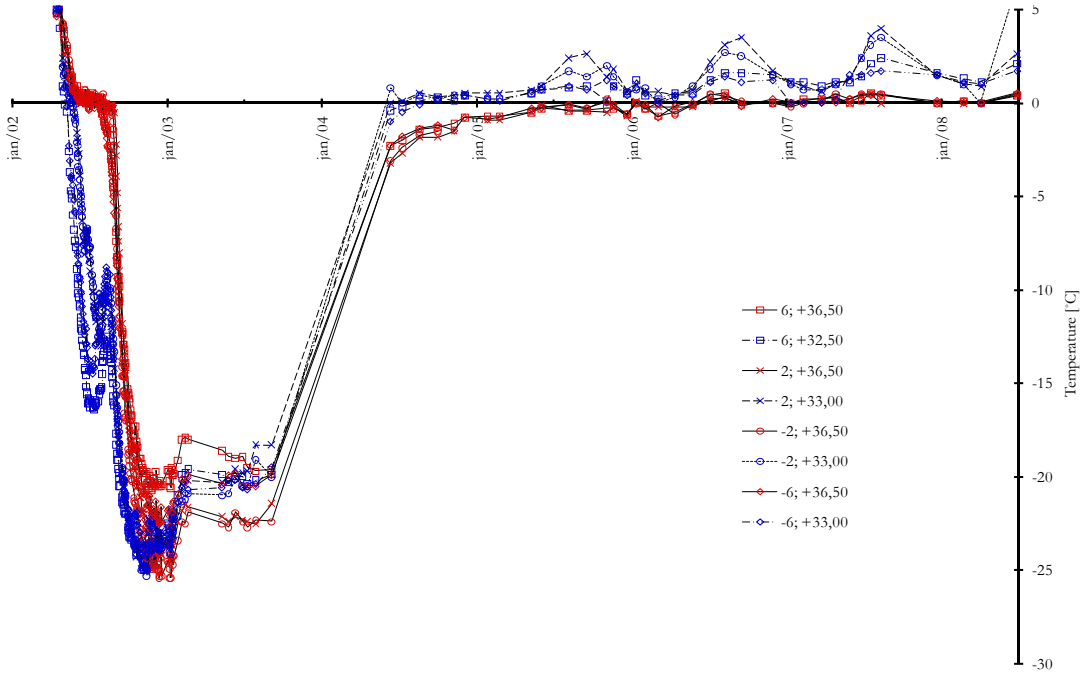

Figure B.8 *The temperature development for chainage13+601 at the Bothnia Line, from April 16th, 2002 to June 26th, 2008. The temperature registrations originate from four temperature sensor casing tubes located, 6 m and 2 m north, and 2 m and 6 m south of the tunnel centre axis. The temperature sensors in each temperature sensor casing tube are placed at the geodetic level +36.50 and +33.00 and 32.50. The temperature sensor casing tubes are noted positive north of the tunnel and refer to the distance to the tunnel centre axis. The temperature of the outside air as well as inflow and return for brine during the freezing of the tunnel is presented*

Catalogue of co-ordinates

The freeze area at the Bothnia Line is limited by chainages 13+520.5 and 13+615, thus, the length of the freeze area is 94.5 m. The temperature casing tubes with the temperature sensors have geodetic data according to Table B.7. The measuring points of the ground level gauges (the top of the invar rods) have the geodetic data presented in Table B.8. The geodetic data of the tunnel for the tunnel roof's theoretical, interior level and the top of rail is documented in Table B.9.

Table B.7 *The designation and catalogue of the temperature casing tubes (TG), as well as the upper edge co-ordinates (x, y) of the temperature casing tubes*

Chainage	Pos rel to TC	Temperature casing tubes (TG) Name according to: Bothnia Line	Lemminkäinen	*x*	*y*	*z*	Distance from tunnel centre axis (horizontal)
13+525	N	TG18	1.1	7 022 523.496	138 412.594		7.59
13+525	N	TG17	1.2	7 022 517.792	138 412.526		1.89
13+525	S	TG16	1.3	7 022 510.225	138 412.697		5.68
13+549	N	TG15	2.1	7 022 522.730	138 436.876		6.44
13+549	S	TG14	2.2A	7 022 513.964	138 436.792		2.32
13+549	S	TG13	2.2B	7 022 513.937	138 437.076		2.35
13+549	S	TG12	2.3	7 022 509.936	138 436.975		6.35
13+549	S	TG11	2.4	7 022 507.276	138 436.970		9.01

Chainage	Pos rel to TC	Temperature casing tubes (TG) Name according to: Bothnia Line	Lemmin-käinen	*x*	*y*	*z*	Distance from tunnel centre axis (horizontal)
13+568.5	N	TG7	3.1	7 022 524.337	138 456.133		7.63
13+568.5	N	TG8	3.2	7 022 520.823	138 456.216		4.11
13+568.5	S	TG9	3.3	7 022 516.545	138 456.193		0.16
13+568.5	S	TG10	3.4	7 022 508.806	138 456.451		7.91
13+579	N	TG6	4.1	7 022 523.103	138 466.858		6.11
13+579			4.2				damaged
13+579	S	TG5	4.3	7 022 507.957	138 467.084		9.03
13+601	N	TG1	5.1	7 022 524.006	138 487.293		6.37
13+601	N	TG2	5.2	7 022 519.647	138 487.513		2.01
13+601	S	TG3	5.3	7 022 515.390	138 487.913		2.26
13+601	S	TG4	5.4	7 022 511.266	138 487.626		6.37

Table B.8 *The designation and catalogue of the ground level gauges (MP), as well as the upper edge co-ordinates (x,y) of the ground level gauges. The z-co-ordinate for the ground level gauges is preliminary*

Chainage	Pos rel to TC	Ground level gauge (MP) Name according to: Bothnia Line	KTH	*x*	*y*	*z (prel)*	Distance from the tunnel centre axis (horizontal)
13+549	*N*	*MP1[Damaged]*	*15N*	*7 022 530.803*	*138 434.728*	*Damaged*	*14.55*
13+549	N	MP2	10N	7 022 526.097	138 436.611	42.254	9.81
13+549	N	MP3	5N	7 022 521.515	138 436.860	42.821	5.23
13+549	N	MP4	2N	7 022 517.936	138 436.641		1.65
13+549	S	MP5	-2S	7 022 514.500	138 436.742	42.908	1.79
13+549	S	MP6	-5S	7 022 511.198	138 436.640	42.826	5.09
13+549	S	MP7	-10S	7 022 506.422	138 436.902	42.627	9.87
13+549	S	PT1	-10PT	7 022 505.703	138 436.885	42.678	10.58
13+549	S	MP8	-10PT	7 022 505.702	138 436.884	42.678	10.59
13+568.5	N	MP14	10N	7 022 526.601	138 457.225		9.87
13+568.5	N	MP13	5N	7 022 521.244	138 457.069		4.52
13+568.5	N	MP12	2N	7 022 518.541	138 457.002	42.815	1.81
13+568.5	S	MP11	-2S	7 022 514.539	138 456.963	42.912	2.19
13+568.5	S	MP10	-5S	7 022 511.471	138 456.809	42.678	5.25
13+568.5	S	PT2	-10PT	7 022 506.498	138 455.898	42.516	10.20
13+568.5	S	MP9	-10PT	7 022 506.497	138 455.899	42.516	10.26
13+568.5	S	MP0015	-10S	7 022 506.459	138 456.847	42.537	10.20
(13+498)	(N)	GPS-F	Fixed point	7 022 523.391	138 385.995	44.424	(7.90)

Table B.9 *Register of theoretical geodetic level for chainages with respective level for interior lining in tunnel roof and top of rail*

Chainage	*x*	*y*	*z*-roof	*z*-rail head
13+525	7 022 515.911	138 412.800	29.843	23.093
13+549	7 022 516.287	138 436.797	30.083	23.333
13+568.5	7 022 516.711	138 456.292	30.278	23.528
13+579	7 022 516.987	138 466.788	30.383	23.633
13+601	7 022 517.680	138 488.777	30.603	23.853

C APPENDIX, JOBFEM ANALYSES

This supplementary chapter shows results from the JOBFEM analyses. The thaw settlement has been analysed in the finite element program JOBFEM. Figure C.1 to Figure C.5 show soil settlement distribution around the tunnel at altered times. The procedure for the thaw settlement analysis has been presented in the chapter analysis and discussions.

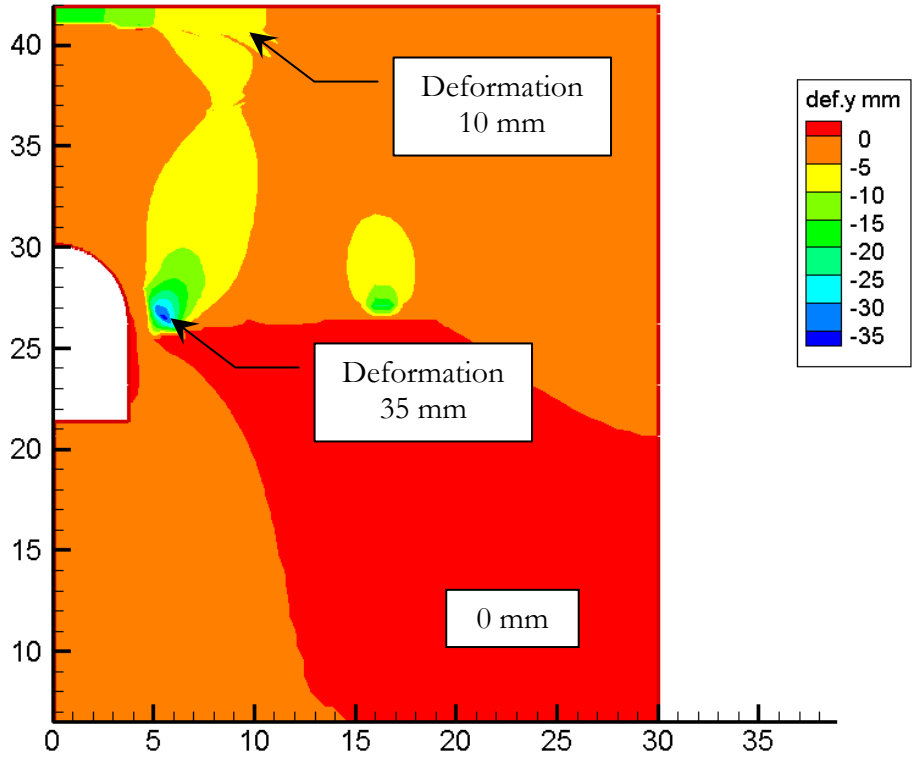

Figure C.1 *Soil settlement distribution around the tunnel 18 months after the cooling device was shut off, i.e. the prognosis for March 2005, based on the measured temperatures at the time of September 2003 and the volumetric strains in oedometer tests. Calculated in JOBFEM*

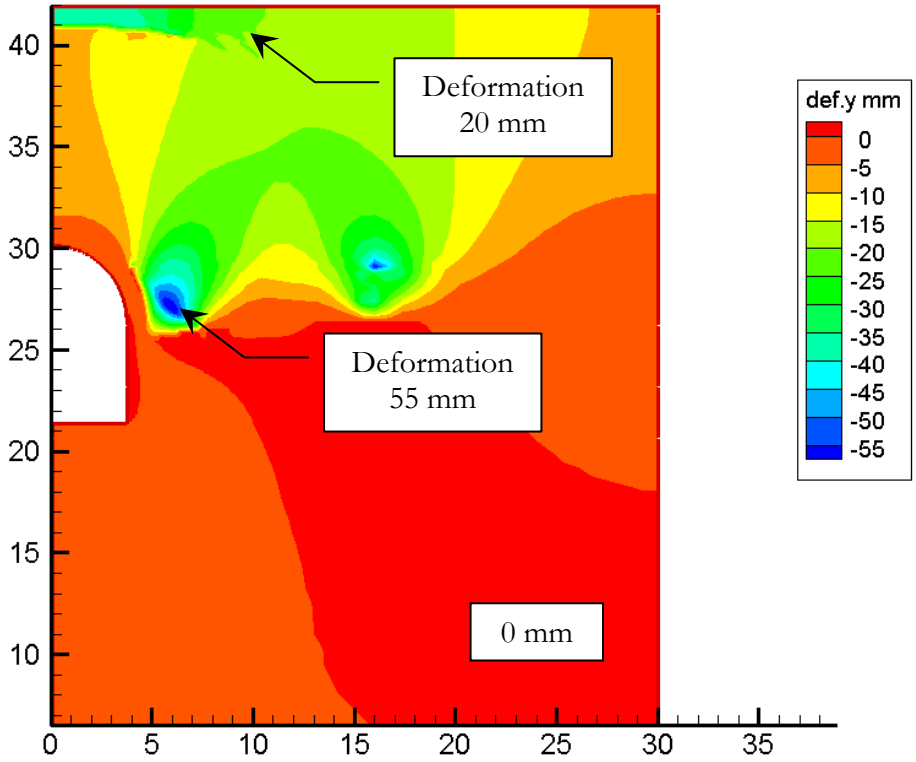

Figure C.2 *Soil settlement distribution around the tunnel 24 months after the cooling device was shut off, i.e. the prognosis for September 2005, based on the measured temperatures at the time of September 2003 and the volumetric strains in oedometer tests. Calculated in JOBFEM*

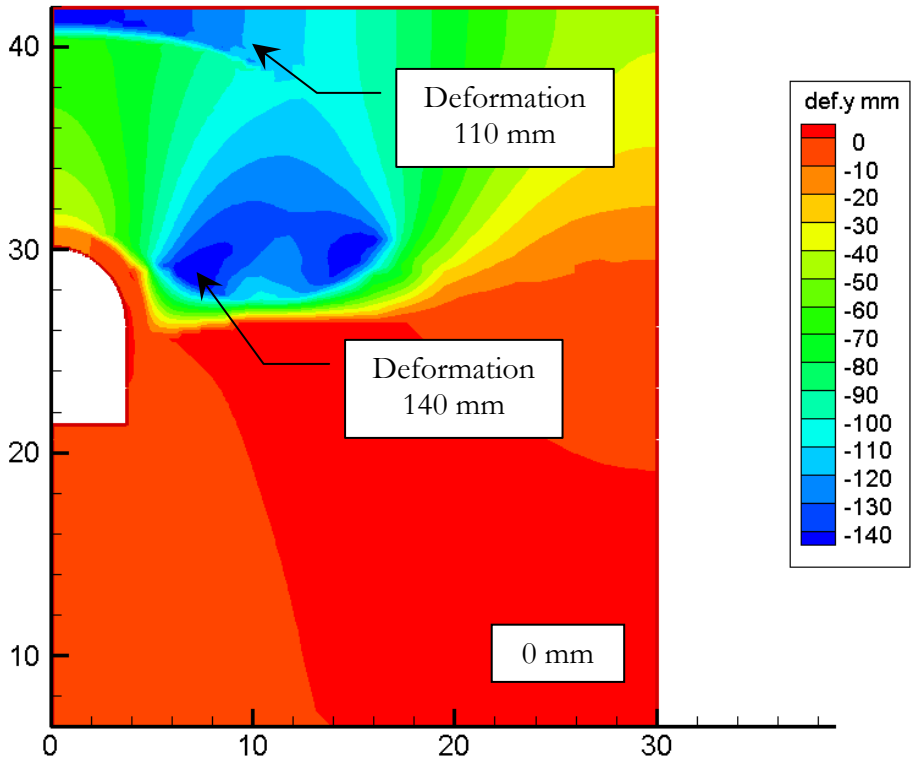

Figure C.3 *Soil settlement distribution around the tunnel 48 months after the cooling device was shut off, i.e. the prognosis for September 2007, based on the measured temperatures at the time of September 2003 and the volumetric strains in oedometer tests. Calculated in JOBFEM*

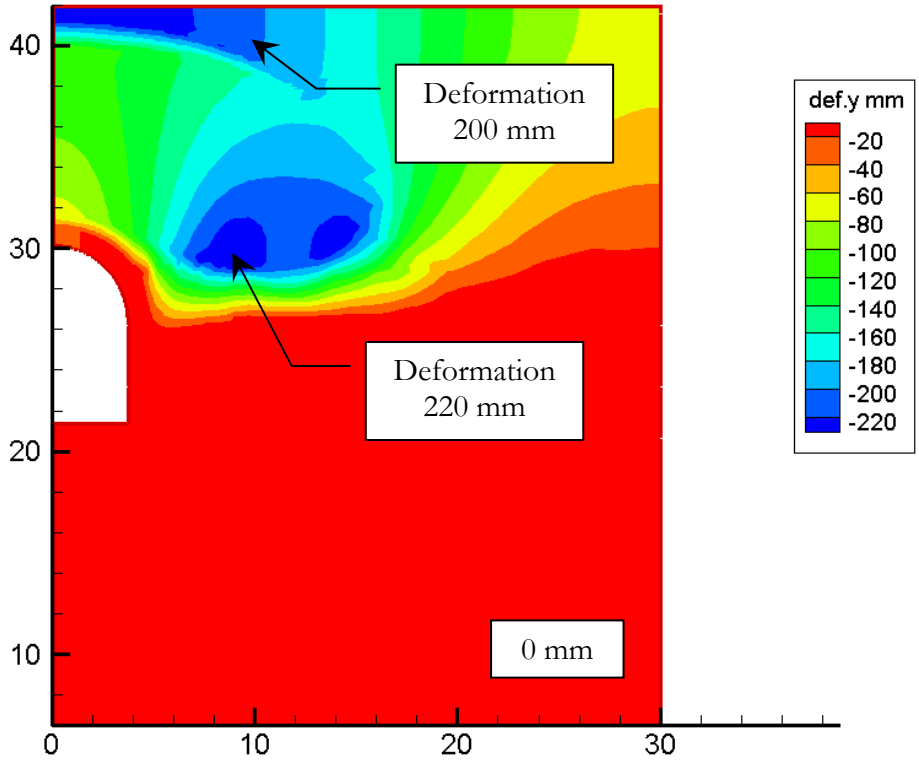

Figure C.4 *Soil settlement distribution around the tunnel 72 months after the cooling device was shut off, i.e. the prognosis for September 2009, based on the measured temperatures at the time of September 2003 and the volumetric strains in oedometer tests. Calculated in JOBFEM*

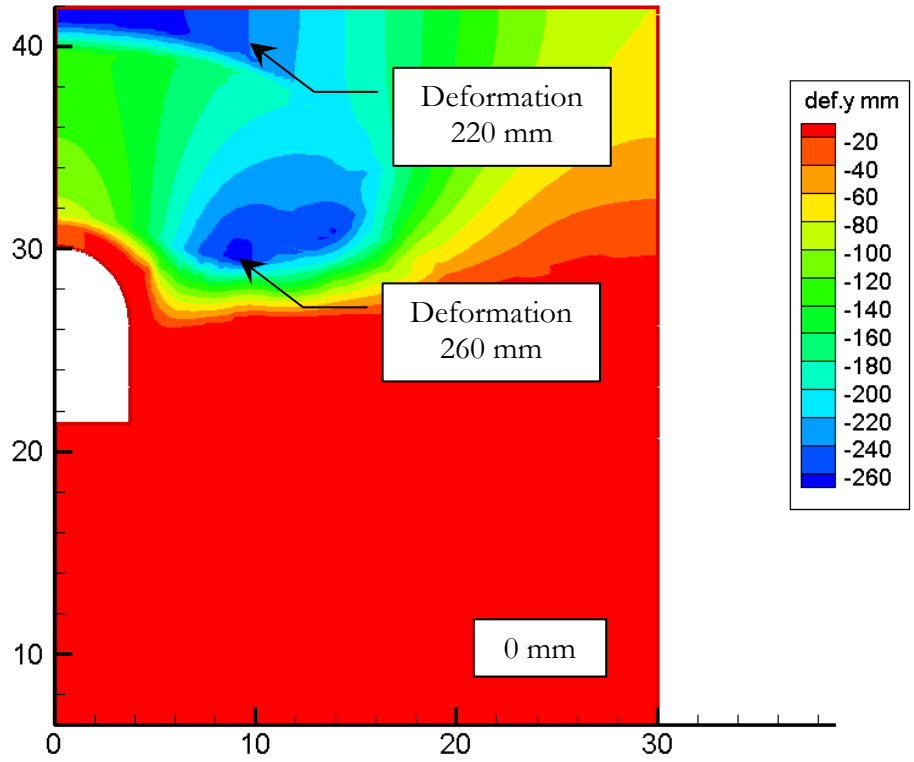

Figure C.5 *Soil settlement distribution around the tunnel 84 months after the cooling device was shut off, i.e. the prognosis for September 2010, based on the measured temperatures at the time of September 2003 and the volumetric strains in oedometer tests. Calculated in JOBFEM*

D APPENDIX, CRS-TESTS

Figure D.1 to Figure D.4 show performed CRS-tests for undisturbed soil and thawed soil collected on August 7th, 2006. Four tests at each depth were performed, i.e. two tests on undisturbed soil and two tests on thawed soil. All tests were performed at normal room temperature (20 °C). Figure D.5 shows the coefficient of consolidation at each depth below ground surface.

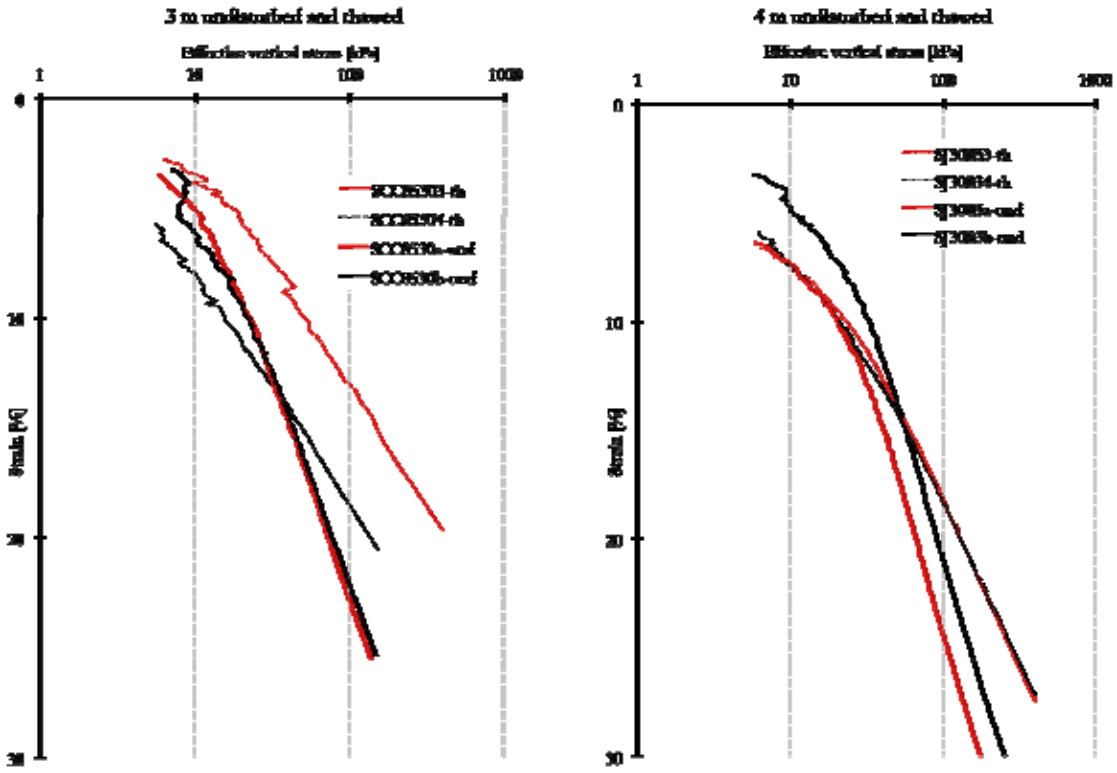

Figure D.1 CRS-tests of soil from 3 m and 4 m depths. "und" denotes undisturbed soil and "th" denotes thawed soil

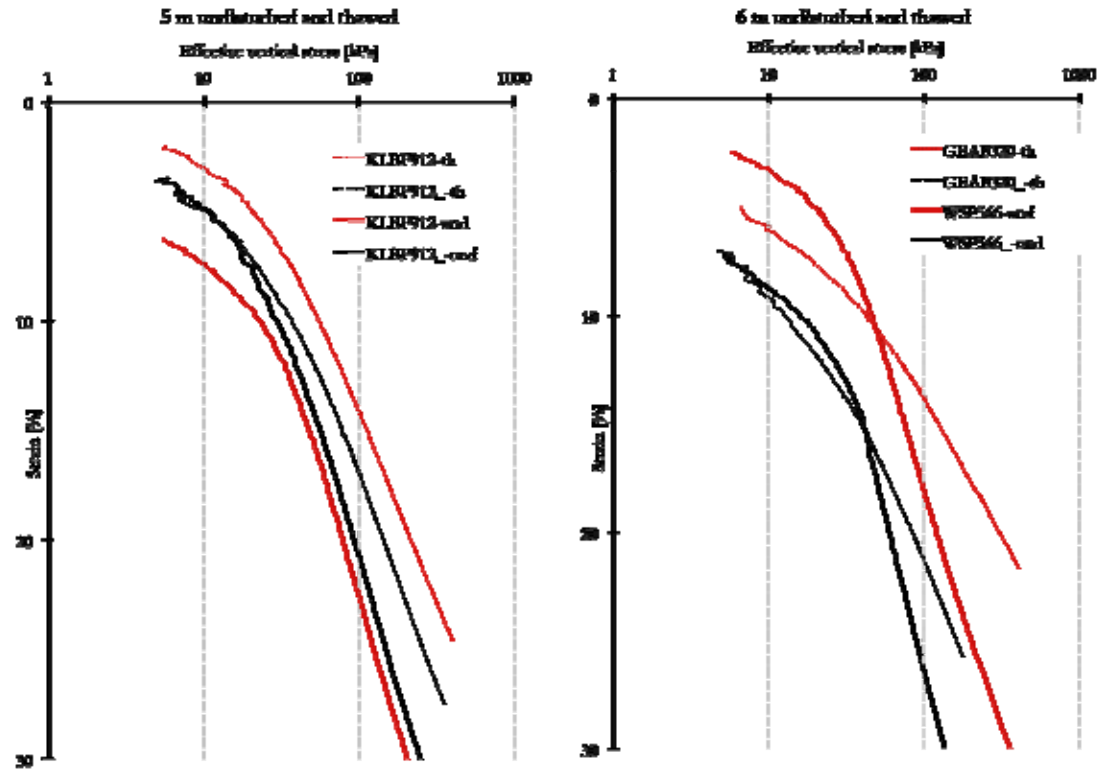

Figure D.2 CRS-tests of soil from 5 m and 6 m depths. "und" denotes undisturbed soil and "th" denotes thawed soil

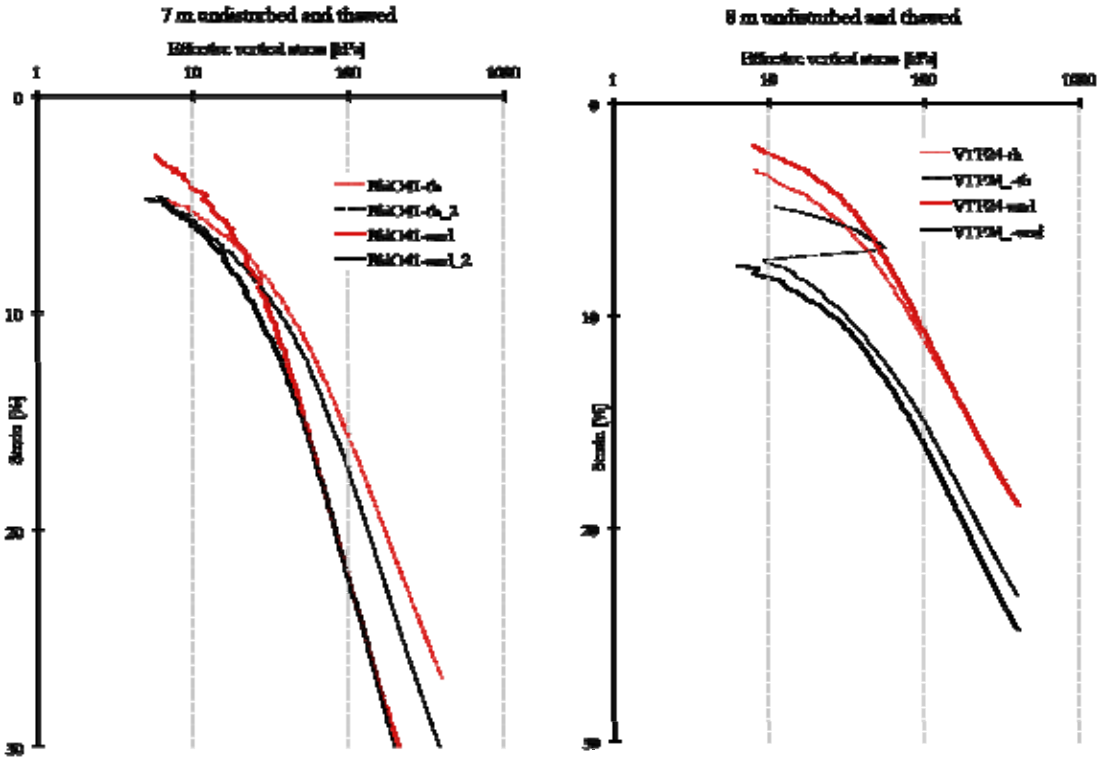

Figure D.3 CRS-tests of soil from 7 m and 8 m depths. "und" denotes undisturbed soil and "th" denotes thawed soil

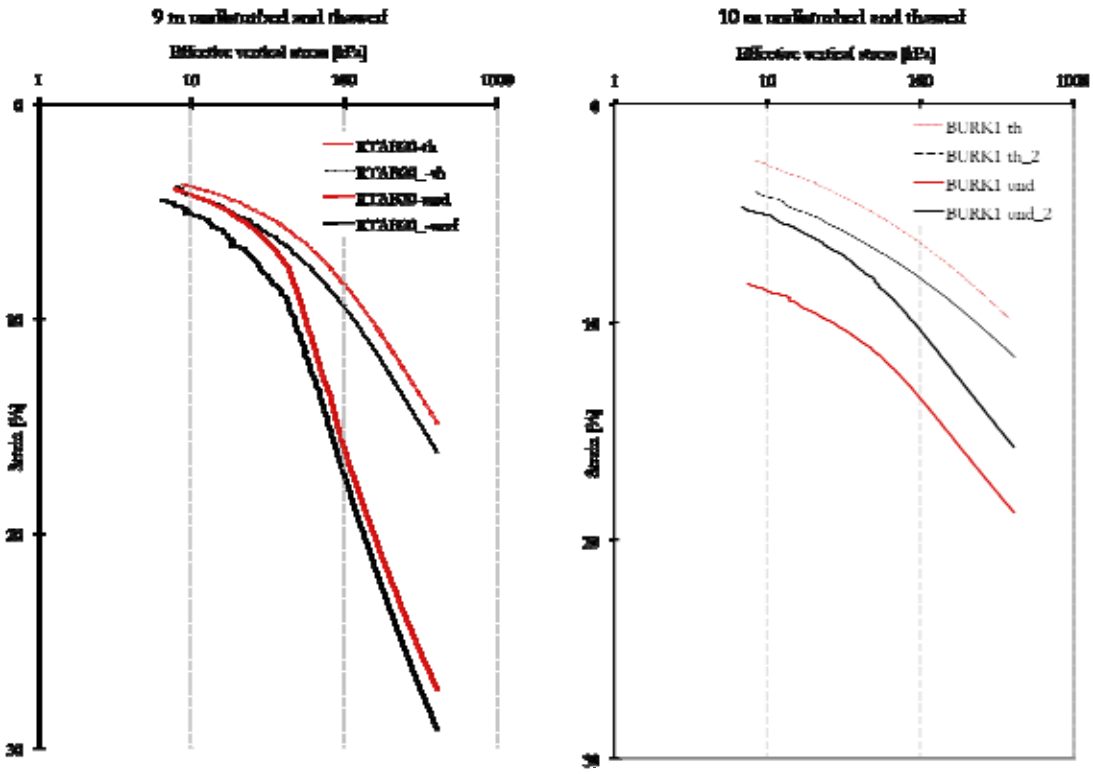

Figure D.4 *CRS-tests of soil from 9 m and 10 m depths. "und" denotes undisturbed soil and "th" denotes thawed soil*

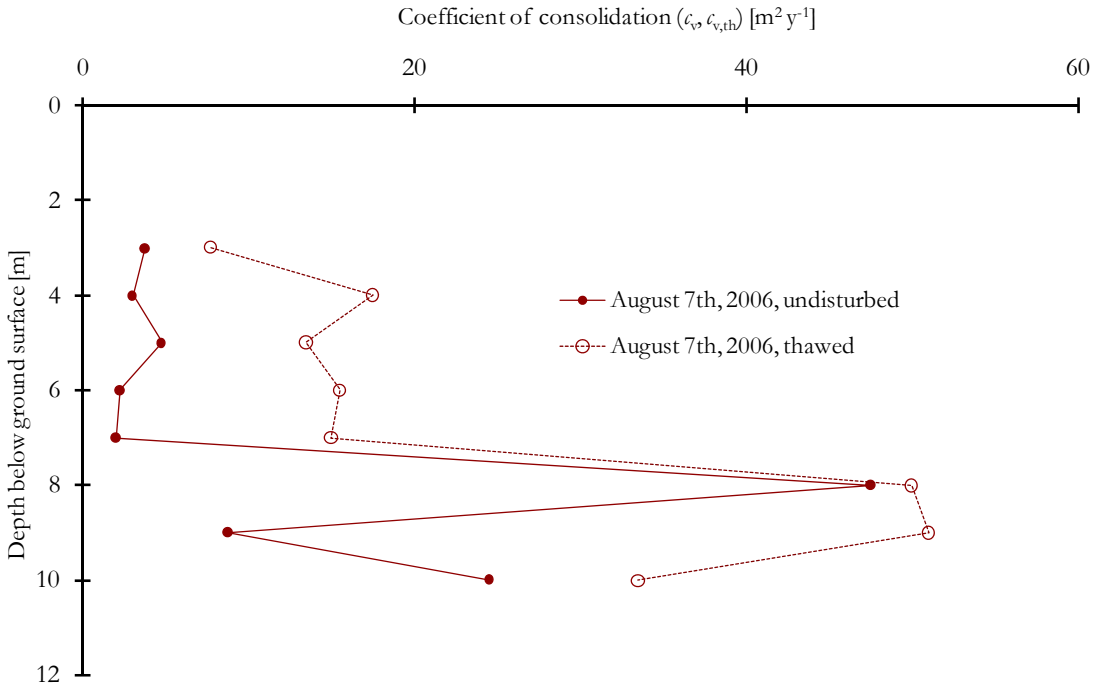

Figure D.5 *Coefficient of consolidation at each depth below ground surface, interpreted from CRS-tests of undisturbed soil and thawed soil from soil collected on August 7th, 2006*